2008-10-14

A Mechanistic Investigation of Nitrogen Evolution in Pulverized Coal Oxy-Fuel Combustion

Andrew John Mackrory
Brigham Young University - Provo

A MECHANISTIC INVESTIGATION OF NITROGEN EVOLUTION IN PULVERIZED COAL OXY-FUEL COMBUSTION

by

Andrew J. Mackrory

A dissertation submitted to the faculty of

Brigham Young University

in partial fulfillment of the requirements for the degree of

Doctor of Philosophy

Department of Mechanical Engineering

Brigham Young University

December 2008

BRIGHAM YOUNG UNIVERSITY

GRADUATE COMMITTEE APPROVAL

of a dissertation submitted by

Andrew J. Mackrory

This dissertation has been read by each member of the following graduate committee and by majority vote has been found to be satisfactory.

Date	Dale R. Tree, Chair
Date	Larry L. Baxter
Date	Thomas H. Fletcher
Date	Matthew R. Jones
Date	Daniel Maynes

BRIGHAM YOUNG UNIVERSITY

As chair of the candidate's graduate committee, I have read the dissertation of Andrew J. Mackrory in its final form and have found that (1) its format, citations, and bibliographical style are consistent and acceptable and fulfill university and department style requirements; (2) its illustrative materials including figures, tables, and charts are in place; and (3) the final manuscript is satisfactory to the graduate committee and is ready for submission to the university library.

Date

Dale R. Tree
Chair, Graduate Committee

Accepted for the Department

Larry L. Howell
Graduate Coordinator

Accepted for the College

Alan R. Parkinson
Dean, Ira A. Fulton College of Engineering and Technology

ABSTRACT

A MECHANISTIC INVESTIGATION OF NITROGEN EVOLUTION IN PULVERIZED COAL OXY-FUEL COMBUSTION

Andrew J. Mackrory

Department of Mechanical Engineering

Doctor of Philosophy

Oxy-fuel combustion is an enabling technology for capture of CO_2 from coal combustion, the economics of which depends strongly on the ability of the process to produce low NO_X emissions. The literature contains many reports of lower NO_X emissions from oxy-fuel combustion but the reasons for this are not fully understood. The objective of this work was to gain understanding of nitrogen evolution under pulverized coal oxy-fuel conditions.

Pulverized coal was burned in a once-through, down-fired, laminar flow reactor. Nitrogen compounds and other combustion species were measured at the reactor centerline as a function of distance from the burner. Dry recycled flue gas was simulated with CO_2 and O_2 was added to form an oxy-fuel oxidizer.

Oxy-fuel combustion measurements were compared to similar experimental data from air-fired cases. In addition, a detailed kinetic model was written and nodel predictions were compared to the experimental data. These comparisons gave insight into the mechanisms of nitrogen evolution under oxy-fuel conditions.

The combustion model matched the experimental data well in many qualitative respects but failed to predict reburning reactions which are believed to be important in both air and oxy-fuel combustion. Model assumptions related to particle size and mixing may be responsible for this difference. Several mechanisms other than reburning are discussed with respect to their importance in the results.

The effect of varying primary combustion zone stoichiometry (depth of staging) was investigated and it was found that oxy-fuel combustion, like air combustion has some depth of staging that produces minimum NO_X. At minimum NO_X conditions in this once-through experiment both air and oxy-fuel combustion converted a similar amount of fuel-bound nitrogen to NO_X, however the minimums were at significantly different stoichiometries.

Relative to air combustion, oxy-fuel combustion was found to exhibit higher concentrations of CO, NH_3, HCN, and hydrocarbons, which indicates a more effective reburning environment exists in oxy-fuel combustion relative to air, even at higher primary stoichiometric ratios. This and other factors such as maximizing the amount of recycled NO_X passing through the fuel-rich flame lead to the conclusion that oxy-fuel combustors should be operated at higher primary stoichiometric ratios than air combustors, which would conveniently also favor high fuel burnout.

ACKNOWLEDGMENTS

My greatest thanks go to Dr. Dale Tree for the last 5½ years of great research and personal growth opportunities. I also wish to express appreciation to my graduate committee for their contribution.

Funding for this work was provided by the United States Department of Energy University Coal Research Program (Award Number DE-FG26-05NT42530) with additional support and technical input from American Air Liquide. Coal samples were donated with the kind help of Joe Hirschi (Illinois Clean Coal Institute), Phil Ott (Freeman Energy), and Vince Conrad and Pete Rosendale (Consol Energy). Significant assistance with experimental equipment and parts fabrication was provided by Kevin Cole and Ken Forster.

Professors Terry Wall (University of Newcastle, Australia) and Adel Sarofim (University of Utah, USA) are appreciated for their insight during conversations at conferences.

Finally, I express my love and thanks to my beautiful wife KaraLynne, my kids Lyman and Corilynn, and my parents for all the sacrifices made by them that have allowed me to be writing this today.

"If I have seen further it is by standing on the shoulders of giants." – Sir Isaac Newton, Letter to Robert Hooke, February 5, 1675

TABLE OF CONTENTS

LIST OF TABLES

LIST OF FIGURES

NOMENCLATURE

a_{ij}	number of atoms of element i in the species j
A	pre-exponential factor or frequency factor
DAF	dry, ash free
E	activation energy
i	summation index for elements
j	summation index for species
k	reaction rate coefficient or in calculation of r, the total number of species in the reactants mixture
l	total number of elements (4 for C, H, N, and O)
$\dot{m}_{coal}$	measured mass flow of coal
$\dot{m}_{prod,wet}$	measured mass flow of wet products
MW_j	molecular weight of species j
MW_N	molecular weight of atomic nitrogen
$MW_{prod,dry}$	average molecular weight of dry products
q	heat transferred
r	chemical equivalence ratio
r^2	square of the correlation coefficient (linear regression) – the percentage of observed variation in the dependent variable explained by variation in the independent variable with the regression equation

R	universal gas constant
SR	stoichiometric ratio - ratio (by mass) of actual oxidizer to oxidizer required for stoichiometric conditions. SR < 1 is fuel-rich; SR > 1 is fuel-lean
T	temperature
V_i^+	positive oxidation state of i^{th} element (C: 4, H: 1)
V_i^-	negative oxidation state of i^{th} element (O: -2)
$X_{NO,dry}$	measured mole fraction of NO_X (dry basis)
Y_j	mass fraction of species j
$Y_{moist,prod,wet}$	mass fraction of condensed liquids (H_2O and H_2SO_4) in a cooled gas sample
$Y_{N,coal}$	mass fraction of nitrogen in coal
η_N	nitrogen conversion efficiency - NO_X normalized by the nitrogen in the coal. If thermal and prompt NO_X formation is negligible this is equal to the formation of NO_X from the fuel-bound nitrogen, hence the term “nitrogen conversion efficiency”. The method of calculation is detailed in Section 3.1.8
μ	average
σ	standard deviation

1 Introduction

1.1 Background

Recently, CO_2 emissions have received much attention as a greenhouse gas responsible for global warming. While the assertion that manmade CO_2 emissions are responsible for global warming is not universally accepted it seems almost certain that regulation of CO_2 is in the near future and technical solutions to mitigate CO_2 emissions will be required. Two of the leading solutions suitable for retrofit to existing pulverized coal-fired power plants are (1) monoethanolamine (MEA) scrubbing technology to separate CO_2 from conventional flue gas; and (2) oxy-fuel combustion to produce a CO_2-rich stream ready for sequestration. Oxy-fuel combustion is the combustion of coal in a mixture of oxygen and recycled flue gas (mostly CO_2 and H_2O) which is required to moderate combustion temperatures and preserve existing convective heat transfer characteristics in retrofit applications. As defined by Buhre et al. (2005), the term oxy-fuel combustion refers to an external flue gas recycle stream, as opposed to oxy-combustion, which uses internal recirculation induced by high-momentum oxygen jets as applied in the glass and steel industries. Often in the literature the terms oxy-fuel and oxy-combustion are used interchangeably and other terms such as "O_2/CO_2 recycle combustion" have been introduced. In this work all references to oxy-fuel combustion

refer to applications with an external recycle stream (or simulated external recycle stream). Figure 1 shows a simplified schematic of an oxy-fuel plant.

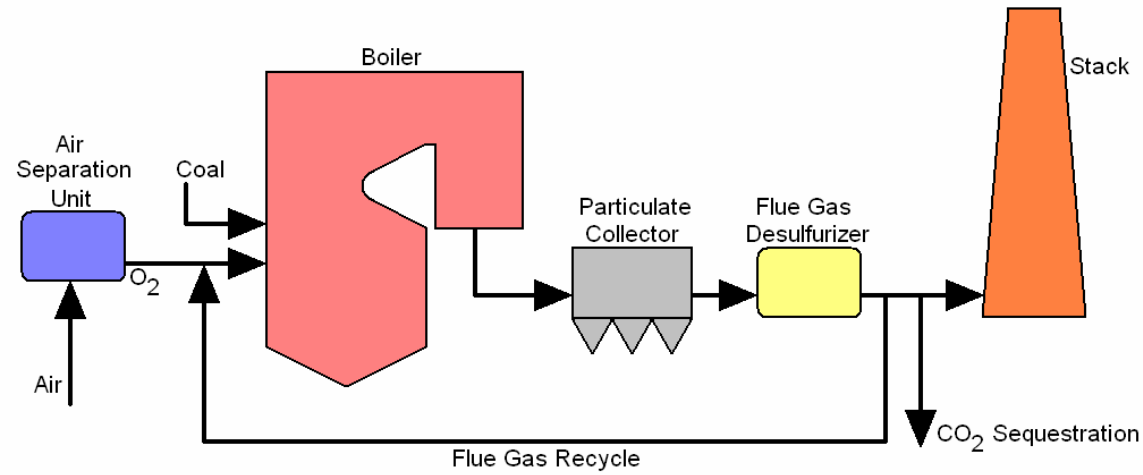

Figure 1. Simplified schematic of a pulverized coal oxy-fuel plant.

It has been noted in pilot scale studies of oxy-fuel combustion that NO_X emissions are reduced (Buhre et al., 2005). In one representative test (Sangras et al., 2004) NO_X emissions relative to baseline air-fired cases were decreased 70%. This reduction is substantial enough that conventional and expensive flue gas treatments such as selective catalytic reduction (SCR) to remove NO_X may become unnecessary. Varagani et al. (2004) concluded that the opportunity to do away with the SCR in oxy-fuel systems is an important factor in the economics of choosing a CO_2 capture technology. Depending of course on site-specific variables and local emissions regulations oxy-fuel combustion may be the lowest cost approach to capture CO_2 (Buhre et al., 2005). The NO_X performance of oxy-fuel is therefore critical to its commercial application.

Most (75-80%) of NO_X emissions from coal-firing originates from nitrogen in the fuel (Kitto and Stultz, 2005). Therefore it could be considered somewhat surprising that

oxy-fuel combustion produces lower NO_X. An important point that has been learned is that the NO_X reduction is not automatic in oxy-fuel combustion. Low-NO_X burners and other combustion devices designed to form N_2 rather than NO are applicable to oxy-fuel combustion (Tan and Croiset, 2005). Without such equipment, oxy-fuel combustion may produce higher NO_X emissions than air-fired cases (Scheffknecht et al., 2007).

Nitrogen evolution during coal combustion has been studied for decades and as a result it is possible to hypothesize possible reasons why oxy-fuel combustion may produce lower NO_X. What follows is a list (not necessarily exhaustive) of possible reasons for the observation of lower NO_X from oxy-fuel combustion. The discussion assumes prior knowledge of common NO_X control methods applied to coal combustion which are described briefly in Appendix A.

- Near-elimination of N_2 in the system: N_2 in a combustion system may be oxidized to NO by the thermal and prompt NO_X mechanisms (Turns, 2000). With atmospheric nitrogen replaced by recycled flue gas, the amount of N_2 available for oxidation is dramatically reduced, but some N_2 may be present in the boiler from air infiltration, N_2 originating from fuel-N, and some N_2 from the air separation unit (Buhre et al. 2005). Thermal and prompt NO_X emissions are already relatively low in most pulverized coal furnaces and so this change may have only a minor effect, but as oxy-fuel combustion has the potential to change temperature and species profiles in the flame it is still of interest to determine how significant these mechanisms are at converting small amounts of N_2 in the boiler to NO.

- Equilibrium considerations: Related to the near-absence of N_2 in the system, calculations show that the equilibrium amount of NO_X in oxy-fuel combustion products is much lower than in air combustion. Even though typical NO_X emissions are at super-equilibrium levels, this reveals that oxy-fuel combustion may have greater potential than air combustion for NO_X destruction.
- Improved attachment of flame to burner: Higher oxygen concentrations in oxygen-enhanced combustion have been reported to better attach the flame to the low-NO_X burner (Bool and Bradley, 2003) resulting in less secondary oxidizer entrainment into the burner's recirculation zone. This reduces oxygen availability during initial combustion of the volatiles and therefore reduces initial NO formation. The oxygen concentration in an oxy-fuel boiler will likewise determine the extent of flame attachment.
- Elevated NO concentrations: The data of Okazaki and Ando (1997) suggest that the presence of NO in the recycled flue gas limits the conversion of fuel-N to NO. Bose et al. (1988) concluded that NO destruction rates in fuel-rich zones are first order with respect to NO. In oxy-fuel combustion the recycled flue gas volume (molar) flow rate is lower than the flow of nitrogen in an air-fired case because the flue gas has higher molecular weight and heat capacity than N_2. This change, together with the recycling of minor species, raises the concentration (relative to air combustion) of all minor species, including NO.
- Reduction of recycled NO_X in the fuel-rich flame zone: Okazaki and Ando (1997) concluded that this was the dominant mechanism of NO_X abatement

(accounting for 50-80% of observed reduction) in oxy-fuel combustion; however their lab-scale experiment had some differences from a practical oxy-fuel combustor (discussed further in the literature review). It is possible that other mechanisms may have increased importance under different conditions.

- Temperature increases: Higher temperatures in the fuel-rich recirculation zone of a low-NO_X burner increase the rate of reduction of NO to N_2. In addition, at higher temperatures the conversion of volatile-N to N_2 is faster than volatile-N to NO conversion (Châtel-Pélage et al., 2004). The near-absence of atmospheric N_2 allows temperature increases to be used to benefit the kinetics without risk of increasing thermal NO_X, which is a problem in oxygen-enhanced combustion that necessitates great care in the method of O_2 injection (Thompson et al., 2004).
- Increased residence times in fuel-rich regions: The higher oxygen concentrations in oxy-fuel combustion should allow deeper staging without flame instability, promoting longer residence times and more fuel-rich stoichiometry in the burner region of the boiler (Kobayashi and Bool, 2005), both favorable conditions for reduction of NO_X. Longer residence times are also caused by the lower gas volume flow rates in oxy-fuel combustion (Sarofim, 2007) and should allow for more nitrogen to be extracted from the char and reduced to N_2 under fuel-rich conditions (Châtel-Pélage et al., 2004).
- Reduced NO formation from char: In addition to the residence time effect just noted, increased temperatures in the devolatilization zone can be expected to increase volatiles yield and to a greater extent the nitrogen content of the

volatiles (Pohl and Sarofim, 1976; Blair et al., 1976). This would decrease the amount of char-N that can be converted to NO in the fuel-lean burnout zone by decreasing both the amount of char, and its relative nitrogen content.

- Enhanced heterogeneous reburning: Depending on the conditions (see literature review) CO may enhance NO_X reduction by char (heterogeneous reburning). CO concentrations in oxy-fuel flames have been reported to be higher than in air flames (Hjärtstam et al., 2007). Increased NO concentrations as discussed above would also be expected to increase the rate of this reaction pathway. Okazaki and Ando (1997) do not consider this mechanism to be significant in pulverized coal combustion on account of low particle density. In Smoot (1993) it is also noted that heterogeneous reactions involving soot have potential to both create and destroy NO_X. Oxy-fuel combustion can change the level of soot formation in a flame due to temperature, residence time, and chemical (CO_2) effects (Sarofim, 2007).
- Increased importance of gasification reactions: The high CO_2 concentrations in oxy-fuel combustion may increase the importance of gasification reactions that are typically neglected in modeling air-fired furnaces. While gasification reactions may not directly affect NO_X mechanisms, species and temperature profiles may change, indirectly affecting the nitrogen chemistry.
- Competition for oxygen: The possible changes to temperature and species concentrations in oxy-fuel combustion may affect the competition for oxygen between hydrocarbons and nitrogen compounds, potentially changing the initial level of NO formation.

The above list conveys some idea of the complexity of nitrogen chemistry in a pulverized coal flame. Understanding of the mechanisms and their relative importance is critical to design of a combustion system. Varagani et al. (2004) observe that the possible independent control of oxygen concentrations in various oxidizer streams in oxy-fuel combustion offers a level of optimization that does not exist in conventional air combustion. Use of air as an oxidizer effectively couples temperature with stoichiometry, whereas control of the oxygen concentration allows combustion temperatures in various boiler locations to be adjusted independent of stoichiometry. This increased potential may only be realized with increased understanding of the mechanisms involved.

While there have been several studies to investigate the lower NO_X emissions of oxy-fuel combustion, the mechanisms are still not understood (Sarofim, 2007). This is not surprising given that our understanding of NO_X chemistry even in idealized combustion conditions in air is incomplete (Glarborg et al., 2003).

1.2 Research Objectives

The objective of this research was to gain increased understanding of the mechanisms responsible for the NO_X reducing behavior of oxy-fuel combustion. This was achieved through experimental measurements of gas species in air and oxy-fuel pulverized coal flames and computational modeling of the experimental setup. A computational model using detailed chemistry was used, and when compared with the measurements, provided insight into the feasibility of various NO_X reduction pathways and an understanding of the ability of state of the art modeling tools to predict the performance of oxy-fuel combustion.

1.3 Scope

The focus of this work is on nitrogen evolution in pulverized coal oxy-fuel combustion and comparable air-fired cases. Flue gas was not recycled in the experiments. Instead, bottled CO_2 was used to simulate dry recycled flue gas. The results are applicable to entrained-flow pulverized coal combustion in general, but the absence of turbulence in the laminar flow experiment is a notable difference from any practical combustor.

The majority of the data presented are in-flame measurements which provide more insight into the physical processes than effluent gas species measurements alone. This, combined with the fact that the experiments are complemented by detailed kinetic modeling, constitute the unique contributions of this work. As noted by Andersson et al. (2007), experimental studies of oxy-fuel combustion NO_X emissions that include computational modeling of the chemistry are rare.

The field of oxy-fuel combustion has a number of important issues presently being considered by researchers, but as these are not directly related to the scope of this work they are not discussed. These areas include, but are not limited to:

- Choice of recycle stream configurations: wet vs. dry recycle, before or after flue gas desulfurization, or combinations thereof.
- Choices related to process economics including oxygen production method and purity.
- The allowable or desirable level of impurities such as NO_X and SO_X in CO_2 captured for sequestration. These levels are not yet determined (Sarofim, 2007).

- Potential for altered corrosion potential in oxy-fuel combustion.
- Whether or not CO_2 capture is wise to pursue. It is possible that how much CO_2 can be sequestered is limited by oxygen availability in the atmosphere and not by CO_2 storage capacity of the planet (Lackner, 2007). This work should not be seen as an endorsement of the capture and storage of CO_2.

The fate of sulfur in the fuel is another important issue. Some relevant points from the literature will be noted and a few sulfur measurements are presented. However interpretation of these data is minimal.

2 Literature Review

The literature relevant to NO_X formation in coal combustion is enormous and therefore no attempt is made here to provide a complete review; rather the focus of this chapter is on points from the literature that are particularly relevant to this work. More complete reviews on certain aspects may be found in the literature as follows:

- Oxy-fuel combustion: Buhre et al. (2005)
- Fuel nitrogen conversion from solid fuels: Glarborg et al. (2003)
- NO_X modeling: Hill and Smoot (2000)
- Nitrogen reactions involving char: Molina et al. (2000)

2.1 Coal Devolatilization and Nitrogen Release

As a coal particle is heated it is decomposed, or pyrolyzed. Volatiles (gas phase species) are given off in a process known as devolatilization. Combustion of the solid residue remaining after devolatilization is known as char oxidation. Badzioch and Hawksley (1970) tested ten bituminous coals and one semi-anthracite feeding them into a laminar flow of hot nitrogen to give industrially relevant pulverized coal heating rates of 25,000-50,000 K/s. They determined that volatiles yield depends on the time-temperature history of the particle and that both the rate of temperature rise and the final temperature attained are important. Some volatiles are reactive with each other and the char, but for

particles suspended in a gas the volatiles are usually removed quickly or diluted with the surrounding gas so there is little reaction during devolatilization. Some of their experiments were conducted with oxygen at concentrations below that required for particle ignition. There was no difference noted in the rate of decomposition between nitrogen and oxygen-nitrogen mixtures which suggests that devolatilization is primarily a thermal process. They also mention that some studies support the hypothesis that char oxidation overlaps devolatilization. This depends on oxygen availability at the surface which in turn is dependent on the rate at which volatiles are being evolved.

Pohl and Sarofim (1976) studied the kinetics of coal nitrogen pyrolysis. Release of nitrogen was concluded to be kinetically controlled and dependent on coal molecular structure. In their work about ten percent of observed coal weight loss occurred before release of nitrogen, but once nitrogen release began it was proportional to incremental weight loss. HCN was thought to be a principal product of coal pyrolysis.

Rates and speciation of volatiles release from pulverized coal particles during pyrolysis was studied by Blair et al. (1976) both experimentally and theoretically. Total mass evolved was strongly dependent on coal composition, but nitrogen evolution was not. Their data suggested a similarity of nitrogen evolution kinetics between coals even when the mass loss between the coals is different. Pyrolysis temperature had a significant effect on distribution of nitrogen between volatiles and char. Nitrogen evolution was more sensitive to temperature than was mass loss for all the coals tested (bituminous and sub-bituminous). Regarding speciation of the volatiles, NO and C_2N_2 were not detected but N_2, HCN, and NH_3 were. Only 15% of the nitrogenous species were contained in these light gases. High boiling point (i.e. greater than 750 °C) compounds contained

about the same percentage of the coal nitrogen as the HCN and so the remainder of nitrogen must therefore have been in the intermediate boiling range compounds or tars. In their review Glarborg et al. (2003) suggest that the amount of nitrogen from primary pyrolysis existing in the tar is 85-100%.

Hill and Smoot (2000) discuss research on nitrogen release and note variation in conclusions in the literature. Some have concluded that lower rank coals yield NH_3, (e.g. Bose et al., 1988) and others that NH_3 is formed from HCN under oxidizing conditions during pyrolysis. Still others have concluded that HCN is the dominant nitrogen product in primary and secondary pyrolysis for a sub-bituminous (low rank) and bituminous (high rank) coal. Secondary pyrolysis refers to the reactions undergone by tar and thermal decomposition of char at high temperature after they are separated during primary pyrolysis (Glarborg et al., 2003).

From the work of Blair et al. (1976) which found most nitrogen release to be contained in the tars, it appears that conclusions that coal releases nitrogen in the form of HCN and NH_3 are not separating primary and secondary pyrolysis in the pathway of nitrogen release. Zhang and Fletcher (2001) studied secondary coal pyrolysis and determined that volatile-N released in the tar may be converted to HCN, or at high temperatures and long residence times where tar has a strong tendency to form soot, the nitrogen may be contained in the soot. NO_X control methods based on combustion modifications rely on the nitrogen being in the gas phase and so incorporation of nitrogen in the soot is undesirable.

Not much is known about the products of soot nitrogen and for bituminous coals as much as 25% of the nitrogen from primary pyrolysis may be incorporated in the soot

in secondary pyrolysis (Glarborg et al., 2003). CO_2 is known to decrease soot formation (Oh and Shin, 2006; Sarofim, 2007), but as noted, increased temperature and residence time favor soot formation. The net effect on soot formation in changing from air to oxy-fuel combustion is unclear.

Zhang and Fletcher (2001) determined that for high tar coals the initial tar release is related to mass release, but low rank (low tar) coals release other light gases such as CO before tar and so initial nitrogen release lags behind the mass release. Light gas nitrogen release (such as HCN) occurred at a later stage than tar nitrogen release and its source was secondary pyrolysis. For the coals they studied (ranging in rank from lignite to high volatile B bituminous) the tar nitrogen release during secondary pyrolysis was largely independent of coal type. From their survey of the literature they discussed the selectivity between HCN and NH_3 and note that the HCN/NH_3 ratio may not affect the amount of NO formed at high temperatures (i.e. pulverized coal combustion), and that it was still not clear whether HCN and NH_3 are released independently or NH_3 is a product of reactions of HCN. HCN was believed to be the dominant nitrogen species from tar cracking. They concluded from their own work that the relative amount of HCN/NH_3 had more to do with reactor type and local gas environment than coal properties.

Release of nitrogen during char burnout is likewise complex. In their review Hill and Smoot (2000) state that several studies have concluded that char oxidation does not release HCN. Thus NO_X from char is not formed from homogeneous oxidation of HCN. Heterogeneous reactions of the char may both form and reduce NO in the char pores before the nitrogen product leaves the char particle. Nitrogen release from char is discussed below in connection with fuel and heterogeneous NO_X mechanisms.

2.2 NO_X Chemical Mechanisms

There are a number of different pathways through which NO_X can be formed and destroyed in combustion. The relative importance of these mechanisms changes with combustion conditions (Glarborg et al., 2003) and so understanding of the mechanisms allows the control of NO_X to be implemented through combustor design. This section outlines important mechanisms that have been described in the literature.

2.2.1 Thermal NO_X

Thermal NO_X is the oxidation of atmospheric nitrogen as described by the extended Zeldovich mechanism in Reaction 1 through Reaction 3 (Turns, 2000).

$$O + N_2 \longleftrightarrow NO + N \qquad \text{[Reaction 1]}$$

$$N + O_2 \longleftrightarrow NO + O \qquad \text{[Reaction 2]}$$

$$N + OH \longleftrightarrow NO + H \qquad \text{[Reaction 3]}$$

The mechanism is most important at elevated temperatures (above 1800 K) due to the high activation energy of Reaction 1, which explains the name of this mechanism. Typically thermal NO_X control strategies are centered on decreasing peak temperatures, sometimes through dilution with recycled flue gas. In addition to temperature-based solutions, thermal NO_X may be prevented by limiting the concentrations of reactants O_2 and N_2. In conventional pulverized coal combustion fuel NO_X dominates (75-80%), but thermal NO_X accounts for most of the remaining NO production (Kitto and Stultz, 2005).

Glarborg et al. (2003) note that high levels of fuel NO_X can inhibit thermal NO_X due to the high NO concentrations increasing the reverse rate of progress for Reaction 1.

2.2.2 Prompt NO_X

The prompt NO_X mechanism, so called because it forms NO_X faster than the thermal mechanism, is described by the Fenimore mechanism and consists of attack of molecular nitrogen by hydrocarbon fragments to form amines or cyano compounds as shown in Reaction 4 and Reaction 5. These nitrogen compounds further react and can eventually form NO (Turns, 2000). There are many elementary reactions involved as demonstrated by the large number of N-containing reactions in the GRI-Mech 3.0 methane combustion mechanism (Smith et al., 2000) shown in Appendix B. The relative importance of different pathways changes with stoichiometry and gas composition. Further discussion may be found in the references.

$$CH + N_2 \longleftrightarrow HCN + N \qquad \text{[Reaction 4]}$$

$$C + N_2 \longleftrightarrow CN + N \qquad \text{[Reaction 5]}$$

Because of the requirement for hydrocarbon fragments, prompt NO_X is more prevalent in fuel-rich flames. Staged combustion applied to pulverized coal is therefore expected to increase prompt NO_X relative to an unstaged furnace, but in coal combustion where the fuel contains on average 1.4% nitrogen by weight (US coals – Sarofim et al., 1978) prompt NO_X is usually negligible relative to fuel NO_X.

2.2.3 Fuel NO_X

Fuel NO_X consists of oxidation of nitrogen originating in the fuel molecular structure. The term does not apply to N_2 in a fuel gas. Sarofim et al. (1978) review research that suggests nitrogen compounds are mostly converted early in the flame to a common intermediate. Experimental evidence points to HCN as one of the most

significant of these. HCN is the dominant stable product at high temperatures (1120-1370 K), but NH_3 has been found to increase in importance in later zones of hydrocarbon flames. Turns (2000) states that once the intermediate compound is formed the same pathways followed for prompt NO_X formation apply to fuel NO_X. Figure 2 illustrates these pathways.

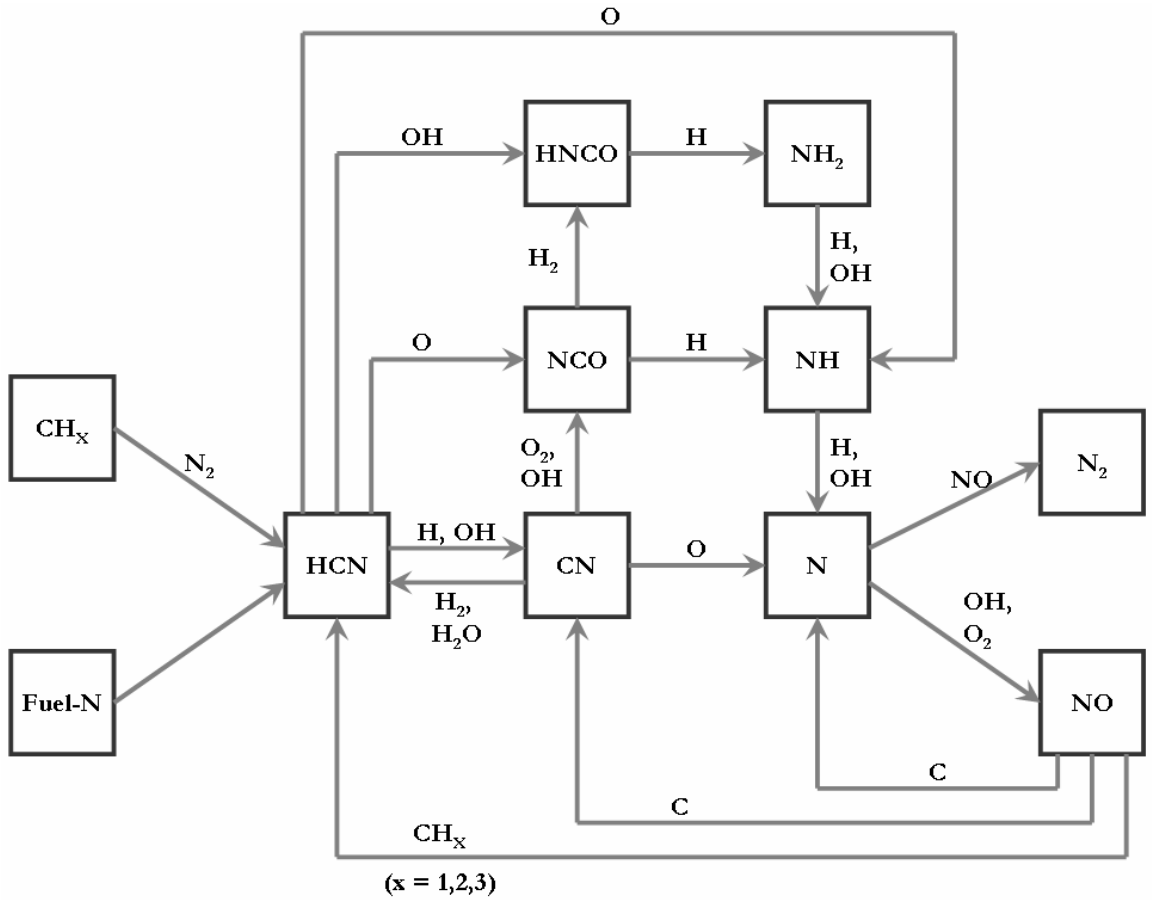

Figure 2. Important pathways of NO formation in the prompt and fuel NO_X mechanisms. The significance of the pathways varies depending on local conditions (redrawn from Bowman, 1992).

Pohl and Sarofim (1976), in determining the conversion efficiency of nitrogen in volatiles and char to NO_X observed that under fuel-rich conditions a lower fraction of

volatiles nitrogen is converted to NO_X. Further, at high furnace temperatures (1500 K) under oxidizing conditions, 60-80% of the NO_X was contributed by the volatiles nitrogen. In other words conversion of nitrogen in the char to NO_X was lower than conversion of volatiles nitrogen to NO_X by a factor of 2-3. It was also found that increasing temperature or residence time for pyrolysis under fuel rich conditions reduced the nitrogen retained in the char. These trends lead directly to strategies for NO_X abatement involving control of local temperature and stoichiometry in the coal flame.

2.2.4 Other Homogeneous NO_X Mechanisms

Sarofim et al. (1978) review work where NO was added to flames and found to form HCN by reaction with hydrocarbons early in the flame. Oxidation of the HCN to NO_X thereafter would be similar to the prompt or fuel NO_X mechanisms. The conversion of NO to HCN is known as reburning. Reburning has importance in coal combustion, and more particularly oxy-fuel combustion where NO is recycled with the flue gas.

Selective non-catalytic reduction (SNCR), reburning, and advanced reburning (see Appendix A) are all relevant NO_X reduction methods with homogeneous chemistry.

Another homogeneous NO_X mechanism in the literature is the N_2O-intermediate mechanism. This mechanism is important in low temperature, fuel-lean flames but is not of importance to coal combustion. It is most typically considered in connection with gas-turbine combustors (Turns, 2000).

2.2.5 Heterogeneous NO_X Mechanisms

There are heterogeneous reactions that can occur between the solids in a coal flame (soot and char) and the nitrogen species. Reduction of NO by char is important in fluidized bed combustion and probably also important inside pulverized coal char as NO

diffuses out of the particle. This may partly explain why conversion of char nitrogen to NO is lower than conversion of volatiles nitrogen to NO. Pohl and Sarofim (1976) concluded that char-N conversion to NO_X is affected by oxygen availability in the pores and not the bulk O_2 concentration.

There have been multiple studies (Chan et al., 1983; Guo, 1997; Aarna and Suuberg, 1999) of char-NO reactions at conditions relevant to fluidized bed combustors. Common conclusions include that reduction of NO by char is first order with respect to NO, and that CO can enhance the rate of reduction. The results of these studies may not apply to pulverized coal combustion as a result of temperature and other differences. Aarna and Suuberg (1999) determined that enhancement of the NO-carbon reaction by CO is lower at high temperatures and in their results was insignificant above 900°C for coal char and other carbons. Char concentration in Guo's packed bed experiment (1997) was 0.1 g/cm^3, and in this work the char concentration was on the order of 1×10^{-5} g/cm^3.

Bose et al. (1988) note that at the time of their work there was some question as to the importance of char-NO reactions in pulverized coal combustion. They used a down-fired, autothermal furnace operating under reducing conditions. Experiments with gaseous fuels yielded similar data to pulverized coal experiments and led to the conclusion that homogeneous chemistry controlled the NO_X reduction. The question of how much NO_X destruction mechanisms depend on coal composition was also investigated. Coal composition was found to be important because of its influence on the temperature and combustion environment and not because of variation in evolved nitrogen species.

Sarofim et al. (1999) present a single particle model that captures the characteristics of NO-char kinetic reactions at pulverized coal combustion conditions. They particularly note the performance of the model in predicting *"the very significant decrease in apparent conversion of char nitrogen to NO with increasing ambient NO concentrations"*. This comment suggests that under oxy-fuel conditions with high NO concentrations and all other things equal, the formation of NO from char should be reduced relative to air combustion.

Molina et al. (2000) reviewed mechanisms and modeling of formation and destruction of NO by char. They note that as primary control methods have improved the importance of this source of NO has grown (see Section 2.2.6 for discussion of primary control methods). Unfortunately, NO formed from char is not easily controlled. They discuss in their review some disagreement on the mechanism of NO reduction on char surfaces, which could be due the importance of different reactions changing with temperature. Some research they reviewed suggests that H_2O and CO_2 (both in elevated concentrations in oxy-fuel) do not affect the rate of NO reduction by char, but more recent studies they reviewed suggest that these gases may affect the population of surface complexes and thereby the final reaction rate. At pulverized coal combustion conditions the dominant product of NO reactions with char is N_2. The reduction reaction(s) can be considered first order with respect to NO and thus their effectiveness will decrease as primary NO_X control methods improve.

Glarborg et al. (2003) observe in their review that there is not much agreement on how much char-N becomes NO with values ranging from 30-100%. Particle concentration and size may have effects that reduce the value by reducing NO in pores or

on other particles. If NO levels are sufficiently high the net effect may be destruction of gas-phase NO as observed by Okazaki et al. (1984) during char burnout in a lean, premixed pulverized fuel flame.

Molina et al. (2004) found that in their entrained flow char experiments (in N_2 or helium-based gas mixtures) that as the bulk NO concentration increased the conversion of char-N to NO decreased. They concluded that homogeneous mechanisms were important to the observed trends, but the simultaneous presence of both homogeneous and heterogeneous mechanisms made it difficult to separate the effects. Local stoichiometry was determined to be a significant factor.

2.2.6 Primary NO_X Control Strategies

Primary NO_X control strategies are defined as combustion modifications that affect the net formation of NO_X in the furnace. They are typically more cost-effective than secondary measures (post-combustion). Often a combination of primary and secondary measures is required to achieve very low emissions. This section discusses the principles behind primary NO_X emission controls. Descriptions of the methods that employ these principles are found in Appendix A.

Sarofim at el. (1978) discuss strategies for controlling NO_X emissions from fuels containing nitrogen based on the knowledge at the time. Fuel-rich conditions are favorable for decreased conversion of fuel-N to NO_X; suggesting staged combustion as an effective technique. Rates of mixing of fuel and oxidizer are also important. Research was referenced where increased NO_X formation was associated with decreased sooting tendency, and sooting tendency can be taken as an index of mixing effectiveness. Slower rates of mixing increase the fraction of fuel that reacts under locally fuel-rich conditions

and thereby reduces conversion of fuel-N to NO_X by the same principle as changes to overall stoichiometry.

Flue gas recirculation to reduce peak flame temperatures is noted to be a relatively ineffective strategy when the fuel nitrogen contribution is dominant (or thermal NO_X is already almost eliminated). Works referenced by Sarofim et al. (1978) concluded that oxidation of coal nitrogen is temperature insensitive over the practical range of temperatures.

NO_X reduction is also discussed by Sarofim et al. (1978) in terms of thermodynamic and kinetic constraints. Typically NO_X levels in flue gases are at super-equilibrium values because furnace conditions are not sufficient in temperature and required species for the NO_X reduction kinetics to function. Increased temperatures in reducing zones may be considered as a tool to overcome the kinetic constraint. At near stoichiometric conditions NO is the thermodynamically preferred form of nitrogen (as opposed to HCN or NH_3) and so staged combustion to create fuel-rich conditions can be thought of as a way to overcome the thermodynamic constraint. They recommend staged combustion, low excess air firing, and high air-preheat to minimize NO_X. More recently oxygen-enhanced combustion has been used to raise temperatures in the reducing zone (Kobayashi and Bool, 2005).

There are trade-offs involved in primary NO_X control strategies. Typically conditions that favor low NO_X are detrimental to high fuel burnout, and CO emissions become an issue. Châtel-Pélage et al. (2004) report that burner stoichiometric ratio (SR) in air combustion usually cannot be reduced below 0.8 for flame stability reasons.

2.3 Use of Oxygen in Combustion

Oxygen enrichment may be used to control temperatures independent of stoichiometry to improve combustion and NO_X performance. Châtel-Pélage et al. (2004) note that oxygen enrichment can allow lower burner stoichiometric ratio while maintaining or increasing temperatures and flame stability.

Baukal (1998) discusses some of the potential changes to a combustion system when oxygen is used to enhance the combustion. When oxygen concentration is increased, flammability limits widen, flame speed and residence time increase, and required ignition energy, ignition temperature, and flue gas volume decrease. Decreases in flue gas volume lead to lower particle entrainment, and increases in trace species concentrations (notably NO_X and SO_X). These changes enhance the ease with which undesirable trace species may be scrubbed from the product gases. Changes to heat transfer are more complex than these simple trends. The important point is made that when using oxygen to enhance a process, the gas analysis results need to be reported in some basis that corrects for differences in the oxidizer. It is also noted that under reducing conditions CO is formed preferentially to NO.

2.4 Selected Air Combustion NO_X Studies

Bose et al. (1988) using a down-fired, autothermal, pulverized coal furnace operating under reducing conditions found that the chemistry differed from equilibrium significantly:

- All measured nitrogen species were at super-equilibrium values.

- The water-gas shift equilibrium did not hold except at the largest residence times. Temperatures calculated using measured species concentrations and assuming water-gas shift equilibrium were lower than measured temperatures.
- The global equilibrium assumption they made for OH did not appear to be generally valid for SR ≥ 0.6 even if residence time was long.

In addition it was found that:

- Their results were consistent with the hypothesis that under oxidative pyrolysis conditions NH_3 comes from HCN which comes from tar nitrogen.
- NO destruction rates were first order with respect to NO and NH_3. They determined that NH_3 was a key intermediate that should be predicted in modeling of NO destruction.
- The addition of NO to the reactants caused increases in HCN and NH_3.
- NO reacts rapidly with hydrocarbons to form HCN, NH_3, and N_2, but only occurs rapidly when hydrocarbon concentrations are high.
- HCN evolved in the post flame appeared to be from the char and not from NO-hydrocarbon reactions, as in the post flame the hydrocarbon concentration was low and NO destruction rates slowed down. Other work reports that HCN is not a product of char oxidation (Hill and Smoot, 2000), but it is possibly a product of secondary pyrolysis of char.
- Reactions from the thermal and prompt NO_X mechanisms of Zeldovich and Fenimore were both important (at different temperature ranges).

Chen et al. (1991) studied advanced reburning (see Appendix A) and report that the temperature window for the process can be widened if the reagent is added under

slightly fuel-rich conditions (e.g. SR = 0.99). Their kinetic modeling suggests that the rich zone acts primarily as a source of CO which is oxidized at the rich-lean transition where burnout air is added and can produce excess OH through chain-branching reactions. The OH is important in reactions with NH_3 that allow the NO to eventually be reacted to N_2. The CO concentration in their experiments was determined to be a key parameter along with NH_3 species and temperature. These results indicate that while major combustion species (CO for example) may not necessarily be directly involved in nitrogen chemistry, the nitrogen chemistry is coupled to the major species combustion through the radicals.

Another important point that may be taken from Chen at al. (1991) is that certain combustion parameters are not necessarily transferable between combustors. In their bench scale experiments they used SR = 0.99 for the reagent injection zone stoichiometry, but in pilot scale studies had to use SR = 1.03 to allow for finite mixing rates and higher CO in the larger furnace. In the oxy-fuel combustion literature there are often reports of oxygen concentrations or other parameters that allowed air combustion to be closely approximated. These values should only be considered valid for the specific furnace configuration studied.

2.5 Oxy-fuel Combustion Studies

Japan has led the way in early research on oxy-fuel combustion. Oxy-fuel experiments reported as early as 1992 by Nakayama et al. indicate reduced NO_X emissions under oxy-fuel conditions.

Kimura et al. (1995) performed a study of combustion characteristics under oxy-fuel conditions using a swirl-stabilized burner firing 100 kg/hr coal. They used positive gage pressure in their furnace to prevent air infiltration, and reported NO_X in terms of a NO_X conversion ratio defined as conversion of fuel-N to NO_X assuming all NO_X is fuel-derived. It was observed that:

- Higher oxygen concentrations (by volume) than in air were required in oxy-fuel combustion to match flame temperatures.
- NO_X in oxy-fuel combustion was reduced to about one fifth the levels in air combustion for conditions where unburned carbon was similar. This improvement was attributed to reburning of recycled NO_X.

Nozaki et al. (1997) in a follow up paper report that NO_X in the flame (mostly recycled NO_X) was reduced rapidly to HCN or NH_3 in the early stages of coal combustion. Oxygen injection at the burner centerline raised near burner gas temperatures, causing increased devolatilization. Formation of NO_X in the flame was concluded to be lower under oxy-fuel conditions.

Okazaki and Ando (1997) are widely referenced in the oxy-fuel literature. Their paper is one of very few that documents a correction made to the NO_X measurement to account for CO_2 interference in a chemiluminescent analyzer (Zabielski et al., 1984). They studied three mechanisms of NO_X reduction in oxy-fuel combustion relative to air and used analytical methods to separate the effects of the mechanisms and quantify the significance of each pathway. The three mechanisms were:

- NO_X reduction by char enhanced by high CO concentrations which themselves come from high CO_2 concentrations. Less than 10% of oxy-fuel

NO_X reduction was attributed to this mechanism. The relative insignificance of it was concluded to be due to low particle density in pulverized coal conditions (particle spacing > 40 diameters).

- Interactions between recycled NO_X and nitrogen released from the fuel. 10-50% of the NO_X reduction effect of oxy-fuel was attributed to this mechanism.
- Reduction of recycled NO_X was determined to be the dominant effect responsible for 50-80% of NO_X reduction relative to air-firing.

While the conclusion that reduction of recycled NO_X is dominant is probably sound, certain aspects of the experiment differed from practical burners and it is possible that mechanisms that may have been unimportant in their work may still be important in oxy-fuel generally. Specifically, these points should be considered:

- Coal volatiles were simulated with CH_4 and NH_3 despite, as noted by the authors, coal volatiles consist of many hydrocarbons. Smoot (1993) suggests (not referring to this experiment) that the presence of CH_4 may exaggerate the prompt NO_X and reburning reactions. In addition, NH_3 is probably not the major nitrogen species from coal pyrolysis. HCN was not used for safety reasons.
- The gases used to simulate volatiles combustion were premixed, removing mixing and transient effects of coal pyrolysis that lead to local variation in stoichiometry.
- Char was simulated with anthracite which is expected to have much lower active surface area than an industrial char (Smith et al., 1994).

Kiga et al. (1997) measured flame speeds for coal flames in O_2/N_2, O_2/CO_2, and O_2/Ar mixtures in a microgravity chamber. They observed that the flame speed was lowest for O_2/CO_2 mixtures with the same volume percent O_2, which was consistent with the greatest effect on flame speed being the specific heat of the gas. Similar flame speeds to air were achieved at 40 volume percent O_2 in CO_2. Industrial scale (100 kg/hr coal) combustion tests using recycled flue gas were also performed. They used a non-dispersive infrared analyzer for NO_X to avoid interference of CO_2. The conversion ratio of fuel nitrogen to NO_X in oxy-fuel was not as sensitive to the depth of staging as it was in air. Some of the small change that was observed was explained by recycled NO_X in the staging gas (overfire oxidizer) not being reduced because of a lack of reactants (hydrocarbons) in that region of the furnace. Oxy-fuel sulfur emissions (SO_2) at the stack were reduced by about 50% relative to air for three different coals. Although the sulfur mass balance could not be closed, the oxy-fuel ash did contain higher levels of sulfur.

Hu et al. (2001) studied the reduction of recycled NO and NO_2 in a high-volatile bituminous coal flame under low recycling ratio (high O_2 concentration in the oxidizer). Less recycled NO was reduced when oxygen concentrations were higher which according to their discussion may be due to consumption of CH fragments by the high O_2 concentration leaving less CH fragments for NO reduction. HCN concentration decreased with increases in recycled NO concentration. This is consistent with a pathway where HCN reacts with NO to form N_2, but from the literature they referenced it appeared that the reaction between CH fragments and NO were more important to the reduction of recycled NO than the HCN + NO pathway. No obvious effect of temperature was found, which may be due to competing effects: increased production of NO with temperature vs.

increased volatiles yield with temperature providing more species for reduction of NO. Recycled NO_2 followed similar trends to NO consistently for this bituminous coal, but in a later work (Hu et al., 2003) a semi-anthracite coal exhibited lower reduction efficiency for NO_2 than NO. Most (95% or greater) NO_X emissions from combustion of pulverized coal in air are NO (Zevenhoven and Kilpinen, 2002).

Sangras et al. (2004) report on oxy-fuel performance in a 1.5 MW_{th} plant where 70% reduction in NO_X was achieved relative to air combustion. They note advantages to oxy-fuel such as reduced flue gas flow rates, less sensible heat loss to the stack, and easier capture of CO_2. The lower NO_X emissions were achieved with air infiltration of about 5% of the total boiler gas flow rate indicating that small amounts of N_2 may not affect the NO_X performance greatly.

Farzan et al. (2005), using the same facility as Sangras et al. (2004), used oxygen and recycled flue gas flow rates to achieve combustion conditions suitable for existing boiler technology. With overall combustion characteristics comparable to air firing, the NO_X emissions were reduced almost 65%. The burner was a scaled-down B&W DRB-4Z low-NO_X burner modified for oxy-fuel combustion. Flame temperatures were prevented from exceeding conventional boiler flame temperatures by more than 60 K to prevent thermal NO_X. It is noted that there is less thermal NO_X because there is less N_2 available, but N_2 was entering the boiler with the oxygen (purity < 100%) and air ingress. The boiler parameters (including burner SR) were optimized for NO_X reduction while maintaining heat transfer similar to the air-fired baseline case. Recycled flue gas ranged from 80-90% of total flue gas. They observed that NO_X emissions decreased with recycled flue gas flow rate, but this was only a slight effect. This trend is opposite to that

reported by Hu et al. (2001) from experiments at much lower recycling ratio. These two results indicate that there may be an optimum level of recycling (or oxygen concentration) for minimum NO_X.

Flame temperatures measured by Farzan et al. (2005) using two-color pyrometry were 1572 and 1633 K for air and oxy-fuel at burner SR's of 0.86 and 1.05 respectively. Flame spectral emittance measurements were also made and the air and oxy-fuel cases were similar with the exception of small regions of the spectrum corresponding to emission from CO_2. The results indicate that the radiation heat transfer from the flame was dominated by soot, coal, and ash particles and the increased CO_2 (and H_2O) concentrations were relatively unimportant.

In furnace areas other than the flame, CO_2 and H_2O may become more important radiators as ash emittance decreases with increased carbon conversion (Nozaki et al., 1997). There is some difference in gas emittance between wet and dry recycled oxy-fuel flue gas, and air-fired flue gas (Khare et al., 2005).

Buhre et al. (2005) review oxy-fuel combustion technology. Oxygen purity of 95-99.5% purity has been used in full-scale testing. Lower oxygen purity requires less energy for the air separation unit, but low levels of N_2 are potentially undesirable. They quote combined modeling and experimental work performed at CANMET in Canada where small amounts of N_2 (3%) significantly decreased the difference in NO_X between air and oxy-fuel combustion. This conclusion may be burner-specific as others (Andersson et al., 2007) have observed only modest increases in NO with air ingress of 4% of feed gas flow.

Khare et al. (2005) reviewed the oxygen levels used by various groups. They note that some of the O_2 required for combustion will come from the recycle stream. The choice between wet and dry recycle streams affects the required oxygen concentration as the heat capacity of the flue gas changes significantly with water content. Flame temperatures depend on mixing rates and other factors beyond oxygen concentration. For the furnace designs they considered, required oxygen concentrations through the burner were estimated to range from 25 to 38% by volume.

Shaddix (2007) explains that due to the competing effects of increased oxygen concentration, and lower diffusion coefficients in CO_2 relative to air, O_2 and CO_2 effects on ignition and devolatilization approximately cancel each other out for 30 vol. % O_2 in CO_2.

Tan and Croiset (2005) note that even though unrecycled flue gas is ideally destined for CO_2 sequestration; NO_X in this stream will probably be released to the atmosphere when the CO_2 is compressed, dehydrated and cooled. It is also possible that a plant may need to temporarily increase power to the grid by shutting down the CO_2 capture train and venting all unrecycled flue gas through the stack. These possibilities underscore the importance of designing the combustion system for low NO_X. They point out that lower NO_X is not automatic or inherent in oxy-fuel combustion and that low-NO_X burner designs should be used. In contrast, Allam et al. (2005) and Sarofim (2007) refer to a process proposed by Air Products and Chemicals, Inc. where high NO_X levels might be beneficial. Increased concentrations of trace species in oxy-fuel (including SO_X, HCl, and mercury) will increase the acid dew point temperature. SO_X and NO_X would be condensed in the CO_2 purification unit as sulfuric and nitric acids and the nitric acid will

react with the mercury to allow its removal with the acids. Regardless of the choice of CO_2 processing method, understanding of the NO_X chemistry is important to produce the desired level of NO_X.

In the experiments of Tan and Croiset (2005) the conversion ratio of SO_2 to SO_3 did not change from air to oxy-fuel combustion, but the accumulation of recycled SO_2 did result in increased SO_3 concentrations. They suspected that higher SO_3 concentrations would threaten boiler integrity and therefore most boiler systems (particularly those that fire high-sulfur coal) would have the flue gas recycled from a point downstream of SO_2 removal.

Scheffknecht et al. (2007) performed unstaged oxy-fuel combustion experiments and report that fuel NO_X emissions increased with O_2 partial pressure. For oxidizer-staged experiments, trends in NO_X with burner SR were the same for air and oxy-fuel combustion. They also achieved effectively 100% reduction of recycled NO_X with a staged combustion test. They measured higher CO near the burner in oxy-fuel relative to air and attributed this to enhanced water-shift and CO_2-shift reactions. Peak measured in-flame CO in air was about 15 vol. % and oxy-fuel about 18 vol. %.

Dhungel et al. (2007) determined that the pathways of NO reduction in oxy-fuel in their experiment were similar to those in air combustion. They present a pathway for NO_X where recycled NO_X is reduced to HCN by reaction with hydrocarbon radicals. It was observed that reduction of recycled NO_X was lower when some of it went through an overfire air port. If the furnace is deeply staged this becomes more of an issue and may be one reason why the optimum burner stoichiometry was higher in oxy-fuel than air in the work reported by Farzan et al. (2005).

Andersson et al. (2007) performed oxy-fuel experiments with associated modeling. Their model made use of the gas-phase fuel-N model of De Soete (1975) and one NO destruction reaction:

$$NO + CO \longleftrightarrow \tfrac{1}{2} N_2 + CO_2 \qquad \text{[Reaction 6]}$$

The nitrogen-containing reactions were modeled with kinetic rate expressions while most other species were assumed to be in chemical equilibrium. CO and O_2 were controlled to agree with experimentally measured values because of their importance to the nitrogen containing reactions.

The model parameters were tuned to match one air and one oxy-fuel case, and thereafter the model correctly predicted a minimum in NO concentration at a point inside the flame for a different oxy-fuel case with higher oxygen concentrations and temperatures. This minimum in the NO profile did not exist in the air and oxy-fuel cases used for model tuning. At the location of the minimum in NO the reported in-flame CO data exhibit dramatic differences in CO (by 7 vol. %) between the two oxy-fuel flames that differ in temperature by only 58 K (1476 and 1534 K) at the point of interest. CO_2 dissociation to form CO becomes significant at about 1500 K which is consistent with the measurements, but another factor is that O_2 was lower when CO was higher and vice versa. Thermal dissociation of CO_2 may therefore not be the only factor in the high CO values. Since CO in the model was controlled to fit measured values it is not clear to what extent CO trends could be predicted, but CO would be critical to predict if Reaction 6 is to be used. It was concluded that the reduction of NO_X in oxy-fuel is due to increased destruction of NO_X, both recycled and otherwise. Stoichiometry was varied and oxy-fuel

was found to be fairly insensitive to stoichiometry in terms of NO_X emissions. As mentioned above, simulated air ingress had only a small effect on NO_X formation.

In the discussion by Skreiberg et al. (2004) Reaction 6 is not believed to be important as an elementary reaction. The more recently published large mechanisms have used lower rates for reaction of NO with CO to form N atoms and so Reaction 6 should be considered a global reaction. In addition, Skreiberg et al. (2004) state that they do not expect that CO under reducing conditions causes a significant reduction in NO below 1400 K.

Hjärtstam et al. (2007) reporting on the same experiments as Andersson et al. (2007) note that stack CO emissions were comparable between air and oxy-fuel cases even when very high levels of CO existed in the oxy-fuel flames. They also report improved attachment of the flame with increasing oxygen concentration in the oxy-fuel cases. Oxygen concentration in the flames was lower when the flame was better attached which is presumably a combined effect of less entrainment of oxygen from the secondary stream and more rapid consumption of the primary oxygen by the fuel.

2.6 Modeling of NO_X in Coal Combustion

Smoot (1993) reviews the relevant literature and discusses combustion modeling, in particular the modeling of NO_X. The reactions of importance change with stoichiometry making it difficult to derive a simple or global model that functions under all combustion conditions. Global modeling is however more efficient computationally and the premise for such an approach is that key intermediates exist through which formation or destruction of NO passes. Experience has shown that HCN, CN, and NH_i

are intermediate nitrogen species derived from fuel nitrogen that may be oxidized to NO or reduced to N_2 through competing pathways. Several global rate models have been correlated to HCN or NH_3. Other important findings reviewed include the existence of OH in super-equilibrium concentrations and that homogeneous rather than heterogeneous reactions control the destruction of NO. A particular global model verified under a variety of conditions was presented. It contains the three thermal NO_X reactions given earlier (Reaction 1 through Reaction 3) and five reactions for fuel NO. Four of these expressions account for oxidation and reduction of the nitrogen intermediates (HCN and NH_3) to NO and N_2, and a fifth reaction models conversion of HCN to NH_3. Some discrepancies between experiments and predictions were noted and attributed to the absence of prompt NO_X and reburning reactions in the model. The agreement observed was used to demonstrate that global or simplified mechanisms may be adequate for NO_X predictions.

Bowman (1997) discusses modeling of gas-phase destruction of NO using reburning and advanced reburning. Sensitivity analysis suggests that radical producing and consuming reactions are important, even dominant, in determining NO destruction rates. Discrepancies between model predictions and experimental results are attributed to reactions that produce radicals missing from the model. The promotion of NO destruction by small amounts of CO in the combustion products as demonstrated by experimental data is noted. Furthermore, modeling studies are discussed that show this is a result of the moist CO oxidation mechanism which produces radicals to sustain the NO reduction process. Specific reactions to which NO formation is most sensitive are chain-branching reactions that produce OH in agreement with the conclusions of Chen et al. (1991).

Hill and Smoot (2000) emphasize that the goal of mathematical models is prediction of trends and that for emissions species, quantitative a priori predictions have generally not been considered possible in the past. Thermal and fuel NO_X reactions are slow relative to fuel oxidation which necessitates kinetic rate expressions in modeling. These are computationally expensive in computational fluid dynamics (CFD) models, but since nitrogen species are typically low in concentration their effect on the flame structure is negligible. This justifies the common approach of decoupling the computation of fluid flow and major species from the nitrogen model which is executed later. Even with this simplification the complex chemistry of the prompt NO_X mechanism is often too computationally expensive to include. Commonly fuel NO_X is modeled by global reactions that consider only competitive oxidation and reduction of an intermediate nitrogen species. This requires a model for the form of nitrogen release (usually as HCN, NH_3, or a combination) and the associated rate of release. After release the intermediate may be oxidized to NO or reduced to N_2 depending on local conditions.

Various global reaction rates have been proposed in the literature. As an example, reactions proposed by De Soete (1975) as given by Hill and Smoot (2000) appear in Table 1. An approach such as that described has been applied to oxy-fuel combustion with *"reasonably accurate engineering predictions"* for NO by Chui et al. (2003) using the scheme of Chui and Hughes (1996).

Table 1. Example of competing oxidation and reduction reactions for a fuel NO_X model (De Soete, 1975 as given by Hill and Smoot, 2000).

Reaction $k = A\exp\left(-E/RT\right)$	A	E (J/g mol)
For HCN as the intermediate:		
$HCN + O_2 \xrightarrow{k} NO + \ldots$	1×10^{10}	280300
$HCN + NO \xrightarrow{k} N_2 + \ldots$	3×10^{12}	251000
For NH_3 as the intermediate:		
$NH_3 + O_2 \xrightarrow{k} NO + \ldots$	4×10^{6}	133900
$NH_3 + NO \xrightarrow{k} N_2 + \ldots$	1.8×10^{8}	113000

One of the most fundamentally-based devolatilization models is the Chemical Percolation Devolatilization (CPD) model (Grant et al., 1989; Fletcher et al., 1992). The CPD model describes devolatilization of rapidly heated coal using percolation lattice statistics to simulate the coal structure. Initial coal lattice characteristics are taken from chemical structural parameters measured with ^{13}C NMR (Nuclear Magnetic Resonance) spectroscopy. One empirical parameter is included that represents the population of char bridges in the parent coal. The devolatilization process depends strongly on the temperature history of the fuel particle as there are competing reactions in the lattice: bridges may be broken to form tar (detachable lattice fragments) and bridges may form through cross linking that can reincorporate fragments back into the char matrix. A strong point of the CPD model is that the kinetic rate parameters are based on data where particle size, temperature, and velocity were directly measured by optical methods (Fletcher, 1989) rather than calculated as in many other models. It is noted that major mass loss occurs during particle heating which explains the sensitivity of devolatilization

to the temperature history of the particle. Particle temperature histories are in turn very sensitive to local gas temperature and particle diameter, heat capacity, and apparent density. Apparent density as used in the model is calculated from total volume and mass of a settled coal sample and includes voids between particles.

The CPD model has been extended more recently by Genetti (1999) and Perry (1999) to include predictions of nitrogen and light gas release, and nitrogen retained in the char. This version of the model is designated CPD-NLG. Genetti also developed a correlation to allow estimation of ^{13}C NMR parameters from ultimate and proximate analysis results which extends the use of the CPD model to coals where ^{13}C NMR data are not available. Badzioch and Hawksley (1970) concluded that the most reliable parameter for representing coal type is the carbon content on a dry, ash free basis as determined by ultimate analysis. Genetti's (1999) correlations are non-linear and use multiple factors, but carbon content is important.

Current models of nitrogen release from char are less sophisticated. Molina et al. (2000) states that at pulverized coal combustion conditions it is believed to be adequate to model only the production of NO from char-N as opposed to other intermediates such as HCN. Commonly, modeling of NO formation from char is done with an intermediate (HCN, NH_3, NO, or a combination) with competitive oxidation and reduction pathways as done for the volatiles, or an empirical efficiency factor for Char-N to NO that may take into account both formation and reduction.

2.7 Summary

Although many studies of NO_X formation from coal in air and oxy-fuel combustion have been conducted there remains much to be learned. Current understanding at the conceptual level of how the combustion environment affects NO_X formation is fairly good and has successfully led to strategies to control NO_X emissions. Knowledge of details is however still not sufficient for computational models to be truly predictive.

Information in the literature can guide the choice of assumptions in modeling however experimental results should be interpreted with care as some conclusions may be experiment or burner specific. This work is intended to provide additional insight into the formation of NO_X in oxy-fuel combustion through combined modeling and in-flame experimental data.

3 Methods

3.1 Experimental Methods

3.1.1 Multi-fuel Flow Reactor

Pulverized coal was burned in a down-fired, refractory-lined, laminar flow reactor referred to as the Multi-fuel Flow Reactor (MFR). The MFR, shown schematically in Figure 3, has nominal inside dimensions of 0.12 x 2 m. Various auxiliary systems are also represented in the figure.

Radial sampling ports (10 mm diameter) are distributed over the length of the reactor as indicated in Figure 3. These allow sampling of gases from the reactor centerline and measurement of wall temperatures using sheathed type-K thermocouples. Small metal blocks were clamped onto the thermocouple sheaths to set the insertion distance and ensure that wall thermocouple positioning was repeatable. Cotton balls were used around the thermocouples and gas sample probe to reduce leaks. The reactor was operated at slight positive pressure so that any leakage would not introduce unmetered air to the combustion process.

The bottom section of the MFR includes a larger sampling port for insertion of a water-cooled fly-ash sampling probe. A few char samples were collected using this probe.

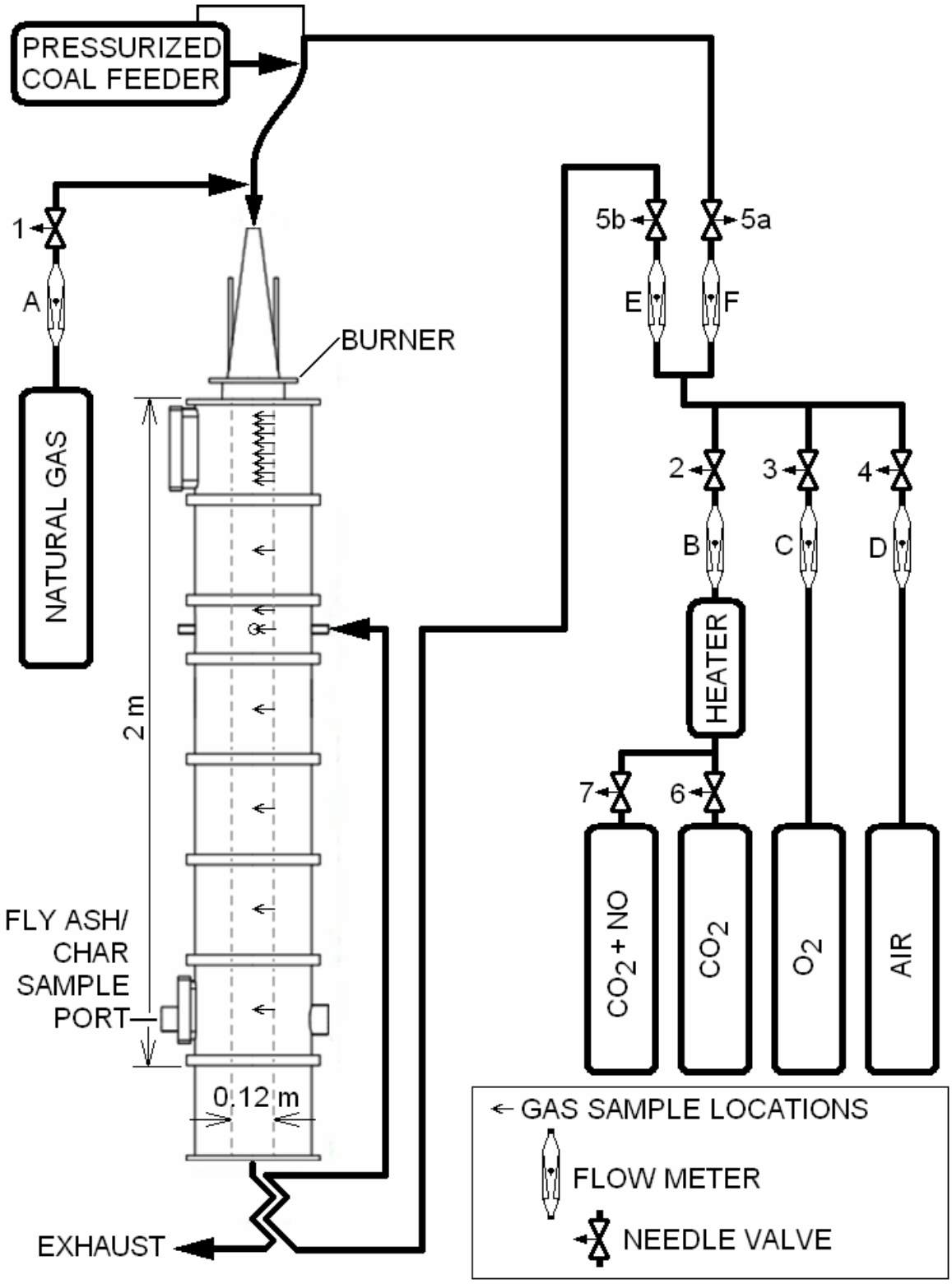

Figure 3. Schematic Diagram of the MFR.

The alumina-silica refractory lining in each reactor section is supported on the outside by a steel cylinder of 350 mm diameter. The steel walls are about 5 mm thick and insulated on the outside with fiber clay to prevent burns from accidental contact. Bolted flanges connect each section to the one above and below. Previous to this work the top three sections were constructed using Kast-O-Lite 30 castable insulation (A.P. Green, Pittsburgh, PA) and the remaining sections with Purolite 30 (National Refractories, Mexico, MO). The two materials are similar in composition and the manufacturers' data sheets give properties over different temperature ranges, which show good agreement where the temperature ranges overlap. A combined table of properties suitable for use in a model is given in Table 2.

Table 2. Thermal conductivity values for the cast refractory.

Temperature (K)	Thermal Conductivity (W/mK)
478	0.52
923	0.55
1143	0.59
1366	0.69
1644	1.12

A quartz window in the top section allowed visual observation of the near-burner region. The opening to the combustion space is about 25 mm wide and extends in the axial direction from the burner face to 200 mm downstream. A slow recirculation flow with some soot and few, if any, entrained particles can be observed in the window cavity during combustion tests. With the exception of this eddy, all flows observed through the window were downward and laminar. The Reynolds number based on reactor diameter

for one of the air-fired experiments was 560, well below the range of values where transition to turbulence occurs.

A number of different reactant flow rates were used for various tests. These are detailed in tables in Section 3.1.12: Experiment Conditions. Some fluctuation did exist in the flow rates. Example flow rate data for the coal and gases are shown in Figure 4 through Figure 9 to demonstrate that these fluctuations were a small percentage of the average flow rates. Average flow rates were steady over time and thus the experiments were considered steady state. To minimize the impact of flow rate fluctuations on the results, gas species and temperature data were averaged over time and only used for analysis when steady.

The coal feed exhibited the highest fluctuation in flow rate of the reactants. Simultaneous coal flow rate and $NO_{(X)}$ concentration data in Figure 5 demonstrate that the percentage fluctuations in gas species measurements are lower than that for the coal feed rate and not sufficiently large to be of concern. The insensitivity of the gas analysis to random variations in the reactant flow rates is partly due to the finite volume of the gas analysis chambers in the analyzers. Even though the gas in the sample line entering the chambers may be changing composition rapidly, the mixing of the sample with gas already in the chamber causes the composition as analyzed to be more stable or representative of the temporal average.

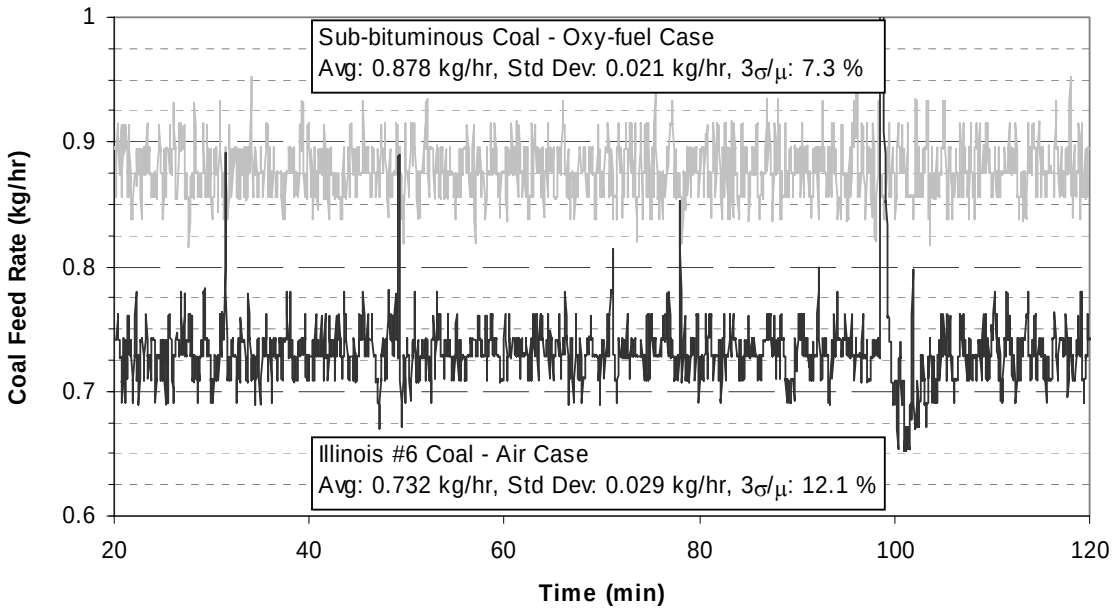

Figure 4. Sample coal feed rate data.

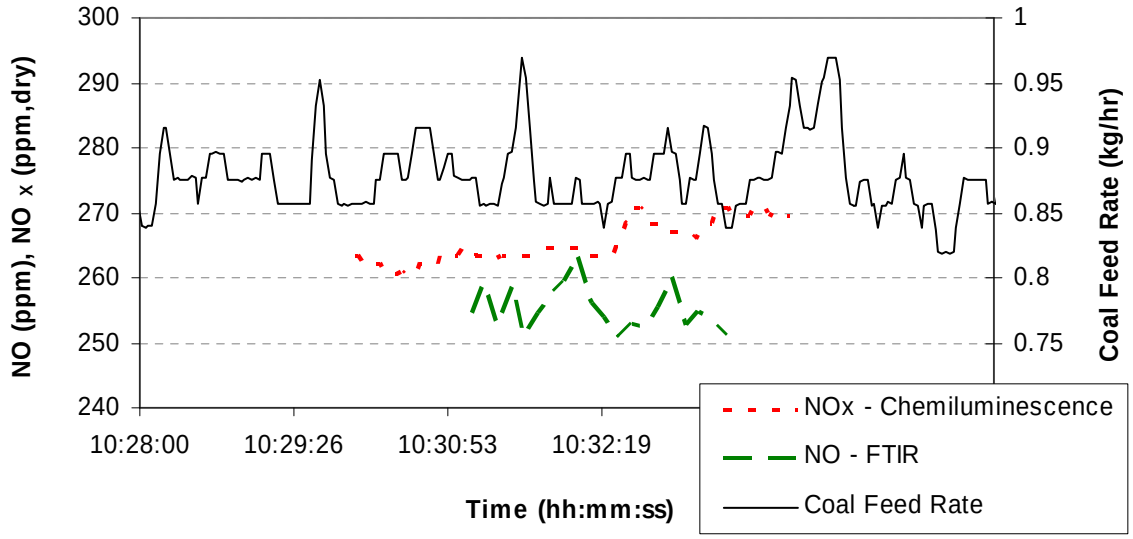

Figure 5. Sample coal feed rate and gas species data taken at the same time to show typical unsteadiness in the gas species measurements that may be partially due to coal feed rate fluctuations.

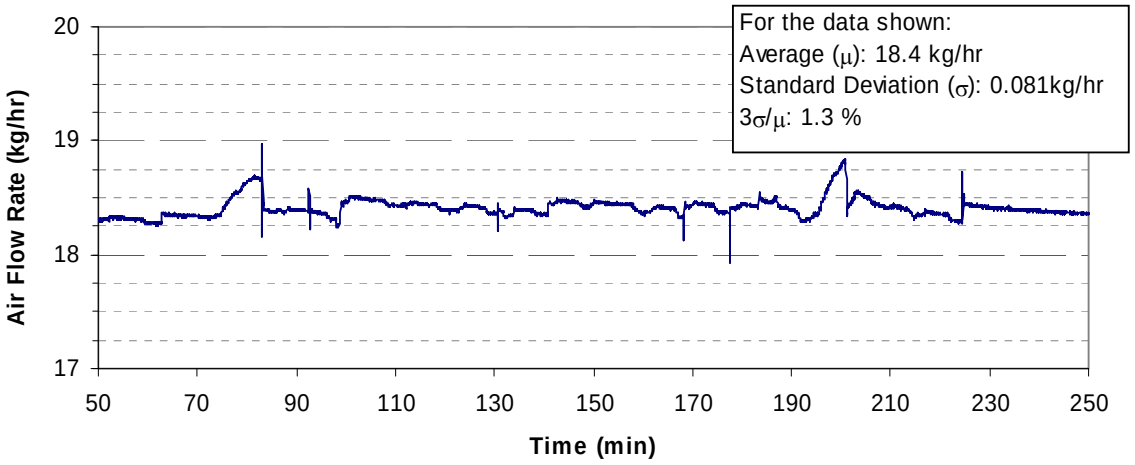

Figure 6. Sample air flow rate data.

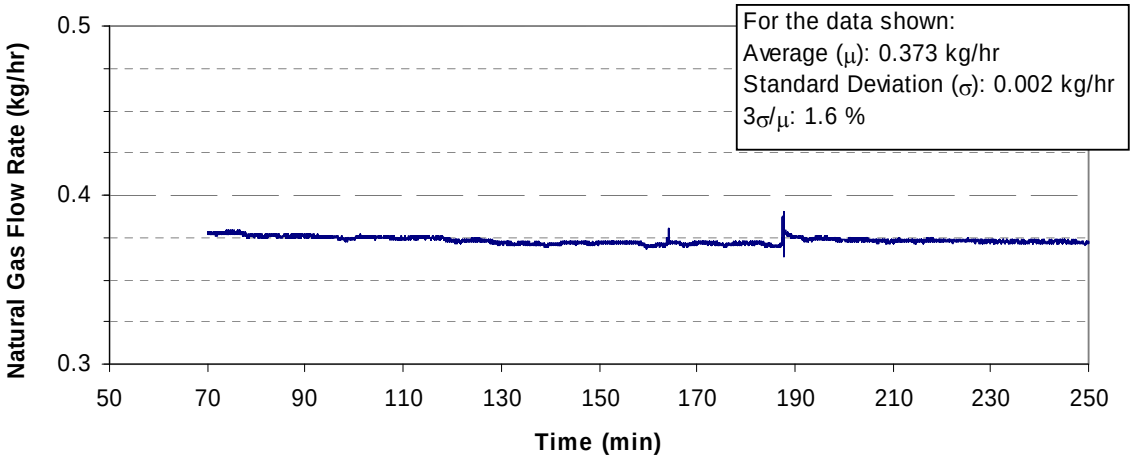

Figure 7. Sample natural gas flow rate data.

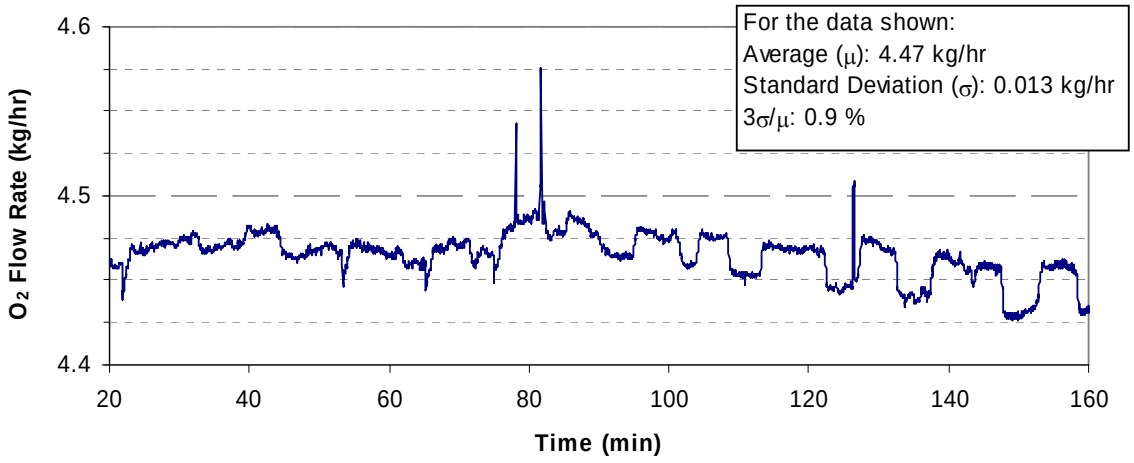

Figure 8. Sample O_2 flow rate data.

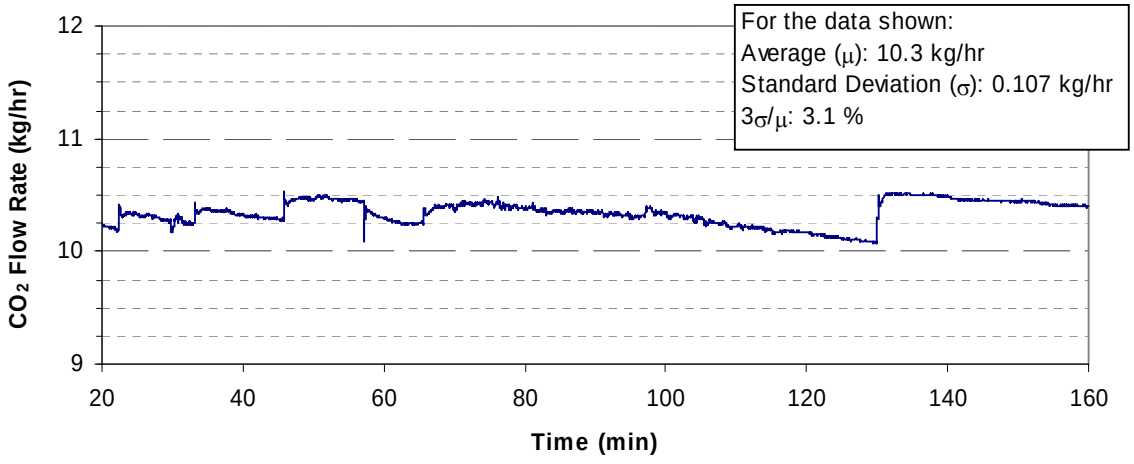

Figure 9. Sample CO_2 flow rate data.

3.1.2 Gaseous Reactants

In the experiments, flue gas was not recycled; rather, bottled CO_2 (≥99% purity) was used to simulate dry flue gas. O_2 (≥99.5% purity) was also supplied from compressed gas bottles. Air was supplied from a compressor. For the O_2, and CO_2, three and five size 200 bottles respectively were connected to a manifold to provide sufficient gas for several hours of operation. An electric immersion heater was used to return the CO_2 cooled by evaporation and expansion to room temperature. All gaseous reactant flows were regulated to 100-200 psig then metered with calibrated choked-flow orifice meters prior to mixing. An electronic data acquisition system processed temperature and pressure measurements from upstream of the orifices to calculate flow rates. Absolute pressure as measured by an on-campus weather station was included in the flow measurement calculations. At the elevation of the university the pressure was typically about 85 kPa. Control of the flow rates was by manual operation of valves.

Oxidizers were mixed separately from fuels and split into primary and burnout oxidizer streams. Two rotameters operating at the same temperature and pressure were used to measure the relative flow rates of primary and burnout oxidizer as controlled by valves 5a and 5b in Figure 3. Calibrated orifices were impractical for this splitting for a couple of reasons: first, one orifice was already positioned upstream and the pressure was too low to produce sonic conditions in an additional orifice; and second, the oxidizer composition would change for different tests which would alter the sonic velocity and make the data processing cumbersome.

The primary stream was mixed with fuels prior to entering the burner and the burnout stream was preheated using waste heat from the exhaust system prior to injection

through four radial ports (about 10 mm in diameter) located 0.67 m from the burner in the axial direction.

Oxy-fuel oxidizers used in this work are referred to as O25, and O30. These are nominally 25 and 30% O_2 by mass (32 and 37% O_2 by volume) with the remainder being CO_2. An O35 oxidizer was used in some early testing but for later tests at lower burner flow rates the higher oxygen concentration produced an excessive flame speed causing the flame to propagate (flashback) upstream above the water cooled plate into the cone above the burner. Lower oxygen concentrations were not used due to problems with flame stability. One oxy-fuel test was conducted using a certified standard mixture of 525 ppm NO in CO_2 to simulate the recycling of NO with the flue gas. Further tests of this type were not conducted due to the high cost of the mixture. The absence of recycled NO in the experiments does allow other mechanisms of NO destruction to be isolated, which for this work is an advantage.

3.1.3 Premixed Burner and Fuel Feeding

Fuel (pulverized coal and natural gas) and primary oxidizer enter the reactor premixed through a water-cooled burner. The steel burner plate is 99 mm in diameter and has 93 holes 5.8 mm in diameter laid out as shown in Figure 10. The plate is 10 mm thick and each hole is cylindrical. Water cooling passages are located between the rows of holes in the plate.

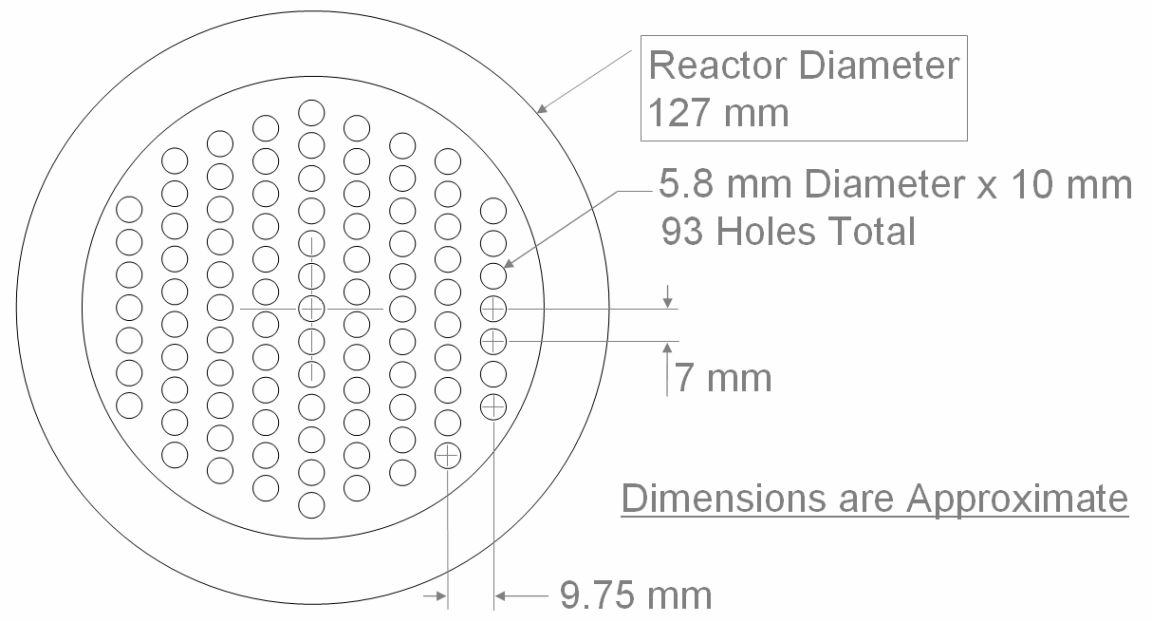

Figure 10. Layout of the holes in the burner face.

Pulverized coal was fed by a single auger Acrison Gravimetric Feeder (Model 406-BDFM) with an Acrison MD-II Series 400 weigh feeder controller. The coal hopper was sealed at the top with a latex gasket and 25 mm thick Plexiglas lid so that the hopper could be pressurized to the pressure of the primary oxidizer line. This was done to prevent air entering the system which would result in uncertain stoichiometry and unwanted nitrogen in the oxy-fuel cases. The packing in the seals where the auger and hopper agitator shafts entered the hopper was adjusted to stop leaks from that location.

The outlet of the pipe surrounding the auger had four fine wires across it as shown in Figure 11 to minimize fluctuations in coal feed rate due to caking of the coal at the end of the pipe.

Figure 11. Outlet of the coal feeder auger pipe showing four fine wires crossing the opening.

Primary oxidizer and coal was mixed in a custom-fabricated vertical mixing chamber (Figure 12) designed to entrain the coal without allowing it to collect in the chamber as had occurred with earlier horizontal designs. A pressure tap from the mixer to the lid of the hopper ensured that no pressure gradient would exist in the auger pipe. Previous experience showed that clumps of coal released from the auger could create a pressure pulse in the reactor as they burned. The pulse would propagate back to the feeder temporarily slowing coal flow through the auger followed by another release of extra coal. This pulsing could produce resonant frequencies that caused uncontrollable flow rates. Equalizing the pressure in the feed line with the hopper seemed to be a key to reducing this pulsing.

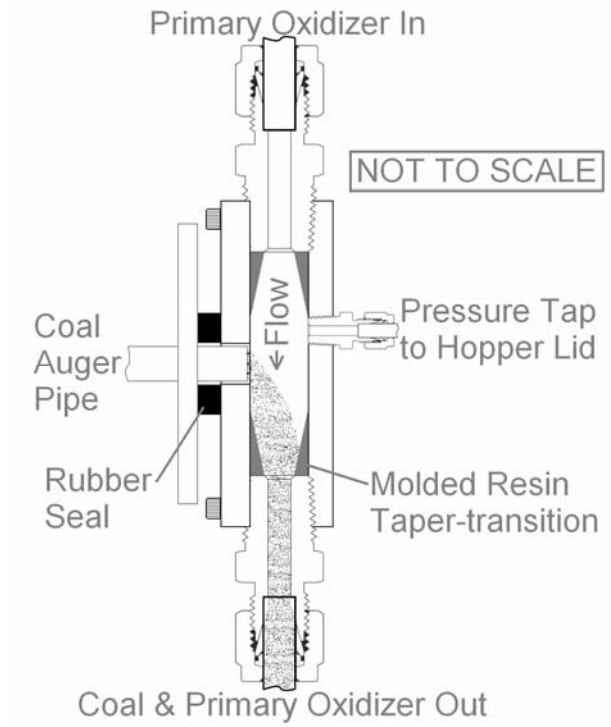

Figure 12. Sketch of the coal-primary oxidizer mixer.

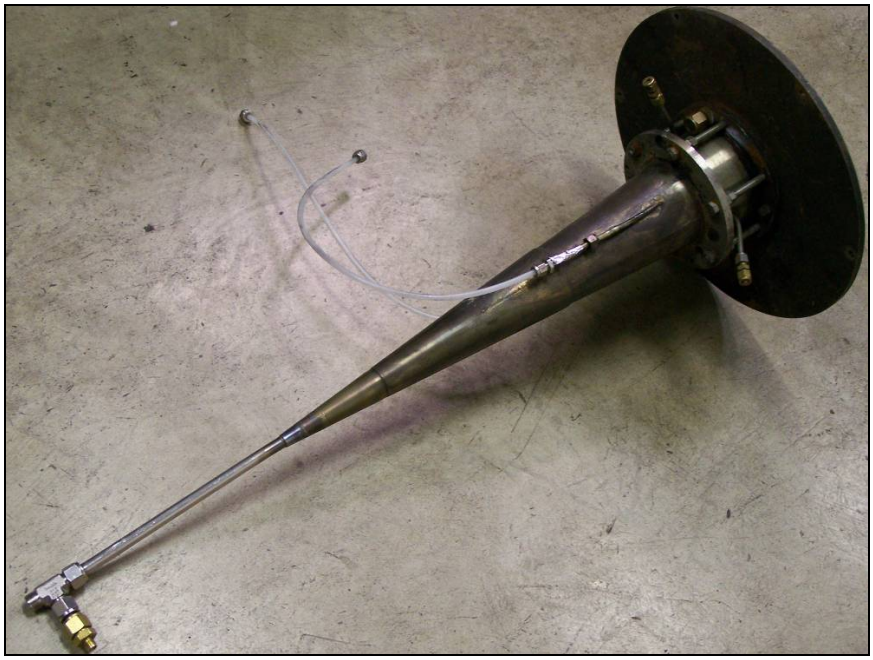

Figure 13. The cone and burner exterior. Coal and primary oxidizer enter through the stainless steel connection at the bottom left of the photograph. Natural gas enters through the brass fitting to the lower right of the stainless steel connection. The white plastic tubing is for water cooling of the burner face. All other fittings are no longer in use.

Natural gas was mixed with the coal-primary oxidizer mixture with a T-connector prior to entering a cone shaped diffuser that connected to the burner (Figure 13). Nominal flow rates for the coal and natural gas were set to about 6 kW_{th} for each fuel for a total of almost 12 kW_{th} (based on higher heating value).

3.1.4 Fuel Properties

Three coals were used in this work: Illinois #6, Pittsburgh #8, and a sub-bituminous coal believed to originate from Wyoming's Powder River Basin. All coals were pulverized and samples sent for analysis by an independent laboratory. Selected coal properties are shown in Table 3. The full lab reports are included in Appendix C. Particle size distributions determined using US Standard sieves are shown in Figure 14.

Table 3. Selected properties of the coals.

	Sub-bituminous	Illinois #6	Pittsburgh #8
Proximate Analysis	**DAF wt%**	**DAF wt%**	**DAF wt%**
Volatile Matter	49.72	44.17	41.96
Fixed Carbon	50.28	55.83	58.04
Ash (wt%, dry)	6.42	9.31	10.67
Higher Heating Value (Btu/lb, DAF)	11981	14226	14785
ASTM Rank	Sub-bituminous A	High-volatile C bituminous	High-volatile A bituminous
Ultimate Analysis	**DAF wt%**	**DAF wt%**	**DAF wt%**
C	70.56	81.88	85.19
H	4.18	4.37	4.87
O	23.63	7.83	4.70
N	1.04	1.27	1.38
S	0.59	4.64	3.86
	100	100	100

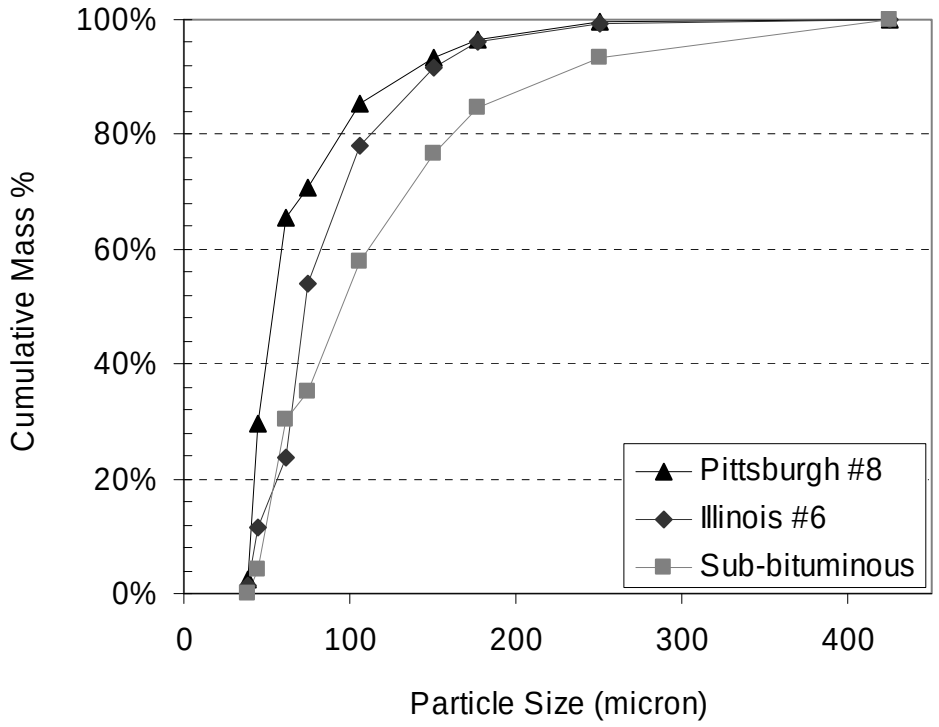

Figure 14. Coal particle size distributions.

Due to continual drying of the coal, moisture analysis was performed just prior to each run to properly calculate stoichiometry based on coal mass flow rate. After most runs an ash sample from the exhaust system was used to determine the level of burnout achieved.

The laboratory natural gas system receives gas from the city natural gas supply. Gas is compressed and stored in tanks connected by a manifold. Although daily gas quality reports are available from the utility, there is uncertainty as to when the gas in the tanks was compressed. Typical gas properties obtained by averaging the gas quality report over the time when most data for this work was taken are listed in Table 4.

Table 4. Approximate composition of the natural gas (Source: Questar Gas Quality Information).

Component	%
N2	0.44
CO2	0.87
C1	92.82
C2	4.07
C3	1.13
IC4	0.22
NC4	0.23
IC5	0.08
NC5	0.05
C6	0.05
C7	0.03
C8	0.01
C9	0
Specific Gravity	0.607
Btu/Cu Ft	1067

3.1.5 Data Acquisition

Prior to data acquisition the reactor would be allowed to heat to a steady state, as determined by wall temperatures. Data was acquired using National Instruments data acquisition hardware and LabVIEW software. Temperatures, reactant flow rates, and gas concentrations were written to a spreadsheet for later analysis. The LabVIEW virtual instrument (vi) was also programmed with a calculator to assist the user in controlling valves 5a and 5b in Figure 3 to set the primary/burnout oxidizer ratio. The user could also enter the rotameter readings for the primary and burnout oxidizer, location of the gas sampling probe, and other parameters so that these were included in the spreadsheet with the measurements. The spreadsheets would later be processed to extract only those gas species measurements that were at steady state.

3.1.6 Exhaust System

Pressure in the reactor was controlled using a variable speed induced draft exhaust fan mounted on the roof of the building. A pressure tap in the reactor wall located 1.2 m from the burner was used to monitor the reactor pressure. Typically experiments were run at positive gage pressure of about 12 Pa to prevent air ingress. When probes were removed, soot and char were observed flowing out of the access ports which confirmed that air ingress was unlikely. The exhaust duct operated at negative gage pressure to prevent leaks of combustion products into the room.

The burnout oxidizer was run through stainless steel tubing in an insulated section of the exhaust system to heat it and improve burnout. Heated oxidizer lines were insulated and oxidizer temperature was measured just upstream of the line splitting to the four radial injection ports. Burnout oxidizer temperatures of almost 300°C could be achieved, depending on the gas flow rates, but could not be independently controlled.

At two locations downstream of the burnout oxidizer heat exchanger the exhaust duct increased in diameter with an annular opening. This opening allowed for room air to enter the exhaust for cooling by dilution. Both locations were at negative gage pressure and no exhaust air leaked into the room. The first opening also served to allow the burnout oxidizer lines to be connected to the heat exchanger. After dilution the flue gases passed through a filter to remove fly ash prior to exiting the building through the roof-mounted fan.

3.1.7 Gas Sampling System

It was discovered in early testing that the gas sample probe previously used with the MFR for NO_X measurements in air-fired, oxidizing conditions could not obtain a

steady NO_X measurement under fuel-rich oxy-fuel conditions. Sample data appear in Figure 15. In addition to this problem the probe showed a tendency to clog with char particles. This probe was essentially a stainless steel tube of about 5 mm inside diameter.

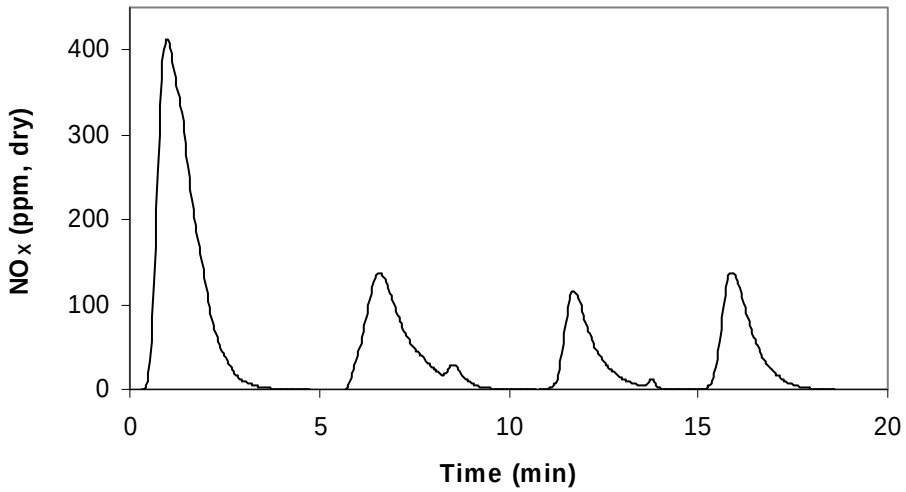

Figure 15. Sample NO_X data obtained by inserting the original gas sample probe four times into the reactor 0.12 m from the burner. After each time the measurement fell to zero the probe was removed, cleared of char using compressed air, and reinserted. Illinois #6 coal, oxidizer: 30% O_2 (by mass), SR = 0.76.

Steady NO_X measurements were obtained if the probe was kept out of the gas stream and sampled gases from near the wall. As a result of this observation it was concluded that the high temperature of the probe when it was placed in the gas stream was sufficient to allow reactions between the gases and the char moving through the probe, and NO reduction by char was probably occurring (Guo, 1997).

A new, air-cooled probe was designed (Figure 16) and steady and repeatable NO_X measurements were obtained as demonstrated by the data in Figure 17. The new probe showed much less tendency to clog with char despite having a smaller inside diameter

than the older probe. The level of cooling with this probe was adjusted by the cooling air flow rate which was maintained at the highest level that would prevent condensation in the sample line. This ensured that reactions would be quenched as quickly as possible inside the probe and that liquid water would not form, dissolving NH_3 before it could be measured.

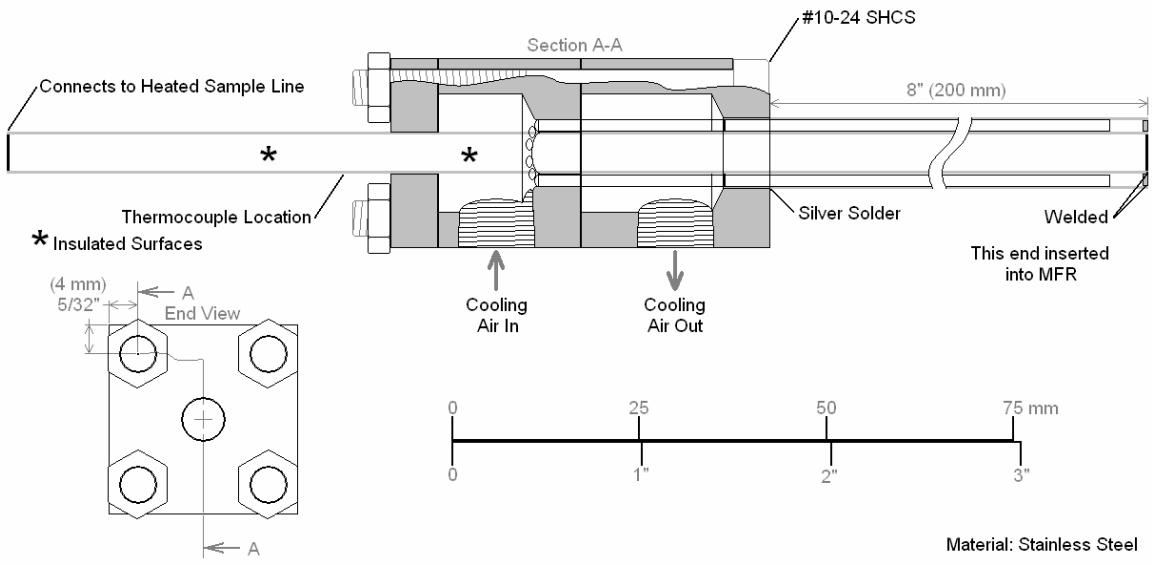

Figure 16. Diagram of the air-cooled gas sample probe. Cooling air flows along the probe length through the small tubes and back between the same tubes.

From the air-cooled probe, gases passed through filter paper to remove particulate, and thence into a Teflon sample line heated to 180°C. This temperature was selected to minimize adsorption of NH_3 onto metal components in the sample line (Damstedt, 2007). The sample flowed through a heated diaphragm pump into an FTIR gas analyzer (MKS MultiGas 2030) with a 5.11 m path length gas cell. Sample lines internal to the analyzer cooled the sample from 180°C to 150°C – the operating temperature of the gas cell. The FTIR analyzer was used for the measurement of CH_4,

C_2H_4, NO, NO_2, N_2O, CO, CO_2, H_2O, SO_2, HCN, and NH_3. These gases were measured on a wet basis with no limits on the measurable concentrations. Calibrations for these gases were supplied by MKS and selection of wave numbers for analysis was checked and adjusted where necessary to avoid interference between gases known to exist in the sample gas. Attempts were made to measure SO_3, but the signal-to-noise ratio was too low for any useful results to be obtained.

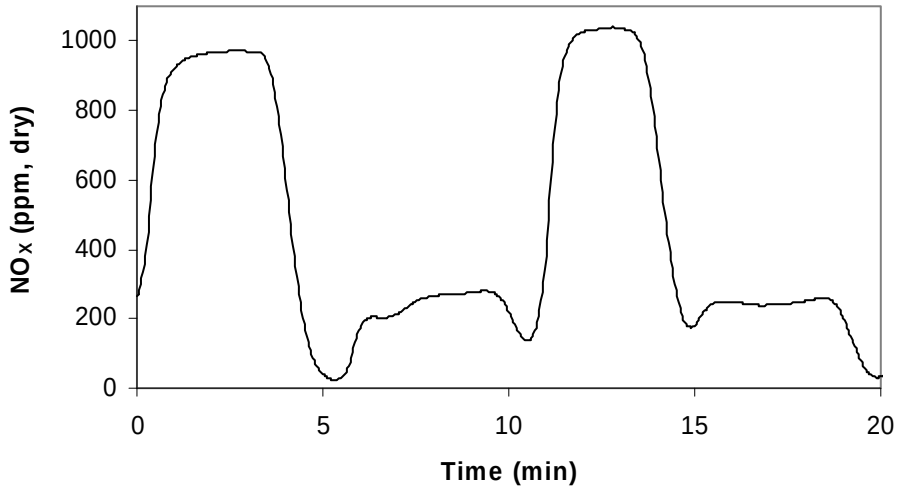

Figure 17. Example of NO_X measurements made in oxy-fuel conditions with the air-cooled sample probe at the reactor centerline. The first and third features correspond to fuel-rich conditions 0.4 m from the burner and demonstrate steady state and repeatable measurements. The other two peaks are from downstream of the burnout oxidizer injection in fuel lean conditions where steady measurements were also obtained. Compare Figure 15.

Downstream of the FTIR gas analyzer the sample lines were not heated. The sample passed through a chamber of desiccant (anhydrous calcium sulfate) followed by a rotameter with a valve for flow rate control and into an HORIBA PG-250 portable gas analyzer that measured O_2, NO_X (total of NO and NO_2), CO (up to 5000 ppm), and CO_2 (up to 20 vol. %) on a dry basis. The sample was then released into the MFR exhaust

system. The HORIBA instrument had an SO_2 sensor, however it was discovered that the desiccant acted as capacitor for SO_2 and so no usable SO_2 measurements were obtained from this sensor. Because the HORIBA instrument was designed for effluent gas measurements from air combustion and not in-flame measurements in air and oxy-fuel combustion, a number of other issues needed to be investigated.

Two O_2 sensors were tested under oxy-fuel conditions with the HORIBA instrument – a galvanic cell, and a zirconium oxide sensor. Initial calibration with a CO_2-based span gas indicated that the galvanic cell would function without significant interference under oxy-fuel conditions; however after running an oxy-fuel experiment for several hours it was observed that the zero point of the sensor had drifted considerably (on the order of 4 vol. % O_2). This CO_2 interference was investigated by calibrating the sensor with N_2-based calibration gases and then exposing the sensor to CO_2 and 20.9 vol. % O_2 in CO_2 for longer periods of time. Results are shown in Figure 18 and indicate that under high CO_2 conditions the galvanic cell sensor was not reliable.

The zirconium oxide sensor was not observed to drift with time exposed to sample gases, but negative O_2 concentrations were often reported by the analyzer for sample gases from fuel-rich regions of the MFR. Testing of the instrument at higher O_2 concentrations indicated little error as indicated by the test result in Figure 19.

Given these problems neither sensor is suitable for in-flame oxy-fuel measurements, but some qualitative information could still be gained from the data as will be noted as results are presented.

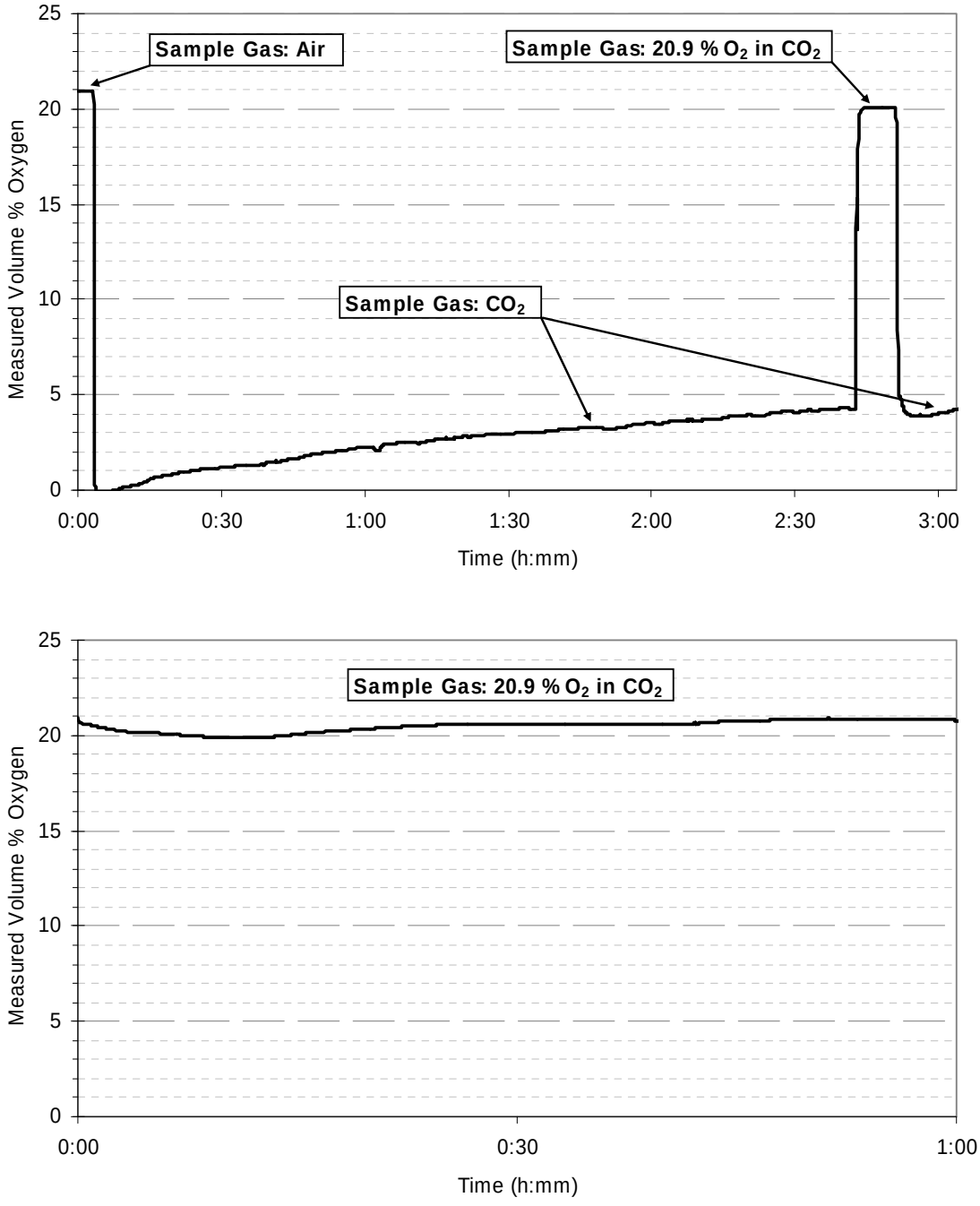

Figure 18. Effects of CO_2 on the galvanic cell O_2 sensor over long periods of time. Top: The zero point of the sensor drifts by more than 4 vol. % O_2 over 3 hours. Bottom: Near the maximum range of the sensor the drift is <1 vol. % O_2.

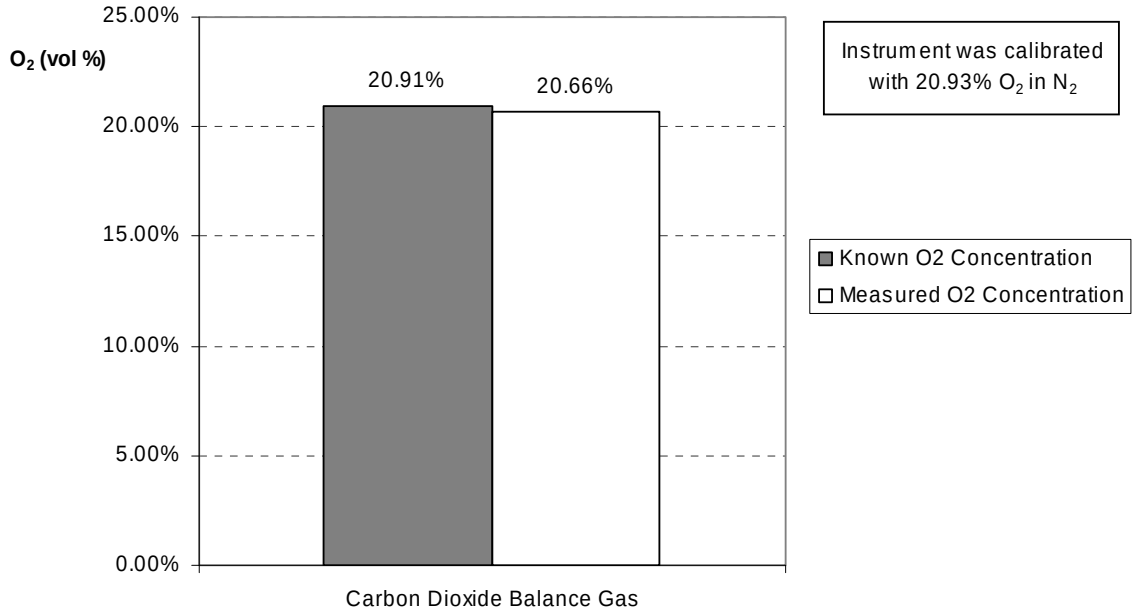

Figure 19. Test of CO_2 interference for the zirconium oxide O_2 sensor using a CO_2-based gas.

The NO detector in the HORIBA instrument is of the chemiluminescent type, which works on the principle that NO can react with O_3 (generated by the analyzer) to form the energized molecule: NO_2* (Reaction 7). NO_2* may then collide with another molecule and give off light as it returns to the normal state (Reaction 8). Measurement of the emitted light provides a signal proportional to the concentration of NO. Unfortunately some molecules such as CO_2 can quench the chemiluminescent reaction (Reaction 9). High levels of CO_2 in a sample gas may result in under-measurements (more than 10% lower) for an instrument calibrated with NO in N_2 (Zabielski et al., 1984).

$$NO + O_3 \xrightarrow{k7} NO_2 * + O_2 \qquad \text{[Reaction 7]}$$

$$NO_2 * + M \xrightarrow{k8} NO_2 + M + h\nu \qquad \text{[Reaction 8]}$$

$$NO_2 * + M \xrightarrow{k9} NO_2 + M \qquad \text{[Reaction 9]}$$

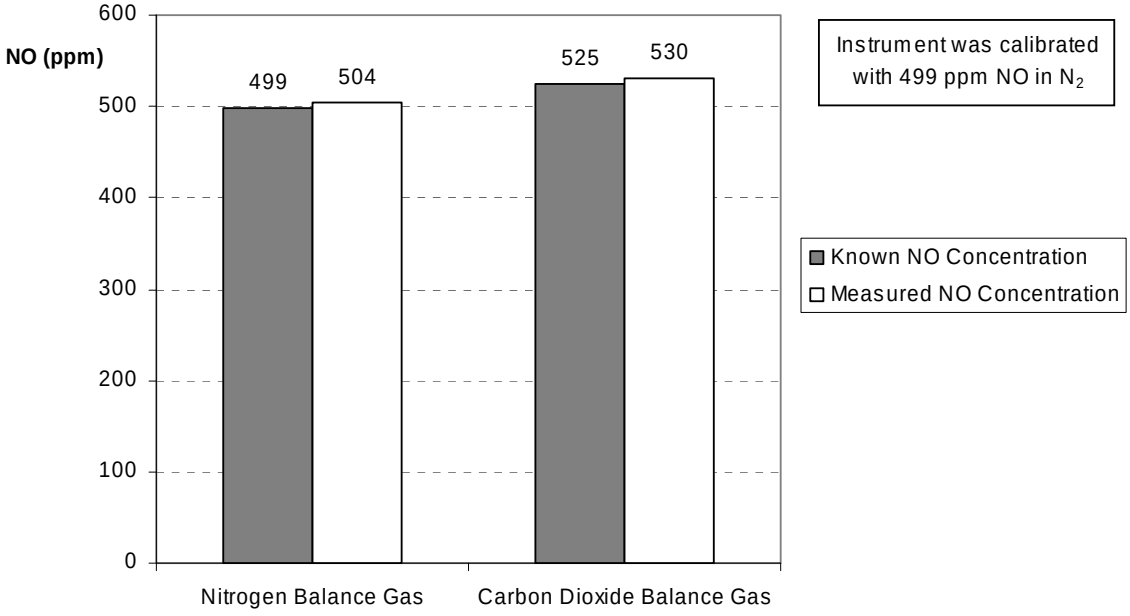

Figure 20. Test of CO_2 interference for the HORIBA NO_X analyzer.

The analyzer was tested using calibration gases based in CO_2 and N_2 to determine the level of CO_2 interference. The interference, if any, was less than the instrument repeatability as seen in Figure 20. Communication from the manufacturer indicated that the sample gas was diluted internal to the analyzer with room air 12:1 specifically to avoid CO_2 interference. The measurement reported for the HORIBA in this work is total NO and NO_2 (collectively NO_X) as the analyzer passes the sample over a catalyst to convert all NO_2 to NO prior to the chemiluminescent analysis. CO_2 and CO are measured by the non-dispersive infrared method (NDIR).

To compare the performance of the two analyzers the simultaneous CO and NO data produced by each was plotted using parity plots shown in Figure 21 through Figure 23. If the analyzers are both accurate the data will lie on a diagonal line from the bottom left to the top right of the plot. For these figures the data from the HORIBA were

converted to a wet basis measurement using the H_2O concentration reported by the FTIR analyzer.

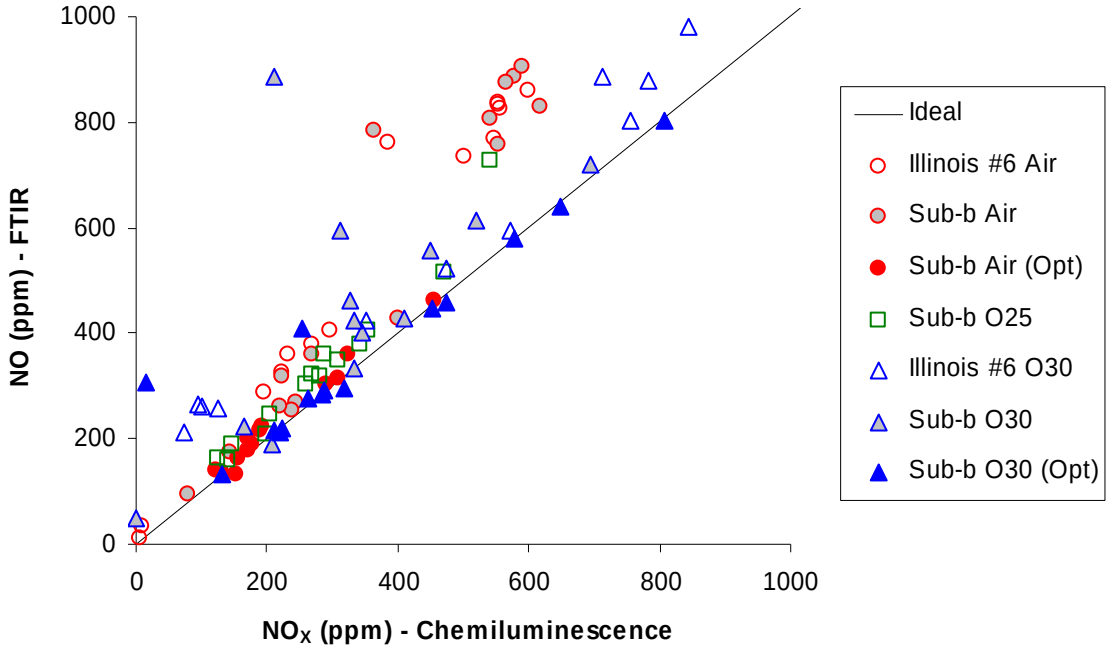

Figure 21. Parity plot for the NO measurements for several combustion cases including air and oxy-fuel combustion in fuel-rich and fuel-lean conditions.

The HORIBA measured NO_X and the FTIR measured NO, but as will be shown in the results the NO_X is dominated by NO. The outliers at the top region of the figure are from fuel-rich regions where many unidentified species exist. As these species were not included in interference calculations by the FTIR software it is expected that the chemiluminescent data is more accurate. For some data points the FTIR measurement is as much as 50% higher. This is discussed further in connection with experimental uncertainty below.

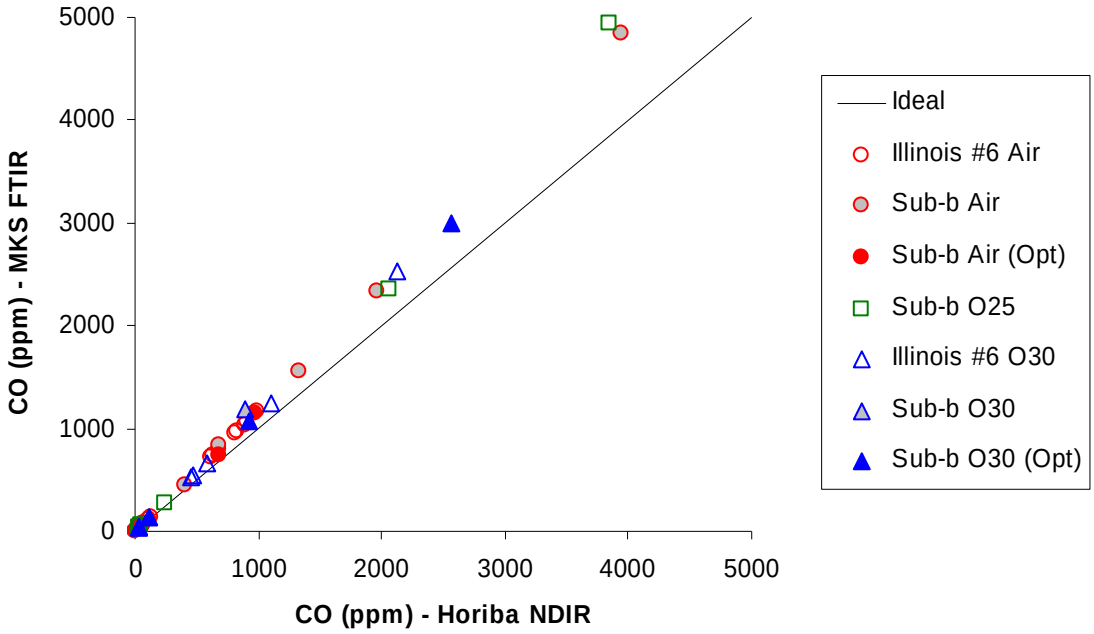

Figure 22. Parity plot for the CO measurements 0- 5000 ppm.

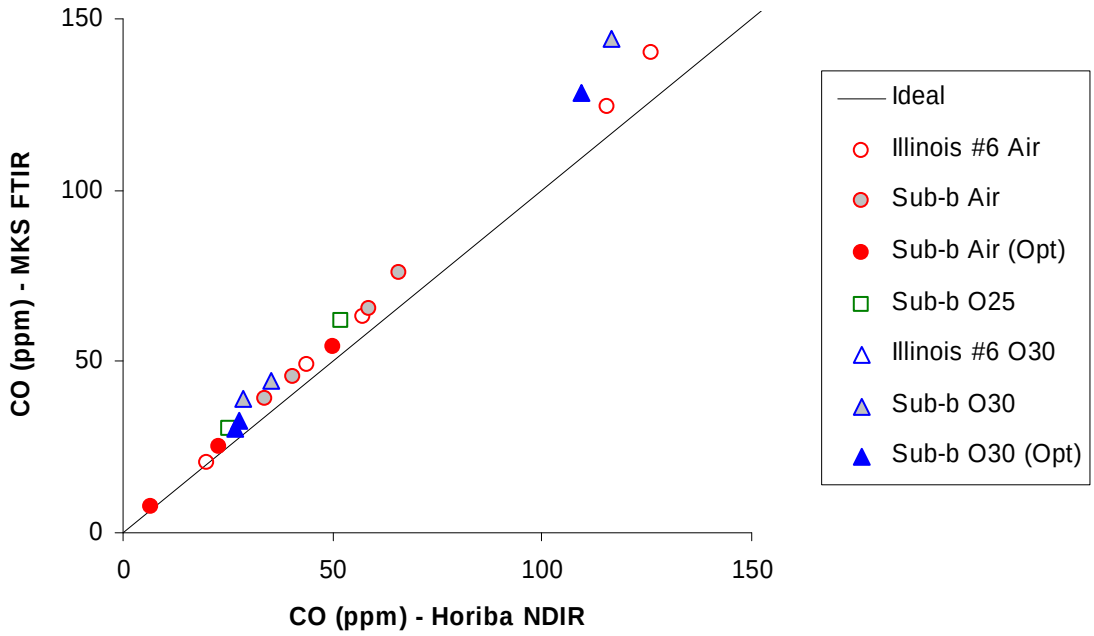

Figure 23. Close up of the 0-150 ppm range of the parity plot shown in Figure 22.

The agreement for the CO data shows a constant offset with the MKS analyzer reading 10-15% higher than the HORIBA. No comparisons could be made above 5000 ppm due to the range limit of the HORIBA instrument.

3.1.8 Nitrogen Conversion Efficiency

Both NO_X concentration and the quantitative amount of NO_X in the combustion gas can be useful in evaluating NO_X formation. Concentration of NO_X is important in the calculation of kinetic rates but is not necessarily a measure of the total amount of NO_X formed. Concentrations are a function of the other gases present and therefore NO_X concentrations can be higher because other gases' quantities are lower (as is the case when N_2 is replaced by CO_2), not because the amount of NO_X has actually increased. To allow a direct comparison of NO_X produced or reduced the measured NO_X values were converted to nitrogen conversion efficiency (η_N). This is the ratio of nitrogen existing as NO_X to the nitrogen supplied by the coal as calculated by Equation 1. If thermal and prompt NO_X are very low, η_N is a measure of the efficiency with which fuel NO_X is formed, hence the term "nitrogen conversion efficiency". If thermal and prompt NO_X are significant however, η_N should be simply considered a normalized measure of NO_X.

$$\eta_N \approx \frac{\dot{m}_{prod,wet}\left(1 - Y_{moist,prod,wet}\right) X_{NO,dry} \dfrac{MW_N}{MW_{prod,dry}}}{\dot{m}_{coal} Y_{N,coal}} \qquad \text{[Eq. 1]}$$

In Equation 1:

- $\dot{m}_{prod,wet}$ and $\dot{m}_{coal}$ are the measured flow rates of wet products and coal respectively

- $Y_{moist,prod,wet}$ is the mass fraction of condensed liquids in the cooled sample (H_2O and H_2SO_4) estimated using the NASA-Glenn CEA2 equilibrium code (Gordon and McBride, 1994)
- $X_{NO,dry}$ is the measured mole fraction of NO_X (dry basis) from the HORIBA gas analyzer
- MW_N and $MW_{prod,dry}$ are the molecular weight of atomic nitrogen and dry products respectively, the latter estimated using the NASA-Glenn CEA2 equilibrium code
- $Y_{N,coal}$ is the mass fraction of nitrogen in the coal on the same basis as $\dot{m}_{coal}$

Ash is considered condensed and inert. The molecular weight of the products in regions where the fuel has not completely reacted is unknown, but was estimated using equilibrium calculations with the assumption that only 70% of the coal mass is reacted upstream of the burnout oxidizer injection. The maximum error associated with the calculation of η_N is 5%. For error bars on plots of η_N, this uncertainty was combined with experimental uncertainty discussed next.

3.1.9 Experimental Uncertainty and Repeatability

The two gas analyzers that were used have different levels of uncertainty and are discussed separately. For the HORIBA instrument used to measure NO_X, CO, CO_2, and O_2 the test results in Figure 20 indicate that the uncertainty due to repeatability is on the order of 1% (5 ppm repeatability error at 500ppm). In the instrument documentation the manufacturer lists the level of uncertainty due to interference of other combustion gases as 1-2%. At the beginning of each experiment the HORIBA analyzer was calibrated using

certified standard gas mixtures, and a further calibration at the end of the day confirmed that the calibration was still valid with the exception of the oxygen sensor problems discussed previously. The measurement error associated with the instrument alone is small compared to variation observed in repeated experiments. Examples of repeated NO_X measurements from the HORIBA analyzer are shown in Figure 24.

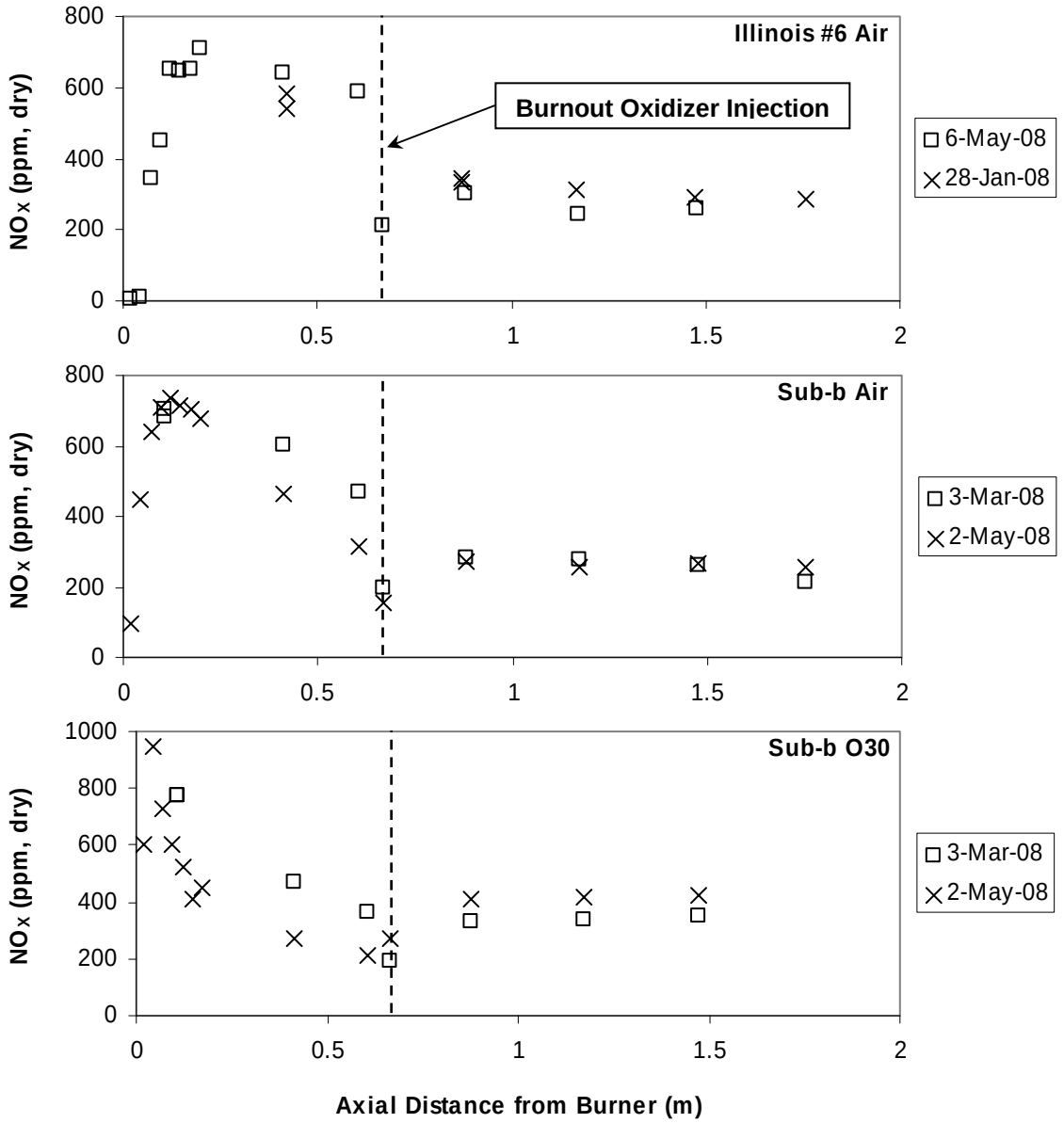

Figure 24. NO_X data (HORIBA) from repeated experiments used to evaluate experiment variability.

Observed variability (defined here as the difference between two measurements as a percentage of their average) ranged from 3-7%, and was 5% on average for measurements made the same day in the same experiment. For measurements recorded on different days for the same experiment the average variability is 22%, however it can be seen in Figure 24 that repeatability is better in the burnout region (average variability = 17%) than it is near the burner (average variability = 31%). It is likely that changes in reactant flow rates that alter gas composition move the flame relative to the burner and gas sample location. Near the burner the steeper gradients in NO_X make the measurement more sensitive to such changes than the measurements in the burnout section where gradients in NO_X are slight or non-existent. As the instrument error is very low compared to the experiment repeatability, the NO_X values measured are believed to be accurate, and the HORIBA thereby provides a good indication of changes in the experiment.

In the presentation of results error bars are placed on some of the plotted nitrogen conversion efficiency data to assist in judging the significance of differences between measurements. The variability in the data in Figure 24 was combined with the 5% uncertainty of calculating η_N, using the root-sum-squares method. For the burnout section of the reactor this gives a total estimated uncertainty of ±18% (rounded). The same procedure was followed for the near burner region and for measurements within the same experiment using the variability values above. As the data points are often densely grouped on plots, error bars are only shown where required by the discussion.

For both analyzers the raw measurements as a function of time were processed to extract only the steady state data at each sampling location. Sample NO_X data from both are shown in Figure 25 to illustrate the selection of data points for each analyzer.

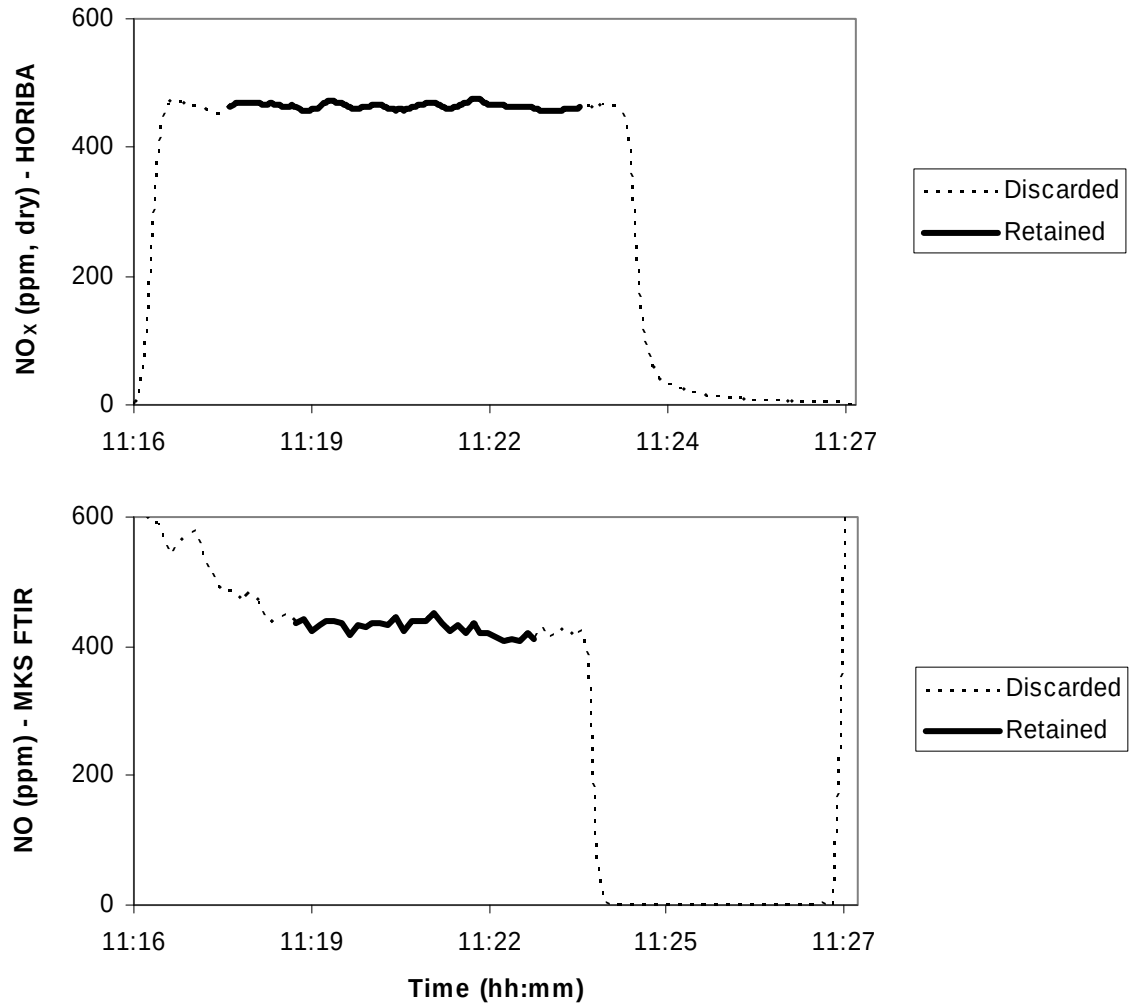

Figure 25. Example simultaneous $NO_{(X)}$ data from both gas analyzers showing steady state portions that were retained and time-averaged to produce measured values for the sampling location.

The manufacturer's calibrations were used for the MKS FTIR with some modifications made by Damstedt (2007) to prevent species interference. To assess accuracy of the FTIR analyzer the data for $NO_{(X)}$ and CO were compared to the corresponding measurements made by the calibrated HORIBA instrument (Section 3.1.7), and a calibration gas consisting of 75 ppm NH_3 in N_2 was passed through the gas sample system. As was discussed previously the CO measurements from the FTIR are

10-15% higher than the values measured by the HORIBA. The FTIR NO measurements are also higher, in some cases by as much as 50%, with more scatter than the CO data. The analysis of the NH_3 calibration gas yielded a measurement of about 95 ppm, an error of 25%.

The FTIR measures the gas concentrations by analyzing the infrared absorbtion spectrum of the mixture. Preloaded calibration spectra are used in conjunction with Classical Least Squares (CLS) analysis to determine the concentrations of each gas. Inherent in the numerical analysis is the risk for instabilities, and occasionally unrealistic (i.e. far outside the range 0-100%) instantaneous values were reported that were later excluded from the data.

Normal experimental noise is illustrated in Figure 26 by a concentration measurement over time for N_2O in where a very low signal-to-noise ratio is evident compared to the simultaneously obtained $NO_{(X)}$ data shown in Figure 25. Noise was handled by time-averaging the measurements.

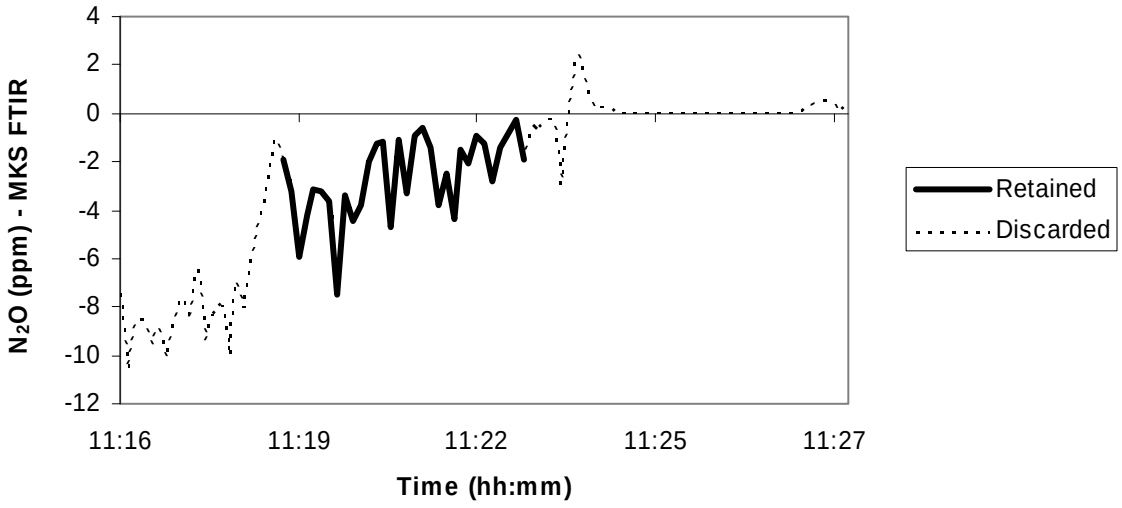

Figure 26. N_20 concentration calculated by the FTIR for the same gas sample as in Figure 25.

Any obviously erroneous data (identified by comparison with data from neighboring sampling locations) were excluded from the results, but the results should still be interpreted in light of the uncertainty noted. Relative changes indicated by the data are believable if larger than the scatter in adjacent data points, but absolute values vary from one gas to another and have only been characterized for CO, NO, and NH_3 as noted above. Low concentration data for species such as N_2O may be dominated by noise and have little meaning as evidenced by the scatter being similar to the magnitude in Figure 26.

3.1.10 Relevance of the Experiment to Practical Burners

A valid question is whether the laminar flow in the MFR has any relevance to practical low-NO_X burners with a swirled, turbulent flame. It is often explained in the literature that the fuel-rich recirculation zone in front of a low-NO_X burner prevents the formation of NO_X with fuel-N forming N_2 instead. What is often not stated is that significant NO can form at the base of the flame and this is reduced through reburning reactions in the recirculation zone. The data of Damstedt (2007) taken from a turbulent, swirled, pulverized coal-air flame support this view as shown in Figure 27. The left of the figure corresponds to the burner position. In the figure, the flame would extend from the left of the figure to the right side of the zone labeled “2”, as indicated by the CO data.

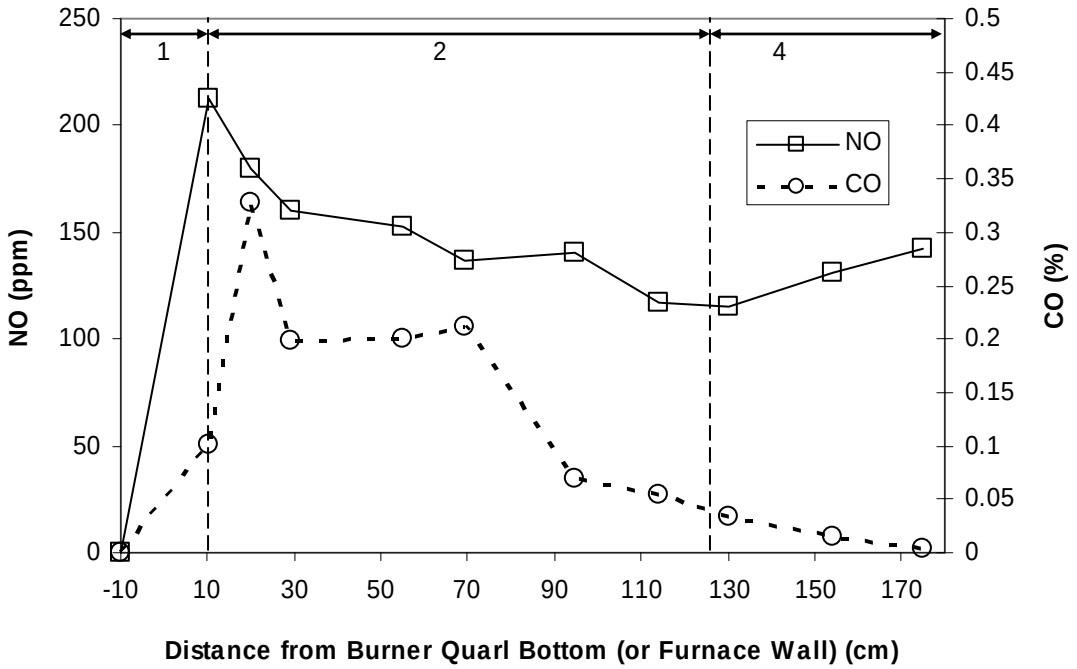

Figure 27. Average axial NO and CO data for a low-NO_X coal burner. Data used with permission from Damstedt (2007).

In considering the evolution of fuel-bound nitrogen in pulverized coal combustion it should be considered that it can pass through as many as four distinct zones in a temporally separated sequence. Figure 27 is labeled with three of the zones (1, 2, and 4).

In zone 1, premixed combustion of the volatiles with the primary air and any air entrained upstream of the flame occurs. During this process NO is formed rapidly but fuel nitrogen is in competition with volatile hydrocarbons for oxygen, which is in short supply. In the second zone, the atmosphere is reducing; causing fuel nitrogen in the volatiles, typically in the form of HCN and NH_3, to be reduced to N_2 while NO formed in zone 1 can be reduced through reburning reactions. Zone 3 is the oxidation of the products evolved in zones 1 and 2 as they mix with secondary air. In zone 3, the remaining HCN and NH_3 can be oxidized to produce NO_X. Zone 3 in Figure 27 occurs

axially at the same location as zone 2, around the perimeter of the flame. Only the net effect of NO formation and destruction are available in the figure. Zone 4 consists of char burnout and cooling of the combustion products from peak reaction temperatures to effluent temperatures. In zone 4, NO_X is rapidly frozen and typically remains constant; however heterogeneous reactions with coal char may both produce and reduce NO_X and high temperatures may create thermal NO_X.

A principle difference between the laboratory flame in this work and full scale boiler flames is the existence of turbulent mixing in industrial flames that produces a wider range of stoichiometries and temperatures. In these experiments, coal and oxidizer are relatively evenly distributed and premixed producing a fuel-rich, premixed zone at the average stoichiometry. In a full-scale boiler, a wide range of fuel-rich pockets would form, some much richer than the average and some leaner. Due to the highly non-linear response of NO_X chemistry to temperature and stoichiometry, the conditions for NO_X reduction found in these experiments should not be expected to be quantitatively the same in turbulent flames.

As will be seen in the results, the axial NO_X profiles for oxidizer-staged combustion in the MFR are qualitatively similar to the NO profile shown in Figure 27 and the same four zones exist. Therefore the results of this work allow the NOX chemistry relevant to an industrial flame to be explored without the complexity associated with turbulence.

3.1.11 Photographs of the Experimental Setup

The purpose of this section is to provide additional understanding of the experimental setup and evidence of important combustion conditions. Figure 28 shows an example of the laminar flow observed near the burner. Figure 29 shows natural gas flames at each of the holes in the burner face. These flames appeared uniform in size and this led to the conclusion that the reactant flows were well distributed over the entire cross section of the reactor. Figure 30 through Figure 32 show the physical appearance of the reactor and burner.

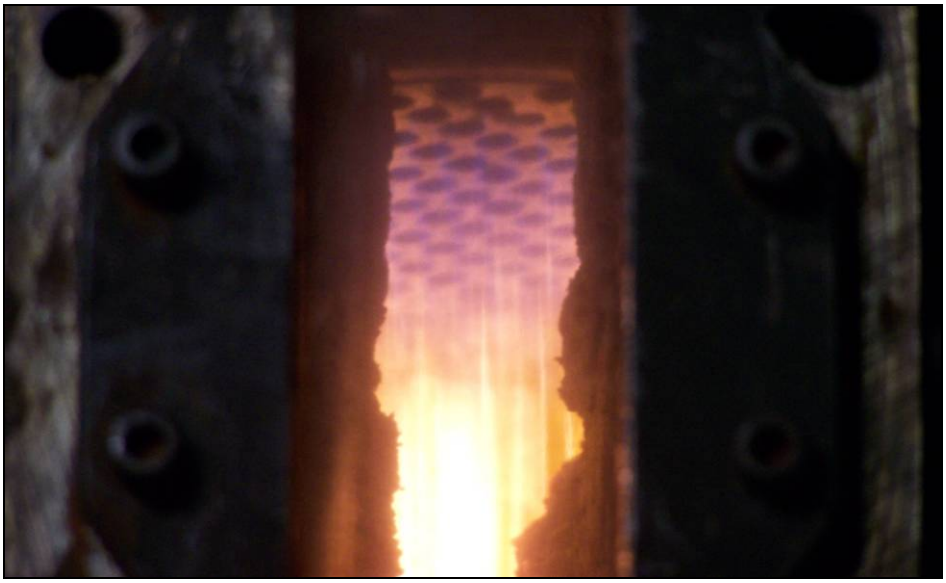

Figure 28. View of the burner through the observation window. Glowing coal particles can be seen here traveling in straight lines as evidence of the laminar flow.

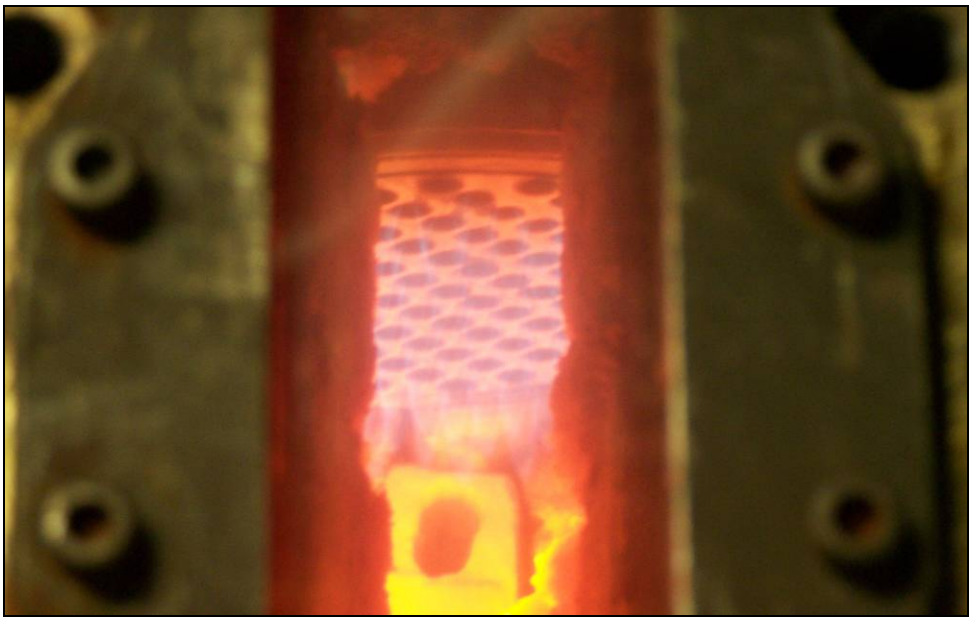

Figure 29. Natural gas flames observed through the window appeared uniform in size across the entire burner face.

Figure 30. The burner face and top flange of the MFR. The cast refractory material fits closely around the burner face. The fact that this water-cooled assembly rests directly on top of the first reactor section is one reason for lower wall temperatures at the top of the reactor.

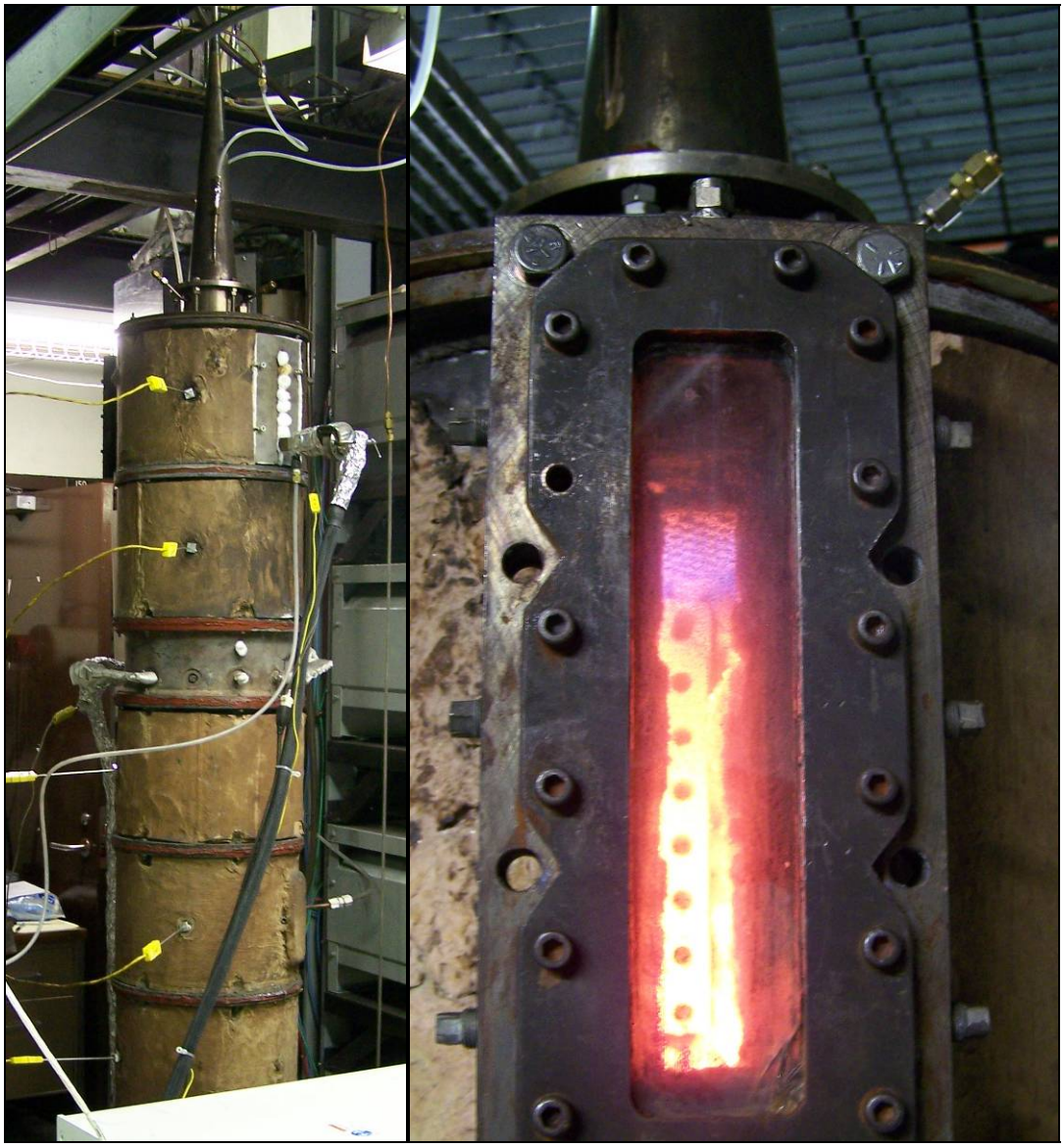

Figure 31. Left: Overall view of the reactor with burner at the top and gas sample probe to the lower right of the top section. The brown covering on the reactor is fiber clay insulation. The shorter section (in the axial direction) that does not have the brown covering is the section where burnout oxidizer is injected. Right: A view through the window showing the closely spaced sampling ports on the opposite side.

Figure 32. Looking down into the MFR with the burner removed reveals ash deposits with colors characteristic of the oxidizing and reducing conditions in different regions of the MFR.

The location of reducing and oxidizing zones in the MFR can be seen in Figure 32. This view looking down the MFR from the burner location shows light colored ash deposits close to the burner characteristic of oxidizing conditions. The fuel-rich section begins within the first section and has dark deposits (from inorganic species and not unburned carbon) which end shortly above the sampling port 0.61 m from the burner. Burnout oxidizer is injected radially at 0.67 m from the burner. The location of the end of the dark deposits and some of the gas sample data shown in the experimental results indicate that oxygen from the burnout oxidizer is transported several centimeters upstream of the injection ports. The surface of the reactor was originally smooth when cast, but has become rough due to deposit buildup. The original surface is still visible in many places and the diameter has not decreased significantly from the original 127 mm.

3.1.12 Experiment Conditions

A number of different experiments were performed using different oxidizers, different coals, and different ratios of primary to burnout oxidizer. The experiment conditions are detailed in Table 5 through Table 11. Each experiment has a unique name consisting of the coal used and the nominal oxidizer composition (Air, O25, O30), followed by a notation for special conditions (if any). The standard experiment was oxidizer-staged i.e. enough oxidizer was diverted from the burner to the burnout oxidizer ports to result in a nominal primary zone SR of 0.75. The notations for special conditions are as follows:

- Unstaged: Unstaged experiments had all reactants flow through the burner.
- Staging: In these experiments the ratio of primary to burnout oxidizer was varied to determine the effect on effluent NO_X concentration.
- (Opt): These experiments were conducted at the ratio of primary to burnout oxidizer that produced minimum effluent NO_X.
- (x ppm NO): To investigate the effect of recycled NO_X, an experiment was conducted using CO_2 doped with 525 ppm NO. The data obtained just prior to the switch from pure CO_2 to doped CO_2 make up the (0 ppm NO) experiment, and that taken with the doped CO_2 make up the (525 ppm NO) experiment.

Table 5. Experiment conditions for unstaged experiments.

Experiment Name: **Illinois #6 Air Unstaged**			
	Flow Rates (kg/hr)		
Reactant	Burner	Burnout Oxidizer	Total
Coal	0.734	-	0.734
Natural Gas	0.373	-	0.373
Air	17.0	-	17.0
Stoichiometric Ratio:	1.06		
Coal Moisture (as fired):	~14 wt%		

Experiment Name: **Illinois #6 O25 Unstaged**			
	Flow Rates (kg/hr)		
Reactant	Burner	Burnout Oxidizer	Total
Coal	0.737	-	0.737
Natural Gas	0.374	-	0.374
O_2	3.92	-	3.92
CO_2	11.6	-	11.6
Stoichiometric Ratio:	1.04		
Coal Moisture (as fired):	~14 wt%		

Experiment Name: **Illinois #6 O30 Unstaged**			
	Flow Rates (kg/hr)		
Reactant	Burner	Burnout Oxidizer	Total
Coal	0.737	-	0.737
Natural Gas	0.378	-	0.378
O_2	3.93	-	3.93
CO_2	9.15	-	9.15
Stoichiometric Ratio:	1.04		
Coal Moisture (as fired):	~14 wt%		

Table 6. Experiment conditions for standard experiments performed with Illinois #6 coal.

Experiment Name: **Illinois #6 Air**			
	Flow Rates (kg/hr)		
Reactant	Burner	Burnout Oxidizer	Total
Coal	0.732	-	0.732
Natural Gas	0.372	-	0.372
Air	11.87	7.13	19.0
Oxidizer to Burnout Oxidizer Ports:	37.5 %		
Primary Stoichiometric Ratio:	0.75		
Burnout Stoichiometric Ratio:	1.21		
Burnout Oxidizer Temperature:	502 K		
Coal Moisture (as fired):	11.3 wt%		

Experiment Name: **Illinois #6 O30**			
	Flow Rates (kg/hr)		
Reactant	Burner	Burnout Oxidizer	Total
Coal	0.729	-	0.729
Natural Gas	0.375	-	0.375
O_2	2.8	1.66	4.46
CO_2	6.5	3.85	10.35
Oxidizer to Burnout Oxidizer Ports:	37.2 %		
Primary Stoichiometric Ratio:	0.76		
Burnout Stoichiometric Ratio:	1.21		
Burnout Oxidizer Temperature:	461 K		
Coal Moisture (as fired):	11.3 wt%		

Table 7. Experiment conditions for experiments performed using pure CO_2 and NO-doped CO_2.

Experiment Name: **Illinois #6 O30 (0 ppm NO)**			
	Flow Rates (kg/hr)		
Reactant	Burner	Burnout Oxidizer	Total
Coal	0.736	-	0.736
Natural Gas	0.376	-	0.376
O_2	2.84	1.63	4.47
CO_2	6.5	3.72	10.22
NO in CO_2:	0 ppm		
Oxidizer to Burnout Oxidizer Ports:	36.4 %		
Primary Stoichiometric Ratio:	0.77		
Burnout Stoichiometric Ratio:	1.21		
Burnout Oxidizer Temperature:	436 K		
Coal Moisture (as fired):	11.7 wt%		

Experiment Name: **Illinois #6 O30 (525 ppm NO)**			
	Flow Rates (kg/hr)		
Reactant	Burner	Burnout Oxidizer	Total
Coal	0.736	-	0.736
Natural Gas	0.377	-	0.377
O_2	2.83	1.61	4.44
CO_2	6.43	3.67	10.10
NO in CO_2:	525.4 ppm		
Oxidizer to Burnout Oxidizer Ports:	36.3 %		
Primary Stoichiometric Ratio:	0.76		
Burnout Stoichiometric Ratio:	1.2		
Burnout Oxidizer Temperature:	435 K		
Coal Moisture (as fired):	11.7 wt%		

Table 8. Experiment conditions for standard experiments with Pittsburgh #8 coal.

Experiment Name: **Pittsburgh #8 Air**			
	Flow Rates (kg/hr)		
Reactant	Burner	Burnout Oxidizer	Total
Coal	0.645	-	0.645
Natural Gas	0.372	-	0.372
Air	10.99	6.51	17.5
Oxidizer to Burnout Oxidizer Ports:	37.2 %		
Primary Stoichiometric Ratio:	0.76		
Burnout Stoichiometric Ratio:	1.2		
Burnout Oxidizer Temperature:	466 K		
Coal Moisture (as fired):	1.51 wt%		

Experiment Name: **Pittsburgh #8 O30**			
	Flow Rates (kg/hr)		
Reactant	Burner	Burnout Oxidizer	Total
Coal	0.644	-	0.644
Natural Gas	0.372	-	0.372
O_2	2.59	1.49	4.08
CO_2	5.80	3.71	9.51
Oxidizer to Burnout Oxidizer Ports:	36.6 %		
Primary Stoichiometric Ratio:	0.76		
Burnout Stoichiometric Ratio:	1.2		
Burnout Oxidizer Temperature:	425 K		
Coal Moisture (as fired):	1.51 wt%		

Table 9. Experiment conditions for standard experiments with sub-bituminous coal.

Experiment Name: **Sub-b Air**			
	Flow Rates (kg/hr)		
Reactant	Burner	Burnout Oxidizer	Total
Coal	0.877	-	0.877
Natural Gas	0.373	-	0.373
Air	11.16	7.24	18.4
Oxidizer to Burnout Oxidizer Ports:	39.3 %		
Primary Stoichiometric Ratio:	0.75		
Burnout Stoichiometric Ratio:	1.23		
Burnout Oxidizer Temperature:	522 K		
Coal Moisture (as fired):	8.46 wt%		

Experiment Name: **Sub-b O25**			
	Flow Rates (kg/hr)		
Reactant	Burner	Burnout Oxidizer	Total
Coal	0.874	-	0.874
Natural Gas	0.373	-	0.373
O_2	2.63	1.65	4.28
CO_2	7.9	4.94	12.84
Oxidizer to Burnout Oxidizer Ports:	38.5 %		
Primary Stoichiometric Ratio:	0.76		
Burnout Stoichiometric Ratio:	1.23		
Burnout Oxidizer Temperature:	522 K		
Coal Moisture (as fired):	8.46 wt%		

Experiment Name: **Sub-b O30**			
	Flow Rates (kg/hr)		
Reactant	Burner	Burnout Oxidizer	Total
Coal	0.878	-	0.878
Natural Gas	0.377	-	0.377
O_2	2.63	1.66	4.29
CO_2	6.18	3.91	10.09
Oxidizer to Burnout Oxidizer Ports:	38.8 %		
Primary Stoichiometric Ratio:	0.75		
Burnout Stoichiometric Ratio:	1.23		
Burnout Oxidizer Temperature:	495 K		
Coal Moisture (as fired):	8.46 wt%		

Table 10. Experiment conditions for the Staging-type experiments.

Experiment Name: **Sub-b Air Staging**			
	Flow Rates (kg/hr)		
Reactant	Burner	Burnout Oxidizer	Total
Coal	0.872	-	0.872
Natural Gas	0.378	-	0.378
Air	Oxidizer split between burner and burnout oxidizer ports was varied		18.4
Oxidizer to Burnout Oxidizer Ports:	18.9, 25.0, 31.9, 34.2, 35.8, 39.6, 42.9, 49.0, 53.8 %		
Primary Stoichiometric Ratios:	1.00, 0.92, 0.84, 0.81, 0.79, 0.74, 0.70, 0.63, 0.57		
Burnout Stoichiometric Ratio:	1.23		
Burnout Oxidizer Temperature:	492, 514, 527, 519, 520, 534, 535, 532, 525 K		
Coal Moisture (as fired):	8.46 wt%		

Experiment Name: **Sub-b O25 Staging**			
	Flow Rates (kg/hr)		
Reactant	Burner	Burnout Oxidizer	Total
Coal	0.878	-	0.878
Natural Gas	0.373	-	0.373
O_2	Oxidizer split between burner and burnout oxidizer ports was varied		4.29
CO_2			12.88
Oxidizer to Burnout Oxidizer Ports:	20.5, 24.8, 31.1, 36.4, 39.3, 46.4 %		
Primary Stoichiometric Ratio:	0.98, 0.93, 0.85, 0.78, 0.75, 0.66		
Burnout Stoichiometric Ratio:	1.23		
Burnout Oxidizer Temperature:	475, 494, 510, 520, 523, 526 K		
Coal Moisture (as fired):	8.46 wt%		

Experiment Name: **Sub-b O30 Staging**			
	Flow Rates (kg/hr)		
Reactant	Burner	Burnout Oxidizer	Total
Coal	0.873	-	0.873
Natural Gas	0.373	-	0.373
O_2	Oxidizer split between burner and burnout oxidizer ports was varied		4.29
CO_2			10.05
Oxidizer to Burnout Oxidizer Ports:	18.8, 25.2, 32.8, 36.0, 39.0, 43.0, 47.1 %		
Primary Stoichiometric Ratio:	1.00, 0.92, 0.83, 0.79, 0.75, 0.70, 0.65		
Burnout Stoichiometric Ratio:	1.24		
Burnout Oxidizer Temperature:	445, 464, 483, 490, 493, 497, 494 K		
Coal Moisture (as fired):	8.46 wt%		

Table 11. Experiment conditions for minimum effluent NO_X.

Experiment Name: **Sub-b Air (Opt)**			
	Flow Rates (kg/hr)		
Reactant	Burner	Burnout Oxidizer	Total
Coal	0.875	-	0.875
Natural Gas	0.373	-	0.373
Air	9.33	9.07	18.4
Oxidizer to Burnout Oxidizer Ports:	49.3 %		
Primary Stoichiometric Ratio:	0.63		
Burnout Stoichiometric Ratio:	1.23		
Burnout Oxidizer Temperature:	514 K		
Coal Moisture (as fired):	8.46 wt%		

Experiment Name: **Sub-b O30 (Opt)**			
	Flow Rates (kg/hr)		
Reactant	Burner	Burnout Oxidizer	Total
Coal	0.876	-	0.876
Natural Gas	0.377	-	0.377
O_2	2.89	1.4	4.29
CO_2	6.77	3.27	10.04
Oxidizer to Burnout Oxidizer Ports:	32.6 %		
Primary Stoichiometric Ratio:	0.83		
Burnout Stoichiometric Ratio:	1.23		
Burnout Oxidizer Temperature:	467 K		
Coal Moisture (as fired):	8.46 wt%		

3.2 Computational Methods

3.2.1 General Description of the Detailed Kinetic Model

The approach taken for detailed kinetic modeling was to simulate the MFR using existing sub-models available in the literature. In order to produce a model that required little adjustment to match experimental data, the emphasis was on fundamental over empirical methods. An advantage of such a model is that it may be used to investigate the relative importance of various NO_X mechanisms by enabling and disabling them and

determining which features of the model are most important to correctly predicting the nitrogen evolution observed experimentally.

A conceptual diagram of the model is shown in Figure 33. The MFR was represented as a plug flow reactor divided into a series of 875 slices (each 2 mm in the axial direction). Each slice was modeled as a continuously-stirred tank reactor (CSTR). In the limit, a series of infinitely-small CSTR's is a plug flow reactor. The size of 2 mm was chosen as the smallest size where the model would predict ignition of the incoming reactants. Grid independence was verified by comparing results from a 4 mm and 2 mm grid spacing model.

The open-source kinetic code Cantera (Goodwin, 2003) was used to integrate the gas-phase reactions in each CSTR. Three gas-phase mechanisms were tested: SKG03 (Skreiberg et al., 2004), GRI-Mech 3.0 (Smith et al., 2000), and GRI-Mech 3.0 + B96 which is the GRI-Mech 3.0 mechanism with advanced reburning reactions from Bowman (1997) added following a similar approach to Xu et al. (2001).

Devolatilization was modeled using the CPD-NLG model (Grant et al., 1989; Fletcher et al., 1992; Genetti, 1999) which includes prediction of nitrogen and light gas species release from the coal. Genetti's correlations to estimate the required ^{13}C NMR parameters for the coal based on proximate and ultimate analyses were employed.

MATLAB was chosen for the main program as Cantera functions can be called from MATLAB. The CPD-NLG model was translated from FORTRAN source code to MATLAB and modified to replace built-in correlations for gas properties (that assumed N_2) with gas mixture properties evaluated by Cantera.

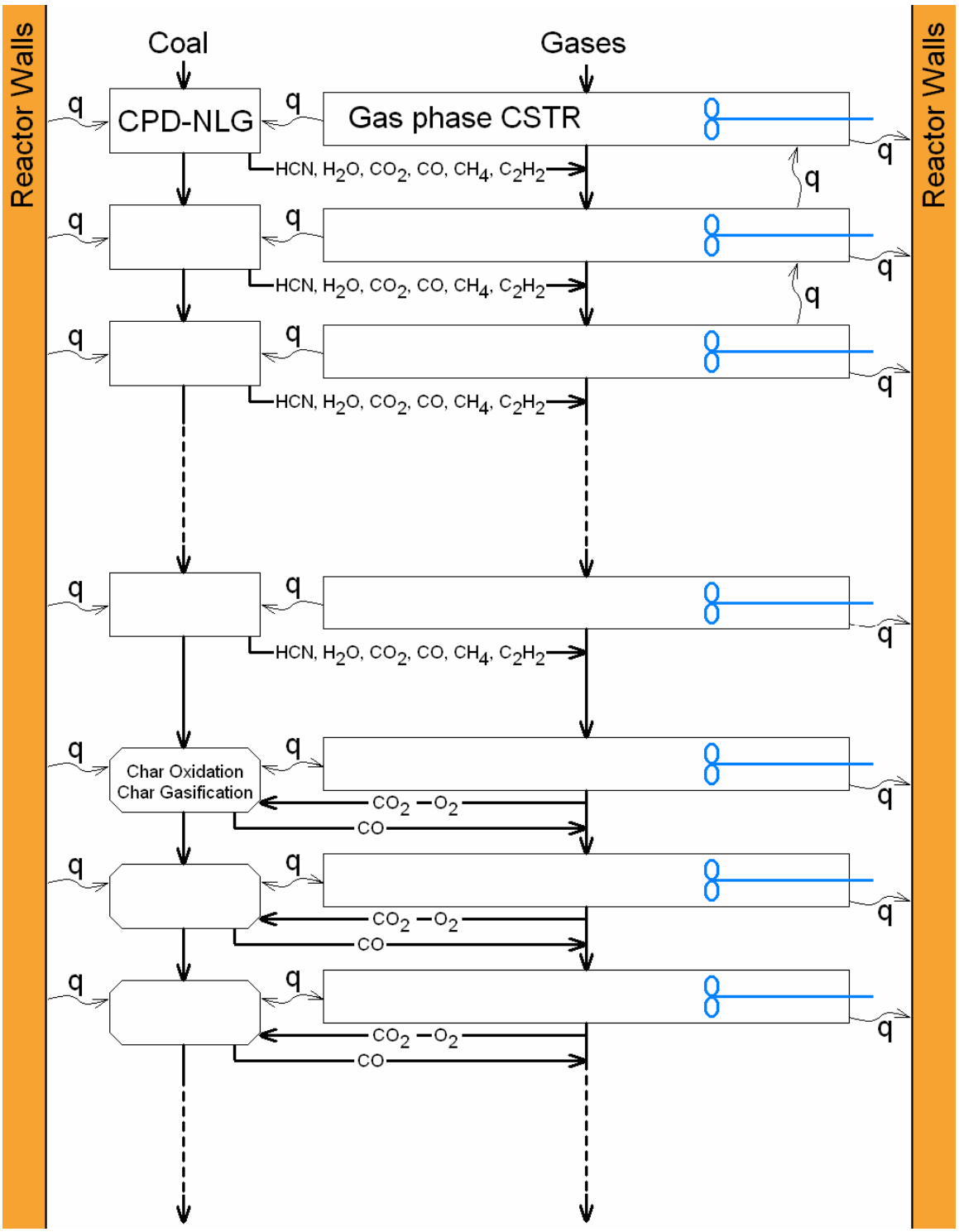

Figure 33. Schematic diagram of the detailed kinetic model. The letter "q" indicates heat transfer.

A char oxidation and gasification (by CO_2) model described in Smoot and Smith (1985) using the data of Goetz et al. (1982) was included. This char reaction model only becomes active after devolatilization is completed.

Each CSTR was solved sequentially with the exception of the first 5 CSTR's which had to be solved simultaneously to model thermal feedback from the natural gas flame necessary for ignition. After each CSTR the gas mixture was altered to account for production of volatiles by the coal or consumption of oxidant and production of CO by the char. The new mixture was then passed downstream to the next CSTR.

Convective heat transfer between gas and particles was modeled as well as radiation between particles and the walls. Measured wall temperatures were used as an input. Radiation heat transfer from the gases was neglected on account of the small reactor cross section (Wall et al., 1979). Convective losses from the gases to the walls and other heat transfer such as radiation from soot and char are handled with an empirically-adjusted factor that was based on matching gas temperature data from a well-characterized natural gas MFR experiment, and gas species measurements (CO) from this work indicative of gas temperature.

3.2.2 Simplifying Assumptions

Key assumptions made in the model were largely based on the literature and included the following:

- Coal particles were spherical and entrained (i.e. particle velocity was equal to gas velocity). A calculation was performed to estimate the terminal velocity of a 115 μm diameter coal particle in hot combustion gases. The result was a predicted velocity of 0.17 m/s for a Reynolds number of 0.07. The estimated

gas velocity was much higher at 1.42 m/s. This assumption greatly simplifies the model.

- All gas products from the coal consisted of species in the kinetic mechanism. Secondary pyrolysis of coal char results in soot and light gases such as H_2, CO, C_2H_2, C_2H_4, and single ring aromatics (Glarborg et al., 2003). The CPD-NLG model predicts some light gases as indicated in Figure 33, and other volatiles were assumed to consist of CH_4 and C_2H_2 in proportions that closed the carbon and hydrogen balances. These balances were based on carbon release being proportional to burnout and hydrogen mass release being a function of burnout as described by Equation 2 and Equation 3. Equation 2 was generated by curve-fitting data from Asay (1982) for a bituminous coal. The equation had an r^2 value of 0.95 for the bituminous data and was a good visual match to a set of sub-bituminous data. This is a significant assumption and is based on assuming that all tars are cracked to form light gases. Soot is therefore neglected, but most, if not all, published NO_X mechanisms in the literature are based on light gases. Bose et al. (1988) concluded that homogeneous chemistry dominated NO_X destruction. Further, if this assumption were not made, the detailed kinetic approach taken would have been impossible.

$$\%H_{released} = -0.5597 \times Burnout^2 + 1.5651 \times Burnout \qquad \text{[Eq. 2]}$$

$$Burnout = 1 - \frac{Char\ Mass\ Flux\ (DAF)}{Initial\ Coal\ Mass\ Flux\ (DAF)} \qquad \text{[Eq. 3]}$$

- Oxygen was assumed to be completely contained in the CPD predictions of CO, H_2O, and CO_2 in accordance with the findings of Niksa (1996).
- Natural gas was modeled as 100% CH_4 as done by Xu et al. (2001). Approximate natural gas composition is given in Table 4 and is mostly methane.
- All nitrogen in the volatiles was in the form of HCN. This matches the majority of observations in the literature as discussed in the literature review.
- Char consisted of C(s) and burned with a shrinking core of constant density and constant ash content with CO as the surface product. These assumptions were used in deriving the rate constants sourced from Goetz et al. (1982) and so needed to be used when applying said constants. Diffusion-limited vs. kinetic-limited char burning did not therefore need to be considered in this model. The experiments of Goetz et al. (1982) were performed at 1 atm over the temperature range of 1250-1730 K with chars prepared in 1750 K N_2 from 200-400 mesh coals, which is applicable to pulverized coal conditions. NO_X formation from char was not included in the model. CO from the char reactions was oxidized to CO_2 by the gas-phase kinetics.
- Sulfur species are neglected.
- No fluid mechanics were modeled as the focus of the model was the devolatilization and gas-phase kinetics. Mixing of burnout oxidizer was assumed to occur in one CSTR. This was initially tried for simplicity in coding and when it did not introduce any model instabilities it was retained.

- For coding simplicity the coal particles were represented with one particle diameter based on the mean diameter for a Rosin-Rammler distribution fit to the measured size distributions.

The full MATLAB source code including the CPD-NLG model is included in Appendix D. The code is heavily commented so that minor details not described in this section are clearly identified in the code.

3.2.3 Gas-phase Mechanisms

Skreiberg et al. (2004) recommend a mechanism known as SKG03 for modeling the reduction of NO by primary measures in biomass combustion, and combustion of coal syngas. It was validated under conditions similar to those in staged combustion.

GRI-Mech 3.0 (Smith et al., 2000) is a collection of 325 elementary reactions involving 53 species. It has been optimized for methane and natural gas combustion over the range 1000-2500 K, 10 Torr to 10 atm, and equivalence ratios from 0.1-5 for premixed systems. Some species such as ethane and propane are included in the species list because they are found in natural gas, but the authors state that the mechanism should not be used for modeling of fuels other than methane and natural gas, even if these species are on the species list. If the reactions are truly elementary then the reactions should be usable in other mechanisms but there are no guarantees. NO formation and reduction (thermal and prompt NO_X, and reburning reactions) are included in the mechanism with the notable exception of the chemistry involved in SNCR. Soot formation is also not described.

Xu et al. (2001) modeled advanced reburning with a reduced mechanism that was derived from the earlier GRI-Mech 2.11 mechanism with advanced reburning reactions

from Bowman (1997) added. This advanced reburning model was used in the PCGC-3 CFD code. The model was activated at the location of NH_3 injection, and upstream of this a global fuel-N mechanism was employed. Agreement with experimental data was determined to be *"reasonably good"*. Given their success it was decided for this work to try the newer GRI-Mech 3.0 mechanism with Bowman's reaction set added. This mechanism is referred to as GRI-Mech 3.0 + B96.

3.2.4 Char Reactions

Both char oxidation by O_2 and char gasification by CO_2 were modeled. Typically in combustion modeling, gasification by CO_2 is neglected because the reaction rate is much slower than oxidation, but in this work it was included because the CO_2 concentrations in oxy-fuel combustion are much higher and the effect of increased CO_2 was of interest. Shaddix and Murphy, 2003 (as referenced by Buhre et al., 2005) found that in oxygen-enriched combustion, CO_2 gasification of the char becomes important at practical temperatures.

The only product considered for the char reactions was CO. Molina et al. (2000) in reviewing char combustion modeling note that while some workers have modeled heterogeneous production of both CO_2 and CO from char, it is known that the major pathway at combustion temperatures is production of CO, and that most CO_2 comes from homogeneous oxidation of CO.

The char reactions were modeled using rates measured by Goetz et al. (1982) for coals from the same US regions as used in this work. The parameters were sourced from Brown et al. (1988) and Smoot and Smith (1985) and are shown in Table 12. Figure 34 shows a visual comparison of the rates of reaction on an Arrhenius plot. It can be seen

from the figure that oxidation is a faster process than gasification, and that rates generally increase with decreasing rank.

Table 12. Char oxidation and gasification parameters used in the model (Goetz et al., 1982).

Coal	Oxidation Rate Parameters		Gasification Rate Parameters	
	A $g/(cm^2 s\ atm_{O_2})$	E (cal/gmol)	A $g/(cm^2 s\ atm_{CO_2})$	E (cal/gmol)
Sub-bituminous	145	19970	1040	42470
Illinois #6	60	17150	12973	56370
Pittsburgh #8	66	20360	1390	53700

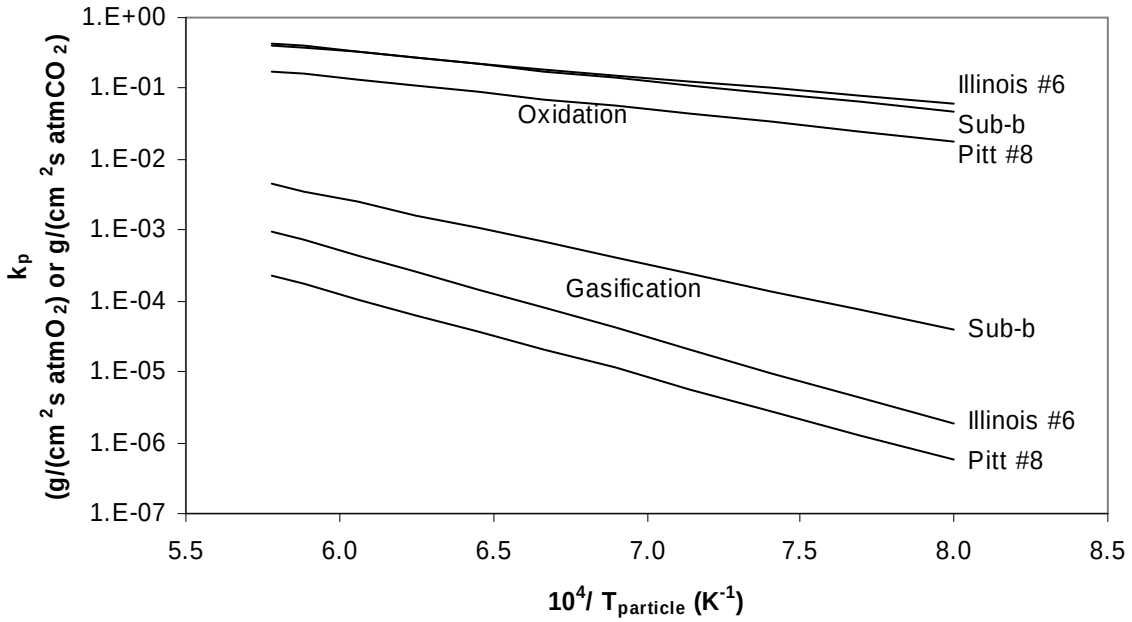

Figure 34. Comparison of rates of char reaction with O_2 (oxidation) and CO_2 (gasification).

Kajitani et al. (2006) studied CO_2 gasification of char in entrained flow gasification and concluded that CO can inhibit the CO_2 gasification, but high partial pressures of CO were required (>0.4 MPa) and the effect is less at high temperatures (>

1400°C). Based on these results this possible effect was neglected in the model and the values from Goetz et al. (1982) were used without modification.

Shaddix and Molina (2007) determined that char combustion rates were lower in a CO_2-based gas. As the surface kinetic rates were nominally the same as in air, the difference was attributed to slower diffusion of O_2 through the CO_2-rich boundary layer. The char model used here is based on bulk gas concentrations and therefore this knowledge could not be incorporated into the model. The error due to this is however minimal as the reported decrease in burning rate is only about 10%.

4 Experimental Results

In this chapter experimental results are presented, but most discussion is delayed until Chapter 6 so that the data can be discussed in connection with model predictions presented in Chapter 5.

4.1 Unstaged Combustion Experiments

The unstaged experiments were conducted by introducing all reactants (premixed) through the burner with an overall SR of 1.04–1.06. Effluent O_2 of 6 vol. % (dry basis) in the Air case was used to estimate burnout at 95%. CO_2 data for the air case shown in Figure 35 indicate that most reaction occurs in the upper half of the MFR.

Figure 36 presents the wall temperature data that indicate comparable heat release profiles for the Air and O25 oxidizers. The higher wall temperature near the burner for the O30 oxidizer suggests earlier heat release and probably higher particle heating rates. As is the case for all figures in this chapter, the lines connecting data points are to assist in visual association between widely spaced data points and do not imply that the plotted parameter follows that path.

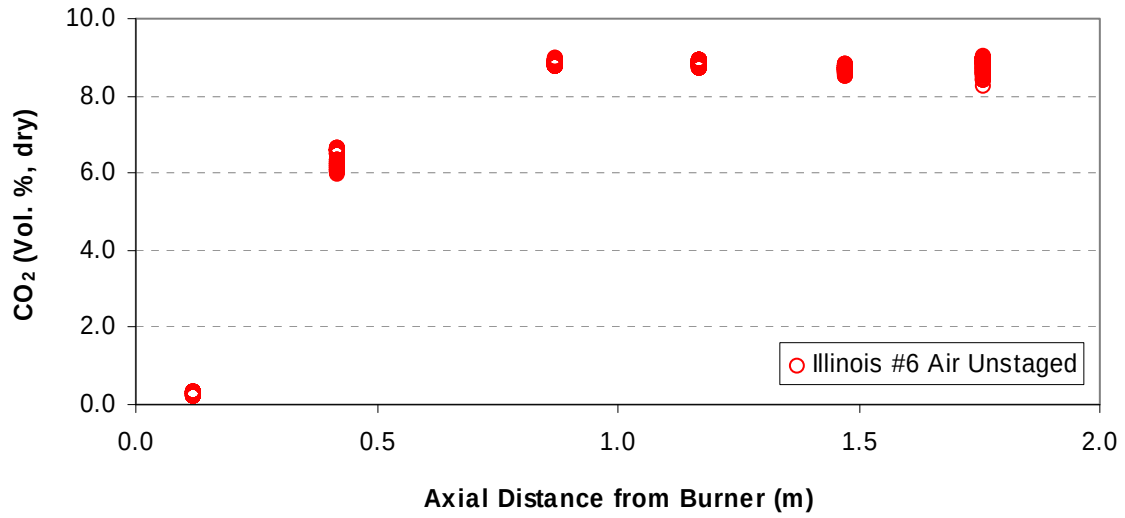

Figure 35. CO_2 data for the Illinois #6 Air Unstaged experiment.

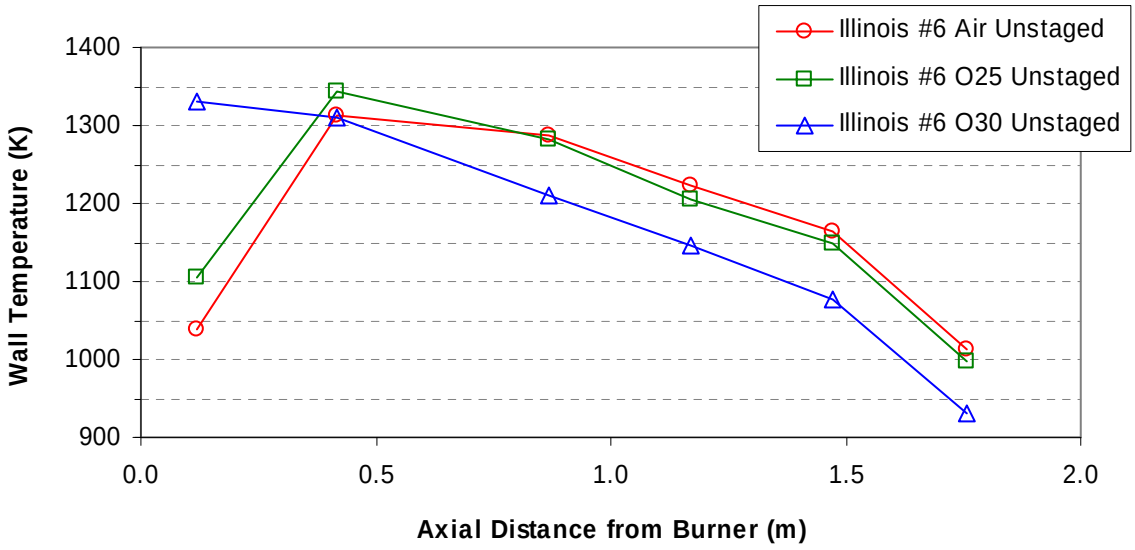

Figure 36. Wall temperature data for the Illinois #6 Unstaged experiments.

NO_X measurements in Figure 37 show higher NO_X concentrations in both oxy-fuel cases relative to the air case. The nitrogen conversion efficiency data removes the effect of the varying diluent and indicates that Air and O30 as oxidizers produce similar effluent NO_X with O25 producing slightly less.

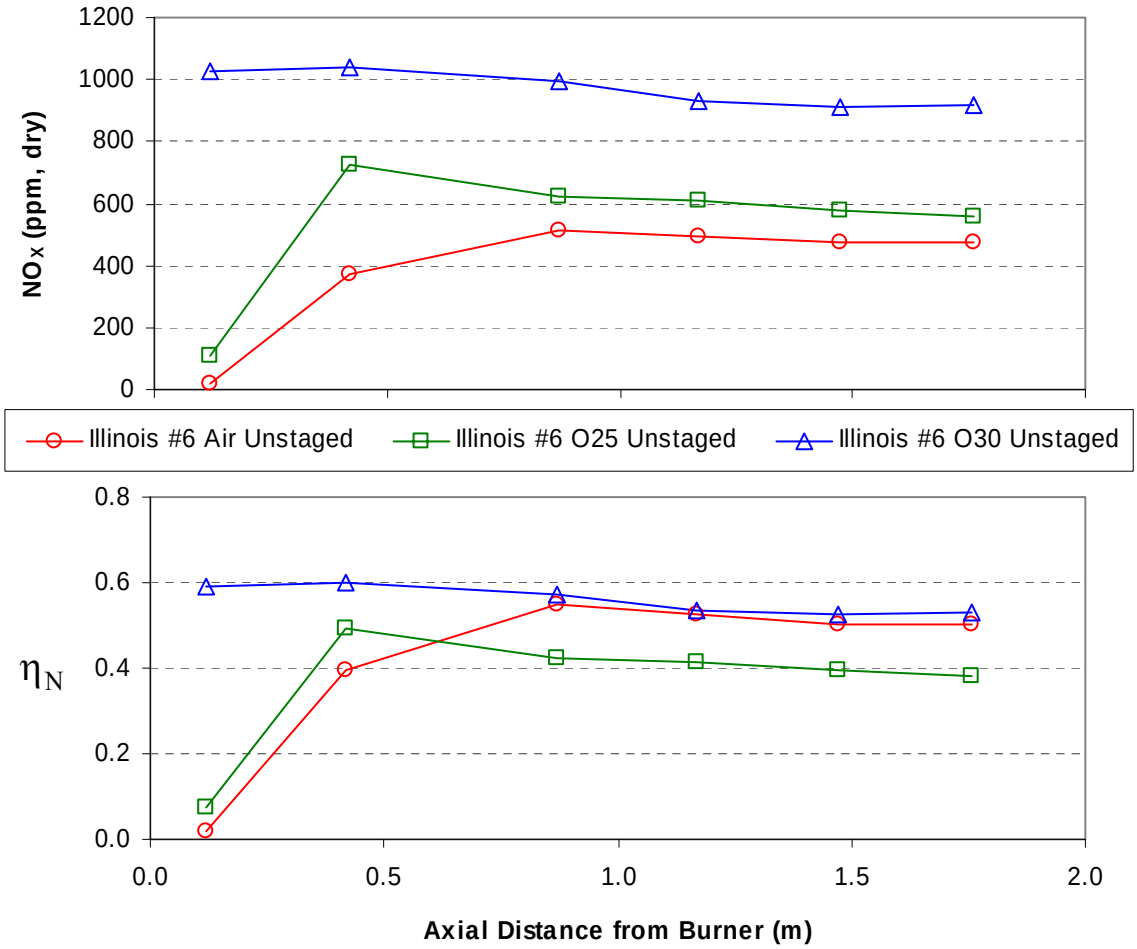

Figure 37. NO_X measurements and corresponding nitrogen conversion efficiency data for the Illinois #6 Unstaged experiments.

A slight decline in NO_X is observed for all cases in the lower half of the reactor. This drop was unexpected because NO reduction by reaction with char or by reverse thermal NO_X reactions was not expected to be significant in this section of the reactor. Other possible explanations include dilution by air leaking into the reactor or by CO_2 production during char oxidation. The CO_2 data in Figure 35 show little rise in this region of the reactor suggesting CO_2 dilution is not the cause. Although initially the reactor was found to leak air inward, the data shown were taken with a positive reactor gage pressure

which eliminated this source of dilution. This leaves little explanation except to conclude that some reduction in NO_X due to char or the thermal mechanism is occurring.

The NO_X data for the O30 oxidizer show that peak NO_X values occur further upstream than for the Air and O25 oxidizers. This is consistent with more rapid combustion as indicated by the wall temperature data. The O25 oxidizer's lower effluent NO_X may also be due to differences in heating rates. A lower heating rate is expected to result in lower nitrogen release with the volatiles. Lower conversion efficiency of char-N to NO (relative to volatiles-N to NO conversion) could thereby cause lower overall NO production.

The slight decline in NO_X in the lower half of the reactor is insufficient to produce the low levels of nitrogen conversion efficiency required by emissions regulations. No notable difference in nitrogen evolution between air and oxy-fuel cases is noted beyond the initial NO_X formation, which may be simply due to differences in particle heating and combustion rates. The remainder of the work focused on oxidizer-staged combustion where a reducing zone was formed near the burner to simulate the performance of a low-NO_X combustion system.

4.2 Char and Fly Ash Analysis - Staged Combustion, Fixed Stoichiometry

For the oxidizer-staged experiments with three coals, an attempt was made to close the nitrogen balance by analyzing the char for residual nitrogen and using these data in combination with NO_X measurements. Figure 38 presents a summary of the results normalized by fuel-N entering the MFR (i.e. in terms of η_N). The figure is based on the

assumption that all measured NO_X originates from fuel-N and that nitrogen not accounted for in the char and NO_X must have left the MFR in the form of N_2. Accuracy of the char-N and burnout measurements is not affected by this assumption. Burnout was determined by ashing particulate from the exhaust system filter and measuring the mass loss (i.e. ash was used as a tracer).

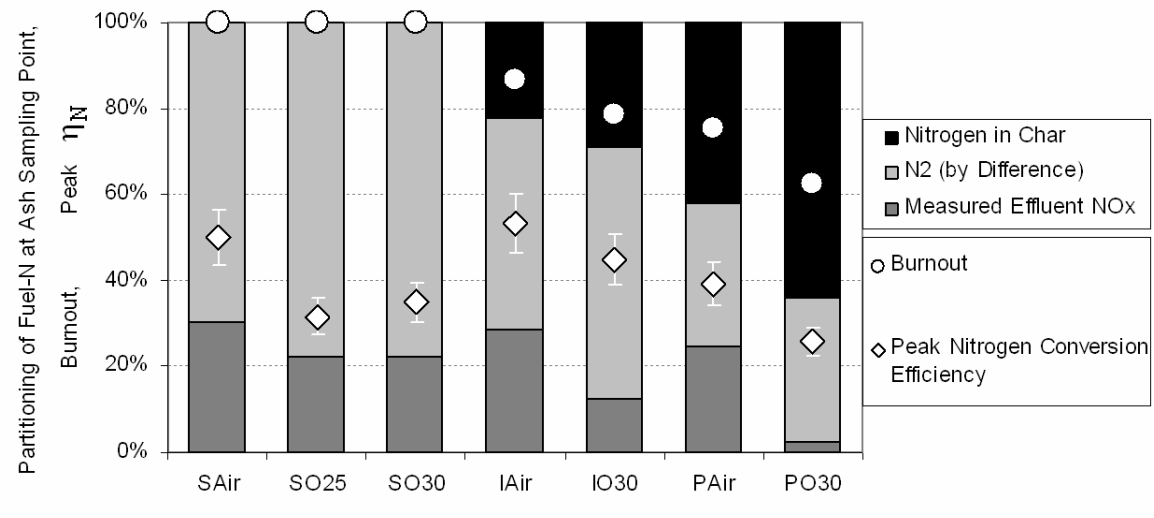

Figure 38. Summary of data showing the fate of fuel nitrogen in oxidizer-staged experiments (assuming all NO_X is fuel NO_X). All data are from the ash sampling location with the exception of the peak nitrogen conversion efficiency which is from the reactor centerline near the burner. The horizontal axis labels indicate the coal by the first letter: S, I, P for sub-bituminous, Illinois #6, and Pittsburgh #8 respectively, followed by the oxidizer type.

By comparing the burnout measurements to the char-N measurements in Figure 38 we see that for the two higher-ranked coals the percent of coal burned is greater than the percent of fuel-N converted. This is consistent with measurements made in developing the CPD-NLG coal devolatilization model that nitrogen release is slightly lower than volatiles release thus resulting in a char that is enriched in nitrogen relative to the parent coal (Genetti, 1999). Only the sub-bituminous coal achieved high burnout;

which was the reason for it being the most extensively studied coal in this work. The O25 and O30 data in the figure for this coal show no difference in peak nitrogen conversion efficiency greater than the level of uncertainty.

Peak η_N in the air cases is higher than in the corresponding oxy-fuel cases for all three coals which may be due to thermal and prompt NO_X formation in addition to fuel NO_X. For all three coals the effluent NO_X emissions are lower in the oxy-fuel cases than the air cases and the higher the rank of the coal, the greater is the difference between the air and oxy-fuel NO_X emissions.

The high level of burnout achieved for the sub-bituminous coal made it possible to submit fly ash samples for mineral analysis without further thermal processing. Results are shown in Figure 39. As expected, the ash generated by combustion differs significantly from the ash prepared under laboratory conditions.

These data show the largest percentage change between air and oxy-fuel is in the sulfur content, with oxy-fuel being higher. Oxy-fuel ash was also higher in calcium by 17% and lower in silicon by 16%. Sarofim (2007) quotes multiple works that measured increased sulfur removal with the ash under oxy-fuel conditions, consistent with this result. The composition differences lead to changes in ash properties such as estimated ash fusion temperature. This topic is outside of the scope of this work, but additional details are available in Appendix C.

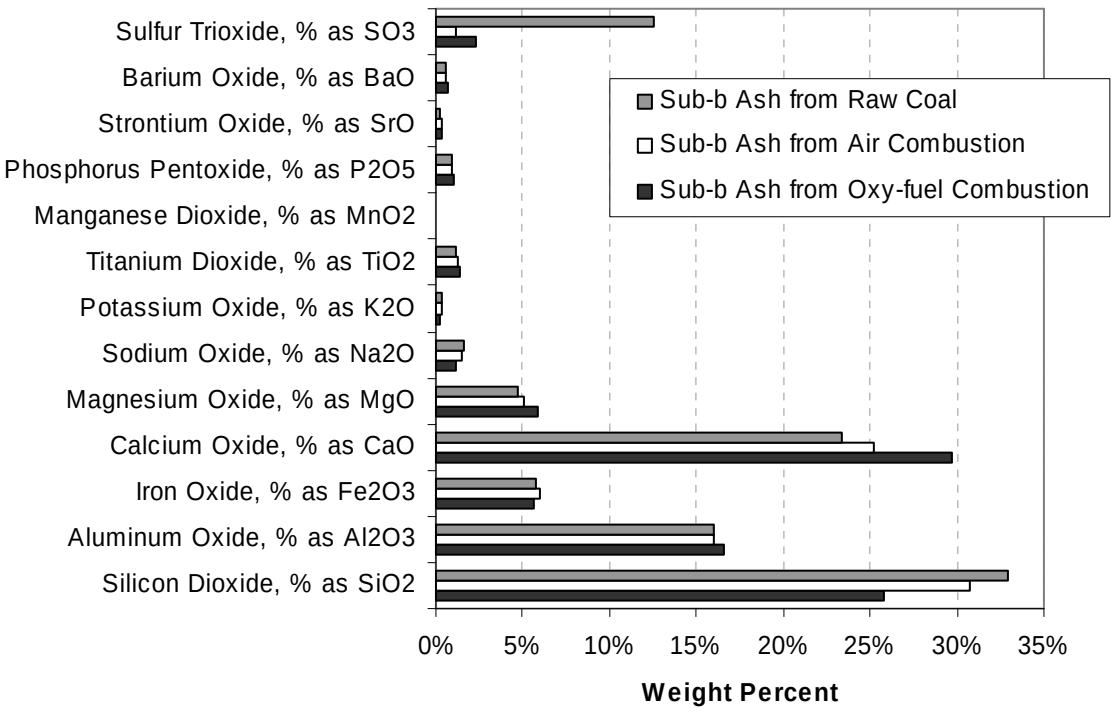

Figure 39. Mineral ash analysis from the parent sub-bituminous coal, and fly ash from air and oxy-fuel staged combustion. The fly ash was obtained from the exhaust system particulate filter. In the oxy-fuel case this was after both O25 and O30 experiments were conducted.

The causes of the NO_X evolution differences between air and oxy-fuel under oxidizer staged combustion were investigated through centerline measurements of NO_X formation and destruction along the length of the reactor. These data make up the remainder of this chapter.

4.3 Gas Species Measurements - Staged Combustion, Fixed Stoichiometry

4.3.1 Pittsburgh #8 Coal

Wall temperature measurements for the Pittsburgh #8 coal are shown in Figure 40. The oxy-fuel case has higher wall temperatures near the burner, lower temperatures

further downstream in the reducing zone, and comparable temperatures to air combustion in the burnout zone.

The oxygen data in Figure 41 (which may be only qualitative as discussed in Section 3.1.7) shows that consumption of oxygen in the primary combustion zone requires some distance downstream from the burner to occur. Some oxygen from burnout oxidizer injection is detected upstream of the injection point, and fairly rapid consumption occurs close to the burnout oxidizer injectors. It appears that little or no combustion occurs further downstream, and the final oxygen levels are consistent with the low level of burnout (Figure 38).

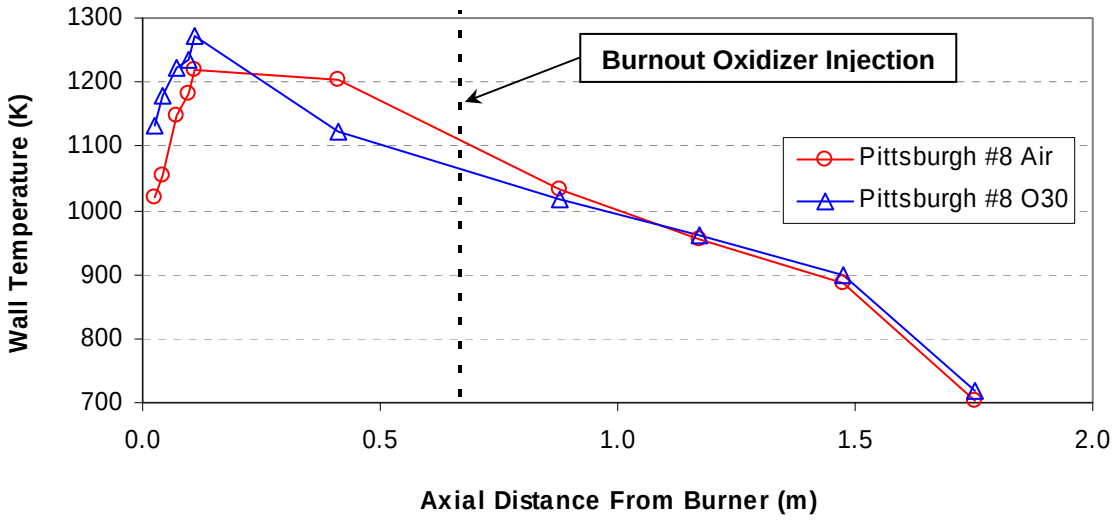

Figure 40. Wall temperature measurements for the Pittsburgh #8 staged combustion experiments.

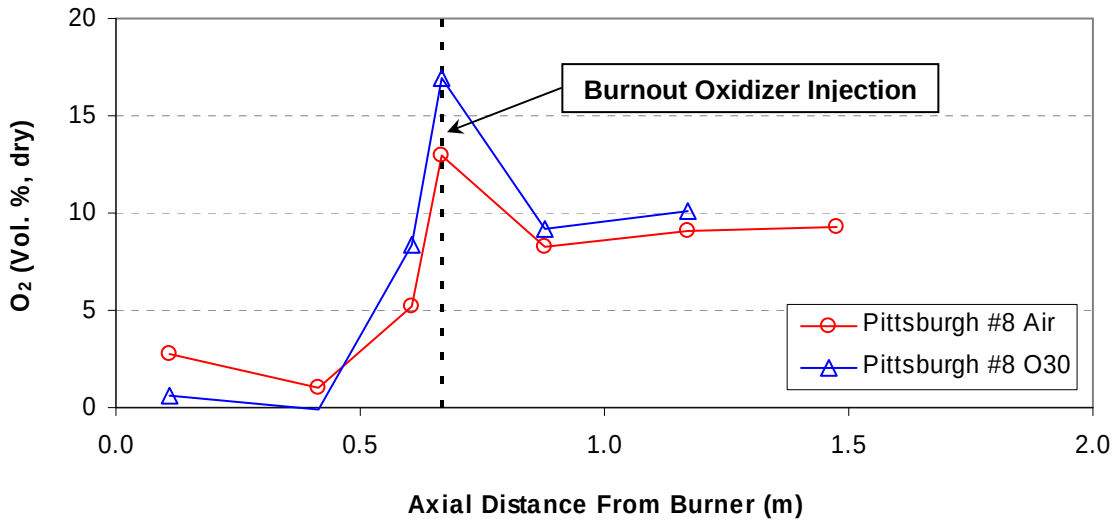

Figure 41. Oxygen measurements for the Pittsburgh #8 staged combustion experiments.

CO measurements (Figure 42) show very high levels of CO (beyond the HORIBA instrument's range of 5000 ppm) in the oxy-fuel reducing zone relative to air combustion. Data downstream of the burnout oxidizer injection are of limited value given the low level of fuel burnout.

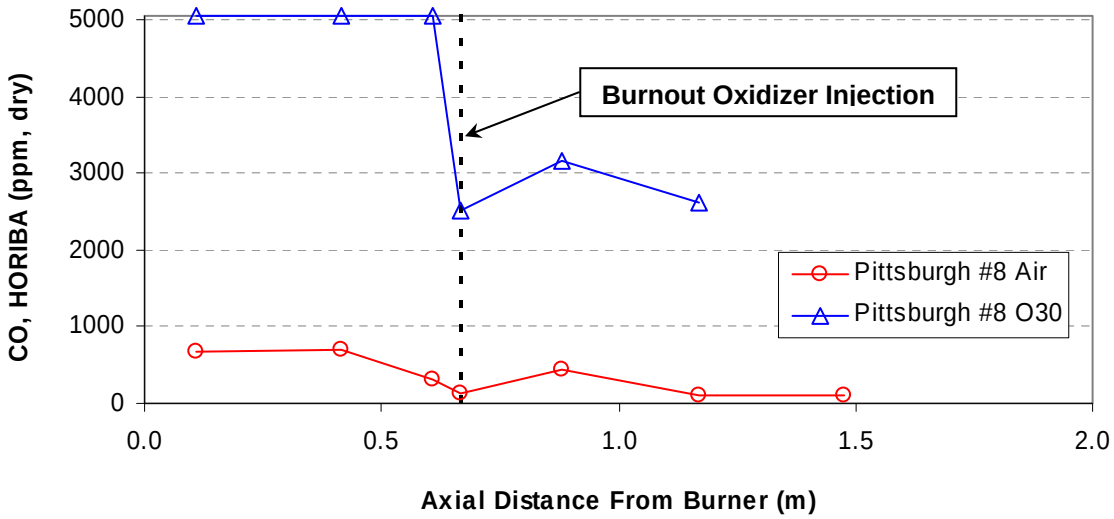

Figure 42. CO data for the Pittsburgh #8 staged combustion experiments.

Measurements of NO_X and corresponding η_N in Figure 43 indicate that the oxy-fuel case produced lower NO_X initially, and had more rapid NO_X destruction prior to burnout oxidizer injection. The air case produced more NO_X than the oxy-fuel case around the burnout injector location, and final NO_X levels were significantly higher than in the oxy-fuel case. The oxy-fuel char retained more nitrogen than the air char (see Figure 38).

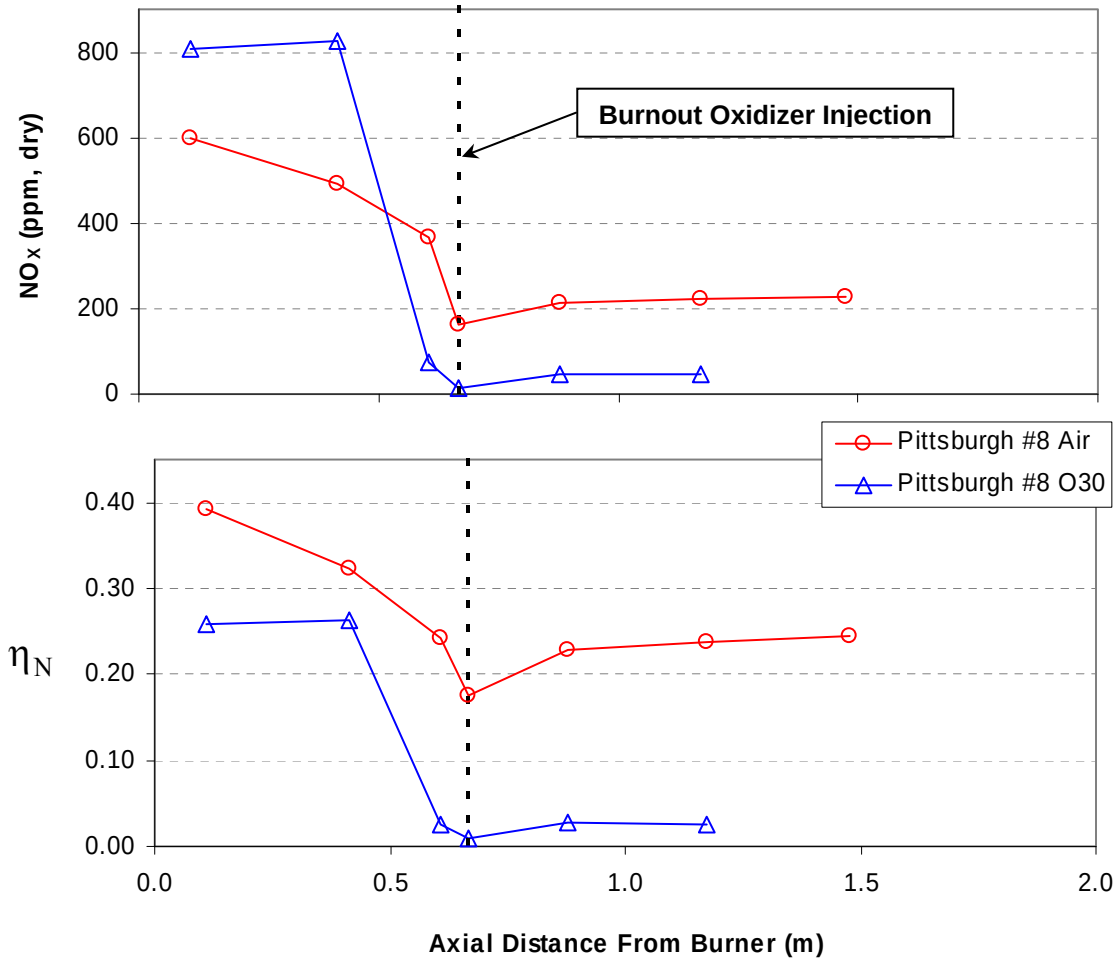

Figure 43. NO_X concentration measurements and corresponding nitrogen conversion efficiency for the Pittsburgh #8 staged combustion experiments (data from HORIBA instrument).

4.3.2 Illinois #6 Coal

Wall temperature profiles and major species (O_2, CO_2, and H_2O) measurements for the Illinois #6 Air and O30 experiments are shown in Figure 44. Like the Pittsburgh #8 wall temperature data the oxy-fuel case relative to air firing has higher temperatures near the burner, cooler temperatures later in the reducing zone and comparable temperatures in the burnout zone.

The O_2 measurements are constant for both air and oxy-fuel cases from 0.2–0.6 m from the burner. Again it is emphasized that these data are qualitative, and thus while the measured value is non-zero, the zero slope over this region in the reactor is believed to indicate that oxygen consumption has stopped due to oxygen being unavailable. Up to 0.2 m from the burner the O_2 appears to be consumed faster in the oxy-fuel case.

The oxy-fuel experiment has higher levels of CO_2 and H_20 as expected with the CO_2 diluent. In the lower half of the reactor the oxy-fuel data show an increase in CO_2 and H_20 while O_2 decreases, consistent with char oxidation. It is not known why the air experiment does not have these characteristics. For oxy-fuel, the sum of O_2, CO_2, and H_2O concentrations is roughly 100% at the exit of the reactor.

Carbon combustion intermediate species (CO, CH_4, and C_2H_4) measurements are presented in Figure 45. The uppermost plot in the figure of CO data measured on a dry basis was limited by the HORIBA instrument to 5000 ppm, but this plot shows better resolution of lower CO levels in the burnout zone than can be seen in the second CO plot obtained from the MKS FTIR instrument. Effluent CO levels are comparable between air and oxy-fuel, but CO is significantly higher in the reducing zone for the oxy-fuel case, at nominally the same SR. CH_4 was only detected for the air case near the burner and could be methane from the natural gas supplied to the burner or from the coal volatiles.

Ethylene (C_2H_4) was detected in higher concentrations in oxy-fuel over most of the reactor. With the exception of the data point at about 45 ppm there appears to be a trend of decreasing ethylene with distance from the burner in the reducing zone.

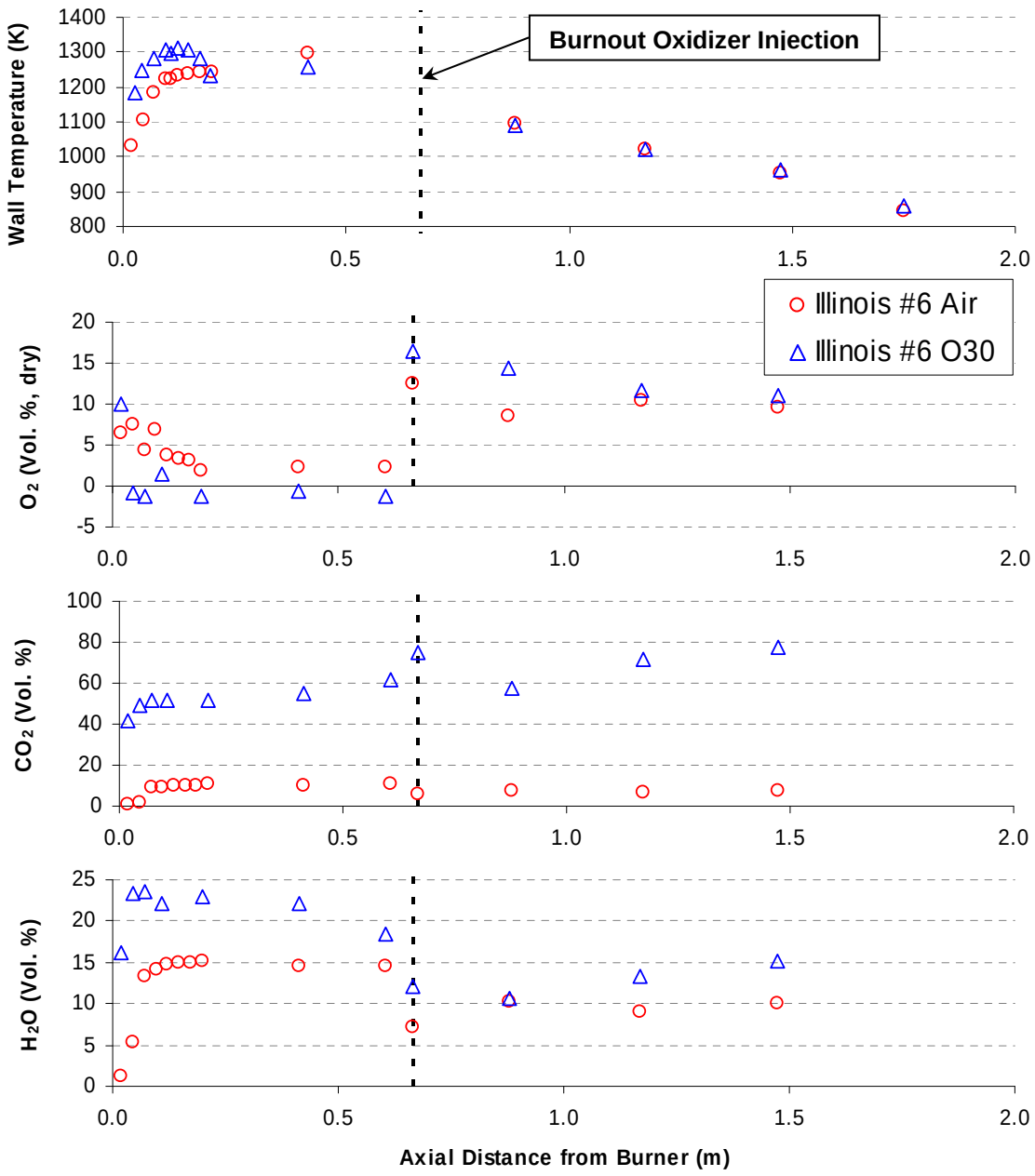

Figure 44. Wall temperatures and major species measurements for the Illinois #6 staged combustion experiments.

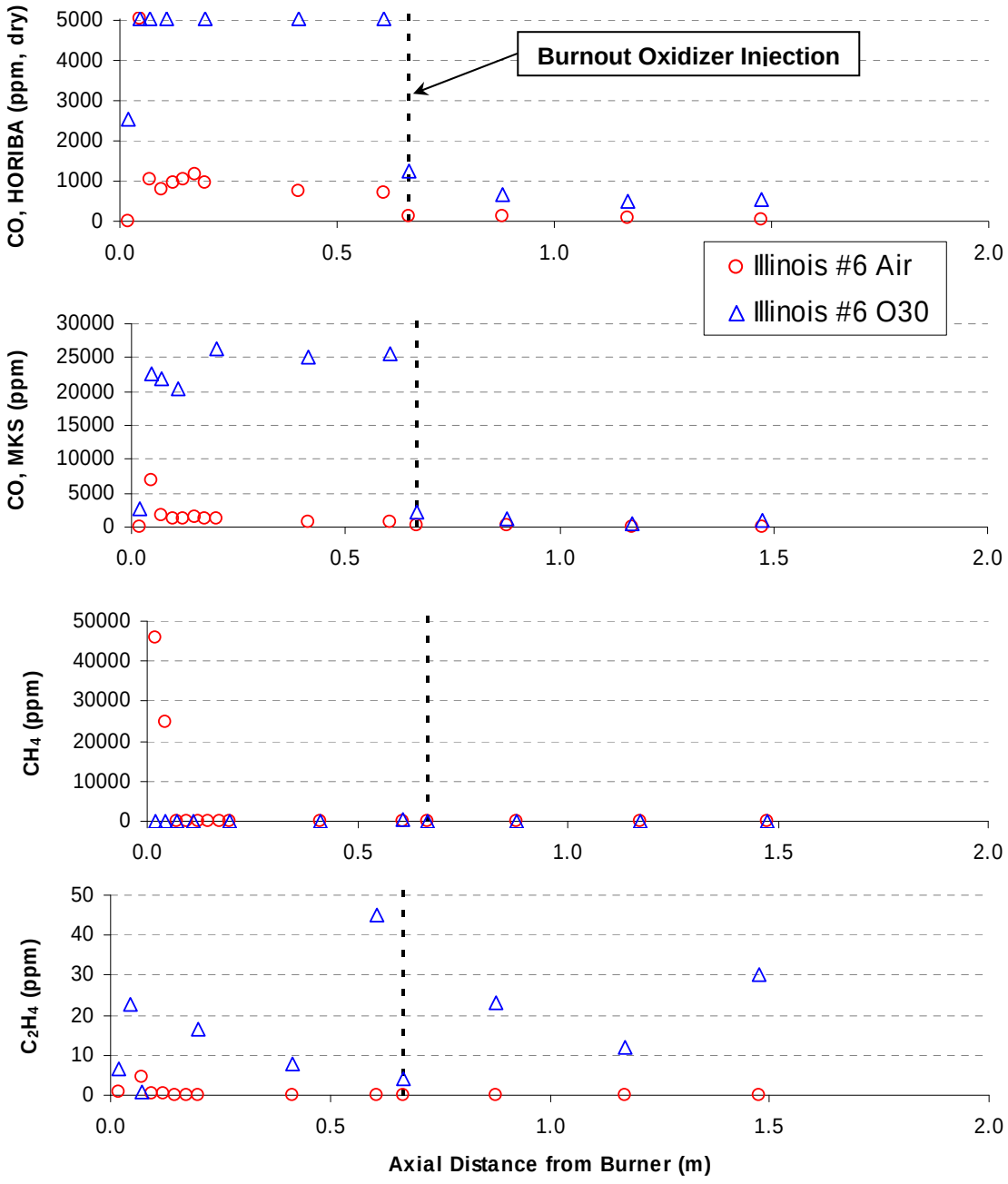

Figure 45. Carbon combustion species for the Illinois #6 staged combustion experiments.

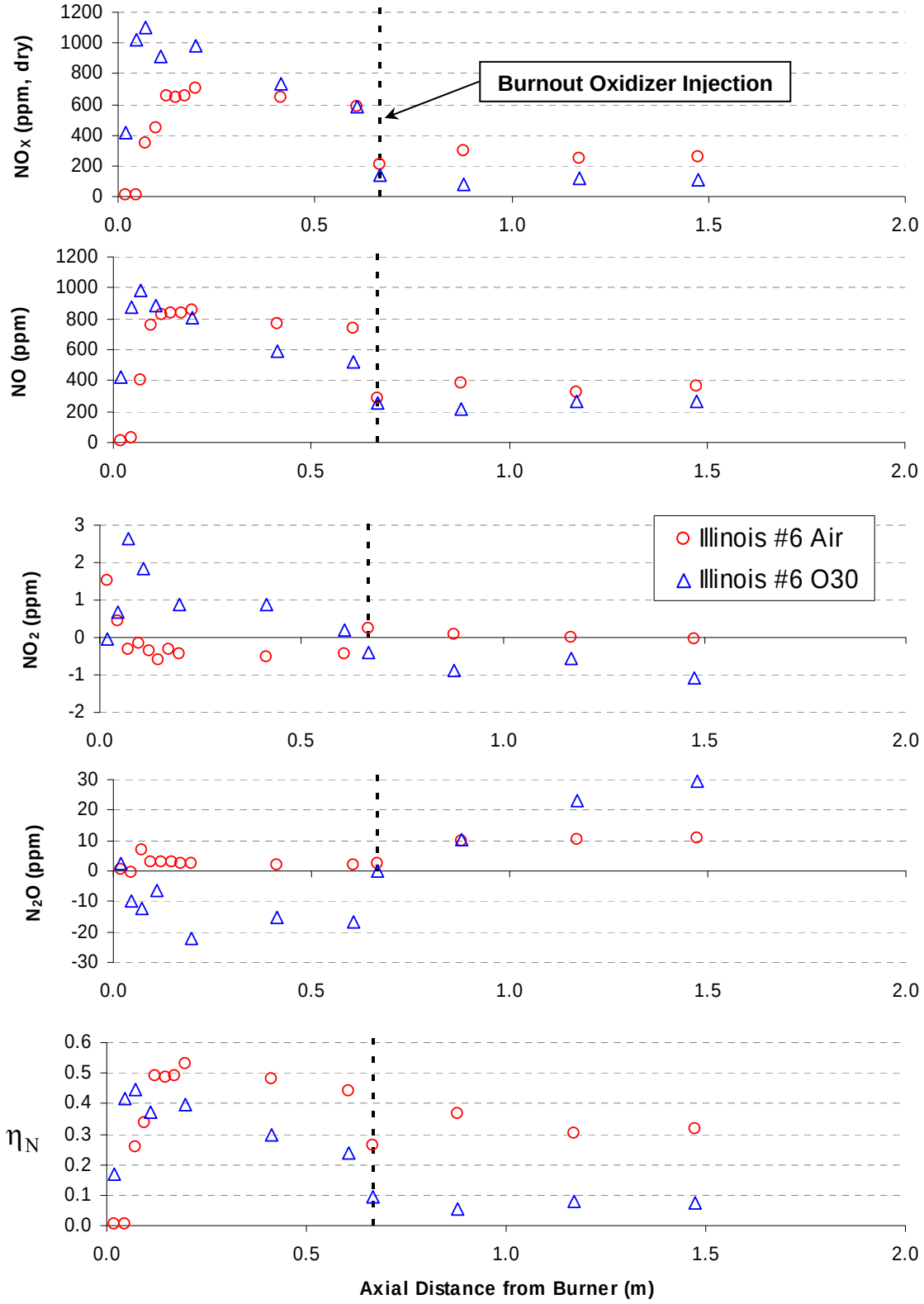

Figure 46. Nitrogen oxides measurements for the Illinois #6 experiments. Nitrogen conversion efficiency was calculated from the HORIBA NO_X data in the top plot.

Measurements of nitrogen oxides in Figure 46 show that the NO_X is predominantly NO. N_2O and NO_2 are in lower concentrations and the measurements have low signal-to-noise ratio as demonstrated by the negative values reported by the instrument. The NO_X data for air show a rapid rise in NO_X after the burner followed by a slower rise before the decline in NO_X associated with the reducing zone. The oxy-fuel case in contrast shows only the rapid rise followed by a decline that is more rapid than that observed for air. At the point of burnout oxidizer injection the air case forms some NO_X but the oxy-fuel case does not. With these differences the oxy-fuel case produced lower effluent NO_X despite the similarity in the initial rapid NO_X formation between air and oxy-fuel seen in the η_N plot at the bottom of the figure.

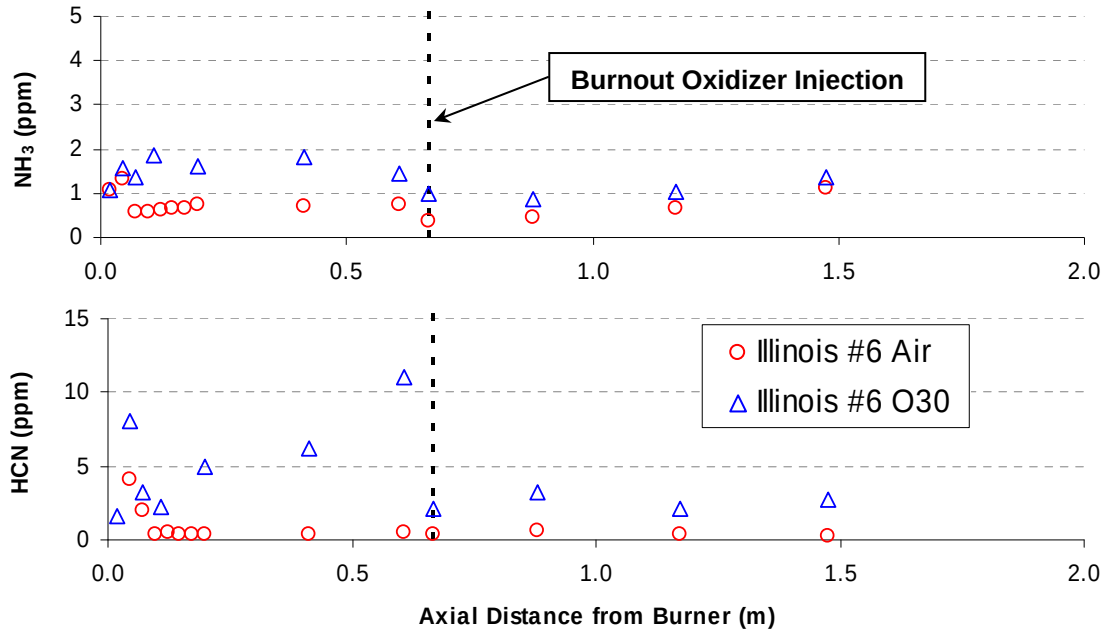

Figure 47. Nitrogen intermediates NH_3 and HCN for the Illinois #6 staged combustion experiments.

Concentrations of the nitrogen intermediate species HCN and NH_3 are plotted in Figure 47. Both species are in low concentrations although higher values were measured under oxy-fuel conditions. For the air case the highest values occur nearest the burner where as for oxy-fuel, HCN and NH_3 are found in measurable amounts throughout the region upstream of burnout oxidizer injection.

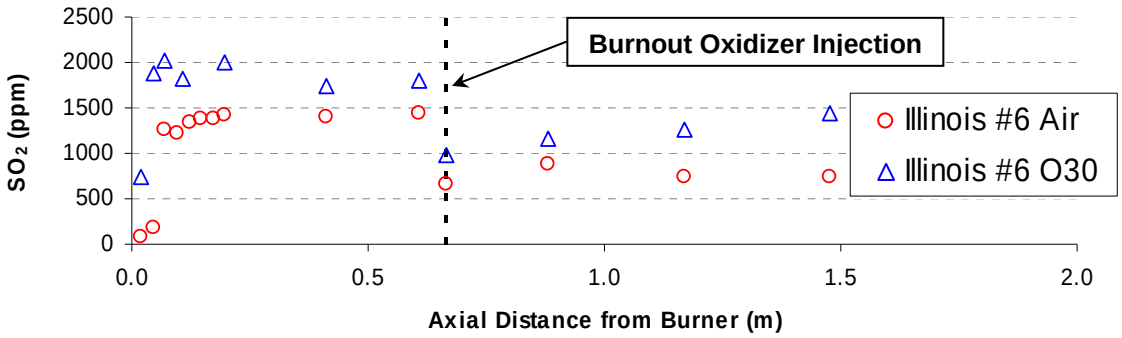

Figure 48. SO_2 concentrations measured in the Illinois #6 staged combustion experiments.

SO_2 concentrations were slightly higher in the oxy-fuel case as shown in Figure 48. It should be noted that these experiments were performed with oxidizer from bottled gases rather than flue gas recycling and thus the values are not representative of SO_2 concentrations to be expected in an industrial situation with a true recycle stream. The increased concentrations are primarily due to lower volumes of diluent (CO_2) in oxy-fuel relative to the N_2 in air. It is noted that unlike NO_X, SO_2 is not reduced in the reducing zone. Because of this behavior SO_2 is not amenable to control by combustion modifications and flue gas treatment is necessary. The drop in SO_2 at 0.67 m from the burner is due to the dilution of the combustion gases with burnout oxidizer.

4.3.3 Illinois #6 Coal with NO in Reactants

The effect of recycled NO on nitrogen evolution was investigated by replacing the CO_2 in the oxidizer with a mixture of 525 ppm NO in CO_2. NO_X was measured with and without NO in the oxidizer with results shown in Figure 49 and Figure 50. A line representing the difference between the two data has been added to assist in evaluating the data. As a result of dilution of the doped CO_2 with oxygen and natural gas, the gas mixture entering the reactor, has 308 ppm more NO than the pure CO_2-based mixture. At the first measurement location, the difference has decreased to only 253 ppm. Since the concentration of NO_X, at the first measurement position is higher than the incoming concentration it appears that NO_X formation is slower or inhibited by NO in the oxidizer. The difference continues to decrease monotonically during a period when both experiments show NO_X reduction. NO_X reduction therefore appears to increase with the presence of NO in the oxidizer. Both of these observed trends are consistent with the rate of NO_X destruction reactions being proportional to NO_X concentration. The rise in NO between 0.41 and 0.6 m from the burner is largely associated with transport of NO upstream from the burnout oxidizer. Evidence of upstream transport is also demonstrated by the increase in O_2 measured over the same space as shown in Figure 50.

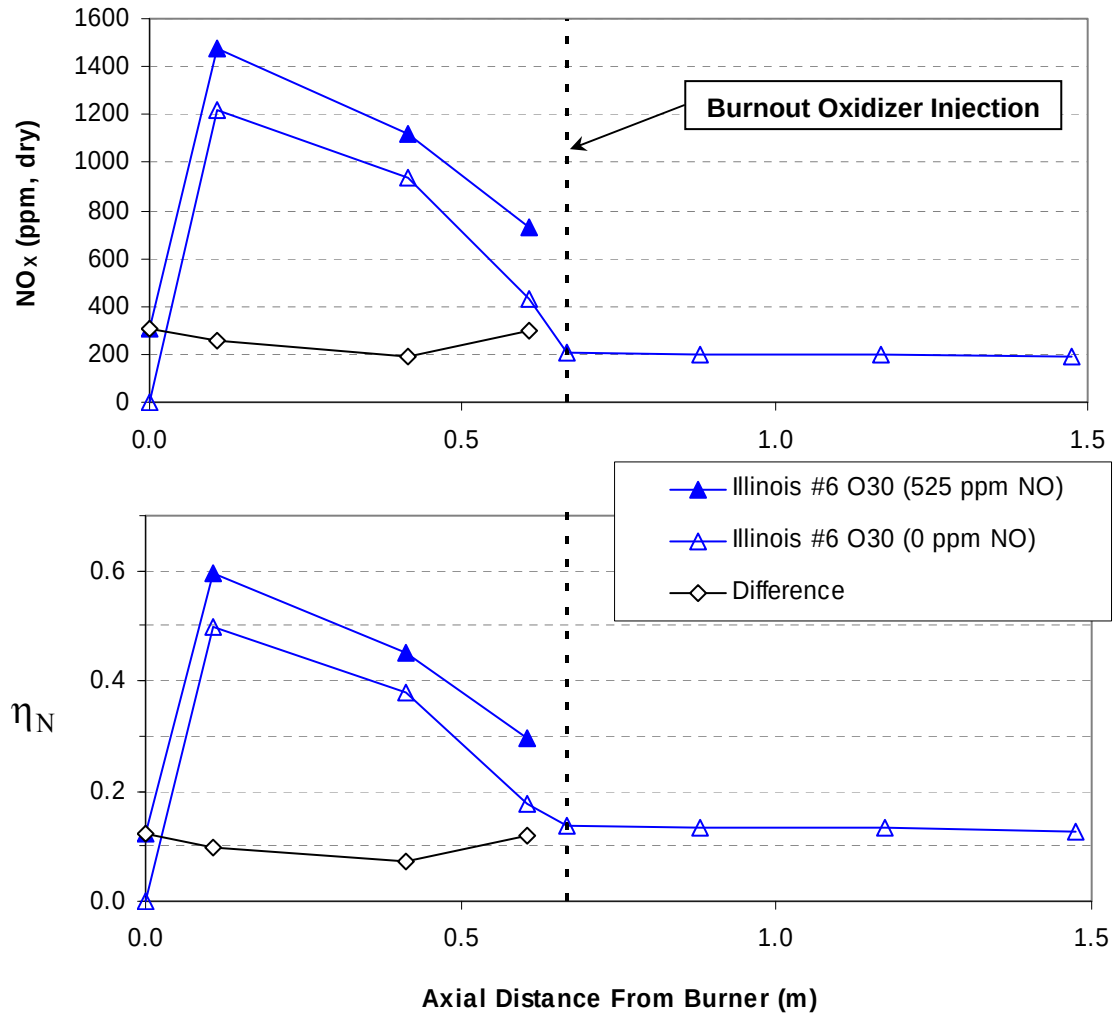

Figure 49. NO_X measurements and nitrogen conversion efficiency with and without NO in the reactants for Illinois #6 coal. Values at 0 m from the burner are calculated from the measured reactant flows as opposed to being directly measured. All data from the HORIBA instrument.

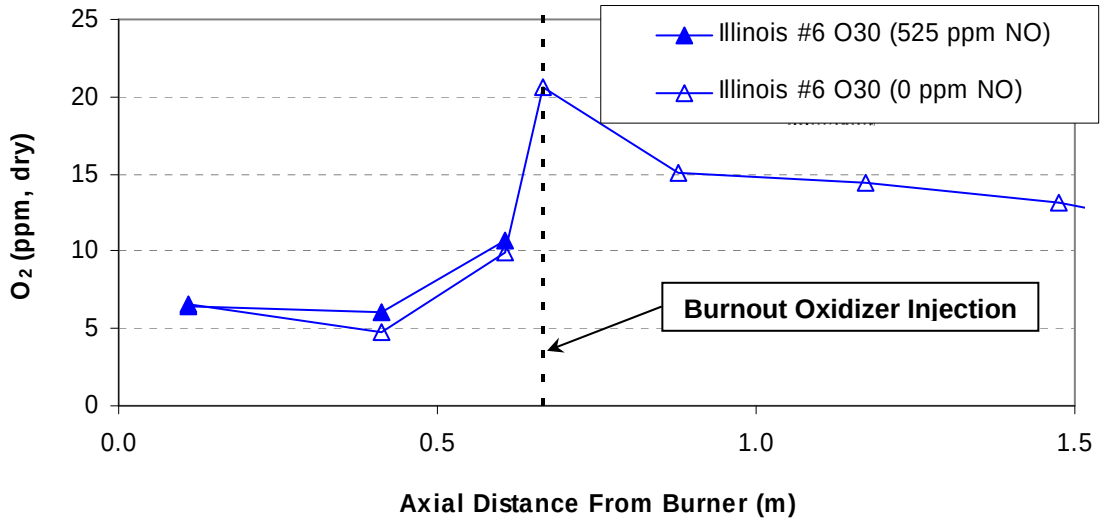

Figure 50. Oxygen concentration measurements for the Illinois #6 experiments with and without NO in the reactants. Note that this data is only qualitative.

4.3.4 Sub-bituminous Coal

Wall temperature and major species data for the sub-bituminous coal staged combustion experiments are shown in Figure 51. Like the two other coals the wall temperatures near the burner are comparable or higher in oxy-fuel than air combustion, and lower in the reducing zone. Unlike the other two coals the oxy-fuel wall temperatures are higher than air combustion in the burnout region.

The O_2 data appear to indicate more rapid consumption of O_2 near the burner in the oxy-fuel cases. CO_2 and H_2O concentrations are higher in oxy-fuel than air cases. For all data the O25 and O30 oxy-fuel cases are more similar to each other than either is to the air case. Beyond these points there is nothing remarkable about the major species data.

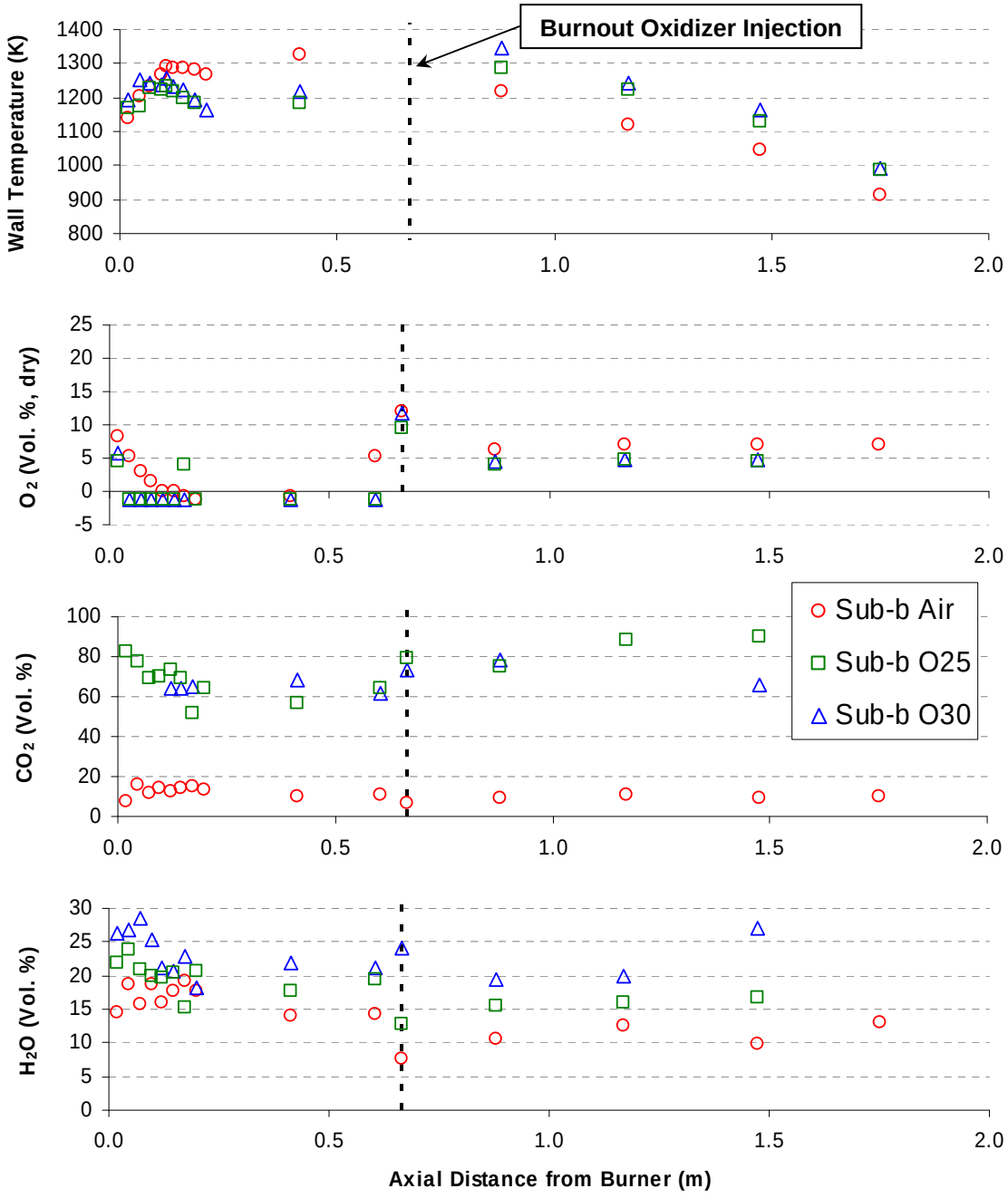

Figure 51. Wall temperatures and major species measurements for the sub-bituminous coal staged combustion experiments.

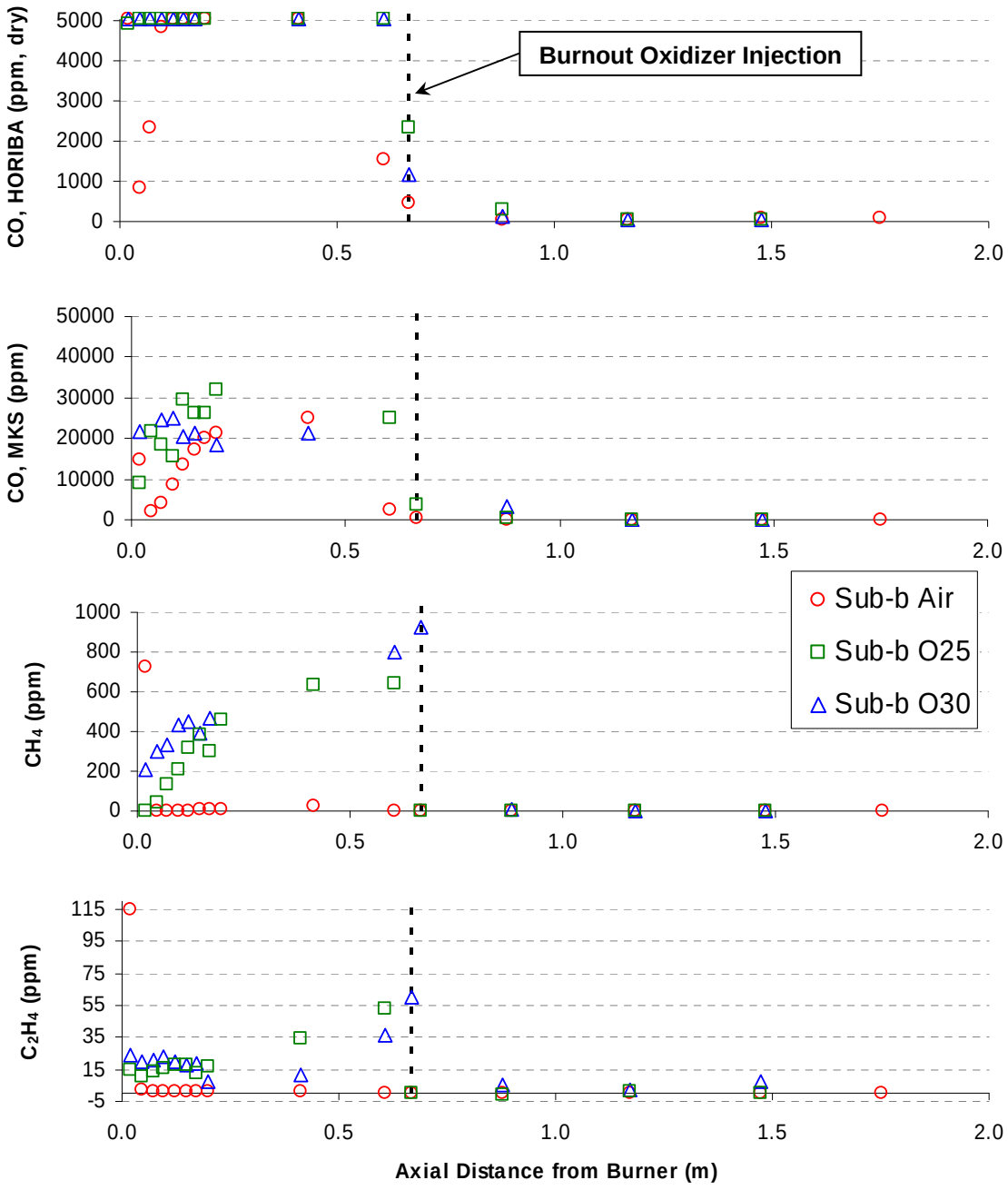

Figure 52. Carbon combustion species for the sub-bituminous coal staged combustion experiments.

CO, methane, and ethylene data are plotted in Figure 52. For the air case there is a peak in CO just downstream of the burner followed by a low value that rises to levels comparable to those in the oxy-fuel case. For the Illinois #6 coal the air case CO was

quite low relative to the values shown here. The oxy-fuel cases have high CO levels throughout the primary combustion zone. All cases have very low effluent CO.

Methane and ethylene are almost non-existent in the air case except very close to the burner. In contrast the oxy-fuel cases have significant amounts of both gases throughout the reducing zone.

Data for the oxides of nitrogen appear in Figure 53. Most features of the data are similar to those observed in the Illinois #6 experiments. The air case has rapid NO formation near the burner followed by slower formation. The oxy-fuel cases also have rapid formation initially, but this is followed by NO_X destruction that begins earlier than in the air case and has a faster rate. NO_X is dominated by NO and the initial levels of rapid NO formation are similar in terms of η_N. Several N_2O data points for the O30 case were discarded as the readings were not steady, despite other species measurements being steady.

Unlike the Illinois #6 coal, effluent NO_X levels for this coal are comparable between air and oxy-fuel. A key difference between the Illinois #6 η_N profile in O30 oxidizer and that of the sub-bituminous coal is the greater formation of NO_X in the sub-bituminous case as burnout oxidizer is injected. In Figure 53 the 18% error bars on the last Air and O30 data points show that the estimated uncertainty is too large to conclude that the oxy-fuel cases produce lower η_N.

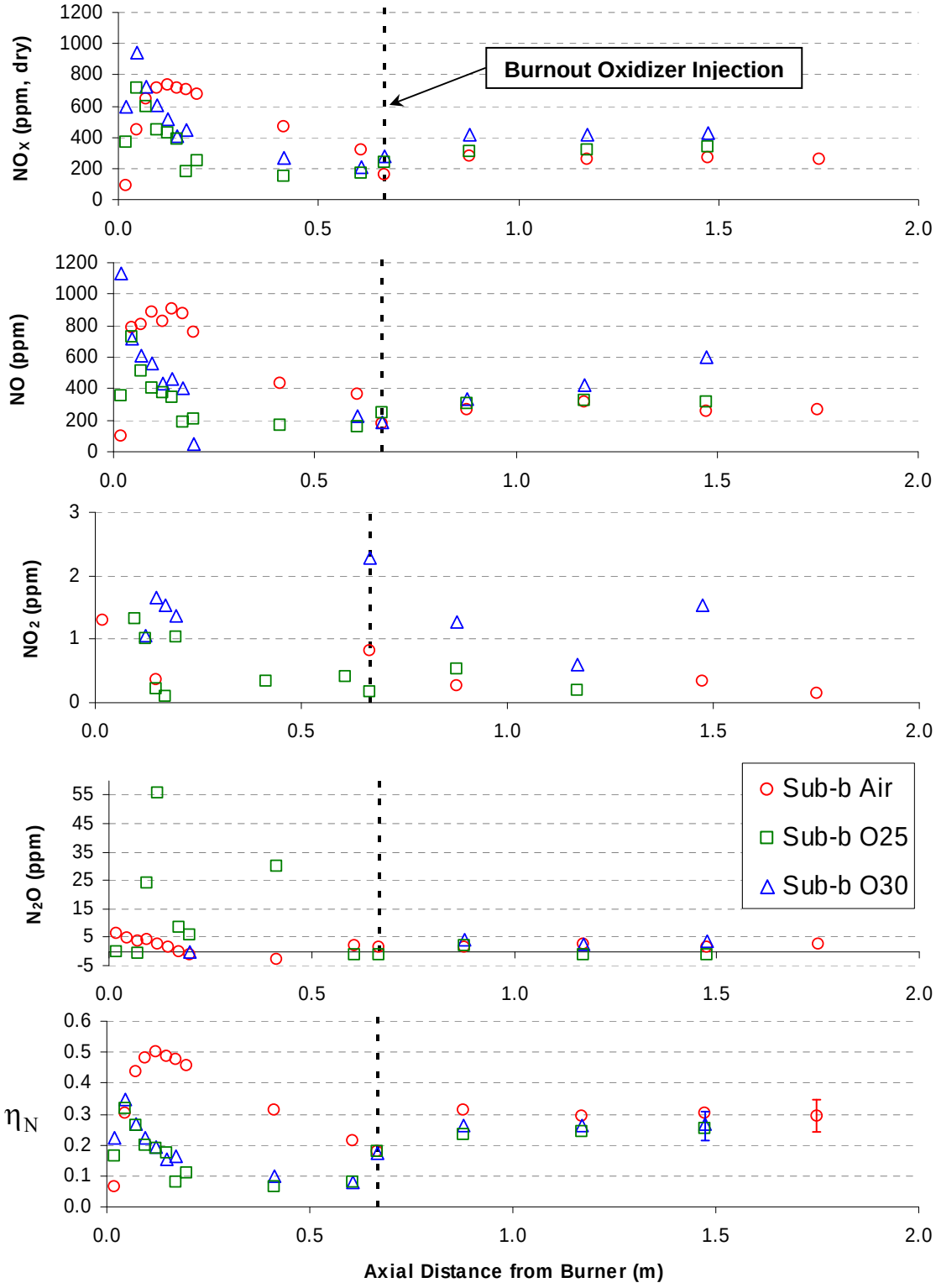

Figure 53. Nitrogen oxides measurements for the sub-bituminous coal experiments. Oxy-fuel data were not taken at 1.75 m from the burner due to experimental difficulties. η_N is calculated from NO_X data in the top plot.

Measurements of the nitrogen intermediates HCN and NH_3 in Figure 54 show that NH_3 is in much greater concentrations with sub-bituminous coal than for Illinois #6. NH_3 tends to increase with distance from the burner. Both HCN and NH_3 are more prevalent in oxy-fuel than air cases. Neither species was detected in significant amounts in the burnout region.

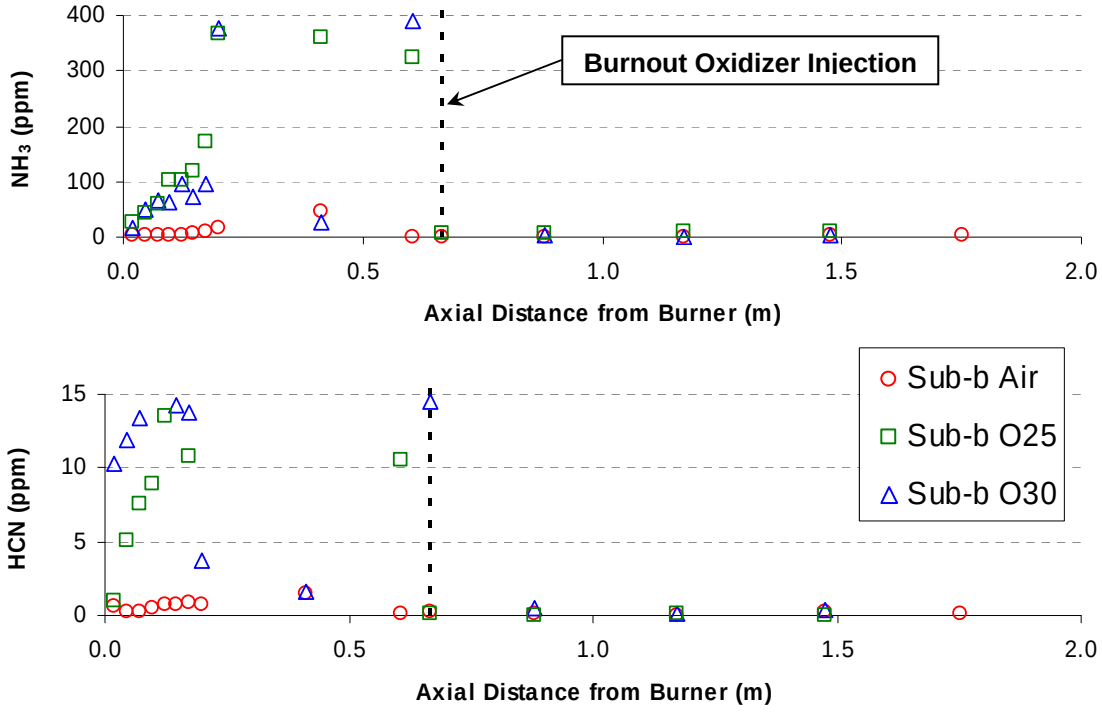

Figure 54. Nitrogen intermediates NH_3 and HCN for the sub-bituminous coal staged combustion experiments.

The results shown up to this point have compared air and oxy-fuel combustion on the basis of identical stoichiometry. In the next section the effect of primary (burner) SR on effluent NO_X was studied. This testing was done to find the conditions for lowest

effluent NO_X in this reactor for air and oxy-fuel so that a detailed comparison could be made of the two combustion types operating under their optimum low-NO_X conditions.

4.4 Effluent NO_X Measurements – Staged Combustion with Varied Stoichiometry

Effluent NO_X as a function of primary zone SR is presented in Figure 55. Total oxidizer flow to the experiment was kept constant while the ratio of primary to burnout oxidizer was changed. As expected there was some level of staging (amount of oxidizer diverted from the burner) that produced minimum NO_X. As primary zone SR decreases, O_2 availability to form NO_X initially is decreased and conditions for NO_X reduction are also created. There is some point however where combustion at the burnout injector location becomes so intense that significant NO_X begins to form and overall NO_X production increases.

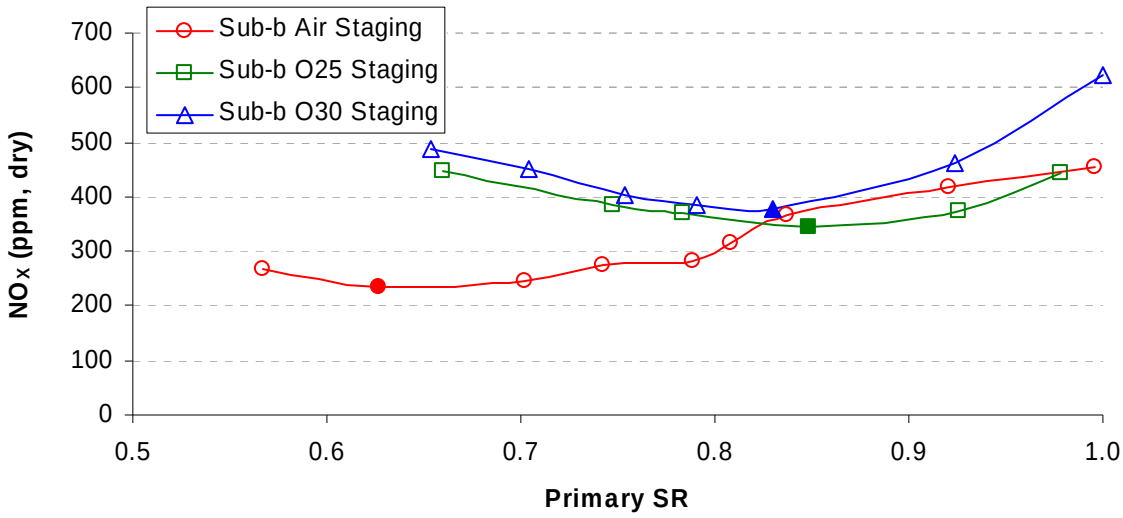

Figure 55. Effluent NO_X measurements for the sub-bituminous coal as a function of primary combustion zone SR.

Figure 56 shows that the primary zone SR for minimum NO_X in oxy-fuel was significantly higher than for air combustion consistent with the higher concentrations of intermediates and more rapid destruction of NO in the reducing zone measured at equal primary SR between air and oxy-firing shown earlier (see Figure 53 and Figure 54). This also suggests that oxy-fuel combustion produces a better reburning environment when NO_X is recycled through the flame in comparison to air combustion. Solid data point markers are used to indicate the conditions of minimum NO_X in the figures. While the minima are similar between oxidizers, at higher values of primary SR, η_N for the oxy-fuel cases are clearly lower than in air at the same primary SR. The data demonstrate that similar η_N can be achieved in air by deeply staging air combustion or staging oxy-fuel combustion to a lesser extent which also favors burnout in oxy-fuel. Note that this is in the absence of recycled NO_X and shows that η_N reduction is favorable in oxy-fuel combustion independent of recycled NO_X. The air combustion NO_X is more sensitive to primary SR than the oxy-fuel cases at high values of primary SR consistent with trends observed by Kiga et al. (1997). As with results already presented there is little difference between the characteristics of the O25 and O30 oxidizers.

Evidence of increased combustion intensity at the location of burnout oxidizer addition as primary SR decreases can be seen in the wall temperature data in Figure 57 through Figure 59. For all three oxidizers the minimum NO_X conditions are at or near the primary SR where wall temperature downstream of burnout oxidizer injection (0.88 m from burner) becomes higher than the wall temperature upstream (0.41 m from burner).

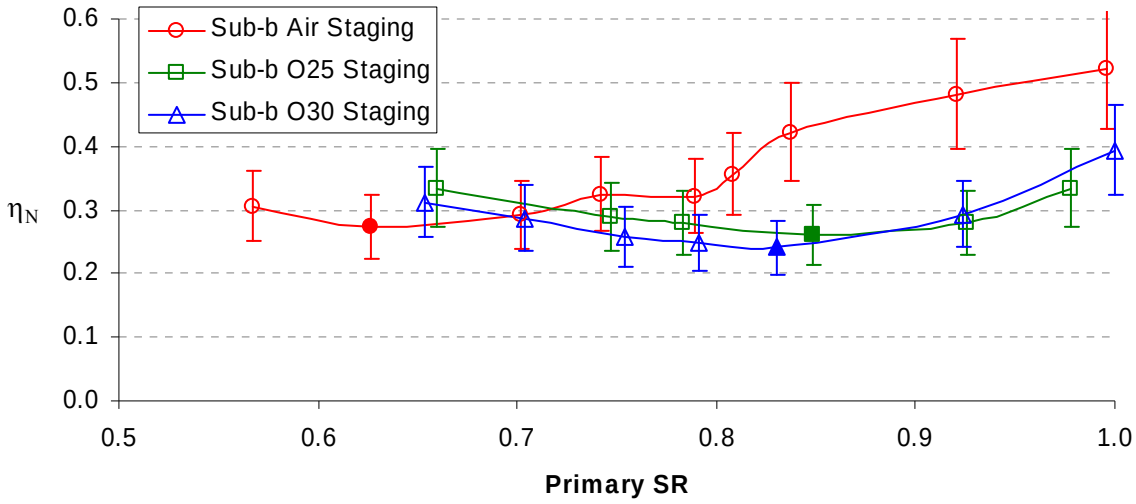

Figure 56. Effluent nitrogen conversion efficiency as a function of primary combustion zone SR. 18% error bars are shown for comparison between Air, O25, and O30. For comparisons within the same oxidizer experiment, the variability is an estimated 5%. An additional 5% uncertainty associated with nitrogen conversion efficiency calculation is not applicable here as the fuel was completely burned for these gas samples.

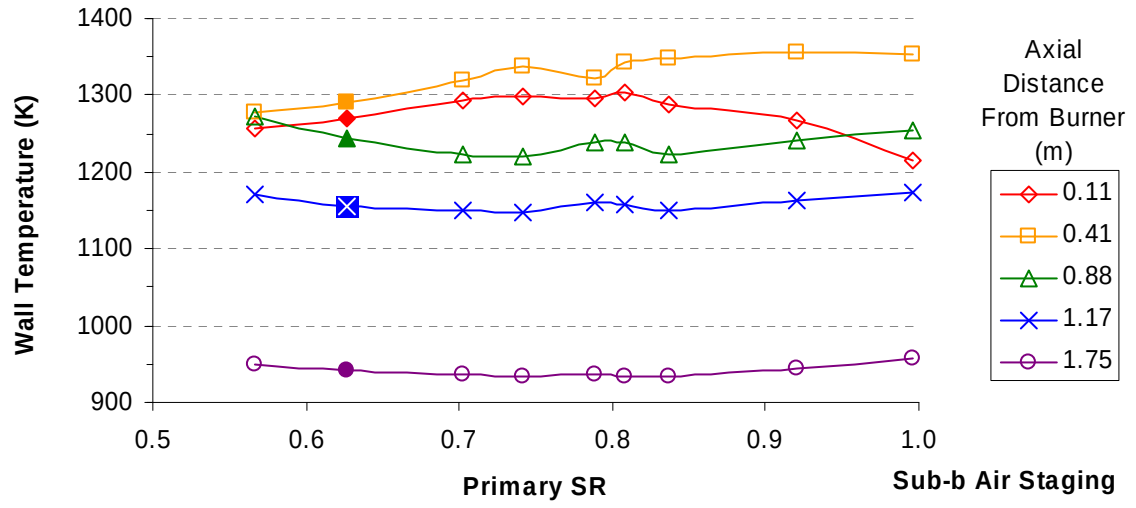

Figure 57. Wall temperature data at various axial locations as a function of primary zone SR for the Sub-b Air Staging experiment.

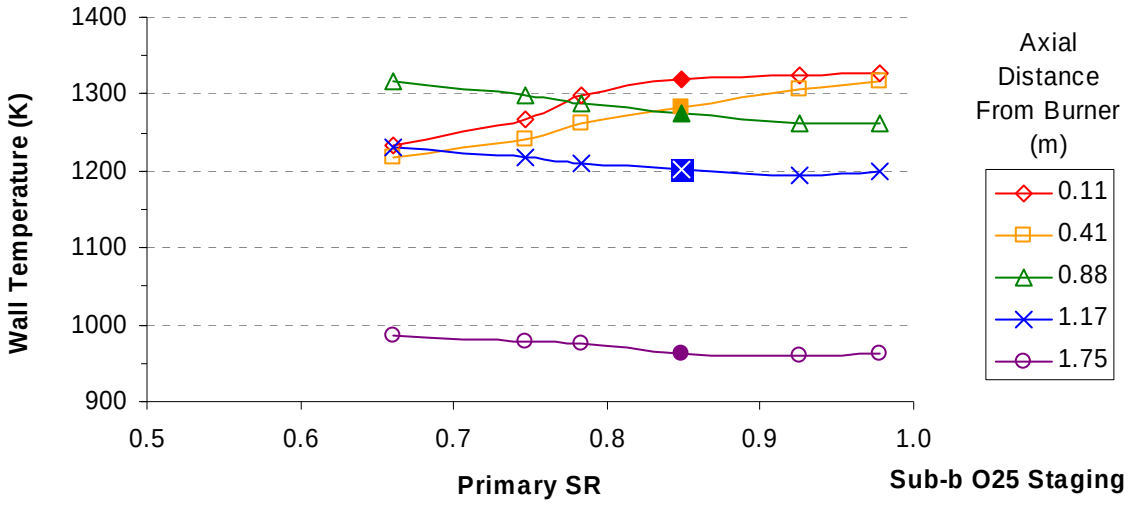

Figure 58. Wall temperature data at various axial locations as a function of primary zone SR for the Sub-b O25 Staging experiment

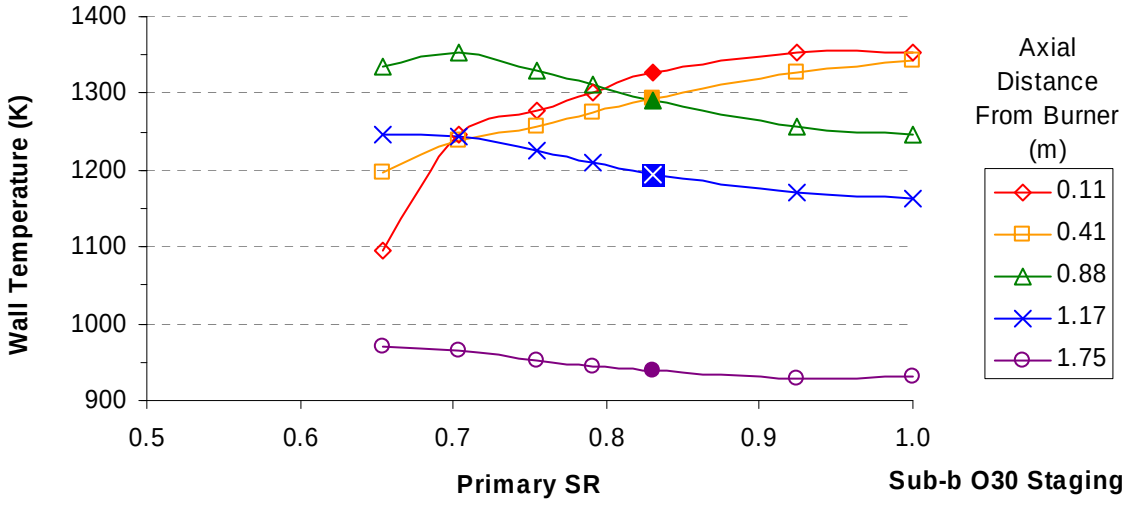

Figure 59. Wall temperature data at various axial locations as a function of primary zone SR for the Sub-b O30 Staging experiment

4.5 Gas Species Measurements - Staged Combustion at Minimum NO_X Conditions

The primary SR's for minimum effluent NO_X that were determined from the results just presented were used to obtain the results reported in this section. High resolution gas sampling measurements and wall temperatures were obtained at these conditions to investigate details of NO_X formation and destruction. Wall temperatures are generally higher overall for the oxy-fuel case as seen in Figure 60. H_2O and CO_2 concentrations in the same figure are also higher for oxy-fuel relative to air combustion as expected. For both air and oxy-fuel the O_2 data near the burner seem inconsistent with neighboring data points and it is hard to tell where the O_2 concentration falls to zero. All of the species data appear to follow trends that do not follow smooth curves but rather show significant scatter among what appears to be clear trends. This reason for this scatter is unexplained but the most likely cause is an unsteady fuel flow rate. From 0.25 m from the burner to the point of burnout oxidizer injection it appears that O_2 is unavailable in both cases.

CO, methane, and ethylene data in Figure 61 show similar trends for the air and oxy-fuel cases in the reducing zone. Oxy-fuel concentrations are typically lower for methane and ethylene, but considering both the differences in molecular weight of the oxidizers, and in primary SR, differences in total mass of CO, methane and ethylene are difficult to judge. The oxy-fuel conditions appear to produce NO_X reduction of a similar quantity to air combustion (Figure 62) even though species indicating the strength of the reducing environment are of similar or lower concentrations.

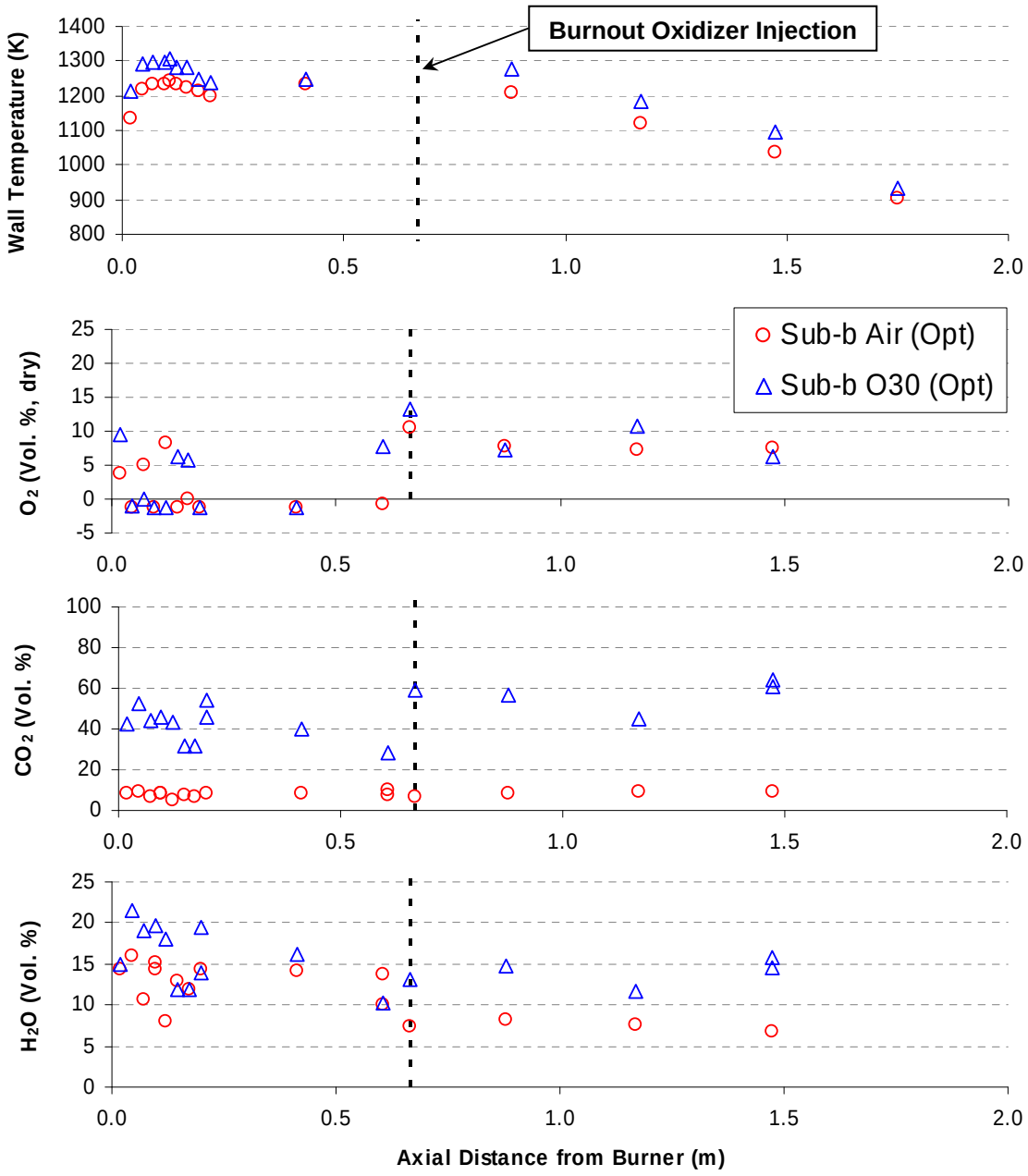

Figure 60. Wall temperatures and major species measurements for the sub-bituminous coal staged combustion experiments at minimum NO_X conditions.

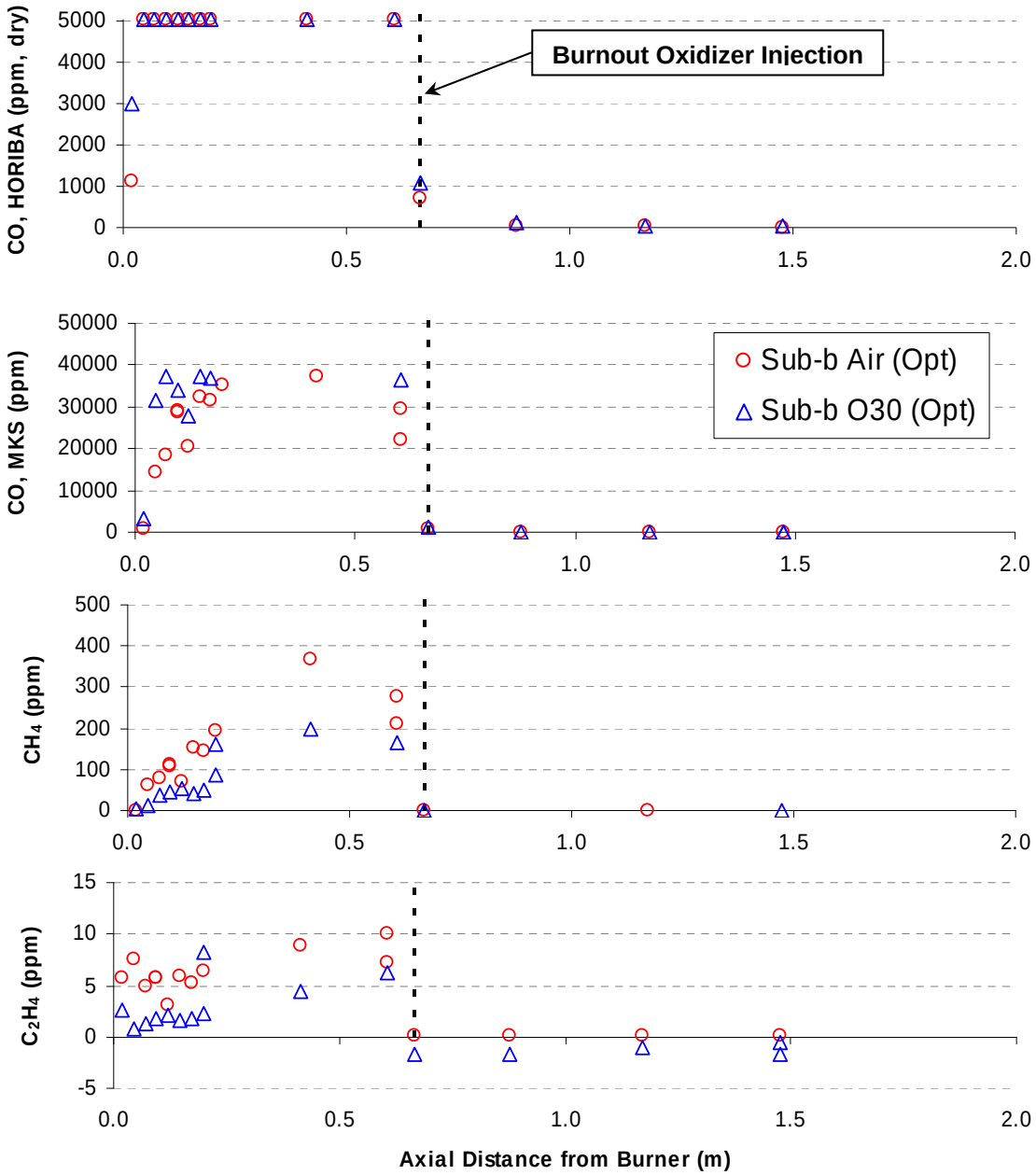

Figure 61. Carbon combustion species for the sub-bituminous coal staged combustion experiments at minimum NO_X conditions.

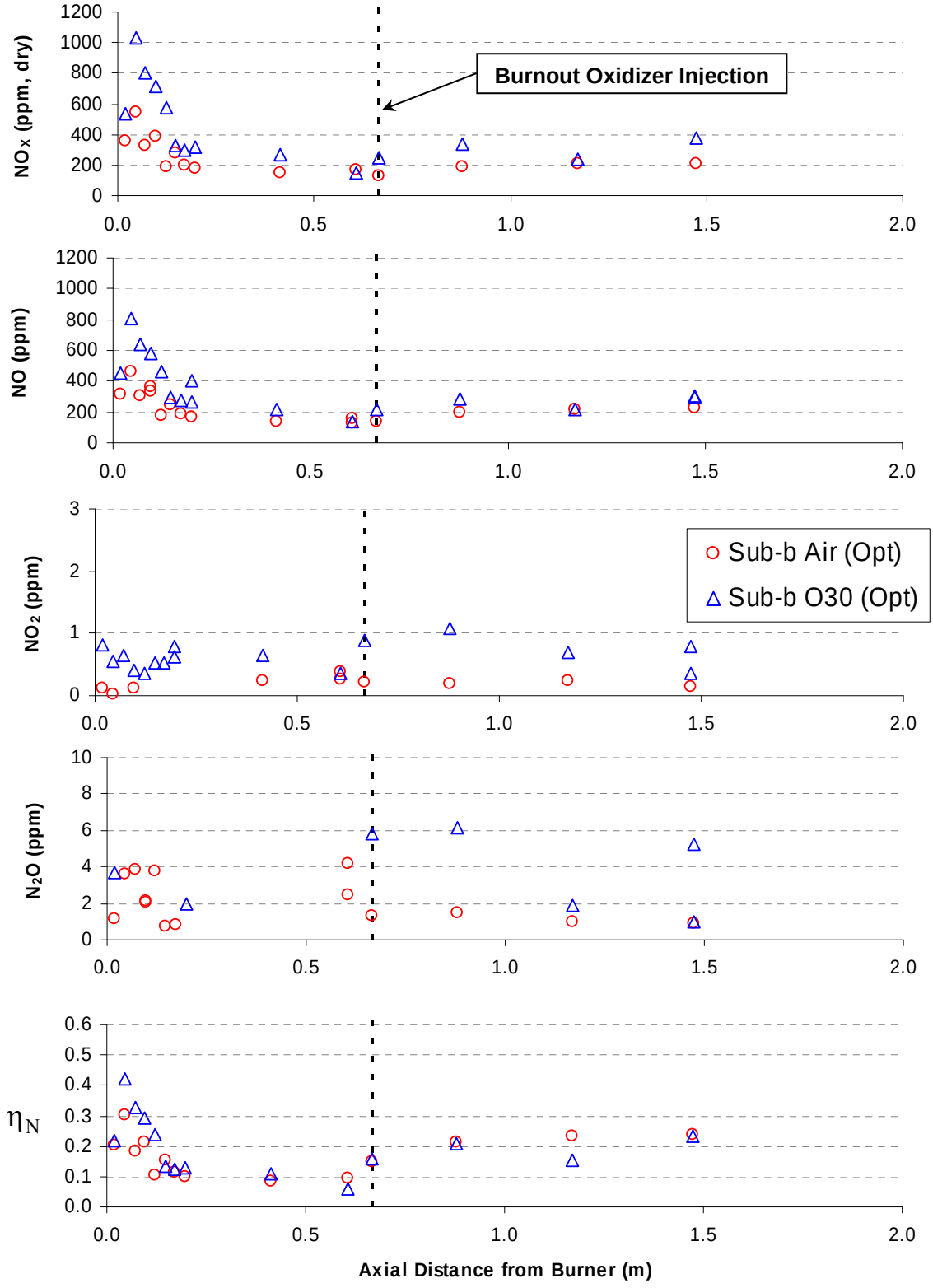

Figure 62. Nitrogen oxides measurements and associated nitrogen conversion efficiency for the sub-bituminous coal experiments at minimum NO_X conditions. Nitrogen conversion efficiency is calculated from the HORIBA NO_X data in the top plot. All other data are from the MKS FTIR.

As with data presented previously, the NO_X measurements in Figure 62 show NO to be the major nitrogen oxide product. Both air and oxy-fuel cases exhibit rapid initial NO_X formation followed by fairly rapid destruction. Any changes in η_N over the lower two-thirds of the reducing zone are much less significant. A notable difference between these data and those shown previously is that the air case here does not have the slow NO_X formation after initial rapid formation. Concentrations of NO are higher in the oxy-fuel case, but in terms of η_N the two cases are quite similar. It is also interesting to note that both cases appear to form some NO_X at the point of secondary oxidizer injection indicating the minimum NO_X occurs even though some NO_X is produced at this location.

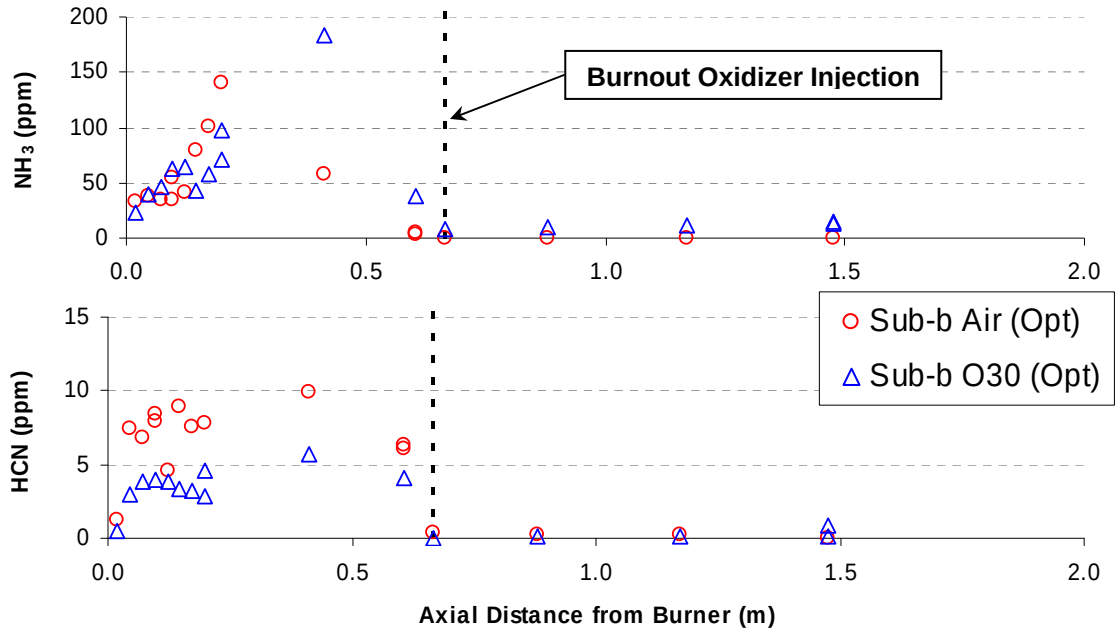

Figure 63. Nitrogen intermediates NH_3 and HCN for the sub-bituminous coal staged combustion experiments at minimum NO_X conditions.

NH_3 concentrations are also similar between air and oxy-fuel combustion as seen in Figure 63. The concentration of NH_3 increases as NO (Figure 62) decreases up to 0.2 m from the burner. Over this same space the HCN concentration is roughly constant. NH_3 is in higher concentrations than HCN (by a factor of 10). The HCN data show low levels between 5 and 10 ppm but they are about twice as high in the air case. As for other experiments these species are only detected upstream of burnout oxidizer injection.

5 Computational Modeling Results

5.1 Equilibrium Calculations

If the NO chemistry was sufficiently fast and radicals were available, the concentration of NO would reach equilibrium. Equilibrium NO_X levels therefore indicate a limit on NO_X reduction by alterations to stoichiometry and temperature. Figure 64 illustrates the trends in equilibrium NO_X as a function of SR and temperature for air and oxy-fuel mixtures. These results were calculated using the NASA-Glenn CEA2 equilibrium code.

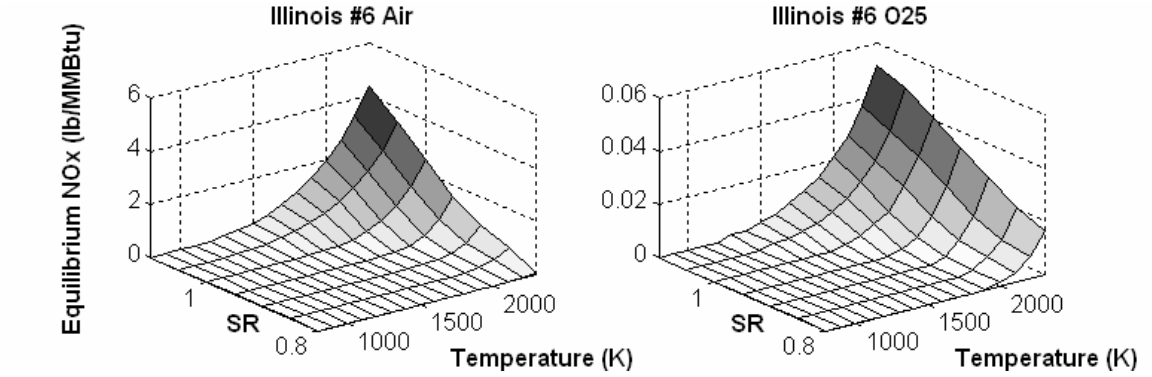

Figure 64. Equilibrium NO_X as a function of temperature and stoichiometry. Note the difference in the vertical scales.

As can be seen in the figure, high levels of NO_X are favored by high temperature, fuel-lean (high SR) conditions for both air and oxy-fuel combustion. The equilibrium levels however are almost two orders of magnitude lower in oxy-fuel than air.

Often in combustion modeling it is assumed that major combustion products have fast chemistry and react to equilibrium as rapidly as the reactants are mixed. NO_X formation on the other hand is characterized by finite rate chemistry and it is kinetic considerations that determine the level of NO_X. The computational model described in Section 3.2 was used to calculate the concentrations of NO predicted by kinetics (using the GRI-Mech 3.0 mechanism) for the Sub-b Air and Sub-b O30 experiments. These predictions are compared to equilibrium NO values and experimental data in Figure 65 and Figure 66.

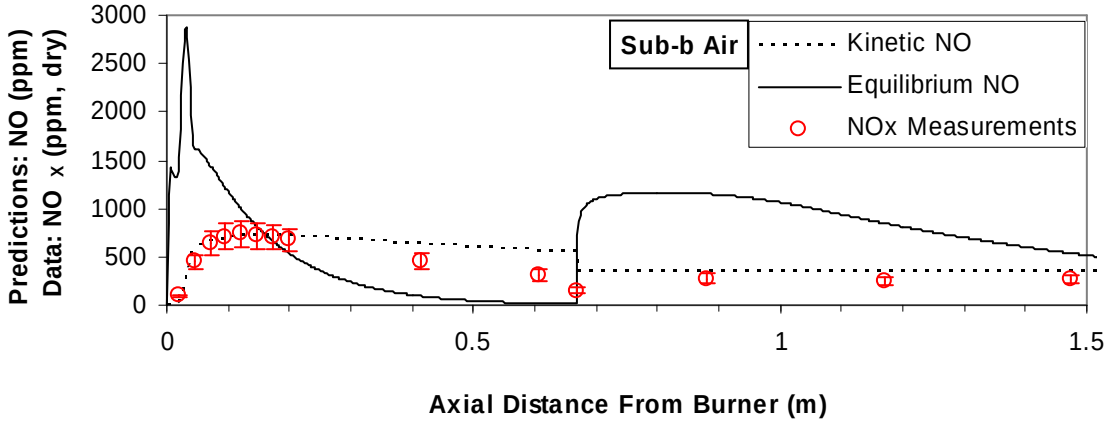

Figure 65. Comparison of experimental NO_X data (HORIBA) with finite rate chemistry model predictions (Kinetic NO) and associated equilibrium NO levels for staged air combustion.

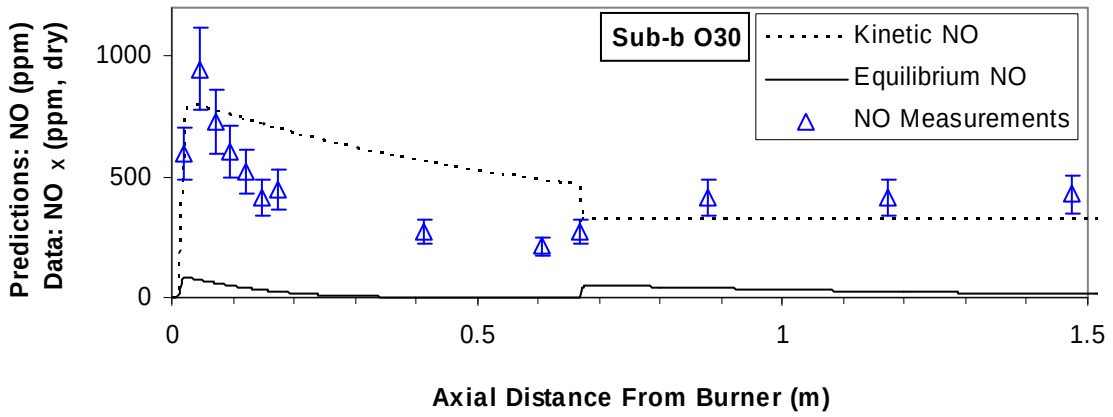

Figure 66. Comparison of experimental NO_X data (HORIBA) with finite rate chemistry model predictions (Kinetic NO) and associated equilibrium NO levels for staged oxy-fuel combustion.

In terms of the shape of the NO_X profile near the burner Figure 65 and Figure 66 show good agreement between kinetic predictions and experimental data. In the air case (Figure 65) the rapid initial NO formation and the slow NO formation that follows occur while NO is at sub-equilibrium levels. Once equilibrium NO levels fall below the actual concentration the decrease in NO begins. The model however suggests that NO reduction is limited by reaction rates and although there is a reduction in NO, it cannot follow the equilibrium curve and NO is frozen at super-equilibrium values for the latter part of the reducing zone.

In the oxy-fuel case the equilibrium NO is at all locations lower than the kinetically-computed and experimental values. This may partially explain why the slow formation of NO after rapid initial formation does not occur in the oxy-fuel cases. The initial formation of super-equilibrium NO is a result of the finite rate nitrogen chemistry. Some insight into the chemistry can be gained from the reaction pathway diagrams in Figure 67 and Figure 68. These diagrams were generated from the kinetic model predictions using the MixMaster application distributed with the Cantera software.

Figure 67 shows that modeled NO is being formed from N, NH, HNO, and NCO with NCO and HNO being the reactants with the dominant pathways as indicated by the uppermost value in the reaction details next to the respective pathway arrows. The relative width of the arrows also provides an indication of pathway importance.

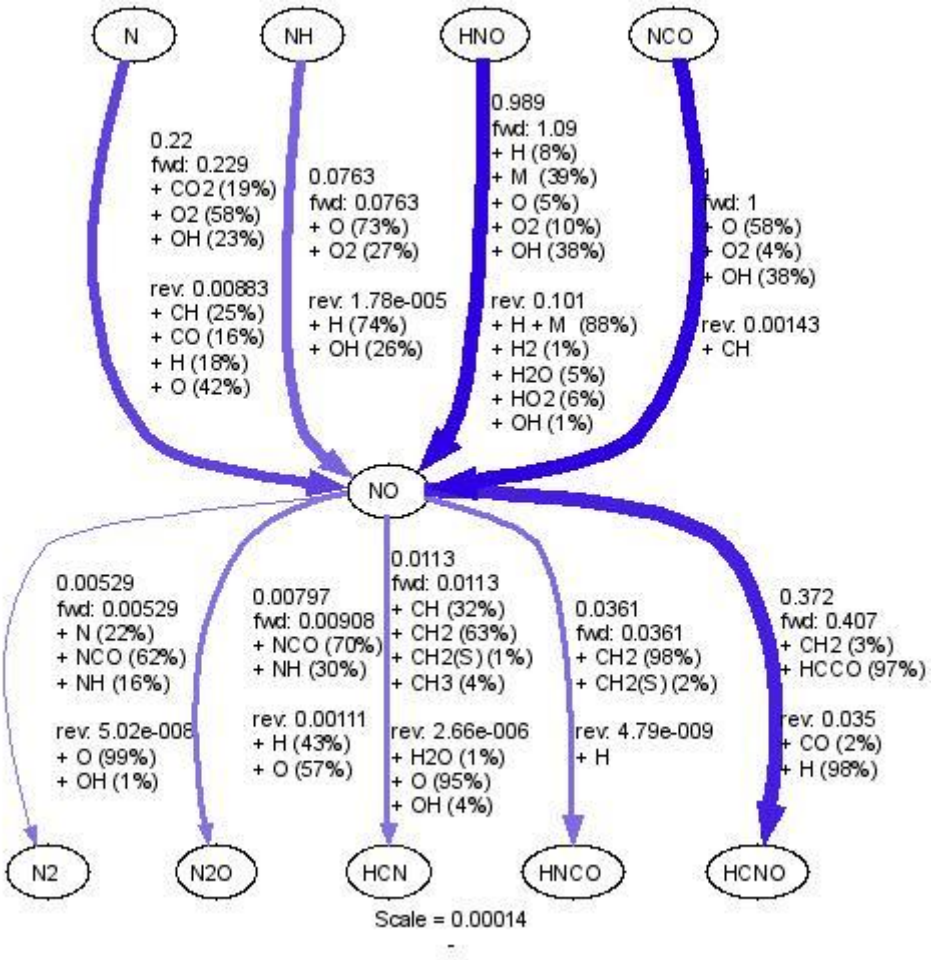

Figure 67. Reaction pathway diagram for NO formation and destruction in the Sub-b O30 model 14 mm from the burner (GRI-Mech 3.0 mechanism).

As indicated in the diagram, NO is also being consumed to form N_2, N_2O, HCN, HNCO, and HCNO. These pathways are of lesser significance at this point in the reactor than the NO formation pathways. In the near-burner region the NO formed is an

intermediate species rather than a final product, but its concentration increases because the reactions producing NO are faster than the reactions that are consuming it. If both reaction sets were fast the NO concentration would remain low.

Figure 68 gives additional insight into the modeled NO formation pathways by showing important nitrogen species in the mechanism including HCN from the volatiles.

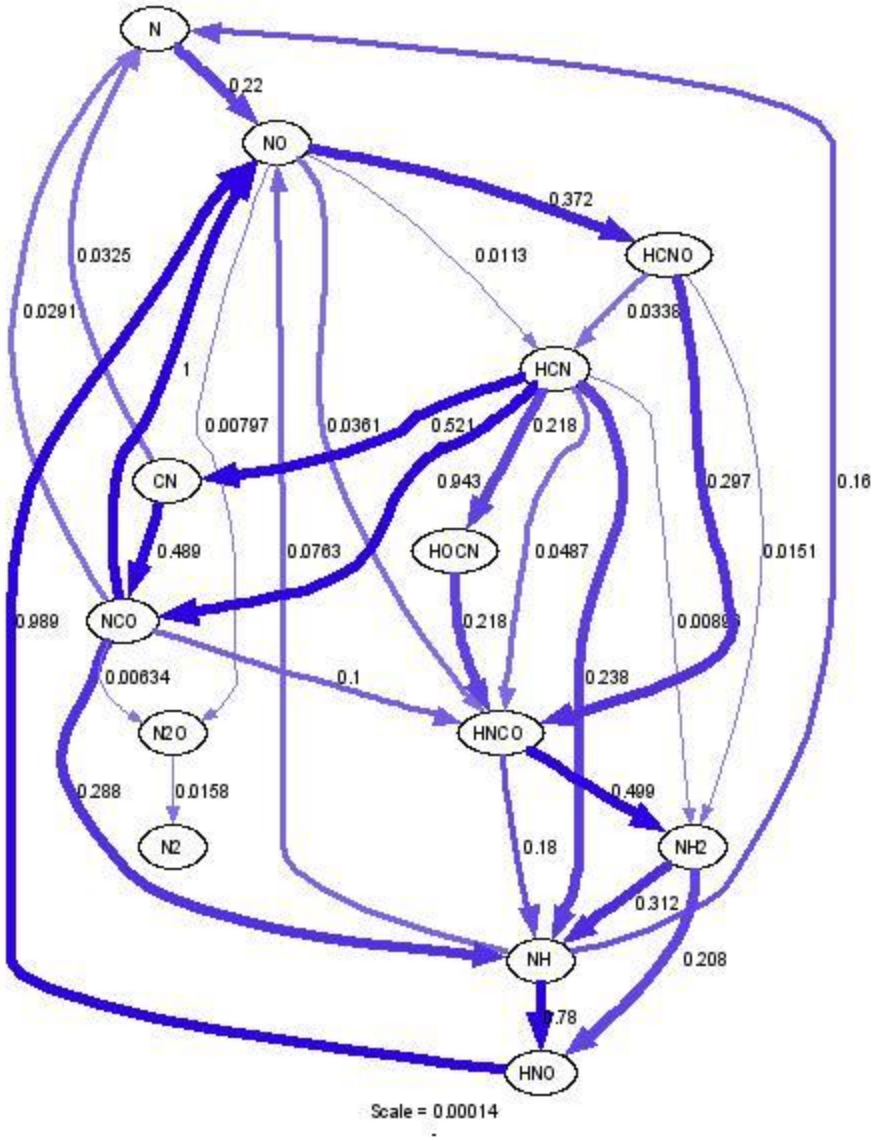

Figure 68. Reaction pathway diagram for N-containing species in the Sub-b O30 model 14 mm from the burner (GRI-Mech 3.0 mechanism).

CO was another species of interest in this work. In contrast to NO, CO levels predicted by the kinetic calculations (GRI-Mech 3.0) closely matched equilibrium values as shown in Figure 69. Comparisons of model predictions with experimental data will be discussed in further detail below.

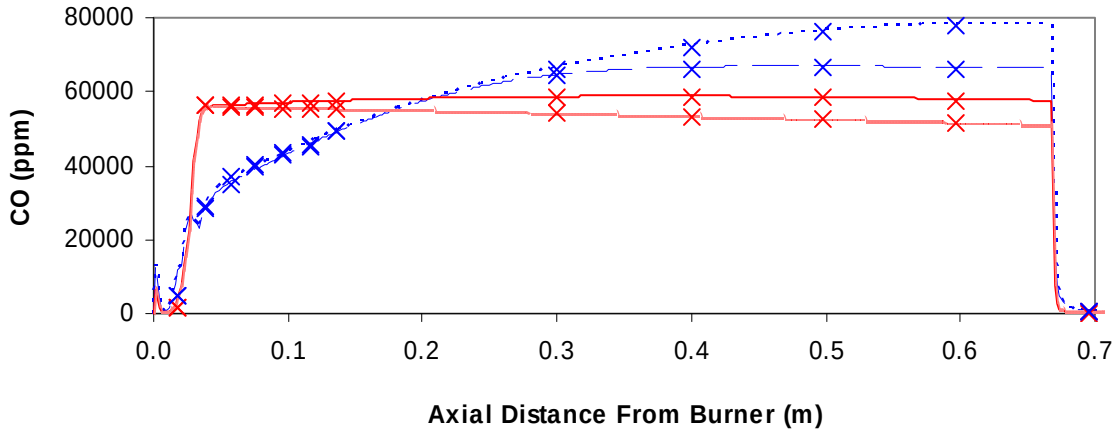

Figure 69. Comparison of CO levels for Sub-b Air and O30 (Opt) cases as calculated by kinetics (lines) and equilibrium (×'s). The purpose of this figure is only to illustrate the agreement between kinetic and equilibrium CO predictions. The specific cases shown are identified in Figure 91.

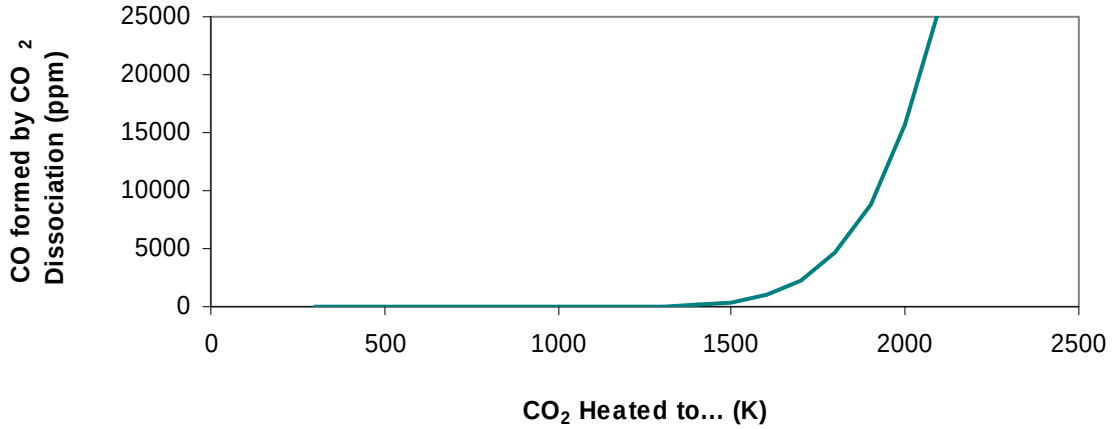

Figure 70. CO formation by thermal dissociation of CO_2 as calculated with NASA-Glenn CEA2 equilibrium code.

CO may be formed by thermal dissociation of CO_2 at high temperatures. Equilibrium calculation results in Figure 70 indicate that this process is extremely temperature sensitive and begins at about 1500 K.

5.2 Comparison of NO Data with Predictions from the Three Gas-phase Mechanisms

With three gas-phase mechanisms (Section 3.2.3), several experiment cases, and tens of species predicted by the model it is impractical to report predictions from all permutations. One gas-phase mechanism was selected by comparing predictions of η_N (the parameter of primary interest) to experimental data. Comparisons for selected experiments appear in Figure 71 through Figure 73.

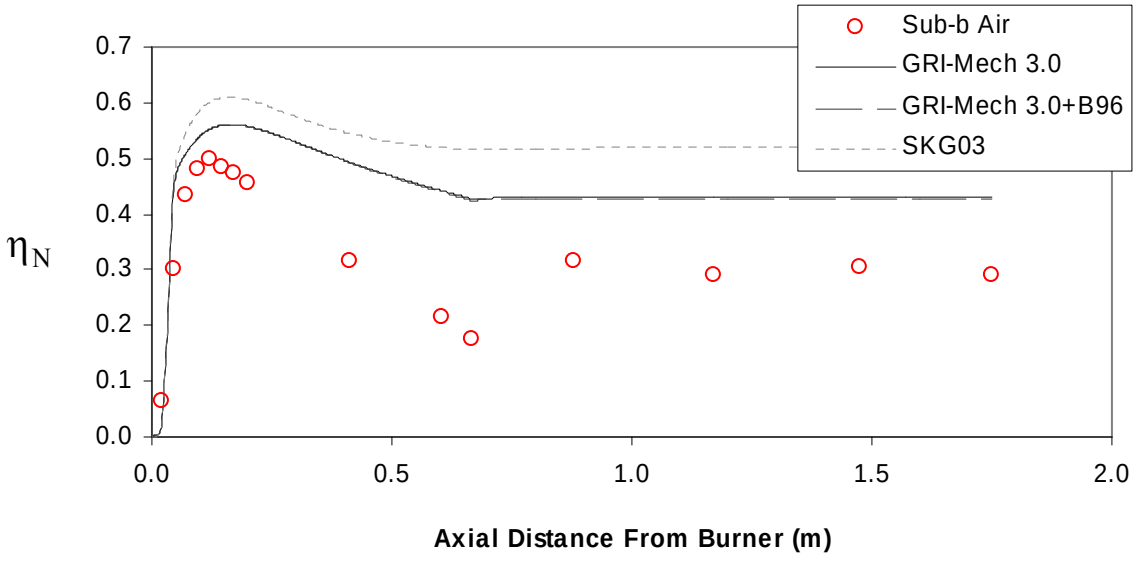

Figure 71. Comparison of nitrogen conversion efficiency predictions for all three gas-phase mechanisms for the Sub-b Air experiment.

The η_N data for the Sub-b Air experiment in Figure 71 exhibits slower NO_X formation following initial rapid formation near the burner. This characteristic is predicted by all three mechanisms, as is the period of NO_X destruction that follows. All mechanisms predict similar levels of initial NO_X formation that are close to the experimental values. The two mechanisms with GRI-Mech reactions are closer to the experimental values than the SKG03 mechanism for this case. Advanced reburning reactions (B96) added to GRI-Mech 3.0 did not make any significant difference to the predictions for the conditions and assumptions in the model. The rate of NO_X destruction is under predicted by all three mechanisms, and the rise in NO_X as burnout oxidizer is added is very slight in the model predictions and well below the experimental values.

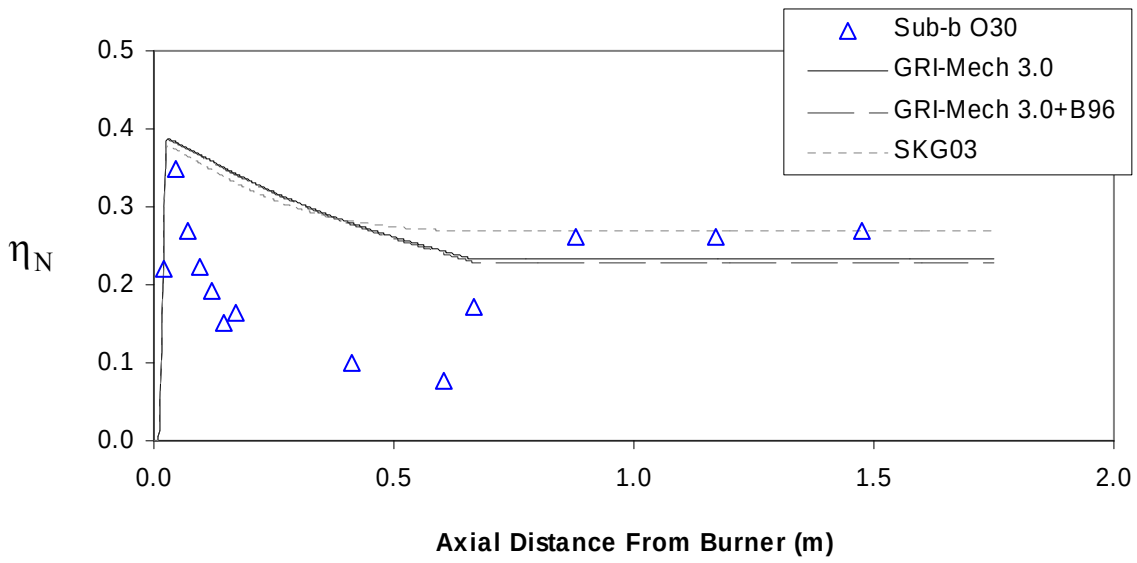

Figure 72. Comparison of nitrogen conversion efficiency predictions for all three gas-phase mechanisms for the Sub-b O30 experiment.

The qualitative agreement between model predictions and experimental data for initial NO_X formation in an oxy-fuel case is also good as shown in Figure 72. As in the

air case the rate of NO_X destruction is under predicted as is the NO_X formation at burnout oxidizer injection. The addition of advanced reburning reactions to GRI-Mech 3.0 again does not change the predictions significantly.

Figure 71 and Figure 72 are typical of the model performance for air and oxy-fuel cases for all three coals and all oxidizers with the exception of one case shown in Figure 73. For the Sub-b Air (Opt) experiment the SKG03 mechanism predicted a similar initial rate of NO_X formation to the other mechanisms but this was followed by a rapid drop in NO_X unique to the SKG03 prediction in this case. This feature is discussed in more detail in section 5.12.

The slight rise in NO_X predicted by the model at the location of burnout oxidizer injection is more noticeable in Figure 73 than previous figures, which is consistent with the more deeply-staged combustion, but lower than the experimentally observed rise.

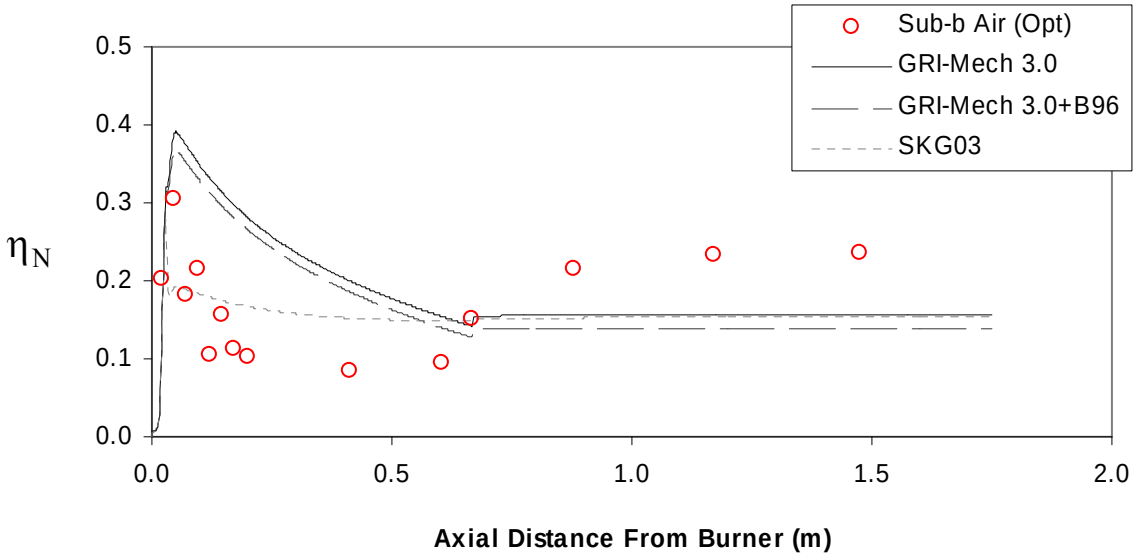

Figure 73. Comparison of nitrogen conversion efficiency predictions for all three gas-phase mechanisms for the Sub-b Air (Opt) experiment.

5.2.1 Choice of Gas-phase Mechanism

In predictions of the shape and location of the NO_X formation profile near the burner, all three mechanisms were qualitatively accurate. The fact that the GRI-Mech 3.0-based mechanisms were often closer quantitatively is considered fortuitous and such may not be the case if the model assumptions were to change. All three mechanisms (in all cases but one) under predicted the rates of NO_X destruction such that no mechanism was clearly superior in this respect. Except where noted, the results in the remainder of this chapter are from the GRI-Mech 3.0 mechanism predictions. This mechanism was selected as it was the least computationally expensive.

5.3 Effect of Recycled NO

The model predictions for the experiments where NO was added to the reactants are shown with the experimental data in Figure 74. The apparently monotonic decrease in the modeled difference between 0 and 525 ppm NO tests would suggest that the initial formation of NO_X is somewhat suppressed in the model predictions by elevated NO concentrations, however the close up view shows that the modeled difference does not decrease much until the NO_X destruction zone begins. The experimental data have insufficient spatial resolution to fully investigate possible suppression of NO formation. Qualitatively the model captures the trends in the available experimental data, with the exception of upstream mixing of NO from the burnout oxidizer (see Section 4.3.3), as fluid mechanics were not included in the model.

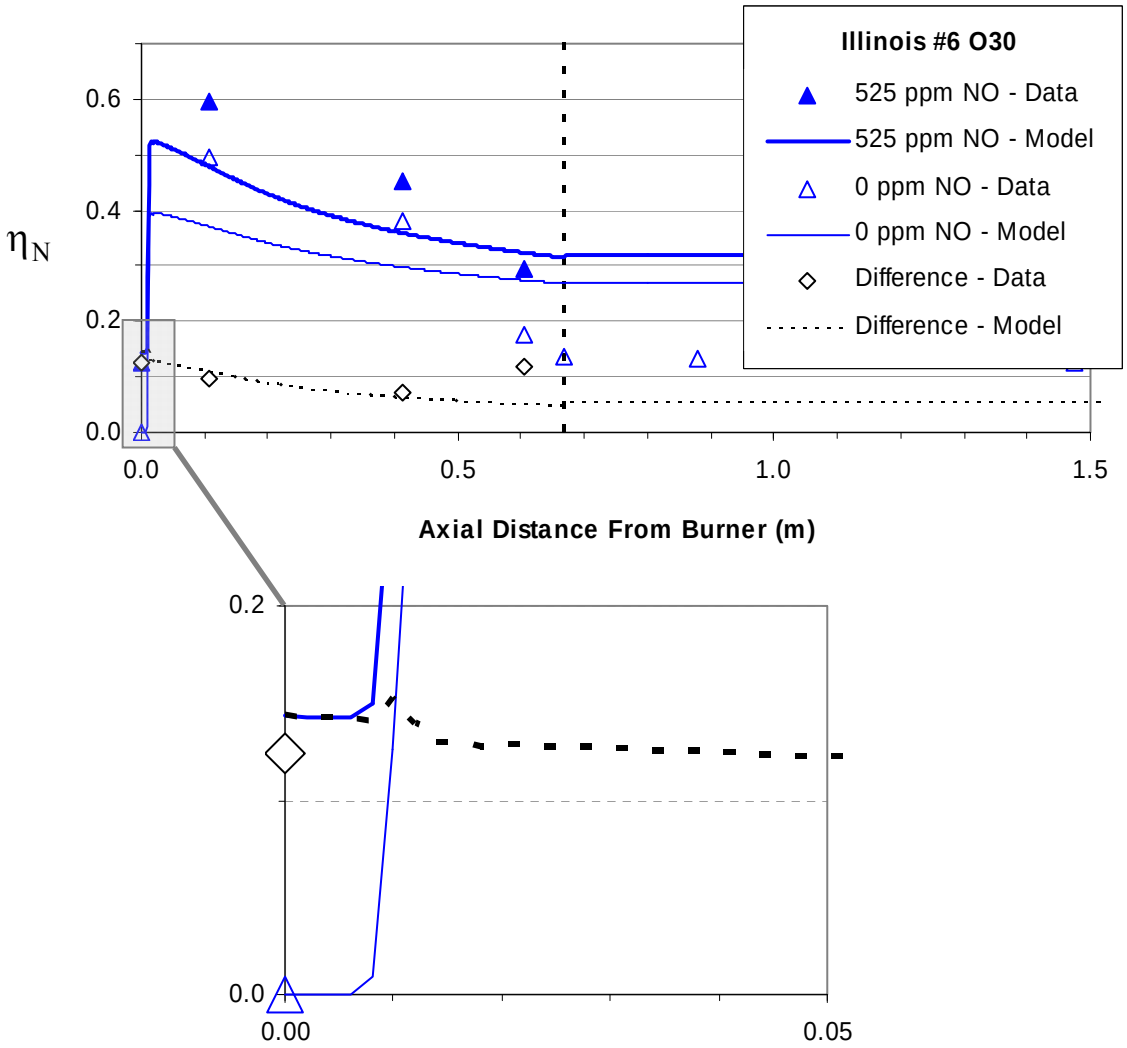

Figure 74. Comparison of model predictions and experimental data for experiments where NO was added to the reactor inlet to simulate recycled NO.

5.4 Effect of Air Infiltration

For practical systems it is expected that some air will enter the combustion space thus adding N_2 to the gas mixture. In the experiments the natural gas contained only about 0.44% N_2 (Table 4) and thus this N_2 was neglected in the modeling. To determine

the predicted effect of air infiltration the model was run with and without N_2 in the reactants and results are shown in Figure 75.

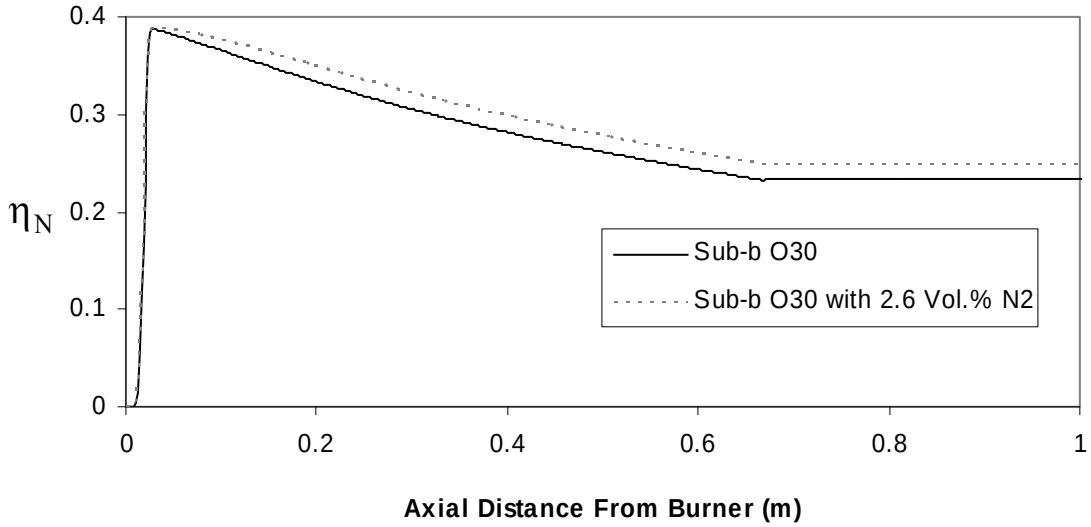

Figure 75. Modeled effect of 2.6 vol. % N_2 in the gaseous reactants for the Sub-b O30 experiment.

The level of N_2 selected (2.6 vol. %) corresponds to air infiltration being 2.6% of total gas mass flow through the burner. As is seen in the figure, this air infiltration is not predicted to significantly increase NO_X. The small increase that is seen is predominantly formed by thermal NO_X reactions.

5.5 Relative Importance of Thermal, Prompt, and Fuel NO_X Mechanisms

A major advantage of a computational model is that individual chemical reactions may be disabled at will to determine the relative significance of different NO_X mechanisms. Thermal NO_X formation is disabled by setting the multiplier in the model

for Reaction 1 through Reaction 3 to zero (reaction multipliers are 1 by default). Likewise for prompt NO_X the multipliers for Reaction 4 and Reaction 5 are set to zero.

For the Sub-b Air case the result of separating the thermal, prompt, and fuel NO_X contributions to NO_X is shown in Figure 76. This modeling exercise predicts that the rapid initial NO_X formation is due to fuel NO_X, and the slower formation thereafter is predominantly thermal NO_X. The model also predicts that thermal NO_X reactions are responsible for most of the predicted NO reduction. Reburning reactions (which are reflected in the fuel NO_X prediction) are of little significance to the modeled NO reduction. Prompt NO_X formation occurs rapidly, fairly close to the burner and is of minor importance compared to the other two mechanisms.

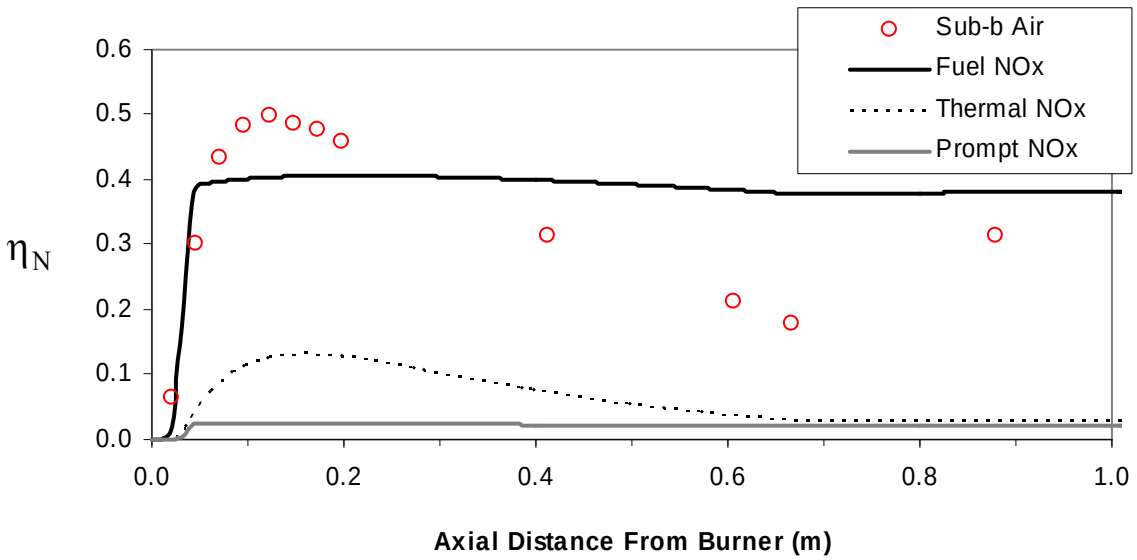

Figure 76. Separated contributions of thermal, prompt, and fuel NO_X predicted by the model for the Sub-b Air case. The experimental data are also plotted.

The same type of model predictions for the Sub-b O30 experiment appear in Figure 77. As with the air case the initial rapid rise in NO_X is attributed to fuel NO_X. The

lack of N_2 results in negligible prompt NO_X, and as with the air case, the majority of predicted NO_X destruction is via thermal NO_X reactions.

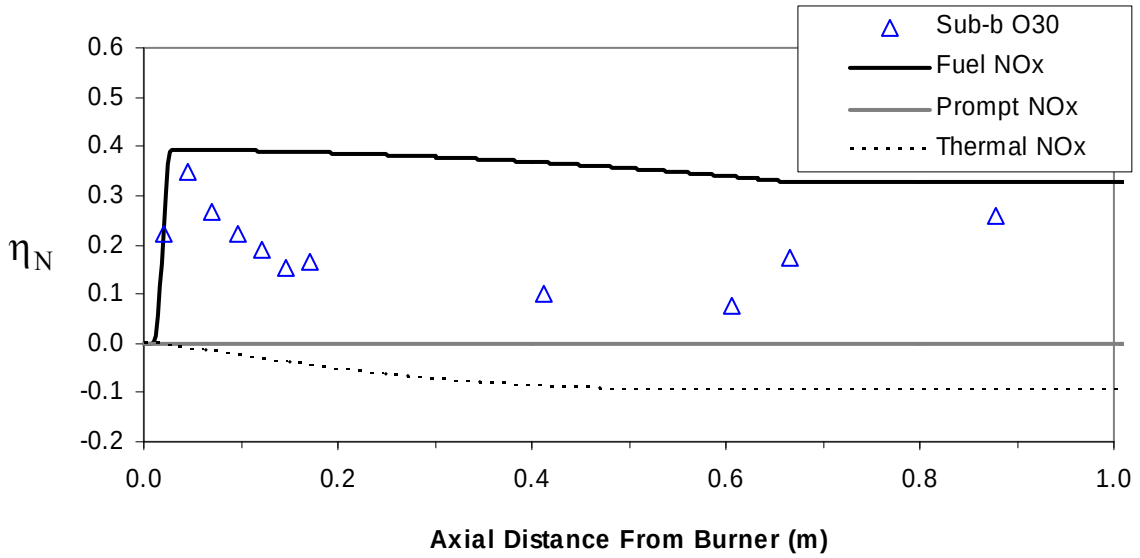

Figure 77. Separated contributions of thermal, prompt, and fuel NO_X predicted by the model for the Sub-b O30 case. Corresponding experimental data are also plotted.

5.6 Flame Characteristics in Devolatilization

Due to the transient release of coal volatiles, the gas-phase stoichiometry changes with distance from the burner. To gain insight into how this might affect nitrogen evolution the model was used to calculate the chemical equivalence ratio (Equation 4, Gordon and McBride, 1994) and this parameter was plotted with other relevant variables in Figure 78. The chemical equivalence ratio is based on elemental oxidation states and is 1 for stoichiometric gas mixtures, greater than 1 for reducing conditions, and less than 1 for oxidizing conditions.

$$r \equiv -\frac{\sum_{i=1}^{l} V_i^{+} \left(\sum_{j=1}^{k} a_{ij} \frac{Y_j}{MW_j} \right)}{\sum_{i=1}^{l} V_i^{-} \left(\sum_{j=1}^{k} a_{ij} \frac{Y_j}{MW_j} \right)} \qquad \text{[Eq. 4]}$$

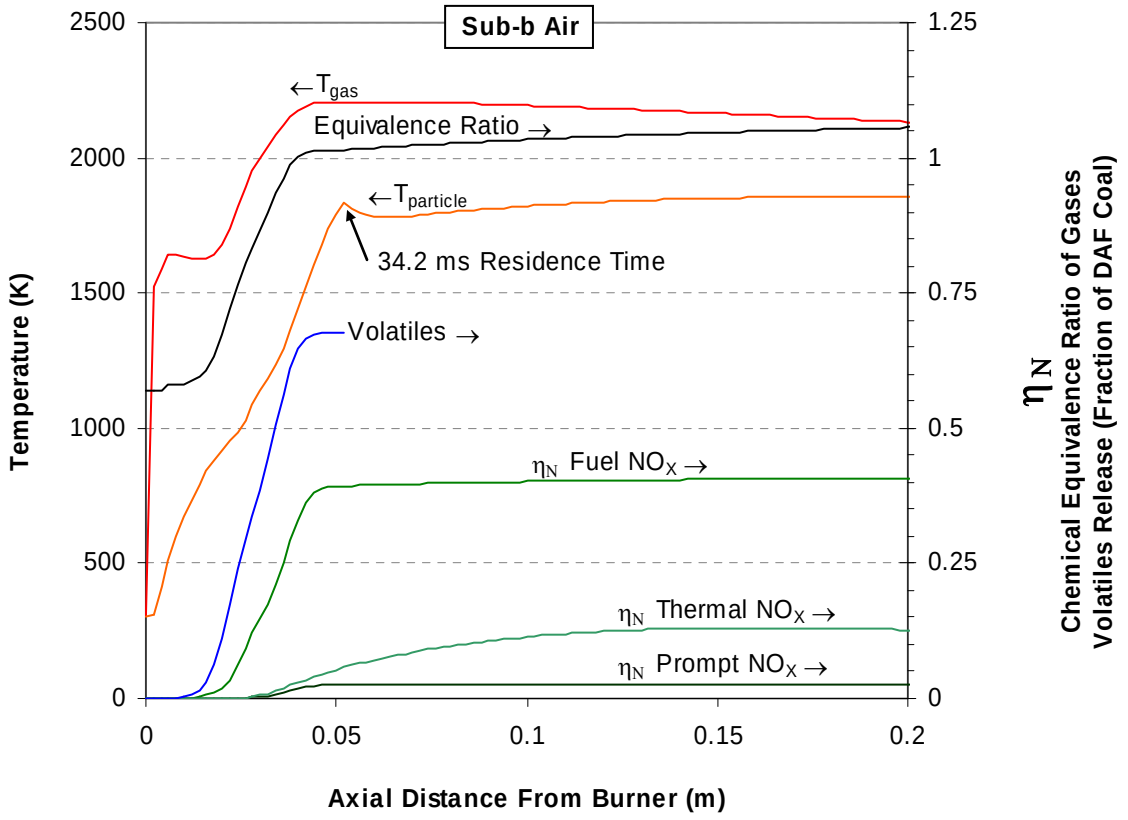

Figure 78. Plot of gas-phase chemical equivalence ratio in the Sub-b Air flame with other important variables.

The modeled gas temperature in Figure 78 has two distinct periods where temperature increases. The first is associated with the natural gas flame that provides heat for coal devolatilization and the second is from combustion of the coal volatiles. Particle temperature lags behind the gas temperature and as a result the coal volatiles are not released in the model until after the natural gas flame. Fuel NO_X formation begins with

the release of volatiles, and thermal NO_X forms further downstream. Prompt NO_X only occurs over a small region corresponding to the location where chemical equivalence ratio changes from oxidizing to reducing values.

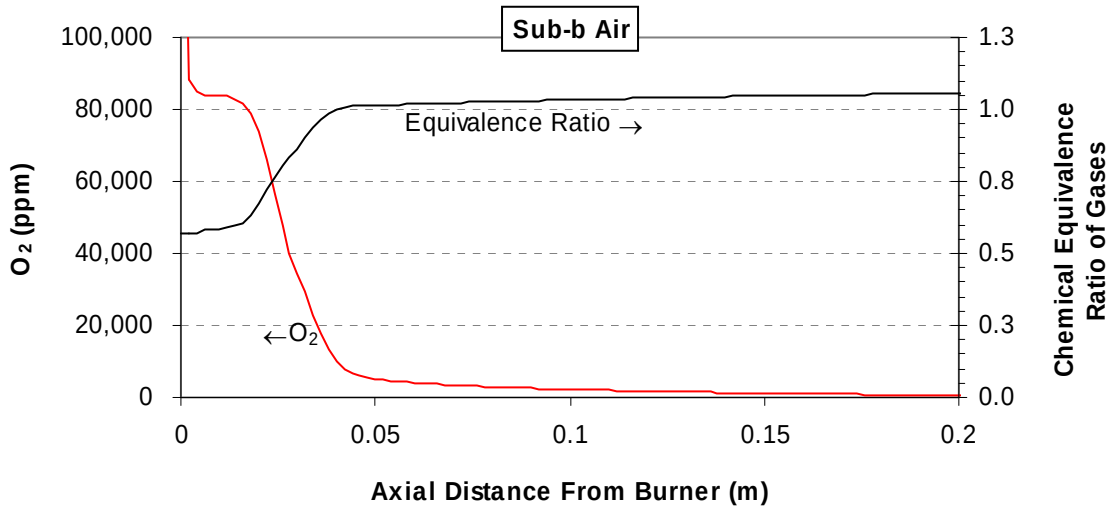

Figure 79. Modeled gas-phase chemical equivalence ratio for the Sub-b Air case plotted with predicted O_2 concentration.

Given the requirement for O_2, It may be somewhat surprising that thermal NO_X would form under chemical equivalence ratios greater than 1, but as seen in Figure 79 the modeled O_2 concentrations are low but non-zero over the region where the chemical equivalence ratio is greater than 1 and thermal NO_X is formed.

The most prevalent radical species predicted by the model are shown in Figure 80. The species profiles all have a valley between the methane and coal volatiles flames locations which indicates that in the model at least these two flames are largely independent. In the experiment the range of particle sizes is expected to cause some overlap, but the peak height (in some cases) and breadth (in all cases) of predicted

volatiles flame radical species profiles is greater than for the methane flame. This may indicate that some overlap may not have a major influence in the volatiles flame radicals pool and resulting NO_X chemistry.

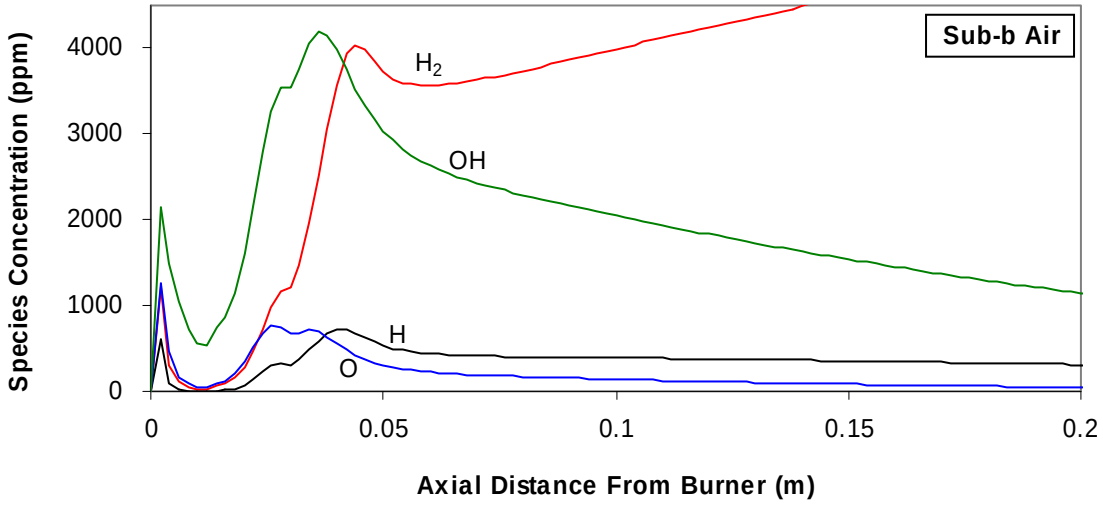

Figure 80. Major radicals species predicted in the Sub-b Air case near the burner.

Figure 81 shows the gas-phase chemical equivalence ratio and other predictions for the Sub-b O30 case. The values of chemical equivalence ratio in the oxy-fuel case are about the same as for the air case indicating that the diluent (N_2 or CO_2) does not affect this chemical measure of stoichiometry. The gas temperature increases occur slightly upstream of their locations in the air case, and particle heat up is slightly faster, but other than this there is little difference between the oxy-fuel and air cases. The dominant predicted radicals for this case are shown in Figure 82 and are also similar to the air case species profiles. Like the air case, some O_2 is predicted in the reducing zone where the chemical equivalence ratio is greater than 1 (Figure 83).

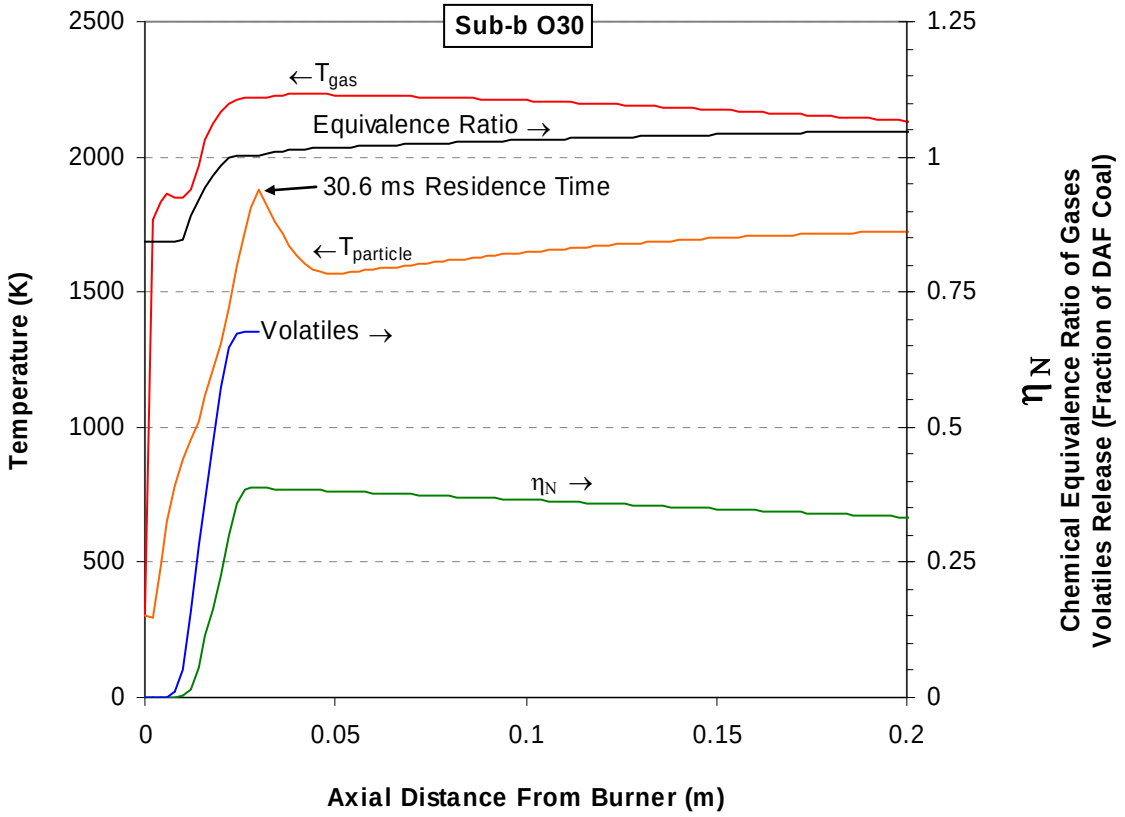

Figure 81. Plot of gas-phase chemical equivalence ratio in the Sub-b O30 flame with other important variables.

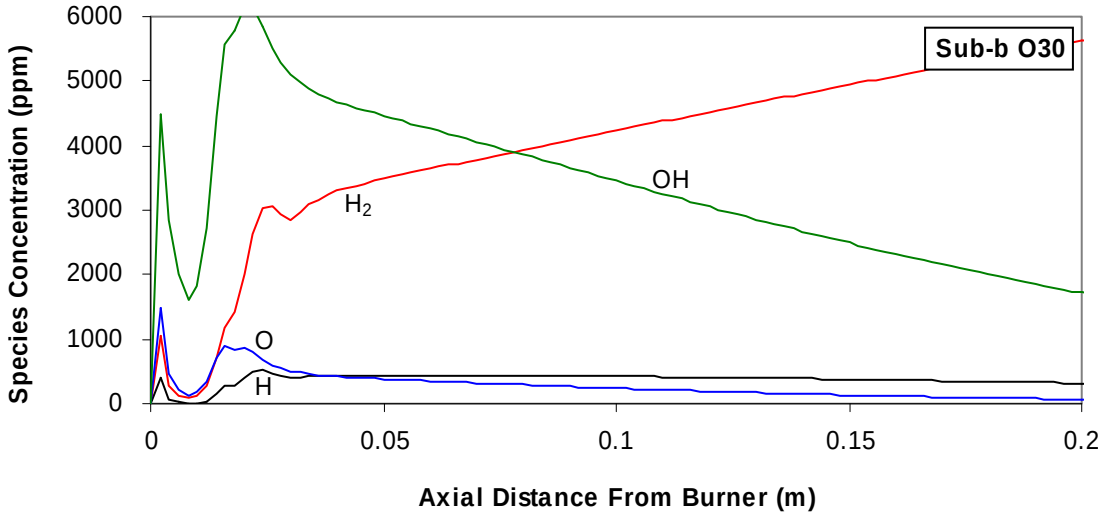

Figure 82. Major radicals species predicted in the Sub-b O30 case near the burner.

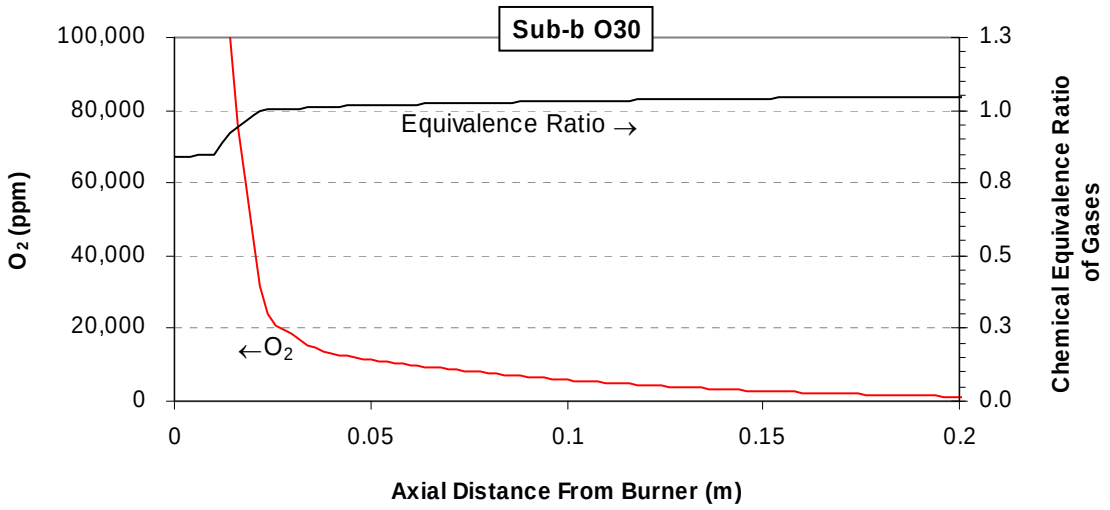

Figure 83. Modeled gas-phase chemical equivalence ratio for the Sub-b O30 case plotted with predicted O_2 concentration.

5.7 Effect of Varied Primary Stoichiometry

The model was used to examine the predicted trends in effluent NO_X with varied primary stoichiometry as was done in the Staging experiments. The model predictions and experimental data are compared in Figure 84. The most important result desired from a modeling study such as this is the primary SR for minimum NO_X. This was not identified by the model as the model results indicate that the minimums would occur at a primary SR below the lowest level tested. One aspect of the experimental data that is however correctly predicted is the greater sensitivity of air combustion NO_X to increases in primary SR.

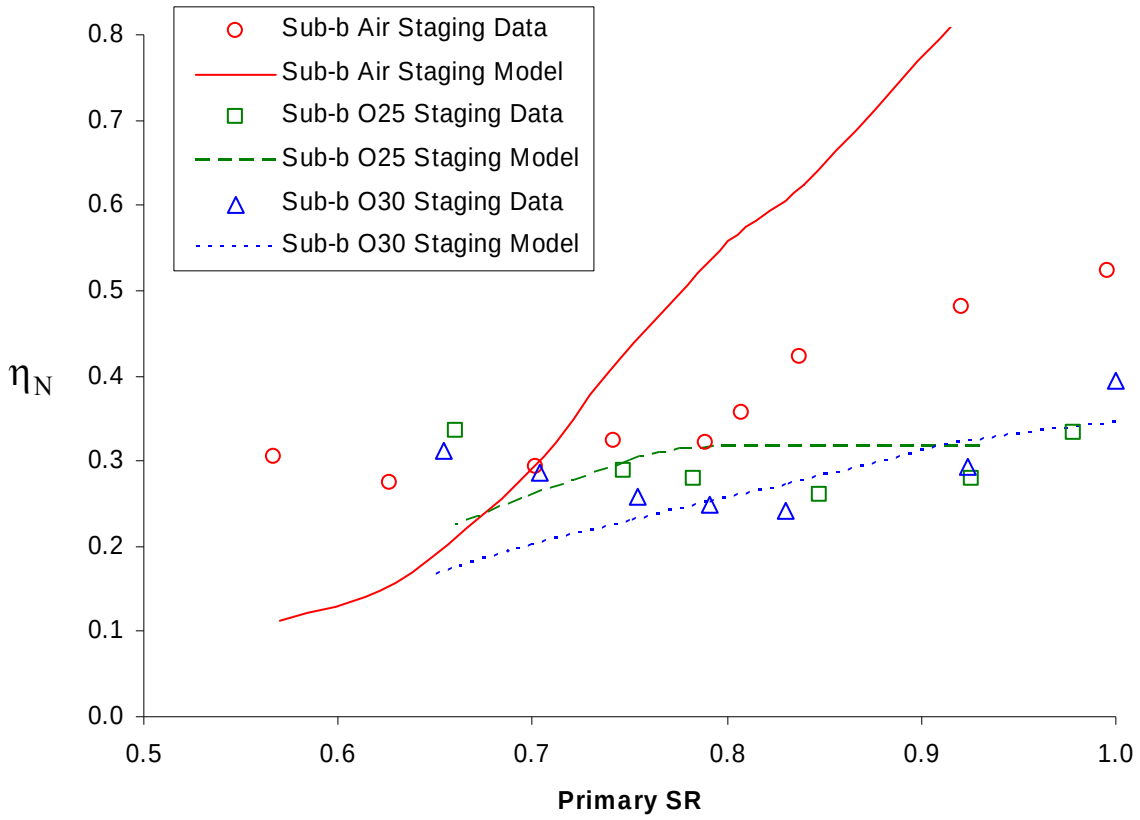

Figure 84. Predicted and measured trends in effluent η_N as a function of primary SR.

The predicted axial η_N profiles for each primary SR were plotted for air (Figure 85) and oxy-fuel (Figure 86). In the case of air it is seen that as primary SR decreases the slow formation of NO_X associated with thermal NO_X formation gradually disappears. The very significant contribution of thermal NO_X at high primary SR appears to explain the greater sensitivity of the air combustion NO_X to the stoichiometry.

Another trend visible in Figure 85 is that as primary SR decreases the predicted NO_X formation at the point of burnout oxidizer injection increases. This NO_X formation is under predicted as already shown in connection with Figure 73. If this NO_X formation were increased by the same multiplier for each stoichiometry, it can be seen that a

minimum in final NO_X versus stoichiometry could be reached in the model as it is observed the data.

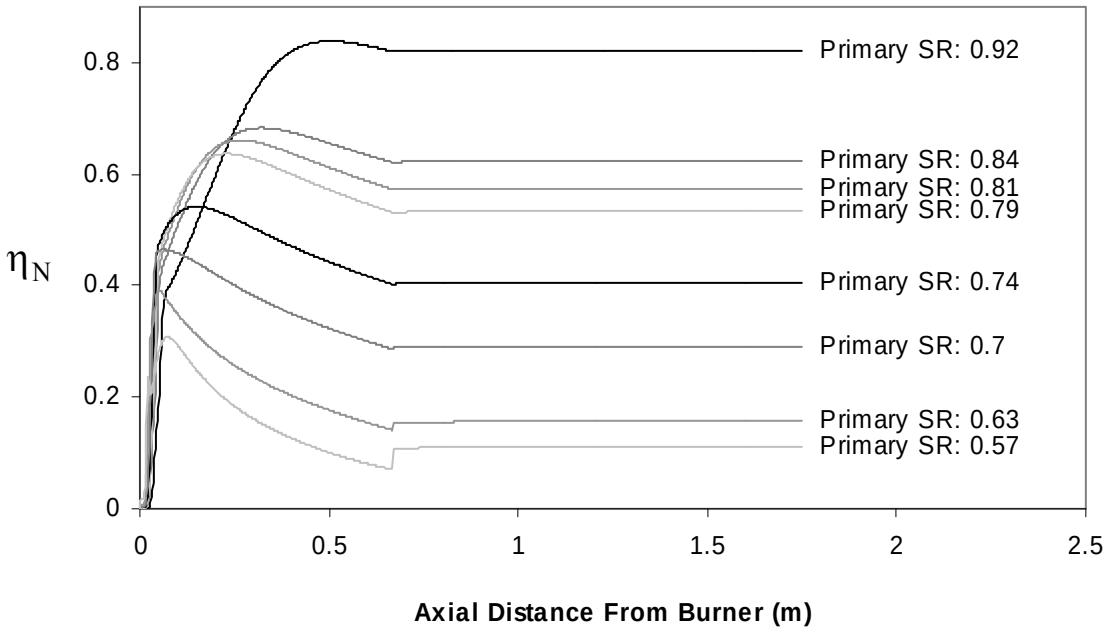

Figure 85. Axial profiles of predicted η_N in air combustion as a function of the depth of staging (or primary SR).

In the model predictions for oxy-fuel shown in Figure 86, the trend of increasing NO_X formation at burnout oxidizer injection with decreased primary SR is also apparent, and as shown previously in Figure 72 is also under predicted. Near the burner the lack the of thermal NO_X formation observed in the air cases at high primary SR appears to be the reason for the lower sensitivity of oxy-fuel NO_X to primary SR.

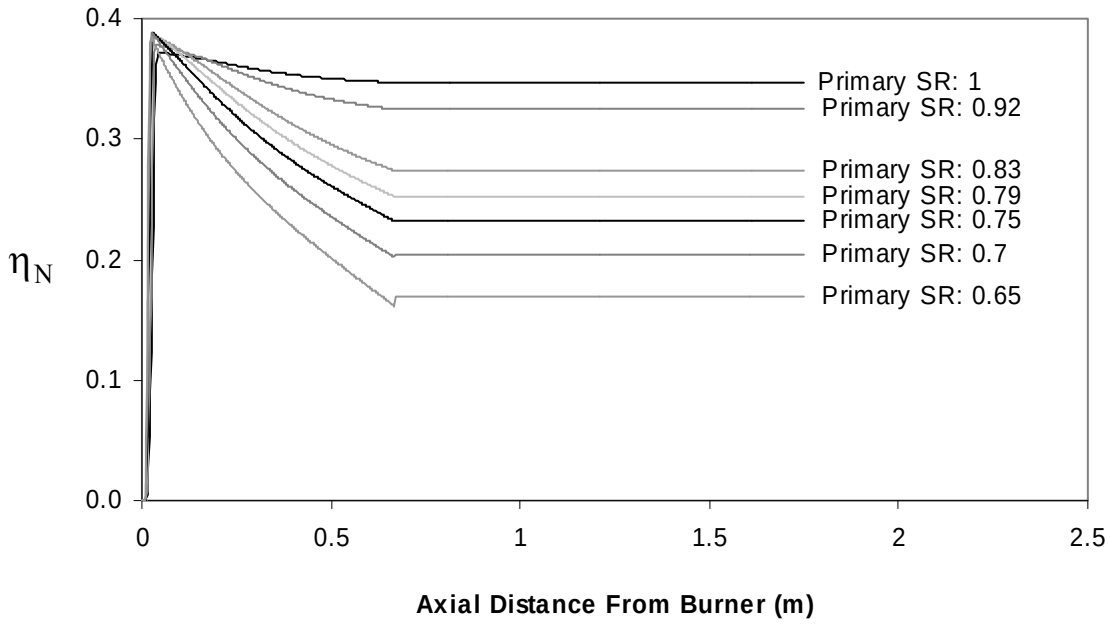

Figure 86. Axial profiles of predicted η_N in oxy-fuel (O30) combustion as a function of the depth of staging (or primary SR).

Close inspection of Figure 85 reveals that the model predicts lower initial NO_X formation with decreasing primary SR over most of the range of stoichiometries (primary SR = 0.92 is an exception). The available experimental data is consistent with this observation as illustrated in Figure 87. For oxy-fuel combustion the same trend is seen in the modeling results but was not observed experimentally. The effect is not as strong in the oxy-fuel model results as in the air cases.

The lower initial NO_X formation in air with lower primary SR may be due to lower nitrogen release from the coal, lower conversion of fuel-N to NO, or a combination. The model results for volatiles and nitrogen release were examined to help determine the relative significance of these reasons. Predictions shown in Table 13 indicate that nitrogen release is not expected to change significantly with primary SR. In general, volatiles and nitrogen release increase with particle heating rate, but with

diminishing returns. At the high heating rates used the volatiles and nitrogen release is at or near the maximum attainable value. This points to lower conversion of fuel-N to NO as the explanation for lower initial NO_X formation at lower primary SR. Lower amounts of oxygen in these cases is probably the cause of the observation.

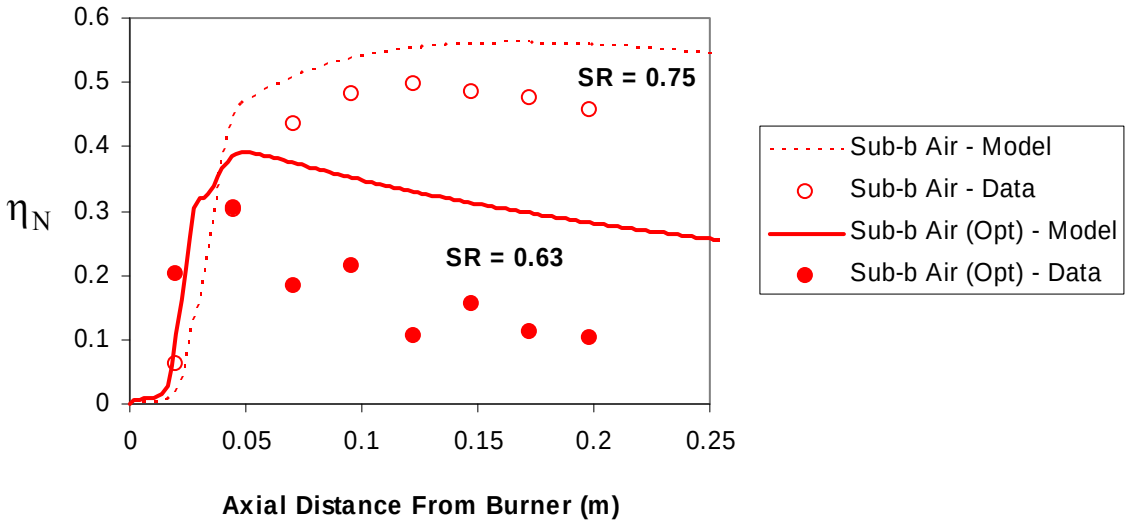

Figure 87. Model predictions and data comparison of initial NO_X formation for Sub-b Air and Sub-b Air (Opt) cases.

Table 13. Fractional volatiles and nitrogen release predictions for the sub-bituminous coal experiments.

Modeled Case	Volatiles Release	Nitrogen Release
Sub-b Air	67.6 %	62.2 %
Sub-b Air (Opt)	67.6 %	62.5 %
Sub-b O30	67.6 %	62.5 %
Sub-b O30 (Opt)	67.6 %	62.3 %

5.8 Model-Data Comparison: CO

A comparison of the experimental data and model predictions for the Illinois #6 Air and O30 CO concentrations is shown in Figure 88. The model does predict the trend of higher CO levels for the oxy-fuel case as seen in the data, but the magnitude of the model prediction is in poor agreement with the data. For the sub-bituminous data and model predictions shown in Figure 89, the predictions are more accurate for the Air and O25 cases but too high for the O30 case. The model includes an empirical heat transfer parameter to account for heat lost through the reactor walls. Knowing that CO should follow equilibrium concentrations, the heat transfer parameter was tuned to force agreement between model predictions of CO and CO data from the Sub-b Air experiment, which explains the good agreement in that case. The chosen value obviously works well for O25 also, but not for the Illinois #6 coal and the Sub-b O30 experiment.

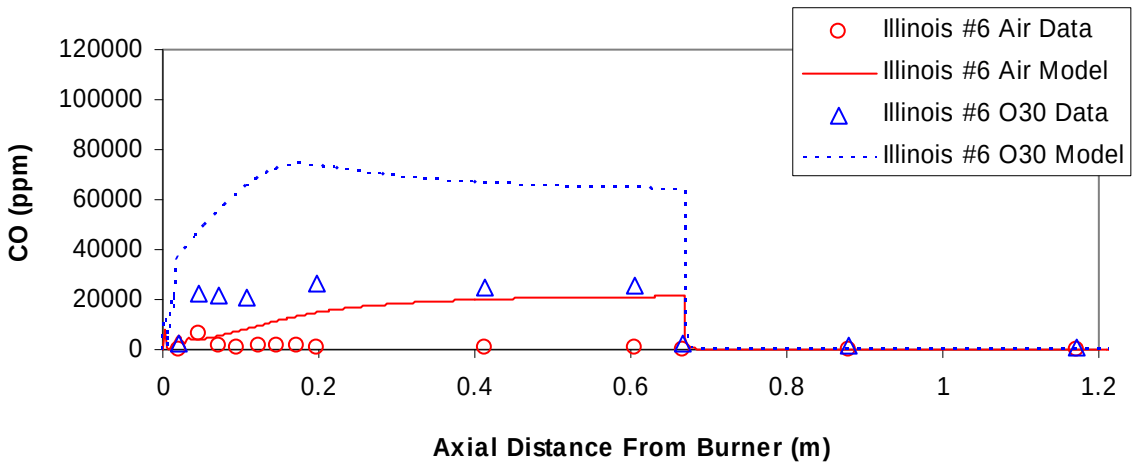

Figure 88. Model predictions and data comparison for CO in Illinois #6 staged combustion.

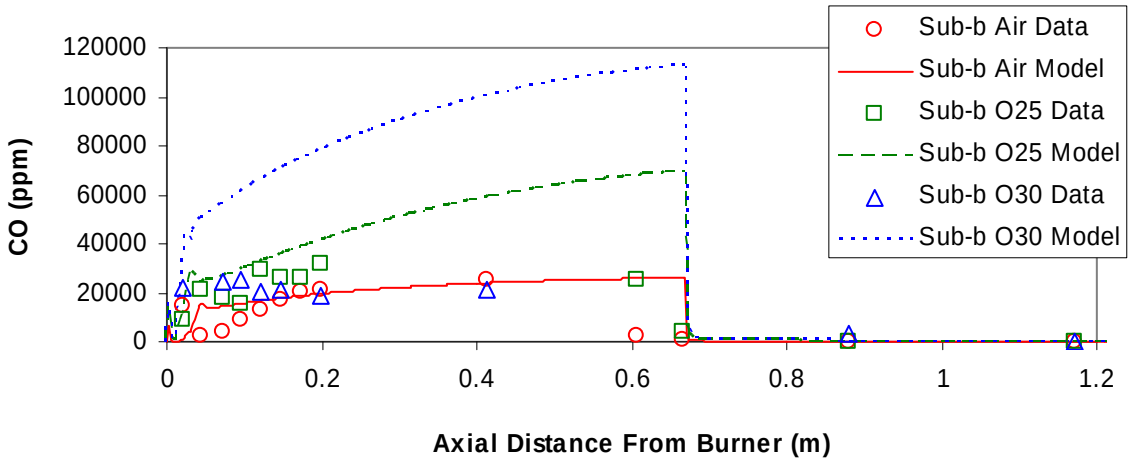

Figure 89. Model predictions and data comparison for CO in Sub-bituminous coal staged combustion.

The same model-data comparison for the sub-bituminous experiments at lowest effluent NO_X conditions is shown in Figure 90. At these markedly different levels of available oxygen in the primary combustion zone CO is similar between the air and oxy-fuel cases in both the model and the experiments.

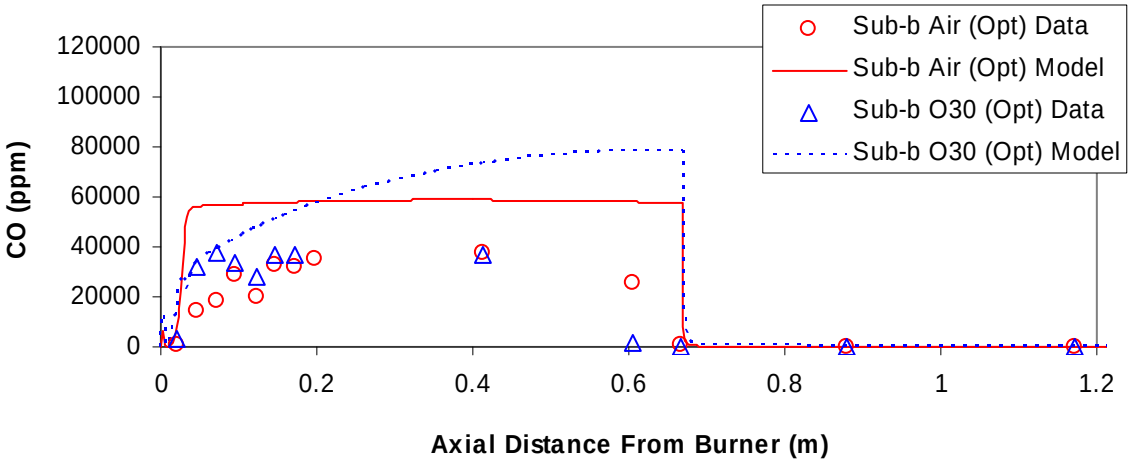

Figure 90. Model predictions and data comparison for CO in Sub-bituminous coal staged combustion at minimum effluent NO_X stoichiometries.

5.8.1 Effect of CO_2 Gasification of the Char on CO Concentrations

Early in the experimental work the high levels of CO observed in the reducing zone for oxy-fuel conditions combined with lower wall temperatures 0.4 m from the burner led to questions as to the cause of the high CO concentrations. Endothermic gasification of the char by CO_2 under oxy-fuel conditions was hypothesized as a possible explanation and this was investigated using the model.

Figure 91 presents model predictions for the same experiments considered in Figure 90 with and without inclusion of the CO_2 gasification reactions. The difference made to the CO levels is not insignificant, but it is small compared to the high level of CO. It appeared from these modeling results and equilibrium calculations for the same model cases presented in Figure 69 that gasification of the char by CO_2 does affect the level of CO, but the effect is minor compared with the CO quantities formed by thermal dissociation of CO_2 as equilibrium is maintained.

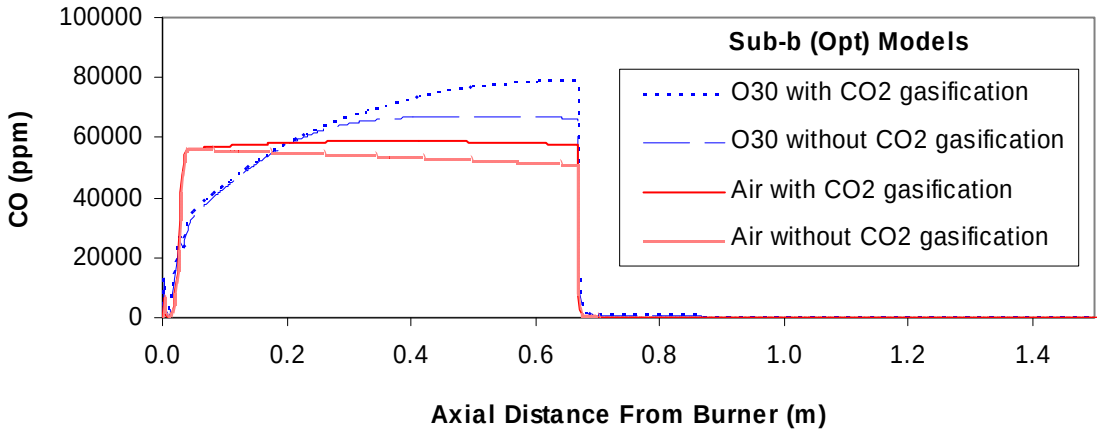

Figure 91. Effect of CO_2 gasification on CO levels in air and oxy-fuel model predictions.

The reasons that enabling or disabling the CO_2 gasification reactions in the model can change the predicted level of CO are that (1) The temperature is slightly lowered by the endothermic reactions; and (2) the production of CO added to the gas phase alters the elemental composition of the gas.

5.9 Effect of CO_2 Gasification of Char on η_N

In the literature review it was noted that moist oxidation of CO may produce radicals that are required by NO_X reduction reactions. As CO_2 gasification of the char is predicted to affect the CO concentration, it is also of interest to determine the effect of char gasification on NO_X. This model prediction is shown in Figure 92 and indicates little effect of the gasification reaction on η_N.

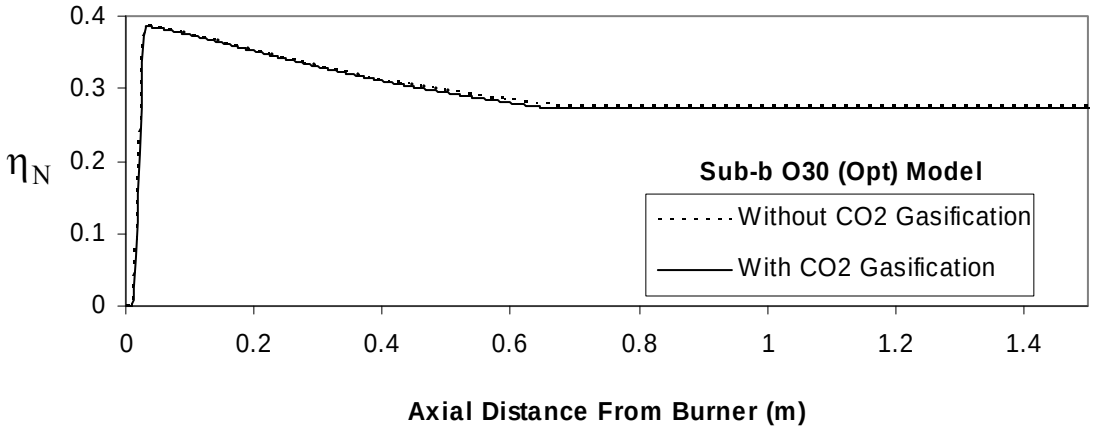

Figure 92. Predicted effect of CO_2 gasification reactions on nitrogen conversion efficiency for the Sub-b O30 (Opt) experiment.

5.10 Model-Data Comparison: NH_3 and HCN

As was done in Section 5.2 for η_N, all three gas-phase mechanisms were compared to the experimental data for HCN and NH_3 prediction accuracy and as before the GRI-Mech 3.0 mechanism was most often closest to the experimental data. All predictions shown in this section were made using the GRI-Mech 3.0 reaction set.

Figure 93 shows model predictions compared to data for sub-bituminous coal staged combustion. The same qualitative trends seen in the data are followed by the model predictions, specifically the rise in NH_3 with distance from the burner, and the higher NH_3 concentration in oxy-fuel relative to air at the same primary SR, and the trend of increasing NH_3 as primary SR decreases for each oxidizer.

In spite of this qualitative agreement, the magnitude of the predicted levels of NH_3 is generally two orders of magnitude too low. The predictions for the Sub-b Air (Opt) case at significantly lower primary SR are also too low, but closer to the data.

In the model predictions the sharp narrow peak in NH_3 near the burner is associated with volatiles release, and the rise in NH_3 downstream is associated with homogeneous nitrogen chemistry. Nitrogen release from char is not modeled. These features appear distinct in the model but not in the experimental data, perhaps because the coal particle size distribution causes overlap of the physical processes in the measured data while a monodisperse distribution is assumed in the model, as will be discussed in more detail in Section 5.11.

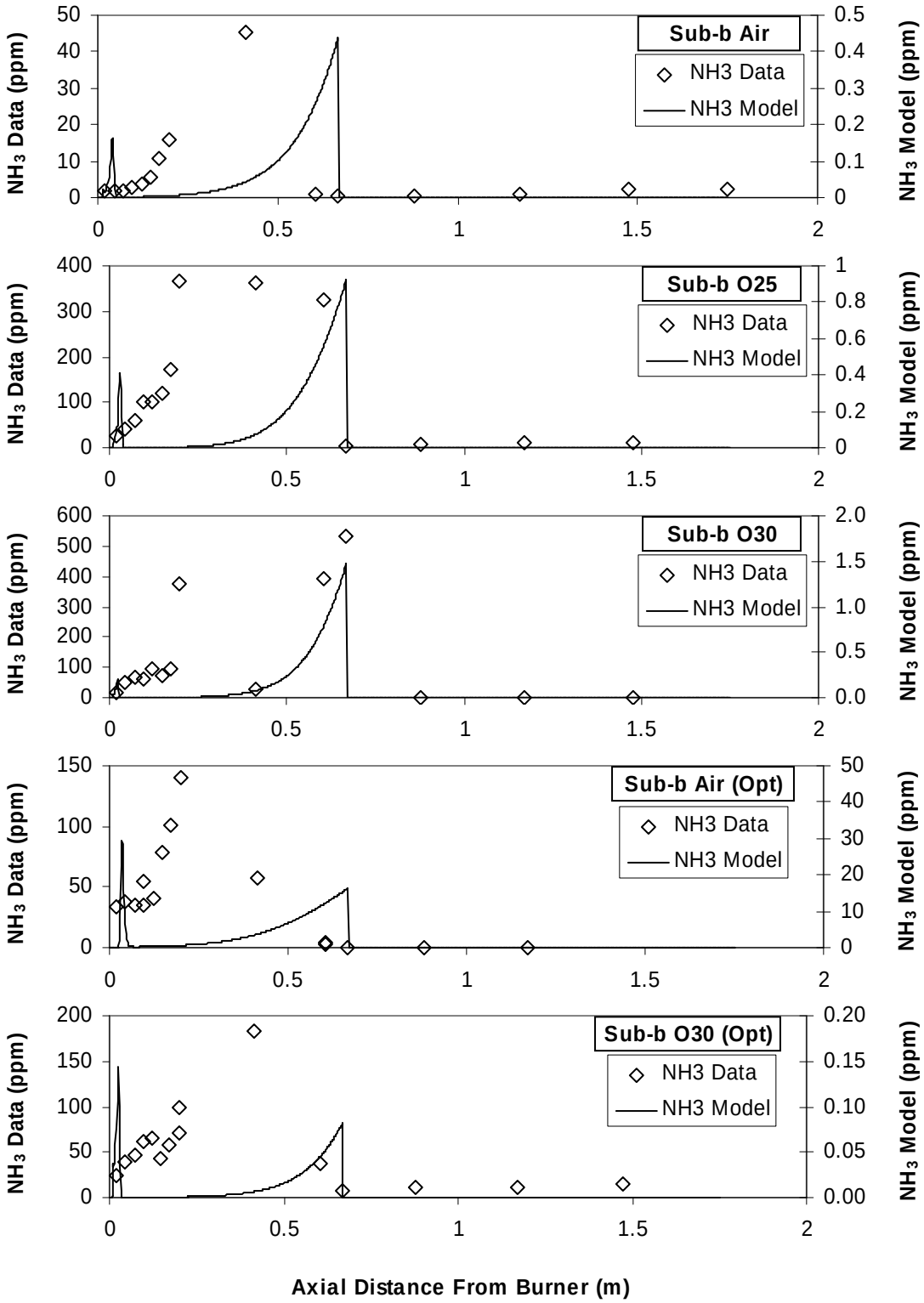

Figure 93. NH_3 model predictions and data for sub-bituminous coal staged combustion.

As observed experimentally, the model predicts lower NH_3 levels for the Illinois #6 coal than for the sub-bituminous coal, but the agreement between the model and data is still poor (Figure 94).

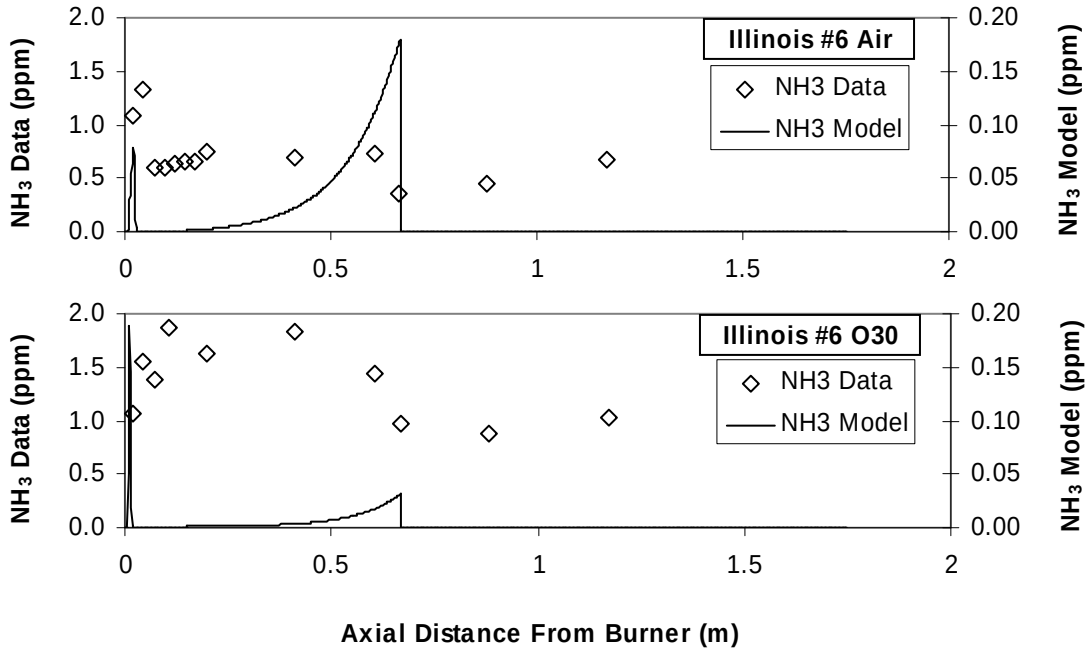

Figure 94. NH_3 model predictions and data for Illinois #6 staged combustion.

The HCN data for the sub-bituminous coal already presented in Sections 4.3.4 and 4.5 showed HCN present throughout the reducing zone. The model predictions for this coal however exhibit a sharp peak in HCN near the burner with no significant HCN elsewhere. The results in Figure 95 are qualitatively representative of all the sub-bituminous cases.

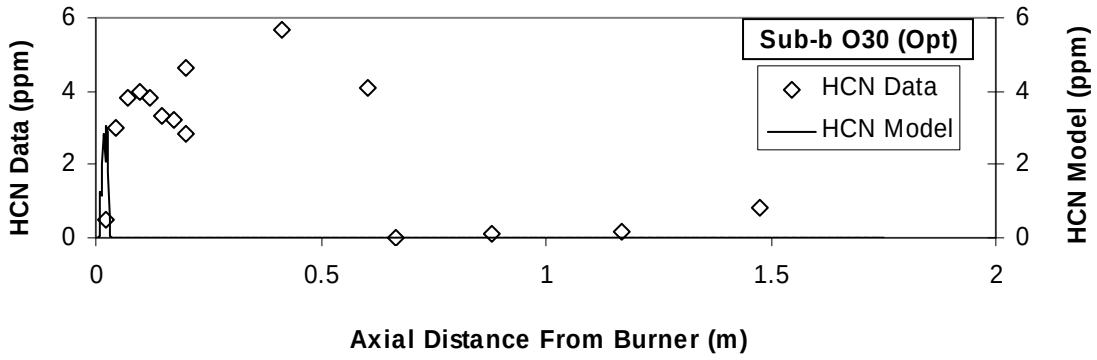

Figure 95. Comparison of HCN model predictions and experimental data for Sub-b O30 (Opt).

For the Illinois #6 coal the model again predicts only a sharp peak in HCN near the burner. As is seen in Figure 96 the model trend somewhat matches the Illinois #6 Air data with a rapid rise and fall in HCN, but not the Illinois #6 O30 data where the model shows a rapid rise and fall but the data shows a small but lingering concentration of HCN.

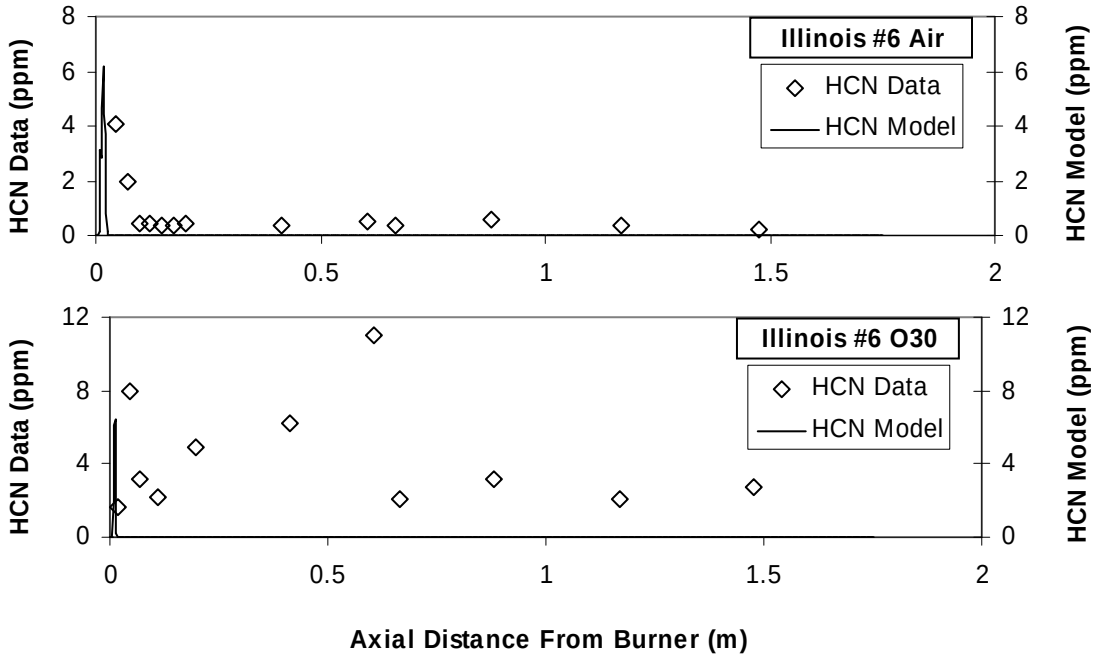

Figure 96. HCN experimental data and model predictions for the Illinois #6 experiments.

5.11 Model-Data Comparison: Hydrocarbons

Experimental data and model predictions for CH_4 in the Sub-b Air and Sub-b Air (Opt) cases appear in Figure 97. Similar information for C_2H_4 is in Figure 98.

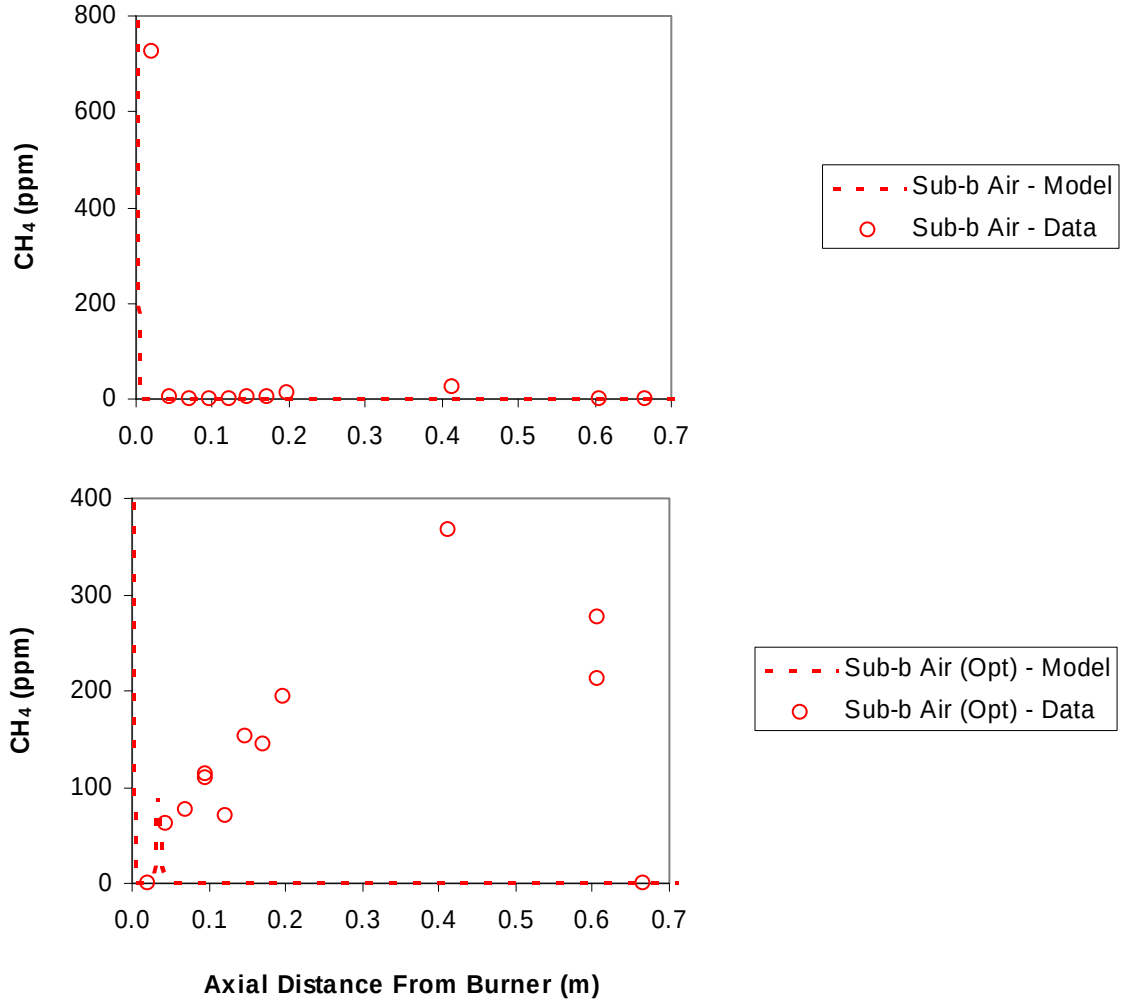

Figure 97. Comparison of model predictions and experimental data for CH_4 in the Sub-b Air and Sub-b Air (Opt) cases.

In these two figures the Sub-b Air case has high levels of both hydrocarbons near the burner. In the model this is associated with the natural gas flame. This high initial hydrocarbon level does not appear in the experimental data for the Sub-b Air (Opt) cases.

A possible reason is that the lower flow rate through the burner moves the flame to a location upstream of the first gas sampling location.

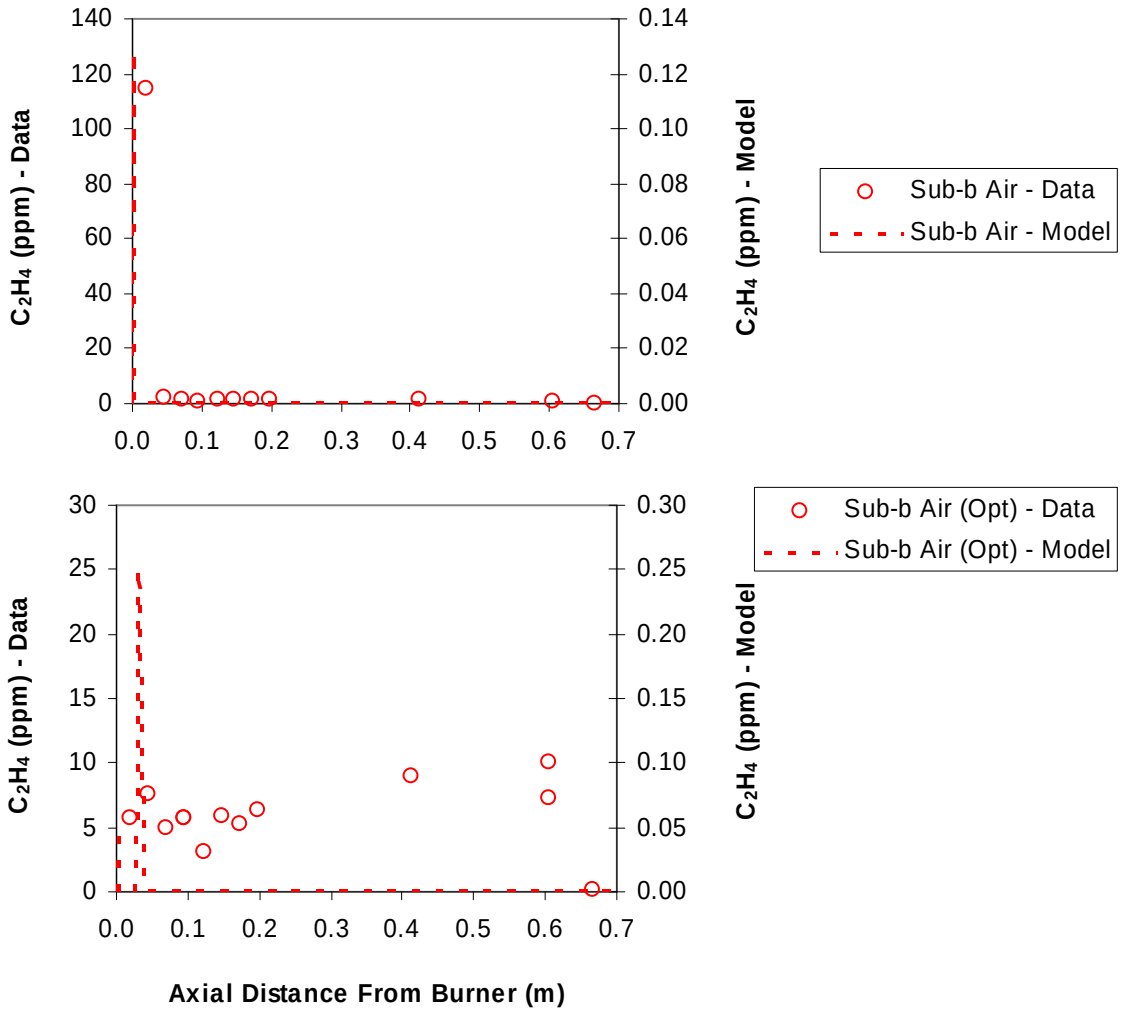

Figure 98. Comparison of model predictions and experimental data for C_2H_4 in the Sub-b Air and Sub-b Air (Opt) cases.

In the model predictions only, the hydrocarbon levels peak again just downstream of the initial high levels. These downstream peaks are associated with the predicted volatiles release from the coal. The size of these peaks is very small in the Sub-b Air case, probably due to high oxygen availability, but they are still present (Figure 99). The

peak width is small and followed by near-zero levels of hydrocarbons, whereas the experimental data has higher levels of hydrocarbons over a broad region.

The Sub-b Air (Opt) case has higher hydrocarbon concentrations than the Sub-b Air case, consistent with the lower primary SR.

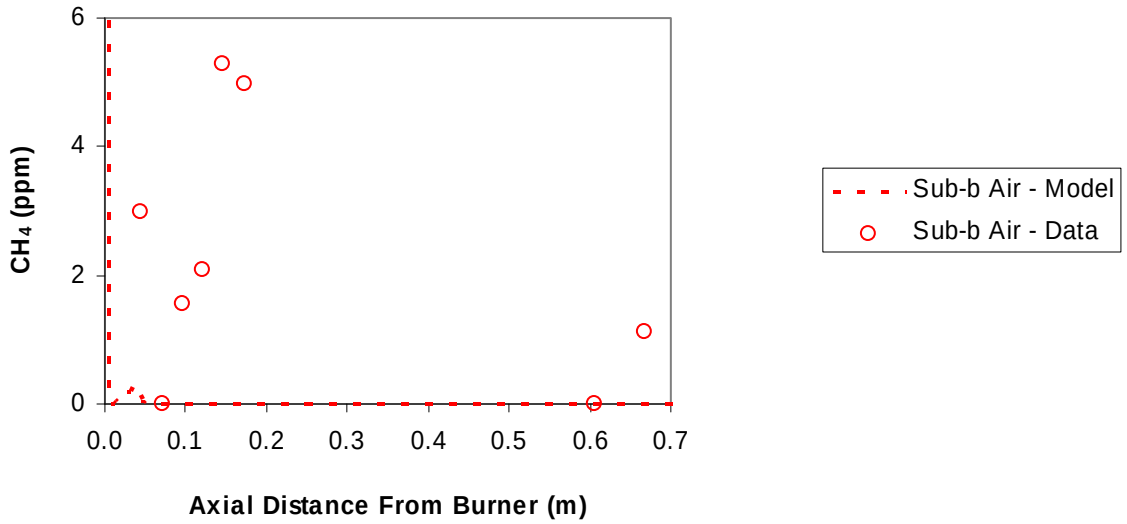

Figure 99. The same data and model predictions shown in the upper plot of Figure 97 but with the vertical axis limits changed to reveal small details in the model prediction near the burner.

The comparison between model predictions of hydrocarbons and experimental data for the Sub-b O30 and Sub-b O30 (Opt) cases displays similar trends to the Air combustion cases shown above. Other hydrocarbons predicted by the model for which there are no experimental measurements (such as CH_3, CH_2, CH, and HCCO) show the same behavior as CH_4 and C_2H_4.

A significant simplifying assumption made in the model is that of a single particle size representing the size distribution in the experiment. To investigate effects of this assumption, two model cases were run for the Sub-b Air (Opt) case using different

particle sizes. The first case followed the standard modeling procedure used in this work of using the mean particle size from the measured particle size distribution (121 μm). The second case assumed 300 μm diameter particles to represent particles near the upper end of the size distribution. A plot of the predicted CH_3 profiles is shown in Figure 100. CH_3 was chosen as a representative hydrocarbon, as most of the hydrocarbons followed similar behavior.

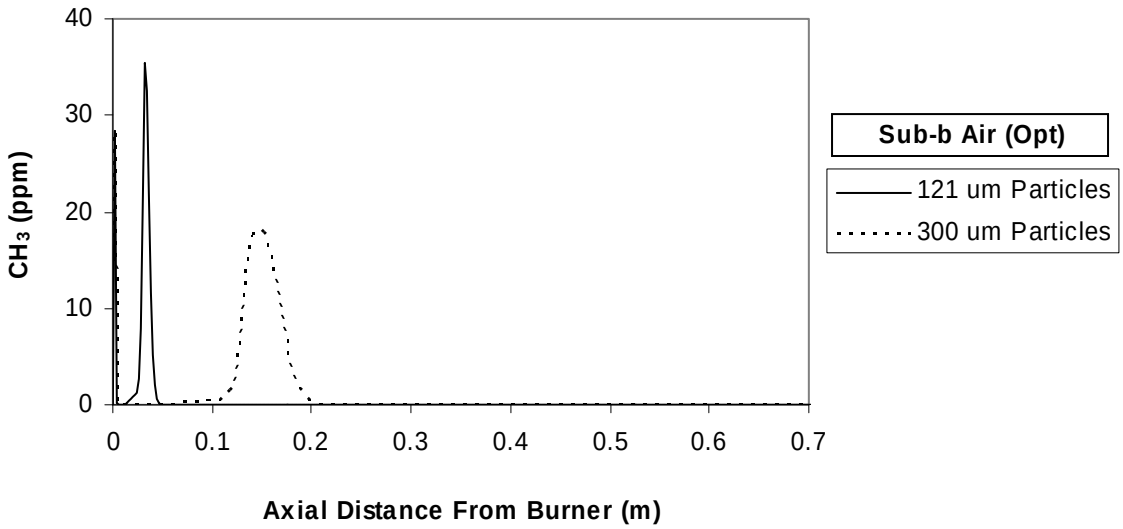

Figure 100. Plot of the predicted CH_3 profile for the Sub-b Air (Opt) case using two different particle sizes.

As is seen in the figure, the CH_3 profiles have two peaks each. A sharp, narrow peak near the burner is associated with the methane flame and further downstream is a wider peak spatially coincident with the modeled release of volatiles. These predictions suggest that if a particle size distribution was included in the model that volatiles would be released over a broad region from 0-0.2 m from the burner for the Sub-b Air (Opt) case, rather than in the first 0.05 m from the burner predicted when only one

representative particle size is used. Smaller particles completing devolatilization early would be expected to consume oxygen by heterogeneous char oxidation while larger particles are still evolving volatiles. Volatiles evolved late from the larger particles would be released under reducing conditions and would probably result in the persistence of hydrocarbons throughout the primary combustion zone as observed in the experimental data.

An additional explanation for poor agreement between the model and the data is the lack of a model for mixing of coal and oxidizer. In the model, the coal is assumed to be perfectly mixed within the oxidizer. In reality, the coal may clump during the feed process and produce spatial or temporal pockets of rich products that require some amount of mixing before reaching the average stoichiometry of the mixture. This would also tend to broaden the region of volatiles release and produce local zones of lower SR in which HCN, NH_3, and hydrocarbons could survive.

5.12 NO_X Reaction Pathways

The MixMaster application was used to evaluate the pathways through which NO is destroyed in the model. For the GRI-Mech 3.0 mechanism, representative pathway diagrams for modeled NO destruction in the Sub-b Air (Opt) and Sub-b O30 (Opt) cases are shown in Figure 101 and Figure 102. It should be noted that these diagrams only show the most significant pathways since there are too many pathways in the mechanism to show all in a practical figure.

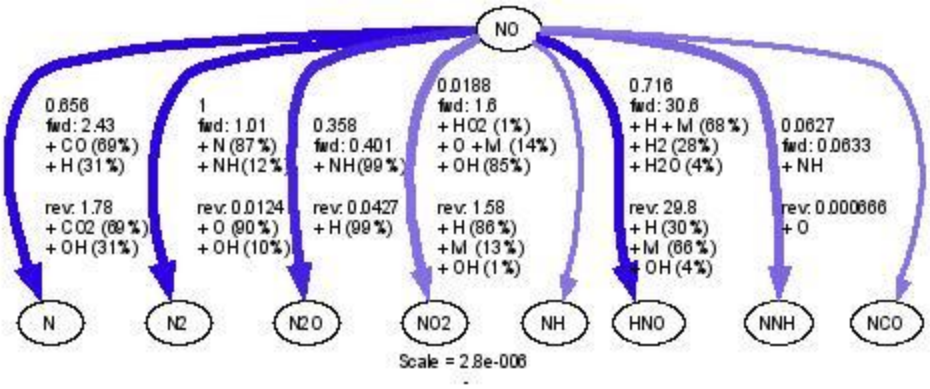

Figure 101. Major modeled NO reaction pathways for the Sub-b Air (Opt) case 152 mm from the burner using GRI-Mech 3.0.

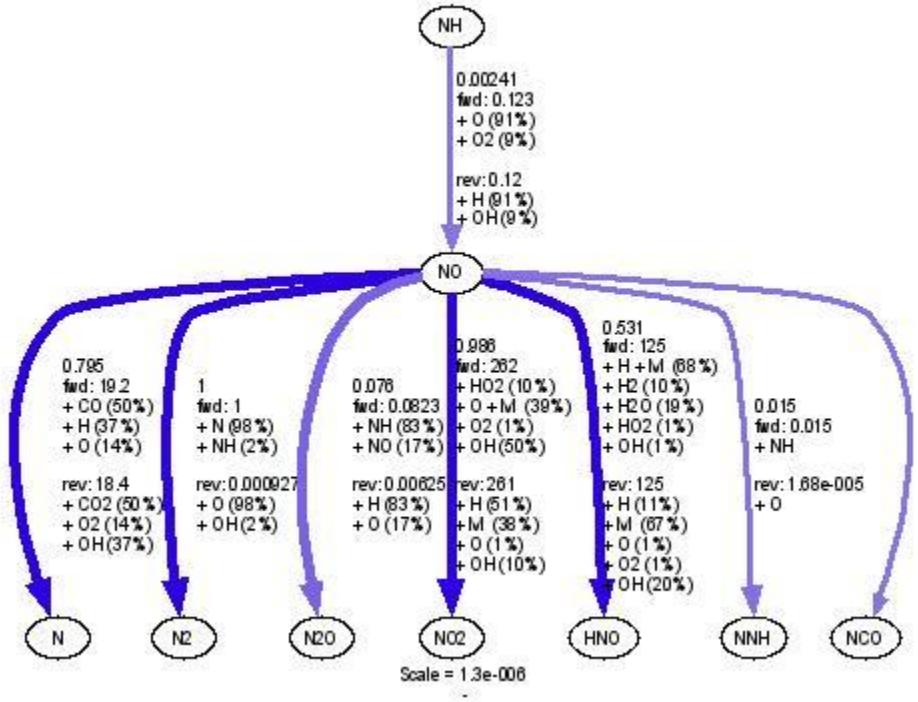

Figure 102. Major modeled NO reaction pathways for the Sub-b O30 (Opt) case 152 mm from the burner using GRI-Mech 3.0.

An important feature of these pathway diagrams is the absence of hydrocarbons in the reactants listed next to the pathway arrows even though the GRI-Mech 3.0

mechanism does include reactions of NO with hydrocarbons. These reburning reactions are listed in Appendix B as reactions 247 through 256 in the mechanism file. Reaction 10 is an example.

$$CH_3 + NO \longleftrightarrow HCN + H_2O \qquad \text{[Reaction 10]}$$

The reason that the reburning reactions do not produce significant NO reduction in the model is a result of the hydrocarbon concentration predictions being near-zero over most of the reactor. As mentioned in connection with Figure 73 in Section 5.2 the SKG03 mechanism displays a unique feature in the predictions for the Sub-b Air (Opt) case. The narrow peak in hydrocarbons associated with the modeled volatiles release occurs at just the right place for reburning reactions to cause a sudden drop in NO. A reaction pathway diagram for this case is shown in Figure 103. The dominant NO destruction pathway here involves reaction of NO with hydrocarbons to produce HCN.

It is reasonable to expect that if the model used a range of particle sizes as discussed in Section 5.11 the hydrocarbon concentrations would be lower than predicted at the single narrow peak and spread over a larger region in space. The resulting NO destruction rate should then decrease relative to that in Figure 73 and also occur over a wider region.

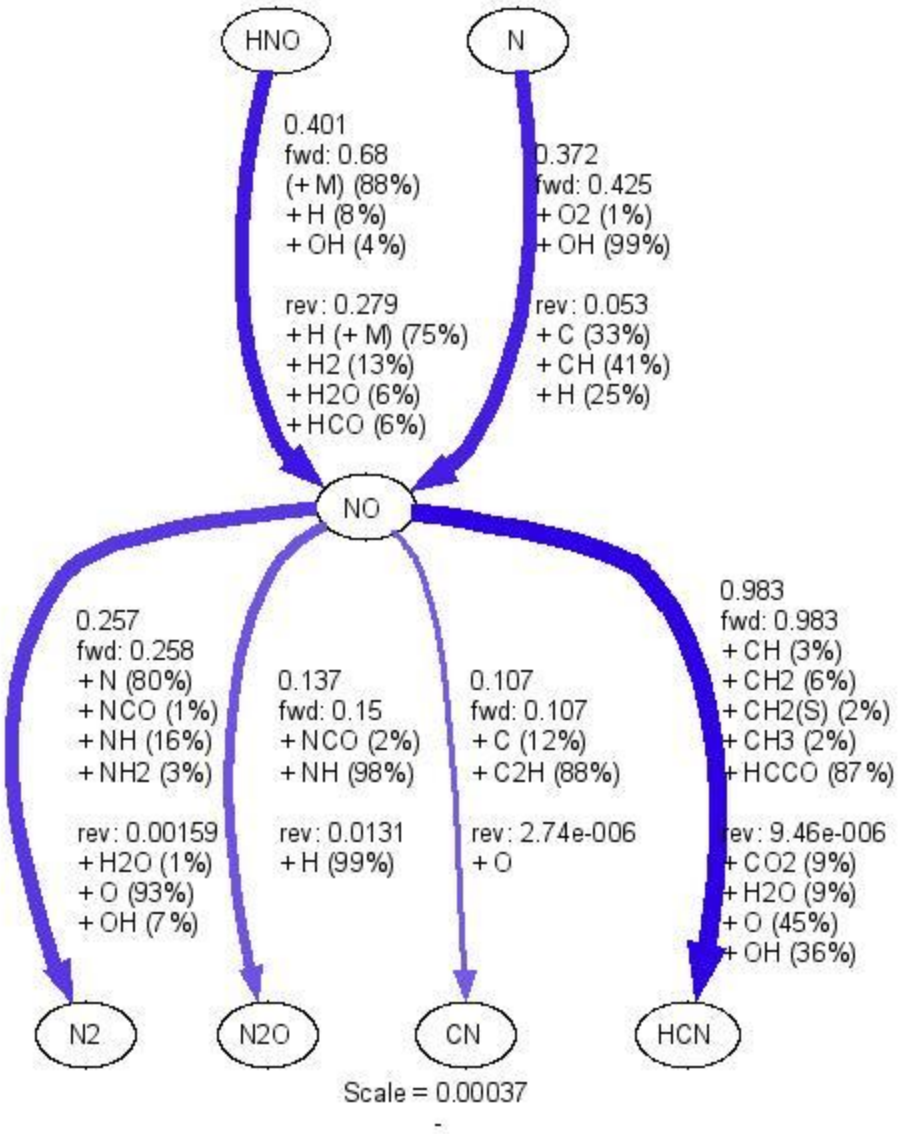

Figure 103. Major modeled NO reaction pathways for the Sub-b Air (Opt) case 32 mm from the burner using the SKG03 mechanism.

6 Discussion

6.1 Unstaged Combustion

The unstaged experiments showed two important features:

- A slight decrease in NO_X during char burnout was the only reduction observed
- Oxy-fuel NO_X concentrations were higher but mass flux of NO_X was comparable for air and oxy-fuel

Reduction of NO_X during char burnout in a fuel-lean premixed flame was also observed by Okazaki et al. (1984), and may be due to heterogeneous reactions. It is expected that this reduction would increase with higher concentrations of NO_X, and thus may be more significant under oxy-fuel conditions. In these experiments the reductions were not noticeably greater under oxy-fuel conditions, and were not significant enough for practical benefits. In agreement with previous research (Tan and Croiset, 2005), these results indicate that low-NO_X combustor designs are required for oxy-fuel combustion in order to reduce NO_X significantly.

Some differences were observed in initial rates of NO_X formation. The O30 oxidizer formed NO_X more rapidly than the Air or O25 oxidizers. The O30 oxidizer also formed the highest amount of NO_X initially. These trends are consistent with expectations

based on higher reaction rates with elevated O_2 concentrations, and enhanced nitrogen release when particle heating rates increase.

6.2 Staged Combustion

6.2.1 Effects of Coal Type

Staged combustion experiments with three different coals (sub-bituminous, Illinois #6, and Pittsburgh #8) exhibited varying differences in effluent NO_X between air and oxy-fuel combustion. For the same SR between air and oxy-fuel combustion, the oxy-fuel combustion produced lower conversions of fuel N to NO_X. Additional experiments with the sub-bituminous coal where the primary SR was varied indicated that there was an optimum primary stoichiometry (at a given secondary stoichiometry) for low effluent NO_X, and that this optimum primary stoichiometry was quite different for air and oxy-fuel combustion. While fuel-oxidizer ratios determine the stoichiometry, as the coal is initially solid, the gas-phase stoichiometry depends on volatiles release. The gas environment in the primary combustion zone for different coals may be different due to volatiles content differences even if the global stoichiometry is the same. It is possible that the differences in nitrogen to NO_X conversion rates observed between coals are due to differences in the coals' volatiles yields. Heterogeneous chemistry is believed to be of only minor importance (Bose et al., 1988; Okazaki and Ando, 1997). Further interpretation of the data from the higher-ranked coals is difficult given the low level of burnout achieved.

6.2.2 High CO Levels in the Flame

As observed by others (including Hjärtstam et al., 2007), higher levels of CO were measured in the fuel-rich region under oxy-fuel conditions than in air combustion when the global stoichiometry of both flames was the same. Under minimum effluent NO_X conditions where the primary stoichiometry of the oxy-fuel case was significantly higher than in air, the levels of CO were comparable. If CO is an important species to produce radicals required in NO reduction reactions (Bowman, 1997), it is significant that oxy-fuel combustion can produce high CO levels without a requirement for strongly fuel-rich conditions as is the case for air combustion.

The equilibrium calculations performed above combined with kinetic modeling suggest that CO levels are at or near equilibrium in the flames and that it is primarily the high CO_2 levels in oxy-fuel that cause the high CO levels. A secondary source of CO is gasification of the char by CO_2 which is traditionally neglected in air combustion modeling, but may become significant under oxy-fuel conditions. Again this is due to the elevated CO_2 levels.

Other research (Andersson et al., 2007) found that the oxygen concentration in the oxy-fuel oxidizer also had an effect on the CO levels in the flame whereas in this work no notable differences were observed between the O25 and O30 oxidizers. In their work the measured gas temperatures were above and below 1500 K where thermal dissociation of CO_2 into CO and other species becomes significant. In this work estimated gas temperatures are well above 1500 K (see for example Figure 78), which is probably why no difference was observed.

6.2.3 Model Performance

One strength of the model used in this work is the general lack of empiricism (with the exception of a heat transfer parameter). Sub-models were used that were independent of specific experiment types with the intention of obtaining predictive results without having to tune the model to match the data. NO_X formation predictions near the burner were qualitatively accurate, and predicted trends in NO_X formation near the burnout oxidizer injection were consistent with expectations. For all three gas-phase mechanisms tested, the rate of NO_X destruction in all cases but one was significantly under predicted. In the one case where the rate was over predicted (see Section 5.2), the faster rate was caused by reburning reactions that were not significant in the other cases due to lack of hydrocarbon availability in the predicted gas mixture. In Section 5.11 it is shown that the prediction of hydrocarbon species by the model is inaccurate which likely stems from the particle size and perfect mixing assumptions. If a particle size distribution and mixing model were added, hydrocarbons required for reburning are expected in the predictions over the first 0.2 m of the reactor and reburning reactions would be expected to play an important role in the model predictions over this region.

In the experimental data (repeated in Figure 104) it is clear that NO_X destruction is faster in the devolatilizing region of the reactor than in the lower portion of the reducing zone from 0.2 to 0.6 m from the burner. From this it appears that reburning reactions are significant in the air and oxy-fuel experiments, and this is the major NO_X reduction feature is not demonstrated by the model.

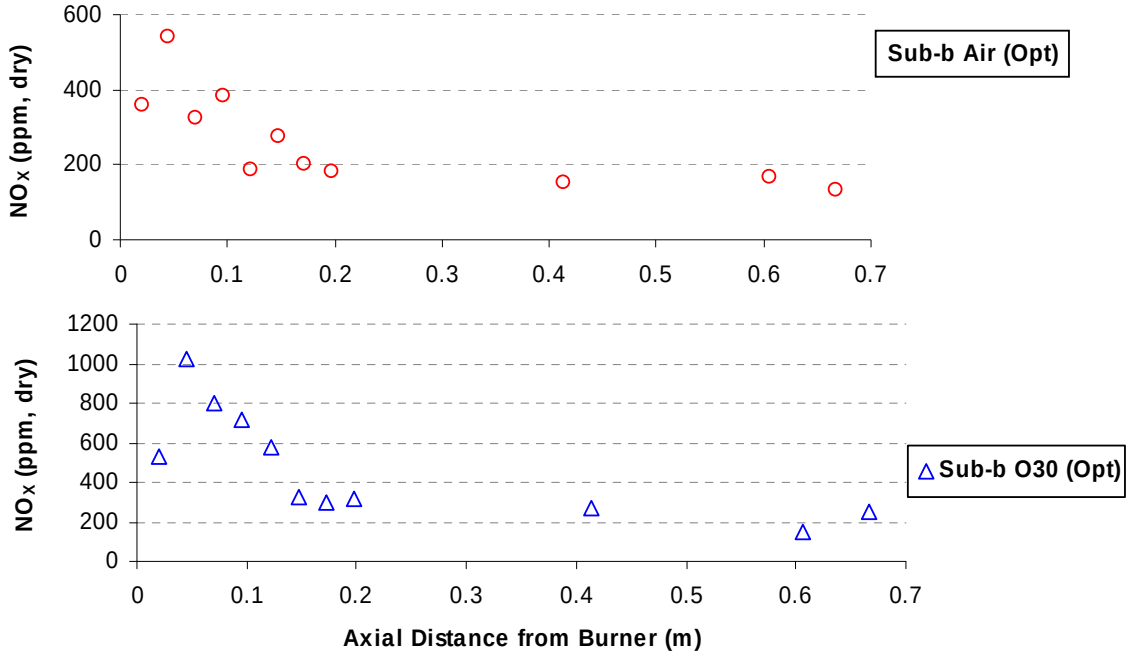

Figure 104. NO_X data for an Air and O30 case showing faster NO_X reduction in the first 0.2 m of the reactor that is attributed to reburning reactions.

Advanced reburning reactions were also insignificant in their effect on the model predictions (Section 5.2) which may again be due to the inaccurate hydrocarbon profiles. Theoretically, in advanced reburning and SNCR, one mole of NH_3 reacts with one mole of NO to produce N_2 and H_2O. Thus the level of ammonia injected in these processes is close to the level of NO_X. In the experimental data for the sub-bituminous coal (Figure 53 and Figure 54) the NH_3 levels are high enough to be comparable to the NO and advanced reburning reactions are possibly of importance. For the Illinois #6 coal the NH_3 levels were low and the same argument would not apply.

With the single particle size used in the model the prediction of initial NO_X formation is quite good. This may be simply fortuitous and may not be true if the particle size modeling was improved. While the GRI-Mech 3.0 mechanism was used most in this

work, it is not clear at this point which mechanism of those tested is most accurate for this type of model.

Inaccuracies in the predictions of NO_X formation at the burnout oxidizer addition are probably due to neglect of mixing effects and turbulence-chemistry interactions.

6.2.4 HCN, NH_3, and Hydrocarbons in the Reducing Zone

The HCN, NH_3, and hydrocarbon (CH_4 and C_2H_4) measurements may be summarized as follows:

- Concentrations were higher in oxy-fuel conditions than air at the same primary SR
- For NH_3, oxy-fuel at high primary SR exhibited similar concentrations to air at low primary SR
- Oxy-fuel combustion at high primary SR had significant levels of HCN and hydrocarbons albeit lower than the levels in air at low primary SR

Nozaki et al. (1997) observed higher HCN and NH_3 levels in their work and attributed this to reduction of recycled NO to form HCN or NH_3 early in the flame. In contrast the present observations were made in the absence of recycled NO, thus necessitating another explanation. Another group (Dhungel et al., 2007 and Scheffknecht et al., 2007) performed experiments without NO_X recycling using a jet/swirl burner and staged combustion. Air and oxy-fuel cases at identical stoichiometry were compared (overall SR of 1.15, burner SR of 0.75) and as observed in this work, HCN and NH_3 concentrations were higher under oxy-fuel conditions. No hydrocarbon measurements were reported, and the differences in HCN and NH_3 did not directly lead to any

conclusions. It was concluded that the pathways of NO destruction in oxy-fuel were similar to those of air combustion.

High concentrations of HCN, NH_3, and hydrocarbon fragments are indicative of an environment suitable for rapid reduction of NO by reburning (Hu et al., 2001) and advanced reburning reactions. The increase in NH_3 with distance from the burner as NO_X decreases is evidence of reburning in the experiments (Figure 62 and Figure 63). These results suggest that oxy-fuel combustion is better able to produce reburning environments than is air combustion. As the model qualitatively predicts some of the trends between air and oxy-fuel concentrations of these species it is likely that the model may be useful to identify the reason for this difference, but the model weaknesses noted should be remedied first. At present the reason for the difference remains unclear, but as discussed above there are multiple observations in the literature to support the hypothesis.

6.3 Importance of Various Mechanisms

The use of a model in this work allowed the effects of various mechanisms to be somewhat isolated for additional insight. In this section some of the possible reasons for lower NO_X emissions from oxy-fuel combustion discussed previously in the Background are revisited in light of the experimental and modeling results.

6.3.1 Near-Elimination of N_2 in the System

In the results presented air combustion showed greater sensitivity to increases in primary SR than oxy-fuel combustion due largely to thermal NO_X formation. This dictates that the primary combustion zone in air be operated at low SR. Unfortunately this usually has a negative impact on fuel conversion. The absence of N_2 to form thermal

NO_X allows an oxy-fuel combustor to operate with higher primary SR and thus achieve higher fuel conversion early in the reactor and higher temperatures conducive to NO_X reduction kinetics. For the sub-bituminous coal in this reactor the primary SR for minimum NO_X in oxy-fuel was 0.83 and for air 0.63. Farzan et al. (2005) also reported optimum NO_X conditions being achieved at increased burner SR for oxy-fuel relative to air.

The model predicted that the thermal NO_X reactions were important in oxy-fuel conditions as the reverse reactions became significant with high NO concentrations and low N_2 concentrations. Thus in a computational model the absence of N_2 should not be used to justify the omission of these reactions. In addition, practical combustors will have some N_2 from air infiltration and other sources. For small amounts of N_2 the model predicted a slight increase in NO formation that was mostly formed through the thermal NO_X pathway. The amount of NO_X formed by small amounts of N_2 was here predicted to be slight, but this may be burner-specific since conflicting reports exist in the literature (see Section 2.5).

6.3.2 Equilibrium Considerations

The experimental data and kinetic model predictions agree on the fact that NO levels are far above equilibrium for both air and oxy-fuel combustion. When stoichiometry was varied to determine minimum NO_X conditions the minimum nitrogen conversion efficiency for air and oxy-fuel were very similar despite equilibrium NO_X being two orders of magnitude lower in oxy-fuel (see Section 5.1). Thus it appears that kinetic limitations are the primary obstacle to overcome in primary NO_X controls under oxy-fuel conditions.

6.3.3 Improved Attachment of Flame to Burner

In the experimental data, high levels of NO_X occurred closer to the burner in the unstaged O30 case relative to the corresponding Air and O25 cases (Figure 37). In addition, wall temperature data in Figure 51 and NO_X measurements in Figure 53 for the sub-bituminous coal indicate that combustion occurs closer to the burner as oxygen concentration in the reactants increases. This is consistent with the observations of Bool and Bradley (2003) and supports the notion that selection of the oxygen concentration in various streams may be used as a tool to control flame attachment and thereby influence NO_X reactions inside the flame.

6.3.4 Reduction of Recycled NO_X in the Fuel-rich Flame Zone

The data obtained when NO was included in the reactants showed more rapid destruction of NO_X in the fuel-rich zone than when NO was not included (Figure 49), and possibly reduced initial formation of NO_X. The increased destruction rate leads to the expectation that a greater amount of NO_X would be reduced if NO_X concentrations increased. In oxy-fuel combustion this should occur when the flue gas is recycled and would be important to determining the level of NO_X exiting the combustion space.

In one test, Scheffknecht et al. (2007) achieved effectively 100% reduction of the recycled NO_X, but this should not be considered automatic in oxy-fuel. Some recycled NO_X may not experience a fuel-rich zone if for example it is passed through overfire air ports. The finding in this work and that of Farzan et al. (2005) that the optimum level of staging for minimum NO_X in oxy-fuel combustion is at a higher primary SR in oxy-fuel than air is important in the discussion of this mechanism. If higher primary SR is used, more of the recycled NO_X will pass through the reducing zone. In addition the flame

intensity where burnout oxidizer is added is reduced at higher primary SR and thus the formation of NO_X at this point should also be reduced. The higher levels of hydrocarbons, HCN, and NH_3 in oxy-fuel reducing zones relative to air combustion at the same primary SR (Section 6.2.4) that have potential to form NO at this location add additional importance to this point.

6.3.5 Temperature Increases

In the Background it was noted that in oxy-fuel combustion the near-absence of atmospheric N_2 allows temperature increases to be used to benefit the NO_X reduction kinetics without risk of increasing thermal NO_X. This appears to have played a role in the experiments here where minimum NO_X conditions in oxy-fuel were at a primary SR that would have yielded significant thermal NO_X in air combustion.

6.3.6 Increased Residence Times in Fuel-rich Regions

The higher oxygen concentrations in oxy-fuel combustion should allow deeper staging without flame instability and hence longer fuel-rich residence times for NO_X destruction. Molecular weight differences between N_2 and CO_2 also promote longer residence times in oxy-fuel combustion. The results of this work however, indicate that deeper staging may not be desirable in oxy-fuel, and increased residence time may have only a slight effect on NO_X if other requirements for NO_X reduction (such as availability of radicals) are not met. In Figure 104 the rate of NO_X reduction is extremely slow in both air and oxy-fuel from 0.2 to 0.6 m from the burner despite high temperatures and reducing conditions.

6.3.7 Increased Importance of Gasification Reactions

Andersson (2007) had some success with a CO-based reaction in a global NO_X reduction model, and Bowman (1997) indicates that moist oxidation of CO may produce radicals required for NO reduction. As indicated by the predicted differences in CO with and without the reaction of CO_2 with char (Figure 91), gasification reactions may change the CO level, but the effect on CO by this mechanism is small compared to the CO levels produced by thermal equilibrium when CO_2 levels are high. It is therefore expected that gasification reactions would not have much impact on oxy-fuel nitrogen chemistry.

6.3.8 Competition for Oxygen

At the same primary zone SR, the rapid initial formation of NO_X in terms of η_N was similar between air and oxy-fuel cases for both the Sub-bituminous and Illinois #6 coals (near-burner data was not obtained for the Pittsburgh #8 coal). Thus there is no indication from these data that the changes to the combustion environment (temperature and species concentrations) between air and oxy-fuel significantly affected the competition for oxygen between hydrocarbons and nitrogen compounds.

6.3.9 Heterogeneous Mechanisms

Reduced NO formation from char and enhanced heterogeneous reburning were discussed in the Background as possible reasons for lower NO_X emissions from oxy-fuel combustion. In the unstaged experiments only a slight decline in NO_X could possibly be attributed to reduction of NO by char. The literature discussed in 2.2.5 also suggests that heterogeneous pathways are of minor importance.

6.4 Application of Results to a Practical Combustor

As mentioned in Section 4.4, at the primary SR that gave the lowest effluent η_N for air and oxy-fuel, the value of η_N was about the same (within uncertainty). At these conditions thermal NO_X formation had been essentially eliminated in the air case and the nitrogen conversion efficiency profiles shown in Figure 62 were qualitatively similar. While these results do give insight into the mechanisms of nitrogen evolution, they cannot be directly applied to an industrial combustor.

The primary SR used to produce minimum NO_X in air combustion is low compared to values used in practice. Higher primary SR is typically required in order to obtain good fuel burnout. As a result of this trade off air-fired burners do produce some thermal NO_X, whereas an oxy-fuel burner would not. This is one of the reasons for lower NO_X release to the environment from an oxy-fuel system. The fact that oxy-fuel combustion may produce its minimum nitrogen conversion efficiency at high primary SR suggests that the trade off between low NO_X and high burnout may not exist for oxy-fuel combustors.

In addition, as defined in this work, effluent η_N is a measure of NO_X at the exit of a once-through combustor (with simulated flue gases in the oxy-fuel cases). In a practical oxy-fuel process more than half of the gas leaving the combustion space may be recycled back to the combustion chamber and thus if η_N at the combustion chamber exit was the same between an air and oxy-fuel process, the oxy-fuel system would be releasing much less NO_X to the environment (or CO_2 capture process) than the air system.

7 Conclusions

Pulverized coal was burned in a down-fired, laminar flow reactor with and without oxidizer staging. Air or mixtures of O_2 and CO_2 were used as oxidizers, and nitrogen and combustion gas species concentrations were measured to gain insight into the differences between NO_X formation in air and oxy-fuel combustion. Additional understanding was obtained by modeling the reactor as a series of ideal reactors with detailed kinetics. Coal volatiles were predicted using the CPD-NLG coal devolatilization model. The following conclusions can be drawn from the results:

- In unstaged premixed combustion, air and oxy-fuel combustion produced similar levels of fuel nitrogen conversion to NO_X. Low NO_X emissions from oxy-fuel combustion are therefore not achieved without staged mixing of oxidizer and fuel as is the case for conventional air combustion.
- Wall temperature and other data indicated higher reaction rates under oxy-fuel conditions than in air.
- While effluent CO levels were comparable between air and oxy-fuel combustion, higher CO concentrations in fuel-rich, oxy-fuel flames were often measured. The computational model suggests that high CO levels observed in oxy-fuel combustion are due to thermodynamic equilibrium. Thermal dissociation of CO_2 becomes significant at about 1500 K which is expected to

lead to strong temperature sensitivity of CO concentrations around this temperature. In oxy-fuel combustion, CO levels are higher than air combustion above 1500 K because of the greater amount of CO_2 available for dissociation reactions. CO may indirectly influence the NO_X chemistry through reactions that increase the concentration of radicals important to NO_X reduction.

- Gasification of char by CO_2 under oxy-fuel conditions has some influence on the level of CO through the thermal effects of the gasification reactions and the effect of additional fuel conversion on the elemental composition of the combustion gases. These gasification reactions may not be insignificant in oxy-fuel conditions as is often assumed to be the case in air combustion but the amount of CO appears to be dominated by equilibrium considerations, not gasification reactions.
- A detailed model of nitrogen evolution under pulverized coal air and oxy-fuel conditions was assembled using existing sub-models from the literature. The CPD-NLG devolatilization model was modified for use in oxy-fuel environments. The CPD-NLG model treats devolatilization as a purely thermal process. Interaction with the N_2 or CO_2-based surroundings is based on gas transport properties and not chemistry. The experimental data obtained are consistent with this model being adequate to describe the devolatilization process under oxy-fuel conditions.
- The homogeneous chemistry used in the model correctly predicts certain qualities of oxy-fuel combustion observed experimentally and shows promise

of greater quantitative accuracy with further development. The success achieved with the model suggests that NO_X formation in oxy-fuel combustion can be described with the existing knowledge base. Further model development is required to determine if the same may be said of NO_X destruction. As is the case with air combustion (Bose et al., 1988), heterogeneous chemistry is believed to be of minor importance to NO_X in pulverized coal oxy-fuel conditions.

- Initial formation of NO_X in the flames was predicted by the model to be controlled by finite rate chemistry for both air and oxy-fuel combustion. Model predictions and experimental data showed good qualitative agreement (good quantitative agreement was thought to be fortuitous).
- Measured values of NO_X formed in oxy-fuel were far above equilibrium. The extremely low equilibrium levels of NO_X in oxy-fuel gas mixtures have little effect on the finite rate NO_X chemistry.
- Thermal NO_X formation was insignificant in the oxy-fuel conditions studied however, it is predicted by the kinetic model to be the primary pathway for NO_X formed from trace amounts of N_2 present (from air infiltration and other sources).
- Destruction of NO_X by the reverse reactions of the thermal NO_X mechanism was predicted by the model to be important under both air and oxy-fuel conditions.
- Destruction of NO_X by reburning reactions was not predicted by the computational model and this was attributed to inaccuracies in hydrocarbon

level predictions. Based on measured hydrocarbon, HCN, and NH_3 data, this pathway is believed to be the dominant means of rapid NO_X destruction observed in the experiments.

- NO_X destruction rates in the fuel-rich zone increased with increased inlet NO concentration caused by supplying NO to the oxidizer. This means that a greater amount of NO_X may be destroyed in a combustion zone supplied with recycled NO_X than in a once-through process. There was insufficient spatial resolution in the experimental data to measure suppression of NO_X formation by increased inlet NO levels, however others have observed this phenomenon (Okazaki and Ando, 1997).
- Air combustion shows greater sensitivity to changes in primary SR than oxy-fuel combustion as the SR is increased. This sensitivity is mostly due to the onset of thermal NO_X formation in air as more oxygen becomes available in the primary combustion zone.
- Both air and oxy-fuel combustion have an optimum level of oxidizer staging for low-NO_X emissions that arises from a trade off between NO_X formation and destruction in the primary combustion zone, and NO_X formation as additional oxidizer is mixed into fuel-rich products.
- The optimum primary SR for oxidizer-staged oxy-fuel combustion for low-NO_X is higher than that for air partially because thermal NO_X formation is not significant under oxy-fuel conditions. The higher optimum primary SR found here is consistent with pilot scale tests in turbulent combustion (Farzan et al., 2005) and has the advantages of more of the recycle stream passing through

the fuel-rich zone for NO_X reburning, a less intense combustion that may form NO_X at the location of burnout oxidizer mixing, and probably improved burnout of the fuel.

- At the same primary SR oxy-fuel flames have higher CO, NH_3, HCN, and hydrocarbons than air flames which likely leads to more rapid reburning of NO_X in oxy-fuel. The high levels of nitrogen intermediates increases the potential to form NO_X as burnout oxidizer is added, providing further reason to use higher primary SR under oxy-fuel conditions.
- In the absence of N_2 to form thermal NO_X in oxy-fuel, high temperatures and higher primary SR can be used to benefit NO_X reduction kinetics without some of the trade offs inherent in air combustion.
- Due to differences in thermal NO_X, reburning rates, and NO_X formation at burnout oxidizer injection, NO_X emissions from a once-through combustor can be lower in oxy-fuel than air combustion, however a further important factor in lower NO_X emissions from oxy-fuel is that a flue gas recycle system only releases a fraction of the furnace exit NO_X to the environment (or CO_2 capture process) while the remainder is sent back to the combustion chamber.

8 Recommendations

8.1 Recommendations for Future Work

The greatest weaknesses of the model presented in this work may stem from the single particle size assumption. To change this assumption would require a massive restructuring of the model to account for different-sized particle streams, and unfortunately this was outside the scope of work. Some of the restructuring would be necessary to prevent the computational cost becoming excessive. If this improvement to the model was made it is expected that hydrocarbon predictions would be dramatically improved, as would predictions of NO_X destruction by reburning and possibly advanced reburning for lower-ranked coals that yield higher NH_3 concentrations. The influence of CO on NO_X reduction may then be more fully investigated.

The documentation of the experiment in this work is intended to be sufficiently detailed that a computational fluid dynamics (CFD) model of the experiment could be completed and global models for NO_X could be tested using the experimental data to validate the model. A CFD model would allow turbulence-chemistry interactions at the location of burnout oxidizer injection to be understood more fully.

As mentioned in the literature review, nitrogen in soot is undesirable because it is not as easily controlled as gas-phase nitrogen. Nitrogen in soot may be the next most

productive source of nitrogen for industry to confront and therefore soot-forming tendencies of oxy-fuel combustion are important to understand. The higher hydrocarbon concentrations in oxy-fuel combustion relative to air combustion at the same SR indicate that soot formation is probably different under oxy-fuel conditions.

8.2 Recommendations for Computational Modeling of NO_X formation in Oxy-fuel Combustion

Given the similarities between the air and oxy-fuel cases studied there is no evidence from the results obtained to expect that simplified NO_X models developed for air combustion will not function equally well under oxy-fuel conditions. Model validation is still required, and in general NO_X models are not yet considered quantitatively predictive, but these points may be useful to the modeler:

- The thermal NO_X reactions (in reverse) appear to be significant under oxy-fuel conditions even though N_2 is largely absent. These reactions should be enabled in an oxy-fuel NO_X model.
- Reburning reactions appear to be the major reason for rapid destruction of NO_X in a fuel rich zone and these should be included also. This will require that hydrocarbons such as CH, CH_2, etc. are predicted by the combustion model. The accuracy of these predictions needs validation as in this work it was found that oxy-fuel combustion has higher levels of hydrocarbons than air combustion at the same stoichiometry.

9 References

Aarna, I., E. M. Suuberg (1999) *The Role of Carbon Monoxide in the NO-Carbon Reaction*, Energy and Fuels, Vol. 13, 1145-1153.

Allam, R. J., R. S. Panesar, V. White, D. Dillon (2005) *Optimising the design of an Oxyfuel-Fired Supercritical PF Boiler*, The 30th International Technical Conference on Coal Utilization and Fuel Systems, April 17-21, 2005, Clearwater, FL.

Andersson, K. (2007) *Combustion Tests and Modeling of the Oxy-fuel Process, An Overview of Research Activities at Chalmers University*, 2nd IEAGHG International Oxy-combustion Workshop, January 25-26, 2007, Windsor, CT.

Andersson, K., F. Normann, F. Johnsson (2007) *Experiments and modeling on oxy-fuel combustion chemistry during lignite firing*, The 32nd International Technical Conference on Coal Utilization and Fuel Systems, June 10-15, Clearwater, FL.

Asay, B. W. (1982) *Effects of Coal Type and Moisture Content on Burnout and Nitrogeneous Pollutant Formation*, Ph.D. Dissertation, Brigham Young University, Provo, UT.

Badzioch, S., P. G. W. Hawksley (1970) *Kinetics of Thermal Decomposition of Pulverized Coal Particles*, Ind. Eng. Chem. Process Des. Develop., Vol. 9, No. 4, 521-530.

Blair, D. W., J. O. L. Wendt, W. Bartok (1976) *Evolution of Nitrogen and Other Species During Controlled Pyrolysis of Coal*, Sixteenth Symposium (International) on Combustion, 475-489, The Combustion Institute, Pittsburgh, PA, 1976.

Bool, L. E., J. Bradley (2003) *NO_X reduction from a 44 MW wall-fired boiler utilizing oxygen enhanced combustion*, The 28th International Conference on Coal Utilization and Fuel Systems, March 10, 2003, Clearwater, FL.

Bose, A. C., K. M. Dannecker, J. O. L. Wendt (1988) *Coal Composition Effects on Mechanisms Governing the Destruction of NO and Other Nitrogenous Species during Fuel-Rich Combustion*, Energy and Fuels 2:301-308.

Baukal, C. E., Editor (1998) *Oxygen-enhanced combustion*, CRC Press LLC (book).

Bowman, C. T. (1992) *Control of Combustion-Generated Nitrogen Oxide Emissions: Technology Driven by Regulations*, Twenty Fourth Symposium (International) on Combustion, The Combustion Institute, Pittsburgh, PA, 859-878.

Bowman, C. T. (1997) *Mechanisms and Modeling of Gas-Phase Aftertreatment Methods for NO Removal from Combustion Products*, Physical and chemical aspects of combustion; a tribute to Irvin Glassman, 29-68, Edited by F. L. Dryer and R. F. Sawyer, Gordon and Breach. (In some citations the year is given as 1996 and the mechanism presented is referred to as "B96").

Brown, B. W., L. D. Smoot, P. J. Smith, P. O. Hedman (1988) *Measurement and Prediction of Entrained-Flow Gasification Processes*, AIChE Journal, Vol. 34, No. 3, 435-446.

Buhre, B. J. P., L. K. Elliott, C. D. Sheng, R. P. Gupta, T. F. Wall (2005) *Oxy-fuel combustion technology for coal-fired power generation*, Progress in Energy and Combustion Science, Vol. 31, 283-307.

Chan, L. K., A. F. Sarofim, J. M. Beer (1983) *Kinetics of the NO-Carbon Reaction at Fluidized Bed Combustor Conditions*, Combustion and Flame, 52:37-45.

Châtel-Pélage, F., P. Pranda, N. Perrin, H. Farzan, S. J. Vecci (2004) *Oxygen-Enrichment for NO_X control in coal-fired utility boilers*, The 29th International Technical Conference on Coal Utilization and Fuel Systems, April 18-22, 2004, Clearwater, FL.

Chen, S. L., R. K. Lyon, W. R. Seeker (1991) *Advanced Non-Catalytic Post Combustion NO_X Control*, Environmental Progress, Vol. 10, No. 3, 182-185.

Chui, E. H., M. A. Douglas, Y. Tan (2003) *Modeling of oxy-fuel combustion for a western Canadian sub-bituminous coal*, Fuel, Vol. 82, 1201–1210.

Chui, E. H., P. M. J. Hughes (1996) *Validation of NO_X and NO_X precursor predictions in coal flames*, Combustion Science and Technology, Vol. 119, 51–75.

Damstedt, B. D. (2007) *Structure and nitrogen chemistry in coal, biomass, and cofiring low-NO_X flames*, Ph.D. Dissertation, Brigham Young University, Provo, UT.

See also:

Damstedt, B., J. M. Pederson, D. Hansen, T. Knighton, J. Jones, C. Christensen, L. Baxter, D. Tree (2007) *Biomass cofiring impacts on flame structure and emissions*, Proceedings of the Combustion Institute, 31, 2813-2820.

De Soete, G. G. (1975) *Overall Reaction Rates of NO and N_2 Formation from Fuel Nitrogen*, Fifteenth Symposium (International) on Combustion, pages 1093-1102, The Combustion Institute.

Dhungel, B., J. Maier, G. Scheffknecht (2007) *Emission Behaviour During Oxy-Coal Combustion*, AIChE 2007 Annual Meeting, November 4-9, Salt Lake City, UT.

Farzan, H., S. J. Vecci, F. Châtel-Pélage, P. Pranda, A. C. Bose (2005) *Pilot-Scale Evaluation of Coal Combustion in an Oxygen-Enriched Recycled Flue Gas*, The 30th International Technical Conference on Coal Utilization and Fuel Systems, April 17-21, 2005, Clearwater, FL.

Fletcher, T. H. (1989) *Time-Resolved Temperature Measurements of Individual Coal Particles During Devolatilization*, Combustion Science and Technology, Vol. 63, 89-105.

Fletcher, T. H., A. R. Kerstein, R. J. Pugmire, M Solum, D. M. Grant (1992) *A Chemical Percolation Model for Devolatilization: Milestone Report*, Sandia Report SAND92-8207, available through National Technical Information Service, May 1992.

Genetti, D. B. (1999) *An Advanced Model of Coal Devolatilization Based on Chemical Structure*, M.S. Thesis, Department of Chemical Engineering, Brigham Young University, Provo, UT.

See also:

Genetti, D., T. H. Fletcher (1999) *Modeling Nitrogen Release during Devolatilization on the Basis of Chemical Structure of Coal*, Energy and Fuels, Vol. 13, 1082-1091.

Genetti, D., T. H. Fletcher, R. J. Pugmire (1999) *Development and Application of a Correlation of ^{13}C NMR Chemical Structural Analyses of Coal Based on Elemental Composition and Volatile Matter Content*, Energy and Fuels, Vol. 13, 60-68.

Glarborg, P., A. D. Jensen, J. E. Johnsson (2003) *Fuel nitrogen conversion in solid fuel fired systems*, Progress in Energy and Combustion Science, Vol. 29, 89-113.

Goetz, G. J., N. Y. Nsakala, R. L. Patel, T. C. Lao (1982) *Combustion and Gasification Characteristics of Chars from Four Commercially Significant Coals of Different Rank*, Combustion Engineering, Inc., Windsor, CT – Brown et al. (1988) and Smoot and Smith (1985) were the sources used for the parameters measured by Goetz et al.

Goodwin, D. G. (2003), *An open-source, extensible software suite for CVD process simulation*, Chemical Vapor Deposition XVI and EUROCVD 14, M. Allendorf, F. Maury and F. Teyssandier, editors, Electrochemical Society, 155-162.

Gordon, S., B. J. McBride (1994) *Computer Program for Calculation of Complex Chemical Equilibrium Compositions and Applications I. Analysis*, NASA Reference Publication 1311, October 1994.

Grant, D. M., R. J. Pugmire, T. H. Fletcher, A. R. Kerstein (1989) *A Chemical Model of Coal Devolatilization Using Percolation Lattice Statistics*, Energy and Fuels, Vol. 3, 175-186.

Guo, F. (1997) *Kinetics and Mechanism of the Reaction of NO with Char: Effects of Coal Rank, Burnout, CaO, and Flue Gases*, Ph.D. Dissertation, Department of Chemical Engineering, Brigham Young University, Provo, UT.

See also:

Guo F., W. Hecker (1996) *Effect of CaO and burnout on the kinetics of NO reduction by Beulah Zap char*, Proc. Combust. Inst. Vol. 26, 2251.

Guo F., W. Hecker (1998) *Kinetics of NO reduction by char: effects of coal rank*, Proc. Combust. Inst. Vol. 27, 3085-3092.

Hill, S. C., L. D. Smoot (2000) *Modeling of nitrogen oxides formation and destruction in combustion systems*, Progress in Energy and Combustion Science, Vol. 26, 417-458.

Hjärtstam, S., K. Andersson, F. Johnsson (2007) *Combustion Characteristics of Lignite-Fired Oxy-Fuel Flames*, The 32nd International Technical Conference on Coal Utilization and Fuel Systems, June 10-15, Clearwater, FL.

Hu, Y. Q., N. Kobayashi, M. Hasatani (2001) *The reduction of recycled-NO_X in coal combustion with O_2/recycled flue gas under low recycling ratio*, Fuel, Vol. 80, 1851-1855.

Hu, Y. Q., N. Kobayashi, M. Hasatani (2003) *Effects of coal properties on recycled-NO_X reduction in coal combustion with O_2/recycled flue* gas, Energy Conversion and Management, Vol. 44, 2331-2340.

Kajitani, S., N. Suzuki, M. Ashizawa, S. Hara (2006) *CO_2 gasification rate analysis of coal char in entrained flow coal gasifier*, Fuel, Vol. 85, 163-169.

Khare, S. P., T. F. Wall, R. P. Gupta, L. K. Elliott, and B. J. P. Buhre (2005) *Retrofitting of Air-Fired pf Plant to Oxy-Fuel: Combustibility and Heat Transfer Impacts*, The 30th International Technical Conference on Coal Utilization and Fuel Systems, April 17-21, 2005, Clearwater, FL, Alternate Title: *Retrofitting of Air-Fired pf Plant to Oxy-Fuel and Associated Oxygen Levels through the Burners and Oxygen Production Requirements*.

Kimura, N., K. Omata, T. Kiga, S. Takano, S. Shikisima (1995) *The Characteristics of Pulverized Coal Combustion in O_2/CO_2 Mixtures for CO_2 Recovery*, Energy Conversion and Management, Vol. 36, 805-808.

Kitto, J. B., S. C. Stultz, editors (2005) *Steam, its generation and use: Edition 41*, The Babcock and Wilcox Company, a McDermott company, ISBN 0-9634570-1-2.

Kobayashi, H., L. E. Bool (2005) *Oxygen enhanced low NO_X combustion*, US Patent No. 6,957,955.

Lackner, K. S. (2007) *Update: CO_2 in the Future*, The 32nd International Technical Conference on Coal Utilization and Fuel Systems, June 10-15, Clearwater, FL.

Merrick, D. (1983) *Mathematical Models of the Thermal Decomposition of Coal 2. Specific Heats and Heats of Reaction*, Fuel, Vol. 62, 540-546.

Molina, A., E. G. Eddings, D. W. Pershing, A. F. Sarofim (2000) *Char nitrogen conversion: implications to emissions from coal-fired utility boilers*, Progress in Energy and Combustion Science, Vol. 26, 507-531.

Molina, A., E. G. Eddings, D. W. Pershing, A. F. Sarofim (2004) *Nitric oxide destruction during coal and char oxidation under pulverized-coal combustion conditions*, Combustion and Flame, Vol. 136, 303-312.

Nakayama, S., Y. Noguchi, T. Kiga, S. Miyamae, U. Maeda, M. Kawai, T. Tanaka, K. Koyata, H. Makino (1992) *Pulverized coal combustion in O_2/CO_2 mixtures on a power plant for CO_2 recovery*, Energy Conversion and Management, Vol. 33, 379-386.

Niksa, S. (1996) *Flashchain Theory for Rapid Coal Devolatilization Kinetics. 7. Predicting the Release of Oxygen Species from Various Coals*, Energy and Fuels, Vol. 10, 173-187.

Nozaki, T., S. Takano, T. Kiga (1997) *Analysis of the Flame Formed During Oxidation of Pulverized Coal by an O_2-CO_2 Mixture*, Energy, Vol. 22, 199-205.

Oh, K. C., H. D. Shin (2006) *The effect of oxygen and carbon dioxide concentration on soot formation in non-premixed flames*, Fuel, Vol. 85, 615–624.

Okazaki, K., H. Shishido, T. Nishikawa, K. Ohtake (1984) *Separation of the basic factors affecting NO formation in pulverized coal combustion*, Twentieth Symposium (International) on Combustion, The Combustion Institute, Pittsburgh, PA, 1381-1389.

Okazaki K., T. Ando (1997) *NO_X Reduction Mechanism in Coal Combustion with Recycled CO_2*, Energy, Vol. 22, 207-215.

Perry, S. T. (1999) *A Global Free-Radical Mechanism for Nitrogen Release During Coal Devolatilization Based on Chemical Structure*, Ph.D. Dissertation, Department of Chemical Engineering, Brigham Young University, Provo, UT.

See also:

Perry, S. T., T. H. Fletcher, M. S. Solum, R. J. Pugmire (2000) *Modeling Nitrogen Evolution during Coal Pyrolysis Based on a Global Free-Radical* Mechanism, Energy and Fuels, Vol. 14, 1094-1102.

Pohl, J. H., A. F. Sarofim (1976) *Devolatilization and Oxidation of Coal Nitrogen*, Sixteenth Symposium (International) on Combustion, 491-501, The Combustion Institute, Pittsburgh, PA, 1976.

Sangras, R. et al. (2004) *Oxycombustion process in pulverized coal-fired boilers: a promising technology for CO_2 capture*, The 29th International Technical Conference on Coal Utilization and Fuel Systems, April 18-22, 2004, Clearwater, FL.

Sarofim, A. F., J. H. Pohl, B.R. Taylor (1978) *Strategies for Controlling Nitrogen Oxide Emissions During Combustion of Nitrogen-Bearing Fuels*, AIChE Symposium Series, Tech. Sess., 74: Kansas City, 1978.

Sarofim, A. F., D. W. Pershing, E. G. Eddings, A. Molina (1999) *NO-char kinetics: Implementation to NO_X emissions*, Mediterranean Combustion Symposium, Antalya, June 20-25, 1999, 72-83.

Sarofim, A. F. (2007) *Oxy-fuel Combustion: Progress and Remaining Issues*, 2nd IEAGHG International Oxy-Combustion Workshop, January 25-26, Windsor, CT.

Scheffknecht, G. J. Maier, B. Dhungel, P. Mönckert (2007) *Investigation of Oxy-Coal Combustion in Semi-technical Test Facilities*, Third International Conference on Clean Coal Technologies for our Future, May 15-17, Cagliari, Sardinia, Italy.

Shaddix, C. R., J. J. Murphy (2003) *Coal Char Combustion Reactivity in Oxy-Fuel Applications*, Twentieth Annual International Pittsburgh Coal Conference, September 15-19, Pittsburgh, PA.

Shaddix, C. (2007) *Coal Particle Ignition, Devolatilisation & Char Combustion Kinetics During Oxy-Combustion*, 2nd IEAGHG International Oxy-Combustion Workshop, January 25-26, Windsor, CT.

See also:

Molina, A., C. Shaddix (2007) *Ignition and devolatilization of pulverized bituminous coal particles during oxygen/carbon dioxide coal combustion*, Proceedings of the Combustion Institute, Vol. 31, 1905-1912.

Shaddix, C., A. Molina (2007) *Effect of CO_2 on Coal Char Combustion Rates in Oxy-fuel Applications*, Pittsburgh Coal Conference, September 10-14, Johannesburg, South Africa.

Skreiberg, Ø., P. Kilpinen, P. Glarborg (2004) *Ammonia chemistry below 1400 K under fuel-rich conditions in a flow reactor*, Combustion and Flame, Vol. 136, 501-518.

Smith, K. L., L. D. Smoot, T. H. Fletcher, R. J. Pugmire (1994) *The Structure and Reaction Processes of Coal*, The Plenum Chemical Engineering Series, Springer, (book).

Smith, G. P., D. M. Golden, M. Frenklach, N. W. Moriarty, B. Eiteneer, M. Goldenberg, C. T. Bowman, R. K. Hanson, S. Song, W. C. Gardiner, Jr., V. V. Lissianski, and Z. Qin (2000) *GRI-Mech 3.0*, http://www.me.berkeley.edu/gri_mech/

Smoot, L. D., P. J. Smith (1985) *Coal combustion and gasification*, The Plenum Chemical Engineering Series, Plenum Press, NY (book).

Smoot, L. D., Editor and co-author (1993) *Fundamentals of Coal Combustion for Clean and Efficient Use*, Elsevier, The Netherlands, (book).

Tan, Y., E. Croiset (2005) *Emissions from Oxy-fuel Combustion of Coal with Flue Gas Recycle*, The 30th International Technical Conference on Coal Utilization & Fuel Systems, April 17 - 21, 2005, Clearwater, FL.

Thompson, D. R., L. E. Bool, J. C. Chen (2004) *Oxygen Enhanced Combustion for NO_X control*, Department of Energy Final Report for Award Number DE-FC26-00NT40756, March 2004.

Turns, S. R. (2000) *An Introduction to Combustion, Concepts and Applications, second edition*, McGraw-Hill (book).

Varagani, R. et al. (2004) *Oxycombustion in pulverized coal-fired boiler: a promising technology for CO_2* capture, Third Annual Conference on Carbon Sequestration, May 3-6, 2004, Alexandria, VA.

Wall, T. F., A. Lowe, L. J. Wibberley, I. McC. Stewart (1979) *Mineral Matter in Coal and the Thermal Performance of Large Boilers*, Progress in Energy and Combustion Science, Vol. 5, No. 1, 1-29.

Xu, H., L. D. Smoot, D. R. Tree, S. C. Hill (2001) *Prediction of Nitric Oxide Destruction by Advanced Reburning*, Energy and Fuels, vol. 15, 541-551.

Zabielski, M. F., D. J. Seery, L. G. Dodge (1984) Influence of Mass Transport and Quenching on Nitric Oxide Chemiluminescent Analysis, Environ. Sci. Technol. 18:88-92.

Zevenhoven, R., P. Kilpinen (2002) *Control of pollutants in flue gases and fuel gases*, 2nd ed., ISBN 951-22-5527-8.

Available July 2008 at:

http://eny.hut.fi/research/combustion_waste/publications/gasbook/index.htm

Zhang, H., T. H. Fletcher (2001) *Nitrogen Transformations during Secondary Coal Pyrolysis*, Energy and Fuels, Vol. 15, 1512-1522.

Appendix A:
Common NO_X Control Techniques in Pulverized Coal Combustion

Many NO_X control techniques function by controlling the local temperature and fuel/air ratio where NO_X reactions occur (Hill and Smoot, 2000). Usually these techniques are used in combination such as low-NO_X burners + overfire air + low excess air. This section gives a basic description of the commercial techniques available for NO_X control. For more detail than given here, Zevenhoven and Kilpinen (2002), and Kitto and Stultz (2005) are recommended sources.

Low Excess Air

The simplest and cheapest way to reduce NO_X is to lower the excess air to the combustion process. It should be noted that when firing solid fuels, even for a fuel-lean combustor, there will be pockets of reactants that are locally more fuel-rich than the total flow. Reducing oxygen availability overall reduces oxygen further in these lower SR pockets which favors reduction of NO_X. Lowering excess air also improves efficiency by minimizing sensible energy loss through the stack. This technique is almost universally applied, but for coal combustion some excess air is always required to compensate for incomplete mixing. Typically a wall-fired boiler operates with about 20% excess air.

Overfire Air (Air Staging)

As reducing conditions favor N_2 over NO, diverting some of the combustion air to a point downstream of the main combustion zone allows most of the fuel to burn under reducing conditions and limits NO_X. At the point of overfire air (OFA) addition, the temperatures are lower and the less intense combustion prevents excessive NO_X formation despite oxygen availability. Sometimes this technique is referred to simply as "staged combustion", but technically, a completely different technique known as reburning (described below) is also staged combustion.

Burners out of service (BOOS) is a form of overfire air used with multiple burner oil or gas-fired furnaces. The lower burners are operated at increased output and the upper burners become essentially OFA ports.

Low NO_X Burners

Low NO_X burners function by creating a reducing zone in front of the burner where most of the combustion occurs. This allows nitrogen released from the fuel early in the combustion process to be reduced to N_2 rather than oxidized to NO. Air going to the burner is divided into different streams referred to as primary and secondary air. The primary air conveys the coal, (usually through the center of the burner) and the secondary air is swirled and introduced through an annulus around the primary air. Centrifugal forces expand the swirling secondary air flow outwards as it enters the furnace creating an adverse pressure gradient that draws hot gases from the furnace back towards the burner. The hot gas ignites the incoming coal and also creates an internal recirculation zone (IRZ). Conditions in the IRZ are reducing because the amount of primary air is

insufficient to burn the fuel and the mixing patterns of secondary air into the IRZ are designed to limit availability of oxygen.

Since the fuel goes through a reducing zone before reaching the fuel-lean burnout zone, this is a form of staged combustion. It is sometimes referred to as aerodynamic or in-flame staging.

Low-NO_X burners are used in wall-fired boilers. In principle, a tangential-fired boiler may be thought of as a very large low-NO_X burner, although the physical means of introducing the reactants differs.

Burner characteristics and fuel properties are strongly coupled such that low NO_X burners are far more effective with high volatiles (low rank) coals (Hill and Smoot, 2000).

Reburning (Fuel Staging)

In reburning or fuel-staging, the main combustion zone is operated overall fuel-lean. Downstream, a small amount of fuel (relative to the total fuel flow) is injected to create a fuel-rich condition and provide hydrocarbon radicals required to convert NO to HCN. Additional oxidizer is then added to burn out the reburning fuel. The lower intensity combustion at this point creates less NO_X than was destroyed in the reburning zone. The reburning fuel does not need to be the same as the main fuel source and is often the startup fuel for the boiler.

Advanced Reburning

Advanced reburning is the combination of reburning with injection of a nitrogen containing reagent such as urea or ammonia to increase the effectiveness of the process.

Selective Non-catalytic Reduction

Selective non-catalytic reduction (SNCR) is the injection of ammonia (NH_3) into fuel-lean flue gases at 850-1000°C. Theoretically one mole of NO in the flue gases will react with one mole of NH_3 to produce water. The amount of reagent therefore needs to be controlled to minimize both NO_X and NH_3 emissions (referred to as "NH_3 slip"). If at the point of NH_3 injection the gas temperatures are too low then NH_3 slip occurs, and if they are too high the NH_3 will form NO. The narrow temperature window for the process presents perhaps the biggest difficulty in application. SNCR is also known as thermal $DeNO_X$.

Selective Catalytic Reduction

Selective catalytic reduction (SCR) is similar to SNCR in that it also involves the injection of NH_3 into the flue gas, however in SCR the flue gas is at about 400°C and a catalyst is used to react the NH_3 with NO to form water. SCR units are expensive and do have problems such as poisoning or plugging of the catalyst by trace species or particulate in the flue gas, but they are extremely effective (90-95% NO_X reduction – Zevenhoven and Kilpinen, 2002).

Fuel Preparation and Delivery

It is noted in Kitto and Stultz (2005) that coal fineness is an important part of a low-NO_X system, as is proper distribution of fuel between multiple burners. This latter point essentially comes down to good control of stoichiometry.

Oxygen-enhanced Combustion

Recently, use of oxygen injected into specific places in the burner has been tested and patented for NO_X control (Bool and Bradley, 2003; Kobayashi and Bool, 2005). The technique works by a combination of increased temperatures in the fuel-rich zone, deeper staging, improved flame attachment to the burner, and increased release of nitrogen from the fuel under reducing conditions.

Other Methods

Other forms of NO_X control exist such as flue gas recirculation, but they are not typically applied to coal combustion. Sometimes the processes described above are referred to by trademarks or other names. OFA ports for example are sometimes called NO_X ports. This section covers only those techniques with the greatest relevance to this work.

Appendix B:
Gas-phase Kinetic Mechanism Files

SKG03 (Skreiberg et al., 2004)

The Cantera tool “ck2cti” was used in this work to convert a CHEMKIN input file for the SKG03 mechanism (Skreiberg et al., 2004) to a Cantera mechanism file named skg03.cti. For brevity, the more compact CHEMKIN input file, rather than the Cantera version is shown below. Units: length: cm, time: s, quantity: mol, activation energy: cal/mol.

```
!
! ************************************************
! *  SKG03 mechanism                             *
! *  Skreiberg, Kilpinen and Glarborg            *
! *  Combustion and Flame 136:501-518, 2004      *
! *  see paper for references                    *
! ************************************************
!
ELEMENTS
H O C N AR
END
SPECIES
CO CO2 NO HCN
H O OH HO2 O2 H2 H2O2 H2O
CH2O HCO
CH4 CH3 CH2 CH2(S) CH C
CH3OH CH3O CH2OH
C2H6 C2H5 C2H4 C2H3 C2H2 C2H C2
CH3HCO CH2HCO CH3CO C2H2OH OCHCHO CH2CO HCCOH HCCO C2O
C2H5CHO C2H5CO
NO2 NO3 HNO HONO H2NO
NH3 NH2 NH N N2H2 NNH N2O
CN NCO HNCO HOCN HCNO C2N2 NCN CH3CN CH2CN H2CN
AR N2
N2H4 N2H3 H2NN
HON HNOH HNNO NH2OH NH2NO
END
THERMO
```

```
!
! SKG03 thermodynamic data
!
HO2               BUR95 H   1O   2   00   00G   200.000  6000.000  1000.000    1
 0.41722659E+01 0.18812098E-02-0.34629297E-06 0.19468516E-10 0.17609153E-15    2
 0.61818851E+02 0.29577974E+01 0.43017880E+01-0.47490201E-02 0.21157953E-04    3
-0.24275961E-07 0.92920670E-11 0.29480876E+03 0.37167010E+01 0.15096500E+04    4
HON          HF MELIUS93H   1N   1O   1    0G   300.000  5000.000 1671.000    01
 3.78577430E+00 2.86062728E-03-1.02423922E-06 1.64463139E-10-9.77943616E-15    2
 2.93319701E+04 3.12193293E+00 3.33656431E+00 2.67682939E-03 5.61801303E-07    3
-1.11362279E-09 2.84076438E-13 2.95979751E+04 5.96343188E+00                   4
HNOH        JWB/94      N   1H   2O   1    0G   300.000  5000.000 1375.000    11
 5.24159962E+00 3.64132385E-03-1.26199882E-06 1.97647403E-10-1.15363360E-14    2
 8.79675199E+03-2.52971854E+00 3.42226363E+00 6.62639079E-03-2.62136579E-06    3
 1.83974483E-10 7.81187077E-14 9.57854837E+03 7.72947399E+00                   4
H2NN       M93/JBPM3 96 N   2H   2    0    0G   300.000  5000.000 1695.000    01
 3.13531032E+00 5.68632569E-03-1.93983467E-06 3.01290501E-10-1.74978144E-14    2
 3.33678346E+04 7.04815840E+00 2.88544262E+00 4.69495999E-03 7.01983230E-07    3
-1.53359038E-09 3.79345858E-13 3.36030690E+04 8.95096779E+00                   4
HNNO          MELIUS    N   2H   1O   1    0G   300.000  5000.000 1389.000    01
 6.24923385E+00 3.26982600E-03-1.14794129E-06 1.81382853E-10-1.06538435E-14    2
 2.53822145E+04-7.09498008E+00 2.40143952E+00 1.26718683E-02-1.00828325E-05    3
 4.10522699E-09-6.79228425E-13 2.66782704E+04 1.34257464E+01                   4
NH2OH       JWB/SAND88  N   1H   3O   1    0G   300.000  5000.000 1412.000    11
 5.12276969E+00 5.73428233E-03-1.86277359E-06 2.78938290E-10-1.57685159E-14    2
-7.42648110E+03-3.34064363E+00 1.59842441E+00 1.54722273E-02-1.24132635E-05    3
 5.50996715E-09-1.00114333E-12-6.34935610E+03 1.50585859E+01                   4
NH2NO          M/JB189  N   2H   2O   1    0G   300.000  5000.000 1376.000    11
 8.29632310E+00 4.68893443E-03-1.88894635E-06 3.25848090E-10-2.03763038E-14    2
 5.26778509E+03-2.04554254E+01 1.30310075E+00 1.94969032E-02-1.34642223E-05    3
 4.29560204E-09-5.24866242E-13 7.86417421E+03 1.76712406E+01                   4
!
! GADM98 thermodynamic data
!
C2H5               83194H   5C   2    0    0G   300.000  4000.000 1400.00    0 1
 0.87349157E+01 0.54537677E-02-0.37647177E-06-0.31297920E-09 0.52844000E-13    2
 0.10265269E+05-0.23104086E+02 0.24398923E+01 0.13747212E-01-0.85500653E-06    3
-0.31469924E-08 0.93754355E-12 0.13158588E+05 0.13099146E+02                   4
C2H3               83194H   3C   2    0    0G   300.000  4000.000 1400.00    0 1
 0.71861677E+01 0.34552682E-02-0.29435373E-06-0.20681942E-09 0.36797774E-13    2
 0.32229627E+05-0.15977573E+02 0.24955740E+01 0.10269993E-01-0.10226917E-05    3
-0.27594382E-08 0.96919825E-12 0.34232813E+05 0.10614626E+02                   4
C2H                83194H   1C   2    0    0G   300.000  4000.000 1400.00    0 1
 0.52086663E+01 0.12875765E-02-0.10398387E-06-0.67526325E-10 0.11751871E-13    2
 0.64697773E+05-0.53721781E+01 0.39396334E+01 0.32114412E-02-0.39412765E-06    3
-0.74782530E-09 0.27493521E-12 0.65224684E+05 0.17814000E+01                   4
CH2(S)             83194H   2C   1    0    0G   300.000  4000.000 1400.00    0 1
 0.40752106E+01 0.15779120E-02-0.10806129E-06-0.84592437E-10 0.14033284E-13    2
 0.50007492E+05-0.15480316E+01 0.35932946E+01 0.13151238E-02 0.30756846E-06    3
 0.42637904E-09-0.34178712E-12 0.50451547E+05 0.17780241E+01                   4
CH2                83194H   2C   1    0    0G   300.000  4000.000 1400.00    0 1
 0.39737520E+01 0.16097502E-02-0.10785119E-06-0.86399922E-10 0.14301196E-13    2
 0.45608973E+05 0.75549729E-01 0.36872995E+01 0.15066403E-02 0.69679857E-07    3
 0.23537297E-09-0.19397147E-12 0.45863672E+05 0.20267601E+01                   4
CH3CN              111596H   3C   2N   1    0G   300.000  3000.000 1000.00    0 1
 0.23924046E+01 0.15618873E-01-0.79120497E-05 0.19372333E-08-0.18611956E-12    2
 0.84999377E+04 0.11145236E+02 0.25197531E+01 0.13567523E-01-0.25764077E-05    3
-0.30893967E-08 0.14288692E-11 0.85533762E+04 0.10920868E+02                   4
CH2CN              111596H   2C   2N   1    0G   300.000  3000.000 1000.00    0 1
 0.46058146E+01 0.94485160E-02-0.47116329E-05 0.11389957E-08-0.10828942E-12    2
 0.29171486E+05 0.10084415E+01 0.25296724E+01 0.18114138E-01-0.18960575E-04    3
 0.11944583E-07-0.32544142E-11 0.29592293E+05 0.10993441E+02                   4
OCHCHO             120596H   2C   2O   2    0G   300.000  3000.000 1000.00    0 1
 0.49087462E+01 0.13182673E-01-0.71416730E-05 0.18461316E-08-0.18525858E-12    2
-0.27116386E+05 0.59148768E+00 0.25068862E+01 0.18899139E-01-0.10302623E-04    3
 0.62607508E-09 0.88114253E-12-0.26427374E+05 0.13187043E+02                   4
C2H2OH HCCO TRAN   121196H   3C   2O   1    0G   300.000  3000.000 1000.00    0 1
 0.57206843E+01 0.10704185E-01-0.50358494E-05 0.11324499E-08-0.10086621E-12    2
 0.12849424E+05-0.47081776E+01 0.81498282E-01 0.31640644E-01-0.34085361E-04    3
 0.18978838E-07-0.41950165E-11 0.14060783E+05 0.22908977E+02                   4
C2H5CO    burcat  T 9/92C   3H   5O   1    0G   298.150  5000.000 1000.00      1
```

```
 0.30445698E+01 0.23236429E-01-0.86317936E-05 0.14799550E-08-0.96860829E-13    2
-0.61787211E+04 0.13122302E+02 0.67368294E+01-0.26945299E-02 0.49927017E-04    3
-0.50025808E-07 0.15011503E-10-0.65703366E+04-0.23398732E+01-0.43321855E+04    4
C2H5CHO   burcat  T 9/92C   3H   6O   1    0G   273.150  5000.000 1000.00      1
 0.33137982E+01 0.26619606E-01-0.10475596E-04 0.18815334E-08-0.12761310E-12    2
-0.25459603E+05 0.96608447E+01 0.76044596E+01-0.86403564E-02 0.73930097E-04    3
-0.79687398E-07 0.28004927E-10-0.25489789E+05-0.67643691E+01-0.23097645E+05    4
CH3CN             111596H   3C   2N   1    0G   300.000  3000.000 1000.00    0 1
 0.23924046E+01 0.15618873E-01-0.79120497E-05 0.19372333E-08-0.18611956E-12    2
 0.84999377E+04 0.11145236E+02 0.25197531E+01 0.13567523E-01-0.25764077E-05    3
-0.30893967E-08 0.14288692E-11 0.85533762E+04 0.10920868E+02                   4
CH2CN             111596H   2C   2N   1    0G   300.000  3000.000 1000.00    0 1
 0.46058146E+01 0.94485160E-02-0.47116329E-05 0.11389957E-08-0.10828942E-12    2
 0.29171486E+05 0.10084415E+01 0.25296724E+01 0.18114138E-01-0.18960575E-04    3
 0.11944583E-07-0.32544142E-11 0.29592293E+05 0.10993441E+02                   4
HNO               pg9601H   1N   1O   1     G  0300.00   5000.00  1000.00      1
 0.03615144E+02 0.03212486E-01-0.01260337E-04 0.02267298E-08-0.01536236E-12    2
 0.11769108E+05 0.04810264E+02 0.02784403E+02 0.06609646E-01-0.09300223E-04    3
 0.09437980E-07-0.03753146E-10 0.12025976E+05 0.09035629E+02                   4
HCN               110193H   1C   1N   1     G  0300.00   4000.00  1000.00      1
 0.03426457E+02 0.03924190E-01-0.01601138E-04 0.03161966E-08-0.02432850E-12    2
 0.01485552E+06 0.03607795E+02 0.02417787E+02 0.09031856E-01-0.01107727E-03    3
 0.07980141E-07-0.02311141E-10 0.01501044E+06 0.08222891E+02                   4
HNCO              110193H   1C   1N   1O   1G  0300.00   4000.00  1400.00      1
 0.06545307E+02 0.01965760E-01-0.01562664E-05-0.01074318E-08 0.01874680E-12    2
-0.01664773E+06-0.01003880E+03 0.03858467E+02 0.06390342E-01-0.09016628E-05    3
-0.01898224E-07 0.07651380E-11-0.01562343E+06 0.04882493E+02                   4
HOCN              110193H   1C   1N   1O   1G  0300.00   4000.00  1400.00      1
 0.06022112E+02 0.01929530E-01-0.01455029E-05-0.01045811E-08 0.01794814E-12    2
-0.04040321E+05-0.05866433E+02 0.03789424E+02 0.05387981E-01-0.06518270E-05    3
-0.01420164E-07 0.05367969E-11-0.03135335E+05 0.06667052E+02                   4
NCO               110193C   1N   1O   1     G  0300.00   4000.00  1400.00      1
 0.06072346E+02 0.09227829E-02-0.09845574E-06-0.04764123E-09 0.09090445E-13    2
 0.01359820E+06-0.08507293E+02 0.03359593E+02 0.05393239E-01-0.08144585E-05    3
-0.01912868E-07 0.07836794E-11 0.01462809E+06 0.06549694E+02                   4
END
REACTIONS
!
! START SKG03 reactions
!
! ************************************************
! *  H2/CO/O2 Subset                             *
! ************************************************
!
O+OH=H+O2                       2.0E+14 -0.4        0 ! *SKG03-1*
O+H2=OH+H                       5.0E+04  2.67    6290 ! *SKG03-2*
OH+H2=H2O+H                     2.1E+08  1.52    3450 ! *SKG03-3*
OH+OH=H2O+O                     4.3E+03  2.7    -2486 ! *SKG03-4*
H+H+M=H2+M                      7.0E+17 -1          0 ! *SKG03-5*
  N2/0/ H2O/0/ H2/0/
H+H+N2=H2+N2                    5.4E+18 -1.3        0 ! *SKG03-5a*
H+H+H2=H2+H2                    1.0E+17 -0.6        0 ! *SKG03-5b*
H+H+H2O=H2+H2O                  1.0E+19 -1          0 ! *SKG03-5c*
H+O+M=OH+M                      6.2E+16 -0.6        0 ! *SKG03-6*
  H2O/5/
H+OH+M=H2O+M                    8.3E+21 -2          0 ! *SKG03-7*
  N2/2.7/ H2O/17/
O+O+M=O2+M                      1.9E+13  0      -1788 ! *SKG03-8*
  N2/1.5/ O2/2.7/ H2O/10/
H+O2(+M)=HO2(+M)                1.5E+12  0.6        0 ! *SKG03-9*
  LOW/3.5E16 -0.41 -1116/
  TROE/0.5 1.E+30 1.E-30/
  N2/1/ H2O/10/ AR/0/
H+O2(+AR)=HO2(+AR)              1.5E+12  0.6        0 ! *SKG03-9a*
  LOW/1.5E15 0 -1000/
  TROE/0.45 1.E+30 1.E-30/
HO2+H=H2+O2                     1.7E+13  0        820 ! *SKG03-10*
HO2+H=OH+OH                     7.1E+13  0        300 ! *SKG03-11*
HO2+H=O+H2O                     3.0E+13  0       1721 ! *SKG03-12*
HO2+O=OH+O2                     3.3E+13  0          0 ! *SKG03-13*
HO2+OH=H2O+O2                   1.9E+16 -1          0 ! *SKG03-14*
```

```
HO2+HO2=H2O2+O2                 1.3E+11  0      -1630 ! *SKG03-15-dup*
DUP
HO2+HO2=H2O2+O2                 4.2E+14  0      11982 ! *SKG03-15-dup*
DUP
H2O2(+M)=OH+OH(+M)              3.0E+14  0      48480 ! *SKG03-16*
  LOW/1.2E17 0 45500/
  TROE/0.5 1.E+30 1.E-30/
  H2O/5/
H2O2+H=HO2+H2                   1.7E+12  0       3755 ! *SKG03-17*
H2O2+H=H2O+OH                   1.0E+13  0       3576 ! *SKG03-18*
H2O2+O=HO2+OH                   6.6E+11  0       4000 ! *SKG03-19*
H2O2+OH=H2O+HO2                 7.8E+12  0       1330 ! *SKG03-20-dup*
  DUP
H2O2+OH=H2O+HO2                 5.8E+14  0       9560 ! *SKG03-20-dup*
  DUP
CO+O(+M)=CO2(+M)                1.8E+10  0       2380 ! *SKG03-21*
  LOW/1.4E24 -2.79 4190/
  H2O/5/
CO+OH=CO2+H                     1.4E+05  1.95    -1347 ! *SKG03-22*
CO+HO2=CO2+OH                   3.0E+13  0      23000 ! *SKG03-23*
CO+O2=CO2+O                     2.5E+12  0      47700 ! *SKG03-24*
!
! ************************************************
! *  H/N/O Subset                                *
! ************************************************
!
NH3+M=NH2+H+M                   2.2E+16  0      93470 ! *SKG03-25*
NH3+H=NH2+H2                    6.4E+05  2.39   10171 ! *SKG03-26*
NH3+O=NH2+OH                    9.4E+06  1.94    6460 ! *SKG03-27*
NH3+OH=NH2+H2O                  2.0E+06  2.04     566 ! *SKG03-28*
NH3+HO2=NH2+H2O2                3.0E+11  0      22000 ! *SKG03-29*
!
NH2+H=NH+H2                     7.2E+05  2.32     799 ! *SKG03-30*
NH2+O=HNO+H                     6.6E+14 -0.5        0 ! *SKG03-31*
NH2+O=NH+OH                     6.8E+12  0          0 ! *SKG03-32*
NH2+OH=NH+H2O                   4.0E+06  2       1000 ! *SKG03-33*
NH2+OH=NH2OH                    3.9E+33 -7       4441 ! *SKG03-34*
NH2+HO2=H2NO+OH                 5.0E+13  0          0 ! *SKG03-35*
NH2+HO2=NH3+O2                  9.2E+05  1.94   -1152 ! *SKG03-36*
NH2+O2=H2NO+O                   2.5E+11  0.48   29586 ! *SKG03-37*
NH2+O2=HNO+OH                   6.2E+07  1.23   35100 ! *SKG03-38*
NH2+NH2=N2H4                    5.6E+48 -11.3   11882 ! *SKG03-39*
NH2+NH2=N2H3+H                  1.2E+12 -0.03   10084 ! *SKG03-40*
NH2+NH2=H2NN+H2                 1.2E+21 -3.08    3680 ! *SKG03-41*
NH2+NH2=NH3+NH                  5.0E+13  0      10000 ! *SKG03-42*
NH2+NH=N2H2+H                   5.0E+13  0          0 ! *SKG03-43*
NH2+NH=NH3+N                    9.2E+05  1.94    2444 ! *SKG03-44*
NH2+N=N2+H+H                    7.0E+13  0          0 ! *SKG03-45*
NH2+NO=NNH+OH                   2.3E+10  0.425   -814 ! *SKG03-46*
NH2+NO=N2+H2O                   2.8E+20 -2.654   1258 ! *SKG03-47*
NH2+NO2=N2O+H2O                 1.6E+16 -1.44     268 ! *SKG03-48*
NH2+NO2=H2NO+NO                 6.5E+16 -1.44     268 ! *SKG03-49*
NH2+H2NO=HNO+NH3                3.0E+12  0       1000 ! *SKG03-50*
NH2+HNO=NH3+NO                  3.6E+06  1.63   -1250 ! *SKG03-51*
NH2+HONO=NH3+NO2                7.1E+01  3.02   -4940 ! *SKG03-52*
!
NH+H=N+H2                       3.0E+13  0          0 ! *SKG03-53*
NH+O=NO+H                       9.2E+13  0          0 ! *SKG03-54*
NH+OH=HNO+H                     2.0E+13  0          0 ! *SKG03-55*
NH+OH=N+H2O                     5.0E+11  0.5     2000 ! *SKG03-56*
NH+O2=HNO+O                     4.6E+05  2       6500 ! *SKG03-57*
NH+O2=NO+OH                     1.3E+06  1.5      100 ! *SKG03-58*
NH+NH=N2+H+H                    2.5E+13  0          0 ! *SKG03-59*
NH+N=N2+H                       3.0E+13  0          0 ! *SKG03-60*
NH+NO=N2O+H                     2.9E+14 -0.4        0 ! *SKG03-61-dup*
DUP
NH+NO=N2O+H                    -2.2E+13 -0.23       0 ! *SKG03-61-dup*
DUP
NH+NO=N2+OH                     2.2E+13 -0.23       0 ! *SKG03-62*
NH+NO2=N2O+OH                   1.0E+13  0          0 ! *SKG03-63*
NH+HONO=NH2+NO2                 1.0E+13  0          0 ! *SKG03-64*
```

```
!
N+OH=NO+H                       3.8E+13  0          0 ! *SKG03-65*
N+O2=NO+O                       6.4E+09  1       6280 ! *SKG03-66*
N+NO=N2+O                       3.3E+12  0.3        0 ! *SKG03-67*
!
N2H4+H=N2H3+H2                  7.0E+12  0       2500 ! *SKG03-68*
N2H4+O=N2H2+H2O                 4.4E+11  0      -1270 ! *SKG03-69*
N2H4+O=N2H3+OH                  6.7E+08  1.5     2851 ! *SKG03-70*
N2H4+OH=N2H3+H2O                4.0E+13  0          0 ! *SKG03-71*
N2H4+NH2=N2H3+NH3               3.9E+12  0       1500 ! *SKG03-72*
!
N2H3=N2H2+H                     3.6E+47 -10.38   69009! *SKG03-73*
N2H3+H=N2H2+H2                  2.4E+08  1.5      -10 ! *SKG03-74*
N2H3+O=N2H2+OH                  1.7E+08  1.5     -646 ! *SKG03-75*
N2H3+O=NH2+HNO                  3.0E+13  0          0 ! *SKG03-76*
N2H3+O=NH2NO+H                  3.0E+13  0          0 ! *SKG03-77*
N2H3+OH=N2H2+H2O                1.2E+06  2      -1192 ! *SKG03-78*
N2H3+OH=H2NN+H2O                3.0E+13  0          0 ! *SKG03-79*
N2H3+OH=NH3+HNO                 1.0E+12  0      15000 ! *SKG03-80*
N2H3+HO2=N2H4+O2                9.2E+05  1.94    2126 ! *SKG03-81*
N2H3+HO2=N2H2+H2O2              1.4E+04  2.69   -1600 ! *SKG03-82*
N2H3+NH2=N2H2+NH3               9.2E+05  1.94   -1152 ! *SKG03-83*
N2H3+NH2=H2NN+NH3               3.0E+13  0          0 ! *SKG03-84*
N2H3+NH=N2H2+NH2                2.0E+13  0          0 ! *SKG03-85*
!
N2H2+M=NNH+H+M                  1.9E+27 -3.05  66107  ! *SKG03-86*
  H2O/7/
N2H2+H=NNH+H2                   8.5E+04  2.63     230 ! *SKG03-87*
N2H2+O=NNH+OH                   3.3E+08  1.5      497 ! *SKG03-88*
N2H2+O=NH2+NO                   1.0E+13  0          0 ! *SKG03-89*
N2H2+OH=NNH+H2O                 5.9E+01  3.4     1360 ! *SKG03-90*
N2H2+NH2=NNH+NH3                8.8E-02  4.05    1610 ! *SKG03-91*
N2H2+NH=NNH+NH2                 2.4E+06  2      -1192 ! *SKG03-92*
N2H2+NO=N2O+NH2                 4.0E+12  0      11922 ! *SKG03-93*
!
H2NN=NNH+H                      3.4E+26 -4.83   46228 ! *SKG03-94*
H2NN+H=NNH+H2                   4.8E+08  1.5     -894 ! *SKG03-95*
H2NN+H=N2H2+H                   7.0E+13  0          0 ! *SKG03-96*
H2NN+O=NNH+OH                   3.3E+08  1.5     -894 ! *SKG03-97*
H2NN+O=NH2+NO                   7.0E+13  0          0 ! *SKG03-98*
H2NN+OH=NNH+H2O                 2.4E+06  2      -1192 ! *SKG03-99*
H2NN+OH=NH2NO+H                 2.0E+12  0          0 ! *SKG03-100*
H2NN+HO2=NH2NO+OH               9.0E+12  0          0 ! *SKG03-101*
H2NN+HO2=NNH+H2O2               2.9E+04  2.69   -1600 ! *SKG03-102*
H2NN+O2=NH2+NO2                 1.5E+12  0       5961 ! *SKG03-103*
H2NN+NH2=NNH+NH3                1.8E+06  1.94   -1192 ! *SKG03-104*
!
NNH=N2+H                        6.5E+07  0          0 ! *SKG03-105*
NNH+H=N2+H2                     1.0E+14  0          0 ! *SKG03-106*
NNH+O=N2O+H                     1.0E+14  0          0 ! *SKG03-107*
NNH+O=N2+OH                     8.0E+13  0          0 ! *SKG03-108*
NNH+O=NH+NO                     5.0E+13  0          0 ! *SKG03-109*
NNH+OH=N2+H2O                   5.0E+13  0          0 ! *SKG03-110*
NNH+O2=N2+HO2                   2.0E+14  0          0 ! *SKG03-111*
NNH+O2=N2+H+O2                  5.0E+13  0          0 ! *SKG03-112*
NNH+NO=N2+HNO                   5.0E+13  0          0 ! *SKG03-113*
NNH+NH2=N2+NH3                  5.0E+13  0          0 ! *SKG03-114*
NNH+NH =N2+NH2                  5.0E+13  0          0 ! *SKG03-115*
!
NH2OH+H=HNOH+H2                 4.8E+08  1.5     6249 ! *SKG03-116*
NH2OH+H=H2NO+H2                 2.4E+08  1.5     5067 ! *SKG03-117*
NH2OH+O=HNOH+OH                 3.3E+08  1.5     3865 ! *SKG03-118*
NH2OH+O=H2NO+OH                 1.7E+08  1.5     3010 ! *SKG03-119*
NH2OH+OH=HNOH+H2O               2.4E+06  2       -328 ! *SKG03-120*
NH2OH+OH=H2NO+H2O               1.2E+06  2       -596 ! *SKG03-121*
NH2OH+HO2=HNOH+H2O2             2.9E+04  2.69    9557 ! *SKG03-122*
NH2OH+HO2=H2NO+H2O2             1.4E+04  2.69    6418 ! *SKG03-123*
NH2OH+NH2=HNOH+NH3              1.8E+06  1.94    3229 ! *SKG03-124*
NH2OH+NH2=H2NO+NH3              9.2E+05  1.94    1888 ! *SKG03-125*
!
H2NO+M=HNO+H+M                  2.8E+24 -2.83   64915 ! *SKG03-126*
```

```
  H2O/10/
H2NO+M=HNOH+M                 1.1E+29 -4      44000 ! *SKG03-127*
  H2O/10/
H2NO+H=HNO+H2                 3.0E+07  2       2000 ! *SKG03-128*
H2NO+H=NH2+OH                 5.0E+13  0          0 ! *SKG03-129*
H2NO+O=HNO+OH                 3.0E+07  2       2000 ! *SKG03-130*
H2NO+OH=HNO+H2O               2.0E+07  2       1000 ! *SKG03-131*
H2NO+HO2=HNO+H2O2             2.9E+04  2.69   -1600 ! *SKG03-132*
H2NO+HO2=NH2OH+O2             2.9E+04  2.69   -1600 ! *SKG03-133*
H2NO+O2=HNO+HO2               3.0E+12  0      25000 ! *SKG03-134*
H2NO+NO=HNO+HNO               2.0E+04  2      13000 ! *SKG03-135*
H2NO+NO2=HONO+HNO             6.0E+11  0       2000 ! *SKG03-136*
!
HNOH+M=HNO+H+M                2.0E+24 -2.84   58934 ! *SKG03-137*
  H2O/10/
HNOH+H=NH2+OH                 4.0E+13  0          0 ! *SKG03-138*
HNOH+H=HNO+H2                 4.8E+08  1.5      378 ! *SKG03-139*
HNOH+O=HNO+OH                 7.0E+13  0          0 ! *SKG03-140-dup*
DUP
HNOH+O=HNO+OH                 3.3E+08  1.5     -358 ! *SKG03-140-dup*
DUP
HNOH+OH=HNO+H2O               2.4E+06  2      -1192 ! *SKG03-141*
HNOH+HO2=HNO+H2O2             2.9E+04  2.69   -1600 ! *SKG03-142*
HNOH+HO2=NH2OH+O2             2.9E+04  2.69   -1600 ! *SKG03-143*
HNOH+O2=HNO+HO2               3.0E+12  0      25000 ! *SKG03-144*
HNOH+NH2=NH3+HNO              1.8E+06  1.94   -1152 ! *SKG03-145*
HNOH+NH2=N2H3+OH              1.0E+01  3.46    -467 ! *SKG03-146*
HNOH+NH2=H2NN+H2O             8.8E+16 -1.08    1113 ! *SKG03-147*
HNOH+NO2=HONO+HNO             6.0E+11  0       2000 ! *SKG03-148*
!
HNO+H=NO+H2                   4.4E+11  0.72     650 ! *SKG03-149*
HNO+O=NO+OH                   2.3E+13  0          0 ! *SKG03-150*
HNO+OH=NO+H2O                 3.6E+13  0          0 ! *SKG03-151*
HNO+O2=HO2+NO                 2.0E+13  0      16000 ! *SKG03-152*
HNO+NO2=HONO+NO               6.0E+11  0       2000 ! *SKG03-153*
HNO+HNO=N2O+H2O               9.0E+08  0       3100 ! *SKG03-154*
!
HON+M=NO+H+M                  5.1E+19 -1.73   16045 ! *SKG03-155*
  H2O/7/  CO2/2/
HON+H=HNO+H                   2.0E+13  0          0 ! *SKG03-156*
HON+H=OH+NH                   2.0E+13  0          0 ! *SKG03-157*
HON+O=OH+NO                   7.0E+13  0          0 ! *SKG03-158*
HON+OH=HONO+H                 4.0E+13  0          0 ! *SKG03-159*
HON+O2=NO2+OH                 1.0E+12  0       4968 ! *SKG03-160*
!
H+NO(+M)=HNO(+M)              1.5E+15 -0.41       0 ! *SKG03-161*
  LOW/2.3E+14 0.206 -1550/
  N2/1.6/ H2O/10/ O2/1.5/ H2/2/ CO2/3/
NO+O(+M)=NO2(+M)              1.3E+15 -0.75       0 ! *SKG03-162*
  LOW/7.5E+19 -1.41 0/
  N2/1.7/ O2/1.5/ H2O/10/
NO+OH(+M)=HONO(+M)            2.0E+12  0       -721 ! *SKG03-163*
  LOW/5.1E+23 -2.51 -68/
  H2O/6.7/
NO+HO2=NO2+OH                 2.1E+12  0       -480 ! *SKG03-164*
!
HONO+H=HNO+OH                 5.6E+10  0.86    5000 ! *SKG03-165*
HONO+H=NO+H2O                 8.1E+06  1.89    3850 ! *SKG03-166*
HONO+O=NO2+OH                 1.2E+13  0       6000 ! *SKG03-167*
HONO+OH=NO2+H2O               4.0E+12  0          0 ! *SKG03-168*
HONO+HONO=NO+NO2+H2O          3.5E-01  3.64   12100 ! *SKG03-169*
!
NO2+H=NO+OH                   8.4E+13  0          0 ! *SKG03-170*
NO2+O=NO+O2                   3.9E+12  0       -238 ! *SKG03-171*
NO2+H2=HONO+H                 4.5E+12  0      27600 ! *SKG03-172*
NO2+HO2=HONO+O2               6.3E+08  1.25    5000 ! *SKG03-173*
NO2+NO2=NO+NO+O2              1.6E+12  0      26123 ! *SKG03-174*
!
NH2NO=N2+H2O                  3.1E+34 -7.11   36283 ! *SKG03-175*
NH2NO+H=HNNO+H2               4.8E+08  1.5     7412 ! *SKG03-176*
NH2NO+O=HNNO+OH               3.3E+08  1.5     4699 ! *SKG03-177*
```

```
NH2NO+OH=HNNO+H2O              2.4E+06  2        -70 ! *SKG03-178*
NH2NO+HO2=HNNO+H2O2            2.9E+04  2.69   12627 ! *SKG03-179*
NH2NO+NH2=HNNO+NH3             1.8E+06  1.94    4540 ! *SKG03-180*
!
N2O(+M)=N2+O(+M)               1.3E+12  0      62570 ! *SKG03-181*
  LOW/4.0E+14 0 56600/
  N2/1.7/ O2/1.4/ H2O/12/
N2O+H=N2+OH                    3.3E+10  0       4729 ! *SKG03-182-dup*
DUP
N2O+H=N2+OH                    4.4E+14  0      19254 ! *SKG03-182-dup*
DUP
N2O+H=HNNO                     1.3E+25 -4.48   10770 ! *SKG03-183*
N2O+O=NO+NO                    9.2E+13  0      27679 ! *SKG03-184*
N2O+O=N2+O2                    3.7E+12  0      15936 ! *SKG03-185*
N2O+OH=N2+HO2                  1.3E-02  4.72   36560 ! *SKG03-186*
N2O+OH=HNO+NO                  1.2E-04  4.33   25080 ! *SKG03-187*
N2O+NO=NO2+N2                  5.3E+05  2.23   46280 ! *SKG03-188*
CO+NO2=CO2+NO                  9.0E+13  0      33800 ! *SKG03-189*
CO+N2O=N2+CO2                  3.2E+11  0      20237 ! *SKG03-190*
CH4+NH2=CH3+NH3                1.5E+03  3.01    9940 ! *SKG03-191*
!
! END SKG03 reactions
!
! ************************************************
! *  GADM98 hydrocarbon/nitrogen mechanism         *
! *  Glarborg, Alzueta, Dam-Johansen,Miller        *
! *  Combustion and Flame 115:1-27, 1998           *
! *  see paper for references                      *
! ************************************************
!
! START GADM98 reactions
!
! ************************************************
! *  H2/O2 Subset - REPLACED                       *
! ************************************************
!
!
! ************************************************
! *  CO Subset - REPLACED                          *
! ************************************************
!
!
! ************************************************
! *  CH2O/HCO Subset                               *
! ************************************************
!
CH2O+M=HCO+H+M                 3.3E+16  0      81000
  H2O/5/
CH2O+H=HCO+H2                  1.3E+08  1.62    2166
CH2O+O=HCO+OH                  1.8E+13  0       3080
CH2O+OH=HCO+H2O                3.4E+09  1.18    -447
CH2O+HO2=HCO+H2O2              3.0E+12  0      13000
CH2O+O2=HCO+HO2                6.0E+13  0      40660
HCO+M=H+CO+M                   1.9E+17 -1      17000
  H2O/5/
HCO+H=CO+H2                    1.2E+13  0.25       0
HCO+O=CO+OH                    3.0E+13  0          0
HCO+O=CO2+H                    3.0E+13  0          0
HCO+OH=H2O+CO                  1.0E+14  0          0
HCO+O2=HO2+CO                  7.6E+12  0        400
!
! ************************************************
! *  CH4/CH3/CH2/CH/C Subset                       *
! ************************************************
!
CH3+H(+M)=CH4(+M)              1.3E+16 -0.63     383
  LOW/1.75E+33 -4.76 2440/
  TROE/0.783 74 2941 6964/
  H2O/8.57/ N2/1.43/
CH4+H=CH3+H2                   1.3E+04  3       8040
CH4+O=CH3+OH                   1.0E+09  1.5     8600
```

```
CH4+OH=CH3+H2O                  1.6E+06  2.1     2460
CH4+HO2=CH3+H2O2                1.8E+11  0      18700
CH4+O2=CH3+HO2                  7.9E+13  0      56000
CH3+H=CH2+H2                    9.0E+13  0      15100
CH2(S)+H2=CH3+H                 7.2E+13  0          0
CH3+O=CH2O+H                    8.4E+13  0          0
CH3+OH=CH2+H2O                  7.5E+06  2       5000
CH2(S)+H2O=CH3+OH               3.0E+15 -0.6        0
CH2OH+H=CH3+OH                  1.0E+14  0          0
CH3O+H=CH3+OH                   1.0E+14  0          0
CH3+OH(+M)=CH3OH(+M)            6.3E+13  0          0
  LOW/1.89E+38 -6.3 3100/
  TROE/0.2105 83.5 5398 8370/
  N2/1.43/ H2O/8.58/
CH3+HO2=CH3O+OH                 8.0E+12  0          0
CH3+O2=CH3O+O                   2.9E+13  0      30480
CH3+O2=CH2O+OH                  1.9E+12  0      20315
CH3+CH3(+M)=C2H6(+M)            2.1E+16 -0.97     620
  LOW /1.26E+50 -9.67 6220/
  TROE/0.5325 151 1038 4970/
  N2/1.43/ H2O/8.59/ H2/2/ CO/2/ CO2/3/
CH3+CH2O=CH4+HCO                7.8E-08  6.1     1967
CH3+HCO=CH4+CO                  1.2E+14  0          0
CH2+H=CH+H2                     1.0E+18 -1.56       0
CH2+O=CO+H+H                    5.0E+13  0          0
CH2+O=CO+H2                     3.0E+13  0          0
CH2+OH=CH+H2O                   1.1E+07  2       3000
CH2+OH=CH2O+H                   2.5E+13  0          0
CH2+O2=CO+H2O                   2.2E+22 -3.3     2867
CH2+O2=CO2+H+H                  3.3E+21 -3.3     2867
CH2+O2=CH2O+O                   3.3E+21 -3.3     2867
CH2+O2=CO2+H2                   2.6E+21 -3.3     2867
CH2+O2=CO+OH+H                  1.6E+21 -3.3     2867
CH2+CO2=CH2O+CO                 1.1E+11  0       1000
CH2+CH4=CH3+CH3                 4.3E+12  0      10030
CH2+CH3=C2H4+H                  4.2E+13  0          0
CH2+CH2=C2H2+H+H                4.0E+13  0          0
CH2+HCCO=C2H3+CO                3.0E+13  0          0
CH2(S)+M=CH2+M                  1.0E+13  0          0
  H/0/ H2O/0/ N2/0/ AR/0/
CH2(S)+N2=CH2+N2                1.3E+13  0        430
CH2(S)+AR=CH2+AR                1.5E+13  0        884
CH2(S)+H=CH2+H                  2.0E+14  0          0
CH2(S)+H2O=CH2+H2O              3.0E+13  0          0
CH2(S)+H=CH+H2                  3.0E+13  0          0
CH2(S)+O=CO+H+H                 3.0E+13  0          0
CH2(S)+OH=CH2O+H                3.0E+13  0          0
CH2(S)+O2=CO+OH+H               7.0E+13  0          0
CH2(S)+CO2=CH2O+CO              3.0E+12  0          0
CH2(S)+CH4=CH3+CH3              4.3E+13  0          0
CH2(S)+CH3=C2H4+H               2.0E+13  0          0
CH2(S)+CH2CO=C2H4+CO            1.6E+14  0          0
CH2(S)+C2H6=CH3+C2H5            1.2E+14  0          0
CH+H=C+H2                       1.5E+14  0          0
CH+O=CO+H                       5.7E+13  0          0
CH+OH=HCO+H                     3.0E+13  0          0
CH+OH=C+H2O                     4.0E+07  2       3000
CH+O2=HCO+O                     3.3E+13  0          0
CH+H2O=CH2O+H                   5.7E+12  0       -751
CH+CO2=HCO+CO                   3.4E+12  0        690
CH+CH4=C2H4+H                   6.0E+13  0          0
CH+CH3=C2H3+H                   3.0E+13  0          0
CH+CH2=C2H2+H                   4.0E+13  0          0
CH+CH2O=CH2CO+H                 9.5E+13  0       -515
CH+HCCO=C2H2+CO                 5.0E+13  0          0
C+OH=CO+H                       5.0E+13  0          0
C+O2=CO+O                       2.0E+13  0          0
C+CH3=C2H2+H                    5.0E+13  0          0
C+CH2=C2H+H                     5.0E+13  0          0
!
! ************************************************
```

```
! *  CH3OH/CH2OH/CH2O Subset                          *
! ************************************************
!
CH3OH+H=CH2OH+H2                1.7E+07  2.1     4868
CH3OH+H=CH3O+H2                 4.2E+06  2.1     4868
CH3OH+O=CH2OH+OH                3.9E+05  2.5     3080
CH3OH+OH=CH2OH+H2O              5.3E+04  2.53     960
CH3OH+OH=CH3O+H2O              1.32E+04  2.53     960
CH3OH+HO2=CH2OH+H2O2            9.6E+10  0       12578
CH2O+H(+M)=CH3O(+M)             5.4E+11  0.454   2600
  LOW/1.54E+30 -4.8 5560/
  TROE/0.758 94 1555 4200/
  N2/1.43/ H2O/8.58/
CH3O+H=CH2O+H2                  2.0E+13  0          0
CH3O+O=CH2O+OH                  1.0E+13  0          0
CH3O+OH=CH2O+H2O                1.0E+13  0          0
CH3O+O2=CH2O+HO2                6.3E+10  0       2600
H+CH2O(+M)=CH2OH(+M)            5.4E+11  0.454   3600
  LOW/0.91E32 -4.82 6530/
  TROE/0.7187 103 1291 4160/
  N2/1.43/ H2O/8.58/ CO/2/ CO2/3/ H2/2/
CH2OH+H=CH2O+H2                 2.0E+13  0          0
CH2OH+O=CH2O+OH                 1.0E+13  0          0
CH2OH+OH=CH2O+H2O               1.0E+13  0          0
CH2OH+O2=CH2O+HO2               1.6E+15 -1          0
 DUP
CH2OH+O2=CH2O+HO2               7.2E+13  0       3577
 DUP
!
! ************************************************
! *  C2H6/C2H5/C2H4/C2H3/C2H2/C2H/C2 Subset        *
! ************************************************
!
C2H6+H=C2H5+H2                  5.4E+02  3.5     5210
C2H6+O=C2H5+OH                  3.0E+07  2       5115
C2H6+OH=C2H5+H2O                7.2E+06  2        864
C2H6+HO2=C2H5+H2O2              1.3E+13  0      20460
C2H6+O2=C2H5+HO2                5.0E+13  0      55000
C2H6+CH3=C2H5+CH4               5.5E-01  4       8300
C2H4+H(+M)=C2H5(+M)             1.1E+12  0.454   1822
  LOW/1.112E+34 -5 4448/
  TROE/0.5 95 95 200/
  H2O/5/
C2H5+H(+M)=C2H6(+M)             5.2E+17 -0.99    1580
  LOW/2.0E+41 -7.08 6685/
  TROE/0.8422 125 2219 6882/
  N2/1.0/ H2O/6/ AR/0.7/
C2H5+H=CH3+CH3                  4.9E+12  0.35       0
C2H5+O=CH3+CH2O                 4.2E+13  0          0
C2H5+O=CH3HCO+H                 5.3E+13  0          0
C2H5+O=C2H4+OH                  3.0E+13  0          0
C2H5+OH=C2H4+H2O                2.4E+13  0          0
C2H5+O2=C2H4+HO2                1.0E+10  0      -2190
C2H5+CH2O=C2H6+HCO              5.5E+03  2.81    5860
C2H5+HCO=C2H6+CO                1.2E+14  0          0
C2H5+CH3=C2H4+CH4               1.1E+12  0          0
C2H5+C2H5=C2H6+C2H4             1.5E+12  0          0
C2H3+H(+M)=C2H4(+M)             6.1E+12  0.27     280
  LOW /0.98E+30 -3.86 3320/
  TROE /0.782 207.5 2663 6095/
  H2/2.85/ CO/2.1/ CO2/2.85/ H2O/7.14/ CH4/2.85/ C2H6/4.29/ N2/1.43/
C2H4+M=C2H2+H2+M                3.5E+16  0.0    71500
  N2/1.5/ H2O/10/
C2H4+H=C2H3+H2                  5.4E+14  0      14900
C2H4+O=CH2HCO+H                 4.7E+06  1.88     180
C2H4+O=CH3+HCO                  8.1E+06  1.88     180
C2H4+O=CH2CO+H2                 6.8E+05  1.88     180
C2H4+OH=C2H3+H2O                2.0E+13  0       5940
C2H4+HO2=CH3HCO+OH              2.2E+12  0      17200
C2H4+O2=CH2HCO+OH               2.0E+08  1.5    39000
C2H4+CH3=C2H3+CH4               5.0E+11  0      15000
```

```
H+C2H2(+M)=C2H3(+M)            3.1E+11  0.58    2590
  LOW/2.254E40 -7.269 6577/
  TROE/0.5 675. 675./
  H2/2/ CO/2/ CO2/3/ H2O/5/
C2H3+H=C2H2+H2                 4.0E+13  0          0
C2H3+O=CH2CO+H                 3.0E+13  0          0
C2H3+OH=C2H2+H2O               2.0E+13  0          0
C2H3+O2=CH2O+HCO               1.1E+23 -3.29    3890
C2H3+O2=CH2HCO+O               2.5E+15 -0.78    3135
C2H3+O2=C2H2+HO2               5.2E+15 -1.26    3310
C2H3+CH2O=C2H4+HCO             5.4E+03  2.81    5860
C2H3+HCO=C2H4+CO               9.0E+13  0          0
C2H3+CH3=C2H2+CH4              2.1E+13  0          0
C2H3+C2H3=C2H4+C2H2            1.5E+13  0          0
C2H2+M=C2H+H+M                 9.1E+30 -3.7   127138
  H2/2/ CO/2/ CO2/3/ H2O/5/
H2+C2H=C2H2+H                  4.1E+05  2.39     864
C2H2+O=CH2+CO                  6.1E+06  2       1900
C2H2+O=HCCO+H                  1.4E+07  2       1900
C2H2+O=C2H+OH                  3.2E+15 -0.6    15000
OH+C2H2=C2H+H2O                3.4E+07  2      14000
OH+C2H2=HCCOH+H                5.0E+05  2.3    13500
OH+C2H2=CH2CO+H                2.2E-04  4.5    -1000
OH+C2H2=CH3+CO                 4.8E-04  4      -2000
OH+C2H2(+M)=C2H2OH(+M)         1.5E+08  1.7     1000
  LOW/1.81E+23  -2  0/
  H2/2/ CO/2/ CO2/3/ H2O/5/
HO2+C2H2=CH2HCO+O              1.0E+12  0      10000
HO2+C2H2=CH2O+HCO              1.0E+12  0      10000
C2H2+O2=HCO+HCO                2.0E+08  1.5    30100
C2+H2=C2H+H                    4.0E+05  2.4     1000
C2H+O=CH+CO                    5.0E+13  0          0
C2H+OH=HCCO+H                  2.0E+13  0          0
C2H+OH=C2+H2O                  4.0E+07  2       8000
C2H+O2=CO+CO+H                 2.5E+13  0          0
C2H+CH4=CH3+C2H2               7.2E+12  0        976
C2+OH=C2O+H                    5.0E+13  0          0
C2+O2=CO+CO                    5.0E+13  0          0
!
! ************************************************
! * CH3HCO/CH2HCO/CH3CO/CH2CO/HCCOH/HCCO/C2O Subset*
! ************************************************
!
CH3HCO=CH3+HCO                 7.1E+15  0      81280
CH3HCO+H=CH3CO+H2              4.1E+09  1.16    2400
CH3HCO+O=CH3CO+OH              5.8E+12  0       1800
CH3HCO+OH=CH3CO+H2O            2.3E+10  0.73   -1110
CH3HCO+HO2=CH3CO+H2O2          3.0E+12  0      12000
CH3HCO+O2=CH3CO+HO2            3.0E+13  0      39000
CH3HCO+CH3=CH3CO+CH4           2.0E-06  5.6     2464
CH2HCO=CH3+CO                  1.0E+13  0      42000
CH2HCO+H=CH3+HCO               1.0E+14  0          0
CH2HCO+H=CH3CO+H               3.0E+13  0          0
CH2HCO+O=CH2O + HCO            5.0E+13  0          0
CH2HCO+OH=CH2CO+H2O            2.0E+13  0          0
CH2HCO+OH=CH2OH+HCO            1.0E+13  0          0
CH2HCO+O2=CH2O+CO+OH           2.2E+11  0       1500
CH2HCO+CH3=C2H5CHO             5.0E+13  0          0
CH2HCO+CH2=C2H4+HCO            5.0E+13  0          0
CH2HCO+CH=C2H3+HCO             1.0E+14  0          0
C2H5+HCO=C2H5CHO               1.8E+13  0          0
C2H5CHO+H=C2H5CO+H2            8.0E+13  0          0
C2H5CHO+O=C2H5CO+OH            7.8E+12  0       1730
C2H5CHO+OH=C2H5CO+H2O          1.2E+13  0          0
C2H5+CO=C2H5CO                 1.5E+11  0       4800
C2H2OH+H=CH2HCO+H              5.0E+13  0          0
C2H2OH+O=OCHCHO+H              5.0E+13  0        0.0
C2H2OH+O2=OCHCHO+OH            1.0E+12  0       5000
CH3CO(+M)=CH3+CO(+M)           2.8E+13  0      17100
  LOW/2.1E+15 0 14000/
  TROE/0.5 1.0E-30 1.0E+30 /
```

```
  H2/2/ CO/2/ CO2/3/ H2O/5/
CH3CO+H=CH3+HCO                 2.1E+13  0          0
CH3CO+H=CH2CO+H2                1.2E+13  0          0
CH3CO+O=CH3+CO2                 1.5E+14  0          0
CH3CO+O=CH2CO+OH                4.0E+13  0          0
CH3CO+OH=CH2CO+H2O              1.2E+13  0          0
CH2+CO(+M)=CH2CO(+M)            8.1E+11  0.5     4510
  LOW/1.88E+33 -5.11 7095/
  TROE/0.5907 275 1226 5185/
  H2/2/ CO/2/ CO2/3/ H2O/8.58/ N2/1.43/
CH2CO+H=CH3+CO                  5.9E+06  2       1300
CH2CO+H=HCCO+H2                 3.0E+07  2      10000
CH2CO+O=CO2+CH2                 1.8E+12  0       1350
CH2CO+O=HCCO+OH                 2.0E+07  2      10000
CH2CO+OH=HCCO+H2O               1.0E+07  2       3000
CH2CO+OH=CH2OH+CO               7.2E+12  0          0
CH2CO+OH=CH3+CO2                3.0E+12  0          0
HCCOH+H=HCCO +H2                3.0E+07  2       1000
HCCOH+OH=HCCO+H2O               1.0E+07  2       1000
HCCOH+O=HCCO+OH                 2.0E+07  3       1900
OCHCHO+M=HCO+HCO+M              1.0E+17  0      58000
OCHCHO+H=CH2O+HCO               3.0E+13  0          0
CH+CO(+M)=HCCO(+M)              5.0E+13  0          0
  LOW/1.88E+28 -3.74 1936/
  TROE/0.5757 237 1652 5069/
  N2/1.43/ H2O/8.58/ CO/2/ CO2/3/ H2/2/
H+HCCO=CH2(S)+CO                1.0E+14  0          0
O+HCCO=H+CO+CO                  1.0E+14  0          0
HCCO+OH=C2O+H2O                 6.0E+13  0          0
HCCO+O2=CO2+CO+H                1.4E+07  1.7     1000
HCCO+O2=CO +CO +OH              2.9E+07  1.7     1000
HCCO+HCCO=C2H2+CO+CO            1.0E+13  0          0
C2O+H=CH+CO                     1.0E+13  0          0
C2O+O=CO+CO                     5.0E+13  0          0
C2O+OH=CO+CO+H                  2.0E+13  0          0
C2O+O2=CO+CO+O                  2.0E+13  0          0
!
! ************************************************
! *  H/N/O Subset - REPLACED                      *
! ************************************************
!
! ************************************************
! *  Cyanide Subset                               *
! ************************************************
!
CN+H2=HCN+H                     3.0E+05  2.45    2237
HCN+O=NCO+H                     1.4E+04  2.64    4980
HCN+O=NH+CO                     3.5E+03  2.64    4980
HCN+O=CN+OH                     2.7E+09  1.58   29200
HCN+OH=CN+H2O                   3.9E+06  1.83   10300
HCN+OH=HOCN+H                   5.9E+04  2.40   12500
HCN+OH=HNCO+H                   2.0E-03  4       1000
HCN+OH=NH2+CO                   7.8E-04  4       4000
HCN+CN=C2N2+H                   1.5E+07  1.71    1530
CN+O=CO+N                       7.7E+13  0          0
CN+OH=NCO+H                     4.0E+13  0          0
CN+O2=NCO+O                     7.5E+12  0       -389
CN+CO2=NCO+CO                   3.7E+06  2.16   26884
CN+NO2=NCO+NO                   5.3E+15 -0.752    344
CN+NO2=CO+N2O                   4.9E+14 -0.752    344
CN+NO2=N2+CO2                   3.7E+14 -0.752    344
CN+HNO=HCN+NO                   1.8E+13  0          0
CN+HONO=HCN+NO2                 1.2E+13  0          0
CN+N2O=NCN+NO                   3.9E+03  2.6     3696
CN+HNCO=HCN+NCO                 1.5E+13  0          0
CN+NCO=NCN+CO                   1.8E+13  0          0
HNCO+M=NH+CO+M                  1.1E+16  0      86000
HNCO+H=NH2+CO                   2.2E+07  1.7     3800
HNCO+O=HNO+CO                   1.5E+08  1.57   44012
HNCO+O=NH+CO2                   9.8E+07  1.41    8524
HNCO+O=NCO+OH                   2.2E+06  2.11   11425
```

```
HNCO+OH=NCO+H2O                 6.4E+05  2       2563
HNCO+HO2=NCO+H2O2               3.0E+11  0      22000
HNCO+O2=HNO+CO2                 1.0E+12  0      35000
HNCO+NH2=NH3+NCO                5.0E+12  0       6200
HNCO+NH=NH2+NCO                 3.0E+13  0      23700
HOCN+H=NCO+H2                   2.0E+07  2       2000
HOCN+O=NCO+OH                   1.5E+04  2.64    4000
HOCN+OH=NCO+H2O                 6.4E+05  2       2563
HCNO+H=HCN+OH                   1.0E+14  0      12000
HCNO+O=HCO+NO                   2.0E+14  0          0
HCNO+OH=CH2O+NO                 4.0E+13  0          0
NCO+M=N+CO+M                    3.1E+16 -0.5    48000
NCO+H=NH+CO                     5.0E+13  0          0
NCO+O=NO+CO                     4.7E+13  0          0
NCO+OH=NO+HCO                   5.0E+12  0      15000
NCO+O2=NO+CO2                   2.0E+12  0      20000
NCO+H2=HNCO+H                   7.6E+02  3       4000
NCO+HCO=HNCO+CO                 3.6E+13  0          0
NCO+NO=N2O+CO                   6.2E+17 -1.73     763
NCO+NO=N2+CO2                   7.8E+17 -1.73     763
NCO+NO2=CO+NO+NO                2.5E+11  0       -707
NCO+NO2=CO2+N2O                 3.0E+12  0       -707
NCO+HNO=HNCO+NO                 1.8E+13  0          0
NCO+HONO=HNCO+NO2               3.6E+12  0          0
NCO+N=N2+CO                     2.0E+13  0          0
NCO+NCO=N2+CO+CO                1.8E+13  0          0
C2N2+O=NCO+CN                   4.6E+12  0       8880
C2N2+OH=HOCN+CN                 1.9E+11  0       2900
NCN+O=CN+NO                     1.0E+14  0          0
NCN+OH=HCN+NO                   5.0E+13  0          0
NCN+H=HCN+N                     1.0E+14  0          0
NCN+O2=NO+NCO                   1.0E+13  0          0
H+CH3CN=HCN+CH3                 4.0E+07  2       2000
H+CH3CN=CH2CN+H2                3.0E+07  2       1000
O+CH3CN=NCO+CH3                 1.5E+04  2.64    4980
OH+CH3CN=CH2CN+H2O              2.0E+07  2       2000
CH2CN+O=CH2O+CN                 1.0E+14  0          0
CN+CH2OH=CH2CN+OH               5.0E+13  0          0
H2CN+M=HCN+H+M                  3.0E+14  0      22000
!
! ************************************************
! *  Subset for CxHyOz+nitrogen species reactions  *
! ************************************************
!
CH2O+NCO=HNCO+HCO               6.0E+12  0          0
CH2O+NO2=HCO+HONO               8.0E+02  2.77   13730
HCO+NO=HNO+CO                   7.2E+12  0          0
HCO+NO2=CO+HONO                 1.2E+23 -3.29    2355
HCO+NO2=H+CO2+NO                8.4E+15 -0.75    1930
HCO+HNO=CH2O+NO                 6.0E+11  0       2000
CH4+CN=CH3+HCN                  6.2E+04  2.64    -437
NCO+CH4=CH3+HNCO                9.8E+12  0       8120
CH3+NO=HCN+H2O                  1.5E-01  3.523   3950
CH3+NO=H2CN+OH                  1.5E-01  3.523   3950
CH3+NO2=CH3O+NO                 1.4E+13  0          0
CH3+N=H2CN+H                    7.1E+13  0          0
CH3+CN=CH2CN+H                  1.0E+14  0          0
CH3+HOCN=CH3CN+OH               5.0E+12  0       2000
CH2+NO=HCN+OH                   2.2E+12  0       -378
CH2+NO=HCNO+H                   1.3E+12  0       -378
CH2+NO2=CH2O+NO                 5.9E+13  0          0
CH2+N=HCN+H                     5.0E+13  0          0
CH2+N2=HCN+NH                   1.0E+13  0      74000
H2CN+N=N2+CH2                   2.0E+13  0          0
CH2(S)+NO=HCN+OH                2.0E+13  0          0
CH2(S)+NO=CH2+NO                1.0E+14  0          0
CH2(S)+HCN=CH3+CN               5.0E+13  0          0
CH+NO2=HCO+NO                   1.0E+14  0          0
CH+NO=HCN+O                     4.8E+13  0          0
CH+NO=HCO+N                     3.4E+13  0          0
CH+NO=NCO+H                     1.9E+13  0          0
```

```
CH+N=CN+H                       1.3E+13  0          0
CH+N2=HCN+N                     3.7E+07  1.42   20723
CH+N2O=HCN+NO                   1.9E+13  0       -511
C+NO=CN+O                       2.0E+13  0          0
C+NO=CO+N                       2.8E+13  0          0
C+N2=CN+N                       6.3E+13  0      46019
C+N2O=CN+NO                     5.1E+12  0          0
C2H6+CN=C2H5+HCN                1.2E+05  2.77   -1788
C2H6+NCO=C2H5+HNCO              1.5E-09  6.89   -2910
C2H4+CN=C2H3+HCN                5.9E+14 -0.24       0
C2H3+NO=C2H2+HNO                1.0E+12  0       1000
C2H3+N=HCN+CH2                  2.0E+13  0          0
C2H2+NCO=HCCO+HCN               1.4E+12  0       1815
C2H+NO=CN+HCO                   2.1E+13  0          0
CH2CO+CN=HCCO+HCN               2.0E+13  0          0
HCCO+NO=HCNO+CO                 7.2E+12  0          0
HCCO+NO=HCN+CO2                 1.6E+13  0          0
HCCO+NO2=HCNO+CO2               1.6E+13  0          0
HCCO+N=HCN+CO                   5.0E+13  0          0
!
! END GADM98 reactions
!
END
→
```

The CHEMKIN SKG03.INP file and CHEMKIN thermodynamic database files were provided by Dr. Peter Glarborg (Technical University of Denmark). A transport properties input file was also required. The file SKG03_tran.dat (shown below) was assembled using the sources indicated in the file comments. Properties for some species were not available and were estimated using values from similar molecules as also indicated in the comments.

```
!!!!!!!!!!!!!!!!!!!!!!!!!!!!!!!!!!!!!!!!!!!!!!!!!!!!!!!!!!!!!!!!!!!!!!!!!!!!!!!!
! SKG03_tran.dat
!
! Collection of transport parameters for SKG03 mechanism
! estimated in some cases using these sources:
! 1) http://homepages.vub.ac.be/~akonnov/science/mechanism/texts/tran0_5.txt
! 2) http://ame-www.usc.edu/research/combustion/combustionkinetics/model_release.html#top
! but...
! 3) mostly from misc_tran.dat (distributed with Cantera) by
!            $Author: hkmoffa $
!            $Date: 2003/09/05 14:45:59 $
!            $Revision: 1.1 $
!
!!!!!!!!!!!!!!!!!!!!!!!!!!!!!!!!!!!!!!!!!!!!!!!!!!!!!!!!!!!!!!!!!!!!!!!!!!!!!!!!
!
!
!-------------------------------------------------------------------------------
!                      epsilon    Sigma     Dipole Polarizability Rotational
!               Config  ------    (Angst)   Moment                Relaxation
!               Param     k
```

```
!------------------------------------------------------------------------
!
AR                0   136.500     3.330     0.000     0.000     0.000
C                 0    71.400     3.298     0.000     0.000     0.000 ! *
C2                1    97.530     3.621     0.000     1.760     4.000
C2O               1   232.400     3.828     0.000     0.000     1.000 ! *
C2H               1   209.000     4.100     0.000     0.000     2.500
C2H2              1   209.000     4.100     0.000     0.000     2.500
C2H2OH            2   224.700     4.162     0.000     0.000     1.000 ! *
C2H3              2   209.000     4.100     0.000     0.000     1.000 ! *
C2H4              2   280.800     3.971     0.000     0.000     1.500
C2H5              2   252.300     4.302     0.000     0.000     1.500
C2H6              2   252.300     4.302     0.000     0.000     1.500
C2N2              1   349.000     4.361     0.000     0.000     1.000 ! OIS
CH                1    80.000     2.750     0.000     0.000     0.000
CH2               1   144.000     3.800     0.000     0.000     0.000
CH2(S)            1   144.000     3.800     0.000     0.000     0.000
CH2CO             2   436.000     3.970     0.000     0.000     2.000
CH2O              2   498.000     3.590     0.000     0.000     2.000
CH2OH             2   417.000     3.690     1.700     0.000     2.000
CH3               1   144.000     3.800     0.000     0.000     0.000
CH3CO             2   436.000     3.970     0.000     0.000     2.000
CH3HCO            2   436.000     3.97      0.000     0.000     2.000 !=CH3CHO from 3
CH2HCO            2   436.000     3.97      0.000     0.000     2.000 !=CH2CHO from 3
CH3CN             2   436.000     3.97      0.000     0.000     2.000 !=CH3CO
CH2CN             2   436.000     3.97      0.000     0.000     2.000 !=CH3CO
C2H5CHO           2   357.000     5.176     0.000     0.000     1.000 !=C4H8 in 1
C2H5CO            2   357.000     5.176     0.000     0.000     1.000 !=C4H8 in 1
CH3O              2   417.000     3.690     1.700     0.000     2.000
CH3OH             2   481.800     3.626     0.000     0.000     1.000 ! SVE
CH4               2   141.400     3.746     0.000     2.600    13.000
CN                1    75.000     3.856     0.000     0.000     1.000 ! OIS
CO                1    98.100     3.650     0.000     1.950     1.800
CO2               1   244.000     3.763     0.000     2.650     2.100
H                 0   145.000     2.050     0.000     0.000     0.000
H2                1    38.000     2.920     0.000     0.790   280.000
H2CN              1   569.000     3.630     0.000     0.000     1.000 ! os/jm
H2NO              2   116.700     3.492     0.000     0.000     1.000 ! JAM
H2O               2   572.400     2.605     1.844     0.000     4.000
H2O2              2   107.400     3.458     0.000     0.000     3.800
HCCO              2   150.000     2.500     0.000     0.000     1.000 ! *
HCCOH             2   436.000     3.970     0.000     0.000     2.000
HCN               1   569.000     3.630     0.000     0.000     1.000 ! OIS
HCO               2   498.000     3.590     0.000     0.000     0.000
HCNO              2   232.400     3.828     0.000     0.000     1.000 ! JAM
HOCN              2   232.400     3.828     0.000     0.000     1.000 ! JAM
HNCO              2   232.400     3.828     0.000     0.000     1.000 ! OIS
HNNO              2   232.400     3.828     0.000     0.000     1.000 ! *
HNO               2   116.700     3.492     0.000     0.000     1.000 ! *
HNOH              2   116.700     3.492     0.000     0.000     1.000 ! JAM
HO2               2   107.400     3.458     0.000     0.000     1.000 ! *
HON               2   116.700     3.492     0.000     0.000     1.000 !=HNO
HONO              2   232.400     3.828     0.000     0.000     1.000 !=HNNO
H2NN              2    71.400     3.798     0.000     0.000     1.000 !=N2H2
N                 0    71.400     3.298     0.000     0.000     0.000 ! *
N2                1    97.530     3.621     0.000     1.760     4.000
N2H2              2    71.400     3.798     0.000     0.000     1.000 ! *
N2H3              2   200.000     3.900     0.000     0.000     1.000 ! *
N2H4              2   205.000     4.230     0.000     4.260     1.500
N2O               1   232.400     3.828     0.000     0.000     1.000 ! *
NCN               1   232.400     3.828     0.000     0.000     1.000 ! OIS
NCO               1   232.400     3.828     0.000     0.000     1.000 ! OIS
NH                1    80.000     2.650     0.000     0.000     4.000
NH2               2    80.000     2.650     0.000     2.260     4.000
NH2OH             2   116.700     3.492     0.000     0.000     1.000 !=HNOH
NH2NO             2   232.400     3.828     0.000     0.000     1.000 !=HNNO
NH3               2   481.000     2.920     1.470     0.000    10.000
NNH               2    71.400     3.798     0.000     0.000     1.000 ! *
NO                1    97.530     3.621     0.000     1.760     4.000
NO2               2   200.000     3.500     0.000     0.000     1.000 ! *
NO3               2   378.400     4.175     0.000     0.000     1.000 !=SO3 from 1
```

```
O                 0    80.000     2.750     0.000     0.000     0.000
O2                1   107.400     3.458     0.000     1.600     3.800
OH                1    80.000     2.750     0.000     0.000     0.000
OCHCHO            2   224.700     4.162     0.000     0.000     1.000 !=C2H2OH
```

GRI-Mech 3.0 Mechanism (Smith et al., 2000) – Filename: gri30.cti

```
#
# Generated from file gri30.inp
# by ck2cti on Mon Aug 25 09:52:57 2003
#
# Transport data from file ../transport/gri30_tran.dat.

units(length = "cm", time = "s", quantity = "mol", act_energy = "cal/mol")


ideal_gas(name = "gri30",
      elements = " O  H  C  N  Ar ",
      species = """ H2  H  O  O2  OH  H2O  HO2  H2O2  C  CH
                    CH2  CH2(S)  CH3  CH4  CO  CO2  HCO  CH2O  CH2OH  CH3O
                    CH3OH  C2H  C2H2  C2H3  C2H4  C2H5  C2H6  HCCO  CH2CO  HCCOH
                    N  NH  NH2  NH3  NNH  NO  NO2  N2O  HNO  CN
                    HCN  H2CN  HCNN  HCNO  HOCN  HNCO  NCO  N2  AR  C3H7
                    C3H8  CH2CHO  CH3CHO """,
      reactions = "all",
      kinetics = "GRI30",
      initial_state = state(temperature = 300.0,
                            pressure = OneAtm)    )

ideal_gas(name = "gri30_mix",
      elements = " O  H  C  N  Ar ",
      species = """ H2  H  O  O2  OH  H2O  HO2  H2O2  C  CH
                    CH2  CH2(S)  CH3  CH4  CO  CO2  HCO  CH2O  CH2OH  CH3O
                    CH3OH  C2H  C2H2  C2H3  C2H4  C2H5  C2H6  HCCO  CH2CO  HCCOH
                    N  NH  NH2  NH3  NNH  NO  NO2  N2O  HNO  CN
                    HCN  H2CN  HCNN  HCNO  HOCN  HNCO  NCO  N2  AR  C3H7
                    C3H8  CH2CHO  CH3CHO """,
      reactions = "all",
      kinetics = "GRI30",
      transport = "Mix",
      initial_state = state(temperature = 300.0,
                            pressure = OneAtm)    )


ideal_gas(name = "gri30_multi",
      elements = " O  H  C  N  Ar ",
      species = """ H2  H  O  O2  OH  H2O  HO2  H2O2  C  CH
                    CH2  CH2(S)  CH3  CH4  CO  CO2  HCO  CH2O  CH2OH  CH3O
                    CH3OH  C2H  C2H2  C2H3  C2H4  C2H5  C2H6  HCCO  CH2CO  HCCOH
                    N  NH  NH2  NH3  NNH  NO  NO2  N2O  HNO  CN
                    HCN  H2CN  HCNN  HCNO  HOCN  HNCO  NCO  N2  AR  C3H7
                    C3H8  CH2CHO  CH3CHO """,
      reactions = "all",
      kinetics = "GRI30",
      transport = "Multi",
      initial_state = state(temperature = 300.0,
                            pressure = OneAtm)    )



#-------------------------------------------------------------------------------
#  Species data
#-------------------------------------------------------------------------------

species(name = "H2",
    atoms = " H:2 ",
    thermo = (
       NASA( [  200.00,  1000.00], [  2.344331120E+00,   7.980520750E-03,
              -1.947815100E-05,   2.015720940E-08,  -7.376117610E-12,
              -9.179351730E+02,   6.830102380E-01] ),
       NASA( [ 1000.00,  3500.00], [  3.337279200E+00,  -4.940247310E-05,
               4.994567780E-07,  -1.795663940E-10,   2.002553760E-14,
              -9.501589220E+02,  -3.205023310E+00] )
             ),
```

```
    transport = gas_transport(
                    geom = "linear",
                    diam =     2.92,
                    well_depth =    38.00,
                    polar =     0.79,
                    rot_relax =   280.00),
    note = "TPIS78"
       )

species(name = "H",
    atoms = " H:1 ",
    thermo = (
       NASA( [  200.00,  1000.00], [  2.500000000E+00,   7.053328190E-13,
               -1.995919640E-15,   2.300816320E-18,  -9.277323320E-22,
                2.547365990E+04,  -4.466828530E-01] ),
       NASA( [ 1000.00,  3500.00], [  2.500000010E+00,  -2.308429730E-11,
                1.615619480E-14,  -4.735152350E-18,   4.981973570E-22,
                2.547365990E+04,  -4.466829140E-01] )
             ),
    transport = gas_transport(
                    geom = "atom",
                    diam =     2.05,
                    well_depth =   145.00),
    note = "L 7/88"
       )

species(name = "O",
    atoms = " O:1 ",
    thermo = (
       NASA( [  200.00,  1000.00], [  3.168267100E+00,  -3.279318840E-03,
                6.643063960E-06,  -6.128066240E-09,   2.112659710E-12,
                2.912225920E+04,   2.051933460E+00] ),
       NASA( [ 1000.00,  3500.00], [  2.569420780E+00,  -8.597411370E-05,
                4.194845890E-08,  -1.001777990E-11,   1.228336910E-15,
                2.921757910E+04,   4.784338640E+00] )
             ),
    transport = gas_transport(
                    geom = "atom",
                    diam =     2.75,
                    well_depth =    80.00),
    note = "L 1/90"
       )

species(name = "O2",
    atoms = " O:2 ",
    thermo = (
       NASA( [  200.00,  1000.00], [  3.782456360E+00,  -2.996734160E-03,
                9.847302010E-06,  -9.681295090E-09,   3.243728370E-12,
               -1.063943560E+03,   3.657675730E+00] ),
       NASA( [ 1000.00,  3500.00], [  3.282537840E+00,   1.483087540E-03,
               -7.579666690E-07,   2.094705550E-10,  -2.167177940E-14,
               -1.088457720E+03,   5.453231290E+00] )
             ),
    transport = gas_transport(
                    geom = "linear",
                    diam =     3.46,
                    well_depth =   107.40,
                    polar =     1.60,
                    rot_relax =     3.80),
    note = "TPIS89"
       )

species(name = "OH",
    atoms = " O:1  H:1 ",
    thermo = (
       NASA( [  200.00,  1000.00], [  3.992015430E+00,  -2.401317520E-03,
                4.617938410E-06,  -3.881133330E-09,   1.364114700E-12,
                3.615080560E+03,  -1.039254580E-01] ),
       NASA( [ 1000.00,  3500.00], [  3.092887670E+00,   5.484297160E-04,
                1.265052280E-07,  -8.794615560E-11,   1.174123760E-14,
                3.858657000E+03,   4.476696100E+00] )
```

```
            ),
    transport = gas_transport(
                    geom = "linear",
                    diam =     2.75,
                    well_depth =    80.00),
    note = "RUS 78"
       )

species(name = "H2O",
    atoms = " H:2  O:1 ",
    thermo = (
       NASA( [  200.00,  1000.00], [  4.198640560E+00,  -2.036434100E-03,
                6.520402110E-06,  -5.487970620E-09,   1.771978170E-12,
               -3.029372670E+04,  -8.490322080E-01] ),
       NASA( [ 1000.00,  3500.00], [  3.033992490E+00,   2.176918040E-03,
               -1.640725180E-07,  -9.704198700E-11,   1.682009920E-14,
               -3.000429710E+04,   4.966770100E+00] )
            ),
    transport = gas_transport(
                    geom = "nonlinear",
                    diam =     2.60,
                    well_depth =   572.40,
                    dipole =     1.84,
                    rot_relax =     4.00),
    note = "L 8/89"
       )

species(name = "HO2",
    atoms = " H:1  O:2 ",
    thermo = (
       NASA( [  200.00,  1000.00], [  4.301798010E+00,  -4.749120510E-03,
                2.115828910E-05,  -2.427638940E-08,   9.292251240E-12,
                2.948080400E+02,   3.716662450E+00] ),
       NASA( [ 1000.00,  3500.00], [  4.017210900E+00,   2.239820130E-03,
               -6.336581500E-07,   1.142463700E-10,  -1.079085350E-14,
                1.118567130E+02,   3.785102150E+00] )
            ),
    transport = gas_transport(
                    geom = "nonlinear",
                    diam =     3.46,
                    well_depth =   107.40,
                    rot_relax =     1.00),
    note = "L 5/89"
       )

species(name = "H2O2",
    atoms = " H:2  O:2 ",
    thermo = (
       NASA( [  200.00,  1000.00], [  4.276112690E+00,  -5.428224170E-04,
                1.673357010E-05,  -2.157708130E-08,   8.624543630E-12,
               -1.770258210E+04,   3.435050740E+00] ),
       NASA( [ 1000.00,  3500.00], [  4.165002850E+00,   4.908316940E-03,
               -1.901392250E-06,   3.711859860E-10,  -2.879083050E-14,
               -1.786178770E+04,   2.916156620E+00] )
            ),
    transport = gas_transport(
                    geom = "nonlinear",
                    diam =     3.46,
                    well_depth =   107.40,
                    rot_relax =     3.80),
    note = "L 7/88"
       )

species(name = "C",
    atoms = " C:1 ",
    thermo = (
       NASA( [  200.00,  1000.00], [  2.554239550E+00,  -3.215377240E-04,
                7.337922450E-07,  -7.322348890E-10,   2.665214460E-13,
                8.544388320E+04,   4.531308480E+00] ),
       NASA( [ 1000.00,  3500.00], [  2.492668880E+00,   4.798892840E-05,
               -7.243350200E-08,   3.742910290E-11,  -4.872778930E-15,
```

```
               8.545129530E+04,   4.801503730E+00] )
            ),
    transport = gas_transport(
                    geom = "atom",
                    diam =     3.30,
                    well_depth =    71.40),
    note = "L11/88"
       )

species(name = "CH",
    atoms = " C:1  H:1 ",
    thermo = (
       NASA( [  200.00,  1000.00], [  3.489816650E+00,   3.238355410E-04,
              -1.688990650E-06,   3.162173270E-09,  -1.406090670E-12,
               7.079729340E+04,   2.084011080E+00] ),
       NASA( [ 1000.00,  3500.00], [  2.878464730E+00,   9.709136810E-04,
               1.444456550E-07,  -1.306878490E-10,   1.760793830E-14,
               7.101243640E+04,   5.484979990E+00] )
            ),
    transport = gas_transport(
                    geom = "linear",
                    diam =     2.75,
                    well_depth =    80.00),
    note = "TPIS79"
       )

species(name = "CH2",
    atoms = " C:1  H:2 ",
    thermo = (
       NASA( [  200.00,  1000.00], [  3.762678670E+00,   9.688721430E-04,
               2.794898410E-06,  -3.850911530E-09,   1.687417190E-12,
               4.600404010E+04,   1.562531850E+00] ),
       NASA( [ 1000.00,  3500.00], [  2.874101130E+00,   3.656392920E-03,
              -1.408945970E-06,   2.601795490E-10,  -1.877275670E-14,
               4.626360400E+04,   6.171193240E+00] )
            ),
    transport = gas_transport(
                    geom = "linear",
                    diam =     3.80,
                    well_depth =   144.00),
    note = "L S/93"
       )

species(name = "CH2(S)",
    atoms = " C:1  H:2 ",
    thermo = (
       NASA( [  200.00,  1000.00], [  4.198604110E+00,  -2.366614190E-03,
               8.232962200E-06,  -6.688159810E-09,   1.943147370E-12,
               5.049681630E+04,  -7.691189670E-01] ),
       NASA( [ 1000.00,  3500.00], [  2.292038420E+00,   4.655886370E-03,
              -2.011919470E-06,   4.179060000E-10,  -3.397163650E-14,
               5.092599970E+04,   8.626501690E+00] )
            ),
    transport = gas_transport(
                    geom = "linear",
                    diam =     3.80,
                    well_depth =   144.00),
    note = "L S/93"
       )

species(name = "CH3",
    atoms = " C:1  H:3 ",
    thermo = (
       NASA( [  200.00,  1000.00], [  3.673590400E+00,   2.010951750E-03,
               5.730218560E-06,  -6.871174250E-09,   2.543857340E-12,
               1.644499880E+04,   1.604564330E+00] ),
       NASA( [ 1000.00,  3500.00], [  2.285717720E+00,   7.239900370E-03,
              -2.987143480E-06,   5.956846440E-10,  -4.671543940E-14,
               1.677558430E+04,   8.480071790E+00] )
            ),
    transport = gas_transport(
```

```
                    geom = "linear",
                    diam =     3.80,
                    well_depth =   144.00),
    note = "L11/89"
       )

species(name = "CH4",
    atoms = " C:1  H:4 ",
    thermo = (
       NASA( [  200.00,  1000.00], [  5.149876130E+00,  -1.367097880E-02,
                4.918005990E-05,  -4.847430260E-08,   1.666939560E-11,
               -1.024664760E+04,  -4.641303760E+00] ),
       NASA( [ 1000.00,  3500.00], [  7.485149500E-02,   1.339094670E-02,
               -5.732858090E-06,   1.222925350E-09,  -1.018152300E-13,
               -9.468344590E+03,   1.843731800E+01] )
             ),
    transport = gas_transport(
                    geom = "nonlinear",
                    diam =     3.75,
                    well_depth =   141.40,
                    polar =     2.60,
                    rot_relax =    13.00),
    note = "L 8/88"
       )

species(name = "CO",
    atoms = " C:1  O:1 ",
    thermo = (
       NASA( [  200.00,  1000.00], [  3.579533470E+00,  -6.103536800E-04,
                1.016814330E-06,   9.070058840E-10,  -9.044244990E-13,
               -1.434408600E+04,   3.508409280E+00] ),
       NASA( [ 1000.00,  3500.00], [  2.715185610E+00,   2.062527430E-03,
               -9.988257710E-07,   2.300530080E-10,  -2.036477160E-14,
               -1.415187240E+04,   7.818687720E+00] )
             ),
    transport = gas_transport(
                    geom = "linear",
                    diam =     3.65,
                    well_depth =    98.10,
                    polar =     1.95,
                    rot_relax =     1.80),
    note = "TPIS79"
       )

species(name = "CO2",
    atoms = " C:1  O:2 ",
    thermo = (
       NASA( [  200.00,  1000.00], [  2.356773520E+00,   8.984596770E-03,
               -7.123562690E-06,   2.459190220E-09,  -1.436995480E-13,
               -4.837196970E+04,   9.901052220E+00] ),
       NASA( [ 1000.00,  3500.00], [  3.857460290E+00,   4.414370260E-03,
               -2.214814040E-06,   5.234901880E-10,  -4.720841640E-14,
               -4.875916600E+04,   2.271638060E+00] )
             ),
    transport = gas_transport(
                    geom = "linear",
                    diam =     3.76,
                    well_depth =   244.00,
                    polar =     2.65,
                    rot_relax =     2.10),
    note = "L 7/88"
       )

species(name = "HCO",
    atoms = " H:1  C:1  O:1 ",
    thermo = (
       NASA( [  200.00,  1000.00], [  4.221185840E+00,  -3.243925320E-03,
                1.377994460E-05,  -1.331440930E-08,   4.337688650E-12,
                3.839564960E+03,   3.394372430E+00] ),
       NASA( [ 1000.00,  3500.00], [  2.772174380E+00,   4.956955260E-03,
               -2.484456130E-06,   5.891617780E-10,  -5.335087110E-14,
```

```
               4.011918150E+03,   9.798344920E+00] )
            ),
    transport = gas_transport(
                    geom = "nonlinear",
                    diam =     3.59,
                    well_depth =   498.00),
    note = "L12/89"
       )

species(name = "CH2O",
    atoms = " H:2  C:1  O:1 ",
    thermo = (
       NASA( [  200.00,  1000.00], [  4.793723150E+00,  -9.908333690E-03,
                3.732200080E-05,  -3.792852610E-08,   1.317726520E-11,
               -1.430895670E+04,   6.028129000E-01] ),
       NASA( [ 1000.00,  3500.00], [  1.760690080E+00,   9.200000820E-03,
               -4.422588130E-06,   1.006412120E-09,  -8.838556400E-14,
               -1.399583230E+04,   1.365632300E+01] )
            ),
    transport = gas_transport(
                    geom = "nonlinear",
                    diam =     3.59,
                    well_depth =   498.00,
                    rot_relax =     2.00),
    note = "L 8/88"
       )

species(name = "CH2OH",
    atoms = " C:1  H:3  O:1 ",
    thermo = (
       NASA( [  200.00,  1000.00], [  3.863889180E+00,   5.596723040E-03,
                5.932717910E-06,  -1.045320120E-08,   4.369672780E-12,
               -3.193913670E+03,   5.473022430E+00] ),
       NASA( [ 1000.00,  3500.00], [  3.692665690E+00,   8.645767970E-03,
               -3.751011200E-06,   7.872346360E-10,  -6.485542010E-14,
               -3.242506270E+03,   5.810432150E+00] )
            ),
    transport = gas_transport(
                    geom = "nonlinear",
                    diam =     3.69,
                    well_depth =   417.00,
                    dipole =     1.70,
                    rot_relax =     2.00),
    note = "GUNL93"
       )

species(name = "CH3O",
    atoms = " C:1  H:3  O:1 ",
    thermo = (
       NASA( [  300.00,  1000.00], [  2.106204000E+00,   7.216595000E-03,
                5.338472000E-06,  -7.377636000E-09,   2.075610000E-12,
                9.786011000E+02,   1.315217700E+01] ),
       NASA( [ 1000.00,  3000.00], [  3.770799000E+00,   7.871497000E-03,
               -2.656384000E-06,   3.944431000E-10,  -2.112616000E-14,
                1.278325200E+02,   2.929575000E+00] )
            ),
    transport = gas_transport(
                    geom = "nonlinear",
                    diam =     3.69,
                    well_depth =   417.00,
                    dipole =     1.70,
                    rot_relax =     2.00),
    note = "121686"
       )

species(name = "CH3OH",
    atoms = " C:1  H:4  O:1 ",
    thermo = (
       NASA( [  200.00,  1000.00], [  5.715395820E+00,  -1.523091290E-02,
                6.524411550E-05,  -7.108068890E-08,   2.613526980E-11,
               -2.564276560E+04,  -1.504098230E+00] ),
```

```
       NASA( [ 1000.00,  3500.00], [  1.789707910E+00,   1.409382920E-02,
               -6.365008350E-06,   1.381710850E-09,  -1.170602200E-13,
               -2.537487470E+04,   1.450236230E+01] )
             ),
    transport = gas_transport(
                    geom = "nonlinear",
                    diam =     3.63,
                    well_depth =   481.80,
                    rot_relax =     1.00),
    note = "L 8/88"
       )

species(name = "C2H",
    atoms = " C:2  H:1 ",
    thermo = (
       NASA( [  200.00,  1000.00], [  2.889657330E+00,   1.340996110E-02,
               -2.847695010E-05,   2.947910450E-08,  -1.093315110E-11,
                6.683939320E+04,   6.222964380E+00] ),
       NASA( [ 1000.00,  3500.00], [  3.167806520E+00,   4.752219020E-03,
               -1.837870770E-06,   3.041902520E-10,  -1.772327700E-14,
                6.712106500E+04,   6.635894750E+00] )
             ),
    transport = gas_transport(
                    geom = "linear",
                    diam =     4.10,
                    well_depth =   209.00,
                    rot_relax =     2.50),
    note = "L 1/91"
       )

species(name = "C2H2",
    atoms = " C:2  H:2 ",
    thermo = (
       NASA( [  200.00,  1000.00], [  8.086810940E-01,   2.336156290E-02,
               -3.551718150E-05,   2.801524370E-08,  -8.500729740E-12,
                2.642898070E+04,   1.393970510E+01] ),
       NASA( [ 1000.00,  3500.00], [  4.147569640E+00,   5.961666640E-03,
               -2.372948520E-06,   4.674121710E-10,  -3.612352130E-14,
                2.593599920E+04,  -1.230281210E+00] )
             ),
    transport = gas_transport(
                    geom = "linear",
                    diam =     4.10,
                    well_depth =   209.00,
                    rot_relax =     2.50),
    note = "L 1/91"
       )

species(name = "C2H3",
    atoms = " C:2  H:3 ",
    thermo = (
       NASA( [  200.00,  1000.00], [  3.212466450E+00,   1.514791620E-03,
                2.592094120E-05,  -3.576578470E-08,   1.471508730E-11,
                3.485984680E+04,   8.510540250E+00] ),
       NASA( [ 1000.00,  3500.00], [  3.016724000E+00,   1.033022920E-02,
               -4.680823490E-06,   1.017632880E-09,  -8.626070410E-14,
                3.461287390E+04,   7.787323780E+00] )
             ),
    transport = gas_transport(
                    geom = "nonlinear",
                    diam =     4.10,
                    well_depth =   209.00,
                    rot_relax =     1.00),
    note = "L 2/92"
       )

species(name = "C2H4",
    atoms = " C:2  H:4 ",
    thermo = (
       NASA( [  200.00,  1000.00], [  3.959201480E+00,  -7.570522470E-03,
                5.709902920E-05,  -6.915887530E-08,   2.698843730E-11,
```

```
                5.089775930E+03,   4.097330960E+00] ),
       NASA( [ 1000.00,  3500.00], [  2.036111160E+00,   1.464541510E-02,
               -6.710779150E-06,   1.472229230E-09,  -1.257060610E-13,
                4.939886140E+03,   1.030536930E+01] )
             ),
    transport = gas_transport(
                     geom = "nonlinear",
                     diam =     3.97,
                     well_depth =   280.80,
                     rot_relax =     1.50),
    note = "L 1/91"
       )

species(name = "C2H5",
    atoms = " C:2  H:5 ",
    thermo = (
       NASA( [  200.00,  1000.00], [  4.306465680E+00,  -4.186588920E-03,
                4.971428070E-05,  -5.991266060E-08,   2.305090040E-11,
                1.284162650E+04,   4.707209240E+00] ),
       NASA( [ 1000.00,  3500.00], [  1.954656420E+00,   1.739727220E-02,
               -7.982066680E-06,   1.752176890E-09,  -1.496415760E-13,
                1.285752000E+04,   1.346243430E+01] )
             ),
    transport = gas_transport(
                     geom = "nonlinear",
                     diam =     4.30,
                     well_depth =   252.30,
                     rot_relax =     1.50),
    note = "L12/92"
       )

species(name = "C2H6",
    atoms = " C:2  H:6 ",
    thermo = (
       NASA( [  200.00,  1000.00], [  4.291424920E+00,  -5.501542700E-03,
                5.994382880E-05,  -7.084662850E-08,   2.686857710E-11,
               -1.152220550E+04,   2.666823160E+00] ),
       NASA( [ 1000.00,  3500.00], [  1.071881500E+00,   2.168526770E-02,
               -1.002560670E-05,   2.214120010E-09,  -1.900028900E-13,
               -1.142639320E+04,   1.511561070E+01] )
             ),
    transport = gas_transport(
                     geom = "nonlinear",
                     diam =     4.30,
                     well_depth =   252.30,
                     rot_relax =     1.50),
    note = "L 8/88"
       )

species(name = "HCCO",
    atoms = " H:1  C:2  O:1 ",
    thermo = (
       NASA( [  300.00,  1000.00], [  2.251721400E+00,   1.765502100E-02,
               -2.372910100E-05,   1.727575900E-08,  -5.066481100E-12,
                2.005944900E+04,   1.249041700E+01] ),
       NASA( [ 1000.00,  4000.00], [  5.628205800E+00,   4.085340100E-03,
               -1.593454700E-06,   2.862605200E-10,  -1.940783200E-14,
                1.932721500E+04,  -3.930259500E+00] )
             ),
    transport = gas_transport(
                     geom = "nonlinear",
                     diam =     2.50,
                     well_depth =   150.00,
                     rot_relax =     1.00),
    note = "SRIC91"
       )

species(name = "CH2CO",
    atoms = " C:2  H:2  O:1 ",
    thermo = (
       NASA( [  200.00,  1000.00], [  2.135836300E+00,   1.811887210E-02,
```

```
               -1.739474740E-05,   9.343975680E-09,  -2.014576150E-12,
               -7.042918040E+03,   1.221564800E+01] ),
       NASA( [ 1000.00,  3500.00], [  4.511297320E+00,   9.003597450E-03,
               -4.169396350E-06,   9.233458820E-10,  -7.948382010E-14,
               -7.551053110E+03,   6.322472050E-01] )
             ),
    transport = gas_transport(
                    geom = "nonlinear",
                    diam =     3.97,
                    well_depth =   436.00,
                    rot_relax =     2.00),
    note = "L 5/90"
       )

species(name = "HCCOH",
    atoms = " C:2  O:1  H:2 ",
    thermo = (
       NASA( [  300.00,  1000.00], [  1.242373300E+00,   3.107220100E-02,
               -5.086686400E-05,   4.313713100E-08,  -1.401459400E-11,
                8.031614300E+03,   1.387431900E+01] ),
       NASA( [ 1000.00,  5000.00], [  5.923829100E+00,   6.792360000E-03,
               -2.565856400E-06,   4.498784100E-10,  -2.994010100E-14,
                7.264626000E+03,  -7.601774200E+00] )
             ),
    transport = gas_transport(
                    geom = "nonlinear",
                    diam =     3.97,
                    well_depth =   436.00,
                    rot_relax =     2.00),
    note = "SRI91"
       )

species(name = "N",
    atoms = " N:1 ",
    thermo = (
       NASA( [  200.00,  1000.00], [  2.500000000E+00,   0.000000000E+00,
                0.000000000E+00,   0.000000000E+00,   0.000000000E+00,
                5.610463700E+04,   4.193908700E+00] ),
       NASA( [ 1000.00,  6000.00], [  2.415942900E+00,   1.748906500E-04,
               -1.190236900E-07,   3.022624500E-11,  -2.036098200E-15,
                5.613377300E+04,   4.649609600E+00] )
             ),
    transport = gas_transport(
                    geom = "atom",
                    diam =     3.30,
                    well_depth =    71.40),
    note = "L 6/88"
       )

species(name = "NH",
    atoms = " N:1  H:1 ",
    thermo = (
       NASA( [  200.00,  1000.00], [  3.492908500E+00,   3.117919800E-04,
               -1.489048400E-06,   2.481644200E-09,  -1.035696700E-12,
                4.188062900E+04,   1.848327800E+00] ),
       NASA( [ 1000.00,  6000.00], [  2.783692800E+00,   1.329843000E-03,
               -4.247804700E-07,   7.834850100E-11,  -5.504447000E-15,
                4.212084800E+04,   5.740779900E+00] )
             ),
    transport = gas_transport(
                    geom = "linear",
                    diam =     2.65,
                    well_depth =    80.00,
                    rot_relax =     4.00),
    note = "And94"
       )

species(name = "NH2",
    atoms = " N:1  H:2 ",
    thermo = (
       NASA( [  200.00,  1000.00], [  4.204002900E+00,  -2.106138500E-03,
```

```
                7.106834800E-06,  -5.611519700E-09,   1.644071700E-12,
                2.188591000E+04,  -1.418424800E-01] ),
       NASA( [ 1000.00,  6000.00], [  2.834742100E+00,   3.207308200E-03,
               -9.339080400E-07,   1.370295300E-10,  -7.920614400E-15,
                2.217195700E+04,   6.520416300E+00] )
             ),
    transport = gas_transport(
                     geom = "nonlinear",
                     diam =     2.65,
                     well_depth =    80.00,
                     polar =     2.26,
                     rot_relax =     4.00),
    note = "And89"
       )

species(name = "NH3",
    atoms = " N:1  H:3 ",
    thermo = (
       NASA( [  200.00,  1000.00], [  4.286027400E+00,  -4.660523000E-03,
                2.171851300E-05,  -2.280888700E-08,   8.263804600E-12,
               -6.741728500E+03,  -6.253727700E-01] ),
       NASA( [ 1000.00,  6000.00], [  2.634452100E+00,   5.666256000E-03,
               -1.727867600E-06,   2.386716100E-10,  -1.257878600E-14,
               -6.544695800E+03,   6.566292800E+00] )
             ),
    transport = gas_transport(
                     geom = "nonlinear",
                     diam =     2.92,
                     well_depth =   481.00,
                     dipole =     1.47,
                     rot_relax =    10.00),
    note = "J 6/77"
       )

species(name = "NNH",
    atoms = " N:2  H:1 ",
    thermo = (
       NASA( [  200.00,  1000.00], [  4.344692700E+00,  -4.849707200E-03,
                2.005945900E-05,  -2.172646400E-08,   7.946953900E-12,
                2.879197300E+04,   2.977941000E+00] ),
       NASA( [ 1000.00,  6000.00], [  3.766754400E+00,   2.891508200E-03,
               -1.041662000E-06,   1.684259400E-10,  -1.009189600E-14,
                2.865069700E+04,   4.470506700E+00] )
             ),
    transport = gas_transport(
                     geom = "nonlinear",
                     diam =     3.80,
                     well_depth =    71.40,
                     rot_relax =     1.00),
    note = "T07/93"
       )

species(name = "NO",
    atoms = " N:1  O:1 ",
    thermo = (
       NASA( [  200.00,  1000.00], [  4.218476300E+00,  -4.638976000E-03,
                1.104102200E-05,  -9.336135400E-09,   2.803577000E-12,
                9.844623000E+03,   2.280846400E+00] ),
       NASA( [ 1000.00,  6000.00], [  3.260605600E+00,   1.191104300E-03,
               -4.291704800E-07,   6.945766900E-11,  -4.033609900E-15,
                9.920974600E+03,   6.369302700E+00] )
             ),
    transport = gas_transport(
                     geom = "linear",
                     diam =     3.62,
                     well_depth =    97.53,
                     polar =     1.76,
                     rot_relax =     4.00),
    note = "RUS 78"
       )
```

```
species(name = "NO2",
    atoms = " N:1  O:2 ",
    thermo = (
       NASA( [  200.00,  1000.00], [  3.944031200E+00,  -1.585429000E-03,
                1.665781200E-05,  -2.047542600E-08,   7.835056400E-12,
                2.896617900E+03,   6.311991700E+00] ),
       NASA( [ 1000.00,  6000.00], [  4.884754200E+00,   2.172395600E-03,
               -8.280690600E-07,   1.574751000E-10,  -1.051089500E-14,
                2.316498300E+03,  -1.174169500E-01] )
             ),
    transport = gas_transport(
                     geom = "nonlinear",
                     diam =     3.50,
                     well_depth =   200.00,
                     rot_relax =     1.00),
    note = "L 7/88"
       )

species(name = "N2O",
    atoms = " N:2  O:1 ",
    thermo = (
       NASA( [  200.00,  1000.00], [  2.257150200E+00,   1.130472800E-02,
               -1.367131900E-05,   9.681980600E-09,  -2.930718200E-12,
                8.741774400E+03,   1.075799200E+01] ),
       NASA( [ 1000.00,  6000.00], [  4.823072900E+00,   2.627025100E-03,
               -9.585087400E-07,   1.600071200E-10,  -9.775230300E-15,
                8.073404800E+03,  -2.201720700E+00] )
             ),
    transport = gas_transport(
                     geom = "linear",
                     diam =     3.83,
                     well_depth =   232.40,
                     rot_relax =     1.00),
    note = "L 7/88"
       )

species(name = "HNO",
    atoms = " H:1  N:1  O:1 ",
    thermo = (
       NASA( [  200.00,  1000.00], [  4.533491600E+00,  -5.669617100E-03,
                1.847320700E-05,  -1.713709400E-08,   5.545457300E-12,
                1.154829700E+04,   1.749841700E+00] ),
       NASA( [ 1000.00,  6000.00], [  2.979250900E+00,   3.494405900E-03,
               -7.854977800E-07,   5.747959400E-11,  -1.933591600E-16,
                1.175058200E+04,   8.606372800E+00] )
             ),
    transport = gas_transport(
                     geom = "nonlinear",
                     diam =     3.49,
                     well_depth =   116.70,
                     rot_relax =     1.00),
    note = "And93"
       )

species(name = "CN",
    atoms = " C:1  N:1 ",
    thermo = (
       NASA( [  200.00,  1000.00], [  3.612935100E+00,  -9.555132700E-04,
                2.144297700E-06,  -3.151632300E-10,  -4.643035600E-13,
                5.170834000E+04,   3.980499500E+00] ),
       NASA( [ 1000.00,  6000.00], [  3.745980500E+00,   4.345077500E-05,
                2.970598400E-07,  -6.865180600E-11,   4.413417300E-15,
                5.153618800E+04,   2.786760100E+00] )
             ),
    transport = gas_transport(
                     geom = "linear",
                     diam =     3.86,
                     well_depth =    75.00,
                     rot_relax =     1.00),
    note = "HBH92"
       )
```

```
species(name = "HCN",
    atoms = " H:1  C:1  N:1 ",
    thermo = (
       NASA( [  200.00,  1000.00], [  2.258988600E+00,   1.005117000E-02,
               -1.335176300E-05,   1.009234900E-08,  -3.008902800E-12,
                1.471263300E+04,   8.916441900E+00] ),
       NASA( [ 1000.00,  6000.00], [  3.802239200E+00,   3.146422800E-03,
               -1.063218500E-06,   1.661975700E-10,  -9.799757000E-15,
                1.440729200E+04,   1.575460100E+00] )
             ),
    transport = gas_transport(
                     geom = "linear",
                     diam =     3.63,
                     well_depth =   569.00,
                     rot_relax =     1.00),
    note = "GRI/98"
       )

species(name = "H2CN",
    atoms = " H:2  C:1  N:1 ",
    thermo = (
       NASA( [  300.00,  1000.00], [  2.851661000E+00,   5.695233100E-03,
                1.071140000E-06,  -1.622612000E-09,  -2.351108100E-13,
                2.863782000E+04,   8.992751100E+00] ),
       NASA( [ 1000.00,  4000.00], [  5.209703000E+00,   2.969291100E-03,
               -2.855589100E-07,  -1.635550000E-10,   3.043258900E-14,
                2.767710900E+04,  -4.444478000E+00] )
             ),
    transport = gas_transport(
                     geom = "linear",
                     diam =     3.63,
                     well_depth =   569.00,
                     rot_relax =     1.00),
    note = "41687"
       )

species(name = "HCNN",
    atoms = " C:1  N:2  H:1 ",
    thermo = (
       NASA( [  300.00,  1000.00], [  2.524319400E+00,   1.596061900E-02,
               -1.881635400E-05,   1.212554000E-08,  -3.235737800E-12,
                5.426198400E+04,   1.167587000E+01] ),
       NASA( [ 1000.00,  5000.00], [  5.894636200E+00,   3.989595900E-03,
               -1.598238000E-06,   2.924939500E-10,  -2.009468600E-14,
                5.345294100E+04,  -5.103050200E+00] )
             ),
    transport = gas_transport(
                     geom = "nonlinear",
                     diam =     2.50,
                     well_depth =   150.00,
                     rot_relax =     1.00),
    note = "SRI/94"
       )

species(name = "HCNO",
    atoms = " H:1  N:1  C:1  O:1 ",
    thermo = (
       NASA( [  300.00,  1382.00], [  2.647279890E+00,   1.275053420E-02,
               -1.047942360E-05,   4.414328360E-09,  -7.575214660E-13,
                1.929902520E+04,   1.073329720E+01] ),
       NASA( [ 1382.00,  5000.00], [  6.598604560E+00,   3.027786260E-03,
               -1.077043460E-06,   1.716665280E-10,  -1.014393910E-14,
                1.796613390E+04,  -1.033065990E+01] )
             ),
    transport = gas_transport(
                     geom = "nonlinear",
                     diam =     3.83,
                     well_depth =   232.40,
                     rot_relax =     1.00),
    note = "BDEA94"
```

```
      )

species(name = "HOCN",
    atoms = " H:1  N:1  C:1  O:1 ",
    thermo = (
       NASA( [  300.00,  1368.00], [  3.786049520E+00,   6.886679220E-03,
               -3.214878640E-06,   5.171957670E-10,   1.193607880E-14,
               -2.826984000E+03,   5.632921620E+00] ),
       NASA( [ 1368.00,  5000.00], [  5.897848850E+00,   3.167893930E-03,
               -1.118010640E-06,   1.772431440E-10,  -1.043391770E-14,
               -3.706533310E+03,  -6.181678250E+00] )
             ),
    transport = gas_transport(
                    geom = "nonlinear",
                    diam =     3.83,
                    well_depth =   232.40,
                    rot_relax =     1.00),
    note = "BDEA94"
       )

species(name = "HNCO",
    atoms = " H:1  N:1  C:1  O:1 ",
    thermo = (
       NASA( [  300.00,  1478.00], [  3.630963170E+00,   7.302823570E-03,
               -2.280500030E-06,  -6.612712980E-10,   3.622357520E-13,
               -1.558736360E+04,   6.194577270E+00] ),
       NASA( [ 1478.00,  5000.00], [  6.223951340E+00,   3.178640040E-03,
               -1.093787550E-06,   1.707351630E-10,  -9.950219550E-15,
               -1.665993440E+04,  -8.382247410E+00] )
             ),
    transport = gas_transport(
                    geom = "nonlinear",
                    diam =     3.83,
                    well_depth =   232.40,
                    rot_relax =     1.00),
    note = "BDEA94"
       )

species(name = "NCO",
    atoms = " N:1  C:1  O:1 ",
    thermo = (
       NASA( [  200.00,  1000.00], [  2.826930800E+00,   8.805168800E-03,
               -8.386613400E-06,   4.801696400E-09,  -1.331359500E-12,
                1.468247700E+04,   9.550464600E+00] ),
       NASA( [ 1000.00,  6000.00], [  5.152184500E+00,   2.305176100E-03,
               -8.803315300E-07,   1.478909800E-10,  -9.097799600E-15,
                1.400412300E+04,  -2.544266000E+00] )
             ),
    transport = gas_transport(
                    geom = "linear",
                    diam =     3.83,
                    well_depth =   232.40,
                    rot_relax =     1.00),
    note = "EA 93"
       )

species(name = "N2",
    atoms = " N:2 ",
    thermo = (
       NASA( [  300.00,  1000.00], [  3.298677000E+00,   1.408240400E-03,
               -3.963222000E-06,   5.641515000E-09,  -2.444854000E-12,
               -1.020899900E+03,   3.950372000E+00] ),
       NASA( [ 1000.00,  5000.00], [  2.926640000E+00,   1.487976800E-03,
               -5.684760000E-07,   1.009703800E-10,  -6.753351000E-15,
               -9.227977000E+02,   5.980528000E+00] )
             ),
    transport = gas_transport(
                    geom = "linear",
                    diam =     3.62,
                    well_depth =    97.53,
                    polar =     1.76,
```

```
                    rot_relax =     4.00),
    note = "121286"
       )

species(name = "AR",
    atoms = " Ar:1 ",
    thermo = (
       NASA( [  300.00,  1000.00], [  2.500000000E+00,   0.000000000E+00,
                0.000000000E+00,   0.000000000E+00,   0.000000000E+00,
               -7.453750000E+02,   4.366000000E+00] ),
       NASA( [ 1000.00,  5000.00], [  2.500000000E+00,   0.000000000E+00,
                0.000000000E+00,   0.000000000E+00,   0.000000000E+00,
               -7.453750000E+02,   4.366000000E+00] )
             ),
    transport = gas_transport(
                    geom = "atom",
                    diam =     3.33,
                    well_depth =   136.50),
    note = "120186"
       )

species(name = "C3H7",
    atoms = " C:3  H:7 ",
    thermo = (
       NASA( [  300.00,  1000.00], [  1.051551800E+00,   2.599198000E-02,
                2.380054000E-06,  -1.960956900E-08,   9.373247000E-12,
                1.063186300E+04,   2.112255900E+01] ),
       NASA( [ 1000.00,  5000.00], [  7.702698700E+00,   1.604420300E-02,
               -5.283322000E-06,   7.629859000E-10,  -3.939228400E-14,
                8.298433600E+03,  -1.548018000E+01] )
             ),
    transport = gas_transport(
                    geom = "nonlinear",
                    diam =     4.98,
                    well_depth =   266.80,
                    rot_relax =     1.00),
    note = "L 9/84"
       )

species(name = "C3H8",
    atoms = " C:3  H:8 ",
    thermo = (
       NASA( [  300.00,  1000.00], [  9.335538100E-01,   2.642457900E-02,
                6.105972700E-06,  -2.197749900E-08,   9.514925300E-12,
               -1.395852000E+04,   1.920169100E+01] ),
       NASA( [ 1000.00,  5000.00], [  7.534136800E+00,   1.887223900E-02,
               -6.271849100E-06,   9.147564900E-10,  -4.783806900E-14,
               -1.646751600E+04,  -1.789234900E+01] )
             ),
    transport = gas_transport(
                    geom = "nonlinear",
                    diam =     4.98,
                    well_depth =   266.80,
                    rot_relax =     1.00),
    note = "L 4/85"
       )

species(name = "CH2CHO",
    atoms = " O:1  H:3  C:2 ",
    thermo = (
       NASA( [  300.00,  1000.00], [  3.409062000E+00,   1.073857400E-02,
                1.891492000E-06,  -7.158583000E-09,   2.867385000E-12,
                1.521476600E+03,   9.558290000E+00] ),
       NASA( [ 1000.00,  5000.00], [  5.975670000E+00,   8.130591000E-03,
               -2.743624000E-06,   4.070304000E-10,  -2.176017000E-14,
                4.903218000E+02,  -5.045251000E+00] )
             ),
    transport = gas_transport(
                    geom = "nonlinear",
                    diam =     3.97,
                    well_depth =   436.00,
```

```
                    rot_relax =     2.00),
    note = "SAND86"
       )

species(name = "CH3CHO",
    atoms = " C:2  H:4  O:1 ",
    thermo = (
       NASA( [  200.00,  1000.00], [  4.729459500E+00,  -3.193285800E-03,
                4.753492100E-05,  -5.745861100E-08,   2.193111200E-11,
               -2.157287800E+04,   4.103015900E+00] ),
       NASA( [ 1000.00,  6000.00], [  5.404110800E+00,   1.172305900E-02,
               -4.226313700E-06,   6.837245100E-10,  -4.098486300E-14,
               -2.259312200E+04,  -3.480791700E+00] )
             ),
    transport = gas_transport(
                    geom = "nonlinear",
                    diam =     3.97,
                    well_depth =   436.00,
                    rot_relax =     2.00),
    note = "L 8/88"
       )



#-----------------------------------------------------------------------------
#  Reaction data
#-----------------------------------------------------------------------------

#  Reaction 1
three_body_reaction( "2 O + M <=> O2 + M",   [1.20000E+17, -1, 0],
         efficiencies = " AR:0.83  C2H6:3  CH4:2  CO:1.75  CO2:3.6  H2:2.4  H2O:15.4 ")

#  Reaction 2
three_body_reaction( "O + H + M <=> OH + M",   [5.00000E+17, -1, 0],
         efficiencies = " AR:0.7  C2H6:3  CH4:2  CO:1.5  CO2:2  H2:2  H2O:6 ")

#  Reaction 3
reaction( "O + H2 <=> H + OH",   [3.87000E+04, 2.7, 6260])

#  Reaction 4
reaction( "O + HO2 <=> OH + O2",   [2.00000E+13, 0, 0])

#  Reaction 5
reaction( "O + H2O2 <=> OH + HO2",   [9.63000E+06, 2, 4000])

#  Reaction 6
reaction( "O + CH <=> H + CO",   [5.70000E+13, 0, 0])

#  Reaction 7
reaction( "O + CH2 <=> H + HCO",   [8.00000E+13, 0, 0])

#  Reaction 8
reaction( "O + CH2(S) <=> H2 + CO",   [1.50000E+13, 0, 0])

#  Reaction 9
reaction( "O + CH2(S) <=> H + HCO",   [1.50000E+13, 0, 0])

#  Reaction 10
reaction( "O + CH3 <=> H + CH2O",   [5.06000E+13, 0, 0])

#  Reaction 11
reaction( "O + CH4 <=> OH + CH3",   [1.02000E+09, 1.5, 8600])

#  Reaction 12
falloff_reaction( "O + CO (+ M) <=> CO2 (+ M)",
         kf = [1.80000E+10, 0, 2385],
         kf0   = [6.02000E+14, 0, 3000],
         efficiencies = " AR:0.5  C2H6:3  CH4:2  CO:1.5  CO2:3.5  H2:2  H2O:6  O2:6 ")

#  Reaction 13
reaction( "O + HCO <=> OH + CO",   [3.00000E+13, 0, 0])
```

```
#  Reaction 14
reaction( "O + HCO <=> H + CO2",   [3.00000E+13, 0, 0])

#  Reaction 15
reaction( "O + CH2O <=> OH + HCO",   [3.90000E+13, 0, 3540])

#  Reaction 16
reaction( "O + CH2OH <=> OH + CH2O",   [1.00000E+13, 0, 0])

#  Reaction 17
reaction( "O + CH3O <=> OH + CH2O",   [1.00000E+13, 0, 0])

#  Reaction 18
reaction( "O + CH3OH <=> OH + CH2OH",   [3.88000E+05, 2.5, 3100])

#  Reaction 19
reaction( "O + CH3OH <=> OH + CH3O",   [1.30000E+05, 2.5, 5000])

#  Reaction 20
reaction( "O + C2H <=> CH + CO",   [5.00000E+13, 0, 0])

#  Reaction 21
reaction( "O + C2H2 <=> H + HCCO",   [1.35000E+07, 2, 1900])

#  Reaction 22
reaction( "O + C2H2 <=> OH + C2H",   [4.60000E+19, -1.41, 28950])

#  Reaction 23
reaction( "O + C2H2 <=> CO + CH2",   [6.94000E+06, 2, 1900])

#  Reaction 24
reaction( "O + C2H3 <=> H + CH2CO",   [3.00000E+13, 0, 0])

#  Reaction 25
reaction( "O + C2H4 <=> CH3 + HCO",   [1.25000E+07, 1.83, 220])

#  Reaction 26
reaction( "O + C2H5 <=> CH3 + CH2O",   [2.24000E+13, 0, 0])

#  Reaction 27
reaction( "O + C2H6 <=> OH + C2H5",   [8.98000E+07, 1.92, 5690])

#  Reaction 28
reaction( "O + HCCO <=> H + 2 CO",   [1.00000E+14, 0, 0])

#  Reaction 29
reaction( "O + CH2CO <=> OH + HCCO",   [1.00000E+13, 0, 8000])

#  Reaction 30
reaction( "O + CH2CO <=> CH2 + CO2",   [1.75000E+12, 0, 1350])

#  Reaction 31
reaction( "O2 + CO <=> O + CO2",   [2.50000E+12, 0, 47800])

#  Reaction 32
reaction( "O2 + CH2O <=> HO2 + HCO",   [1.00000E+14, 0, 40000])

#  Reaction 33
three_body_reaction( "H + O2 + M <=> HO2 + M",   [2.80000E+18, -0.86, 0],
         efficiencies = " AR:0  C2H6:1.5  CO:0.75  CO2:1.5  H2O:0  N2:0  O2:0 ")

#  Reaction 34
reaction( "H + 2 O2 <=> HO2 + O2",   [2.08000E+19, -1.24, 0])

#  Reaction 35
reaction( "H + O2 + H2O <=> HO2 + H2O",   [1.12600E+19, -0.76, 0])

#  Reaction 36
reaction( "H + O2 + N2 <=> HO2 + N2",   [2.60000E+19, -1.24, 0])
```

```
#  Reaction 37
reaction( "H + O2 + AR <=> HO2 + AR",   [7.00000E+17, -0.8, 0])

#  Reaction 38
reaction( "H + O2 <=> O + OH",   [2.65000E+16, -0.6707, 17041])

#  Reaction 39
three_body_reaction( "2 H + M <=> H2 + M",   [1.00000E+18, -1, 0],
        efficiencies = " AR:0.63  C2H6:3  CH4:2  CO2:0  H2:0  H2O:0 ")

#  Reaction 40
reaction( "2 H + H2 <=> 2 H2",   [9.00000E+16, -0.6, 0])

#  Reaction 41
reaction( "2 H + H2O <=> H2 + H2O",   [6.00000E+19, -1.25, 0])

#  Reaction 42
reaction( "2 H + CO2 <=> H2 + CO2",   [5.50000E+20, -2, 0])

#  Reaction 43
three_body_reaction( "H + OH + M <=> H2O + M",   [2.20000E+22, -2, 0],
        efficiencies = " AR:0.38  C2H6:3  CH4:2  H2:0.73  H2O:3.65 ")

#  Reaction 44
reaction( "H + HO2 <=> O + H2O",   [3.97000E+12, 0, 671])

#  Reaction 45
reaction( "H + HO2 <=> O2 + H2",   [4.48000E+13, 0, 1068])

#  Reaction 46
reaction( "H + HO2 <=> 2 OH",   [8.40000E+13, 0, 635])

#  Reaction 47
reaction( "H + H2O2 <=> HO2 + H2",   [1.21000E+07, 2, 5200])

#  Reaction 48
reaction( "H + H2O2 <=> OH + H2O",   [1.00000E+13, 0, 3600])

#  Reaction 49
reaction( "H + CH <=> C + H2",   [1.65000E+14, 0, 0])

#  Reaction 50
falloff_reaction( "H + CH2 (+ M) <=> CH3 (+ M)",
        kf = [6.00000E+14, 0, 0],
        kf0   = [1.04000E+26, -2.76, 1600],
        falloff = Troe(A = 0.562, T3 = 91, T1 = 5836, T2 = 8552),
        efficiencies = " AR:0.7  C2H6:3  CH4:2  CO:1.5  CO2:2  H2:2  H2O:6 ")

#  Reaction 51
reaction( "H + CH2(S) <=> CH + H2",   [3.00000E+13, 0, 0])

#  Reaction 52
falloff_reaction( "H + CH3 (+ M) <=> CH4 (+ M)",
        kf = [1.39000E+16, -0.534, 536],
        kf0   = [2.62000E+33, -4.76, 2440],
        falloff = Troe(A = 0.783, T3 = 74, T1 = 2941, T2 = 6964),
        efficiencies = " AR:0.7  C2H6:3  CH4:3  CO:1.5  CO2:2  H2:2  H2O:6 ")

#  Reaction 53
reaction( "H + CH4 <=> CH3 + H2",   [6.60000E+08, 1.62, 10840])

#  Reaction 54
falloff_reaction( "H + HCO (+ M) <=> CH2O (+ M)",
        kf = [1.09000E+12, 0.48, -260],
        kf0   = [2.47000E+24, -2.57, 425],
        falloff = Troe(A = 0.7824, T3 = 271, T1 = 2755, T2 = 6570),
        efficiencies = " AR:0.7  C2H6:3  CH4:2  CO:1.5  CO2:2  H2:2  H2O:6 ")

#  Reaction 55
reaction( "H + HCO <=> H2 + CO",   [7.34000E+13, 0, 0])
```

```
#  Reaction 56
falloff_reaction( "H + CH2O (+ M) <=> CH2OH (+ M)",
         kf = [5.40000E+11, 0.454, 3600],
         kf0   = [1.27000E+32, -4.82, 6530],
         falloff = Troe(A = 0.7187, T3 = 103, T1 = 1291, T2 = 4160),
         efficiencies = " C2H6:3  CH4:2  CO:1.5  CO2:2  H2:2  H2O:6 ")

#  Reaction 57
falloff_reaction( "H + CH2O (+ M) <=> CH3O (+ M)",
         kf = [5.40000E+11, 0.454, 2600],
         kf0   = [2.20000E+30, -4.8, 5560],
         falloff = Troe(A = 0.758, T3 = 94, T1 = 1555, T2 = 4200),
         efficiencies = " C2H6:3  CH4:2  CO:1.5  CO2:2  H2:2  H2O:6 ")

#  Reaction 58
reaction( "H + CH2O <=> HCO + H2",   [5.74000E+07, 1.9, 2742])

#  Reaction 59
falloff_reaction( "H + CH2OH (+ M) <=> CH3OH (+ M)",
         kf = [1.05500E+12, 0.5, 86],
         kf0   = [4.36000E+31, -4.65, 5080],
         falloff = Troe(A = 0.6, T3 = 100, T1 = 90000, T2 = 10000),
         efficiencies = " C2H6:3  CH4:2  CO:1.5  CO2:2  H2:2  H2O:6 ")

#  Reaction 60
reaction( "H + CH2OH <=> H2 + CH2O",   [2.00000E+13, 0, 0])

#  Reaction 61
reaction( "H + CH2OH <=> OH + CH3",   [1.65000E+11, 0.65, -284])

#  Reaction 62
reaction( "H + CH2OH <=> CH2(S) + H2O",   [3.28000E+13, -0.09, 610])

#  Reaction 63
falloff_reaction( "H + CH3O (+ M) <=> CH3OH (+ M)",
         kf = [2.43000E+12, 0.515, 50],
         kf0   = [4.66000E+41, -7.44, 14080],
         falloff = Troe(A = 0.7, T3 = 100, T1 = 90000, T2 = 10000),
         efficiencies = " C2H6:3  CH4:2  CO:1.5  CO2:2  H2:2  H2O:6 ")

#  Reaction 64
reaction( "H + CH3O <=> H + CH2OH",   [4.15000E+07, 1.63, 1924])

#  Reaction 65
reaction( "H + CH3O <=> H2 + CH2O",   [2.00000E+13, 0, 0])

#  Reaction 66
reaction( "H + CH3O <=> OH + CH3",   [1.50000E+12, 0.5, -110])

#  Reaction 67
reaction( "H + CH3O <=> CH2(S) + H2O",   [2.62000E+14, -0.23, 1070])

#  Reaction 68
reaction( "H + CH3OH <=> CH2OH + H2",   [1.70000E+07, 2.1, 4870])

#  Reaction 69
reaction( "H + CH3OH <=> CH3O + H2",   [4.20000E+06, 2.1, 4870])

#  Reaction 70
falloff_reaction( "H + C2H (+ M) <=> C2H2 (+ M)",
         kf = [1.00000E+17, -1, 0],
         kf0   = [3.75000E+33, -4.8, 1900],
         falloff = Troe(A = 0.6464, T3 = 132, T1 = 1315, T2 = 5566),
         efficiencies = " AR:0.7  C2H6:3  CH4:2  CO:1.5  CO2:2  H2:2  H2O:6 ")

#  Reaction 71
falloff_reaction( "H + C2H2 (+ M) <=> C2H3 (+ M)",
         kf = [5.60000E+12, 0, 2400],
         kf0   = [3.80000E+40, -7.27, 7220],
         falloff = Troe(A = 0.7507, T3 = 98.5, T1 = 1302, T2 = 4167),
         efficiencies = " AR:0.7  C2H6:3  CH4:2  CO:1.5  CO2:2  H2:2  H2O:6 ")
```

```
#  Reaction 72
falloff_reaction( "H + C2H3 (+ M) <=> C2H4 (+ M)",
         kf = [6.08000E+12, 0.27, 280],
         kf0   = [1.40000E+30, -3.86, 3320],
         falloff = Troe(A = 0.782, T3 = 207.5, T1 = 2663, T2 = 6095),
         efficiencies = " AR:0.7  C2H6:3  CH4:2  CO:1.5  CO2:2  H2:2  H2O:6 ")

#  Reaction 73
reaction( "H + C2H3 <=> H2 + C2H2",   [3.00000E+13, 0, 0])

#  Reaction 74
falloff_reaction( "H + C2H4 (+ M) <=> C2H5 (+ M)",
         kf = [5.40000E+11, 0.454, 1820],
         kf0   = [6.00000E+41, -7.62, 6970],
         falloff = Troe(A = 0.9753, T3 = 210, T1 = 984, T2 = 4374),
         efficiencies = " AR:0.7  C2H6:3  CH4:2  CO:1.5  CO2:2  H2:2  H2O:6 ")

#  Reaction 75
reaction( "H + C2H4 <=> C2H3 + H2",   [1.32500E+06, 2.53, 12240])

#  Reaction 76
falloff_reaction( "H + C2H5 (+ M) <=> C2H6 (+ M)",
         kf = [5.21000E+17, -0.99, 1580],
         kf0   = [1.99000E+41, -7.08, 6685],
         falloff = Troe(A = 0.8422, T3 = 125, T1 = 2219, T2 = 6882),
         efficiencies = " AR:0.7  C2H6:3  CH4:2  CO:1.5  CO2:2  H2:2  H2O:6 ")

#  Reaction 77
reaction( "H + C2H5 <=> H2 + C2H4",   [2.00000E+12, 0, 0])

#  Reaction 78
reaction( "H + C2H6 <=> C2H5 + H2",   [1.15000E+08, 1.9, 7530])

#  Reaction 79
reaction( "H + HCCO <=> CH2(S) + CO",   [1.00000E+14, 0, 0])

#  Reaction 80
reaction( "H + CH2CO <=> HCCO + H2",   [5.00000E+13, 0, 8000])

#  Reaction 81
reaction( "H + CH2CO <=> CH3 + CO",   [1.13000E+13, 0, 3428])

#  Reaction 82
reaction( "H + HCCOH <=> H + CH2CO",   [1.00000E+13, 0, 0])

#  Reaction 83
falloff_reaction( "H2 + CO (+ M) <=> CH2O (+ M)",
         kf = [4.30000E+07, 1.5, 79600],
         kf0   = [5.07000E+27, -3.42, 84350],
         falloff = Troe(A = 0.932, T3 = 197, T1 = 1540, T2 = 10300),
         efficiencies = " AR:0.7  C2H6:3  CH4:2  CO:1.5  CO2:2  H2:2  H2O:6 ")

#  Reaction 84
reaction( "OH + H2 <=> H + H2O",   [2.16000E+08, 1.51, 3430])

#  Reaction 85
falloff_reaction( "2 OH (+ M) <=> H2O2 (+ M)",
         kf = [7.40000E+13, -0.37, 0],
         kf0   = [2.30000E+18, -0.9, -1700],
         falloff = Troe(A = 0.7346, T3 = 94, T1 = 1756, T2 = 5182),
         efficiencies = " AR:0.7  C2H6:3  CH4:2  CO:1.5  CO2:2  H2:2  H2O:6 ")

#  Reaction 86
reaction( "2 OH <=> O + H2O",   [3.57000E+04, 2.4, -2110])

#  Reaction 87
reaction( "OH + HO2 <=> O2 + H2O",   [1.45000E+13, 0, -500],
         options = 'duplicate')

#  Reaction 88
```

```
reaction( "OH + H2O2 <=> HO2 + H2O",   [2.00000E+12, 0, 427],
         options = 'duplicate')

#  Reaction 89
reaction( "OH + H2O2 <=> HO2 + H2O",   [1.70000E+18, 0, 29410],
         options = 'duplicate')

#  Reaction 90
reaction( "OH + C <=> H + CO",   [5.00000E+13, 0, 0])

#  Reaction 91
reaction( "OH + CH <=> H + HCO",   [3.00000E+13, 0, 0])

#  Reaction 92
reaction( "OH + CH2 <=> H + CH2O",   [2.00000E+13, 0, 0])

#  Reaction 93
reaction( "OH + CH2 <=> CH + H2O",   [1.13000E+07, 2, 3000])

#  Reaction 94
reaction( "OH + CH2(S) <=> H + CH2O",   [3.00000E+13, 0, 0])

#  Reaction 95
falloff_reaction( "OH + CH3 (+ M) <=> CH3OH (+ M)",
         kf = [2.79000E+18, -1.43, 1330],
         kf0   = [4.00000E+36, -5.92, 3140],
         falloff = Troe(A = 0.412, T3 = 195, T1 = 5900, T2 = 6394),
         efficiencies = " C2H6:3  CH4:2  CO:1.5  CO2:2  H2:2  H2O:6 ")

#  Reaction 96
reaction( "OH + CH3 <=> CH2 + H2O",   [5.60000E+07, 1.6, 5420])

#  Reaction 97
reaction( "OH + CH3 <=> CH2(S) + H2O",   [6.44000E+17, -1.34, 1417])

#  Reaction 98
reaction( "OH + CH4 <=> CH3 + H2O",   [1.00000E+08, 1.6, 3120])

#  Reaction 99
reaction( "OH + CO <=> H + CO2",   [4.76000E+07, 1.228, 70])

#  Reaction 100
reaction( "OH + HCO <=> H2O + CO",   [5.00000E+13, 0, 0])

#  Reaction 101
reaction( "OH + CH2O <=> HCO + H2O",   [3.43000E+09, 1.18, -447])

#  Reaction 102
reaction( "OH + CH2OH <=> H2O + CH2O",   [5.00000E+12, 0, 0])

#  Reaction 103
reaction( "OH + CH3O <=> H2O + CH2O",   [5.00000E+12, 0, 0])

#  Reaction 104
reaction( "OH + CH3OH <=> CH2OH + H2O",   [1.44000E+06, 2, -840])

#  Reaction 105
reaction( "OH + CH3OH <=> CH3O + H2O",   [6.30000E+06, 2, 1500])

#  Reaction 106
reaction( "OH + C2H <=> H + HCCO",   [2.00000E+13, 0, 0])

#  Reaction 107
reaction( "OH + C2H2 <=> H + CH2CO",   [2.18000E-04, 4.5, -1000])

#  Reaction 108
reaction( "OH + C2H2 <=> H + HCCOH",   [5.04000E+05, 2.3, 13500])

#  Reaction 109
reaction( "OH + C2H2 <=> C2H + H2O",   [3.37000E+07, 2, 14000])
```

```
#  Reaction 110
reaction( "OH + C2H2 <=> CH3 + CO",   [4.83000E-04, 4, -2000])

#  Reaction 111
reaction( "OH + C2H3 <=> H2O + C2H2",   [5.00000E+12, 0, 0])

#  Reaction 112
reaction( "OH + C2H4 <=> C2H3 + H2O",   [3.60000E+06, 2, 2500])

#  Reaction 113
reaction( "OH + C2H6 <=> C2H5 + H2O",   [3.54000E+06, 2.12, 870])

#  Reaction 114
reaction( "OH + CH2CO <=> HCCO + H2O",   [7.50000E+12, 0, 2000])

#  Reaction 115
reaction( "2 HO2 <=> O2 + H2O2",   [1.30000E+11, 0, -1630],
         options = 'duplicate')

#  Reaction 116
reaction( "2 HO2 <=> O2 + H2O2",   [4.20000E+14, 0, 12000],
         options = 'duplicate')

#  Reaction 117
reaction( "HO2 + CH2 <=> OH + CH2O",   [2.00000E+13, 0, 0])

#  Reaction 118
reaction( "HO2 + CH3 <=> O2 + CH4",   [1.00000E+12, 0, 0])

#  Reaction 119
reaction( "HO2 + CH3 <=> OH + CH3O",   [3.78000E+13, 0, 0])

#  Reaction 120
reaction( "HO2 + CO <=> OH + CO2",   [1.50000E+14, 0, 23600])

#  Reaction 121
reaction( "HO2 + CH2O <=> HCO + H2O2",   [5.60000E+06, 2, 12000])

#  Reaction 122
reaction( "C + O2 <=> O + CO",   [5.80000E+13, 0, 576])

#  Reaction 123
reaction( "C + CH2 <=> H + C2H",   [5.00000E+13, 0, 0])

#  Reaction 124
reaction( "C + CH3 <=> H + C2H2",   [5.00000E+13, 0, 0])

#  Reaction 125
reaction( "CH + O2 <=> O + HCO",   [6.71000E+13, 0, 0])

#  Reaction 126
reaction( "CH + H2 <=> H + CH2",   [1.08000E+14, 0, 3110])

#  Reaction 127
reaction( "CH + H2O <=> H + CH2O",   [5.71000E+12, 0, -755])

#  Reaction 128
reaction( "CH + CH2 <=> H + C2H2",   [4.00000E+13, 0, 0])

#  Reaction 129
reaction( "CH + CH3 <=> H + C2H3",   [3.00000E+13, 0, 0])

#  Reaction 130
reaction( "CH + CH4 <=> H + C2H4",   [6.00000E+13, 0, 0])

#  Reaction 131
falloff_reaction( "CH + CO (+ M) <=> HCCO (+ M)",
         kf = [5.00000E+13, 0, 0],
         kf0   = [2.69000E+28, -3.74, 1936],
         falloff = Troe(A = 0.5757, T3 = 237, T1 = 1652, T2 = 5069),
         efficiencies = " AR:0.7  C2H6:3  CH4:2  CO:1.5  CO2:2  H2:2  H2O:6 ")
```

```
#  Reaction 132
reaction( "CH + CO2 <=> HCO + CO",   [1.90000E+14, 0, 15792])

#  Reaction 133
reaction( "CH + CH2O <=> H + CH2CO",   [9.46000E+13, 0, -515])

#  Reaction 134
reaction( "CH + HCCO <=> CO + C2H2",   [5.00000E+13, 0, 0])

#  Reaction 135
reaction( "CH2 + O2 => OH + H + CO",   [5.00000E+12, 0, 1500])

#  Reaction 136
reaction( "CH2 + H2 <=> H + CH3",   [5.00000E+05, 2, 7230])

#  Reaction 137
reaction( "2 CH2 <=> H2 + C2H2",   [1.60000E+15, 0, 11944])

#  Reaction 138
reaction( "CH2 + CH3 <=> H + C2H4",   [4.00000E+13, 0, 0])

#  Reaction 139
reaction( "CH2 + CH4 <=> 2 CH3",   [2.46000E+06, 2, 8270])

#  Reaction 140
falloff_reaction( "CH2 + CO (+ M) <=> CH2CO (+ M)",
         kf = [8.10000E+11, 0.5, 4510],
         kf0   = [2.69000E+33, -5.11, 7095],
         falloff = Troe(A = 0.5907, T3 = 275, T1 = 1226, T2 = 5185),
         efficiencies = " AR:0.7  C2H6:3  CH4:2  CO:1.5  CO2:2  H2:2  H2O:6 ")

#  Reaction 141
reaction( "CH2 + HCCO <=> C2H3 + CO",   [3.00000E+13, 0, 0])

#  Reaction 142
reaction( "CH2(S) + N2 <=> CH2 + N2",   [1.50000E+13, 0, 600])

#  Reaction 143
reaction( "CH2(S) + AR <=> CH2 + AR",   [9.00000E+12, 0, 600])

#  Reaction 144
reaction( "CH2(S) + O2 <=> H + OH + CO",   [2.80000E+13, 0, 0])

#  Reaction 145
reaction( "CH2(S) + O2 <=> CO + H2O",   [1.20000E+13, 0, 0])

#  Reaction 146
reaction( "CH2(S) + H2 <=> CH3 + H",   [7.00000E+13, 0, 0])

#  Reaction 147
falloff_reaction( "CH2(S) + H2O (+ M) <=> CH3OH (+ M)",
         kf = [4.82000E+17, -1.16, 1145],
         kf0   = [1.88000E+38, -6.36, 5040],
         falloff = Troe(A = 0.6027, T3 = 208, T1 = 3922, T2 = 10180),
         efficiencies = " C2H6:3  CH4:2  CO:1.5  CO2:2  H2:2  H2O:6 ")

#  Reaction 148
reaction( "CH2(S) + H2O <=> CH2 + H2O",   [3.00000E+13, 0, 0])

#  Reaction 149
reaction( "CH2(S) + CH3 <=> H + C2H4",   [1.20000E+13, 0, -570])

#  Reaction 150
reaction( "CH2(S) + CH4 <=> 2 CH3",   [1.60000E+13, 0, -570])

#  Reaction 151
reaction( "CH2(S) + CO <=> CH2 + CO",   [9.00000E+12, 0, 0])

#  Reaction 152
reaction( "CH2(S) + CO2 <=> CH2 + CO2",   [7.00000E+12, 0, 0])
```

```
#  Reaction 153
reaction( "CH2(S) + CO2 <=> CO + CH2O",   [1.40000E+13, 0, 0])

#  Reaction 154
reaction( "CH2(S) + C2H6 <=> CH3 + C2H5",   [4.00000E+13, 0, -550])

#  Reaction 155
reaction( "CH3 + O2 <=> O + CH3O",   [3.56000E+13, 0, 30480])

#  Reaction 156
reaction( "CH3 + O2 <=> OH + CH2O",   [2.31000E+12, 0, 20315])

#  Reaction 157
reaction( "CH3 + H2O2 <=> HO2 + CH4",   [2.45000E+04, 2.47, 5180])

#  Reaction 158
falloff_reaction( "2 CH3 (+ M) <=> C2H6 (+ M)",
         kf = [6.77000E+16, -1.18, 654],
         kf0   = [3.40000E+41, -7.03, 2762],
         falloff = Troe(A = 0.619, T3 = 73.2, T1 = 1180, T2 = 9999),
         efficiencies = " AR:0.7  C2H6:3  CH4:2  CO:1.5  CO2:2  H2:2  H2O:6 ")

#  Reaction 159
reaction( "2 CH3 <=> H + C2H5",   [6.84000E+12, 0.1, 10600])

#  Reaction 160
reaction( "CH3 + HCO <=> CH4 + CO",   [2.64800E+13, 0, 0])

#  Reaction 161
reaction( "CH3 + CH2O <=> HCO + CH4",   [3.32000E+03, 2.81, 5860])

#  Reaction 162
reaction( "CH3 + CH3OH <=> CH2OH + CH4",   [3.00000E+07, 1.5, 9940])

#  Reaction 163
reaction( "CH3 + CH3OH <=> CH3O + CH4",   [1.00000E+07, 1.5, 9940])

#  Reaction 164
reaction( "CH3 + C2H4 <=> C2H3 + CH4",   [2.27000E+05, 2, 9200])

#  Reaction 165
reaction( "CH3 + C2H6 <=> C2H5 + CH4",   [6.14000E+06, 1.74, 10450])

#  Reaction 166
reaction( "HCO + H2O <=> H + CO + H2O",   [1.50000E+18, -1, 17000])

#  Reaction 167
three_body_reaction( "HCO + M <=> H + CO + M",   [1.87000E+17, -1, 17000],
         efficiencies = " C2H6:3  CH4:2  CO:1.5  CO2:2  H2:2  H2O:0 ")

#  Reaction 168
reaction( "HCO + O2 <=> HO2 + CO",   [1.34500E+13, 0, 400])

#  Reaction 169
reaction( "CH2OH + O2 <=> HO2 + CH2O",   [1.80000E+13, 0, 900])

#  Reaction 170
reaction( "CH3O + O2 <=> HO2 + CH2O",   [4.28000E-13, 7.6, -3530])

#  Reaction 171
reaction( "C2H + O2 <=> HCO + CO",   [1.00000E+13, 0, -755])

#  Reaction 172
reaction( "C2H + H2 <=> H + C2H2",   [5.68000E+10, 0.9, 1993])

#  Reaction 173
reaction( "C2H3 + O2 <=> HCO + CH2O",   [4.58000E+16, -1.39, 1015])

#  Reaction 174
falloff_reaction( "C2H4 (+ M) <=> H2 + C2H2 (+ M)",
```

```
        kf = [8.00000E+12, 0.44, 86770],
        kf0   = [1.58000E+51, -9.3, 97800],
        falloff = Troe(A = 0.7345, T3 = 180, T1 = 1035, T2 = 5417),
        efficiencies = " AR:0.7  C2H6:3  CH4:2  CO:1.5  CO2:2  H2:2  H2O:6 ")

#  Reaction 175
reaction( "C2H5 + O2 <=> HO2 + C2H4",   [8.40000E+11, 0, 3875])

#  Reaction 176
reaction( "HCCO + O2 <=> OH + 2 CO",   [3.20000E+12, 0, 854])

#  Reaction 177
reaction( "2 HCCO <=> 2 CO + C2H2",   [1.00000E+13, 0, 0])

#  Reaction 178
reaction( "N + NO <=> N2 + O",   [2.70000E+13, 0, 355])

#  Reaction 179
reaction( "N + O2 <=> NO + O",   [9.00000E+09, 1, 6500])

#  Reaction 180
reaction( "N + OH <=> NO + H",   [3.36000E+13, 0, 385])

#  Reaction 181
reaction( "N2O + O <=> N2 + O2",   [1.40000E+12, 0, 10810])

#  Reaction 182
reaction( "N2O + O <=> 2 NO",   [2.90000E+13, 0, 23150])

#  Reaction 183
reaction( "N2O + H <=> N2 + OH",   [3.87000E+14, 0, 18880])

#  Reaction 184
reaction( "N2O + OH <=> N2 + HO2",   [2.00000E+12, 0, 21060])

#  Reaction 185
falloff_reaction( "N2O (+ M) <=> N2 + O (+ M)",
        kf = [7.91000E+10, 0, 56020],
        kf0   = [6.37000E+14, 0, 56640],
        efficiencies = " AR:0.625  C2H6:3  CH4:2  CO:1.5  CO2:2  H2:2  H2O:6 ")

#  Reaction 186
reaction( "HO2 + NO <=> NO2 + OH",   [2.11000E+12, 0, -480])

#  Reaction 187
three_body_reaction( "NO + O + M <=> NO2 + M",   [1.06000E+20, -1.41, 0],
        efficiencies = " AR:0.7  C2H6:3  CH4:2  CO:1.5  CO2:2  H2:2  H2O:6 ")

#  Reaction 188
reaction( "NO2 + O <=> NO + O2",   [3.90000E+12, 0, -240])

#  Reaction 189
reaction( "NO2 + H <=> NO + OH",   [1.32000E+14, 0, 360])

#  Reaction 190
reaction( "NH + O <=> NO + H",   [4.00000E+13, 0, 0])

#  Reaction 191
reaction( "NH + H <=> N + H2",   [3.20000E+13, 0, 330])

#  Reaction 192
reaction( "NH + OH <=> HNO + H",   [2.00000E+13, 0, 0])

#  Reaction 193
reaction( "NH + OH <=> N + H2O",   [2.00000E+09, 1.2, 0])

#  Reaction 194
reaction( "NH + O2 <=> HNO + O",   [4.61000E+05, 2, 6500])

#  Reaction 195
reaction( "NH + O2 <=> NO + OH",   [1.28000E+06, 1.5, 100])
```

```
#  Reaction 196
reaction( "NH + N <=> N2 + H",   [1.50000E+13, 0, 0])

#  Reaction 197
reaction( "NH + H2O <=> HNO + H2",   [2.00000E+13, 0, 13850])

#  Reaction 198
reaction( "NH + NO <=> N2 + OH",   [2.16000E+13, -0.23, 0])

#  Reaction 199
reaction( "NH + NO <=> N2O + H",   [3.65000E+14, -0.45, 0])

#  Reaction 200
reaction( "NH2 + O <=> OH + NH",   [3.00000E+12, 0, 0])

#  Reaction 201
reaction( "NH2 + O <=> H + HNO",   [3.90000E+13, 0, 0])

#  Reaction 202
reaction( "NH2 + H <=> NH + H2",   [4.00000E+13, 0, 3650])

#  Reaction 203
reaction( "NH2 + OH <=> NH + H2O",   [9.00000E+07, 1.5, -460])

#  Reaction 204
reaction( "NNH <=> N2 + H",   [3.30000E+08, 0, 0])

#  Reaction 205
three_body_reaction( "NNH + M <=> N2 + H + M",   [1.30000E+14, -0.11, 4980],
         efficiencies = " AR:0.7  C2H6:3  CH4:2  CO:1.5  CO2:2  H2:2  H2O:6 ")

#  Reaction 206
reaction( "NNH + O2 <=> HO2 + N2",   [5.00000E+12, 0, 0])

#  Reaction 207
reaction( "NNH + O <=> OH + N2",   [2.50000E+13, 0, 0])

#  Reaction 208
reaction( "NNH + O <=> NH + NO",   [7.00000E+13, 0, 0])

#  Reaction 209
reaction( "NNH + H <=> H2 + N2",   [5.00000E+13, 0, 0])

#  Reaction 210
reaction( "NNH + OH <=> H2O + N2",   [2.00000E+13, 0, 0])

#  Reaction 211
reaction( "NNH + CH3 <=> CH4 + N2",   [2.50000E+13, 0, 0])

#  Reaction 212
three_body_reaction( "H + NO + M <=> HNO + M",   [4.48000E+19, -1.32, 740],
         efficiencies = " AR:0.7  C2H6:3  CH4:2  CO:1.5  CO2:2  H2:2  H2O:6 ")

#  Reaction 213
reaction( "HNO + O <=> NO + OH",   [2.50000E+13, 0, 0])

#  Reaction 214
reaction( "HNO + H <=> H2 + NO",   [9.00000E+11, 0.72, 660])

#  Reaction 215
reaction( "HNO + OH <=> NO + H2O",   [1.30000E+07, 1.9, -950])

#  Reaction 216
reaction( "HNO + O2 <=> HO2 + NO",   [1.00000E+13, 0, 13000])

#  Reaction 217
reaction( "CN + O <=> CO + N",   [7.70000E+13, 0, 0])

#  Reaction 218
reaction( "CN + OH <=> NCO + H",   [4.00000E+13, 0, 0])
```

```
#  Reaction 219
reaction( "CN + H2O <=> HCN + OH",   [8.00000E+12, 0, 7460])

#  Reaction 220
reaction( "CN + O2 <=> NCO + O",   [6.14000E+12, 0, -440])

#  Reaction 221
reaction( "CN + H2 <=> HCN + H",   [2.95000E+05, 2.45, 2240])

#  Reaction 222
reaction( "NCO + O <=> NO + CO",   [2.35000E+13, 0, 0])

#  Reaction 223
reaction( "NCO + H <=> NH + CO",   [5.40000E+13, 0, 0])

#  Reaction 224
reaction( "NCO + OH <=> NO + H + CO",   [2.50000E+12, 0, 0])

#  Reaction 225
reaction( "NCO + N <=> N2 + CO",   [2.00000E+13, 0, 0])

#  Reaction 226
reaction( "NCO + O2 <=> NO + CO2",   [2.00000E+12, 0, 20000])

#  Reaction 227
three_body_reaction( "NCO + M <=> N + CO + M",   [3.10000E+14, 0, 54050],
         efficiencies = " AR:0.7  C2H6:3  CH4:2  CO:1.5  CO2:2  H2:2  H2O:6 ")

#  Reaction 228
reaction( "NCO + NO <=> N2O + CO",   [1.90000E+17, -1.52, 740])

#  Reaction 229
reaction( "NCO + NO <=> N2 + CO2",   [3.80000E+18, -2, 800])

#  Reaction 230
three_body_reaction( "HCN + M <=> H + CN + M",   [1.04000E+29, -3.3, 126600],
         efficiencies = " AR:0.7  C2H6:3  CH4:2  CO:1.5  CO2:2  H2:2  H2O:6 ")

#  Reaction 231
reaction( "HCN + O <=> NCO + H",   [2.03000E+04, 2.64, 4980])

#  Reaction 232
reaction( "HCN + O <=> NH + CO",   [5.07000E+03, 2.64, 4980])

#  Reaction 233
reaction( "HCN + O <=> CN + OH",   [3.91000E+09, 1.58, 26600])

#  Reaction 234
reaction( "HCN + OH <=> HOCN + H",   [1.10000E+06, 2.03, 13370])

#  Reaction 235
reaction( "HCN + OH <=> HNCO + H",   [4.40000E+03, 2.26, 6400])

#  Reaction 236
reaction( "HCN + OH <=> NH2 + CO",   [1.60000E+02, 2.56, 9000])

#  Reaction 237
falloff_reaction( "H + HCN (+ M) <=> H2CN (+ M)",
         kf = [3.30000E+13, 0, 0],
         kf0   = [1.40000E+26, -3.4, 1900],
         efficiencies = " AR:0.7  C2H6:3  CH4:2  CO:1.5  CO2:2  H2:2  H2O:6 ")

#  Reaction 238
reaction( "H2CN + N <=> N2 + CH2",   [6.00000E+13, 0, 400])

#  Reaction 239
reaction( "C + N2 <=> CN + N",   [6.30000E+13, 0, 46020])

#  Reaction 240
reaction( "CH + N2 <=> HCN + N",   [3.12000E+09, 0.88, 20130])
```

```
#  Reaction 241
falloff_reaction( "CH + N2 (+ M) <=> HCNN (+ M)",
         kf = [3.10000E+12, 0.15, 0],
         kf0   = [1.30000E+25, -3.16, 740],
         falloff = Troe(A = 0.667, T3 = 235, T1 = 2117, T2 = 4536),
         efficiencies = " AR:1  C2H6:3  CH4:2  CO:1.5  CO2:2  H2:2  H2O:6 ")

#  Reaction 242
reaction( "CH2 + N2 <=> HCN + NH",   [1.00000E+13, 0, 74000])

#  Reaction 243
reaction( "CH2(S) + N2 <=> NH + HCN",   [1.00000E+11, 0, 65000])

#  Reaction 244
reaction( "C + NO <=> CN + O",   [1.90000E+13, 0, 0])

#  Reaction 245
reaction( "C + NO <=> CO + N",   [2.90000E+13, 0, 0])

#  Reaction 246
reaction( "CH + NO <=> HCN + O",   [4.10000E+13, 0, 0])

#  Reaction 247
reaction( "CH + NO <=> H + NCO",   [1.62000E+13, 0, 0])

#  Reaction 248
reaction( "CH + NO <=> N + HCO",   [2.46000E+13, 0, 0])

#  Reaction 249
reaction( "CH2 + NO <=> H + HNCO",   [3.10000E+17, -1.38, 1270])

#  Reaction 250
reaction( "CH2 + NO <=> OH + HCN",   [2.90000E+14, -0.69, 760])

#  Reaction 251
reaction( "CH2 + NO <=> H + HCNO",   [3.80000E+13, -0.36, 580])

#  Reaction 252
reaction( "CH2(S) + NO <=> H + HNCO",   [3.10000E+17, -1.38, 1270])

#  Reaction 253
reaction( "CH2(S) + NO <=> OH + HCN",   [2.90000E+14, -0.69, 760])

#  Reaction 254
reaction( "CH2(S) + NO <=> H + HCNO",   [3.80000E+13, -0.36, 580])

#  Reaction 255
reaction( "CH3 + NO <=> HCN + H2O",   [9.60000E+13, 0, 28800])

#  Reaction 256
reaction( "CH3 + NO <=> H2CN + OH",   [1.00000E+12, 0, 21750])

#  Reaction 257
reaction( "HCNN + O <=> CO + H + N2",   [2.20000E+13, 0, 0])

#  Reaction 258
reaction( "HCNN + O <=> HCN + NO",   [2.00000E+12, 0, 0])

#  Reaction 259
reaction( "HCNN + O2 <=> O + HCO + N2",   [1.20000E+13, 0, 0])

#  Reaction 260
reaction( "HCNN + OH <=> H + HCO + N2",   [1.20000E+13, 0, 0])

#  Reaction 261
reaction( "HCNN + H <=> CH2 + N2",   [1.00000E+14, 0, 0])

#  Reaction 262
reaction( "HNCO + O <=> NH + CO2",   [9.80000E+07, 1.41, 8500])
```

```
#  Reaction 263
reaction( "HNCO + O <=> HNO + CO",   [1.50000E+08, 1.57, 44000])

#  Reaction 264
reaction( "HNCO + O <=> NCO + OH",   [2.20000E+06, 2.11, 11400])

#  Reaction 265
reaction( "HNCO + H <=> NH2 + CO",   [2.25000E+07, 1.7, 3800])

#  Reaction 266
reaction( "HNCO + H <=> H2 + NCO",   [1.05000E+05, 2.5, 13300])

#  Reaction 267
reaction( "HNCO + OH <=> NCO + H2O",   [3.30000E+07, 1.5, 3600])

#  Reaction 268
reaction( "HNCO + OH <=> NH2 + CO2",   [3.30000E+06, 1.5, 3600])

#  Reaction 269
three_body_reaction( "HNCO + M <=> NH + CO + M",   [1.18000E+16, 0, 84720],
         efficiencies = " AR:0.7  C2H6:3  CH4:2  CO:1.5  CO2:2  H2:2  H2O:6 ")

#  Reaction 270
reaction( "HCNO + H <=> H + HNCO",   [2.10000E+15, -0.69, 2850])

#  Reaction 271
reaction( "HCNO + H <=> OH + HCN",   [2.70000E+11, 0.18, 2120])

#  Reaction 272
reaction( "HCNO + H <=> NH2 + CO",   [1.70000E+14, -0.75, 2890])

#  Reaction 273
reaction( "HOCN + H <=> H + HNCO",   [2.00000E+07, 2, 2000])

#  Reaction 274
reaction( "HCCO + NO <=> HCNO + CO",   [9.00000E+12, 0, 0])

#  Reaction 275
reaction( "CH3 + N <=> H2CN + H",   [6.10000E+14, -0.31, 290])

#  Reaction 276
reaction( "CH3 + N <=> HCN + H2",   [3.70000E+12, 0.15, -90])

#  Reaction 277
reaction( "NH3 + H <=> NH2 + H2",   [5.40000E+05, 2.4, 9915])

#  Reaction 278
reaction( "NH3 + OH <=> NH2 + H2O",   [5.00000E+07, 1.6, 955])

#  Reaction 279
reaction( "NH3 + O <=> NH2 + OH",   [9.40000E+06, 1.94, 6460])

#  Reaction 280
reaction( "NH + CO2 <=> HNO + CO",   [1.00000E+13, 0, 14350])

#  Reaction 281
reaction( "CN + NO2 <=> NCO + NO",   [6.16000E+15, -0.752, 345])

#  Reaction 282
reaction( "NCO + NO2 <=> N2O + CO2",   [3.25000E+12, 0, -705])

#  Reaction 283
reaction( "N + CO2 <=> NO + CO",   [3.00000E+12, 0, 11300])

#  Reaction 284
reaction( "O + CH3 => H + H2 + CO",   [3.37000E+13, 0, 0])

#  Reaction 285
reaction( "O + C2H4 <=> H + CH2CHO",   [6.70000E+06, 1.83, 220])

#  Reaction 286
```

```
reaction( "O + C2H5 <=> H + CH3CHO",   [1.09600E+14, 0, 0])

#  Reaction 287
reaction( "OH + HO2 <=> O2 + H2O",   [5.00000E+15, 0, 17330],
         options = 'duplicate')

#  Reaction 288
reaction( "OH + CH3 => H2 + CH2O",   [8.00000E+09, 0.5, -1755])

#  Reaction 289
falloff_reaction( "CH + H2 (+ M) <=> CH3 (+ M)",
         kf = [1.97000E+12, 0.43, -370],
         kf0   = [4.82000E+25, -2.8, 590],
         falloff = Troe(A = 0.578, T3 = 122, T1 = 2535, T2 = 9365),
         efficiencies = " AR:0.7  C2H6:3  CH4:2  CO:1.5  CO2:2  H2:2  H2O:6 ")

#  Reaction 290
reaction( "CH2 + O2 => 2 H + CO2",   [5.80000E+12, 0, 1500])

#  Reaction 291
reaction( "CH2 + O2 <=> O + CH2O",   [2.40000E+12, 0, 1500])

#  Reaction 292
reaction( "CH2 + CH2 => 2 H + C2H2",   [2.00000E+14, 0, 10989])

#  Reaction 293
reaction( "CH2(S) + H2O => H2 + CH2O",   [6.82000E+10, 0.25, -935])

#  Reaction 294
reaction( "C2H3 + O2 <=> O + CH2CHO",   [3.03000E+11, 0.29, 11])

#  Reaction 295
reaction( "C2H3 + O2 <=> HO2 + C2H2",   [1.33700E+06, 1.61, -384])

#  Reaction 296
reaction( "O + CH3CHO <=> OH + CH2CHO",   [5.84000E+12, 0, 1808])

#  Reaction 297
reaction( "O + CH3CHO => OH + CH3 + CO",   [5.84000E+12, 0, 1808])

#  Reaction 298
reaction( "O2 + CH3CHO => HO2 + CH3 + CO",   [3.01000E+13, 0, 39150])

#  Reaction 299
reaction( "H + CH3CHO <=> CH2CHO + H2",   [2.05000E+09, 1.16, 2405])

#  Reaction 300
reaction( "H + CH3CHO => CH3 + H2 + CO",   [2.05000E+09, 1.16, 2405])

#  Reaction 301
reaction( "OH + CH3CHO => CH3 + H2O + CO",   [2.34300E+10, 0.73, -1113])

#  Reaction 302
reaction( "HO2 + CH3CHO => CH3 + H2O2 + CO",   [3.01000E+12, 0, 11923])

#  Reaction 303
reaction( "CH3 + CH3CHO => CH3 + CH4 + CO",   [2.72000E+06, 1.77, 5920])

#  Reaction 304
falloff_reaction( "H + CH2CO (+ M) <=> CH2CHO (+ M)",
         kf = [4.86500E+11, 0.422, -1755],
         kf0   = [1.01200E+42, -7.63, 3854],
         falloff = Troe(A = 0.465, T3 = 201, T1 = 1773, T2 = 5333),
         efficiencies = " AR:0.7  C2H6:3  CH4:2  CO:1.5  CO2:2  H2:2  H2O:6 ")

#  Reaction 305
reaction( "O + CH2CHO => H + CH2 + CO2",   [1.50000E+14, 0, 0])

#  Reaction 306
reaction( "O2 + CH2CHO => OH + CO + CH2O",   [1.81000E+10, 0, 0])
```

```
#  Reaction 307
reaction( "O2 + CH2CHO => OH + 2 HCO",   [2.35000E+10, 0, 0])

#  Reaction 308
reaction( "H + CH2CHO <=> CH3 + HCO",   [2.20000E+13, 0, 0])

#  Reaction 309
reaction( "H + CH2CHO <=> CH2CO + H2",   [1.10000E+13, 0, 0])

#  Reaction 310
reaction( "OH + CH2CHO <=> H2O + CH2CO",   [1.20000E+13, 0, 0])

#  Reaction 311
reaction( "OH + CH2CHO <=> HCO + CH2OH",   [3.01000E+13, 0, 0])

#  Reaction 312
falloff_reaction( "CH3 + C2H5 (+ M) <=> C3H8 (+ M)",
         kf = [9.43000E+12, 0, 0],
         kf0   = [2.71000E+74, -16.82, 13065],
         falloff = Troe(A = 0.1527, T3 = 291, T1 = 2742, T2 = 7748),
         efficiencies = " AR:0.7  C2H6:3  CH4:2  CO:1.5  CO2:2  H2:2  H2O:6 ")

#  Reaction 313
reaction( "O + C3H8 <=> OH + C3H7",   [1.93000E+05, 2.68, 3716])

#  Reaction 314
reaction( "H + C3H8 <=> C3H7 + H2",   [1.32000E+06, 2.54, 6756])

#  Reaction 315
reaction( "OH + C3H8 <=> C3H7 + H2O",   [3.16000E+07, 1.8, 934])

#  Reaction 316
reaction( "C3H7 + H2O2 <=> HO2 + C3H8",   [3.78000E+02, 2.72, 1500])

#  Reaction 317
reaction( "CH3 + C3H8 <=> C3H7 + CH4",   [9.03000E-01, 3.65, 7154])

#  Reaction 318
falloff_reaction( "CH3 + C2H4 (+ M) <=> C3H7 (+ M)",
         kf = [2.55000E+06, 1.6, 5700],
         kf0   = [3.00000E+63, -14.6, 18170],
         falloff = Troe(A = 0.1894, T3 = 277, T1 = 8748, T2 = 7891),
         efficiencies = " AR:0.7  C2H6:3  CH4:2  CO:1.5  CO2:2  H2:2  H2O:6 ")

#  Reaction 319
reaction( "O + C3H7 <=> C2H5 + CH2O",   [9.64000E+13, 0, 0])

#  Reaction 320
falloff_reaction( "H + C3H7 (+ M) <=> C3H8 (+ M)",
         kf = [3.61300E+13, 0, 0],
         kf0   = [4.42000E+61, -13.545, 11357],
         falloff = Troe(A = 0.315, T3 = 369, T1 = 3285, T2 = 6667),
         efficiencies = " AR:0.7  C2H6:3  CH4:2  CO:1.5  CO2:2  H2:2  H2O:6 ")

#  Reaction 321
reaction( "H + C3H7 <=> CH3 + C2H5",   [4.06000E+06, 2.19, 890])

#  Reaction 322
reaction( "OH + C3H7 <=> C2H5 + CH2OH",   [2.41000E+13, 0, 0])

#  Reaction 323
reaction( "HO2 + C3H7 <=> O2 + C3H8",   [2.55000E+10, 0.255, -943])

#  Reaction 324
reaction( "HO2 + C3H7 => OH + C2H5 + CH2O",   [2.41000E+13, 0, 0])

#  Reaction 325
reaction( "CH3 + C3H7 <=> 2 C2H5",   [1.92700E+13, -0.32, 0])
```

GRI-Mech 3.0 + B96 Mechanism – Filename: gri30_b96.cti

The GRI-Mech 3.0 mechanism was used as the basis for the GRI3.0+B96 mechanism and thus the mechanism files have mostly the same content. Only the changes made to the GRI-Mech 3.0 file (shown above) are shown for this mechanism.

Different file header and N_2H_2 added to species lists:

```
# Generated from file gri30.inp
# by ck2cti on Mon Aug 25 09:52:57 2003
# Bowman 1996 reactions added Aug 2007 by Andrew Mackrory
# and one set of duplicate reactions from B96 combined into one to avoid
# a negative pre-exponential factor. Source for Bowman (1997) reactions was
# the PhD dissertation of Hongjie Xu, BYU 1999, Provo, UT, USA.
# Transport data from file ../transport/gri30_tran.dat.

units(length = "cm", time = "s", quantity = "mol", act_energy = "cal/mol")


ideal_gas(name = "gri30_b96",
      elements = " O  H  C  N  Ar ",
      species = """ H2  H  O  O2  OH  H2O  HO2  H2O2  C  CH
                    CH2  CH2(S)  CH3  CH4  CO  CO2  HCO  CH2O  CH2OH  CH3O
                    CH3OH  C2H  C2H2  C2H3  C2H4  C2H5  C2H6  HCCO  CH2CO  HCCOH
                    N  NH  NH2  NH3  NNH  NO  NO2  N2O  HNO  CN
                    HCN  H2CN  HCNN  HCNO  HOCN  HNCO  NCO  N2  AR  C3H7
                    C3H8  CH2CHO  CH3CHO N2H2 """,
      reactions = "all",
      initial_state = state(temperature = 300.0,
                            pressure = OneAtm)    )

ideal_gas(name = "gri30_b96_mix",
      elements = " O  H  C  N  Ar ",
      species = """ H2  H  O  O2  OH  H2O  HO2  H2O2  C  CH
                    CH2  CH2(S)  CH3  CH4  CO  CO2  HCO  CH2O  CH2OH  CH3O
                    CH3OH  C2H  C2H2  C2H3  C2H4  C2H5  C2H6  HCCO  CH2CO  HCCOH
                    N  NH  NH2  NH3  NNH  NO  NO2  N2O  HNO  CN
                    HCN  H2CN  HCNN  HCNO  HOCN  HNCO  NCO  N2  AR  C3H7
                    C3H8  CH2CHO  CH3CHO N2H2 """,
      reactions = "all",
      transport = "Mix",
      initial_state = state(temperature = 300.0,
                            pressure = OneAtm)    )


ideal_gas(name = "gri30_b96_multi",
      elements = " O  H  C  N  Ar ",
      species = """ H2  H  O  O2  OH  H2O  HO2  H2O2  C  CH
                    CH2  CH2(S)  CH3  CH4  CO  CO2  HCO  CH2O  CH2OH  CH3O
                    CH3OH  C2H  C2H2  C2H3  C2H4  C2H5  C2H6  HCCO  CH2CO  HCCOH
                    N  NH  NH2  NH3  NNH  NO  NO2  N2O  HNO  CN
                    HCN  H2CN  HCNN  HCNO  HOCN  HNCO  NCO  N2  AR  C3H7
                    C3H8  CH2CHO  CH3CHO N2H2 """,
      reactions = "all",
      transport = "Multi",
      initial_state = state(temperature = 300.0,
                            pressure = OneAtm)    )
```

N_2H_2 Species data added at end of the relevant section:

```
#-----------------------------------------------------------------------------
#  Species data
#-----------------------------------------------------------------------------

species(name = "N2H2",
    atoms = " N:2  H:2 ",
    thermo = (
       NASA( [  200.00,  1000.00], [  4.910660160E+00,  -1.077918660E-02,
                3.865164410E-05,  -3.865016280E-08,   1.348521000E-11,
                2.422427270E+04,   9.102797030E-02] ),
       NASA( [ 1000.00,  6000.00], [  1.311150860E+00,   9.001872720E-03,
               -3.149118660E-06,   4.814496900E-10,  -2.718979830E-14,
                2.478641670E+04,   1.640910850E+01] )
             ),
    transport = gas_transport(
                     geom = "nonlinear",
                     diam =     3.798,
                     well_depth =    71.4,
                     polar =     0.00,
                     rot_relax =     1.00),
    note = "L 5/90"
       )
```

Reactions added:

```
#-----------------------------------------------------------------------------
#  Reaction data
#-----------------------------------------------------------------------------

#  Reaction 326
reaction( "NH2 + O <=> NO + H2",   [0.5E+13, 0, 0])

#  Reaction 327
reaction( "NH2 + NO <=> NNH + OH",   [0.28E+14, -0.55, 0])

#  Reaction 328
reaction( "NH2 + NO <=> N2 + H2O",   [0.13E+17, -1.338, -533.87])

#  Reaction 329
reaction( "NNH + NO <=> N2 + HNO",   [0.5E+14, 0, 0])

#  Reaction 330
reaction( "NNH + NH2 <=> N2 + NH3",   [0.5E+14, 0, 0])

#  Reaction 331
reaction( "NNH + NH <=> N2 + NH2",   [0.5E+14, 0, 0])

#  Reaction 332
reaction( "NNH + O <=> N2O + H",   [0.10E+15, 0, 0])

#  Reaction 333
reaction( "HNO + NH2 <=> NH3 + NO",   [0.2E+14, 0, 1000])

#  Reaction 334
reaction( "HNO + HNO <=> N2O + H2O",   [0.395E+13, 0, 5000])

#  Reaction 335
```

```
reaction( "HNO + NO <=> N2O + OH",   [0.2E+13, 0, 26000])

#  Reaction 336
reaction( "NH2 + NH <=> N2H2 + H",   [0.15E+16, -0.5, 0])

#  Reaction 337
reaction( "NH + NH <=> N2 + H + H",   [0.25E+14, 0, 0])

#  Reaction 338
reaction( "NH2 + N <=> N2 + H + H",   [0.72E+14, 0, 0])

#  Reaction 339
three_body_reaction( "N2H2 + M <=> NNH + H + M",   [0.5E+17, 0, 50000],
         efficiencies = " H2O:15  O2:2  N2:2  H2:2 ")

#  Reaction 340
reaction( "N2H2 + H <=> NNH + H2",   [0.5E+14, 0, 1000])

#  Reaction 341
reaction( "N2H2 + O <=> NH2 + NO",   [0.10E+14, 0, 0])

#  Reaction 342
reaction( "N2H2 + O <=> NNH + OH",   [0.2E+14, 0, 1000])

#  Reaction 343
reaction( "N2H2 + OH <=> NNH + H2O",   [0.10E+14, 0, 1000])

#  Reaction 344
reaction( "N2H2 + NO <=> N2O + NH2",   [0.3E+13, 0, 0])

#  Reaction 345
reaction( "N2H2 + NH <=> NNH + NH2",   [0.10E+14, 0, 1000])

#  Reaction 346
reaction( "N2H2 + NH2 <=> NH3 + NNH",   [0.10E+14, 0, 1000])

#  Reaction 347
reaction( "NH2 + NH2 <=> N2H2 + H2",   [0.50E+12, 0, 0])

#  Reaction 348
reaction( "NH2 + O2 <=> HNO + OH",   [0.45E+13, 0, 25000])

#  Reaction 349
reaction( "NCO + NO2 <=> N2O + CO2",   [0.58E+15, -0.7, 0],
         options = 'duplicate')

#  Reaction 350
reaction( "NH + HNCO <=> NH2 + NCO",   [0.3E+14, 0, 23700])

#  Reaction 351
reaction( "NH2 + HNCO <=> NH3 + NCO",   [0.10E+13, 0, 6955])

#  Reaction 352
reaction( "HO2 + HNCO <=> NCO + H2O2",   [2.04E+6, 2.04, 566])

#  Reaction 353
reaction( "NH3 + HO2 <=> NH2 + H2O2",   [0.3E+12, 0, 22000])

#  Reaction 354
reaction( "NH2 + NO2 <=> N2O + H2O",   [0.284E+19, -2.2, 0])

#  Reaction 355
reaction( "NH + NO2 <=> N2O + OH",   [0.1E+14, 0, 0])

#  Reaction 356
reaction( "NH2 + NH2 <=> NH + NH3",   [0.5E+14, 0, 10000])

#  Reaction 357
reaction( "NH2 + HO2 <=> NH3 + O2",   [0.43E+14, 0, 0])
```

Reaction 328 was originally expressed as a pair of duplicate reactions with different kinetic constants as follows:

```
#  Reaction 328  (47 in B97, 3 in Xu's B96)
reaction( "NH2 + NO <=> N2 + H2O",   [0.13E+17, -1.25, 0],
         options = 'duplicate')

#  Reaction 329  (48 in B97, 4 in Xu's B96)
reaction( "NH2 + NO <=> N2 + H2O",   [-0.28E+14, -0.55, 0],
         options = 'duplicate')
```

The negative pre-exponential factor for what was originally reaction 329 caused errors in Cantera. To avoid this problem reaction 329 was deleted and reaction 328's kinetic parameters were changed to approximate the combined effect of the duplicate reactions.

Appendix C:
Coal and Fly Ash Analysis Reports

Copies of the coal and fly ash sample analysis reports appear in this section in the order outlined in Table C1.

Table C1. List of coal and fly ash sample analysis reports in Appendix C.

Coal	Sample ID in Report	Analysis and Sample Type
Sub-bituminous	PRB Raw	Proximate and Ultimate Analysis with Chloride Sample Type: As received coal
	PRB Raw	Mineral Ash Analysis Sample Type: As received coal
	PRB Air	Mineral Ash Analysis Sample Type: Fly-ash from air combustion
	PRB Oxy	Mineral Ash Analysis Sample Type: Fly-ash from oxy-fuel combustion
Illinois #6	BYU-OXY-IL6	Proximate, Ultimate, Chloride, and Mineral Ash Analysis Sample Type: As received coal
	Ill 6 Air	Ultimate Analysis Sample Type: Char from air combustion
	Ill 6 Oxy	Ultimate Analysis Sample Type: Char from oxy-fuel combustion
Pittsburgh #8	BYU-OXY-PT8	Proximate, Ultimate, Chloride, and Mineral Ash Analysis Sample Type: As received coal
	Pitt 8 Air	Ultimate Analysis Sample Type: Char from air combustion
	Pitt 8 Oxy	Ultimate Analysis Sample Type: Char from oxy-fuel combustion

Andrew Mackrory
BYU Mechanical Engineering Dept.
435 CTB
Provo, UT 84602

Date: March 27, 2008
Request Number: 25233
Date Received: 3-13-08
Matrix: Raw Coal
Lab Number: L3945
Sample ID: PRB Raw

REPORT OF ANALYSIS

Proximate Analysis Method: ASTM D-5142	As Received wt%	Moisture Free wt%	MAF Basis wt%
Moisture	8.55	******	******
Ash	5.87	6.42	******
Volatile Matter	42.55	46.53	49.72
Fixed Carbon	43.03	47.05	50.28
Total	100.00	100.00	100.00

Ultimate Analysis Method: ASTM D5142/5373			
Moisture	8.55	******	******
Hydrogen	3.58	3.91	4.18
Carbon	60.38	66.03	70.56
Nitrogen	0.89	0.97	1.04
Sulfur	0.50	0.55	0.59
Oxygen	20.23	22.12	23.63
Ash	5.87	6.42	******
Total	100.00	100.00	100.00

Heating Value, Btu/lb Method: ASTM D-5865	10,253	11,212	11,981

Hydrogen and Oxygen values reported do not include hydrogen and oxygen in the free moisture associated with the sample.

Method: XRF

Chloride, wt.%	0.002

Monte L. Ellis
Laboratory Manager

MLE:tab

WYOMING ANALYTICAL LABORATORIES, INC.
1660 Harrison St. Wallaramie@wal-lab.com (307) 742-7995
Laramie, WY 82070 Fax: (307) 721-8956

Andrew Mackrory
BYU Mechanical Engineering Dept.
435 CTB
Provo, UT 84602

Date: March 20, 2008
Request Number: 25233
Date Received: 3-13-08
Matrix: Raw Coal
Lab Number: L3945
Sample ID: PRB Raw

COAL ASH ANALYSIS

wt% as Received Basis

	Method: ASTM D-4326 (XRF)
Silicon Dioxide, % as SiO2	33.57
Aluminum Oxide, % as Al2O3	16.28
Iron Oxide, % as Fe2O3	5.82
Calcium Oxide, % as CaO	23.80
Magnesium Oxide, % as MgO	4.79
Sodium Oxide, % as Na2O	1.61
Potassium Oxide, % as K2O	0.30
Titanium Dioxide, % as TiO2	1.20
Manganese Dioxide, % as MnO2	0.02
Phosphorus Pentoxide, % as P2O5	0.97
Strontium Oxide, % as SrO	0.28
Barium Oxide, % as BaO	0.56
Sulfur Trioxide, % as SO3	12.86

Moisture	0.10
Dry Ash	0.41

Alkalies as Na20	1.81
Base to Acid Ratio	0.71
Silic Ratio	0.49
T250, ^{0}F	2163

MLE:tab

Monte L. Ellis
Laboratory Manager

WYOMING ANALYTICAL LABORATORIES, INC.
1660 Harrison St. Laramie, WY 82070
Wallaramie@wal-lab.com
(307) 742-7995
Fax: (307) 721-8956

Andrew Mackrory
BYU Mechanical Engineering Dept.
435 CTB
Provo, UT 84602

Date: March 20, 2008
Request Number: 25233
Date Received: 3-13-08
Matrix: Coal Ash
Lab Number: L3943
Sample ID: PRB Air

COAL ASH ANALYSIS

wt% as Received Basis

	Method: ASTM D-4326 (XRF)
Silicon Dioxide, % as SiO_2	31.32
Aluminum Oxide, % as Al_2O_3	16.29
Iron Oxide, % as Fe_2O_3	6.11
Calcium Oxide, % as CaO	25.78
Magnesium Oxide, % as MgO	5.13
Sodium Oxide, % as Na_2O	1.47
Potassium Oxide, % as K_2O	0.39
Titanium Dioxide, % as TiO_2	1.35
Manganese Dioxide, % as MnO_2	0.03
Phosphorus Pentoxide, % as P_2O_5	0.89
Strontium Oxide, % as SrO	0.35
Barium Oxide, % as BaO	0.56
Sulfur Trioxide, % as SO_3	1.22

Moisture	0.28
Dry Ash	9.75

Alkalies as Na20	1.73
Base to Acid Ratio	0.79
Silic Ratio	0.46
T250, ^0F	2185

MLE:tab

Monte L. Ellis
Laboratory Manager

WYOMING ANALYTICAL LABORATORIES, INC.
1660 Harrison St. Wallaramie@wal-lab.com (307) 742-7995
Laramie, WY 82070 Fax: (307) 721-8956

Andrew Mackrory
BYU Mechanical Engineering Dept.
435 CTB
Provo, UT 84602

Date: March 20, 2008
Request Number: 25233
Date Received: 3-13-08
Matrix: Coal Ash
Lab Number: L3944
Sample ID: PRB Oxy

COAL ASH ANALYSIS

wt% as Received Basis

	Method: ASTM D-4326 (XRF)
Silicon Dioxide, % as SiO2	26.29
Aluminum Oxide, % as Al2O3	16.97
Iron Oxide, % as Fe2O3	5.74
Calcium Oxide, % as CaO	30.29
Magnesium Oxide, % as MgO	6.01
Sodium Oxide, % as Na2O	1.23
Potassium Oxide, % as K2O	0.26
Titanium Dioxide, % as TiO2	1.41
Manganese Dioxide, % as MnO2	0.02
Phosphorus Pentoxide, % as P2O5	1.10
Strontium Oxide, % as SrO	0.40
Barium Oxide, % as BaO	0.68
Sulfur Trioxide, % as SO3	2.32

Moisture	0.17
Dry Ash	6.08

Alkalies as Na20	1.40
Base to Acid Ratio	0.97
Silic Ratio	0.38
T250, ^{0}F	2335

MLE:tab

Monte L. Ellis
Laboratory Manager

WYOMING ANALYTICAL LABORATORIES, INC.
1660 Harrison St. Laramie, WY 82070
Wallaramie@wal-lab.com
(307) 742-7995
Fax: (307) 721-8956

Dr. Dale Tree
BYU Mechanical Engineering
435 CTB
Provo, UT 84602

Date: March 14, 2006
Request Number: 22933
Lab Number: K4382
Sample ID: BYU-OXY 1L6

REPORT OF ANALYSIS

Proximate Analysis:	As Received Wt%	Moisture Free wt%	MAF Basis wt%
Moisture	14.22	******	******
Ash	7.99	9.31	******
Volatile Matter	34.36	40.06	44.17
Fixed Carbon	43.43	50.63	55.83
Total	100.00	100.00	100.00

Ultimate Analysis:			
Moisture	14.22	******	******
Hydrogen	3.40	3.96	4.37
Carbon	63.70	74.26	81.88
Nitrogen	0.99	1.15	1.27
Sulfur	3.61	4.21	4.64
Oxygen	6.09	7.10	7.83
Ash	7.99	9.31	******
Total	100.00	100.00	100.00

Heating Value, Btu/lb	11067	12902	14226

Chloride, mg/kg	1,336

Mineral Ash Analysis ignited ash, wt%	
Silicon, as SiO2	49.81
Aluminum, as Al203	17.65
Iron, as Fe203	18.99
Calcium, as CaO	5.55
Magnesium, as MgO	1.22
Sodium, as Na2O	1.89
Potassium, as k2O	2.18
Titanium, as TiO2	0.92
Manganese, as Mn02	0.05
Phosphorus, as P205	0.19
Strontium, as SrO	0.06
Barium, as BaO	0.08
Sulfur, as S03	1.41
Total	100.00

T250, F	2370
Silica Ratio	65.91
Base/Acid Ratio	0.44
Si/Al Ratio	2.82
Dolomite Ratio	22.7
% Acidic	69.63
% Basic	30.37
Alkalies, as Na20	1.89
Ash Type	bituminous
Slagging Index	0
Fouling Index	****
Lbs S/MM Btu	3.26
Lbs SO2/MM Btu	6.52
Lbs ash/MM Btu	7.22

Digitally signed by Monte L. Ellis
DN: cn=Monte L. Ellis, o=WAL, ou=Laramie, c=US
Date: 2006.03.20 15:35:41 -07'00'

Monte L. Ellis
Laboratory Manager

MLE:tab

WYOMING ANALYTICAL LABORATORIES, INC.
1660 Harrison St. Laramie, WY 82070
Wallaramie@wal-lab.com
(307) 742-7995
Fax: (307) 721-8956

Andrew Mackrory
BYU Mechanical Engineering Dept.
435 CTB
Provo, UT 84602

Date: March 27, 2008
Request Number: 25233
Date Received: 3-13-08
Matrix: Coal Char

REPORT OF ANALYSIS

Lab Number	L3941		
Sample ID	**III 6 Air**		
Ultimate Analysis Method: ASTM D5142/5373	As Received wt%	Moisture Free wt%	MAF Basis wt%
Moisture	2.61	******	******
Hydrogen	1.61	1.65	2.91
Carbon	46.10	47.34	83.40
Nitrogen	1.18	1.21	2.13
Sulfur	2.73	2.80	4.93
Oxygen	3.66	3.76	6.63
Ash	42.11		******
Total	100.00	100.00	100.00

Lab Number	L3942		
Sample ID	**III 6 Oxy**		
Ultimate Analysis Method: ASTM D5142/5373	As Received wt%	Moisture Free wt%	MAF Basis wt%
Moisture	9.04	******	******
Hydrogen	2.39	2.63	3.88
Carbon	43.27	47.57	70.23
Nitrogen	1.07	1.18	1.74
Sulfur	3.02	3.32	4.90
Oxygen	11.86	13.03	19.25
Ash	29.35	32.27	******
Total	100.00	100.00	100.00

Hydrogen and Oxygen values reported do not include hydrogen and oxygen in the free moisture associated with the sample.

MLE:tab

Monte L. Ellis
Laboratory Manager

WYOMING ANALYTICAL LABORATORIES, INC.
1660 Harrison St. Wallaramie@wal-lab.com (307) 742-7995
Laramie, WY 82070 Fax: (307) 721-8956

Dr. Dale Tree
BYU Mechanical Engineering
435 CTB
Provo, UT 84602

Date: March 14, 2006
Request Number: 22933
Lab Number: K4383
Sample ID: BYU-OXY PT8

REPORT OF ANALYSIS

Proximate Analysis:	As Received Wt%	Moisture Free wt%	MAF Basis wt%
Moisture	2.57	******	******
Ash	10.40	10.67	******
Volatile Matter	36.52	37.48	41.96
Fixed Carbon	50.51	51.85	58.04
Total	100.00	100.00	100.00

Ultimate Analysis:			
Moisture	2.57	******	******
Hydrogen	4.24	4.35	4.87
Carbon	74.14	76.1	85.19
Nitrogen	1.20	1.23	1.38
Sulfur	3.36	3.45	3.86
Oxygen	4.09	4.20	4.70
Ash	10.40	10.67	******
Total	100.00	100.00	100.00

Heating Value, Btu/lb	12868	13207	14785

Chloride, mg/kg	643

Mineral Ash Analysis ignited ash, wt%	
Silicon, as SiO2	46.39
Aluminum, as Al203	22.75
Iron, as Fe203	21.71
Calcium, as CaO	2.76
Magnesium, as MgO	0.74
Sodium, as Na2O	0.49
Potassium, as k2O	2.30
Titanium, as TiO2	1.11
Manganese, as Mn02	0.02
Phosphorus, as P205	0.51
Strontium, as SrO	0.11
Barium, as BaO	0.07
Sulfur, as S03	1.04
Total	100.00

T250, F	2412
Silica Ratio	64.79
Base/Acid Ratio	0.4
Si/Al Ratio	2.04
Dolomite Ratio	12.5
% Acidic	71.5
% Basic	28.5
Alkalies, as Na20	0.49
Ash Type	bituminous
Slagging Index	0
Fouling Index	****
Lbs S/MM Btu	2.61
Lbs SO2/MM Btu	5.22
Lbs ash/MM Btu	8.08

Digitally signed by Monte L. Ellis
DN: cn=Monte L. Ellis, o=WAL, ou=Laramie, c=US
Date: 2006.03.20 15:35:54 -07'00'

Monte L. Ellis
Laboratory Manager

MLE:tab

WYOMING ANALYTICAL LABORATORIES, INC.
1660 Harrison St. Laramie, WY 82070
Wallaramie@wal-lab.com
(307) 742-7995
Fax: (307) 721-8956

Andrew Mackrory
BYU Mechanical Engineering Dept.
435 CTB
Provo, UT 84602

Date: March 27, 2008
Request Number: 25233
Date Received: 3-13-08
Matrix: Coal Char

REPORT OF ANALYSIS

Lab Number	L3939		
Sample ID	**Pitt 8 Air**		
Ultimate Analysis Method: ASTM D5142/5373	As Received wt%	Moisture Free wt%	MAF Basis wt%
Moisture	1.21	******	******
Hydrogen	1.45	1.47	2.18
Carbon	58.99	59.71	88.49
Nitrogen	1.56	1.58	2.34
Sulfur	2.04	2.06	3.05
Oxygen	2.62	2.66	3.94
Ash	32.13	32.52	******
Total	100.00	100.00	100.00

Lab Number	L3940		
Sample ID	**Pitt 8 Oxy**		
Ultimate Analysis Method: ASTM D5142/5373	As Received wt%	Moisture Free wt%	MAF Basis wt%
Moisture	1.71	******	******
Hydrogen	1.02	1.04	1.37
Carbon	67.21	68.38	90.12
Nitrogen	1.76	1.79	2.36
Sulfur	1.99	2.02	2.66
Oxygen	2.60	2.65	3.49
Ash	23.71	24.12	******
Total	100.00	100.00	100.00

Hydrogen and Oxygen values reported do not include hydrogen and oxygen in the free moisture associated with the sample.

MLE:tab

Monte L. Ellis
Laboratory Manager

WYOMING ANALYTICAL LABORATORIES, INC.
1660 Harrison St. Wallaramie@wal-lab.com (307) 742-7995
Laramie, WY 82070 Fax: (307) 721-8956

Appendix D:
MATLAB Source Code

MATLAB/Cantera source code for the detailed kinetic model of the MFR appears in this appendix. The code below may be cut and pasted directly into the MATLAB editor from the electronic version of this document (available from www.etd.byu.edu). The input file should be changed to suit the case being modeled and the main program file (MFR_Model.m) edited in one location (as marked by the comments) to reflect the name of the new input file and desired output filename. Other instructions related to the use of the code may be found in comments in the code (comments are preceded by the % symbol).

Sub_bit_Air_Input.m – Sample Input Script for MFR_model.m

```
%---INPUT SCRIPT FOR MFR Coal Combustion Model-----------------------------

% Reactant Flow Rates:
NG_in = 0.373; % kg/hr Natural Gas (assumed 100% CH4)
COAL = 0.877;  % kg/hr coal (including moisture and ash)
               % see below for more coal-related variables
Primary = 0.607;   % fraction of oxidizer to primary combustion zone
% NOTE: The following 4 variables are flow rates through the burner (i.e.
% excluding burnout oxidizer)
Air_in = 18.42*Primary; % kg/hr Air (assumed 1 mole O2 to 3.76 moles N2)
O2_in = 0*Primary; % kg/hr Bottled O2 (assumed 100% pure)
CO2_in = 0*Primary; % kg/hr Bottled CO2 (assumed 100% pure)
N2_in = 0*Primary; % kg/hr Bottled N2 (assumed 100% pure)

NO_doping = 0; % ppm NO in the CO2 reactant streams

% Experiment conditions:
P = 85000; % Pressure (Pa) at BYU's elevation
T1 = 300; % initial gas temperature (K)
T2 = 522; % Burnout Oxidizer Pre-heat Temperature (K)
d = 0.127; % diameter of MFR reactor (m)
k_wall = 400;   % This empirical heat transfer parameter is tuned to match
```

```
                % experimental data to account for all heat transfer from
                % the combustion that is not explicitly modeled elsewhere.
                % This value is linked to the value of the variable Length
                % (defined below).
                % For a methane-air case, 500 should be used with 0.002 m
                % value for Length
                % For coal-cases with Length = 0.002 m, 400 is recommended

WallX = [0;             % Locations of wall temperature measurements (m)
         0.020;         % The code interpolates when wall temperatures are
         0.045;         % required between these locations.
         0.071;         % (linear interpolation)
         0.096;
         0.122;
         0.147;
         0.172;
         0.198;
         0.413;
         0.879;
         1.171;
         1.475;
         1.751];

twallvector = [400;     % Wall temperature measurements (K)
               1140;    %  - must correspond to WallX locations.
               1203;
               1235;
               1269;
               1286;
               1285;
               1280;
               1268;
               1324;
               1216;
               1118;
               1046;
               914];

% Variables related to the gas phase reactions:
thermal = 1; % multiplier for thermal NOx mechanism reactions
prompt = 1;  % multiplier for prompt NOx mechanism reactions
             % (0 to disable, 1 to enable)

mechanism =  1; % Selection of gas phase chemistry mechanism
                % 1 = GRI-Mech 3.0
                % 2 = GRI-Mech 3.0 + B96 (includes advanced reburning)
                % 3 = SKG03

% Variables related to the numerical modeling:
TR1 = 2000; % initial guessed temperature of the CSTR's in ignition network
dt = 0.01;  % time step for CSTR network integration (seconds)
            % integration continues until steady state is reached (as
            % measured by temperature change being less than a tolerance
tolerance = 1e-8; % tolerance on the change in temperature between time
                  % steps to steady state.
number_reactors = 5; % number of CSTR's in ignition network
Length = 0.002;                 % length of CSTR's in network (m)
                                % usually 0.002 m - Grid Independence was
                                % verified for 0.002 m
                                % Note that if this is changed then the
                                % value of k_wall needs to be changed also
Length2 = Length; % Length of CSTR's after ignition network (see also
                  %  comments for Length above)

% Variables related to the CPDCP-NLG coal devolatilization model:
    % Radiation Heat Transfer Parameters:

    % emissivity of:
    emiss = [0.4;    % burner
             0.5;    % walls
             0.999   % exhaust tube (a cavity)
```

```
        0.7];   % particle

tbnr = 400.0;    % burner face temperature (K)

texit = 900.0;   % exhaust tube temperature (K)

% Time Step Parameters:
timax = 2.0;      % maximum devolatilization time modeled (seconds)
%-------------------------------------------------------------------------
% Proximate and Ultimate Analysis Data for Coal:
% Stored in array yelem in the order: CHNOS, dry, ash-free mass
% fractions

yelem = [0.7056; 0.0418; 0.0104; 0.2363; 0.0059];

ASTMvol = 49.72;    % DAF basis (0 < ASTMvol < 100)
                    % Only required if C13 NMR data will be estimated

%-------------------------------------------------------------------------
% C13 NMR Structural Data for Coal:
% Note: If C13 NMR data are unavailable for your coal, the correlation
% of Genetti and Fletcher will be used to estimate these parameters
% using yelem and ASTMvol (defined above) - if this is the case, set
% mw1 to zero to activate the correlation. The correlation code is in
% the main progam file.
%   Genetti, D., "An Advanced Model of Coal Devolatilization Based on
%   Chemical Structure," M.S. Thesis, Brigham Young University (1998).
mw1 = 0;      % average molecular weight per aromatic cluster
                % (includes side chains)
                % SET TO ZERO TO ACTIVATE C13 NMR CORRELATION:
                % i.e.    mw1 = 0;
p0 = 0;        % ratio of bridges to total attachments
c0 = 0;      % char bridge population
sigp1 = 0;      % this is the coordination number sigma+1 (number of
                % total attachments per cluster)
mdel = 0;      % average molecular weight per side chain
%-------------------------------------------------------------------------
rhop = 0.7;  % initial particle apparent density (g/cm^3). As explained
             % by Fletcher (Comb. Sci. Tech., 63, 89-105, 1989), this
             % parameter is artificially lowered in order to match
             % measured particle temperatures. This may indicate that
             % the reported particle heat capacities are too high, or
             % else that the Sandia flow reactor had radial temperature
             % gradients near the injector that influenced the heating
             % characteristics.
             % Note that apparent density is calculated from total
             % measured coal mass divided by TOTAL volume, so the
             % volume includes voids between particles, and pores in
             % the coal.

dp = 121.0e-4;  % particle diameter (cm)

swell = 0.0; % swelling factor (dpf/dp0 - 1) dpf = final/max diameter
             % dp0 = initial diameter
            % Note that this swelling is not the swelling of coal when
            % placed in a solvent, rather it is swelling of the coal
            % when it softens during heating and escaping gases cause
            % expansion of the softened material. This parameter is
            % heating rate dependent. It is probably near-zero for high
            % rank anthracites and low rank lignites and subbituminous
            % coals, but important for medium rank coals - see the book
            % by K. Lee Smith et al. (1994): The Structure and Reaction
            % Processes of Coal, pg 211.

delhv = -100.0; % Heat of pyrolysis (cal/g), negative indicates
                %  endothermic
                % Nominally -100.0 cal/g

omegaw = 0.0846; % mass fraction of moisture in the parent coal
                 % (as received, i.e. including ash)
```

```
    omegaa = 0.0602; % mass fraction of ash in the parent coal (as received)

% Variables related to the char oxidation and gasification model:
COAL_Type = 1;
                % 1 = Wyoming Sub-bituminous
                % 2 = Illinois #6
                % 3 = Pittsburgh #8

gasification = 1; % Char gasification by CO2: 1 = enable, 0 = disable
Q_reactO2_x = 0; % Fraction (0-1) of heterogeneous O2 reaction heat to char
                 % Nominally 0 because 0.5 and 1.0 gave problems - need to
                 % adjust in the future possibly.
Q_reactCO2_x = 0; % Fraction (0-1) of heterogeneous O2 reaction heat to char
                 % Nominally 0 because 0.5 and 1.0 gave problems - need to
                 % adjust in the future possibly.

%---------END OF USER INPUT SCRIPT-----------------------------------------
```

MFR_Model.m – Main Program File for Detailed Kinetic Model

```
% This is a MATLAB + Cantera model of pulverized coal combustion in BYU's
%  MFR combustion research facility. The model consists of four parts:
% 1. A series network of Cantera CSTR's with heat transfer between them for
%    ignition of the reactants.
% 2. A Cantera CSTR in a loop that acts as a series of CSTR's without heat
%    transfer between them to model the MFR post-ignition. Having heat
%    transfer between CSTR's is too computationally expensive for a large
%    number of CSTR's
% 3. The CPDCP-NLG coal devolatilization model to provide estimated
%    devolatilization products to the CSTR's in 1 and 2 above.
% 4. A char oxidation and CO2 gasification model that begins once
%    devolatilization is complete.
%
%      (NOTE: This model mostly uses metric units, but the CPD model does
%      not. Information is passed in terms of dimensionless quantities, or
%      is converted where necessary). The char reactions model uses a
%      mixture of units as detailed in the comments and the list of
%      variables at the and of the code.
%
% For more information and instructions, see the comments in the code and:
%
% Mackrory, A. J. (2008) A MECHANISTIC INVESTIGATION OF NITROGEN EVOLUTION
%  IN PULVERIZED COAL OXY-FUEL COMBUSTION, Ph.D. Dissertation, Brigham
%  Young University, Mechanical Engineering Department, December 2008,
%  Provo, UT, U.S.A
%
% Coded by Andrew Mackrory using:
%   MATLAB Version: 7.4.0 (R2007a)
%   Cantera Version: 1.7.1

%---ASSOCIATED SUBROUTINES (m-files)-------------------------------------
% heatap.m - calculates ash heat capacity
% heatcp.m - calculates the heat capacity of a DAF coal particle from
                % Merrick's (1983) correlations
% cpdcp_nlg.m - this is the CPD model which uses these subroutines as
                % described in the cpdcp_nlg comments:
                    % at.m
                    % d.m
                    % flash.m
                    % gamln.m
                    % heatap.m
                    % heatcp.m
                    % inverf.m
                    % lightgas.m
                    % perkp.m
                    % perks.m
                    % xxx.m
                    % yyy.m
% An input script such as Sub_bit_Air_Input.m is also required. It's name
```

```
% may be changed to anything provided the script is called in the code
% below where indicated.

%---CANTERA FUNCTIONS USED IN THE CODE-------------------------------------
% So that these functions may be differentitated from variable names, the
% following is a list of Cantera functions called by this model:
% NOTE: MATLAB is case-sensitive
%
% advance
% air
% cleanup
% cp_mass
% density
% elementIndex
% enthalpy_mass
% GRI30  - creates a gas object using the GRI30.cti mechanism file
% GRI30_B96  - creates a gas object using the GRI30_B96 mechanism file (not
%   distributed with Cantera)
% insert
% install
% MassFlowController
% massFraction
% massFractions
% meanMolarMass
% mixDiffCoeffs
% molecularWeights
% moleFraction
% moleFractions
% nAtoms
% nSpecies
% oneatm
% pressure
% Reactor
% ReactorNet
% Reservoir
% setArea
% setInitialVolume
% setMassFlowRate
% setMultiplier
% setThermalResistance
% setValveCoeff
% SKG03 - creates a gas object using the SKG03.cti mechanism file (not
%   distributed with Cantera)
% speciesIndex
% speciesName
% temperature
% thermalConductivity
% Valve
% viscosity
% Wall

%---IMPORTANT ASSUMPTIONS--------------------------------------------------
% Key assumptions made in the model are largely based on established
% practices in the literature and include the following:
    % Coal particles are entrained (i.e. particle velocity is equal to gas
    %  velocity).
    % All gas products from the coal consist of species in the gas-phase
    %  kinetic mechanism.
    % Natural gas is modeled as 100% CH4
    % All nitrogen in the volatiles is in the form of HCN.
    % Char consists of C(s) and burns with a shrinking core of constant
    %  density and constant ash content with CO as the surface product.
    %  These assumptions were used in deriving the rate constants sourced
    %  from the literature.
    % NO formation from char was not included in the model.
    % Sulfur is ignored.
    % CO from the char reactions was oxidized to CO2 by the gas phase
    %  kinetics.
    % Fluid mechanics were not modeled as the focus of the model was the
    %  devolatilization and gas phase kinetics.
    % Mixing of burnout oxidizer was assumed to occur in one CSTR
```

```
    %  (i.e. intense mixing).
    % The coal particles were represented with one particle diameter based
    %  on the mean diameter for a Rosin-Rammler Distribution fit to the
    %  measured particle size distributions.
% More detailed information on these assumptions and references to the
% literature are available in the dissertation referenced above.

%---VARIABLES-------------------------------------------------------------
% An alphabetic list of variables appears at the end of the code.

%---BEGINNING OF CODE-----------------------------------------------------
clear;      % Clear MATLAB workspace
clc;        % and command window
cleanup;    % Clear Cantera objects in memory

%---RUN INPUT SCRIPT AND SPECIFY OUTPUT FILE------------------------------
% Comment out all but one line:
    % txt is the appropriate filename extension for the output file
    % for use in Microsoft Excel - output is tab-delimited text

Sub_bit_Air_Input; output = 'Sub_bit_Air_Output.txt';
% Sub_bit_O25_Input; output = 'Sub_bit_O25_Output.txt';
% Sub_bit_O30_Input; output = 'Sub_bit_O30_Output.txt';
% Sub_bit_Air_Opt_Input; output = 'Sub_bit_Air_Opt_Output.txt';
% Sub_bit_O30_Opt_Input; output = 'Sub_bit_O30_Opt_Output.txt';
% Illinois6_Air_Input; output = 'Illinois6_Air_Output.txt';
% Illinois6_O30_Input; output = 'Illinois6_O30_Output.txt';
% Illinois6_O30_0ppm_Input; output = 'Illinois6_O30_0ppm_Output.txt';
% Illinois6_O30_525ppm_Input; output = 'Illinois6_O30_525ppm_Output.txt';
% Pitt8_Air_Input; output = 'Pitt8_Air_Output.txt';
% Pitt8_O30_Input; output = 'Pitt8_O30_Output.txt';

%---OPTIONAL C13 NMR PARAMETER ESTIMATION---------------------------------
% (see notes in input script)
if (mw1 == 0)
    yelem = yelem.*100; % convert to percentages for this section of code
    % Estimate C13 NMR parameters as follows:
    %    Declare c (vector of empirical coefficients):
    %    Estimate parameter using c, yelem, and ASTMvol
    %    Move on to next parameter and repeat
    %    Order: mdel, mw1, p0, sigp1, c0
    c = [421.957;
         -8.64692;
         0.0463894;
         -8.47272;
         1.18173;
         1.15366;
         -0.0434024;
         0.556772;
         -0.00654575];

    mdel = c(1)+c(2)*yelem(1)+c(3)*yelem(1)^2+c(4)*yelem(2)+...
           c(5)*yelem(2)^2+c(6)*yelem(4)+c(7)*yelem(4)^2+c(8)*ASTMvol+...
           c(9)*ASTMvol^2;

    c = [1301.41;
         16.3879;
         -0.187493;
         -454.773;
         51.7109;
         -10.072;
         0.0760827;
         1.36022;
         -0.0313561];

    mw1 = c(1)+c(2)*yelem(1)+c(3)*yelem(1)^2+c(4)*yelem(2)+...
          c(5)*yelem(2)^2+c(6)*yelem(4)+c(7)*yelem(4)^2+c(8)*ASTMvol+...
          c(9)*ASTMvol^2;

    c = [0.489809;
         -0.00981566;
```

```
          0.000133046;
          0.155483;
          -0.0243873;
          0.00705248;
          0.000219163;
          -0.0110498;
          0.000100939];

    p0 = c(1)+c(2)*yelem(1)+c(3)*yelem(1)^2+c(4)*yelem(2)+...
         c(5)*yelem(2)^2+c(6)*yelem(4)+c(7)*yelem(4)^2+c(8)*ASTMvol+...
         c(9)*ASTMvol^2;

    c = [-52.1054;
         1.63872;
         -0.0107548;
         -1.23688;
         0.0931937;
         -0.165673;
         0.00409556;
         0.00926097;
         -8.26717E-05];

    sigp1 = c(1)+c(2)*yelem(1)+c(3)*yelem(1)^2+c(4)*yelem(2)+...
            c(5)*yelem(2)^2+c(6)*yelem(4)+c(7)*yelem(4)^2+c(8)*ASTMvol+...
            c(9)*ASTMvol^2;

    if yelem(1) > 85.9
        c0 = min(0.1183*yelem(1)-10.16,0.36);
    else
        if yelem(4) > 12.5
        c0 = min(0.014*yelem(4)-0.175,0.15);
        else
        c0 = 0;
        end
    end

    yelem = yelem./100; % Undo percent conversion
    clear c;
end
%---END OF OPTIONAL C13 NMR PARAMETER ESTIMATION--------------------------

% Setup for calculation of chemical equivalence ratio
% Positive Oxidation States for C,H,N,& O in that order
V_plus = [4 1 0 0];
% Negative Oxidation States for C,H,N,& O in that order
V_minus = [0 0 0 -2];

% Coefficients of element i in species j:
if mechanism == 1
    gas = GRI30('Mix');
elseif mechanism == 2
    gas = GRI30_B96('Mix');
elseif mechanism == 3
    gas = SKG03;
end
CHNOIndex(1) = elementIndex(gas,'C');
CHNOIndex(2) = elementIndex(gas,'H');
CHNOIndex(3) = elementIndex(gas,'N');
CHNOIndex(4) = elementIndex(gas,'O');

% Locations of key species in Cantera gas mixture objects:
H2OIndex = speciesIndex(gas,'H2O');
CO2Index = speciesIndex(gas,'CO2');
CH4Index = speciesIndex(gas,'CH4');
COIndex = speciesIndex(gas,'CO');
C2H2Index = speciesIndex(gas,'C2H2');
HCNIndex = speciesIndex(gas,'HCN');
NOIndex = speciesIndex(gas,'NO');
NO2Index = speciesIndex(gas,'NO2');
O2Index = speciesIndex(gas,'O2');
N2Index = speciesIndex(gas,'N2');
```

```
for j = 1:nSpecies(gas)
    for i = 1:4
        aij(j,i) = nAtoms(gas,j,CHNOIndex(i));
    end
end
clear gas

press = P/oneatm;   % Note: This does affect the pressure used in the CPD
                    % sub-model too.

Area = 0.25*pi*d^2; % Cross section area of reactor tube (m^2)
for i = 1:number_reactors
    Volume(i) = Area * Length; % volume of each CSTR (m^3)
end

% convert coal flow rate to kg/s
COAL = COAL * (1/3600);
% Convert other reactant input to molar flow rates
m_dot(1:number_reactors) = (NG_in + Air_in + O2_in + CO2_in + N2_in)/3600;
          % kg/s mass flow - gas only (coal volatiles added later in code)
NG = NG_in/(12.011+4*1.0079); % moles/hr Natural Gas (assumed 100% CH4)
O2 = (O2_in/(2*15.999) + (1/(1+3.76))*(Air_in/28.851));
                              % moles/hr O2 from air and bottle
CO2 = (CO2_in/(12.011+2*15.999)); % moles/hr bottled CO2

NO = (NO_doping/1000000)*CO2; % moles/hr NO in the CO2

N2 = (N2_in/(2*14.007) + (3.76/(1+3.76))*(Air_in/28.851));
                              % moles/hr N2 from air and bottled sources
composition = ['CH4:',num2str(NG),',O2:',num2str(O2),...
               ',CO2:',num2str(CO2),',N2:',num2str(N2),...
               ',NO:',num2str(NO)];

particles = (COAL*1000)/(rhop*(4/3)*pi*(dp/2)^3);
                                % number of coal particles per second

%---BEGINNING OF IGNITION PART OF CODE-------------------------------------
% Create the Gas objects using the selected gas-phase mechanism:
for i = 1:number_reactors
    if mechanism == 1
        gas(i) = GRI30('Mix');
    elseif mechanism == 2
        gas(i) = GRI30_B96('Mix');
    elseif mechanism ==3
        gas(i) = SKG03;
    end

    set(gas(i),'T',T1,'P',P,'X',composition);

    if mechanism == 3
        % set multiplier for Thermal NOx Mechanism
        setMultiplier(gas(i),74,thermal);
        setMultiplier(gas(i),73,thermal);
        setMultiplier(gas(i),72,thermal);
        % set multiplier for Prompt NOx Fenimore Mechanism
        setMultiplier(gas(i),507,prompt);
        setMultiplier(gas(i),503,prompt);
    else
        % set multiplier for Thermal NOx Mechanism
        setMultiplier(gas(i),178,thermal);
        setMultiplier(gas(i),179,thermal);
        setMultiplier(gas(i),180,thermal);
        % set multiplier for Prompt NOx Fenimore Mechanism
        setMultiplier(gas(i),239,prompt);
        setMultiplier(gas(i),240,prompt);
    end
end

% dummy gas used for property evaluation at film temperatures
if mechanism == 1
```

```
    dummygas = GRI30('Mix');
elseif mechanism == 2
   dummygas = GRI30_B96('Mix');
elseif mechanism == 3
    dummygas = SKG03;
end

% Create upstream reservoirs that will supply the CSTR's with the products
% from the previous CSTR after each iteration (dt).
for i = 1:number_reactors
    upstream(i) = Reservoir(gas(i));
end

% Now set the gases to the initial temperature of the CSTR's, and create
% the reactor objects.
% Set their volumes. In this model, the reactor volume is fixed, and
% pressure is mantained by a valve at the outlet of each CSTR.
for i = 1:number_reactors
    set(gas(i),'T',TR1,'P',P);
    cstr(i) = Reactor(gas(i));
    setInitialVolume(cstr(i),Volume(i));
end

% Create a reservoir to represent the environment, and initialize its
% temperature.
ambient = air;
set(ambient,'T',300,'P',P);
env = Reservoir(ambient);

% Create heat-conducting walls between the CSTR's and the
% environment. Set their area, and overall heat transfer
% coefficients.
for i = 1:number_reactors
    w(i) = Wall;
    install(w(i),cstr(i),env);
    setArea(w(i),pi*d*Length);
    R = log(0.180/(d/2))/(2*pi*Length*k_wall);
    setThermalResistance(w(i),R);
end

% Create heat-conducting walls between the CSTR's themselves.
for i = 1:(number_reactors-1)
   gw(i) = Wall;
   install(gw(i),cstr(i),cstr(i+1));
   setArea(gw(i),Area);
   k_gas = 0.5*(thermalConductivity(gas(i))+thermalConductivity(gas(i+1)));
   R = Length/(k_gas*Area);
   setThermalResistance(gw(i),R);
end

% Connect the upstream reservoirs to the CSTR's with mass flow
% controllers (constant mdot at each one). Set the mass flow rates.
for i = 1:number_reactors
    mfc(i) = MassFlowController;
    install(mfc(i),upstream(i), cstr(i));
    setMassFlowRate(mfc(i),m_dot(i));
end

% Now create downstream reservoirs to exhaust into.
for i = 1:number_reactors
    exhaust(i) = air;
    set(exhaust(i),'T',300,'P',P);
    downstream(i) = Reservoir(exhaust(i));
end

% Connect the CSTR's to the downstream reservoirs with valves, and
% set the coefficient sufficiently large to keep the reactor pressures
% close to the downstream pressure of exhaust.
for i = 1:number_reactors
    v(i) = Valve;
    install(v(i),cstr(i),downstream(i));
```

```
    setValveCoeff(v(i), 1.0);
end

% create the network
for i = 1:number_reactors
    network_cell_array(i) = {cstr(i)};
end
network = ReactorNet(network_cell_array);

% create vector of locations for variables of interest
position(1) = 0;
for i = 2:number_reactors+1
    position(i) = Length+position(i-1);
end

% create arrays for estimation of volatiles species
Cgoal = zeros(1,number_reactors+1);
Hgoal = zeros(1,number_reactors+1);
C_nlg = Cgoal;
H_nlg = Hgoal;
Cdiff = Cgoal;
Hdiff = Hgoal;

% initialize figure for iteration control
figure; subplot(2,1,1); hold on;
title('Temperature Profile - use to check for correct model function');
ylabel('Gas Temperature (K)');
xlabel('Axial Position of CSTR''s (m)');
subplot(2,1,2)
text(0,1,'Choose "Yes" to keep iterating.');
text(0,0.75,'Iterate until max change in T is very small (<1e-5),');
text(0,0.5,'...then select No to continue calculations.');
text(0,0.25,'Select Cancel to end program if T is too low (no ignition)');
axis off;
subplot(2,1,1);

% now integrate in time to a steady state (in a while loop)
tme = 0.0;
n = 0;
iterate = true;
ButtonName = 'Yes';
CPU_time = 0;
delta_max = 1;
while iterate
    n = n + 1; % n counts the iterations
    tme = tme + dt;
    t0 = cputime;
    advance(network, tme);
    CPU_time = CPU_time + (cputime - t0);
    CPU_time_per_step = CPU_time/n;

    % get variables for CPD input
    tgas(1) = temperature(upstream(1));
    for i = 2:number_reactors+1
        tgas(i) = temperature(gas(i-1));
    end
    if n == 1
        tp = tgas;
    end

    tfilm = 0.5*(tp + tgas);

    velocity(1) = m_dot(1)/(density(upstream(1))*Area);
    rhogas(1) = density(upstream(1));
    set(dummygas,'T',tfilm(1),'P',P,'X',composition);
    xwbvector(1) = moleFraction(dummygas,'H2O');
    ugvector(1) = viscosity(dummygas);
    kgvector(1) = thermalConductivity(dummygas);
    DiffCoeffs = mixDiffCoeffs(dummygas);
    diffwvector(1) = DiffCoeffs(H2OIndex); % Mixture-averaged diffusion
                                           % coefficient (m^2/s)
```

```
clear DiffCoeffs;
cpgvector(1) = cp_mass(dummygas);
prgas(1) = ugvector(1)*cpgvector(1)/kgvector(1);

for i = 2:number_reactors+1
    velocity(i) = m_dot(i-1)/(density(gas(i-1))*Area);
    rhogas(i) = density(gas(i-1));
    xwbvector(i) = moleFraction(gas(i-1),'H2O');
    set(dummygas,'T',tfilm(i),'P',P,'Y',massFractions(gas(i-1)));
    ugvector(i) = viscosity(dummygas);
    kgvector(i) = thermalConductivity(dummygas);
    DiffCoeffs = mixDiffCoeffs(dummygas);
    diffwvector(i) = DiffCoeffs(H2OIndex); % Mixture-averaged diffusion
                                           % coefficient (m^2/s)
    clear DiffCoeffs;
    cpgvector(i) = cp_mass(dummygas);
    prgas(i) = ugvector(i)*cpgvector(i)/kgvector(i);
end

% call CPD model here (unit conversions are in this function call)
[tms,xm,tp,tg,fvol,fchar,fcross,ftar,fmet,trate,mwchar,yNsite,...
  fnt,fnchar,fntar,fnhcn,fntot,fgas,ffgas,yygas,yf,water,convheat,...
  dpout] = cpdcp_nlg(twallvector,tbnr,texit,timax,yelem,mw1,p0,c0,...
  sigp1,mdel,position*100,tgas,position*100,velocity*100,press,...
  tgas(1),velocity(1)*100,rhop,dp,swell,omegaw,omegaa,rhogas/1000,...
  xwbvector,ugvector*10,kgvector/418.4,diffwvector*0.01^2,...
  cpgvector*2.38846e-4,prgas,emiss,d*50,WallX*100);

y(n,1) = temperature(upstream(1));
for i = 1:number_reactors
    y(n,i+1) = temperature(gas(i));
end

if n > 1
    delta_max = max(abs((y(n,:)-y(n-1,:))));
    plot(position,y(n,:),'bo');
    ButtonName = questdlg(['Iterate Again? Max Temp Change = ',...
                  num2str(delta_max),' K ',...
                  '(CPU time so far: ',num2str(CPU_time),', = ',...
                  num2str(CPU_time_per_step),' seconds per step'], ...
                  'ITERATION CONTROL');
    pause(0.1);
end

switch ButtonName,
    case 'Yes',
        % adjust the thermal conductivity between CSTR's
        for i = 1:(number_reactors-1)
            k_gas = 0.5*(thermalConductivity(gas(i))+...
                                        thermalConductivity(gas(i+1)));
            R = Length/(k_gas*Area);
            setThermalResistance(gw(i),R);
        end

        % calculate mass flows of existing gases + volatiles + water
        % (this is evaporated water, not light gas water)
        for i = 2:number_reactors
            m_dot(i) = m_dot(i-1) + ...
                        (fvol(i)-fvol(i-1))*COAL*(1-omegaa-omegaw)-...
                         COAL*(water(i)-water(i-1));
            setMassFlowRate(mfc(i),m_dot(i));
        end
        i = number_reactors+1;
        m_dot(i) = m_dot(i-1) + ...
                        (fvol(i)-fvol(i-1))*COAL*(1-omegaa-omegaw)-...
                         COAL*(water(i)-water(i-1));

        % Estimate unknown species in volatiles (kg/s units)
        % Step 1, work out what elemental mass release should be (C, H)
        % Assumptions:
            % C mass release is proportional to total mass release
```

```
    %       (Asay, 1982)
    % H mass release is according to a curve fit to the data
    %       of Asay (1982).
    % O mass release is entirely in the CPD predictions of CO
    %       H2O and CO2 (Niksa, 1996).
for i = 2:number_reactors+1
    Cgoal(i) = COAL*(1-omegaa-omegaw)*yelem(1)*fvol(i)...
                    -Cgoal(i-1);

    Hgoal(i) = COAL*(1-omegaa-omegaw)*yelem(2)*...
                ((-0.5597)*fvol(i)^2 + 1.5651*fvol(i))...
                    -Hgoal(i-1);
end

% Step 2, work out what elemental mass release is predicted by
% cpdcp_nlg in H2O, CO2, CH4, CO, and HCN (assume all N release
% is HCN)
for i = 2:number_reactors+1
    C_nlg(i) = ffgas(2,i)*fvol(i)*COAL*(1-omegaa-omegaw)*...
               (12.011/(12.011+2*15.999))+...  % CO2
               ffgas(3,i)*fvol(i)*COAL*(1-omegaa-omegaw)*...
               (12.011/(12.011+4*1.0079))+...  % CH4
               ffgas(4,i)*fvol(i)*COAL*(1-omegaa-omegaw)*...
               (12.011/(12.011+15.999))+...    % CO
               fntot(i)*yelem(3)*COAL*(1-omegaa-omegaw)*...
               (12.011/14.007)-...             % HCN
               C_nlg(i-1);

    H_nlg(i) = ffgas(1,i)*fvol(i)*COAL*(1-omegaa-omegaw)*...
               (2*1.0079/(2*1.0079+15.999))+... % H2O
               ffgas(3,i)*fvol(i)*COAL*(1-omegaa-omegaw)*...
               (4*1.0079/(12.011+4*1.0079))+... % CH4
               fntot(i)*yelem(3)*COAL*(1-omegaa-omegaw)*...
               (1.0079/14.007)-...              % HCN
               H_nlg(i-1);
end

% Step 3, use the difference to get amounts of C and H to
% add (that presumably come from other light gases and cracked
% tars)
Cdiff = Cgoal - C_nlg;
Hdiff = Hgoal - H_nlg;

% Step 4, assume that the other light gas and cracked tar are
% made up of CH4 and C2H2. Calculate the C/H molar ratio and
% use this to choose the proportions of these two gases to make
% that ratio. Make a new array of all estimated volatiles.
CHratio = (Cdiff/12.011)./(Hdiff/1.0079);
ffgas2 = zeros(6,number_reactors+1);
for i = 2:number_reactors+1
   MolarProportionCH4 = (CHratio(i)-1)/(0.25-1);
   MWunknowns = MolarProportionCH4*(12.011+4*1.0079)+...
                (1-MolarProportionCH4)*2*(12.011+1.0079);
   MassProportionCH4 = MolarProportionCH4*(12.011+4*1.0079)/...
                       MWunknowns; % in other light gas and tar

   % The values in ffgas are modifed and stored in ffgas2
   % which has these species in its rows:
   % H2O, CO2, CH4, CO, C2H2, and HCN in kg of species per kg
   % of volatiles. After this there are no volatiles of unknown
   % or unestimated composition.
   ffgas2(1,i) = ffgas(1,i); % H2O
                             % (excludes evaporated moisture)

   ffgas2(2,i) = ffgas(2,i); % CO2

   ffgas2(4,i) = ffgas(4,i); % CO
   if fvol(i) == 0
       ffgas2(6,i) = 0; %HCN
       ffgas2(3,i) = 0; %CH4
   else
```

```
                ffgas2(6,i) = (fntot(i)*COAL*(1-omegaa-omegaw)*...
                           yelem(3)*(1.0079+12.011+14.007)/(14.007))/...
                           (COAL*(1-omegaa-omegaw)*fvol(i));% HCN
                ffgas2(3,i) = ffgas(3,i) + ...
                           (MassProportionCH4*(ffgas(5,i))*COAL*...
                           (1-omegaa-omegaw))/...
                           (fvol(i)*COAL*(1-omegaa-omegaw));  % CH4
             end
             ffgas2(5,i) = 1-(ffgas2(6,i)+sum(ffgas2(1:4,i)));
                                % C2H2 (by difference)
          end
          % ffgas & ffgas2 = fraction of total volatiles that is a
          % particular species

          % move products downstream, mixing in the volatiles calculated
          % above
          for i = 2:number_reactors
              % get the existing gas composition from previous
              % reactor into kg/s units:
              ExistingGas = m_dot(i-1)*massFractions(gas(i-1));

              % get the gases to be added into kg/s units:
              AddedGas = zeros(size(ExistingGas));
              AddedGas(H2OIndex) = ffgas2(1,i)*(fvol(i)-fvol(i-1))*...
                                   COAL*(1-omegaa-omegaw)+...
                                   (water(i-1)-water(i))*COAL;
                                % H2O (light gas) and evaporated moisture
              AddedGas(CO2Index) = ffgas2(2,i)*(fvol(i)-fvol(i-1))*...
                                   COAL*(1-omegaa-omegaw); % CO2
              AddedGas(CH4Index) = ffgas2(3,i)*(fvol(i)-fvol(i-1))*...
                                   COAL*(1-omegaa-omegaw); % CH4
              AddedGas(COIndex) = ffgas2(4,i)*(fvol(i)-fvol(i-1))*...
                                  COAL*(1-omegaa-omegaw); % CO
              AddedGas(C2H2Index) = ffgas2(5,i)*(fvol(i)-fvol(i-1))*...
                                    COAL*(1-omegaa-omegaw); % C2H2
              AddedGas(HCNIndex) = ffgas2(6,i)*(fvol(i)-fvol(i-1))*...
                                   COAL*(1-omegaa-omegaw); % HCN

              % add the two compositions from above and insert the gas
              % into the next reactor (Heat transfer for volatiles to be
              % added to code later)
              mixture = ExistingGas + AddedGas;

              % lower enthalpy of gas to account for heating of particles
              % by convection
              H = enthalpy_mass(gas(i-1)); %J/kg
              % convheat is in J/particle per second
              H = H - (0.5*(convheat(i)+convheat(i-1)))*...
                       particles*(1/1000)*(tms(i)-tms(i-1))/(m_dot(i-1));
              set(dummygas,'H',H,'P',P,'MassFractions',mixture);
              insert(upstream(i),dummygas);
          end

        case 'No',
            iterate = false;
            close(gcf);
        case 'Cancel',
            close(gcf);
            return; % stop program
    end % switch
end % while

% get some variables ready for output
pressurevector(1) = pressure(upstream(1));
for i = 2:number_reactors+1
    pressurevector(i) = pressure(gas(i-1));
end
%---END OF IGNITION PART OF CODE-----------------------------------------

Length = Length2;
% Calculate chemical equivalence ratios for ignition section and
```

```
% predictions for direct comparison to measurements (NOx, CO, O2, CO2)
MWmix(1) = 1/(sum(massFractions(upstream(1))./molecularWeights(gas(1))'));
nj = massFractions(upstream(1))./molecularWeights(gas(1))';
for k = 1:4
    bi(k) = sum(aij(:,k).*nj');
end
V_p = sum(V_plus.*bi);
V_m = sum(V_minus.*bi);
r(1) = -V_p/V_m;

Yi = massFractions(upstream(1));
YWater = Yi(H2OIndex);
XWater = YWater*MWmix(1)/(2*1.0079+15.999);
YNO = Yi(NOIndex);
YNO2 = Yi(NO2Index);
YCO = Yi(COIndex);
YO2 = Yi(O2Index);
YCO2 = Yi(CO2Index);

XNO = YNO*MWmix(1)/(14.007+15.999);
XNO2 = YNO2*MWmix(1)/(14.007+2*15.999);
XCO = YCO*MWmix(1)/(12.011+15.999);
XO2 = YO2*MWmix(1)/(2*15.999);
XCO2 = YCO2*MWmix(1)/(12.011+2*15.999);

NOx_ppm_dry(1) = 1000000*(XNO + XNO2)/(1-XWater);
CO_ppm_dry(1) = 1000000*XCO/(1-XWater);
O2_vol_dry(1) = 100*XO2/(1-XWater);
CO2_vol_dry(1) = 100*XCO2/(1-XWater);
NCE(1) = (YNO*(14.007/(14.007+15.999))+YNO2*(14.007/(14.007+2*15.999)))*...
          m_dot(1)/(COAL*(1-omegaa-omegaw)*yelem(3));

for j = 2:number_reactors+1
    MWmix(j) = meanMolarMass(gas(j-1));
    nj = (1/MWmix(j))*moleFractions(gas(j-1));
    for k = 1:4
        bi(k) = sum(aij(:,k).*nj);
    end
    V_p = sum(V_plus.*bi);
    V_m = sum(V_minus.*bi);
    r(j) = -V_p/V_m;

    Xi = moleFractions(gas(j-1));
    XWater = Xi(H2OIndex);
    XNO = Xi(NOIndex);
    XNO2 = Xi(NO2Index);
    XCO = Xi(COIndex);
    XO2 = Xi(O2Index);
    XCO2 = Xi(CO2Index);

    NOx_ppm_dry(j) = 1000000*(XNO + XNO2)/(1-XWater);
    CO_ppm_dry(j) = 1000000*XCO/(1-XWater);
    O2_vol_dry(j) = 100*XO2/(1-XWater);
    CO2_vol_dry(j) = 100*XCO2/(1-XWater);

    Yi = massFractions(gas(j-1));
    YNO = Yi(NOIndex);
    YNO2 = Yi(NO2Index);
    NCE(j) = (YNO*(14.007/(14.007+15.999))+YNO2*...
             (14.007/(14.007+2*15.999)))*m_dot(j-1)/...
             (COAL*(1-omegaa-omegaw)*yelem(3));
end

%---START WRITING RESULTS TO FILE----------------------------------------
% File header
fid = fopen(output, 'wt');
fprintf(fid,'BYU MFR Coal Combustion Model\r');
fprintf(fid,'*****************************\r');
fprintf(fid,'* Coded by: Andrew Mackrory *\r');
timedata = fix(clock);
fprintf(fid,['Date: ',date,' \r']);
```

```
fprintf(fid,['Time: ',num2str(timedata(4)),':',...
                        num2str(timedata(5)),' \r\r']);
fprintf(fid,'Model Inputs\r');
fprintf(fid,'============\r');
fprintf(fid,['Methane Through Burner: ',num2str(NG_in),' kg/hr\r']);
fprintf(fid,['Coal: ',num2str(COAL*3600),' kg/hr\r']);
if COAL_Type == 1
    fprintf(fid,'Coal Name: Wyoming Subbituminous\r');
elseif COAL_Type == 2
    fprintf(fid,'Coal Name: Illinois #6\r');
elseif COAL_Type == 3
    fprintf(fid,'Coal Name: Pittsburgh #8\r');
end
fprintf(fid,['Burner Air: ',num2str(Air_in),' kg/hr\r']);
fprintf(fid,['Burner Bottled O2: ',num2str(O2_in),' kg/hr\r']);
fprintf(fid,['Burner Bottled CO2: ',num2str(CO2_in),' kg/hr\r']);
fprintf(fid,['Burnout Air: ',num2str((Air_in/Primary)*(1-Primary)),...
                                                        ' kg/hr\r']);
fprintf(fid,['Burnout Bottled O2: ',...
                       num2str((O2_in/Primary)*(1-Primary)),' kg/hr\r']);
fprintf(fid,['Burnout Bottled CO2: ',...
                      num2str((CO2_in/Primary)*(1-Primary)),' kg/hr\r']);
fprintf(fid,['NO in CO2: ',num2str(NO_doping),' ppm\r']);

fprintf(fid,['Initial Gas Temperature: ',num2str(T1),' K\r']);
fprintf(fid,['Burnout Oxidizer Temperature: ',num2str(T2),' K\r']);
fprintf(fid,['Pressure: ',num2str(press),' atm\r\r']);
if mechanism == 1
    fprintf(fid,'Gas Phase Mechanism: GRI 3.0\r');
elseif mechanism == 2
    fprintf(fid,'Gas Phase Mechanism: GRI 3.0 + B96\r');
elseif mechanism == 3
    fprintf(fid,'Gas Phase Mechanism: SKG03\r');
end
if thermal == 0
    fprintf(fid,'Thermal NOx Mechanism Disabled\r');
elseif thermal == 1
    fprintf(fid,'Thermal NOx Mechanism Enabled\r');
end
if prompt == 0
    fprintf(fid,'Prompt NOx Mechanism Disabled\r\r');
elseif prompt == 1
    fprintf(fid,'Prompt NOx Mechanism Enabled\r\r');
end
if gasification == 0
    fprintf(fid,'Char gasification by CO2 Disabled\r\r');
elseif gasification == 1
    fprintf(fid,'Char gasification by CO2 Enabled\r\r');
end
fprintf(fid,['Percent of O2 Char Oxidation Energy to Char: ',...
             num2str(Q_reactO2_x),'\r']);
fprintf(fid,['Percent of CO2 Char Gasification Energy from Char: ',...
             num2str(Q_reactCO2_x),'\r\r']);
fprintf(fid,['Burner Emissivity: ',num2str(emiss(1)),'\r']);
fprintf(fid,['Reactor Wall Emissivity: ',num2str(emiss(2)),'\r']);
fprintf(fid,['Exhaust Tube Emissivity: ',num2str(emiss(3)),'\r']);
fprintf(fid,['Coal Particle Emissivity: ',num2str(emiss(4)),'\r']);
fprintf(fid,['Burner Temperature: ',num2str(tbnr),' K\r']);
fprintf(fid,['Exhaust Tube Temperature: ',num2str(texit),' K\r']);
fprintf(fid,'Reactor Wall Temperature Profile (m, K):\r');
for i = 1:length(WallX)
   fprintf(fid,[num2str(WallX(i)),'\t',num2str(twallvector(i)),'\r']);
end
fprintf(fid,['\rk_wall ',...
               '(Empirical Wall Thermal Conductivity Parameter): ',...
                       num2str(k_wall),'\r']);
fprintf(fid,['\rCoal Ultimate Analysis: (DAF wt%%)\r',...
                              'C: ',num2str(yelem(1)*100),...
                            '\rH: ',num2str(yelem(2)*100),...
                            '\rN: ',num2str(yelem(3)*100),...
                            '\rO: ',num2str(yelem(4)*100),...
```

```
                            '\rS: ',num2str(yelem(5)*100),...
                            ' (Not used in model)\r\r']);
fprintf(fid,['Coal Moisture Content (as received): ',...
                                          num2str(omegaw*100),'%%\r']);
fprintf(fid,['Coal Ash Content (as received): ',...
                                          num2str(omegaa*100),'%%\r']);
if ASTMvol ~= 0
    fprintf(fid,['ASTM Volatiles (DAF): ',num2str(ASTMvol),' %%\r\r']);
    fprintf(fid,'Estimated C13 NMR Parameters for Coal:\r');
    fprintf(fid,['mw1: ',num2str(mw1),'\r']);
    fprintf(fid,['p0: ',num2str(p0),'\r']);
    fprintf(fid,['c0: ',num2str(c0),'\r']);
    fprintf(fid,['sigp1: ',num2str(sigp1),'\r']);
    fprintf(fid,['mdel: ',num2str(mdel),'\r\r']);
else
    fprintf(fid,'\r\r\rC13 NMR Parameters for Coal:\r');
    fprintf(fid,['mw1: ',num2str(mw1),'\r']);
    fprintf(fid,['p0: ',num2str(p0),'\r']);
    fprintf(fid,['c0: ',num2str(c0),'\r']);
    fprintf(fid,['sigp1: ',num2str(sigp1),'\r']);
    fprintf(fid,['mdel: ',num2str(mdel),'\r\r']);
end

fprintf(fid,['Initial Particle Apparent Density: ',num2str(rhop),...
                                                        ' g/cm^3\r']);
fprintf(fid,['Initial Particle Diameter: ',num2str(dp*1e4),' um\r']);
fprintf(fid,['Swelling Factor: ',num2str(swell),'\r\r']);
fprintf(fid,'Gas species are reported as mass fractions below.\r\r');

% write molecular weights of species to output file for easy conversion
% from mass fractions to mole fractions with a spreadsheet
fprintf(fid,'\t\tMolecular Weight of Species (kg/kmol):');
MW = molarMasses(gas(1));
for i = 1:nSpecies(gas(1))
    fprintf(fid,strcat('\t%d'),MW(i));
end
fprintf(fid,'\r');

fprintf(fid,['Axial Position (m)\tGas Temperature (K)\t',...
             'Gas Pressure (Pa)\t']);

for i = 1:nSpecies(gas(1))
    text = speciesName(gas(1),i);
    fprintf(fid,'%s\t',text{1,1});
end

fprintf(fid,['Gas Mass Flow (kg/s)\tResidence Time (ms)',...
             '\tParticle Temperature (K)\tfvol\tfchar\tfcross\tftar\t',...
             'fmet\t Trate\tMW\tNsite\tNchar\tfnchar\tfntar\tfnhcn\t',...
             'fntot\tfgas\tfH2O\tfCO2\tfCH4\tfCO\tfOth',...
             '\tyH2O\tyCO2\tyCH4\tyCO\tyOther\tXgas\tCoal Moisture %%',...
             '\tO2 Consumptionby Char (kg/s)',...
             '\tCO2 Consumption by Char (kg/s)\tDAF Char Flux (kg/s)',...
             '\tGas Phase Chemical Equivalence Ratio',...
             '\tNOx (ppm, excluding H2O)\tCO (ppm, excluding H2O)',...
             '\tO2 (vol%%, excluding H2O)\tCO2 (vol%%, excluding H2O)',...
             '\tNitrogen Conversion Efficiency\tMW of Gas mixture',...
             '\tParticle Diameter (um)\r']);

% write model predictions from ignition section of MFR
i = 1;
fprintf(fid,strcat('%d\t %d\t %d\t'),position(i),tgas(i),...
                                          pressurevector(i));
for j = 1:nSpecies(gas(1))
    fprintf(fid,'%d\t',massFraction(upstream(1),speciesName(gas(1),j)));
end

fprintf(fid,strcat('%d\t %d\t %d\t %d\t %d\t %d\t %d\t %d\t %d\t',...
                   '%d\t %d\t %d\t %d\t %d\t %d\t %d\t %d\t %d\t',...
                   '%d\t %d\t %d\t %d\t %d\t %d\t %d\t %d\t %d\t',...
                   '%d\t %d\t\t\t\t %d\t %d\t %d\t %d\t %d\t',...
```

```
                    '%d\t %d\t %d\r'),...
                    m_dot(i),tms(i),tp(i),fvol(i),fchar(i),fcross(i),...
                    ftar(i),fmet(i),trate(i),mwchar(i),yNsite(i),...
                    fnt(i),fnchar(i),fntar(i),fnhcn(i),fntot(i),...
                    fgas(i),ffgas(1,i),ffgas(2,i),ffgas(3,i),...
                    ffgas(4,i),ffgas(5,i),...
                    yygas(1,i),yygas(2,i),yygas(3,i),yygas(4,i),...
                    yygas(5,i),yf(i),water(i)*100,r(i),NOx_ppm_dry(i),...
                    CO_ppm_dry(i),O2_vol_dry(i),CO2_vol_dry(i),NCE(i),...
                    MWmix(i),dpout(i)*10000);

for i = 2:number_reactors+1
    fprintf(fid,strcat('%d\t %d\t %d\t'),position(i),tgas(i),...
                                            pressurevector(i));
    for j = 1:nSpecies(gas(1))
        fprintf(fid,'%d\t',massFraction(cstr(i-1),speciesName(gas(1),j)));
    end

    fprintf(fid,strcat('%d\t %d\t %d\t %d\t %d\t %d\t %d\t %d\t %d\t',...
                       '%d\t %d\t %d\t %d\t %d\t %d\t %d\t %d\t %d\t',...
                       '%d\t %d\t %d\t %d\t %d\t %d\t %d\t %d\t %d\t',...
                       '%d\t %d\t\t\t\t %d\t %d\t %d\t %d\t %d\t %d\t',...
                       '%d\t %d\r'),...
                       m_dot(i-1),tms(i),tp(i),fvol(i),fchar(i),...
                       fcross(i),ftar(i),fmet(i),trate(i),mwchar(i),...
                       yNsite(i),fnt(i),fnchar(i),fntar(i),fnhcn(i),...
                       fntot(i),fgas(i),ffgas(1,i),ffgas(2,i),...
                       ffgas(3,i),ffgas(4,i),ffgas(5,i),yygas(1,i),...
                       yygas(2,i),yygas(3,i),yygas(4,i),yygas(5,i),...
                       yf(i),water(i)*100,r(i),NOx_ppm_dry(i),...
                       CO_ppm_dry(i),O2_vol_dry(i),CO2_vol_dry(i),...
                       NCE(i),MWmix(i),dpout(i)*10000);
end

%---BEGINNING OF POST-IGNITION MODEL-----------------------------------------
% set up CSTR and initial conditions
i = number_reactors + 1;  % i is the variable that keeps track of the
                          % CSTR number from now on.
if mechanism == 1
    maingas = GRI30('Mix');
elseif mechanism == 2
    maingas = GRI30_B96('Mix');
elseif mechanism == 3
    maingas = SKG03;
end

if mechanism == 3
    % set multiplier for Thermal NOx Mechanism
    setMultiplier(maingas,74,thermal);
    setMultiplier(maingas,73,thermal);
    setMultiplier(maingas,72,thermal);
    % set multiplier for Prompt NOx Fenimore Mechanism
    setMultiplier(maingas,507,prompt);
    setMultiplier(maingas,503,prompt);
else
    % set multiplier for Thermal NOx Mechanism
    setMultiplier(maingas,178,thermal);
    setMultiplier(maingas,179,thermal);
    setMultiplier(maingas,180,thermal);
    % set multiplier for Prompt NOx Fenimore Mechanism
    setMultiplier(maingas,239,prompt);
    setMultiplier(maingas,240,prompt);
end

ExistingGas = m_dot(i-1)*massFractions(gas(i-1));
% get the gases to be added into kg/s units:
AddedGas = zeros(size(ExistingGas));
AddedGas(H2OIndex) = ffgas2(1,i)*(fvol(i)-fvol(i-1))*...
                     COAL*(1-omegaa-omegaw)+...
                     (water(i-1)-water(i))*COAL;
                     % H2O (light gas) and evaporated moisture
```

```
AddedGas(CO2Index) = ffgas2(2,i)*(fvol(i)-fvol(i-1))*...
                     COAL*(1-omegaa-omegaw); % CO2
AddedGas(CH4Index) = ffgas2(3,i)*(fvol(i)-fvol(i-1))*...
                     COAL*(1-omegaa-omegaw); % CH4
AddedGas(COIndex) = ffgas2(4,i)*(fvol(i)-fvol(i-1))*...
                    COAL*(1-omegaa-omegaw); % CO
AddedGas(C2H2Index) = ffgas2(5,i)*(fvol(i)-fvol(i-1))*...
                      COAL*(1-omegaa-omegaw); % C2H2
AddedGas(HCNIndex) = ffgas2(6,i)*(fvol(i)-fvol(i-1))*...
                     COAL*(1-omegaa-omegaw); % HCN

m_dot(i) = m_dot(i-1) + ...
           (fvol(i)-fvol(i-1))*COAL*(1-omegaa-omegaw) - ...
            COAL*(water(i)-water(i-1));

% add the two compositions from above and insert the gas
% into the next reactor (Heat transfer for volatiles to be
% added to code later)
mixture = ExistingGas + AddedGas;
% lower enthalpy of gas to account for heating of particles
% by convection
H = enthalpy_mass(gas(i-1)); %J/kg
% convheat is in J/particle per second
H = H - (0.5*(convheat(i)+convheat(i-1)))*...
         particles*(1/1000)*(tms(i)-tms(i-1))/(m_dot(i-1));
set(maingas,'H',H,'P',P,'MassFractions',mixture);

% clear old objects from ignition section:
clear upstream gas mfc cstr v downstream exhaust gw w network
% create new reactor network objects for this section of code:
% follows same procedure as above code
upstream = Reservoir(maingas);
insert(upstream,maingas);
cstr = Reactor(maingas);
setInitialVolume(cstr,Volume(end));
w = Wall;
install(w,cstr,env);
setArea(w,pi*d*Length);
R = log(0.180/(d/2))/(2*pi*Length*k_wall);
setThermalResistance(w,R);
mfc = MassFlowController;
install(mfc,upstream,cstr);
setMassFlowRate(mfc,m_dot(end));
exhaust = air;
set(exhaust,'T',300,'P',P);
downstream = Reservoir(exhaust);
v = Valve;
install(v,cstr,downstream);
setValveCoeff(v,1.0);
network_cell_array = {cstr};
network = ReactorNet(network_cell_array);

% start loop for reactors
tme = 0;
devol_incomplete = true;
while devol_incomplete
    i = i + 1 %#ok<NOPTS>
    position(i) = position(i-1) + Length;

    % integrate the CSTR long enough to reach steady state
    count = 1;
    old_T = temperature(cstr);
    delta_T = 1;
    while (delta_T > tolerance) || (count < 3)
        tme = tme + dt;
        advance(network, tme);
        new_T = temperature(cstr);
        delta_T = abs(new_T-old_T);
        old_T = new_T;
        count = count + 1;
    end
```

```
% update last point in output data variables
tfilm = 0.5*(tp + tgas);
tgas(i) = temperature(maingas);
pressurevector(i) = pressure(maingas);

% calculate/estimate properties required for CPD model
velocity(i) = m_dot(i-1)/(density(upstream)*Area);
rhogas(i) = density(upstream);
xwbvector(i) = moleFraction(maingas,'H2O');
set(dummygas,'T',tfilm(i-1),'P',P,'Y',massFractions(upstream));
ugvector(i) = viscosity(dummygas);
kgvector(i) = thermalConductivity(dummygas);
DiffCoeffs = mixDiffCoeffs(dummygas);
diffwvector(i) = DiffCoeffs(H2OIndex);
           % Mixture-averaged diffusion coefficient (m^2/s) for water
clear DiffCoeffs;
cpgvector(i) = cp_mass(dummygas);
prgas(i) = ugvector(i)*cpgvector(i)/kgvector(i);

% Call the CPD model
[tms,xm,tp,tg,fvol,fchar,fcross,ftar,fmet,trate,mwchar,yNsite,...
   fnt,fnchar,fntar,fnhcn,fntot,fgas,ffgas,yygas,yf,water,convheat,...
   dpout] = cpdcp_nlg(twallvector,tbnr,texit,timax,yelem,mw1,p0,c0,...
   sigp1,mdel,position*100,tgas,position*100,velocity*100,press,...
   tgas(1),velocity(1)*100,rhop,dp,swell,omegaw,omegaa,...
   rhogas/1000,xwbvector,ugvector*10,kgvector/418.4,...
   diffwvector*0.01^2,cpgvector*2.38846e-4,prgas,emiss,d*50,WallX*100);

% check if devolatilization is complete
if ((fvol(i)- fvol(i-1)) <= 1e-4) && (fvol(i) > 0.4)
    devol_incomplete = false;
end

% Add the products of devolatilization to the CSTR products
m_dot(i) = m_dot(i-1) + ...
           (fvol(i)-fvol(i-1))*COAL*(1-omegaa-omegaw) - ...
           COAL*(water(i)-water(i-1));
setMassFlowRate(mfc,m_dot(i));

Cgoal(i) = COAL*(1-omegaa-omegaw)*yelem(1)*fvol(i)...
                            -Cgoal(i-1);

Hgoal(i) = COAL*(1-omegaa-omegaw)*yelem(2)*...
                       ((-0.5597)*fvol(i)^2 + 1.5651*fvol(i))...
                            -Hgoal(i-1);

C_nlg(i) = ffgas(2,i)*fvol(i)*COAL*(1-omegaa-omegaw)*...
           (12.011/(12.011+2*15.999))+...  % CO2
           ffgas(3,i)*fvol(i)*COAL*(1-omegaa-omegaw)*...
           (12.011/(12.011+4*1.0079))+...  % CH4
           ffgas(4,i)*fvol(i)*COAL*(1-omegaa-omegaw)*...
           (12.011/(12.011+15.999))+...    % CO
           fntot(i)*yelem(3)*COAL*(1-omegaa-omegaw)*...
           (12.011/14.007)-...             % HCN
           C_nlg(i-1);

H_nlg(i) = ffgas(1,i)*fvol(i)*COAL*(1-omegaa-omegaw)*...
           (2*1.0079/(2*1.0079+15.999))+... % H2O
           ffgas(3,i)*fvol(i)*COAL*(1-omegaa-omegaw)*...
           (4*1.0079/(12.011+4*1.0079))+... % CH4
           fntot(i)*yelem(3)*COAL*(1-omegaa-omegaw)*...
           (1.0079/14.007)-...              % HCN
           H_nlg(i-1);

Cdiff = Cgoal - C_nlg;
Hdiff = Hgoal - H_nlg;

CHratio = (Cdiff/12.011)./(Hdiff/1.0079);

MolarProportionCH4 = (CHratio(i)-1)/(0.25-1);
```

```
MWunknowns = MolarProportionCH4*(12.011+4*1.0079)+...
            (1-MolarProportionCH4)*2*(12.011+1.0079);
MassProportionCH4 = MolarProportionCH4*(12.011+4*1.0079)/...
                  MWunknowns; % in other light gas and tar


% The ffgas array is now modifed and becomes ffgas2
% which has these species in its rows:
% H2O, CO2, CH4, CO, C2H2, and HCN. After this there are no
% volatiles of unestimated composition.
ffgas2(1,i) = ffgas(1,i); % H2O
                        % (excludes evaporated moisture)

ffgas2(2,i) = ffgas(2,i); % CO2

ffgas2(4,i) = ffgas(4,i); % CO
ffgas2(6,i) = (fntot(i)*COAL*(1-omegaa-omegaw)*yelem(3)*...
             (1.0079+12.011+14.007)/(14.007))/...
             (COAL*(1-omegaa-omegaw)*fvol(i)); % HCN

ffgas2(3,i) = ffgas(3,i) + ...
   (MassProportionCH4*(ffgas(5,i))*COAL*(1-omegaa-omegaw))/...
   (fvol(i)*COAL*(1-omegaa-omegaw));  % CH4

ffgas2(5,i) = 1-(ffgas2(6,i)+sum(ffgas2(1:4,i)));
                  % C2H2 (by difference)

ExistingGas = m_dot(i-1)*massFractions(maingas);

% get the gases to be added into kg/s units:
AddedGas = zeros(size(ExistingGas));
AddedGas(H2OIndex) = ffgas2(1,i)*(fvol(i)-fvol(i-1))*...
                     COAL*(1-omegaa-omegaw)+...
                     (water(i-1)-water(i))*COAL;
                     % H2O (light gas) and evaporated moisture
AddedGas(CO2Index) = ffgas2(2,i)*(fvol(i)-fvol(i-1))*...
                     COAL*(1-omegaa-omegaw); % CO2
AddedGas(CH4Index) = ffgas2(3,i)*(fvol(i)-fvol(i-1))*...
                     COAL*(1-omegaa-omegaw); % CH4
AddedGas(COIndex) = ffgas2(4,i)*(fvol(i)-fvol(i-1))*...
                    COAL*(1-omegaa-omegaw); % CO
AddedGas(C2H2Index) = ffgas2(5,i)*(fvol(i)-fvol(i-1))*...
                      COAL*(1-omegaa-omegaw); % C2H2
AddedGas(HCNIndex) = ffgas2(6,i)*(fvol(i)-fvol(i-1))*...
                     COAL*(1-omegaa-omegaw); % HCN

% add the two compositions from above and insert the gas
% into the next reactor (Heat transfer for volatiles to be
% added to code later - ie heat brought into gas by volatiles
mixture = ExistingGas + AddedGas;
% lower enthalpy of gas to account for heating of particles
% by convection
H = enthalpy_mass(maingas); %J/kg
% convheat is in J/particle per second
H = H - (0.5*(convheat(i)+convheat(i-1)))*...
         particles*(1/1000)*(tms(i)-tms(i-1))/(m_dot(i-1));
set(maingas,'H',H,'P',P,'MassFractions',mixture);
insert(upstream,maingas);

% Calculate chemical equivalence ratio for reactor i
MWmix(i) = meanMolarMass(maingas);
nj = (1/MWmix(i))*moleFractions(maingas);
for k = 1:4
    bi(k) = sum(aij(:,k).*nj);
end
V_p = sum(V_plus.*bi);
V_m = sum(V_minus.*bi);
r(i) = -V_p/V_m;

Xi = moleFractions(maingas);
XWater = Xi(H2OIndex);
```

```
    XNO = Xi(NOIndex);
    XNO2 = Xi(NO2Index);
    XCO = Xi(COIndex);
    XO2 = Xi(O2Index);
    XCO2 = Xi(CO2Index);

    NOx_ppm_dry(i) = 1000000*(XNO + XNO2)/(1-XWater);
    CO_ppm_dry(i) = 1000000*XCO/(1-XWater);
    O2_vol_dry(i) = 100*XO2/(1-XWater);
    CO2_vol_dry(i) = 100*XCO2/(1-XWater);

    Yi = massFractions(maingas);
    YNO = Yi(NOIndex);
    YNO2 = Yi(NO2Index);
    NCE(i) = (YNO*(14.007/(14.007+15.999))+...
             YNO2*(14.007/(14.007+2*15.999)))*...
             m_dot(i-1)/(COAL*(1-omegaa-omegaw)*yelem(3));

    % Output data point to file
    fprintf(fid,strcat('%d\t %d\t %d\t'),position(i),tgas(i),...
                                              pressurevector(i));
    for j = 1:nSpecies(maingas)
        fprintf(fid,'%d\t',massFraction(cstr,speciesName(maingas,j)));
    end

    fprintf(fid,strcat('%d\t %d\t %d\t %d\t %d\t %d\t %d\t %d\t %d\t',...
                       '%d\t %d\t %d\t %d\t %d\t %d\t %d\t %d\t %d\t',...
                       '%d\t %d\t %d\t %d\t %d\t %d\t %d\t %d\t %d\t',...
                       '%d\t %d\t\t\t\t %d\t %d\t %d\t %d\t %d\t %d\t',...
                       '%d\t %d\r'),...
                       m_dot(i-1),tms(i),tp(i),fvol(i),fchar(i),...
                       fcross(i),ftar(i),fmet(i),trate(i),mwchar(i),...
                       yNsite(i),fnt(i),fnchar(i),fntar(i),fnhcn(i),...
                       fntot(i),fgas(i),ffgas(1,i),ffgas(2,i),...
                       ffgas(3,i),ffgas(4,i),ffgas(5,i),yygas(1,i),...
                       yygas(2,i),yygas(3,i),yygas(4,i),yygas(5,i),...
                       yf(i),water(i)*100,r(i),NOx_ppm_dry(i),...
                       CO_ppm_dry(i),O2_vol_dry(i),CO2_vol_dry(i),...
                       NCE(i),MWmix(i),dpout(i)*10000);
end

% Update particle diameter to account for swelling during devolatilization
dp = dpout(end);
m_dot(i) = m_dot(i-1);

% Calculate mass flux of DAF CHAR (kg/s) and ASHratio (kg_ash/kg_DAF_CHAR)
% in the CHAR
% (Char is assumed C(s) for remainder of code)
% (Ash percentage in char is assumed to remain constant - shrinking core
% model - ash assumed shed from surface of char as char reacts)
CHAR = COAL*(1-omegaa-omegaw)*fchar(i);
ASHratio = COAL*omegaa/(CHAR);

% Calculate density of char (including ash) - this remains constant in the
% shrinking core model employed by Goetz et al. in their data reduction
% (according to Smith and Smoot)
% kg/m^3
rhoCHAR = (COAL*(1-omegaw)*fchar(i))/(particles*((4/3)*pi*(dp/200)^3));
% (dp in cm)

% Post-devolatilization model (prior to burnout oxidizer addition)
% Models char (C(s)) oxidation and gasification by O2 and CO2 respectively

% Set kinetic constants for the char (Values from Goetz et al. (1982) as
% presented in "Coal Combustion and Gasification" Chapter 4 by Smoot and
% Smith)
gas_const = 1.987; % cal/gmol.K
sigma = 1.335e-12; % cal/s cm^2 K^4 radiation constant

% Get vector of wall temps (interpolated from measurements in input file)
max_position = WallX(end);
```

```
max_index = floor(max_position/Length);
j = 1;
Current_position = 0;
twall = zeros(1,max_index);
for k = 1:max_index
    twall(k) = ((Current_position-WallX(j))/(WallX(j+1)-WallX(j)))*...
                (twallvector(j+1)-twallvector(j))+twallvector(j);

    Current_position = Current_position + Length;

    % Update interpolation index if necessary
    if (Current_position > WallX(j+1))
            j = j + 1;
    end
 end

if COAL_Type == 1
    AO2 = 145; % g/(cm2s atmO2)
               %Units are g/s of O2 consumed per unit char external surface
               %area per atmosphere of O2 partial pressure
    EAO2 = 19970; % cal/gmole (units to match R units)
    ACO2 = 1040*gasification; % g/(cm2s atmCO2)
    EACO2 = 42470; % cal/gmole
elseif COAL_Type == 2
    AO2 = 60; % g/(cm2s atmO2)
               %Units are g/s of O2 consumed per unit char external surface
               %area per atmosphere of O2 partial pressure
    EAO2 = 17150; % cal/gmole (units to match R units)
    ACO2 = 12973*gasification; % g/(cm2s atmCO2)
    EACO2 = 56368; % cal/gmole

elseif COAL_Type == 3
    AO2 = 66; % g/(cm2s atmO2)
               %Units are g/s of O2 consumed per unit char external surface
               %area per atmosphere of O2 partial pressure
    EAO2 = 20360; % cal/gmole (units to match R units)
    ACO2 = 1390*gasification; % g/(cm2s atmCO2)
    EACO2 = 53700; % cal/gmole
end
% C(s) + O2 -> CO
% C(s) + CO2 -> 2CO   (This reaction may be disabled by setting
%                      gasification = 0)

if mechanism == 1
    chargas = GRI30('Mix');
elseif mechanism == 2
    chargas = GRI30_B96('Mix');
elseif mechanism == 3
    chargas = SKG03;
end

while (position(end) < 0.667)
    i = i + 1 %#ok<NOPTS>
    position(i) = position(i-1) + Length;

    % Calculate surface area of particles in previous reactor section
    if CHAR < 0
        A_char = 0;
    else
        A_char = particles*(tms(i-1)-tms(i-2))*(0.001)*4*pi*(dp/2)^2; %cm^2
    end
    % Calculate rate of oxidizer consumption in previous reactor section
    % kp units: g of oxidizer consumed per second per unit char surface
    %           area (in cm^2) per atm of oxidizer
    kpO2 = AO2*exp(-EAO2/(gas_const*tp(i-1)));
    kpCO2 = ACO2*exp(-EACO2/(gas_const*tp(i-1)));

    % rpo units: kg/s oxidizer consumed (in previous reactor section)
    % Minimum of:
    %  1. oxidizer consumption predicted by kinetic rate
    %  2. oxidizer available
```

```
ExistingGas = m_dot(i-1)*massFractions(maingas); % kg/s
AddedGas = zeros(size(ExistingGas));
rpoO2 = min([0.001*kpO2*A_char*moleFraction(maingas,'O2')*P/101325;
             ExistingGas(O2Index)]); % kg/s
rpoCO2 = min([0.001*kpCO2*A_char*moleFraction(maingas,'CO2')*P/101325;
              ExistingGas(CO2Index)]); % kg/s

% Particle heating from convection and radiation (and some fraction of
% heat of char reaction)
% Estimated heat capacity of the char (using same methods as CPD model)
% get daf coal heat capacity
[cpc] = heatcp(tp(i-1),yelem);  % cal/g/K
% get ash heat capacity
[cpa] = heatap(tp(i-1));  % cal/g/K
% combine heat capacities
cp = (CHAR*cpc + (ASHratio*CHAR)*cpa)/(CHAR*(1+ASHratio));
% convert to J/kg/K
cp = cp*4186.8;
% Radiation heat exchange with reactor walls (copied from CPD function
% and therefore has cm, cal, g units
z = position(i)*100;  % distance from burner (cm)
        % distance from exhaust will be (200-z) because reactor is 2m
        % long
% set up areas, etc of radiation enclosure
A(1) = pi*(d*50)^2; % burner (Area vector = same order as emiss vector)
A(2) = 2*pi*(d*50)*200; % walls
A(3) = A(1); % exhaust
A(4) = A_char; % particles
Temp(1) = tbnr;
Temp(2) = twall(i-1);
Temp(3) = texit;
Temp(4) = tp(i-1);
F(4,1) = 0.5*(1-(1/(1+((d*50)/z)^2)^0.5)); %disk to sphere view factor
F(4,3) = 0.5*(1-(1/(1+((d*50)/(200-z))^2)^0.5)); %same as above
F(4,2) = 1 - (F(4,1) + F(4,3)); % by summation rule
% by reciprocity:
    F(1,4) = F(4,1)*A(4)/A(1);
    F(2,4) = F(4,2)*A(4)/A(2);
    F(3,4) = F(4,3)*A(4)/A(3);

qrad = emiss(4)*( F(1,4)*A(1)*emiss(1)*sigma*Temp(1)^4+...
                  F(2,4)*A(2)*emiss(2)*sigma*Temp(2)^4+...
                  F(3,4)*A(3)*emiss(3)*sigma*Temp(3)^4-...
                         A(4)*sigma*Temp(4)^4); % cal/s


Q_rad = qrad*4.1868; % J/s
% Convection heat exchange with the gas
nu = 2;  % Assumes entrained particles - Reynolds number is zero
rtot = 1000*(rpoO2*12.011/31.998 + rpoCO2*12.011/44.009);
b = cp_mass(maingas)*2.38846e-4*(rtot)/...
    (2.0*pi*dp*thermalConductivity(maingas)/418.4);
if (b >= 1.e-4)
    blow = b/(exp(b)-1);
else
    blow = 1.0;
end
h = blow*nu*(thermalConductivity(maingas)/418.4)/dp;
qconv = h*A_char*(tgas(i-1)-tp(i-1)); % cal/s
Q_conv = qconv*4.1868; % J/s
% Some fraction (Q_react_x) of Heat released by reaction
% 6908557 J/kg_O2 for 2C(s) + O2 -> 2CO
% -3918744 J/kg_CO2 for C(s) + CO2 -> 2CO (negative means endothermic)
% Assume some fraction of heat goes into char, char temp will be
% adjusted and CO is released at the new particle temperature for
% mixing with the gas phase
Q_react = Q_reactO2_x*(6908557*rpoO2) -...
          Q_reactCO2_x*(3918744*rpoCO2); % J/s
Q_total = Q_rad + Q_conv + Q_react; % J/s
tp(i) = tp(i-1) + (Q_total/(CHAR+COAL*omegaa))/cp;
```

```
% Remove consumed oxidizer from maingas and add products (CO) at
% particle temperature

% Heat released to the CO product gas by reaction
Q_react = (1-Q_reactO2_x)*(6908557*rpoO2) -...
          (1-Q_reactCO2_x)*(3918744*rpoCO2); % J/s
AddedGas(COIndex) = 2*rpoO2*28.01/31.998+2*rpoCO2*28.01/44.009; %kgCO/s
set(chargas,'T',tp(i),'P',P,'MassFractions',AddedGas);
H_in = enthalpy_mass(chargas)*sum(AddedGas)+Q_react; % J/s
AddedGas(COIndex) = 0;
AddedGas(O2Index) = rpoO2;
AddedGas(CO2Index) = rpoCO2;
set(chargas,'T',tgas(i-1),'P',P,'MassFractions',AddedGas);
H_out = enthalpy_mass(chargas)*sum(AddedGas); % J/s
H_old = enthalpy_mass(maingas)*sum(ExistingGas); % J/s
AddedGas(COIndex) = 2*rpoO2*28.01/31.998 + 2*rpoCO2*28.01/44.009;
AddedGas(O2Index) = -rpoO2;
AddedGas(CO2Index) = -rpoCO2;
mixture = AddedGas + ExistingGas; % kg/s
H_new = (H_old + H_in - H_out)/sum(mixture); % J/kg
if CHAR < 0
    % do nothing
else
    set(maingas,'H',H_new,'P',P,'MassFractions',mixture);
end
insert(upstream,maingas);

% Remove C(s) mass from char and update gas mass flow rate and particle
% diameter
CHAR = CHAR - (rpoO2*2*12.011/31.998 + rpoCO2*12.011/44.009); % kgC/s
m_dot(i) = sum(mixture);
setMassFlowRate(mfc,m_dot(i));
dp = 200*(((3/(4*pi))*CHAR*(1+ASHratio)/(particles*rhoCHAR))^(1/3));

% integrate the CSTR long enough to reach steady state
count = 1;
old_T = temperature(cstr);
delta_T = 1;
while ((delta_T > tolerance) || (count < 3)) && (count < 10000)
    tme = tme + dt;
    advance(network, tme);
    new_T = temperature(cstr);
    delta_T = abs(new_T-old_T);
    old_T = new_T;
    count = count + 1;
end
count %#ok<NOPTS>
% update last point in output data variables
tgas(i) = temperature(maingas);
pressurevector(i) = pressure(maingas);

velocity(i) = m_dot(i-1)/(density(upstream)*Area);
tms(i) = tms(i-1) + 1000*(Length/velocity(i));
% Calculate chemical equivalence ratio for reactor i
MWmix(i) = meanMolarMass(maingas);
nj = (1/MWmix(i))*moleFractions(maingas);
for k = 1:4
    bi(k) = sum(aij(:,k).*nj);
end
V_p = sum(V_plus.*bi);
V_m = sum(V_minus.*bi);
r(i) = -V_p/V_m;

Xi = moleFractions(maingas);
XWater = Xi(H2OIndex);
XNO = Xi(NOIndex);
XNO2 = Xi(NO2Index);
XCO = Xi(COIndex);
XO2 = Xi(O2Index);
XCO2 = Xi(CO2Index);
```

```
    NOx_ppm_dry(i) = 1000000*(XNO + XNO2)/(1-XWater);
    CO_ppm_dry(i) = 1000000*XCO/(1-XWater);
    O2_vol_dry(i) = 100*XO2/(1-XWater);
    CO2_vol_dry(i) = 100*XCO2/(1-XWater);

    Yi = massFractions(maingas);
    YNO = Yi(NOIndex);
    YNO2 = Yi(NO2Index);
    NCE(i) = (YNO*(14.007/(14.007+15.999))+YNO2*...
             (14.007/(14.007+2*15.999)))*...
             m_dot(i-1)/(COAL*(1-omegaa-omegaw)*yelem(3));
    % Output data point to file
    fprintf(fid,strcat('%d\t %d\t %d\t'),position(i),tgas(i),...
                                            pressurevector(i));

    for j = 1:nSpecies(maingas)
        fprintf(fid,'%d\t',massFraction(cstr,speciesName(maingas,j)));
    end

    fprintf(fid,strcat('%d\t %d\t %d\t\t\t\t\t\t\t\t\t\t\t\t\t\t\t\t\t\t',...
                       '\t\t\t\t\t\t\t\t\t\t %d\t %d\t %d\t %d\t',...
                       '%d\t %d\t %d\t %d\t %d\t %d\t %d\r'),...
                      m_dot(i-1),tms(i),tp(i),rpoO2,rpoCO2,CHAR,r(i),...
                      NOx_ppm_dry(i),CO_ppm_dry(i),O2_vol_dry(i),...
                      CO2_vol_dry(i),NCE(i),MWmix(i),dp*10000);
end

% Final Code Section: Burnout Oxidizer Added for Char Burnout
% (instant or intense mixing is assumed)
ExistingGas = m_dot(i-1)*massFractions(maingas); % kg/s
H_Primary = enthalpy_mass(maingas)*sum(ExistingGas); % J/s
AddedGas = zeros(size(ExistingGas));
AddedGas(O2Index) = (O2_in/Primary)*(1-Primary)+...
              0.232999715*(Air_in/Primary)*(1-Primary);
AddedGas(N2Index) = ((1-0.232999715)*(Air_in/Primary)+(N2_in/Primary))...
    *(1-Primary);
AddedGas(CO2Index) = (CO2_in/Primary)*(1-Primary);
if AddedGas(CO2Index) > 0
    AddedGas(NOIndex) = ((NO_doping/1000000)*(14.007+15.999)/...
                         (12.011+2*15.999))/AddedGas(CO2Index);
end
AddedGas = AddedGas/3600; % convert to kg/s
set(chargas,'T',T2,'P',P,'MassFractions',AddedGas);
H_Burnout = enthalpy_mass(chargas)*sum(AddedGas); % J/s
mixture = ExistingGas+AddedGas; % kg/s
H_new = (H_Primary + H_Burnout)/sum(mixture); % J/kg
set(maingas,'H',H_new,'P',P,'MassFractions',mixture);
m_dot(i) = sum(mixture);

while (position(end) < (WallX(end)-Length))
    i = i + 1 %#ok<NOPTS>
    position(i) = position(i-1) + Length;

    % Calculate area of particles in previous reactor section
    if CHAR < 0
        A_char = 0;
    else
        A_char = particles*(tms(i-1)-tms(i-2))*(0.001)*4*pi*(dp/2)^2; %cm^2
    end
    % Calculate rate of oxidizer consumption in previous reactor section
    % kp units: g of oxidizer consumed per second per unit char surface
    %           area (in cm^2) per atm of oxidizer
    kpO2 = AO2*exp(-EAO2/(gas_const*tp(i-1)));
    kpCO2 = ACO2*exp(-EACO2/(gas_const*tp(i-1)));

    % rpo units: kg/s oxidizer consumed (in previous reactor section)
    % Minimum of:
    %  1. oxidizer consumption predicted by kinetic rate
    %  2. oxidizer available
    ExistingGas = m_dot(i-1)*massFractions(maingas); % kg/s
    AddedGas = zeros(size(ExistingGas));
```

```
rpoO2 = min([0.001*kpO2*A_char*moleFraction(maingas,'O2')*P/101325;
             ExistingGas(O2Index)]); % kg/s
rpoCO2 = min([0.001*kpCO2*A_char*moleFraction(maingas,'CO2')*P/101325;
              ExistingGas(CO2Index)]); % kg/s

% Particle heating from convection and radiation (and some fraction of
% heat of char reaction)
% Estimated heat capacity of the char (using same methods as CPD model)
% get daf coal heat capacity
[cpc] = heatcp(tp(i-1),yelem);  % cal/g/K
% get ash heat capacity
[cpa] = heatap(tp(i-1));  % cal/g/K
% combine heat capacities
cp = (CHAR*cpc + (ASHratio*CHAR)*cpa)/(CHAR*(1+ASHratio));
% convert to J/kg/K
cp = cp*4186.8;
% Radiation heat exchange with reactor walls (copied from CPD function
% and therefore has cm, cal, g units)
z = position(i)*100;  % distance from burner (cm)
         % distance from exhaust will be (200-z) because reactor is 2m
         % long
% set up areas, etc of radiation enclosure
A(1) = pi*(d*50)^2; % burner (Area vector = same order as emiss vector)
A(2) = 2*pi*(d*50)*200; % walls
A(3) = A(1); % exhaust
A(4) = A_char; % particles
Temp(1) = tbnr;
Temp(2) = twall(i-1);
Temp(3) = texit;
Temp(4) = tp(i-1);
F(4,1) = 0.5*(1-(1/(1+((d*50)/z)^2)^0.5)); %disk to sphere view factor
F(4,3) = 0.5*(1-(1/(1+((d*50)/(200-z))^2)^0.5)); %same as above
F(4,2) = 1 - (F(4,1) + F(4,3)); % by summation rule
% by reciprocity:
    F(1,4) = F(4,1)*A(4)/A(1);
    F(2,4) = F(4,2)*A(4)/A(2);
    F(3,4) = F(4,3)*A(4)/A(3);

qrad = emiss(4)*( F(1,4)*A(1)*emiss(1)*sigma*Temp(1)^4+...
                  F(2,4)*A(2)*emiss(2)*sigma*Temp(2)^4+...
                  F(3,4)*A(3)*emiss(3)*sigma*Temp(3)^4-...
                         A(4)*sigma*Temp(4)^4); % cal/s

Q_rad = qrad*4.1868; % J/s
% Convection heat exchange with the gas
nu = 2;  % Assumes entrained particles - Reynolds number is zero
rtot = 1000*(rpoO2*12.011/31.998 + rpoCO2*12.011/44.009);
b = cp_mass(maingas)*2.38846e-4*(rtot)/...
    (2.0*pi*dp*thermalConductivity(maingas)/418.4);
if (b >= 1.e-4)
    blow = b/(exp(b)-1);
else
    blow = 1.0;
end
h = blow*nu*(thermalConductivity(maingas)/418.4)/dp;
qconv = h*A_char*(tgas(i-1)-tp(i-1)); % cal/s
Q_conv = qconv*4.1868; % J/s
% Some fraction (Q_react_x) of Heat released by reaction
% 6908557 J/kg_O2 for 2C(s) + O2 -> 2CO
% -3918744 J/kg_CO2 for C(s) + CO2 -> 2CO (negative means endothermic)
% Assume some fraction of heat goes into char, char temp will be
% adjusted and CO is released at the new particle temperature for
% mixing with the gas phase
Q_react = Q_reactO2_x*(6908557*rpoO2) -...
          Q_reactCO2_x*(3918744*rpoCO2); % J/s
Q_total = Q_rad + Q_conv + Q_react; % J/s
tp(i) = tp(i-1) + (Q_total/(CHAR+COAL*omegaa))/cp;

% Remove consumed oxidizer from maingas and add products (CO) at
% particle temperature
```

```
% Heat released to the CO product gas by reaction
Q_react = (1-Q_reactO2_x)*(6908557*rpoO2) -...
          (1-Q_reactCO2_x)*(3918744*rpoCO2); % J/s
AddedGas(COIndex) = 2*rpoO2*28.01/31.998+2*rpoCO2*28.01/44.009; %kgCO/s
set(chargas,'T',tp(i),'P',P,'MassFractions',AddedGas);
H_in = enthalpy_mass(chargas)*sum(AddedGas)+Q_react; % J/s
AddedGas(COIndex) = 0;
AddedGas(O2Index) = rpoO2;
AddedGas(CO2Index) = rpoCO2;
set(chargas,'T',tgas(i-1),'P',P,'MassFractions',AddedGas);
H_out = enthalpy_mass(chargas)*sum(AddedGas); % J/s
H_old = enthalpy_mass(maingas)*sum(ExistingGas); % J/s
AddedGas(COIndex) = 2*rpoO2*28.01/31.998 + 2*rpoCO2*28.01/44.009;
AddedGas(O2Index) = -rpoO2;
AddedGas(CO2Index) = -rpoCO2;
mixture = AddedGas + ExistingGas; % kg/s
H_new = (H_old + H_in - H_out)/sum(mixture); % J/kg
if CHAR < 0
    % do nothing
else
    set(maingas,'H',H_new,'P',P,'MassFractions',mixture);
end
insert(upstream,maingas);

% Remove C(s) mass from char and update gas mass flow rate and particle
% diameter
CHAR = CHAR - (rpoO2*2*12.011/31.998 + rpoCO2*12.011/44.009); % kgC/s
m_dot(i) = sum(mixture);
setMassFlowRate(mfc,m_dot(i));
dp = 200*(((3/(4*pi))*CHAR*(1+ASHratio)/(particles*rhoCHAR))^(1/3));

% integrate the CSTR long enough to reach steady state
count = 1;
old_T = temperature(cstr);
delta_T = 1;
while ((delta_T > tolerance) || (count < 3)) && (count < 10000)
    tme = tme + dt;
    advance(network, tme);
    new_T = temperature(cstr);
    delta_T = abs(new_T-old_T);
    old_T = new_T;
    count = count + 1;
end
count %#ok<NOPTS>
% update last point in output data variables
tgas(i) = temperature(maingas);
pressurevector(i) = pressure(maingas);

velocity(i) = m_dot(i-1)/(density(upstream)*Area);
tms(i) = tms(i-1) + 1000*(Length/velocity(i));
% Calculate chemical equivalence ratio for reactor i
MWmix(i) = meanMolarMass(maingas);
nj = (1/MWmix(i))*moleFractions(maingas);
for k = 1:4
    bi(k) = sum(aij(:,k).*nj);
end
V_p = sum(V_plus.*bi);
V_m = sum(V_minus.*bi);
r(i) = -V_p/V_m;

Xi = moleFractions(maingas);
XWater = Xi(H2OIndex);
XNO = Xi(NOIndex);
XNO2 = Xi(NO2Index);
XCO = Xi(COIndex);
XO2 = Xi(O2Index);
XCO2 = Xi(CO2Index);

NOx_ppm_dry(i) = 1000000*(XNO + XNO2)/(1-XWater);
CO_ppm_dry(i) = 1000000*XCO/(1-XWater);
O2_vol_dry(i) = 100*XO2/(1-XWater);
```

```
    CO2_vol_dry(i) = 100*XCO2/(1-XWater);

    Yi = massFractions(maingas);
    YNO = Yi(NOIndex);
    YNO2 = Yi(NO2Index);
    NCE(i) = (YNO*(14.007/(14.007+15.999))+YNO2*...
             (14.007/(14.007+2*15.999)))*...
             m_dot(i-1)/(COAL*(1-omegaa-omegaw)*yelem(3));

    % Output data point to file
    fprintf(fid,strcat('%d\t %d\t %d\t'),position(i),tgas(i),...
                                            pressurevector(i));

    for j = 1:nSpecies(maingas)
        fprintf(fid,'%d\t',massFraction(cstr,speciesName(maingas,j)));
    end

    fprintf(fid,strcat('%d\t %d\t %d\t\t\t\t\t\t\t\t\t\t\t\t\t\t\t\t\t',...
                       '\t\t\t\t\t\t\t\t\t\t %d\t %d\t %d\t %d\t',...
                       '%d\t %d\t %d\t %d\t %d\t %d\t %d\r'),...
                      m_dot(i-1),tms(i),tp(i),rpoO2,rpoCO2,CHAR,r(i),...
                      NOx_ppm_dry(i),CO_ppm_dry(i),O2_vol_dry(i),...
                      CO2_vol_dry(i),NCE(i),MWmix(i),dp*10000);
end

% close the output file
fclose(fid);

%---LIST OF VARIABLES (alphabetical)----------------------------------------
% Note that MATLAB is case-sensitive.
%
% Units specified here are as at the first instance of the variable in the
% code (such as the user-input values). Unit conversions are noted in the
% code when they are changed.
%
% A - array of areas used in radiation heat transfer calculations (cm^2)
% A_char - surface area of char (cm^2)
% ACO2 - pre-exponential factor for char gasification by CO2
                % (g/(cm2s atmCO2)
% AddedGas - vector of mass flow rates of species to be added to the gas
                % mixture due to coal devolatilization and heterogeneous
                % reactions (kg/s)
% aij - an array of the number of atoms of C, H, N, and O in the species in
                % the gas objects - species in rows, number of CHNO atoms
                % in columns
% Air_in - flow rate of air through the burner (kg/hr)
% ambient - a gas mixture object used to create the env reservoir
% AO2 - pre-exponential factor for char oxidiation (g/(cm2s atmO2))
% Area - cross sectional area of reactor (m^2)
% ASHratio - (kg_ash/kg_DAF_CHAR) in the CHAR
% ASTMvol - ASTM proximate analysis volatiles, DAF (0 < ASTMvol < 100)
% b - transfer number for effects of high mass transfer
% bi - intermediate variable in calculation of r
% blow - blowing factor = b/(exp(b)-1) for effects of high mass transfer
% ButtonName - yes, no, or cancel result of asking user whether to continue
                % iterations in ignition section of code
% c - vector of empirical coefficients used when estimating C13 NMR
                % parameters from proximate and ultimate analysis results
% c0 - char bridge population (C13 NMR parameter)
% C2H2Index - Index of the species in the gas mixture Cantera objects
% Cdiff - the difference between the carbon release predicted by CPD and
                % the amount of carbon release expected from correlation
                % with total mass loss
% Cgoal - the target amount of carbon release from volatiles correlated
                % with total mass release
% CH4Index - Index of the species in the gas mixture Cantera objects
% CHAR - mass flux of DAF CHAR (kg/s)
% chargas - Cantera gas mixture object used for char reactions section of
                % model
% CHNOIndex - indices for the elements in the Cantera objects
% CHratio - the CH ratio of the volatiles not predicted as specific species
```

```
                % by the CPD model
% C_nlg - the carbon release predicted by the CPD model
% CO2 - moles/hr bottled CO2
% CO2_in - flow rate of bottled CO2 through the burner (kg/hr)
% CO2_vol_dry - CO2 expressed in units of vol% on a water-free basis
% COIndex - Index of the species in the gas mixture Cantera objects
% CO_ppm_dry - CO expressed in units of ppm on a water-free basis
% CO2Index - Index of the species in the gas mixture Cantera objects
% COAL - flow rate of pulverized coal through burner (kg/hr)
% COAL_Type - 1, 2, or 3 to determine which char reaction parameters will
                % be used:
                    % 1 = Wyoming Sub-bituminous
                    % 2 = Illinois #6
                    % 3 = Pittsburgh #8
% composition - string containing details of initial gas composition
% convheat - convective heat transferred to particles (CPD model)
% count - counts iterations to get CSTR to steady state
% cp - particle heat capacity (J/kg-K and cal/g-K depending on context)
% cpa - ash heat capacity (cal/g-K)
% cpc - DAF char heat capacity (cal/g-K)
% cpgvector - mass-based heat capacity of gas (J/kg-K)
% CPU_time - stores the total time CPU is used in ignition part of model
% CPU_time_per_step - store the average time per iteration that the CPU is
                % used during the ignition part of the model
% cstr - a Cantera reactor object
% Current_position - variable used in linear interpolation of wall
                % temperature data
% d - reactor diameter (m)
% delhv - heat of pyrolysis (cal/g), negative indicates endothermic,
                % nominally -100.0 cal/g
% delta_max - the maximum temperature change between iterations
% delta_T - change in temperature from 1 iteration
% devol_incomplete - logical variable that tracks whether devolatilization
                % is complete or not
% DiffCoeffs - mixture-averaged diffusion coefficents (m^2/s)
% diffwvector - mixture-averaged diffusion coefficient (m^2/s) for water
% downstream - a Cantera reservoir object connected to the outlet of each
                % CSTR
% dp - coal particle diameter (only 1 value is used to represent all
                % particles)
% dpout - coal particle diameter from CPD model
% dt - time step for CSTR network integration (s)
% dummygas - a gas mixture object used for property evaluation at film
                % temperatures
% EACO2 - activation energy for char gasification by CO2 (cal/gmole)
% EAO2 - activation energy for char oxidation (cal/gmole)
% emiss - emissivity (gray) values for radiation calculations as defined in
                % input file comments
% env - a reservoir that represents the ambient environment that absorbs
                % heat transferred through the reactor external walls
% exhaust - Cantera gas object used to create constant pressure reservoirs
                % downstream of each CSTR
% ExistingGas - vector of mass flow rates of species in the gas mixture
                % (kg/s)
% F - array of radiation view factors
% fchar - equals 1 - fvol. See cpdcp_nlg for more details
% fcross - fraction of original D.A.F. coal that was metaplast and
                % crosslinked into the char matrix
% ffgas     the fraction of total mass release (i.e. volatiles) that is
%             h2o, co2, ch4, co, and other light gases.
% ffgas2 - ffgas modified to include unknown volatiles estimated as a
                % mixture of CH4 and C2H2
% fgas - mass fraction of D.A.F. coal evolved as light gas
% fid - pointer to output file
% fmet - mass fraction of D.A.F. coal existing as metaplast
% fnchar - fraction of original nitrogen remaining in char (and metaplast)
% fnhcn - fraction of original nitrogen released as light gas (by
                % difference: 1 - fnchar - fntar)
% fnt - nitrogen content of char and metaplast
% fntar - fraction of original nitrogen released as tar
% fntot - total fractional release of nitrogen
```

```
% ftar - mass fraction of D.A.F. coal evolved as tar
% fvol - mass fraction of D.A.F. coal evolved as volatiles (light gas +
                % tar)
% gas - a gas mixture object
% gas_const - The universal gas constant in cal/gmol.K
% gasification - 1 or 0 values respectively determine whether char
                % gasification by CO2 is modeled or not
% gw - a Cantera wall object between adjacent CSTR's to model conduction
                % heat transfer between the gases in each CSTR
% h - convective heat transfer coefficient
% H - enthalpy of gas mixture (J/kg)
% H2OIndex - Index of the species in the gas mixture Cantera objects
% HCNIndex - Index of the species in the gas mixture Cantera objects
% Hdiff - the difference between the hydrogen release predicted by CPD and
                % the amount of hydrogen release expected from correlation
                % with total mass loss
% Hgoal - the target amount of hydrogen release from volatiles correlated
                % with total mass release
% H_in - enthalpy from heterogeneous reactions and CO from the same (J/s)
% H_new - enthalpy of gas phase mixture after heterogeneous reactions (J/s)
                % or after mixing of burnout and primary streamss
% H_nlg - the hydrogen release predicted by the CPD model
% H old - enthalpy of existing gas phase mixture before char reactions
                % are calculated (J/s)
% H_out - enthalpy leaving the gas phase with O2 and CO2 consumed by the
                % char (J/s)
% H_Primary - enthalpy of primary reactants just before burnout oxidizer
                % is added (J/s)
% H_Burnout - enthalpy of burnout oxidizer stream (J/s)
% i - index used in loops
% iterate - a logical variable that causes iteration to continue while true
% j - index used in loops
% k_gas - gas thermal conductivity (W/m.K)
% k_wall - thermal conductivity for reactor wall (W/m.K) Value is empirical
                % and linked to the value of Length and Length2
% kgvector - vector of gas thermal conductivity (W/m.K)
% kpCO2 - rate coefficient for CO2 gasification of char (g of oxidizer
                % consumed per second per unit char surface area (in cm^2)
                % per atm of oxidizer)
% kpO2 - rate coefficient for oxidation of char (g of oxidizer consumed per
                % second per unit char surface area (in cm^2) per atm of
                % oxidizer)
% Length - axial length of CSTR's in ignition section of model
% Length2 - axial length of CSTR's in post-ignition sections of model
% maingas - Cantera gas mixture object used for post-ignition model
% MassProportionCH4 - the mass proportion of CH4 in CH4 and C2H2 mixture
                % that makes up the volatiles not predicted by CPD model
% max_index - number of points in linear iterpolation of wall temperature
                % data
% max_position - the last axial position point in the wall temperature data
% mdel - average molecular weight per side chain (C13 NMR parameter)
% mechanism - 1, 2, or 3 to select from the available gas-phase mechanisms:
                % 1 = GRI-Mech 3.0
                % 2 = GRI-Mech 3.0 + B96 (includes advanced reburning)
                % 3 = SKG03
% mfc - mass flow controller Cantera object
% mixture - vector of mass flow rates of species in the gas mixture passed
                % to the next CSTR (kg/s)
% m_dot - gas phase mass flow (kg/s)
% MolarProportionCH4 - the molar proportion of CH4 in CH4 and C2H2 mixture
                % that makes up the volatiles not predicted by CPD model
% mw1 - average molecular weight per aromatic cluster (C13 NMR parameter)
% mwchar - like mw1, but for char. Initially it is set to mw1
% MWmix - mixture molecular weight
% MWunknowns - the mixture molecular weight of the volatiles not predicted
                % by CPD model
% n - iteration counter
% N2 - moles/hr N2 in the reactants
% N2_in - flow rate of bottled N2 (not air N2) through the burner (kg/hr)
% N2Index - Index of the species in the gas mixture Cantera objects
% NCE - conversion efficiency of fuel nitrogen converted to NO + NO2
```

```
                % assuming all NO + NO2 originates from fuel nitrogen
% network - a Cantera object that holds the reactor networks
% network_cell_array - an array of CSTR reactor networks. Each network
                % consists of the upstream reservoir, followed by the mass
                % flow controller, the CSTR, the valve and the downstream
                % reservoir
% new_T - temperature of CSTR after an iteration
% NG - moles/hr natural gas (CH4)
% NG_in - flow rate of natural gas through burner (kg/hr)
% nj - intermediate variable in calculation of r
% NO - moles/hr NO in the CO2 reactant stream
% NO_doping - ppm NO in the CO2 reactant streams
% NOIndex - Index of the species in the gas mixture Cantera objects
% NO2Index - Index of the species in the gas mixture Cantera objects
% NOx_ppm_dry - NO + NO2 expressed in units of ppm on a water-free basis
% nu - Nusselt number
% number_reactors - number of CSTR's in ignition section of model
% O2 - moles/hr O2 (from all reactants - air and bottled O2)
% O2_in - flow rate of bottled O2 (not air O2) through the burner (kg/hr)
% O2_vol_dry - O2 expressed in units of vol% on a water-free basis
% O2Index - Index of the species in the gas mixture Cantera objects
% old_T - temperature of CSTR before iteration
% omegaa - mass fraction of ash in the parent coal (as received)
% omegaw - mass fraction of moisture in the parent coal (as received)
% output - string containing name of output file
% P - pressure (Pa)
% p0 - ratio of bridges to total attachments (C13 NMR parameter)
% particles - number of coal particles per second
% position - vector of CSTR locations along the MFR axis
% press - pressure in atmospheres
% pressurevector - vector of CSTR pressures (Pa)
% prgas - Prandtl number of gas
% Primary - fraction of total oxidizer through the burner (0 < Primary < 1)
% prompt - multiplier for prompt NOx mechanism reactions (0 or 1)
% qconv - convective heat transer rate (cal/s)
% Q_conv - qconv converted to J/s
% qrad - radiation heat transfer rate (cal/s)
% Q_rad - qrad converted to J/s
% Q_react - rate of heat from heterogeneous reactions (J/s)
% Q_reactO2_x - Fraction (0 to 1) of heterogeneous O2 reaction heat to char
                % Nominally 0 because 0.5 and 1.0 gave problems in testing
% Q_reactCO2_x - as for Q_reactO2_x, but for CO2 gasification
% Q_total - total heat rate to char from heterogeneous reactions, and heat
                % transfer (radiatve and convective)
% r - chemical equivalence ratio (r>1 means fuel-rich, r=1 is
                % stoichiometric, r<1 means fuel-lean)
% R - thermal resistance (calculated from k_wall or k_gas depending on
                % context
% rhoCHAR - density of char (including ash) (kg/m^3)
% rhogas - gas density (kg/m^3)
% rhop - initial particle apparent density (g/cm^3) - see additional
                % comments in input script
% rpoCO2 - rate of CO2 consumption by CO2 gasification (kg/s)
% rpoO2 - rate of O2 consumption by oxidation (kg/s)
% rtot - total rate of char consumption (kg/s) by char oxidation and
                % gasification
% sigma - a radiation constant (cal/s cm^2 K^4)
% sigp1 - sigma + 1 is the number of total attachments per cluster (C13 NMR
                % parameter)
% swell - swelling factor (dpf/dp0 - 1) where dpf = final/max diameter and
                % dp0 = initial diameter. See additional comments in the
                % input script
% t0 - the time at the start of iteration
% T1 - initial gaseous reactant temperature (K) (through the burner)
% T2 - temperature of preheated burnout oxidizer (K)
% tbnr - burner face temperature (K)
% Temp - temperatures used in radiation heat transfer calculations
% texit - exhaust pipe temperature (K)
% tfilm - film temperature (average of gas and particle temperatures) (K)
% tg - gas temperature (K)
% tgas - gas temperature (K)
```

```
% thermal - multiplier for thermal NOx mechanism reactions (0 or 1)
% timax - maximum allowable devolatilization time for CPD model
% timedata - time of day that output file is started
% tme - cumulative integration time for reactor networks
% tms - time in milliseconds from CPD model
% tolerance - maximum allowable change in temperature between time steps of
                % CSTR integration to force steady state conditions
% tp - particle temperature (K)
% TR1 - initial guess of temperature for CSTR's in ignition section (K)
% trate - particle heating rate (K/s)
% twall - linearly interpolated wall temperatures
% twallvector - wall temperatures used as an input (K) - see WallX
% ugvector - vector of gas viscosity (g/(m.s) = Pa.s)
% upstream - reservoir upstream of a CSTR containing the gas mixture
                % entering that CSTR
% v - a Cantera valve object between a CSTR and its downstream reservoir -
                % set to maintain constant pressure in the CSTR
% V_m - intermediate variable in calculation of r
% V_minus - negative Oxidation States for C,H,N,& O in that order
% V_p - intermediate variable in calculation of r
% V_plus - positive oxidation states for C,H,N,& O in that order
% velocity - gas (and particle) velocity (m/s)
% Volume - volume of CSTR's (m^3)
% w - a Cantera wall object installed between the cstr's and the
                % environment, env
% WallX - axial locations of wall temperatures used as an input (m)
% water - water content of particles
% XCO - mole fraction of CO
% XCO2 - mole fraction of CO2
% Xi - mole fractions of species in gas mixture
% xm - Particle position (m) from CPD model
% XNO - mole fraction of NO
% XNO2 - mole fraction of NO2
% XO2 - mole fraction of O2
% XWater - mole fraction of water
% xwbvector - vector of bulk gas water concentration (units: mole fraction)
% y - gas temperature (used in calculating temperature changes during
                % iteration
% YCO - mass fraction of CO
% YCO2 - mass fraction of CO2
% yelem - DAF mass fractions of CHNOS for the coal in a 5 element vector,
                % each element between 0 and 1
% yf - A CPD indicator of the fraction of total light gas that has been
                % released. The look up table on light gas composition is
                % based on yf. Called Xgas in Genetti's MS thesis - see the
                % thesis for more detail.
% Yi - mass fractions of gas mixtures in upstream reservoirs
% YNO - mass fraction of NO
% YNO2 - mass fraction of NO2
% yNsite - variable from CPD model (undocumented)
% YO2 - mass fraction of O2
% Ywater - mass fraction of water in upstream reservoir
% yygas - the fractions of light gas release that is h20, co2, ch4, co and
                % other light gases.
% z - distance from burner (cm)
```

cpdcp_nlg.m – CPD Model Function

```
function [tmsout,xmout,tpout,tgout,fvolout,fcharout,fcrossout,...
          ftarout,fmetout,trateout,mwcharout,yNsiteout,fntout,fncharout,...
          fntarout,fnhcnout,fntotout,fgasout,ffgasout,yygasout,...
          yfout,waterout,convheatout,dpout]...
          =cpdcp_nlg(twallvector,tbnr,texit,timax,yelem,mw1,p0,c0,sigp1,...
          mdel,xt,tgc,zv,vpz,press,tg,vg,rhop,dp,swell,omegaw,omegaa,...
          rhogas,xwbvector,ugvector,kgvector,...
          diffwvector,cpgvector,prgas,emiss,rad,WallX)

% This file is the main function file for the cpdcp-nlg model for the
% Cantera-MATLAB model of the MFR combustion facility at BYU. See commments
```

```
% in the code for more information.
% Coded by Andrew Mackrory.
%-------------------------------------------------------------------------
% The cpdcp-nlg devolatilization model was originally written in FORTRAN
% 77. The function of this code is essentially identical to the FORTRAN
% version, but the following points should be noted regarding changes made
% to the code in translation:
%
% 1. In matlab .* is an operator and so all decimal points were preceded
% and followed by at least one numeral to avoid confusion:
%       e.g. FORTRAN: 1.  MATLAB: 1.0
%       e.g. FORTRAN: .1  MATLAB: 0.1
% 2. MATLAB is case sensitive so all code was changed to lower case with a
% few exceptions such as L, L0, and PI. The L's were made uppercase
% to avoid confusion with the numeral 1 and PI was made uppercase to avoid
% confusion with the MATLAB function pi.
% 3. The C13 NMR parameter correlation of Genetti and Fletcher was added
% for use in cases where C13 NMR data are unavailable.
% (see cpdcp_nlg_input.m).
% 4. Single precision variables were the most common variable type used in
% the FORTRAN version of the code. MATLAB uses double precision variables
% almost exclusively resulting in slight differences in results as should
% be expected (rounding error is changed).
% 5. A list of variables with explanations of what most of them are was
% added to the comments.
% 6. Additional comments were added. Original FORTRAN comments can be
% recognized by the FORTRAN comment indicator "c" at the start of each
% comment line. Be sure to read the original file header below.
% 7. Parentheses were added to some expressions to enhance readability.
% 8. Some minor bugs were fixed and the style of some sections of code was
% changed to my own programming style (Andrew Mackrory).
%
% Translation from FORTRAN to the MATLAB m-file format was performed by
% Andrew Mackrory at Brigham Young University in 2007.
% andrew.mackrory@gmail.com
% No liability etc. is assumed for the use of the code as outlined in the
% original FORTRAN file header comments below.
%-------------------------------------------------------------------------
% Original file header comments from the FORTRAN source code (1999):
% c  This is the CPDCP-NLG model
% c
% c  This model was developed by Sandia National Laboratories under
% c  FWP 0709 for the Department of Energy's Pittsburgh Energy
% c  Technology Center and the DOE Division of Engineering and Geosciences
% c  through the Office of Basic Energy Sciences;
% c  and by the University of Utah through funding from
% c  the Advanced Combustion Engineering Research Center (ACERC), which
% c  is principally sponsored by the National Science Foundation, the
% c  State of Utah, and by a consortium of industrial companies.
% c  The code will not be formally licensed.  Neither the U.S. or the
% c  DOE, nor any of their employees, makes any warranty, express or
% c  implied, or assumes any legal liability or responsibility for the
% c  accuracy, completeness, or usefulness of any information, apparatus,
% c  product, or process disclosed, or represents that its use would
% c  infringe privately owned rights.
% c
% c  The CPD model is intended to solve pyrolysis rate equations
% c  based on a percolative bond-breaking scheme.  This version includes
% c  the flash distillation program to distinguish between tar and
% c  metaplast. This program also includes a crosslinking scheme.
% c  (January, 1991)
% c
% c  Most recent modifications to this model include (a) the nitrogen
% c  release model of Perry, (b) the model of Genetti to break the light
% c  gas into species based on a correlation, and (c) slight modification
% c  to mdel to account for the mass associated with c0.
% c  These modifications were made at BYU by Dominic Genetti in his
% c  M.S. thesis work (1999) and Steve Perry in his Ph.D. work (1999).
% c
% c  This version is coupled with a solver for the particle energy and
% c   momentum equations.
```

```
% c       units are g,K,cm,s,cal
% c
% c   A blowing correction to the heat transfer model is employed.
% c
% c   Merrick heat capacity correlations are used
% c

%-------------------------------------------------------------------------
% SUBROUTINES
% The following functions are called by this main program or eachother:
%
% at.m
%   - function required by lightgas.m to calculate area of triangle
% d.m
%   - function required by lightgas.m to calculate distance (for
%   interpolation)
% flash.m
%   - the flash distillation program that distinguishes between tar and
%   metaplast.
% gamln.m
%   - a program to calculate the ln of the gamma function
% heatap.m
%   - calculates ash heat capacity
% heatcp.m
%   - calculates the heat capacity of a D.A.F. coal particle from
%   Merrick's correlations
% inverf.m
%   - calculates the number of standard deviations from the mean
%   corresponding to the area under the standard normal probability curve
% lightgas.m
%   - calculates the distribution of light gas species based on a look up
%   table of reference data
% perkp.m
%   - calculates fractions of tar, and gas
% perks.m
%   - the meat of the devolatilization model
% xxx.m
%   - function required by lightgas.m for interpolation
% yyy.m
%   - function required by lightgas.m for interpolation
%
%-------------------------------------------------------------------------
% The variables used in this script and the related Cantera code that calls
% this function are defined here:
% These definitions do not necessarily apply to variables in the
% subroutines, fac being a good example of same name, different function in
% perkp than in this code.
% LIST OF VARIABLES in this script (alphabetic)
% ab        pre-exponential factor (unitless) for labile bridge
%             dissociation rate
% ac        pre-exponential factor (unitless) for composite rate constant
% acr       pre-exponential factor (unitless) for crosslinking rate
% ag        pre-exponential factor (unitless) for gas release rate
% aind      chemical structure parameter
% aind0     chemical structure parameter (initial value)
% alfa      mass of ash per particle (stays constant during pyrolysis)
% alfc      mass of D.A.F. portion of particle
% alfc0     initial value of alfc
% alfcp     same as alfc, but used in predictor step
% alfw      mass of water per particle
% alfwp     same as alfw, but used in predictor step
% alpha     particle mass (as received, i.e. moist)
% alphap    this variable was the same as alpha and was removed from the
%             code. (This comment is only here for reference).
% an        pre-exponential factor (unitless) for nitrogen release by high
%             temperature decomposition (slow)
% ans       This variable will be generated by MATLAB when certain commands
%             are executed. May be useful if you are debugging.
% ap        surface area of spherical particle
% arad      pre-exponential factor (unitless) for nitrogen attack by free
%             radical (fast)
```

```
% ASTMvol   dry, ash free ASTM volatile wt% (used for optional C13 NMR
%             parameter correlation in cpdcp_nlg_input.m)
% b         transfer number for effects of high mass transfer
% blow      blowing factor = b/(exp(b)-1) for effects of high mass transfer
% bloww     blowing factor for water evaporation (just like blow):
%             bloww = bw/(exp(bw)-1)s
% bw        transfer number for water evaporation
% c         vector for storing empirical correlation coefficients for
%             optional C13 NMR parameter correlation in cpdcp_nlg_input.m
% c0        char bridge population (C13 NMR parameter)
% cp        specific heat capacity of particle
% cpa       specific heat capacity of ash
% cpc       specific heat capacity of the D.A.F. portion of the particle
%             (char)
% cpg       specific heat capacity of gas
% cpw       specific heat capacity of water, 1 cal/g-K
% del2      chemical structure parameter
% delhv     heat of pyrolysis (cal/g), negative indicates endothermic
%             nominally -100.0 cal/g
% delhw     heat of vaporization for water (cal/g) at 1 atm, negative
%             indicates endothermic
% diffw     diffusion coefficient of water in the gas
% dp        particle diameter (cm)
% dp0       initial particle diameter (cm)
% dt        time step (seconds)
% dtmax     maximum time step (seconds)
% dvdt      rate of mass loss of char due to volatile release
% dy1       change in y(1) over a single time step - used to determine if a
%             change in time step is necessary
% eb0       activation energy (cal) for labile bridge dissociation rate
% ebsig     standard deviation of activation energy for labile bridge
%             dissociation rate
% ec0       activation energy (cal) for composite rate constant
% ecr       activation energy (cal) for crosslinking rate
% eg0       activation energy (cal) for gas release rate
% egsig     standard deviation of activation energy for gas release rate
% emiss     emissivity of particle and other surfaces in reactor
% en0       activation energy (cal) for nitrogen release by high
%             temperature decomposition (slow)
% ensig     standard deviation of activation energy for nitrogen release by
%             high temperature decomposition (slow)
% erad      activation energy (cal) for nitrogen attack by free radical
%             (fast)
% F(i,j)    view factor for radiation heat transfer
% fchar     equals 1 - fvol, so it's what's left of the D.A.F. coal after
%             the light gas and tar leaves. NOTE that this includes
%             metaplast (fmet) calculated by the flash subroutine. In some
%             versions of CPD this is "fsolid" instead of "fchar".
% fcross    fraction of original D.A.F. coal that was metaplast and
%             crosslinked into the char matrix
% fcrossold same as fcross, but the last value of fcross calculated
% ffgas     the fraction of total mass release (i.e. volatiles) that is
%             h2o, co2, ch4, co, and other light gases.
% fgas      mass fraction of D.A.F. coal evolved as light gas
% fgasold   fgasold  is the value from the last time the flash subroutine
%             was called (see fgasold2). Coded in this main script to
%             preserve its value between successive calls of the flash
%             subroutine.
% fgasold2  fgasold2 is the value at the previous time step in the flash
%             subroutine (see fgasold). Coded in this main script to
%             preserve its value between successive calls of the flash
%             subroutine.
% fid       file identifier for output file
% fmet      mass fraction of D.A.F. coal existing as metaplast
% fmetold   same as fmet, but the value from earlier calculation/iteration
% fnca0     initial mass fraction of nitrogen in site (aromatic)
% fnchar    fraction of original nitrogen remaining in char (and metaplast)
%             (see comment above for fchar)
% fnhcn     fraction of original nitrogen released as light gas (by
%             difference: 1 - fnchar - fntar)
% fnit      D.A.F. mass fraction of nitrogen in original coals
```

```
% fnt       nitrogen content of char and metaplast
% fntar     fraction of original nitrogen released as tar
% fntot     total fractional release of nitrogen
% fracr     fraction to account for reduction of metaplast by crosslinking
%             in latest time step
% fstable   initial fraction of mw decay with no radical n attack) as
%             explained in this quote from Perry et al., "Modeling Nitrogen
%             Evolution During Coal Pyrolysis", Energy & Fuels, vol. 14,
%             no. 5, 2000 page 1099:
%                 "It was assumed that the radicals formed during the
%                 initial 3% of light gas release were stable (i.e.,
%                 fstable = 0.03). this means that Nsite was assumed to
%                 remain at the value in the parent coal until the
%                 molecular weight per cluster had decayed to 97% of the
%                 coal value. It is not clear whether this empiricism is
%                 really necessary, although it seems to fit the available
%                 data for high-rank coals somewhat better than using
%                 fstable = 0, consistent with the concept of the formation
%                 of a pool of free radicals before steady state is
%                 reached."
%           In some documentation the variable "fst" is mentioned. fst is
%           NOT the same thing as fstable. fst is explained in the MS
%           Thesis of Genetti (BYU, April 1999). fstable is explained in
%           the PhD Dissertation of Perry (BYU, December 1999).
%           The value of 0.03 should be used for fstable.
% ft        weight fraction of each tar bin
% ftold     ftold  is the value from the last time the flash subroutine
%             was called (see ftold2). Coded in this main script to
%             preserve its value between successive calls of the flash
%             subroutine.
%             ftold(i) = weight fraction of each tar bin
% ftold2    ftold2 is the value at the previous time step in the flash
%             subroutine (see ftold). Coded in this main script to
%             preserve its value between successive calls of the flash
%             subroutine.
% ftar      mass fraction of D.A.F. coal evolved as tar
% ftarold   ftarold  is the value from the last time the flash subroutine
%             was called (see ftarold2). Coded in this main script to
%             preserve its value between successive calls of the flash
%             subroutine.
% ftarold2  ftarold2 is the value at the previous time step in the flash
%             subroutine (see ftarold). Coded in this main script to
%             preserve its value between successive calls of the flash
%             subroutine.
% ftart     wt fraction tar, gas, and char? - this definition from comment
%             in perkp subroutine
% fvol      mass fraction of D.A.F. coal evolved as volatiles
%             volatiles = light gas + tar
% g         980.0 cm/s - gravitational acceleration constant
% g0        chemical structure coefficient
% gasmw     presumably the molecular weight of gas given off - calculated
%             from chemical structure coefficients
% h         convective heat transfer coefficient
% heat      heat (rate) required for pyrolysis and water evaporation
% i         iteration or time step counter
% ik        index used in a for loop
% inside    (Logical) - when true, O/C and H/C ratios are inside the bounds
%             of the library coals in the lightgas subroutine.
% intar     (Logical) - when true, tar molecular weight distribution is
%             calculated in subroutine perkp.
% ipred     True (or 1) when on the predictor step (logical)
% ip        array index for property interpolation
% iv        array index for velocity interpolation
% ix        array index for temperature interpolation
% j         index used in for loops
% kg        thermal conductivity of the gas (units: cal/cm/s/c)
% L         number of labile bridges - see y
%             (upper case to avoid confusion with the number one)
% L0        chemical structure coefficient = p0-c0
%             (upper case to avoid confusion with the number ten)
% lib       (integer) The number of the library coal (1-12) used in the
```

```
%             lightgas subroutine. If lib = 13 or 14 this corresponds to
%             the two extremes of the H/C vs O/C coalification diagram.
% ma          chemical structure coefficient - see code
% machar      a char nmr parameter calculated from machar = mwchar-sigp1*mdel
% mb          chemical structure coefficient - see code
% mdel        average molecular weight per side chain (C13 NMR parameter)
% metold      metold  is the value from the last time the flash subroutine
%             was called (see metold2). Coded in this main script to
%             preserve its value between successive calls of the flash
%             subroutine.
%             metold(i) = mass fraction of coal contained in metaplast of
%                         mer size i
% metold2     metold2 is the value at the previous time step in the flash
%             subroutine (see metold). Coded in this main script to
%             preserve its value between successive calls of the flash
%             subroutine.
% mt          molecular weight of each tar bin
% mw1         average molecular weight per aromatic cluster (includes side
%             chains) (C13 NMR parameter)
% mwchar      like mw1, but for char. Initially it is set to mw1
% mwcharold   like mwchar, but used for... initially set to mwchar
% nmax        number of terms in expansion for mol. wt. distribution
% nu          Nusselt number for particle
% nv          number of particle velocity data points
% nx          number of gas temperature data points
% omegaa      mass fraction of ash in the parent coal (as received)
% omegaw      mass fraction of moisture in the parent coal
%             (as received, i.e. including ash)
% output      filename of file where results are saved
% p0          ratio of bridges to total attachments (C13 NMR parameter)
% PI          stores value of pi (upper case signifies it is different to
%             the MATLAB function pi, which returns the value of pi)
% pr          Prandtl number of the gas
% press       pressure (atm)
% pstar       chemical structure coefficient
% qconv       rate of convective particle heating
% qrad        rate of radiative particle heating
% qbnr        rate of radiative particle heating from the burner face
% qexit       rate of radiative particle heating from the exhaust
% qwall       rate of radiative particle heating from the wall
% r2          radiation view factor calculation parameter
% r3          radiation view factor calculation parameter
% rad         reactor radius
% ratecr      cross linking rate
% rba         chemical structure coefficient
% re          Reynolds number of flow around particle
% rg          universal gas constant rg = 1.987 cal/gmole.K
% rhog        gas density
% rhop        initial particle apparent density (g/cm^3). See more detailed
%             comment in cpdcp_nlg_input.m
% rtot        Total rate of mass loss (volatiles and water)
% rtotp       predicted total rate of mass loss (volatiles and water)
% rw          water evaporation rate
% rwp         same as rw, but in predictor step
% sig         chemical structure coefficient = sigp1-1
% siginv      chemical structure coefficient
% sigma       Stefan-Boltzmann constant (for radiation heat transfer)
% sigp1       sig+1 is the coordination number (number of total attachments)
% small       a constant small number for comparisons and making small
%             adjustments to variables
% swell       swelling factor (dpf/dp0 - 1) dpf = final/max diameter. See
%             more detailed comment in cpdcp_nlg_input.m
% tarold      tarold  is the value from the last time the flash subroutine
%             was called (see tarold2). Coded in this main script to
%             preserve its value between successive calls of the flash
%             subroutine.
% tarold2     tarold2 is the value at the previous time step in the flash
%             subroutine (see tarold). Coded in this main script to
%             preserve its value between successive calls of the flash
%             subroutine.
% tg          Gas temperature (K)
```

```
% tgc       Gas temperatures (data as function of position in reactor) (K)
% tbnr      burner temperature (K)
% timax     maximum devolatilization time modeled (seconds)
% time      time (in seconds). The independent variable of the main
%             calculation loop.
% tms       time converted to milliseconds for output
% tp        Particle temperature
% tpred     Predicted particle temperature
% trate     Particle heating rate (K/s)
% tratep    Predicted particle heating rate (K/s)
% texit     exhaust tube temperature (K)
% twall     reactor wall temperature (K)
% ug        gas viscosity (units: g/(cm.s))
% vg        gas velocity
% vp        Particle velocity
% vpp       Predicted particle velocity
% vpz       velocities of particles along z axis (cm/s) (1-d flow of gas
%             and particles assumed)
% x         Particle position (cm)
% xm        Particle position (x) converted to meters for output
% xoc       O/C Molar Ratio
% xp        Particle position (cm) on the predictor step
% xt        z axis locations of gas temperatures (cm) and other properties
% xw0       particle surface water concentration (mole fraction)
% xwb       bulk flow water concentration (mole fraction)
% y         a four element array:
%             y(1) = L       labile bridges
%             y(2) = del     ends
%             y(3) = c       char links
%             y(4) = mass fraction of nitrogen in site (aromatic)
%                    (initially fnca0)
% yelem     5 element array stores dry, ash-free mass fractions of
%             C, H, N, O, S, in that order.
%             per cluster) (C13 NMR parameter)
% yf        A CPD indicator of the fraction of total light gas that has
%             been released. The look up table on light gas composition is
%             based on yf. Called Xgas in Genetti's MS thesis - see the
%             thesis for more detail.
% yhc       H/C Molar Ratio
% ynchar    the nitrogen remaining in the char and metaplast
% yntar     fraction of original nitrogen released as tar
% yp        yp(i) = derivative of y(i) in time
% ypp       same as yp, but used on the predictor step
% ypred     same as y, but used on the predictor step
% yygas     the fractions of light gas release that is h20, co2, ch4, co
%             and other light gases.
% z         Particle position (cm) in radiation calculations
% zero      a constant (0) used for comparisons
% zv        z axis locations of particle velocities (cm)

% define constants
g = 980;
delhw = -540.0;
cpw = 1.0;
rg = 1.987;     % cal/gmole K
PI = 3.14159;
pr = prgas(1);
nmax = 20;  % documentation says this is usually 20
zero = 0.0;
small = 1.0e-7;

dt = 10.0e-6;     % initial time steps (seconds)
dtmax = 50.0e-6;  % maximum time step (seconds)

% KINETIC PARAMETERS
% In these definitions, ? stands for a "subscript" letter:
    % a?'s are pre-exponential factors (unitless)
    % e?'s are activation energies (cal)
            % (sometimes have a zero at end of variable name)
    % e?sig's are standard deviations of activation energies (cal)
% subscript letters:
```

```
    % b is for the labile bridge dissociation rate
    % c is for composite rate constant
                %(ec = 0 so ac = rho, the composite rate constant)
    % g is for gas release rate
    % cr is for crosslinking rate
    % rad is for nitrogen attack by free radical (fast)
    % n is for nitrogen release by high temperature decomposition (slow)
ab = 2.602e15;
eb0 = 55400;
ebsig = 1800;
%
ac = 0.9;
ec0 = 0;
%
ag = 3.0e15;
eg0 = 69000;
egsig = 8100;
%
acr = 3.0e15;
ecr = 65000;
%
arad = 18.4;
erad = 6000;
%
an = 5.5e7;
en0 = 90000;
ensig = 0;
%
fstable = 0.03; % fstable (initial fraction of mw decay with no radical N
                % attack) see the comments in the variable list above for
                % more detail. Set equal to 0.03

delhv = -100.0; % heat of pyrolysis (cal/g), negative indicates endothermic
                % nominally -100.0 cal/g

% The next ten variables are used in the flash subroutine and are passed in
% and out to store them for the next time flash is called:
metold = zeros(1,nmax);
ftold = zeros(1,nmax);
tarold = zeros(1,nmax);
fgasold = 0.0;
ftarold = 0.0;
metold2 = zeros(1,nmax);
ftold2 = zeros(1,nmax);
tarold2 = zeros(1,nmax);
fgasold2 = 0.0;
ftarold2 = 0.0;

% initialization of variables
yp = zeros(4,1);
ypp = zeros(4,1);
ypred = zeros(4,1);
intar = false;
ftar = 0.0;
fgas = 0.0;
fchar = 1.0;
tms = 0.0;
blow = 1.0;
ix = 1.0;
iv = 1.0;
ip = 1.0;
ipT = 1.0;
x = 0.0;
xm = 0.01*x;
nx = length(tgc);
nv = length(vpz);
lib = uint8(0);

% Initialize output arrays and non-zero initial values
tmsout = zeros(size(xt));
xmout = zeros(size(xt));
```

```
tpout = zeros(size(xt));
tgout = zeros(size(xt));
fvolout = zeros(size(xt));
fcharout = zeros(size(xt));
fcrossout = zeros(size(xt));
ftarout = zeros(size(xt));
fmetout = zeros(size(xt));
trateout = zeros(size(xt));
mwcharout = zeros(size(xt));
yNsiteout = zeros(size(xt));
fntout = zeros(size(xt));
fncharout = zeros(size(xt));
fntarout = zeros(size(xt));
fnhcnout = zeros(size(xt));
fntotout = zeros(size(xt));
fgasout = zeros(size(xt));
ffgasout = zeros(5,length(xt));
yygasout = zeros(5,length(xt));
yfout = zeros(size(xt));
tpout(1) = tg;
tgout(1) = tg;
fcharout(1) = 1;
mwcharout(1) = mw1;
yNsiteout(1) = fstable;
fntout(1) = yelem(3);
fncharout(1) = 1;
waterout = zeros(size(xt));
                    % mass fraction of moisture in ash-containing coal
waterout(1) = omegaw;
convheatout = zeros(size(xt));
% set output "trigger" to 2
outputnow = 2;

% c  Save initial char NMR parameters as coal NMR parameters
% c  (char parameters calculated independent of those using
% c  empirical correlation for mdel)
mwchar = mw1;
mwcharold = mwchar;
machar = mwchar-sigp1*mdel;

% c  adjust mdel to correct for c0 (Steve Perry, May 1999)
mdel = mdel/(1.0-c0);

% c  empirical correlation to allow a small portion of alpha-carbon to
% c  stay with the aromatic cluster
mdel = mdel-7;

% c  Now calculate other chemical structure coefficients
L0 = p0 - c0;
mb = 2.0*mdel;
ma = mw1-sigp1*mdel;
sig = sigp1-1;
rba = mb/ma;
fnit = yelem(3);
fnt = fnit;
fnca0 = fnit*mw1/machar;
dp0 = dp;

% c   initialize variables
y(1) = L0;
y(2) = 2.0*(1.0-c0-L0);
y(3) = c0;
y(4) = fnca0;
aind0 = L0 + (1.0-c0-L0);
siginv = 1.0/sig;
pstar = 0.5*siginv;
yntar = 0.0;
yf = 0.0;
inside = true;
fcross = 0.0;
```

```
% c   calculate initial particle velocity
% assumes particle is at the gas temperature at this point
tp = tg;
rhog = rhogas(1);
ug = ugvector(1);
kg = kgvector(1);
cpg = cpgvector(1);
diffw = diffwvector(1);

% also it is assumed that initial particle velocity is equal to initial gas
% velocity:
vp = vg;

fvol = 0.0;
fmet = 0.0;
rtot = 0.0;
xwb = xwbvector(1);
time = 0.0;

% c  for now, assume that the apparent density is indicative of the as
% c  received coal.
alpha = ((4/3)*PI*(dp/2)^3)*rhop;
alfa = alpha*omegaa;
alfw = alpha*omegaw;
alfc = alpha*(1-omegaa-omegaw);
alfc0 = alfc;
ap = PI*dp^2;
re = rhog*abs(vp-vg)*dp/ug;
nu = 2.0 + 0.6*re^0.5*pr^0.333;
h = nu*kg/dp;
sigma = 1.335e-12;              % cal/s cm^2 K^4
heat = 0.0;
% c   calculate O/C and H/C ratios for light gas model
xoc = (yelem(4)/16)/(yelem(1)/12);
yhc = yelem(2)/(yelem(1)/12);

% get daf coal heat capacity
[cpc] = heatcp(tp,yelem);
% get ash heat capacity
[cpa] = heatap(tp);

fntar = 0.0;
cp = (alfc*cpc + alfa*cpa + alfw*cpw)/(alpha);

% START OF MAIN CALCULATION LOOP
i = 0; % iteration counter
breakout = false;
while (time < timax)&&(breakout == false)
    i = i+1;
    % ccccccccccccccccccccccccccccccccccccccccccccccccccccccccccccccccccccccc
    % c
    % c PREDICTOR STEP
    % c
    % ccccccccccccccccccccccccccccccccccccccccccccccccccccccccccccccccccccccc
    fvolold = fvol;
    fcrossold = fcross;
    fmetold = fmet;
    xp = x + vp*dt;
    % calculate gas temperature
    if (xp <= xt(nx))
        tg = (xt(ix+1)-xp)/(xt(ix+1)-xt(ix))*(tgc(ix)-tgc(ix+1))+tgc(ix+1);
    else
%         fprintf('\rReached end of gas temperature correlation\r');
        breakout = true;  % exits the while loop under this condition
    end
    if (inside == false)
%         fprintf('\r!!!!!!!!!!!WARNING!!!!!!!!!!!!!!!!!\r');
%         fprintf('O/C and H/C ratios are outside the\r');
%         fprintf('bounds of the library coals.\r');
%         fprintf('Estimation of light gas distribution\r');
%         fprintf('is based on library coal No. %u \r',lib);
```

```
    end
    if (tg > 4000.)
        fprintf('\r!!!!!!!!!!!WARNING!!!!!!!!!!!!!!!!\r');
        fprintf(' Gas temperature too high---- %d K\r',tg);
    end
    % c interpolate to get particle velocity from given velocities
    if (xp <= zv(nv))
        vpp = (zv(iv+1)-xp)/(zv(iv+1)-zv(iv))*(vpz(iv)-vpz(iv+1))...
                +vpz(iv+1);
    else
%       fprintf('Reached end of particle velocity correlation\r');
      breakout = true;  % exits the while loop under this condition
    end
    % interpolate to get other properties
    if (xp <= zv(nv))
        rhog = (xt(ip+1)-xp)/(xt(ip+1)-xt(ip))*(rhogas(ip)-rhogas(ip+1))...
                +rhogas(ip);
        ug = (xt(ip+1)-xp)/(xt(ip+1)-xt(ip))*(ugvector(ip)-...
                ugvector(ip+1))+ugvector(ip);
        kg = (xt(ip+1)-xp)/(xt(ip+1)-xt(ip))*(kgvector(ip)-...
                kgvector(ip+1))+kgvector(ip);
        cpg = (xt(ip+1)-xp)/(xt(ip+1)-xt(ip))*(cpgvector(ip)-...
                cpgvector(ip+1))+cpgvector(ip);
        diffw = (xt(ip+1)-xp)/(xt(ip+1)-xt(ip))*(diffwvector(ip)-...
                diffwvector(ip+1))+diffwvector(ip);
        xwb = (xt(ip+1)-xp)/(xt(ip+1)-xt(ip))*(xwbvector(ip)-...
                xwbvector(ip+1))+xwbvector(ip);
        pr =  (xt(ip+1)-xp)/(xt(ip+1)-xt(ip))*(prgas(ip)-...
                prgas(ip+1))+prgas(ip);
        twall = (WallX(ipT+1)-xp)/(WallX(ipT+1)-WallX(ipT))*...
                  (twallvector(ipT)-twallvector(ipT+1))+twallvector(ipT);
    else
%       fprintf('\rReached end of property correlations\r');
      breakout = true;  % exits the while loop under this condition
    end

    % Reynolds number set to zero here because as coded, this model
    % assumes gas velocity = particle velocity:
    %     vlag = (vpp-vg);
    %     re = rhog*abs(vlag)*dp/ug;
    re = 0.0;


    % c energy equation
    % c--   convection
    nu = 2 + 0.6*re^0.5*pr^0.333;
    b = cpg*(rtot)/(2.0*PI*dp*kg);
    if (b >= 1.e-4)
        blow = b/(exp(b)-1);
    else
        blow = 1.0;
    end
    h = blow*nu*kg/dp;
    qconv = h*ap*(tg-tp);
    % c--   mass transfer
    if (alfw > 0)
        bw = (rtot)/(2*PI*dp*diffw*rhog);
        if (bw>=1.e-4)
            bloww = bw/(exp(bw)-1);
        else
            bloww = 1.0;
        end
    else
        bloww = 1.0;
    end
    % CHANGE THIS NEXT SECTION TO SUIT GEOMETRY OF SPECIFIC REACTORS:
    % c--    radiation
    z = xp;  % distance from burner (cm)
             % distance from exhaust will be (200-z) because reactor is 2m
             % long
    % set up areas, etc of radiation enclosure
```

```
Area(1) = PI*rad^2; % burner (Area vector = same order as emiss vector)
Area(2) = 2*PI*rad*200; % walls
Area(3) = Area(1); % exhaust
Area(4) = ap; % particle
Temp(1) = tbnr;
Temp(2) = twall;
Temp(3) = texit;
Temp(4) = tp;
% avoid divide by zero:
if z <= 0
    F(4,1) = 0.5;
else
    F(4,1) = 0.5*(1-(1/(1+(rad/z)^2)^0.5)); %disk to sphere view factor
end
F(4,3) = 0.5*(1-(1/(1+(rad/(200-z))^2)^0.5)); %same as above
F(4,2) = 1 - (F(4,1) + F(4,3)); % by summation rule
% by reciprocity:
    F(1,4) = F(4,1)*Area(4)/Area(1);
    F(2,4) = F(4,2)*Area(4)/Area(2);
    F(3,4) = F(4,3)*Area(4)/Area(3);

qrad = emiss(4)*( F(1,4)*Area(1)*emiss(1)*sigma*Temp(1)^4+...
                  F(2,4)*Area(2)*emiss(2)*sigma*Temp(2)^4+...
                  F(3,4)*Area(3)*emiss(3)*sigma*Temp(3)^4-...
                        Area(4)*sigma*Temp(4)^4); % cal/s
% END OF SECTION TO CHANGE TO SUIT GEOMETRY OF SPECIFIC REACTORS
% THERE IS ANOTHER SECTION TO CHANGE BELOW

% c--    water evaporation rate
% using Antoine vapor pressure correlation
if (alfw > 0)
    xw0 = exp(18.3036-3816.44/(tp-46.13))/(760*press);
    % In above line, (760*press) was previously just 760 in the FORTRAN
    % source code. The pressure was added to the equation to allow for
    % pressures other than 1 atm.
    xw0 = min(xw0,1.0);
    xw0 = max(xw0,0.0);
    rwp = bloww*2*rhog*diffw*PI*dp*(xw0-xwb)/(1.0-xw0);
else
    rwp = 0;
end
% c--  coal pyrolysis rate
[ypp] = perks(y,ypp,tp,L0,c0,ab,eb0,ebsig,ac,ec0,ag,eg0,egsig,...
                            rg,fnca0,an,en0,ensig);

% c  free radical light gas nitrogen release mechanism
if ((mw1-mwchar)/mw1 > fstable)
    ypp(4) = ypp(4) - y(4)*arad*exp(-erad/rg/tp)*...
                       (mwcharold-mwchar)/mwchar*machar/mwchar/dt;
         % This needs some parentheses to avoid ambiguity
end

% c component mass conservation
for j = 1:4
     ypred(j) = y(j) + dt*ypp(j);
     ypred(j) = max(ypred(j),zero);
end

% c  crosslinking rate
fracr = 1.0;
if ((fmetold > small) && (acr > 0.0))
    ratecr = acr*exp(-ecr/rg/tp)*fmetold*dt;
    fracr = 1.0 - ratecr/fmetold;
    fmet = fmetold - ratecr;
    fcross = fcrossold + ratecr;
    if (fmet < 0.0)
        fcross = fcrossold + fmet;
        fmet = 0.0;
        fracr = 0.0;
    end
end
```

```
    % c  get product distribution from ypred array
    if(ypred(1) > small)
        intar = true;
    end

    [ftar,ftart,fgas,ft,mt] = perkp(ypred,ftar,intar,ma,rba,c0,...
                                          sig,siginv,nmax,pstar);

    intar = false;
    gasmw = rba*ma/2.0;

    % c  flash distillation
    if(fgas >= 1.0e-5)
        ipred = true;
        [ftar,fmet,metold,metold2,ftold,ftold2,...
          tarold,tarold2,fgasold,fgasold2,ftarold,ftarold2] = ...
          flash(fgas,gasmw,ft,mt,fracr,tp,press,nmax,zero,small,ipred,...
          metold,metold2,ftold,ftold2,tarold,tarold2,fgasold,fgasold2,...
          ftarold,ftarold2);
    elseif (fgas < 1.0e-5)
        fmet = ftart;
        ftar = 0.0;
    end
    fvol = fgas + ftar;
    fchar = 1.0 - fvol;
    dvdt = (fvol - fvolold)/dt*alfc0;
    % c  done with pyrolysis rate!
    rtotp = dvdt + rwp;
    heat = dvdt*delhv + rwp*delhw;

    % c calculate heat capacity
    % get daf coal heat capacity
    [cpc] = heatcp(tp,yelem);
    % get ash heat capacity
    [cpa] = heatap(tp);

    cp = (alfc*cpc + alfa*cpa + alfw*cpw)/(alpha);

    tratep = (qconv + qrad + heat)/(alpha*cp);
    tpred = tp + tratep*dt;

    % c component mass conservation
    alfwp = alfw - rwp*dt;
    alfcp = fchar * alfc0;
    alfcp = max(alfcp,0.0);
    alfwp = max(alfwp,0.0);
    alpha = (alfcp + alfa + alfwp);
    omegaa = alfa/alpha;
    % c  particle swelling
    L = ypred(1);
    dp = dp0 * (1.0 + swell*(1.0-L/L0));
    ap = PI * dp^2;
    % c particle density changes during devolatilization
    rhop = alpha/((4.0/3.0)*PI*(dp/2)^3);

    % ccccccccccccccccccccccccccccccccccccccccccccccccccccccccccccccccc
    % c
    % c CORRECTOR STEP
    % c
    % ccccccccccccccccccccccccccccccccccccccccccccccccccccccccccccccccc
    x = x + 0.5*(vpp+vp)*dt;
    % c   interpolate to get gas temperature
    if (x <= xt(nx))
        tg = (xt(ix+1)-x)/(xt(ix+1)-xt(ix))*(tgc(ix)-tgc(ix+1))+tgc(ix+1);
    else
%         fprintf('\rReached end of gas temperature correlation\r');
        breakout = true;
    end
    % c interpolate to get particle velocity
    if (x <= zv(nv))
```

```
        vp = (zv(iv+1)-x)/(zv(iv+1)-zv(iv))*(vpz(iv)-vpz(iv+1))+vpz(iv+1);
    else
%         fprintf('\rReached end of particle velocity correlation\r');
        breakout = true;
    end

    % interpolate to get other properties
    if (x <= zv(nv))
        rhog = (xt(ip+1)-xp)/(xt(ip+1)-xt(ip))*(rhogas(ip)-rhogas(ip+1))...
                  +rhogas(ip);
        ug = (xt(ip+1)-xp)/(xt(ip+1)-xt(ip))*(ugvector(ip)-...
                  ugvector(ip+1))+ugvector(ip);
        kg = (xt(ip+1)-xp)/(xt(ip+1)-xt(ip))*(kgvector(ip)-...
                  kgvector(ip+1))+kgvector(ip);
        cpg = (xt(ip+1)-xp)/(xt(ip+1)-xt(ip))*(cpgvector(ip)-...
                  cpgvector(ip+1))+cpgvector(ip);
        diffw = (xt(ip+1)-xp)/(xt(ip+1)-xt(ip))*(diffwvector(ip)-...
                  diffwvector(ip+1))+diffwvector(ip);
        xwb = (xt(ip+1)-xp)/(xt(ip+1)-xt(ip))*(xwbvector(ip)-...
                  xwbvector(ip+1))+xwbvector(ip);
        pr =  (xt(ip+1)-xp)/(xt(ip+1)-xt(ip))*(prgas(ip)-...
                  prgas(ip+1))+prgas(ip);
        twall = (WallX(ipT+1)-xp)/(WallX(ipT+1)-WallX(ipT))*...
                    (twallvector(ipT)-twallvector(ipT+1))+twallvector(ipT);
    else
%       fprintf('\rReached end of property correlations\r');
      breakout = true;  % exits the while loop under this condition
    end

    % If you had gas velocities, this is where you would use them:
    % Reynolds number set to zero here because as coded, this model has no
    % input fo gas velocity. It is assumed that the gas velocity is equal
    % to the particle velocity:
    %     vlag = (vp-vg);
    %     re = rhog*abs(vlag)*dp/ug;
    re = 0.0;

    % c energy equation
    % c
    % c--    convection
    nu = 2.0 + 0.6*re^0.5*pr^0.333;
    b = cpg*(rtotp)/(2.0*PI*dp*kg);
    if (b >= 1.0e-4)
        blow = b/(exp(b)-1);
    else
        blow = 1.0;
    end
    h = blow*nu*kg/dp;
    qconv = h*ap*(tg-tpred);
    % c--   mass transfer
    if (alfw > 0.0)
        bw = (rtotp)/(2.0*PI*dp*diffw*rhog);
        if (bw >= 1.0e-4)
            bloww = bw/(exp(bw)-1);
        else
            bloww = 1.0;
        end
    else
        bloww = 1.0;
    end
    % CHANGE THIS NEXT SECTION TO SUIT GEOMETRY OF SPECIFIC REACTORS:
    % c--    radiation
    z = x;   % distance from burner (cm)
             % distance from exhaust will be (200-z) because reactor is 2m
             % long
    % set up areas, etc of radiation enclosure
    Area(1) = PI*rad^2; % burner (Area vector = same order as emiss vector)
    Area(2) = 2*PI*rad*200; % walls
    Area(3) = Area(1); % exhaust
    Area(4) = ap; % particle
    Temp(1) = tbnr;
```

```
    Temp(2) = twall;
    Temp(3) = texit;
    Temp(4) = tpred;
    % avoid divide by zero:
    if z <= 0
        F(4,1) = 0.5; % limiting value of view factor F(4,1)
    else
        F(4,1) = 0.5*(1-(1/(1+(rad/z)^2)^0.5)); %disk to sphere view factor
    end
    F(4,3) = 0.5*(1-(1/(1+(rad/(200-z))^2)^0.5)); %same as above
    F(4,2) = 1 - (F(4,1) + F(4,3)); % by summation rule
    % by reciprocity:
        F(1,4) = F(4,1)*Area(4)/Area(1);
        F(2,4) = F(4,2)*Area(4)/Area(2);
        F(3,4) = F(4,3)*Area(4)/Area(3);

    qrad = emiss(4)*( F(1,4)*Area(1)*emiss(1)*sigma*Temp(1)^4+...
                      F(2,4)*Area(2)*emiss(2)*sigma*Temp(2)^4+...
                      F(3,4)*Area(3)*emiss(3)*sigma*Temp(3)^4-...
                             Area(4)*sigma*Temp(4)^4); % cal/s
    % END OF SECTION TO CHANGE TO SUIT GEOMETRY OF SPECIFIC REACTORS

    % c--    water evaporation rate
    % using Antoine vapor pressure correlation
    if (alfw > 0)
        xw0 = exp(18.3036-3816.44/(tpred-46.13))/(760*press);
        % In above line, (760*press) was previously just 760 in the FORTRAN
        % source code. The pressure was added to the equation to allow for
        % pressures other than 1 atm.

        xw0 = min(xw0,1.0);
        xw0 = max(xw0,0.0);
        rw = bloww*2.0*rhog*diffw*PI*dp*(xw0-xwb)/(1.0-xw0);
    else
        rw = 0;
    end
    % c--  coal pyrolysis rate
    [yp] = perks(ypred,yp,tpred,L0,c0,ab,eb0,ebsig,ac,ec0,ag,eg0,egsig,...
                                rg,fnca0,an,en0,ensig);

    % c   time step control
    if (y(1) > 5.0e-3)
        dy1 = dt*0.5*(yp(1)+ypp(1));
    else
        dy1 = dt*0.5*(yp(3)+ypp(3));
    end
    if (abs(dy1) < 0.001)
        dt = dt*2;
        if (dt < dtmax)
%           fprintf('\rAt time = %d dt changed to %d\r',time,dt);
        end
    elseif (abs(dy1) > 0.02)
        dt = 0.01/abs(dy1)*dt;
%       fprintf('\rAt time = %d dt changed to %d\r',time,dt);
    end
    dt = min(dt,dtmax);

    % c  free radical light gas nitrogen release mechanism
      if ((mw1-mwchar)/mw1 > fstable)
          yp(4)=yp(4)-y(4)*arad*exp(-erad/rg/tp)*...
              (mwcharold-mwchar)/mwchar*machar/mwchar/dt;
      end
    % c component mass conservation
    for j = 1:4
        y(j) = y(j) + dt*0.5*(yp(j)+ypp(j));
        y(j) = max(zero,y(j));
    end

    % c  update current and old mwchar
    mwcharold = mwchar;
    g0 = 2.0*(1.0-y(1)-c0)-y(2);
```

```
mwchar = mw1-g0*mdel*sigp1/2.0;
% c  crosslinking rate
fracr = 1.0;
if ((fmetold > small) && (acr > 0.0))
    ratecr = acr*exp(-ecr/rg/tpred)*fmetold*dt;
    fracr = 1.0-ratecr/fmetold;
    fmet = fmetold-ratecr;
    fcross = fcrossold+ratecr;
    if (fmet<0.0)
        fcross = fcrossold + fmet;
        fmet = 0.0;
        fracr = 0.0;
    end
end

% c  get product distribution from y array
if(y(1) > small)
    intar = true;
end
[ftar,ftart,fgas,ft,mt] = perkp(y,ftar,intar,ma,rba,c0,...
                                          sig,siginv,nmax,pstar);
gasmw = rba*ma/2.0;
% c  flash distillation
if (fgas >= small)
    ipred = false;
    [ftar,fmet,metold,metold2,ftold,ftold2,...
      tarold,tarold2,fgasold,fgasold2,ftarold,ftarold2] = ...
      flash(fgas,gasmw,ft,mt,fracr,tpred,press,nmax,zero,small,...
      ipred,metold,metold2,ftold,ftold2,tarold,tarold2,fgasold,...
      fgasold2,ftarold,ftarold2);
elseif (fgas < 1.0e-5)
    fmet = ftart;
    ftar = 0.0;
end
intar = false;
fvol = fgas + ftar;
fchar = 1.0 - fvol;
dvdt = (fvol-fvolold)/dt*alfc0;
% c  done with pyrolysis rate!
rtot = dvdt + rwp;
heat = dvdt*delhv + rwp*delhw;

% c calculate heat capacity
% get daf coal heat capacity
[cpc] = heatcp(tpred,yelem);
% get ash heat capacity
[cpa] = heatap(tpred);
cp = (alfcp*cpc + alfa*cpa + alfw*cpw)/(alpha);

trate = (qconv + qrad + heat)/(alpha*cp);
tp = tp + 0.5*(trate+tratep)*dt;

alfw = alfw - rw*dt;
alfc = fchar*alfc0;
alfc = max(alfc,0.0);
alfw = max(alfw,0.0);
alpha = (alfc + alfa + alfw);
omegaa = alfa/alpha;

% c particle diameter changes due to swelling during devolatilization
L = y(1);
del2 = y(2)/2.0;
aind = del2 + L;
dp = dp0*(1.0 + swell*(1.0-L/L0));
ap = PI*dp^2;

% c  nitrogen release calculations
% c  calculate tar nitrogen yield
% c  (assumes tar is released before light gas and HCN)
yntar = yntar + (ftar-ftarold)*fnt;
ftarold = ftar;
```

```
    % c  nitrogen content of char and metaplast
    fnt = y(4)*machar/mwchar;
    % c  nitrogen remaining in char
    % since the way fchar is coded is fchar = char AND metaplast, ynchar is
    % the nitrogen remaining in the char and metaplast
    ynchar = fchar*fnt;
    % c  fraction of original nitrogen remaining in char
    % (and metaplast) - see comment above
    fnchar = ynchar/fnit;
    % c  fraction of original nitrogen released as tar
    fntar = yntar/fnit;
    % c  fraction of original nitrogen released as light gas (diff.)
    fnhcn = 1.0 - fnchar - fntar;
    % c  total fractional release of nitrogen
    fntot = (fnit - fnt*fchar)/fnit;

    % c  distribute light gas into H2O, CO2, CO, CH4, & other HC's

    % c  yf is a CPD indicator of the fraction of total light gas
    % c   that has been released. The look up table on light gas
    % c   composition is based on yf.
    % See Genetti's MS Thesis for more info. In his thesis, yf is called
    % Xgas.
    yf = 1 - aind/aind0;
    [yygas,inside,lib] = lightgas(yf,xoc,yhc);

    % c  calculate fraction of total mass release that is h2o, co2, ch4,
    % c   co, and other light gases
    % This comment is confusing. Here's the explanation:
    % yygas stores the fractions of light gas release that is h20, co2,
    % ch4, co and other light gases. ffgas stores the fraction of total
    % mass release (i.e. volatiles) that is h2o, co2, ch4, co, and other
    % light gases.
    ffgas = zeros(5,1);
    for ik = 1:5
         ffgas(ik) = fgas*yygas(ik);
    end

    % c particle density changes during devolatilization
    rhop = alpha/((4.0/3.0)*PI*(dp/2)^3);

    time = time + dt;
    tms = time*1000.0;

    if (time >= timax)
        breakout = true;
    end
    % c   check to see if interpolation indices need update
    if (x > xt(ix+1))
        ix = ix + 1;
%         if (ix >= 50)
%             break
%         end
    end
    if (x > zv(iv+1))
        iv = iv + 1;
        ip = ip + 1;
%         if (iv >= 50)
%             break
%         end
    end
    if (x > WallX(ipT+1))
        ipT = ipT + 1;
    end
    % store data in output arrays if appropriate
    xm = 0.01*x;
    yNsite = y(4);
    if x >= xt(outputnow)
            tmsout(outputnow) = tms;
            xmout(outputnow) = xm;
            tpout(outputnow) = tp;
```

```
            tgout(outputnow) = tg;
            fvolout(outputnow) = fvol;
            fcharout(outputnow) = fchar;
            fcrossout(outputnow) = fcross;
            ftarout(outputnow) = ftar;
            fmetout(outputnow) = fmet;
            trateout(outputnow) = trate;
            mwcharout(outputnow) = mwchar;
            yNsiteout(outputnow) = yNsite;
            fntout(outputnow) = fnt;
            fncharout(outputnow) = fnchar;
            fntarout(outputnow) = fntar;
            fnhcnout(outputnow) = fnhcn;
            fntotout(outputnow) = fntot;
            fgasout(outputnow) = fgas;
            ffgasout(:,outputnow) = ffgas;
            yygasout(:,outputnow) = yygas;
            yfout(outputnow) = yf;
            waterout(outputnow) = alfw/alpha;
            convheatout(outputnow) = qconv*(4.1868); % Watts/particle
            dpout(outputnow) = dp;
        outputnow = outputnow + 1;
    end
end % end of while loop
```

at.m – subroutine for CPD Model

```
function [tri_area] = at(aa,bb,cc)
% Function required by lightgas.m to calculate area of triangle
tri_area = 0.5*bb*cc*(1-((bb^2+cc^2-aa^2)/(2*bb*cc))^2)^0.5;
```

d.m – subroutine for CPD Model

```
function [dist] = d(x2,x1,y2,y1)
% Function required by lightgas.m to calculate distance
dist = ((x2-x1)^2+(y2-y1)^2)^0.5;
```

flash.m – subroutine for CPD Model

```
function [ftar,fmet,metold,metold2,ftold,ftold2,...
          tarold,tarold2,fgasold,fgasold2,ftarold,ftarold2] = ...
          flash(fgas,gasmw,ft,mt,fracr,temp,press,nmax,zero,small,ipred,...
          metold,metold2,ftold,ftold2,tarold,tarold2,fgasold,fgasold2,...
          ftarold,ftarold2)

% c  ipred = true only on predictor step, when old values are updated

% Initialize values of some variables:
ntot = nmax + 1;
a = 87058;
b = 299;
G = 0.5903;
x3 = 0.2;
x2 = 0.3;
x = zeros(1,ntot);
y = zeros(1,ntot);
k = zeros(1,ntot);
L = zeros(1,ntot);
v = zeros(1,ntot);
xmw = zeros(1,ntot);
f = zeros(1,ntot);
z = zeros(1,ntot);
pv = zeros(1,ntot);
converged = false;

% c  xxxold2 is the value at the previous time step, while
% c  xxxold  is the value from the last time the subroutine was called
```

```
% c  metold(i) = mass fraction of coal contained in metaplast of mer size i
% c  fracr = fraction to account for reduction of metaplast by crosslinking
% c          in latest time step
% c
% c  renormalize in tar fragment data to molar basis
% c  f(i) = moles of mer i
% c  ft(i) = mass of mer i

ftot = 0.0;
for i = 1:nmax
    i1=i+1;
    xmw(i1) = mt(i);
    if (ipred)
        ftold2(i) = ftold(i);
        metold2(i) = metold(i);
        tarold2(i) = tarold(i);
        fgasold2 = fgasold;
        ftarold2 = ftarold;
    end
    dif = ft(i) - ftold2(i);
    dif = max(dif,zero);
    f(i1) = (dif+metold2(i)*fracr)/mt(i);
    ftold(i) = ft(i);
    ftot = ftot + f(i1);
end
f(1) = (fgas-fgasold2)/gasmw;
f(1) = max(f(1),0.);
fgasold = max(fgas,fgasold2);
xmw(1) = gasmw;
ftot = ftot + f(1);

% c  Get mole fraction of components in the feed stream
% c  and compute equilibrium constants k(i) from vapor pressure and
% c  Raoults law expression
sum = 0.0;
for ii = 1:ntot
    sum = sum + f(ii);
    pv(ii) = a*exp(-b*xmw(ii)^G/temp);
    k(ii) = pv(ii)/press;
    if (k(ii) < 0.001)
        k(ii) = 0.0;
    end
end

if (sum <= 1.0e-8)
    return
end

for ii = 1:ntot
    z(ii) = f(ii)/sum;
end

% c  use the Rachford-Rice formulation for flash distillation
% c  x = v/f, first guess
x1 = x3;
% c  calculate sum (eq. 11-24, Separation Processes, by King, 1971)
f1 = 0.0;
for ii = 1:ntot
    f1 = f1 + z(ii)*(k(ii)-1)/((k(ii)-1)*(x1)+1);
end

% c  secant method for convergence
if (x2 == x1)
    x2 = x1 + 0.005;
end
for iter = 1:100
    % c  calculate sum (eq. 11-24, separation processes, by King, 1971)
    f2 = 0.0;

    for ii = 1:ntot
        f2 = f2 + z(ii)*(k(ii)-1)/((k(ii)-1)*(x2)+1);
```

```
    end

    if ((abs(f2) <= small) || (abs(f2-f1) <= small^2))
        converged = true;
        break
    end

    x3 = x2 - f2*(x2-x1)/(f2-f1);

    if (x3 > 1.0)
        x3 = 1.0 - small^2;
    end

    if (x3 < 0.0)
        x3 = 0.0 + small^2;
    end

    if (x3 == x2)
        fprintf('\r Problem---f(v/f) not converged, but x3=x2 \r');
        fprintf('x3 = %d \r', x3);
        fprintf('x2 = %d \r', x2);
        if (x2 >= small)
            x3 = x2 - small;
        else
            x3 = x2 + small;
        end
    end

    if ((x2 <= 1.0e-5) && (x1 <= 1.0e-5))
        x2 = 1.0e-7;
        converged = true;
        break
    end

    if ((x2 >= 0.9999) && (x1 >= 0.9999))
        x2 = 0.9999;
        converged = true;
        break
    end

    f1 = f2;
    x1 = x2;

    % c  under-relax solution (especially near the v/f=1 limit
    x2 = 0.2*x2 + 0.8*x3;
end

if (converged == false)
%     fprintf('\r Convergence not achieved in flash distillation\r');
%     fprintf('\r last two guesses for v/f were:\r');
%     fprintf('x3 = %d \r', x3);
%     fprintf('x2 = %d \r', x2);
    ftar = ftarold2;
    fmet = 0;
    return
end

% c  now calculate molecular weight distributions on a
% c  light-gas free basis, wt fractions
vtot = ftot * x2;
ltot = ftot - vtot;
vol = vtot/ltot;
sumx = 0.0;
sumy = 0.0;
% xmwtot = 0.0;
ttot = 0.0;
for ii = 2:ntot
    i = ii-1;
    L(ii) = f(ii)/(1.0 + k(ii)*vol);
    v(ii) = f(ii) - L(ii);
    x(ii) = L(ii)*xmw(ii);
```

```
    y(ii) = v(ii)*xmw(ii);
    metold(i) = max(x(ii),zero);
    tarold(i) = tarold2(i) + y(ii);
%     xmwtot = xmwtot + tarold(i)*xmw(ii);
    ttot = ttot + tarold(i);
    sumx = sumx + x(ii);
    sumy = sumy + y(ii);
end

% This code commented out because xmwtot is an unused variable elsewhere
% Same applies to other places where xmwtot appears
% if (ttot > 0.0)
%     xmwtot = xmwtot/ttot;
% end

for ii = 2:ntot
    if (sumx ~= 0.0)
        x(ii) = x(ii)/sumx;
    end
    if (sumy ~= 0.0)
        y(ii) = y(ii)/sumy;
    end
end

ftar = ftarold2 + sumy;
% ftarold = ftar;  % This should only be executed later in cpdcp_nlg.m
                   % because of the way ftarold is passed back to the
                   % calling program. This is different to the FORTRAN
                   % source code, but the results for fntar are all zero
                   % for the MATLAB version if this line is not commented
                   % out.
fmet = sumx;
```

gamln.m – subroutine for CPD Model

```
function [y] = gamln(x)
% c   this is a program to calculate the ln of the gamma function,
% c   taken from Abramowitz, p. 257, 6.1.41
PI = 3.14159;
y = (x-0.5)*log(x)-x+0.5*log(2.0*PI)+1.0/(12.0*x)-1.0/(360.0*x^3)+...
        1.0/(1260.0*x^5)-1.0/(1680.0*x^7);

% original FORTRAN code:
% gamln = (x-.5)*alog(x)-x+.5*alog(2.*PI)+1./(12.*x)...
%              -1./(360.*x**3)+1./(1260.*x**5)-1./(1680.*x**7)
% Note that in Fortran 77 "alog" is a function that returns the natural
% logarithm. The a at the beginning of alog is there to start the name of
% the function with a letter commonly associated with real rather than
% integer values.
```

heatap.m – subroutine for CPD Model

```
function [cpa] = heatap(tp)
% c  calculates ash heat capacity
% c   tp          particle temperature (k)
% c   cpa         ash heat capacity (cal/g/k)
% c   rgas        gas constant (1.987 cal/g/k)
cpa = (754+0.586*(tp-273))/(4.184e3);
```

heatcp.m – subroutine for CPD Model

```
function [cp] = heatcp(tp,yelem)
% c  this program calculates the heat capacity of a particle from Merrick's
% c  correlations.
% c  calculates daf coal heat capacity
% c   tp          particle temperature (k)
% c   cp          particle heat capacity (cal/g/k)
```

```
% c   u(i)        atomic weights of elements
% c   y(i)        mass fractions of elements (c,h,n,o,s)
% c   rgas        gas constant (1.987 cal/gmole/k)
% c   rgasj       gas constant (8314.3 j/kg/k)


u = [12.0; 1.0; 14.0; 16.0; 32.0];
rgas = 1.987;
% commented out because unused:
% rgasj = 8314.3;

% c  calculate mean atomic weight, a
a = 0.0;
for i = 1:5
    a = a+(yelem(i)/u(i));
end
a = 1/a;
f1 = 380/tp;
f2 = 1800./tp;
cp = rgas/a*((exp(f1)/((exp(f1)-1)/f1)^2)+2*(exp(f2)/((exp(f2)-1)/f2)^2));

% there used to be a separate function called g1:
% g1=exp(z)/((exp(z)-1)/z)^2;
% and  cp was calculated as cp = rgas/a *(g1(f1)+2.*g1(f2));
% this was changed to the version above to remove the requirement for the
% g1 function
```

inverf.m – subroutine for CPD Model

```
function [x] = inverf(y)
% c this program calculates the inverse of the area under the normal curve.
% c if y=area(x), then given y, this program will calculate x.
% c a table lookup is performed.
% Calculates the number of standard deviations (x) from the mean
%   corresponding to the area under the standard normal probability curve
%   from -infinity to x.

xx = [3.4; 3.2; 3.; 2.8; 2.6; 2.4; 2.2; 2.0; 1.8;
      1.6; 1.4; 1.2;1.0; 0.8; 0.6; 0.4; 0.2; 0.0];
yy = [0.9997; 0.9993; 0.9987; 0.9974; 0.9953; 0.9918; 0.9861; 0.9772;
      0.9641; 0.9452; 0.9192; 0.8849; 0.8413; 0.7881; 0.7257; 0.6554;
      0.5793; 0.5];

fac = 1.0;

% c  check to see if y is within range
% c      if(y<0.0228)then
% c         x = -2.0
% c         return

if (y < 0.0003)
    x = -3.4;
    return
elseif (y < 0.5)
    yp = 1.0-y;
    fac = -1.0;
elseif (y > 0.9997)
    x = 3.5;
    return
else
    yp = y;
end

% c  search for range
for i = 18:-1:1
    if (yp <= yy(i-1))
        x = xx(i) + (yp-yy(i))*(xx(i-1)-xx(i))/(yy(i-1)-yy(i));
        x = fac*x;
        return
    end
```

```
end
```

lightgas.m – subroutine for CPD Model

```
function [yygas,inside,lib] = lightgas(yf,xoc,yhc)
% c  ---------------------------------------------------------------------
% c  --------------light gas distribution model-----------------------
% c  ---------------------------------------------------------------------
% c  this program calculates the distribution of light gas species
% c  based on a look up table of reference data
% USAGE:
% [yygas,inside,lib] = lightgas(yf,xoc,yhc);

% c ********************************************************************
% c ****************light gas distribution reference library************
% c ********************************************************************
%
% c  this library can be moved outside of submodel as long as
% c  it is linked to the light gas sub-model
%
% c  xz = the index used in correlation.  In the main program it
% c  corresponds to variable "yf"

% c  f*** = fraction of light gas that is species ***

% c  The data is organized in the following order with 12 ordered
% c  pairs for each species (ordered with xz)

% c  Each table is organized in rows in the following order
% c       1 Lower Kittaning (Chen)
% c       2 Pocahontas #3 (ANL)
% c       3 Upper Freeport (ANL)
% c       4 Pittsburgh (Chen)
% c       5 Lewis Stockton (ANL)
% c       6 Utah Blind Canyon (ANL)
% c       7 Illinois #6 (ANL)
% c       8 Illinois #6 (Chen)
% c       9 Wyodak (ANL)
% c       10 Beulah Zap (ANL)
% c       11 Dietz (Chen)
% c       12 PSOC 1448 (Serio)
% When lib is 13 or 14, the library coal is Rhein Braun or Hongay
% respectively:
%     From Genetti's MS Thesis pg 81: "The light gas composition of
%     extremely high rank coals was estimated based on the measured light
%     gas composition of the pyrolysis products of an anthracite coal,
%     known as Hongay, reported by Xu and Tomita. The light gas composition
%     of extremely low rank coals was estimated based on data on a lignite,
%     known as Rhein Braun, also reported by Xu and Tomita."


% c  reference data for xz = yf, the fractional light gas released
xz = [0,0.04,0.11,0.14,0.21,0.27,0.34,0.675,0.9,1.0,0,0;
      0,0.161,0.442,0.663,0.777,0.874,0.921,0.967,1.0,0,0,0;
      0,0.022,0.20,0.430,0.526,0.64,0.787,0.875,0.927,0.955,1.0,0;
      0,0.04,0.12,0.15,0.23,0.29,0.36,0.68,0.9,1.0,0,0;
      0,0.018,0.058,0.21,0.417,0.572,0.696,0.778,0.821,0.883,0.932,1.0;
      0,0.052,0.144,0.291,0.498,0.639,0.746,0.859,0.925,0.949,0.966,1.0;
      0,0.063,0.178,0.33,0.506,0.612,0.706,0.813,0.895,0.94,1.0,0;
      0,0.04,0.12,0.15,0.23,0.29,0.36,0.68,0.9,1.0,0,0;
      0,0.061,0.146,0.374,0.535,0.622,0.714,0.8,0.883,0.931,0.964,1.0;
      0,0.034,0.087,0.179,0.316,0.472,0.585,0.694,0.777,0.872,0.935,1.0;
      0,0.04,0.12,0.16,0.25,0.31,0.37,0.68,0.9,1.0,0,0;
      0,0.02,0.055,0.17,0.313,0.434,0.546,0.716,0.874,0.935,0.973,1.0];

% c  fraction of light gas that is water
fh2o = [0.772,0.772,0.738,0.455,0.371,0.304,0.290,0.273,0.218,0.218,0,0;
   0.699,0.632,0.299,0.269,0.247,0.249,0.236,0.225,0.226,0,0,0;
   0,0,0.35,0.297,0.301,0.299,0.284,0.291,0.306,0.297,0.283,0;
   0.636,0.636,0.646,0.550,0.436,0.320,0.186,0.199,0.195,0.195,0,0;
```

```
   1.0,0.983,0.754,0.488,0.413,0.385,0.373,0.382,0.377,0.362,0.367,0.348;
   0.665,0.636,0.604,0.508,0.435,0.409,0.383,0.362,0.351,0.343,0.342,0.339;
   0.763,0.737,0.698,0.572,0.527,0.470,0.438,0.411,0.411,0.396,0.378,0;
   0.748,0.748,0.637,0.704,0.490,0.446,0.348,0.268,0.266,0.266,0,0;
   0,0,0.385,0.461,0.396,0.369,0.344,0.323,0.292,0.277,0.266,0.257;
   0,0,0.197,0.267,0.26,0.333,0.361,0.369,0.346,0.306,0.285,0.267;
   0.521,0.521,0.55,0.523,0.511,0.46,0.414,0.388,0.313,0.313,0,0;
   0,0,0.291,0.335,0.264,0.271,0.261,0.211,0.171,0.160,0.153,0.149];

% c  fraction of light gas that is carbon dioxide
fco2 = [0,0,0,0.174,0.174,0.167,0.129,0.102,0.071,0.071,0,0;
   0.259,0.234,0.113,0.086,0.097,0.109,0.116,0.118,0.122,0,0,0;
   0.333,0.327,0.070,0.052,0.057,0.06,0.059,0.062,0.066,0.08,0.115,0;
   0.194,0.194,0.152,0.117,0.116,0.122,0.081,0.092,0.065,0.065,0,0;
   0,0,0,0.122,0.103,0.086,0.083,0.082,0.085,0.086,0.093,0.128;
   0.332,0.318,0.165,0.141,0.120,0.108,0.105,0.119,0.120,0.122,0.125,0.130;
   0.229,0.221,0.125,0.09,0.07,0.073,0.083,0.133,0.132,0.13,0.147,0;
   0.111,0.111,0.142,0.175,0.149,0.155,0.136,0.122,0.133,0.133,0,0;
   0.98,0.984,0.55,0.345,0.317,0.285,0.286,0.277,0.273,0.264,0.254,0.255;
   0.993,0.989,0.786,0.572,0.519,0.416,0.375,0.345,0.335,0.32,0.303,0.299;
   0.363,0.363,0.353,0.325,0.321,0.35,0.318,0.251,0.249,0.249,0,0;
   1.0,0.983,0.448,0.179,0.104,0.09,0.104,0.151,0.166,0.160,0.158,0.154];

% c  fraction of light gas that is methane
fch4 = [0.203,0.203,0.078,0.160,0.180,0.219,0.258,0.294,0.320,0.320,0,0;
        0.041,0.037,0.388,0.389,0.359,0.332,0.323,0.307,0.299,0,0,0;
        0.667,0.655,0.42,0.454,0.444,0.419,0.382,0.353,0.331,0.321,0.306,0;
        0.055,0.055,0.073,0.088,0.116,0.124,0.170,0.15,0.189,0.189,0,0;
        0,0,0.188,0.195,0.234,0.243,0.224,0.21,0.2,0.186,0.177,0.167;
        0,0,0.11,0.155,0.176,0.172,0.185,0.173,0.163,0.159,0.156,0.151;
        0,0,0.075,0.136,0.159,0.178,0.174,0.157,0.143,0.141,0.132,0;
        0.02,0.02,0.026,0.042,0.045,0.049,0.064,0.1,0.128,0.128,0,0;
        0,0,0,0.029,0.048,0.067,0.069,0.072,0.069,0.066,0.063,0.061;
        0,0,0,0,0.035,0.05,0.061,0.058,0.057,0.053,0.049,0.046;
        0.01,0.01,0.011,0.016,0.011,0.021,0.023,0.035,0.06,0.06,0,0;
        0,0,0.216,0.262,0.362,0.327,0.307,0.25,0.203,0.189,0.182,0.177];

% c  fraction of light gas that is carbon monoxide
fco = [0,0,0.157,0.121,0.141,0.112,0.139,0.085,0.145,0.145,0,0;
       0,0,0,0.057,0.097,0.109,0.124,0.15,0.153,0,0,0;
       0,0,0,0,0,0.024,0.078,0.097,0.099,0.104,0.099,0;
       0.083,0.083,0.038,0.066,0.032,0.168,0.286,0.324,0.313,0.313,0,0;
       0,0,0,0,0.055,0.091,0.124,0.131,0.142,0.171,0.168,0.162;
       0,0,0,0.028,0.093,0.129,0.142,0.162,0.181,0.191,0.193,0.195;
       0,0,0,0.075,0.099,0.122,0.139,0.133,0.148,0.167,0.177,0;
       0.101,0.101,0.173,0.054,0.219,0.247,0.335,0.349,0.28,0.280,0,0;
       0,0,0.055,0.115,0.151,0.168,0.172,0.2,0.236,0.264,0.287,0.298;
       0,0,0,0.133,0.142,0.150,0.15,0.173,0.206,0.265,0.307,0.331;
       0.096,0.096,0.066,0.113,0.123,0.13,0.2,0.281,0.334,0.334,0,0;
       0,0,0,0.084,0.078,0.115,0.130,0.191,0.262,0.294,0.311,0.322];

% Transpose arrays above (necessary for FORTRAN to MATLAB translation
% without retyping all the data by hand as was done for the 'out'
% array below):
xz = xz';
fh2o = fh2o';
fco2 = fco2';
fch4 = fch4';
fco = fco';


% c       ************************************************************
% c       **********end of reference library*************************
% c       ************************************************************

% c  ***************************************************************
% c  *******determine the appropriate triangle for interpolation**********
% c  ***************************************************************

% c define the equations of line, distance and area
% These equations were moved into the function files yyy.m, xxx.m, d.m,
```

```
% and at.m:
        % yyy(aa,xd,bb)=aa*xd+bb;
        % xxx(aa,yd,bb)=(yd-bb)/aa;
        % d(x2,x1,y2,y1)=((x2-x1)^2+(y2-y1)^2)^0.5;
        % at(aa,bb,cc)=0.5*bb*cc*(1-((bb^2+cc^2-aa^2)/(2*bb*cc))^2)^0.5;

% c  initialize variables
x = xoc;
y = yhc;
ind = yf;

% c  look up table of the reference points of the triangular mesh
xx = [0.0177734,0.0203654,0.0659401,0.0773465,0.0893623,0.1077369,...
      0.1305803,0.1357569,0.1803479,0.2093441,0.2603201,0.0687];
yy = [0.6717240,0.5810955,0.6550527,0.8088697,0.7575807,0.8506428,...
      0.7671163,0.8523190,0.8499221,0.7890888,0.8572938,0.863];

% c  look up table for a and b of equations of all triangle sides
a = [-34.965,1.6228,-0.34612,2.3021,1.7337,1.1993,4.3774,...
     -4.2685,0.23134,5.0647,1.3746,-3.6565,0.059818,16.459,...
     1.6638,-0.05375,0.27897,-2.0979,0.092179,1.3380,3.7559,...
     -6.2604,-0.31655];
b = [1.2932,0.54805,0.67788,0.63081,0.54074,0.65041,0.36641,...
     1.1390,0.73691,0.30499,0.70255,1.2446,0.84420,-1.3821,...
     0.54985,0.85962,0.73069,1.2283,0.83330,0.50899,0.60497,...
     1.2931,0.88475];

% c  look up table for the three sides that correspond to each triangle
s1 = [1,3,4,7,8,10,12,14,15,18,21,22];
s2 = [2,7,6,5,10,9,14,15,17,20,4,11];
s3 = [3,6,8,9,11,12,13,16,18,19,22,23];

% c  loop to find the appropriate triangle for interpolation
m=0;
inside = true;
for i = 1:12
    z1=xxx(a(s1(i)),y,b(s1(i)));
    z2=xxx(a(s2(i)),y,b(s2(i)));
    z3=yyy(a(s3(i)),x,b(s3(i)));
    if ((x >= z1) && (x <= z2) && (y <= z3))
        m=i;
        break
    end
end
% this if statement moved outside of above loop for speed:
if((i == 12) && (m == 0.0))
%     fprintf('\rOne or both ratios are out of bounds\r');
    inside = false;
else
%     fprintf('\rTriangle = %d',m);
end

% c  ^^^^^^^^^^^^^^^^^^^^^^^^^^^^^^^^^^^^*
% c  ^^^^^^^^*triangular interpolation^^^^^^^^^^^^
% c  ^^^^^^^^^^^^^^^^^^^^^^^^^^^^^^^^^^^^*
if (inside)
    % c  This interpolation scheme is taken from Zhao et al., 25th Symp.
    % c  on Comb. (Int.), 1994/pp. 553-560.

    % c  look up table for points 1,2, and 3 for each triangle
    p1 = [2,3,1,3,5,5,7,7,7,10,1,4];
    p2 = [1,1,4,5,4,6,6,8,9,9,12,12];
    p3 = [3,5,5,7,6,7,8,9,10,11,4,6];

    % c  calculate the length of each side
    ds1 = d(xx(p1(i)),xx(p2(i)),yy(p1(i)),yy(p2(i)));
    ds2 = d(xx(p3(i)),xx(p1(i)),yy(p3(i)),yy(p1(i)));
    ds3 = d(xx(p3(i)),xx(p2(i)),yy(p3(i)),yy(p2(i)));
    ds4 = d(x,xx(p2(i)),y,yy(p2(i)));
    ds5 = d(xx(p1(i)),x,yy(p1(i)),y);
    ds6 = d(xx(p3(i)),x,yy(p3(i)),y);
```

```
    % c  calculate the area of each triangle used in interpolation scheme
    a1 = at(ds1,ds2,ds3);
    a2 = at(ds1,ds5,ds4);
    a3 = at(ds5,ds2,ds6);

    % c  calculate s and r, the weighted fraction of two of the points
    % c  the weighted fraction of other point will be 1-r-s
    s = a2/a1;
    r = a3/a1;

    % c       ^^^^^^^^^^^^^^^^^^^^^^^^^^^^^^
    % c       ^^^^^^*calculate light gas distribution^^^^^^^*
    % c       ^^^^^^^^^^^^^^^^^^^^^^^^^^^^^^

    % c  n is the number of order pairs of data for coals 1-12
    % n = [10,9,11,10,12,12,11,10,12,12,10,12];
    % line above (n = [...) commented out because it is not used

    % c  Loop to calculate the light gas composition of each reference
    % c  coal (point) of triangle.  This is accomplished using linear
    % c  interpolation between points in reference library

    % c  j specifies the point (1,2, or 3) of the triangle selected above
    ygas = zeros(4,3);
    for j = 1:3
        if (j == 1)
            lib=p1(i);
        elseif (j == 2)
            lib=p2(i);
        else
            lib=p3(i);
        end

        % c  do loop to find the two xz points that surround ind

        for ii = 1:12
            if (ind >= xz(ii,lib) && ind <= xz(ii+1,lib))
                break
            end
        end

    % c       for ygas(k,j)
    % c             k=1;fh2o
    % c             k=2;fco2
    % c             k=3;fch4
    % c             k=4;fco
    % c             k=5;other light gases (HC's, H2, parafins, olefins)

    % c  linear interpolation to find reference values as a function of ind

        ygas(1,j)=((ind-xz(ii+1,lib))/(xz(ii,lib)-xz(ii+1,lib)))*...
                    fh2o(ii,lib)+((ind-xz(ii,lib))/(xz(ii+1,lib)-...
                    xz(ii,lib)))*fh2o(ii+1,lib);
        ygas(2,j)=((ind-xz(ii+1,lib))/(xz(ii,lib)-xz(ii+1,lib)))*...
                    fco2(ii,lib)+((ind-xz(ii,lib))/(xz(ii+1,lib)-...
                    xz(ii,lib)))*fco2(ii+1,lib);
        ygas(3,j)=((ind-xz(ii+1,lib))/(xz(ii,lib)-xz(ii+1,lib)))*...
                    fch4(ii,lib)+((ind-xz(ii,lib))/(xz(ii+1,lib)-...
                    xz(ii,lib)))*fch4(ii+1,lib);
        ygas(4,j)=((ind-xz(ii+1,lib))/(xz(ii,lib)-xz(ii+1,lib)))*...
                    fco(ii,lib)+((ind-xz(ii,lib))/(xz(ii+1,lib)-...
                    xz(ii,lib)))*fco(ii+1,lib);
    end
end

if (inside)
    % c       ^^^^^^^^^^^^^^^^^^^^^^^^^^^^^^
    % c       ^^^*calculate gas composition from library coals^^^^*
    % c       ^^^^^^^^^^^^^^^^^^^^^^^^^^^^^^
```

```
    % c  yygas(k) = the fraction of light gas that is k
    % c  1=h20, 2=co2, 3=ch4, 4=co
    yygas = zeros(5,1);
    for k = 1:4
        yygas(k) = (1-r-s)*ygas(k,1) + r*ygas(k,2) + s*ygas(k,3);
    end
else
    % c       ^^^^^^^^^^^^^^^^^^^^^^^^^^^^^^
    % c       ^^*estimate composition for coals outside mesh^^^^^^
    % c       ^^^^^^^^^^^^^^^^^^^^^^^^^^^^^^
    out = [0,0.085,0.12,0.155,0.222,0,0,0.05,0.066,0.175,0,0.222,0.285,0;
 0.085,0.12,0.155,0.222,0.285,0.089,0.05,0.175,0.175,0.222,0.175,1,1,0.175;
 0.835,0.835,0.835,0.835,0.75,0.75,0.63,0.63,0.69,0,0.55,0,0.75,0;
 1.5,1.5,1.5,1.5,1.5,0.835,0.75,0.69,0.835,0.835,0.63,0.75,1.5,0.55;
 12,6,8,9,11,4,1,3,7,10,2,10,13,14];

    for kk = 1:14
        if((x > out(1,kk)) && (x <= out(2,kk)))
            if((y >= out(3,kk)) && (y < out(4,kk)))
                lib = out(5,kk);
                if (lib == 13)
                    yygas(1) = 0.24;
                    yygas(2) = 0.37;
                    yygas(3) = 0.06;
                    yygas(4) = 0.28;
                    break
                end
                if (lib == 14)
                    yygas(1) = 0.18;
                    yygas(2) = 0.08;
                    yygas(3) = 0.37;
                    yygas(4) = 0.18;
                    break
                end
                % c  do loop to find the two xz points that surround ind

                for ii = 1:12
                    if((ind >= xz(ii,lib)) && (ind <= xz(ii+1,lib)))
                        break
                    end
                end

                % c  linear interpolation to find reference values
                %                                       as a function of ind

                yygas(1)=((ind-xz(ii+1,lib))/(xz(ii,lib)-xz(ii+1,lib)))*...
                          fh2o(ii,lib)+((ind-xz(ii,lib))/(xz(ii+1,lib)-...
                          xz(ii,lib)))*fh2o(ii+1,lib);
                yygas(2)=((ind-xz(ii+1,lib))/(xz(ii,lib)-xz(ii+1,lib)))*...
                          fco2(ii,lib)+((ind-xz(ii,lib))/(xz(ii+1,lib)-...
                          xz(ii,lib)))*fco2(ii+1,lib);
                yygas(3)=((ind-xz(ii+1,lib))/(xz(ii,lib)-xz(ii+1,lib)))*...
                          fch4(ii,lib)+((ind-xz(ii,lib))/(xz(ii+1,lib)-...
                          xz(ii,lib)))*fch4(ii+1,lib);
                yygas(4)=((ind-xz(ii+1,lib))/(xz(ii,lib)-xz(ii+1,lib)))*...
                          fco(ii,lib)+((ind-xz(ii,lib))/(xz(ii+1,lib)-...
                          xz(ii,lib)))*fco(ii+1,lib);
                break
            end
        end
    end

% these lines are commented out to speed up execution:
%     fprintf('\rLight gas distribution is based on ref. # %d\r',lib);
%     fprintf('\rO/C = %d\rH/C = %d',x,y);
end

yygas(5) = 1 - yygas(1) - yygas(2) - yygas(3) - yygas(4);
```

perkp.m – subroutine for CPD Model

```
function [ftar,ftart,fgas,ft,mt] = perkp(y,ftar,intar,ma,rba,c0,...
                                                  sig,siginv,nmax,pstar)
% USAGE:
% [ftar,ftart,fgas,ft,mt] = perkp(y,ftar,intar,ma,rba,c0,...
%                                       sig,siginv,nmax,pstar);
%
% c   calculates fractions of tar, and gas from p, sig, L, and c

L = y(1);
del = y(2);
c = y(3);
p = L + c;

if (intar)
    if(p > 0.9999)
        delfac = 1.0;
    else
        delfac = del/(1.0-p);
    end
    a = 1.0 + rba*(L/p + (sig-1.0)/4.0*delfac);
    b = (delfac/2.0 - L/p);
    % find pstar
    pstar0 = pstar;
    pinv = siginv+1.0e-4;
    if(p >= 0.9999)
        pstar = 0.0;
    elseif (p >= pinv)
        for i = 1:25
            f = pstar*(1-pstar)^(sig-1) - p*(1-p)^(sig-1);
            fp = (1-pstar)^(sig-1)-pstar*(sig-1)*(1-pstar)^(sig-2);
            ppstar = pstar - f/fp;
            err = abs(1.0 - ppstar/pstar);
            if (err <= 1.0e-4)
                break
            end
            pstar = ppstar;
        end
        if (err > 1.0e-4)
            fprintf('\r!!!!!!!!!!!WARNING!!!!!!!!!!!!!!!!!\r');
            fprintf('pstar did not converge\r');
            fprintf(' p = %d \r sig = %d \r pstar = %d \r',p,sig,pstar);
        end
    else
        pstar = p;
    end

    % c  check to see if pstar is in the right range
    if ((pstar < 0.0)||((p ~= pstar) && (pstar >= siginv)))
        fprintf('\r!!!!!!!!!!!WARNING!!!!!!!!!!!!!!!!!\r');
        fprintf('Error--pstar out of acceptable ranges!\r');
        fprintf(' pstar = %d \r',pstar);
        fprintf(' p = %d \r sig = %d \r pstar0 = %d \r',p,sig,pstar0);
        return
    end

    sfac = (sig+1.0)/(sig-1.0);
    fp = (pstar/p)^(sfac);
    kp = (pstar/p)^sfac*(1.0-(sig+1)/2.0*pstar);

    % c  calculate wt fraction tar, gas, and char
    ftart = 2.0*(a*fp + rba*b*kp)/(2.0+rba*(1.0-c0)*(sig+1.0));
else
    ftart = 0;
end

tarfac = 1.0 - ftar;
g1 = (2.0*(1.0 - p) - del);
```

```
g2 = 2.0*(c - c0);
g0 = g1 + g2;

mgas = rba*ma*g0*(sig+1)/4.0*tarfac;
mtot = ma + rba*ma*(sig+1)/2.0 *(1.0 - c0);
fgas = mgas/mtot;

ft = zeros(1,nmax); % preallocated for speed
mt = zeros(1,nmax); % preallocated for speed

% c  calculate tar molecular weight distribution
if (intar)
    ftsum = 0.0;

    for n = 1:nmax
        tn = n*(sig - 1.0) + 2;
        xm = n*sig+1.0;
        yk = n-1.0;
        xm1 = xm+1.0;
        % c  gamln is the solution to the gamma function in
        %                                          the sandia math library
        fg1 = gamln(xm1);
        if (fg1 <= 1.0e-10)
            fgam = 0.0;
        else
            yk1 = yk + 1.0;
            fg2 = gamln(yk1);
            xmyk = xm - yk + 1.0;
            fg3 = gamln(xmyk);
            fgam = exp(fg1 - fg2 - fg3);
        end
        bnn = (sig+1.0)/(n*sig+1.0)*fgam;
        qn = bnn*(p^(n-1))*((1-p)^tn)/n;
        % c  ft(n) = weight fraction of each tar bin
        ft(n) = 2.0*(n*a*qn + rba*b*qn)/(2.0 + rba*(1.0-c0)*(sig+1.0));
        ftsum = ftsum + ft(n);
        % c  check to not divide by zero
        if (p <= 1.0e-9)
            fac = 0;
        else
            fac = L/p;
        end
        tst = 1.0-p;
        if (tst <= 1.0e-9)
            fac1 = 0.0;
        else
            fac1 = del/(1.0-p);
        end
        % c  mt(n) = molecular weight of each tar bin
        mt(n) = n*ma + (n-1)*rba*ma*fac + tn*rba*ma/4.0*fac1;
    end
end
```

perks.m – subroutine for CPD Model

```
function [yp] = perks(y,yp,t,L0,c0,ab,eb0,ebsig,ac,ec0,ag,eg0,egsig,...
                                rg,fnca0,an,en0,ensig)
% USAGE:
%  [yp] = perks(y,yp,t,L0,c0,ab,eb0,ebsig,ac,ec0,ag,eg0,egsig,...
%                   rg,fnca0,an,en0,ensig);
% c  This subroutine is the meat of the devolatilization model
% y  A four element array:
%       y(1) = l       labile bridges
%       y(2) = del     ends
%       y(3) = c       char links
%       y(4) = fnca    mass fraction of nitrogen in site (aromatic)
% c  yp(i) = derivative of y(i) in time
%    t = temperature

fx = 0.0;
```

```
L = y(1);
del = y(2);
c = y(3);
fnca = y(4);
p = L+c;
g1 = 2.0*(1-p)-del;
g2 = 2.0*(c-c0);
g0 = g1+g2;

% c  calculate current activation energy using error function solution
if (c0 < 1.0)
    fx = (g0/(1.0-c0))/2.0;
%   originally this was fx = g0/(1.0-c0)/2.0
%   parentheses added to avoid ambiguity
end

x = inverf(fx);

eg = eg0 + x*egsig;

if (fnca0 > 0)
    fx = 1.0 - fnca/fnca0;
end

x = inverf(fx);

en = en0 + x*ensig;

if (L0 > 0.0)
    fx = 1.0 - L/L0;
end

x = inverf(fx);

eb = eb0 + x*ebsig;
ec = ec0;

% c  calculate rate constants
rt = rg*t;
kb = ab*exp(-eb/rt);
rho = ac*exp(-ec/rt);
kg = ag*exp(-eg/rt);
kn = an*exp(-en/rt);

% c  calculate rate of destruction of labile bridges
yp(1) = -(kb)*L;

% c  calculate rate of formation of ends (danglers)
yp(2) = 2.0*rho*kb*L/(rho+1.0) - kg*del;

% c  calculate rate of formation of char
yp(3) = kb*L/(rho+1.0);

% c  calculate rate of high t (slow) nitrogen loss (as hcn)
yp(4) = -kn*fnca;
```

xxx.m – subroutine for CPD Model

```
function [linex] = xxx(aa,yd,bb)
% Function required by lightgas.m to calculate line
linex = (yd-bb)/aa;
```

yyy.m – subroutine for CPD Model

```
function [liney] = yyy(aa,xd,bb)
% Function required by lightgas.m to calculate line
liney = aa*xd+bb;
```

Appendix E:
Tabulated Experimental Results

All experimental data plotted in the body of the dissertation is tabulated in this appendix. Experimental conditions for each set of results appear in Section 3.1.12 and may be cross-referenced using the experiment names. In the tables “Z” represents the axial distance from the burner. Any missing values in the table indicate that a steady measurement was not obtained.

Table E1. Experimental measurements for the Illinois #6 Air Unstaged case.

Experiment Name:		Illinois #6 Air Unstaged					
Wall Temperatures		HORIBA Gas Analyzer					
Z (m)	T (K)	Z (m)	NO_X (ppm, dry)	CO (ppm, dry)	CO_2 (Vol%, dry)	O_2 (Vol%, dry)	η_N
0.121	1038	0.121	17	859	0.27	18.84	0.02
0.419	1313	0.419	370	159	6.37	8.51	0.39
0.870	1288	0.870	516	60	8.83	5.61	0.55
1.168	1223	1.168	495	70	8.81	5.84	0.53
1.473	1163	1.473	474	89	8.68	6.08	0.50
1.759	1012	1.759	473	122	8.77	5.96	0.50

Table E2. Experimental measurements for the Illinois #6 O25 Unstaged case.

Experiment Name:		Illinois #6 O25 Unstaged					
Wall Temperatures		HORIBA Gas Analyzer					
Z (m)	T (K)	Z (m)	NO_X (ppm, dry)	CO (ppm, dry)	CO_2 (Vol%, dry)	O_2 (Vol%, dry)	η_N
0.121	1104	0.121	108	over	over	25.28	0.07
0.419	1342	0.419	725	324	over	15.49	0.49
0.870	1282	0.870	621	231	over	20.28	0.42
1.168	1205	1.168	608	234	over	21.92	0.41
1.473	1149	1.473	580	261	over	16.91	0.40
1.759	996	1.759	557	331	over	23.85	0.38

Table E3. Experimental measurements for the Illinois #6 O30 Unstaged case.

Experiment Name:		Illinois #6 O30 Unstaged					
Wall Temperatures		HORIBA Gas Analyzer					
Z (m)	T (K)	Z (m)	NO_X (ppm, dry)	CO (ppm, dry)	CO_2 (Vol%, dry)	O_2 (Vol%, dry)	η_N
0.121	1330	0.121	1028	349	over	18.07	0.59
0.419	1310	0.419	1039	422	over	16.86	0.60
0.870	1211	0.870	996	233	over	17.04	0.57
1.168	1146	1.168	929	262	over	20.01	0.54
1.473	1077	1.473	911	419	over	19.42	0.52
1.759	932	1.759	917	360	over	11.58	0.53

Table E4. Experimental measurements for the Illinois #6 Air case.

Experiment Name:	Illinois #6 Air										
Wall Temperatures		**HORIBA Gas Analyzer**									
Z (m)	T (K)	Z (m)	NO_X (ppm, dry)	CO (ppm, dry)	CO_2 (Vol%, dry)	O_2 (Vol%, dry)	η_N				
0.02	1034	0.02	7	20	0.65	6.41	0.01				
0.045	1104	0.045	9	over	2.12	7.41	0.01				
0.071	1183	0.071	343	1027	11.08	4.42	0.26				
0.096	1223	0.096	450	789	9.30	6.93	0.34				
0.108	1221	0.122	653	945	11.71	3.67	0.49				
0.122	1233	0.147	649	1062	11.95	3.39	0.49				
0.147	1236	0.172	651	1171	12.21	3.11	0.49				
0.172	1244	0.198	708	972	13.14	1.93	0.53				
0.198	1242	0.413	642	735	12.99	2.32	0.48				
0.413	1296	0.606	586	721	13.05	2.31	0.44				
0.879	1094	0.667	212	124	5.74	12.54	0.26				
1.171	1023	0.879	300	140	8.64	8.53	0.37				
1.475	953	1.171	245	63	7.22	10.51	0.30				
1.751	846	1.475	260	49	7.80	9.65	0.32				
MKS FTIR Gas Analyzer											
	ppm									Vol%	
Z (m)	CO	CH_4	C_2H_4	HCN	NH_3	NO	NO_2	N_2O	SO_2	CO_2	H_2O
0.020	20	45788	1	0	1	12	2	1	80	0.56	1.25
0.045	6778	24795	206	4	1	34	0	0	189	1.77	5.31
0.071	1658	15	4	2	1	405	0	7	1254	8.86	13.36
0.096	1191	-1	0	0	1	760	0	3	1219	9.02	14.09
0.122	1238	-2	0	0	1	827	0	3	1350	9.91	14.83
0.147	1436	1	0	0	1	833	-1	3	1378	9.89	14.87
0.172	1270	-4	0	0	1	837	0	3	1375	10.13	14.96
0.198	1182	-3	0	0	1	859	0	3	1425	10.47	15.23
0.413	818	-1	0	0	1	770	-1	2	1395	10.34	14.49
0.606	825	3	0	1	1	733	0	2	1449	10.70	14.52
0.667	132	8	0	0	0	287	0	2	655	5.58	7.07
0.879	143	20	0	1	0	380	0	10	884	7.84	10.15
1.171	63	0	0	0	1	325	0	10	734	6.92	8.97
1.475	50	-5	0	0	1	359	0	11	744	7.51	9.99

Table E5. Experimental measurements for the Illinois #6 O30 case.

Experiment Name:	Illinois #6 O30						
Wall Temperatures		**HORIBA Gas Analyzer**					
Z (m)	T (K)	Z (m)	NO_X (ppm, dry)	CO (ppm, dry)	CO_2 (Vol%, dry)	O_2 (Vol%, dry)	η_N
0.025	1185	0.02	420	2539	over	10.07	0.17
0.044	1249	0.045	1021	over	over	-0.77	0.41
0.07	1283	0.071	1104	over	over	-1.22	0.45
0.095	1306	0.108	917	over	over	1.40	0.37
0.108	1297	0.198	978	over	over	-1.24	0.40
0.121	1311	0.413	736	over	over	-0.64	0.30
0.146	1307	0.606	582	over	over	-1.21	0.24
0.171	1282	0.667	142	1255	over	16.41	0.10
0.197	1233	0.879	82	656	over	14.30	0.06
0.413	1259	1.171	117	520	over	11.76	0.08
0.879	1088	1.475	113	552	over	10.98	0.08
1.171	1023						
1.475	961						
1.751	860						

MKS FTIR Gas Analyzer											
	ppm									Vol%	
Z (m)	CO	CH_4	C_2H_4	HCN	NH_3	NO	NO_2	N_2O	SO_2	CO_2	H_2O
0.020	2582	29	7	2	1	423	0	2	736	41.85	16.28
0.045	22565	101	23	8	2	877	1	-10	1886	49.47	23.29
0.071	21822	5	1	3	1	980	3	-12	2020	51.71	23.49
0.108	20402	-4	-1	2	2	886	2	-6	1823	51.88	22.20
0.198	26346	135	16	5	2	804	1	-22	1992	51.71	22.91
0.413	25013	74	8	6	2	593	1	-15	1748	54.79	22.13
0.606	25557	327	45	11	1	522	0	-16	1803	61.63	18.41
0.667	2128	6	4	2	1	257	0	0	981	75.29	12.06
0.879	1213	99	23	3	1	213	-1	10	1153	57.63	10.70
1.171	602	55	12	2	1	261	-1	23	1268	71.74	13.23
1.475	1066	130	30	3	1	265	-1	29	1449	77.27	15.21

Table E6. Experimental measurements for the Illinois #6 O30 (0 ppm NO) case.

Experiment Name:		Illinois #6 O30 (0 ppm NO)					
Wall Temperatures		HORIBA Gas Analyzer					
Z (m)	T (K)	Z (m)	NO_X (ppm, dry)	CO (ppm, dry)	CO_2 (Vol%, dry)	O_2 (Vol%, dry)	η_N
0.025	1185	0.108	1222	over	over	6.56	0.50
0.044	1249	0.413	933	over	over	4.82	0.38
0.07	1283	0.606	435	3297	over	9.88	0.18
0.095	1306	0.667	206	858	over	20.68	0.14
0.108	1260	0.879	201	486	over	15.10	0.13
0.121	1311	1.171	199	445	over	14.43	0.13
0.146	1307	1.475	188	360	over	13.17	0.13
0.171	1282	1.751	106	834	over	10.93	0.07
0.197	1233						
0.413	1255						
0.879	1057						
1.171	983						
1.475	913						
1.751	749						

Table E7. Experimental measurements for the Illinois #6 O30 (525 ppm NO) case.

Experiment Name:		Illinois #6 O30 (525 ppm NO)					
Wall Temperatures		HORIBA Gas Analyzer					
Z (m)	T (K)	Z (m)	NO_X (ppm, dry)	CO (ppm, dry)	CO_2 (Vol%, dry)	O_2 (Vol%, dry)	η_N
0.108	1265	0.108	1476	over	over	6.44	0.59
0.413	1248	0.413	1123	over	over	6.07	0.45
0.879	1052	0.606	734	4577	over	10.66	0.30
1.171	980						
1.475	910						
1.751	746						

Table E8. Experimental measurements for the Pittsburgh #8 Air case.

Experiment Name:		Pittsburgh #8 Air					
Wall Temperatures		HORIBA Gas Analyzer					
Z (m)	T (K)	Z (m)	NO_X (ppm, dry)	CO (ppm, dry)	CO_2 (Vol%, dry)	O_2 (Vol%, dry)	η_N
0.025	1020	0.108	597	684	11.88	2.77	0.39
0.044	1055	0.413	492	692	13.61	1.03	0.32
0.07	1148	0.606	369	305	10.54	5.18	0.24
0.095	1181	0.667	162	130	4.99	12.93	0.17
0.108	1218	0.879	212	436	8.49	8.23	0.23
0.121	1206	1.171	222	98	7.72	9.10	0.24
0.146	1190	1.475	227	100	7.55	9.27	0.24
0.171	1050						
0.197	1122						
0.413	1205						
0.879	1032						
1.171	954						
1.475	887						
1.751	702						

Table E9. Experimental measurements for the Pittsburgh #8 O30 case.

Experiment Name:		Pittsburgh #8 O30					
Wall Temperatures		HORIBA Gas Analyzer					
Z (m)	T (K)	Z (m)	NO_X (ppm, dry)	CO (ppm, dry)	CO_2 (Vol%, dry)	O_2 (Vol%, dry)	η_N
0.025	1131	0.108	806	over	over	0.64	0.26
0.044	1178	0.413	827	over	over	-0.07	0.26
0.07	1222	0.606	76	over	over	8.33	0.02
0.095	1234	0.667	15	2509	over	16.99	0.01
0.108	1273	0.879	49	3159	over	9.19	0.03
0.121	1205	1.171	44	2625	over	10.11	0.02
0.146	1238						
0.171	1184						
0.197	1037						
0.413	1123						
0.879	1016						
1.171	960						
1.475	899						
1.751	718						

Table E10. Experimental measurements for the Sub-b Air case.

Experiment Name:	Sub-b Air						
Wall Temperatures		**HORIBA Gas Analyzer**					
Z (m)	T (K)	Z (m)	NO_X (ppm, dry)	CO (ppm, dry)	CO_2 (Vol%, dry)	O_2 (Vol%, dry)	η_N
0.02	1140	0.02	94	over	7.18	8.19	0.06
0.045	1203	0.045	446	845	11.30	5.20	0.30
0.071	1235	0.071	640	2329	13.29	2.99	0.43
0.096	1269	0.096	711	4845	14.45	1.38	0.48
0.108	1290	0.122	736	over	14.99	0.06	0.50
0.122	1286	0.147	716	over	15.06	-0.07	0.49
0.147	1285	0.172	701	over	15.24	-0.78	0.48
0.172	1280	0.198	675	over	15.24	-1.23	0.46
0.198	1268	0.413	464	over	13.57	-0.71	0.31
0.413	1324	0.606	315	1557	12.39	5.25	0.21
0.879	1216	0.667	154	442	7.21	11.96	0.18
1.171	1118	0.879	274	45	12.18	6.19	0.31
1.475	1046	1.171	254	39	11.33	7.09	0.29
1.751	914	1.475	265	65	11.60	6.93	0.30
		1.751	253	76	11.23	7.08	0.29

MKS FTIR Gas Analyzer											
	ppm									Vol%	
Z (m)	CO	CH_4	C_2H_4	HCN	NH_3	NO	NO_2	N_2O	SO_2	CO_2	H_2O
0.020	14879	727	115	1	2	94	1	6	29	7.49	14.51
0.045	2119	3	2	0	2	784	0	5	68	15.67	18.70
0.071	4098	-1	1	0	2	807	0	4	123	12.02	15.68
0.096	8607	2	1	0	3	885	0	4	140	13.93	18.60
0.122	13343	2	1	1	4	829	-1	3	155	12.45	15.89
0.147	17288	5	1	1	5	905	0	2	204	14.21	17.68
0.172	20227	5	2	1	11	874	0	0	221	14.86	19.23
0.198	21113	11	1	1	16	758	0	-1	219	13.50	17.80
0.413	24975	25	1	2	45	429	0	-3	189	9.64	13.94
0.606	2475	-1	1	0	1	361	0	2	171	10.90	14.17
0.667	569	1	0	0	1	174	1	1	94	6.67	7.70
0.879	49	1	0	0	1	269	0	1	131	9.35	10.58
1.171	36	0	0	0	1	320	0	3	147	11.02	12.51
1.475	74	-3	0	0	2	255	0	2	121	8.96	9.91
1.751	85	-2	0	0	2	263	0	3	82	9.70	12.98

Table E11. Experimental measurements for the Sub-b O25 case.

Experiment Name:	Sub-b O25						
Wall Temperatures		**HORIBA Gas Analyzer**					
Z (m)	T (K)	Z (m)	NO_X (ppm, dry)	CO (ppm, dry)	CO_2 (Vol%, dry)	O_2 (Vol%, dry)	η_N
0.02	1168	0.02	367	4936	over	4.49	0.16
0.045	1175	0.045	711	over	over	-1.24	0.32
0.071	1229	0.071	593	over	over	-1.24	0.26
0.096	1222	0.096	441	over	over	-1.24	0.20
0.108	1233	0.122	427	over	over	-1.24	0.19
0.122	1217	0.147	386	over	over	-1.24	0.17
0.147	1198	0.172	174	over	over	4.12	0.08
0.172	1183	0.198	251	over	over	-1.23	0.11
0.413	1185	0.413	151	over	over	-1.23	0.07
0.879	1286	0.606	173	over	over	-1.23	0.08
1.171	1221	0.667	236	2356	over	9.50	0.18
1.475	1128	0.879	309	278	over	3.92	0.23
1.751	989	1.171	321	62	over	4.74	0.24
		1.475	336	31	over	4.62	0.25

MKS FTIR Gas Analyzer											
	ppm									Vol%	
Z (m)	CO	CH_4	C_2H_4	HCN	NH_3	NO	NO_2	N_2O	SO_2	CO_2	H_2O
0.020	8858	3	15	1	25	358	-1	0	77	82.86	21.93
0.045	21581	45	10	5	42	728	-1	-15	180	77.38	23.88
0.071	18362	137	14	8	61	514	0	-1	149	69.29	20.79
0.096	15404	207	16	9	101	404	1	24	108	69.69	19.88
0.122	29660	320	18	13	101	377	1	56	96	73.16	19.69
0.147	26081	379	17	15	119	347	0		116	69.58	20.29
0.172	26385	298	13	11	173	189	0	9	73	51.26	15.22
0.198	31817	461	16	16	365	207	1	6	95	63.89	20.60
0.413		637	35	16	361	163	0	30	75	57.04	17.69
0.606	24929	638	53	11	324	160	0	-1	115	64.58	19.35
0.667	3856	-1	1	0	5	247	0	-1	171	79.53	12.77
0.879	317	1	-1	0	7	304	1	2	209	75.10	15.41
1.171	96	-2	1	0	10	321	0	-1	169	88.17	15.97
1.475	54	-3	0	0	9	317	0	-1	138	90.32	16.68

Table E12. Experimental measurements for the Sub-b O30 case.

Experiment Name:	Sub-b O30						
Wall Temperatures		**HORIBA Gas Analyzer**					
Z (m)	T (K)	Z (m)	NO_X (ppm, dry)	CO (ppm, dry)	CO_2 (Vol%, dry)	O_2 (Vol%, dry)	η_N
0.02	1196	0.02	600	over	over	5.76	0.22
0.045	1253	0.045	947	over	over	-1.23	0.35
0.071	1243	0.071	728	over	over	-1.23	0.27
0.096	1238	0.096	603	over	over	-1.23	0.22
0.108	1255	0.122	521	over	over	-1.23	0.19
0.122	1234	0.147	411	over	over	-1.23	0.15
0.147	1224	0.172	448	over	over	-1.23	0.17
0.172	1195	0.413	271	over	over	-1.23	0.10
0.198	1163	0.606	211	over	over	-1.23	0.08
0.413	1219	0.667	273	1180	over	11.85	0.17
0.879	1345	0.879	413	144	over	4.46	0.26
1.171	1244	1.171	416	44	over	4.73	0.26
1.475	1162	1.475	426	39	over	4.73	0.27
1.751	994						

MKS FTIR Gas Analyzer											
	ppm									Vol%	
Z (m)	CO	CH_4	C_2H_4	HCN	NH_3	NO	NO_2	N_2O	SO_2	CO_2	H_2O
0.020	21645	209	24	10	16	1132	11		138		26.24
0.045		300	20	12	50	719	62		121		26.78
0.071	24731	329	21	13	66	613			115		28.47
0.096	25073	430	23	16	64	556	11		123		25.41
0.122	20523	452	20	15	94	429	1		93	64.52	21.23
0.147	21376	392	18	14	72	462	2		97	64.16	20.76
0.172		464	19	14	96	401	2		58	64.60	22.86
0.198	18647		8	4	378	50	1	0	33		18.24
0.413	21225		11	2	27		0		67	67.96	21.89
0.606		800	36	18	390	223	0		84	61.76	21.14
0.667		928	60	15	532	188	2		112	73.35	24.18
0.879	3209	5	5	0	2	333	1	4	291	78.72	19.43
1.171	188	3	3	0	1	423	1	2	387		19.99
1.475	102	2	8	0	2	597	2	4	485	66.08	27.05

Table E13. Experimental measurements for the Sub-b Air Staging case.

Experiment Name:		Sub-b Air Staging				
Percent Oxidizer to Burnout Oxidizer Ports	Primary SR	Wall Temperatures (K) – Distance From Burner				
		0.11 m	0.41 m	0.88 m	1.17 m	1.75 m
18.9	1.00	1214	1354	1254	1172	957
25.0	0.92	1267	1355	1241	1164	946
31.9	0.84	1289	1349	1224	1150	934
34.2	0.81	1305	1341	1239	1158	935
35.8	0.79	1295	1323	1239	1161	936
39.6	0.74	1299	1338	1221	1149	935
42.9	0.70	1294	1319	1224	1150	937
49.0	0.63	1269	1290	1243	1156	942
53.8	0.57	1258	1277	1273	1171	949
Percent Oxidizer to Burnout Oxidizer Ports	Primary SR	HORIBA Gas Analyzer (1.475 m from Burner)				
		NO_X (ppm, dry)	CO (ppm, dry)	CO_2 (Vol%, dry)	O_2 (Vol%, dry)	η_N
18.9	1.00	454	2	11.25	6.05	0.52
25.0	0.92	418	5	11.50	5.81	0.48
31.9	0.84	365	17	11.38	5.93	0.42
34.2	0.81	314	27	11.83	5.48	0.36
35.8	0.79	283	29	11.82	5.44	0.32
39.6	0.74	273	17	11.07	6.45	0.32
42.9	0.70	247	12	10.95	6.51	0.29
49.0	0.63	234	0	11.21	6.18	0.27
53.8	0.57	268	-3	11.68	5.56	0.30

Table E14. Experimental measurements for the Sub-b O25 Staging case.

Experiment Name:		Sub-b O25 Staging				
Percent Oxidizer to Burnout Oxidizer Ports	**Primary SR**	**Wall Temperatures (K) – Distance From Burner**				
		0.11 m	**0.41 m**	**0.88 m**	**1.17 m**	**1.75 m**
20.5	0.98	1328	1316	1261	1198	963
24.8	0.93	1325	1306	1261	1195	959
31.1	0.85	1319	1283	1274	1202	964
36.4	0.78	1298	1263	1287	1210	974
39.3	0.75	1266	1242	1297	1218	979
46.4	0.66	1234	1219	1317	1230	986
Percent Oxidizer to Burnout Oxidizer Ports	**Primary SR**	**HORIBA Gas Analyzer (1.475 m from Burner)**				
		NO_X (ppm, dry)	CO (ppm, dry)	CO_2 (Vol%, dry)	O_2 (Vol%, dry)	η_N
20.5	0.98	444	101	over	3.66	0.33
24.8	0.93	373	118	over	3.86	0.28
31.1	0.85	344	89	over	3.71	0.26
36.4	0.78	371	81	over	3.87	0.28
39.3	0.75	385	74	over	4.06	0.29
46.4	0.66	447	71	over	4.17	0.33

Table E15. Experimental measurements for the Sub-b O30 Staging case.

Experiment Name:		Sub-b O30 Staging				
Percent Oxidizer to Burnout Oxidizer Ports	**Primary SR**	**Wall Temperatures (K) – Distance From Burner**				
		0.11 m	**0.41 m**	**0.88 m**	**1.17 m**	**1.75 m**
18.8	1.00	1354	1343	1246	1164	931
25.2	0.92	1352	1328	1256	1172	930
32.8	0.83	1326	1294	1290	1194	938
36.0	0.79	1301	1276	1311	1210	945
39.0	0.75	1278	1257	1329	1226	952
43.0	0.70	1246	1238	1352	1243	964
47.1	0.65	1096	1196	1334	1246	971
Percent Oxidizer to Burnout Oxidizer Ports	**Primary SR**	**HORIBA Gas Analyzer (1.475 m from Burner)**				
		NO_X (ppm, dry)	CO (ppm, dry)	CO_2 (Vol%, dry)	O_2 (Vol%, dry)	η_N
18.8	1.00	621	74	over	4.80	0.39
25.2	0.92	463	56	over	5.05	0.29
32.8	0.83	377	49	over	4.57	0.24
36.0	0.79	386	56	over	4.57	0.25
39.0	0.75	405	64	over	4.63	0.26
43.0	0.70	452	79	over	4.43	0.29
47.1	0.65	489	184	over	4.54	0.31

Table E16. Experimental measurements for the Sub-b Air (Opt) case.

Experiment Name:	Sub-b Air (Opt)						
Wall Temperatures		**HORIBA Gas Analyzer**					
Z (m)	T (K)	Z (m)	NO_X (ppm, dry)	CO (ppm, dry)	CO_2 (Vol%, dry)	O_2 (Vol%, dry)	η_N
0.02	1134	0.02	360	1145	10.94	3.74	0.20
0.045	1217	0.045	543	over	12.99	-1.23	0.30
0.071	1230	0.071	326	over	8.27	5.11	0.18
0.096	1235	0.096	384	over	11.05	-1.23	0.21
0.108	1245	0.122	187	over	5.90	8.27	0.10
0.122	1231	0.147	277	over	10.24	-1.23	0.16
0.147	1223	0.172	200	over	9.25	-0.03	0.11
0.172	1214	0.198	181	over	11.05	-1.23	0.10
0.198	1200	0.413	152	over	11.68	-1.23	0.08
0.413	1234	0.606	169	over	12.54	-0.68	0.09
0.879	1207	0.667	131	730	7.41	10.45	0.15
1.171	1121	0.879	187	54	9.67	7.68	0.22
1.475	1034	1.171	204	25	10.05	7.22	0.23
1.751	903	1.475	206	7	9.75	7.61	0.24

MKS FTIR Gas Analyzer											
	ppm									Vol%	
Z (m)	CO	CH_4	C_2H_4	HCN	NH_3	NO	NO_2	N_2O	SO_2	CO_2	H_2O
0.020	1002	1	6	1	33	314	0	1	52	8.03	14.27
0.045	14309	62	8	7	38	463	0	4	124	9.29	15.99
0.071	18458	77	5	7	35	302	0	4	94	6.51	10.70
0.096	29236	113	6	8	54	359	0	2	124	8.46	15.15
0.096	28637	108	6	8	35	335	0	2	119	8.10	14.31
0.122	20356	69	3	5	41	179	0	4	65	4.70	8.00
0.147	32549	153	6	9	79	244	0	1	89	7.59	12.84
0.172	31651	145	5	8	101	188	0	1	60	6.88	11.85
0.198	35193	194	6	8	140	163	0	-4	40	7.99	14.36
0.413	37337	367	9	10	58	137	0	-9	27	8.45	14.20
0.606	21954	213	7	6	3	131	0	4		7.57	10.01
0.606	29571	277	10	6	4	162	0	2	131	9.91	13.83
0.667	842	1	0	0	0	141	0	1	84	6.70	7.29
0.879	61	-3	0	0	0	199	0	1	90	8.46	8.10
1.171	28	1	0	0	0	215	0	1	88	8.88	7.58
1.475	12	-4	0	0	0	222	0	1	69	8.92	6.74

Table E17. Experimental measurements for the Sub-b O30 (Opt) case.

Experiment Name:	Sub-b O30 (Opt)						
Wall Temperatures		**HORIBA Gas Analyzer**					
Z (m)	T (K)	Z (m)	NO_X (ppm, dry)	CO (ppm, dry)	CO_2 (Vol%, dry)	O_2 (Vol%, dry)	η_N
0.02	1215	0.02	532	3005	over	9.39	0.22
0.045	1292	0.045	1028	over	over	-0.97	0.42
0.071	1299	0.071	800	over	over	0.10	0.33
0.096	1296	0.096	718	over	over	-1.23	0.29
0.122	1284	0.122	579	over	over	-1.23	0.24
0.147	1281	0.147	327	over	over	6.35	0.13
0.172	1249	0.172	300	over	over	5.83	0.12
0.198	1239	0.198	315	over	over	-1.23	0.13
0.108	1305	0.413	267	over	over	-1.22	0.11
0.413	1246	0.606	145	over	over	7.86	0.06
0.879	1278	0.667	252	1069	over	13.19	0.16
1.171	1182	0.879	334	128	over	7.37	0.21
1.475	1094	1.171	240	31	over	10.79	0.15
1.751	931	1.475	373	33	over	6.16	0.24

MKS FTIR Gas Analyzer											
	ppm									Vol%	
Z (m)	CO	CH_4	C_2H_4	HCN	NH_3	NO	NO_2	N_2O	SO_2	CO_2	H_2O
0.020	3262	5	3	0	24	449	1	4	100	42.81	14.88
0.045	31702	11	1	3	39	802	1	-14	229	52.38	21.44
0.071	37342	36	1	4	47	640	1	-19	214	44.43	19.13
0.096	33913	45	2	4	62	578	0	-16	216	45.69	19.57
0.122	27725	52	2	4	65	459	0	-20	176	43.08	17.96
0.147	37098	40	2	3	44	293	1	-21	112	31.59	11.81
0.172	36742	49	2	3	57	278	1	-22	111	32.06	11.97
0.198		87	2	5	98	407	1	-4	159	45.87	19.56
0.198		159	8	3	72	266	1	2	54	54.11	13.89
0.413		198	4	6	184	221	1	-19	77	40.04	16.13
0.606	36564	166	6	4	37	134	0	-23	63	28.49	10.19
0.667	1264	0	-2	0	8	213	1	6	184	59.41	13.21
0.879	137	-2	-2	0	11	282	1	6	250	56.64	14.86
1.171	38	-4	-1	0	12	217	1	2	172	44.65	11.68
1.475	59	-2	0	1	14	296	0	1	174	64.23	14.45
1.475	42	-4	-2	0	13	307	1	5	235	60.92	15.72